WILEY-VCH

Edited by
Bartolo Gabriele

Carbon Monoxide in Organic Synthesis

Carbonylation Chemistry

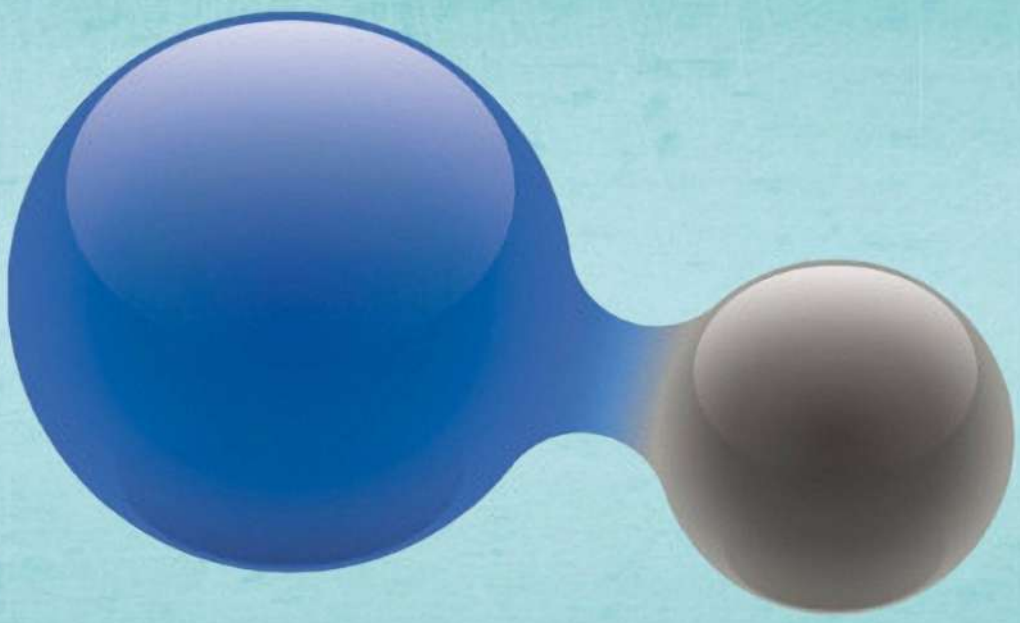

Carbon Monoxide in Organic Synthesis

Carbon Monoxide in Organic Synthesis

Carbonylation Chemistry

Edited by
Bartolo Gabriele

WILEY-VCH

Editor

Prof. Bartolo Gabriele
University of Calabria
Department of Chemistry & Chemical Technologies
Via Pietro Bucci 12/C
87036 Arcavacata di Rende (CS)
Italy

Cover Image: © azatvaleev/Getty Images

Library of Congress Card No.: applied for

British Library Cataloguing-in-Publication Data
A catalogue record for this book is available from the British Library.

Bibliographic information published by the Deutsche Nationalbibliothek
The Deutsche Nationalbibliothek lists this publication in the Deutsche Nationalbibliografie; detailed bibliographic data are available on the Internet at <http://dnb.d-nb.de>.

Print ISBN: 978-3-527-34795-7
ePDF ISBN: 978-3-527-82933-0
ePub ISBN: 978-3-527-82934-7
oBook ISBN: 978-3-527-82935-4

Typesetting Straive, Chennai, India

Printed on acid-free paper

10 9 8 7 6 5 4 3 2 1

This book is dedicated to the memory of my beloved parents, Giuseppe Gabriele and Anna La Valle.

Contents

Preface

This book is dedicated to the use of carbon monoxide as a C-1 building block in organic synthesis. The incorporation of carbon monoxide into an organic substrate to give a carbonyl compound is called "carbonylation." Carbonylation reactions, discovered in 1930s thanks to the pioneering work by Roelen and Reppe, are now established as a most powerful methodology for the direct synthesis of carbonyl derivatives using the simplest and readily available C-1 unit. Impressive progress has been made in this field at both industrial and academic levels, so nowadays carbonylations are widely applied not only for the production of industrially relevant, relatively simple carbonyl compounds but also for the preparation of complex molecular architectures and even as key steps in natural product synthesis.

I have been involved in this fascinating area of research for many years, with particular interest in palladium-catalyzed processes. After my degree in chemistry at the University of Calabria with a thesis on Pd(II)-catalyzed alkyne carbonylation (1990), in 1991, I joined the group of Professors Gian Paolo Chiusoli and Mirco Costa at the University of Parma for a research stage. At that time, the use of CO as C-1 unit in synthesis was among the primary research interests of Professors Chiusoli and Costa, and I was very happy to be involved in this emerging research area. Since then, I continued to work in this field during my PhD (at the University of Calabria, with Professor Giuseppe Salerno) and then in the course my independent career.

Therefore, at the end 2019, when Dr. Anne Brennführer invited me to submit a book proposal on carbonylation chemistry for Wiley-VCH, I was very happy to accept. I was aware that other important and excellent books had been published before (the most recent one in 2014). However, I was convinced that a new updated book in this field, organized in a different way with respect to those already published, could be useful to the scientific community. In fact, a new book could be of interest not only for those researchers directly involved in carbonylation chemistry (from both academia and industry) but also for researchers, postdocs, and PhD students interested in the most recent trends in organic synthesis.

Most carbonylation processes are catalyzed by transition metal species. Different from the previous books on carbonylations, which were organized on the basis of the process type or the nature of the carbonylated product obtained, this book has been structured according to the metal promoting the carbonylation process. The aim of this kind of classification was to help the reader to better focus on the catalytic

abilities and specificities of different metal catalysts in promoting various kinds of carbonylations. However, considering the increasing importance of metal-free carbonylation reactions (radical carbonylations, in particular), a final chapter has been also devoted to this emerging area of research.

The book contributors are leading scientists in the field, who have kindly accepted my invitation to spend some of their time for the realization of this exciting project, and I extend my warmest thanks to them. I also would like to thank very much the Wiley-VCH editors, in particular Dr. Anne Brennführer and Ms. Katherine Wong, for the kind invitation to edit this book and for their invaluable cooperation and support throughout the entire preparation of the book.

I hope you will enjoy reading the book at least as much as I have enjoyed in editing it!

Arcavacata di Rende (CS)
January 18, 2021 *Bartolo Gabriele*

1

Introduction: Carbon Monoxide as Synthon in Organic Synthesis

Bartolo Gabriele

University of Calabria, Laboratory of Industrial and Synthetic Organic Chemistry (LISOC), Department of Chemistry and Chemical Technologies, Via Pietro Bucci 12/C, 87036 Arcavacata di Rende, Italy

This book discusses the synthesis of carbonylated compounds by introducing the carbonyl function into an organic substrate (carbonylation) employing the simplest C-1 unit as carbonylating agent, carbon monoxide. Carbon monoxide is a largely available feedstock. It is produced industrially by partial oxidation of petroleum hydrocarbons and steam reforming of light hydrocarbons (including natural gas) or gasification of coal to give syngas (CO and H_2) [1]. In the future, it is expected that a growing amount of carbon monoxide will be available from renewable feedstocks, such as biowastes and CO_2 [2]. CO is also the simplest unit that, upon insertion into an organic substrate, can be directly transformed, without atom loss, into a carbonyl group. It is therefore a desirable and useful building block in synthesis to produce high value-added industrially relevant molecules and fine chemicals.

Carbonylation reactions were disclosed in the 1930s by the seminal works of Roelen [3] and Reppe [4] (who also coined the term "carbonylation") for industrial applications. Since then, the scientific progress in this field has been enormous, thanks, in particular, to the development of more and more selective and efficient catalysts. These catalysts are able to promote a plethora of carbonylations under mild conditions, which can be applied to a large variety of organic substrates. Accordingly, carbonylations with CO have become increasingly more and more important, at the industrial and academic level, as testified by the considerable number of books [5–12] and reviews [13–115] dedicated to this topic and by the increasing number of industrial patents and scientific publications.

As said above, the *incorporation of carbon monoxide into an organic substrate* to give a carbonyl compound is called *carbonylation*. Interestingly, during the last years, considerable effort has been made by the scientific community to use CO surrogates as indirect carbonylating agents or as *in situ* sources of CO (both in industry and in academia, to avoid the direct handling of gaseous and toxic CO). In this book, several representative examples of CO surrogates will also be presented and discussed. Although CO surrogates can be interesting from a practical point of view, it should

Carbon Monoxide in Organic Synthesis: Carbonylation Chemistry,
First Edition. Edited by Bartolo Gabriele.

still be considered that carbon monoxide is cheaper than its surrogates and that carbonylations with CO occur with a higher atom economy.

Carbon monoxide possesses the strongest bond currently known (257.3 kcal/mol) [116]. This bond is only weakly polarized in the direction of carbon (the experimental dipole moment is 0.122 D) [117]. These characteristics make carbon monoxide a relatively stable and inert molecule. Consequently, CO can be attacked by highly reactive species, such as free radicals, carbocations, and strong nucleophiles (like alkoxides, amide anions, and organolithium reagents) (Scheme 1.1). These reactions form acyl radicals, acyl carbocations, and $[NuCO]^-$ intermediates (alkoxycarbonyl anions, carbamoyl anions, and acyl anions). They evolve toward forming the final carbonylation product depending on the nature of reactants and reaction conditions (Scheme 1.1).

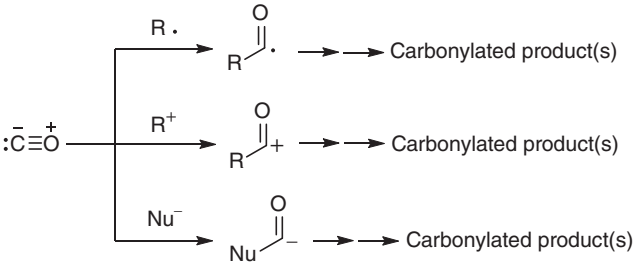

Scheme 1.1 Reactions of carbon monoxide with free radicals, carbocations, or strong nucleophiles (such as RO^-, R_2N^-, RLi).

However, the most common way to activate CO in carbonylation reactions under relatively mild conditions is metal coordination. In fact, upon coordination to a metal center M, the carbon atom becomes more electrophilic. It accordingly becomes susceptible to attack even by a relatively weak nucleophile, either external or coordinated to the metal (Scheme 1.2; formal charges are omitted for clarity). When occurring within the coordination sphere of the metal, this process is called *migratory insertion*. In this case, the metal also favors the attack to coordinated CO for entropic reasons. In either case (external attack, Scheme 1.2a, or migratory insertion, Scheme 1.2b), the coordinated carbon monoxide is transformed into a species in which the carbonyl group is bonded to M, and whose particular structure depends, apart from the metal, on the nature of the nucleophile. Thus, if the nucleophilic species is a carbon group (alkyl, alkenyl, or aryl) σ-bonded to the metal undergoing migratory insertion, an acyl- or aroyl-metal species is formed. On the other hand, oxygen and nitrogen nucleophiles will lead to hydroxycarbonyl-, alkoxycarbonyl-, or carbamoyl-metal complexes, respectively (Scheme 1.2).

These intermediates' fate will depend on the nature of the metal and of the reactants taking part in the carbonylation process and on reaction conditions. In most cases, the final carbonylated organic product is formed with the release of the metal, either in its original or in a different oxidation state. In the first case, a catalytic cycle is directly attained. In contrast, in the second case, the metal species must be reported in its original oxidation state (using a suitable redox agent) to achieve a catalytic process. For example, an acyl- or aroyl-metal intermediate R(CO)–M[+*n*]–X

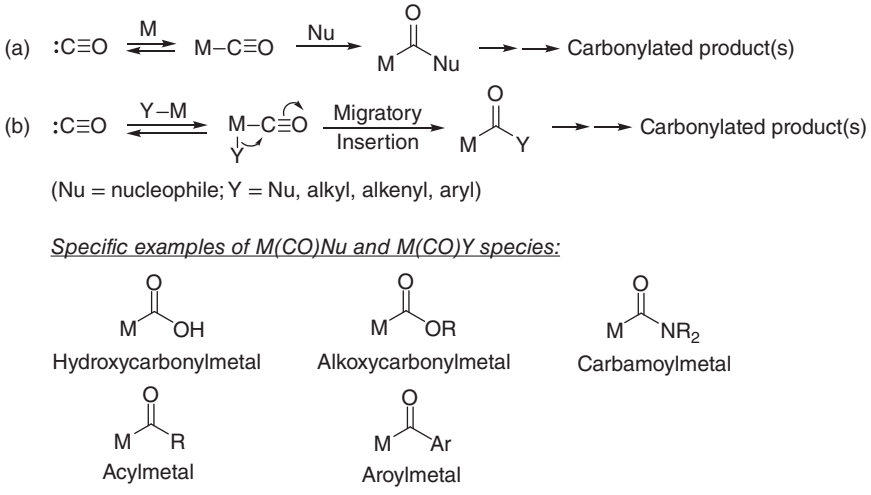

Scheme 1.2 Carbon monoxide coordinated to a metal center becomes more susceptible to nucleophilic attack, either intermolecularly (a) or intramolecularly (*migratory insertion*) (b).

(X^- = halide or other ligands, with M in the oxidation state [+n]) may undergo a nucleophilic attack by a nucleophile NuH (like water, alcohol, or an amine), with the formation of the carbonylated product R(CO)Nu (such as a carboxylic acid, an ester, or an amide), HX, and the reduced metal M[+(n−2)] (reductive displacement or nucleophilic displacement; Scheme 1.3).

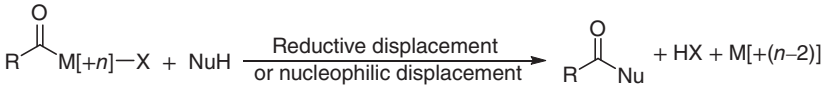

Scheme 1.3 An acyl- or aroyl-metal intermediate (R = carbon group) undergoing reductive displacement (also called nucleophilic displacement).

If the metal initiated the process in its [+(n−2)] oxidation state (for example, by oxidative addition of R–X to the metal center to give R–M[+n]–X followed by CO migratory insertion), a catalytic cycle is directly achieved (Scheme 1.4). On the other hand, if the metal initiated the process in its [+n] oxidation state (for example, by metalation of R–H by M[+n]X_2 with the formation of R–M[+n]–X + HX, followed by CO migratory insertion), the use of a suitable external oxidant is necessary to reconvert the reduced metal M[+(n−2)] to M[+n] and realize a catalytic process

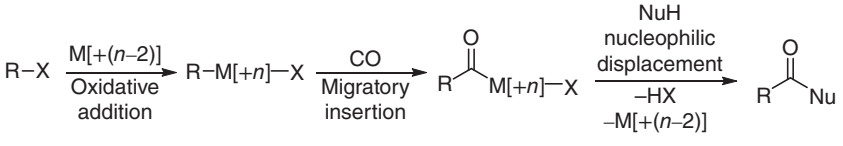

Scheme 1.4 An example of catalytic carbonylation process in which the metal is eliminated at the end of the process in its original oxidation state.

(Scheme 1.5). Clearly, from a practical and economical point of view, the occurrence of a carbonylative catalytic cycle is highly desirable. In the last decades, there has been considerable attention to developing more and more robust and efficient metal catalysts, also heterogeneous and/or with the possibility of being effectively recycled.

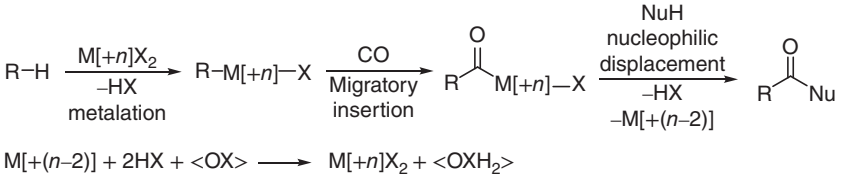

Scheme 1.5 An example of catalytic carbonylation process in which the metal is reduced at the end of the process and is reoxidized to its original oxidation state by the action of an external oxidant.

The nucleophilic attack of NuH to an acyl- or aroyl-metal intermediate (either inter- or intramolecular) is a common and important process by which the final carbonylated compound is delivered in a carbonylation reaction. This process is called *reductive displacement* or *nucleophilic displacement*. The exact mechanism this step may take place depends on reaction conditions, and, in particular, if the carbonylation process is done under acidic, neutral, or basic conditions. Under acidic and neutral conditions, the nucleophile tends to attack the carbonyl (possibly protonated) of the R(CO)–M[+n]–X complex, with the formation of a tetrahedral intermediate. This intermediate undergoes β-H elimination from the H–O–C–MX moiety to give R(CO)Nu and a metal hydride species H–M[+n]–X, in equilibrium with M[+(n−2)] + HX (*addition–elimination mechanism*, Scheme 1.6a). On the other hand, under basic conditions, NuH (possibly in its anionic Nu^- form) preferably attacks the metal center, with formal elimination of X^- and formation

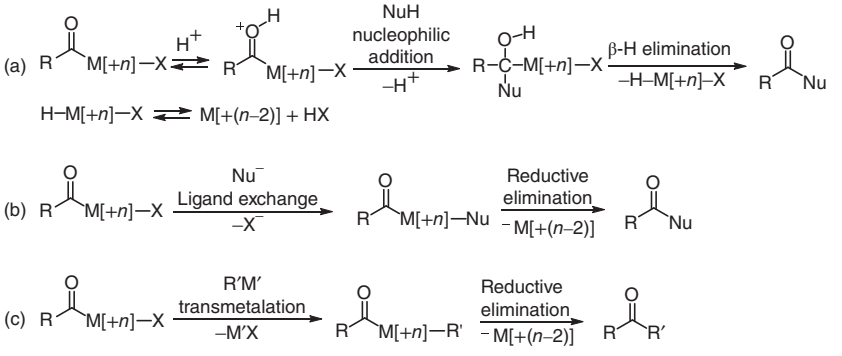

Scheme 1.6 Possible mechanistic pathways in the nucleophilic displacement step: (a) nucleophilic attack to the carbonyl followed by β-H elimination from the H–O–C–MX unit (*addition–elimination mechanism*); (b) nucleophilic attack to the metal center followed by reductive elimination (*ligand exchange mechanism*); (c) reaction with an organometallic reagent R′M′ followed by reductive elimination (*transmetalation mechanism*).

of the R(CO)–M[+n]–Nu complex. Reductive elimination then leads to R(CO)Nu and M[+(n−2)] (*ligand exchange mechanism*; Scheme 1.6b). This latter case also occurs when the R(CO)–M[+n]–X species is attacked by an organometallic reagent R′M′ with the formation of M′X and R(CO)–M[+n]–R′ that undergoes reductive elimination to give R(CO)R′ (as occurs in the so-called carbonylative cross-coupling reactions) (*transmetalation mechanism*; Scheme 1.6c).

Depending on the exact stoichiometry of the process, carbonylations can be broadly classified into *direct*, *substitutive*, *additive*, *oxidative*, and *reductive carbonylations*. In *direct carbonylation*, carbon monoxide is formally inserted into an A—B bond of an organic substrate to give a carbonylated product bearing the A(CO)B functionality (Scheme 1.7a). An example is the direct catalytic carbonylation of methanol to acetic acid (Scheme 1.7b), a particularly important industrial process.

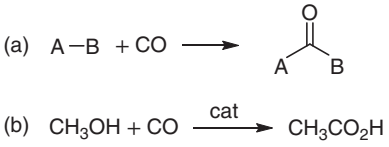

Scheme 1.7 A generic direct carbonylation process (a) and direct carbonylation of methanol to acetic acid (b).

On the other hand, *substitutive carbonylation* corresponds to the formal substitution of a certain functional group W of an organic substrate with a carbonylic functional group (CO)Z (Scheme 1.8a). An example is given by the substitutive carbonylation of an allyl alcohol RCH=CHCH$_2$OH carried out with CO and an alcohol (R′OH) to give a β,γ-unsaturated ester with water as coproduct, as shown in Scheme 1.8b.

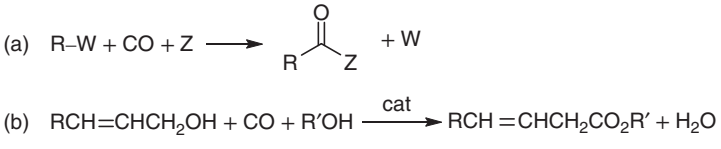

Scheme 1.8 A generic substitutive carbonylation process (a) and substitutive carbonylation of allyl alcohols to β,γ-unsaturated esters (b).

Additive carbonylation is a process in which carbon monoxide, together with an H–Y species (Y = hydrogen or a nucleophilic group), adds to an unsaturated carbon–carbon bond, as exemplified in Scheme 1.9a for the double bond. Examples are given by the hydroformylation of olefins (in which Y = H, with the formal addition to the double bond of a hydrogen atom on one carbon and the formyl group on the other one, Scheme 1.9b) or the Reppe alkoxycarbonylation of an olefin with CO and an alcohol (Y = OR′, with the formal addition to the double bond of a hydrogen atom on one carbon and the alkoxycarbonyl group on the other one, Scheme 1.9c).

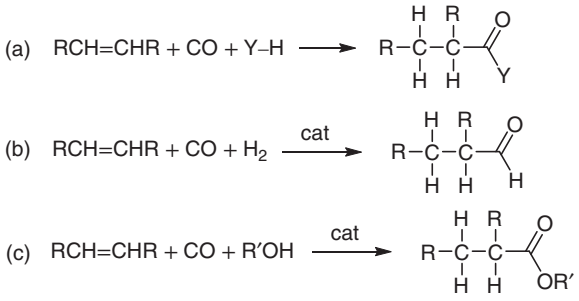

Scheme 1.9 A generic additive carbonylation process for an olefin (a), additive carbonylation of an olefin with H_2 (hydroformylation) (b), and additive carbonylation of an olefin with an alcohol (Reppe carbonylation) (c).

In an oxidative carbonylation reaction, the process occurs with the formal simultaneous elimination of molecular hydrogen from the substrate(s) (Scheme 1.10a). Although a few examples are known in the literature in which molecular hydrogen is indeed formed as the reaction coproduct, in the majority of the cases, the process, promoted by a metal catalyst M[+n], occurs with simultaneous reduction of the metal by two units and with the concomitant formation of 2 mol of H^+ (Scheme 1.10b). A process like this is not catalytic unless a suitable external oxidant (able to reconvert the reduced metal into its original oxidation state, Scheme 1.10c) is added among the reactants (Scheme 1.10d). An example is the PdI_2-catalyzed oxidative dialkoxycarbonylation of alkynes to give maleic diesters carried out with molecular oxygen as the external oxidant, as shown in Scheme 1.11.

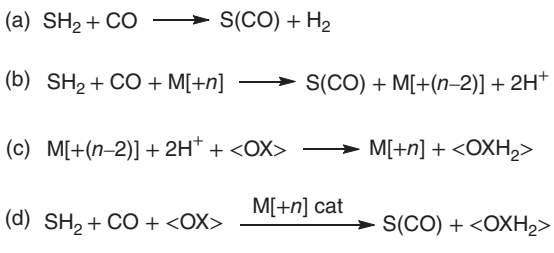

Scheme 1.10 A generic oxidative carbonylation process (a) with the elimination of molecular hydrogen from substrate(s) SH_2 and formation of carbonylated product(s) S(CO) or (b) with reduction by two units of a metal species promoting the process or (d) carried out in the presence of an external oxidant, able to reconvert the promoting metal in its original oxidation state (c). The combination between the stoichiometric process (b) with metal reoxidation (c) gives the reaction (d) catalytic in the metal.

On the other hand, *reductive carbonylation* is when molecular hydrogen is formally inserted together with CO into the organic reactant(s) (Scheme 1.12a). The hydroformylation reaction of olefins, shown in Scheme 1.9b, is the most important example in which molecular hydrogen is used as a coreactant. A more complex example is given by the reductive carbonylation of alkynes, in which molecular hydrogen is formally released from the water-shift reaction ($CO + H_2O \rightarrow CO_2 + H_2$)

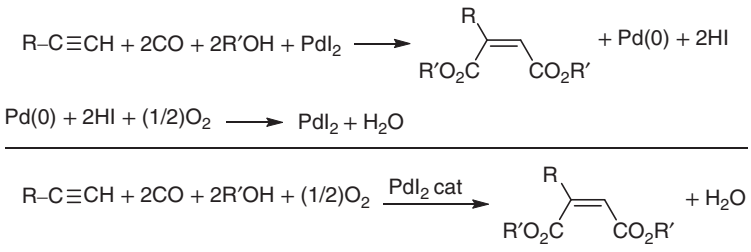

Scheme 1.11 PdI_2-catalyzed oxidative dialkoxycarbonylation of alkynes to maleic diesters. The catalytic process is the result of the combination between the dialkoxycarbonylation process occurring with reduction of PdI_2 to Pd(0) followed by reoxidation of Pd(0) to PdI_2 by the action of the external oxidant (molecular oxygen).

and reduces one carbonyl unit into a $–CH_2O–$ moiety within the final unsaturated γ-lactone ring (Scheme 1.12b).

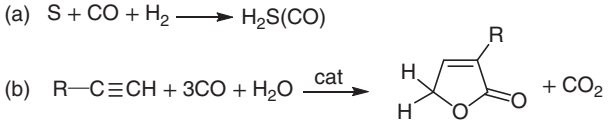

Scheme 1.12 (a) A generic reductive carbonylation process with molecular hydrogen as reducing agent and (b) reductive carbonylation of alkynes to furan-2(5*H*)-ones (in which H_2 is formally produced *in situ* by the water-shift reaction, $CO + H_2O \rightarrow CO_2 + H_2$).

The major emphasis of the book is based on the increasing importance and versatility of transition metal-catalyzed carbonylation processes. The book represents the first attempt to present carbonylations based on the kind of metal promoting the carbonylation process rather than on the carbonylation process type or the carbonylated product's nature. Part I of the book deals with carbonylations promoted by first-row transition metal catalysts (cobalt, nickel, manganese, iron, copper). Part II describes carbonylations promoted by second-row transition metal catalysts (ruthenium, rhodium, palladium, other second-row metals). Carbonylation promoted by third-row transition metal catalysts is discussed in Part III. Chapter 11 is also devoted to metal-free carbonylation processes.

References

1 Reimert, R., Marschner, F., Renner, H.-J., Boll, W., Supp, E., Brejc, M., Liebner, W., and Schaub, G. (2011). Gas production, 2. In: *Ullmann's Encyclopedia of Industrial Chemistry* (eds. H. Baltes, W. Göpel and J. Hesse), 423–479. Weinheim, Germany: Wiley-VCH.

2 Karl, J. and Pröll, T. (2018). *Renewable Sustainable Energy Rev.* 98: 64–78.

3 Roelen, O. (Rührchemie AG) (1938). Verfahren zur Herstellung von sauerstoffhaltigen Verbindungen. German Patent 849548, filed 20 September 1938 and issued 15 September 1952.

4 Reppe, W. (IG Farben) (1939). Verfahren zur Herstellung von Acrylsaeure oder ihren Substitutionserzeugnissen. German Patent 855110, filed 02 August 1939 and issued 10 November 1952.
5 Falbe, J. (ed.) (1970). *Carbon Monoxide in Organic Synthesis*. Berlin: Springer-Verlag.
6 Falbe, J. (ed.) (1980). *New Syntheses with Carbon Monoxide*. Berlin, Germany: Springer-Verlag.
7 Colquhoun, H.M., Thompson, D.J., and Twigg, M.V. (1991). *Carbonylation – Direct Synthesis of Carbonyl Compounds*. New York, NY: Plenum Press.
8 Beller, M. (ed.) (2006). Catalytic carbonylation reactions. In: *Topics in Organometallic Chemistry*, vol. 18, 1–272. Berlin, Germany: Springer.
9 Kollár, L. (ed.) (2008). *Modern Carbonylation Methods*. Weinheim, Germany: Wiley-VCH.
10 Beller, M. and Wu, X.-F. (2013). *Transition Metal Catalyzed Carbonylation Reactions – Carbonylative Activation of C–X Bonds*. Berlin, Germany: Springer.
11 Tambade, P., Bhanage, B., and Patil, Y. (2014). *Studies in Catalytic Carbonylation Reactions*. Riga, Latvia: LAP Lambert Academic Publishing.
12 Wu, X.-F. and Beller, M. (eds.) (2016). Transition metal catalyzed Carbonylative synthesis of heterocycles. In: *Topics in Heterocyclic Chemistry*, vol. 42, 1–166. Berlin: Springer.
13 Ren, Z., Lyu, Y., Song, X., and Ding, Y. (2020). *Appl. Catal., A* 595: 117488.
14 Nogi, K. and Yorimitsu, H. (2020). *Chem. Asian J.* 15: 441–449.
15 Kalck, P., Le Berre, C., and Serp, P. (2020). *Coord. Chem. Rev.* 402, UNSP 213078.
16 Jones, D.J., Lautens, M., and McGlacken, G.P. (2019). *Nat. Catal.* 2: 843–851.
17 Perrone, S., Troisi, L., and Salomone, A. (2019). *Eur. J. Org. Chem.*: 4626–4643.
18 Zhao, S. and Mankad, N.P. (2019). *Catal. Sci. Technol.* 9: 3603–3613.
19 Mancuso, R., Della Ca', N., Veltri, L., Ziccarelli, I., and Gabriele, B. (2019). *Catalysts* 9: 610.
20 Peng, J.-B., Geng, H.-Q., and Wu, X.-F. (2019). *Chem* 5: 526–552.
21 Urban, B., Papp, M., and Skoda-Foldes, R. (2019). *Curr. Green Chem.* 6: 78–95.
22 Ma, K., Martin, B.S., Yin, X., and Dai, M.J. (2019). *Nat. Prod. Rep.* 36: 174–219.
23 Nielsen, D.U., Neumann, K.T., Lindhardt, A.T., and Skrydstrup, T. (2019). *J. Labelled Compd. Radiopharm.* 61: 949–987.
24 Xu, F.N. and Han, W. (2019). *Chin. J. Org. Chem.* 38: 2519–2533.
25 Taddei, C. and Gee, A.D. (2019). *J. Labelled Compd. Radiopharm.* 61: 237–251.
26 Matsubara, H., Kawamoto, T., Fukuyama, T., and Ryu, I. (2018). *Acc. Chem. Res.* 51: 2023–2035.
27 Gabriele, B. (2018). Synthesis of heterocycles by palladium-catalyzed carbonylative reactions. In: *Advances in Transition-Metal Mediated Heterocyclic Synthesis* (eds. D. Solé and I. Fernández), 55–127. London, UK: Academic Press/Elsevier.
28 Gabriele, B. (2018). *Targets in Heterocyclic Systems*, vol. 22 (eds. O.A. Attanasi, P. Merino and D. Spinelli), 41–55. Rome, Italy: Italian Chemical Society.
29 Peng, J.-B. and Wu, X.-F. (2018). *Angew. Chem. Int. Ed.* 57: 1152–1160.
30 Li, Y., Hu, Y., and Wu, X.-F. (2018). *Chem. Soc. Rev.* 47: 172–194.

31 Albano, G. and Aronica, L.A. (2017). *Eur. J. Org. Chem.*: 7204–7221.
32 Piens, N. and D'hooghe, M. (2017). *Eur. J. Org. Chem.*: 5943–5960.
33 Shen, C. and Wu, X.-F. (2017). *Chem. Eur. J.* 23: 2973–2978.
34 Pineiro, M., Dias, L.D., Damas, L., Aquino, G.L.B., Calvete, M.J.F., and Pereira, M.M. (2017). *Inorg. Chim. Acta* 455: 364–377.
35 Peng, J.B., Qi, X., and Wu, X.-F. (2017). *Synlett* 28: 175–194.
36 Feng, J.-B. and Wu, X.-F. (2017). *Adv. Heterocycl. Chem.* 121: 207–246.
37 Zhu, Z., Zhang, W., and Gao, Z. (2016). *Progr. Chem.* 28: 1626–1633.
38 Song, H., Kang, M., Jin, R., Jin, F., and Chen, J. (2016). *Progr. Chem.* 28: 1313–1327.
39 Zoeller, J.R. (2016). *Org. Process Res. Dev.* 20: 1016–1025.
40 Gehrtz, P.H., Hirschbeck, V., Ciszek, B., and Fleischer, I. (2016). *Synthesis* 48: 1573–1596.
41 Friis, S.D., Lindhardt, A.T., and Skrydstrup, T. (2016). *Acc. Chem. Res.* 49: 594–605.
42 Kalck, P. and Urrutigoity, M. (2015). *Inorg. Chim. Acta* 431: 110–121.
43 Rahman, O. (2015). *J. Labelled Compd. Radiopharm.* 58: 86–98.
44 Cavinato, G. and Toniolo, L. (2014). *Molecules* 19: 15116–15161.
45 Fang, W., Zhu, H., Deng, Q., Liu, S., Liu, X., Shen, Y., and Tu, T. (2014). *Synthesis* 46: 1689–1708.
46 Sumino, S., Fusano, A., Fukuyama, T., and Ryu, I. (2014). *Acc. Chem. Res.* 47: 1563–1574.
47 Wu, X.-F., Fang, X., Wu, L., Jackstell, R., Neumann, H., and Beller, M. (2014). *Acc. Chem. Res.* 47: 1041–1053.
48 Kealey, S., Gee, A., and Miller, P.W. (2014). *J. Labelled Compd. Radiopharm.* 57: 195–201.
49 Fukuyama, T., Totoki, T., and Ryu, I. (2014). *Green Chem.* 16: 2042–2050.
50 Wu, L., Fang, X., Liu, Q., Jackstell, Beller, M., and Wu, X.-F. (2014). *ACS Catal.* 4: 2977–2989.
51 Gadge, S.T. and Bhanage, B.M. (2014). *RSC Adv.* 4: 10367–10389.
52 Wu, X.-F., Neumann, H., and Beller, M. (2013). *ChemSusChem* 6: 229–241.
53 Wu, X.-F., Neumann, H., and Beller, M. (2013). *Chem. Rev.* 113: 1–35.
54 Gabriele, B., Mancuso, R., and Salerno, G. (2012). *Eur. J. Org. Chem.*: 6825–6839.
55 Diebolt, O., van Leeuwen, P.W.N.M., and Kamer, P.C.J. (2012). *ACS Catal.* 2: 2357–2370.
56 Fan, Q., Liu, J., Chen, J., and Xia, C. (2012). *Chin. J. Catal.* 33: 1435–1447.
57 Wu, X.-F. and Neumann, H. (2012). *ChemCatChem* 4: 447–458.
58 Liu, Q., Zhang, H., and Lei, A. (2011). *Angew. Chem. Int. Ed.* 50: 10788–10799.
59 Omae, I. (2011). *Coord. Chem. Rev.* 255: 139–160.
60 Occhiato, E.G., Scarpi, D., and Prandi, C. (2010). *Heterocycles* 80: 697–724.
61 Haynes, A. (2010). *Adv. Catal.* 53: 1–45.
62 Liu, J., Chen, J., Sun, W., and Xia, C. (2010). *Chin. J. Catal.* 31: 1–11.
63 Brennführer, A., Neumann, H., and Beller, M. (2009). *ChemCatChem* 1: 28–41.

64 Brennführer, A., Neumann, H., and Beller, M. (2009). *Angew. Chem. Int. Ed.* 48: 4114–4133.
65 Ragaini, F. (2009). *Dalton Trans.*: 6251–6266.
66 Barnard, C.F.J. (2008). *Organometallics* 27: 5402–5422.
67 Chaudhari, R.V. (2008). *Curr. Opin. Drug Discovery Dev.* 11: 820–828.
68 Veige, A.S. (2008). *Polyhedron* 27: 3177–3189.
69 Boyarskii, V.P. (2008). *Russ. J. Gen. Chem.* 78: 1742–1753.
70 Liu, M., Wu, Y., Du, Z, Yuan, H., and Ge, J. (2008). *Chin. J. Catal.* 29: 489–496.
71 Diaz, D.J., Darko, A.K., and McElwee-White, L. (2007). *Eur. J. Org. Chem.*: 4453–4465.
72 Langstom, B., Itsenko, O., and Rahman, O. (2007). *J. Labelled Compd. Radiopharm.* 50: 794–810.
73 Church, T.L., Getzler, Y.D.Y.L., Byrne, C.M., and Coates, G.W. (2007). *Chem. Commun.*: 657–674.
74 Shibata, T. (2006). *Adv. Synth. Catal.* 348: 2328–2336.
75 Vasapollo, G. and Mele, G. (2006). *Curr. Org. Chem.* 10: 1397–1421.
76 Ragaini, F., Cenini, S., Gallo, E., Caselli, A., and Fantauzzi, S. (2006). *Curr. Org. Chem.* 10: 1479–1510.
77 Ungvary, F. (2005). *Coord. Chem. Rev.* 249: 2946–2961.
78 Trzeciak, A.M. and Ziolkowski, J.J. (2005). *Coord. Chem. Rev.* 249: 2308–2322.
79 Muzart, J. (2005). *Tetrahedron* 61: 9423–9463.
80 Park, K.H. and Chung, Y.K. (2005). *Synlett*: 545–559.
81 Gibson, S.E. and Mainolfi, N. (2005). *Angew. Chem. Int. Ed.* 44: 3022–3037.
82 Gabriele, B., Salerno, G., Costa, M., and Chiusoli, G.P. (2004). *Curr. Org. Chem.* 8: 919–946.
83 Vizer, S.A., Yerzhanov, K.B., Al Quntar, A.A.A., and Dembitsky, V.M. (2004). *Tetrahedron* 60: 5499–5538.
84 Green, M.J., Cavell, K.J., Edwards, P.G., Tooze, R.P., Skelton, B.W., and White, A.H. (2004). *Dalton Trans.*: 3251–3260.
85 Thomas, C.M. and Suss-Fink, G. (2004). *Coord. Chem. Rev.* 243: 125–142.
86 Cornils, B. and Herrmann, W.A. (2003). *J. Catal.* 216: 23–31.
87 des Abbayes, H. and Salaun, J.Y. (2003). *Dalton Trans.*: 1041–1052.
88 Gabriele, B., Salerno, G., Costa, M., and Chiusoli, G.P. (2003). *J. Organomet. Chem.* 687: 219–228.
89 Skoda-Foldes, R. and Kollár, L. (2002). *Curr. Org. Chem.* 6: 1097–1119.
90 Kiss, G. (2001). *Chem. Rev.* 101: 3435–3456.
91 del Rio, I., Claver, C., and van Leeuwen, P.W.N.M. (2001). *Eur. J. Inorg. Chem.*: 2719–2738.
92 Bertoux, F., Monflier, E., Castanet, Y., and Mortreux, A. (1999). *J. Mol. Catal. A: Chem.* 143: 11–22.
93 Wender, I. (1996). *Fuel Process. Technol.* 48: 189–297.
94 Ragaini, F. and Cenini, S. (1996). *J. Mol. Catal. A: Chem.* 109: 1–25.
95 Ryu, I. and Sonoda, N. (1996). *Angew. Chem. Int. Ed.* 35: 1050–1066.
96 Beller, M., Cornils, B., Frohning, C.D., and Kohlpaintner, C.W. (1995). *J. Mol. Catal. A: Chem.* 104: 17–85.

97 Khumtaveeporn, K. and Alper, H. (1995). *Acc. Chem. Res.* 28: 414–422.
98 Yamamoto, A. (1995). *Bull. Chem. Soc. Jpn.* 68: 433–446.
99 Tsuji, J. and Mandai, T. (1993). *J. Organomet. Chem.* 451: 15–21.
100 Ford, P.C., Ryba, D.W., and Belt, S.T. (1993). *Adv. Chem.* 238: 27–43.
101 Lin, J.J. and Knifton, J.F. (1992). *Adv. Chem. Ser. D* 230: 235–247.
102 Ojima, A., Zhang, Z., Korda, A., Ingallina, P., and Clos, N. (1992). *Adv. Chem. Ser. D* 230: 277–296.
103 Braca, G., Galletti, A.M.R., Sbrana, G., and Trabuco, E. (1992). *Adv. Chem. Ser. D* 230: 309–322.
104 Moloy, K.G. and Wegman, R.W. (1992). *Adv. Chem. Ser. D* 230: 323–338.
105 Zoeller, J.R., Cloyd, J.D., Lafferty, N.L., Nicely, V.A., Polichnowski, S.W., and Cook, S.L. (1992). *Adv. Chem. Ser. D* 230: 377–394.
106 Oswald, A.A., Hendriksen, D.E., Kastrup, R.V., and Mozeleski, E.J. (1992). *Adv. Chem. Ser. D*: 395–418.
107 Chiusoli, G.P. (1991). *Transition Met. Chem.* 16: 553–564.
108 Iwasaki, M., Ishii, Y., and Hidai, M. (1991). *J. Synth. Org. Chem. Jpn.* 49: 909–918.
109 Jenner, G. (1989). *Appl. Catal.* 50: 99–118.
110 Lapidus, A.L. and Pirozhkov, S.D. (1989). *Usp. Khim.* 58: 197–233.
111 Collin, J. (1988). *Bull. Soc. Chim. Fr.* 6: 976–981.
112 Gulevich, Y.V., Bumagin, N.A., and Beletskaya, I.P. (1988). *Usp. Khim.* 57: 529–561.
113 Chiusoli, G.P. (1987). *Transition Met. Chem.* 12: 89–96.
114 Narayana, C. and Periasamy, M. (1985). *Synthesis*: 253–268.
115 Brown, H.C. (1969). *Acc. Chem. Res.* 2: 65–72.
116 Liu, Y.-R. (2007). *Comprehensive Handbook of Chemical Bond Energies*. Boca Raton, FL: Taylor and Francis.
117 Scuseria, G.E., Miller, M.D., Jensen, F., and Geertsen, J. (1991). *J. Chem. Phys.* 94: 6660–6663.

Part I

Carbonylations Promoted by First Row Transition Metal Catalysts

2

Cobalt-Catalyzed Carbonylations

Jérôme Volkman and Philippe Kalck

University of Toulouse UPS-INP, Composante ENSIACET de l'Institut National Polytechnique de Toulouse, Laboratoire de Chimie de Coordination du CNRS UPR 8241, 4 allée Emile Monso, 31030 Toulouse Cedex 4, France

2.1 Introduction

The production of methane catalyzed by reduced nickel from carbon monoxide and hydrogen was discovered by Paul Sabatier and Jean-Baptiste Sanderens [1]. This seminal work was followed by numerous studies on the conversion of charcoal into hydrocarbons by the hydrogenation of carbon monoxide [2]. In the 1920s, Franz Fischer and Hans Tropsch carried out these investigations at the Kaiser-Wilhelm-Institut für Kohlenforschung at Mülheim an der Ruhr, Germany. Synthetic fuels were produced using iron- and cobalt-based catalysts operating at atmospheric pressure and at temperatures below 300 °C. Otto Roelen, assistant to F. Fischer since 1924, was in charge of building the first pilot plant in 1927. He then moved to the Research Laboratory of Ruhrchemie AG at Oberhausen where the first industrial plant was operating. On 26 July 1938, he decided to recycle ethylene in the Fischer–Tropsch synthesis to increase the formation of longer-chain hydrocarbons. Otto Roelen and his assistant Alfred Landgraf observed the formation of propanal as a main constituent of the conversion of equal volumes of $CH_2{=}CH_2/CO/H_2$. This transformation was carried out over a fixed bed operating at 150 °C and 100 bar with a cobalt catalyst along with magnesia and thoria promoters supported on kieselguhr. This reaction was further extended to various alkenes, and the corresponding aldehydes were synthesized as main products. Six weeks after the first experiment, a patent application was filed on 19 September 1938 and only delivered in 1952 [3]. Two patents however appeared earlier in the United States [4] and France [5]. The Fischer–Tropsch reaction was described in 1940 [6], then by O. Roelen himself [7], and later in many papers, patents, and reviews or book chapters, which are cited by recent references [8–10].

Furthermore, carbon monoxide was shown to react with methanol to produce acetic acid as early as 1913 [11]. Reppe and his research group at I. G. Farben and then BASF patented the catalytic activity of iron, cobalt, and nickel in the presence of an iodide copper salt to carbonylate methanol into acetic acid and methyl acetate.

Carbon Monoxide in Organic Synthesis: Carbonylation Chemistry,
First Edition. Edited by Bartolo Gabriele.

Most examples were focused on nickel at 230–340 °C and 180–200 bar [12]. BASF and later British Celanese intensely worked on the carbonylation reaction at high pressures and temperatures using cobalt or nickel carbonyls in the presence of iodine or iodide salts. This resulted in many patent claims [13]. The corrosion issues encountered when using iodide promoters were only solved in the latter part of the 1950s, when the highly resistant Mo–Ni alloys (Hastelloy®) were developed [14]. However, the toxicity of the $Ni(CO)_4$ produced during the reaction was such that only the cobalt powder/CuI system was further developed, even though it is less efficient (16% acetic acid and 54% methyl acetate) [15]. Even under harsh operating conditions (250 °C and 680 bar) [12], the selectivity to acetic acid was 90% based on methanol and 70% based on CO, mainly due to the water–gas shift (WGS) reaction (Eq. (2.1)) [15, 16]:

$$CO + H_2O \longrightarrow CO_2 + H_2 \tag{2.1}$$

This cobalt-catalyzed methanol carbonylation was industrialized by BASF in 1960 and commercialized in 1963. Twenty years later, two plants were operating in Germany (50 000 t/y) and in the United States (Louisiana, Borden Co plant, 65 000 t/y). This process was abandoned due to the high-pressure conditions and the mediocre selectivity by comparison with the rhodium Monsanto process [14, 16].

Thus, CO and transition metal complexes as a reagent and catalysts have been used to mainly produce large quantities of hydrocarbons and useful intermediates such as acetic acid and aldehydes. Recently, we can observe a renewed interest in first-row transition metal catalysis and particularly in the use of cobalt in fine chemistry and pharmaceutical industry [17, 18]. In this context, the development of efficient catalysts in chemo-, regio-, and even diastereo- or enantioselective syntheses of high-value products is quite challenging.

This chapter will analyze the recent use of carbon monoxide in conjunction with cobalt catalysts to obtain intermediates or target products in fine chemistry. We will be focusing on the main concepts that govern the catalysis of these reactions and the synthetic strategies that can be anticipated.

2.2 Carbon Monoxide and Its Surrogates

The CO/H_2 synthetic gas (syngas) was initially obtained for the Fischer–Tropsch process by coal gasification through partial oxidation reactions at atmospheric pressure and around 200 °C [2, 19]. Syngas was then converted into higher hydrocarbons that were used as fuel [20, 21]. Today, various carbon sources are used for gasification: coal, natural gas, petroleum and petroleum residues, biomass feedstocks, and municipal solid wastes [22–25]. Currently, syngas (and from it CO or H_2) is produced by large industrial plants to manufacture various compounds on large scale. It is necessary to purify syngas since it contains sulfur species (H_2S and COS), HCl, NH_3, HCN, CO_2, and volatile derivatives of various metals such as Hg, As, and Se. Since the

first Fischer–Tropsch unit operated in 1936 at Ruhrchemie AG, this process has been continuously improved and is still today producing large amounts of hydrocarbons. Cobalt catalysts are still utilized and preferred over iron and nickel catalysts; indeed, they are characterized by their long-lasting stability, high activity and selectivity for heavy hydrocarbons, and low WGS activity. In 2011, the last gas-to-liquid plant started up in Qatar (Shell Pearl GTL) and in 2012 reached its full capacity of 7 million t/y [26].

However, transport of carbon monoxide via pipelines is quite difficult, in particular due to the high toxicity of this gas [27, 28]. Still, small fine chemistry units, not always in close proximity of large plants, require access to pure carbon monoxide for their carbonylation reactions. Its production on site is therefore necessary, and many have opted for CO surrogates. Such strategy has also been adopted in several academic research laboratories. Various abundant and cheap molecules can thus be utilized to generate high-purity CO or CO/H_2 within the carbonylation reactor [29, 30]. In particular, formaldehyde or its polymer, paraformaldehyde, which contain 93.3 wt% of CO, allows to perform carbonylation reactions [31–34]. In particular, hydroformylation reactions are carried out by decomposing HCHO into CO/H_2 or by oxidative addition on the metal center to generate an [H–M–CHO] active species. Similarly, formic acid, methyl formate, formamides, formic anhydride, chloroform, and methanol, among others [27–30], have been reported as good sources of CO or syngas. Both formaldehyde and methanol have also been utilized [35]. Higher-molecular-weight aldehydes and alcohols from biomass can generate syngas. All these reactions using surrogates have been reviewed [29–39]. Large amounts of syngas are also produced from CO_2 from the reaction with H_2 via the reversed WGS (Eq. (2.2)) catalyzed by ruthenium complexes supported on weakly acidic alumina [27, 28]:

$$CO_2 + H_2 \longrightarrow CO + H_2O \tag{2.2}$$

In addition, $[Mo(CO)_6]$ in the presence of 1,8-diazabicyclo[5.4.0]undec-7-ene (DBU) is a source of CO [40]. $[Cr(CO)_6]$, $[W(CO)_6]$, and $[Co_2(CO)_8]$ complexes are also efficient CO sources. Furthermore, labeled ^{13}CO carbonylations can be carried out using ^{13}C-labeled pivaloyl chloride via its decomposition by a palladium(0) complex in a two-chamber system (a release and a consumption chamber) [41]. Labeling with ^{11}C and ^{14}C of bioactive compounds has extended the ^{13}C carbonylation reactions [42]. Recently, crystalline 9-methyl-9*H*-fluorene-9-carbonyl chloride and methyldiphenylsilacarboxylic acid, obtained from labeled CO_2, were shown to release labeled CO [43].

Finally, the greenhouse gas mixture of CH_4 and CO_2 can be cleanly converted into syngas via the "dry reforming of methane" on nickel–cobalt-supported catalysts operating at around 900 °C [44, 45]. Another strategy is to operate the photocatalytic or photoelectrochemical reduction of CO_2 and H_2O in the presence of heterogeneous semiconductor-based catalysts [46]. This approach may be opening a new route to produce high-purity CO for fine chemistry and pharmaceutical plants.

2.3 Hydroformylation of Alkenes

Otto Roelen discovered the cobalt-catalyzed hydrocarbonylation of ethene and by extension of various alkenes to yield the corresponding aldehydes. The formal addition of a hydrogen atom and a formyl group to a C=C double bond led to the name *hydroformylation*. Except for ethene, a linear (*l*) aldehyde and a branched (*b*) aldehyde are produced (Scheme 2.1). The following schemes that represent hydroformylation reactions are color-coded with CO in red and H_2 in blue.

The hydroformylation of olefins with syngas is the principal route to C_3–C_{15} aldehydes, which are converted into alcohols, acids, or other derivatives. By far the most important industrial product is (*l*)-butanal for plasticizer alcohols, followed by C_6–C_{13} aldehydes (*l* and *b*). In addition, methyl-2-propanal, (*l*)-pentanal, and C_{12}–C_{18} aldehydes are synthesized for the production of detergent alcohols. In 1980, the cobalt-catalyzed hydroformylation of propene and heavier alkenes was detailed by Cornils in Falbe's book [47]. More recently, reviews and book chapters have appeared mainly focused on the mechanism of this reaction [48–50] and the reactivity of metal carbonyl species and industrial applications [51–54].

The initial hydroformylation processes catalyzed by cobalt carbonyls were carried out under high pressure (300 bar) to produce a mixture of aldehydes and hydrogenated alkenes. By the end of the 1960s, most plants running the cobalt process were operating under severe conditions (200–450 bar and 140–180 °C).

A modified process was developed by the addition of a trialkylphosphine ligand (mainly PBu_3) to perform the hydroformylation of propene at about 50 bar. This process also gave improved selectivity for the preferred (*l*)-butanal with an isomeric *l*:*b* ratio of 7 : 1, instead of 3 : 1. Furthermore, Shell and Sasol introduced sterically hindered phosphabicyclononane ligands to further improve the *l*:*b* ratio (Chart 2.1) [55–60]. These bulky ligands [57] are particularly interesting, notably the two phobanes [4.2.1] and [3.3.1] and the 4,8-dimethyl-2-phosphabicyclo[3.3.1]nonane. High conversion of oct-1-ene (95%) and linearity in nonanol (90%) are obtained.

An innovative approach was reported by Stanley and coworkers, using a monomeric cationic hydridocobalt(II) complex [61]. The high activity of cationic Co(II) bisphosphine catalysts allows to operate under moderate pressure and temperature. For example, a [Co(acac)(diethylphosphinoethane)](BF_4) solution in dimethoxytetraglyme (1 mM) can be activated at 140 °C under 34 bar of 1 : 1 CO:H_2 for five minutes. Hex-1-ene (1 M) was converted at 100 °C and 10 bar into heptanal with a turnover number of 68 in 1 hour and 619 in 29 hours. The *l*:*b* aldehyde ratio

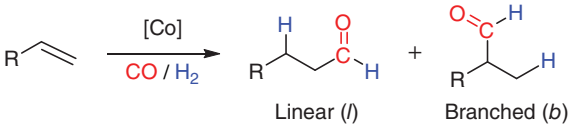

Scheme 2.1 General hydroformylation transformation of a terminal alkene yielding a linear (*l*) aldehyde and a branched (*b*) aldehyde.

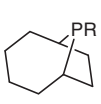

Phoban[4.2.1]

Phoban[3.3.1]

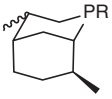

4,8-Dimethyl-2-phospha-bicyclo[3.3.1]nonane

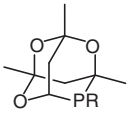

1,3,5,7-Tetramethyl-2,4,6-trioxa-8-phosphatricyclo[3.3.1.13,7]decane

Chart 2.1 Sterically hindered phosphabicyclononane ligands. Sources: Mason and van Winkle [55], Van Winkle et al. [56], Bungu et al. [57], Eberhard et al. [58], Steynberg et al. [59], Polas et al. [60].

is 0.8 and no alkane and alcohol were detected. Interestingly, operating at 140 °C and 30 bar, 2,3-dimethyl-but-2-ene and 4-methyl-pent-2-ene were converted into the corresponding aldehydes with some isomerization.

Since the 1970s, the emergence of Rh-catalyzed hydroformylation reactions has taken a paramount importance for light alkenes (C_2–C_5) due to the low temperatures and pressures utilized, as well as the improved chemo- and regioselectivities [28, 47, 54, 62–64]. However, cobalt catalysts are still used industrially in some hydroformylation applications, particularly for the production of plasticizer alcohols from ethylene oligomers, butene dimers, and propene trimers. Indeed, for heavier alkenes requiring higher operating temperatures, rhodium complexes are unstable.

Concerning the mechanism of the cobalt-catalyzed hydroformylation reaction, the $[Co(H)(CO)_3]$ has been established as the active species (Eq. (2.3)). This result was confirmed by many theoretical calculations and kinetic studies validating the catalytic cycle proposed by Heck and Breslow [65–71]:

$$Co_2(CO)_8 \underset{}{\overset{H_2}{\rightleftharpoons}} 2\,[Co(H)(CO)_4] \underset{CO}{\rightleftharpoons} 2\,[Co(H)(CO)_3] \qquad (2.3)$$

The $[Co(H)(CO)_4]$ resting state complex is prepared under pressure of syngas (CO/H_2) from various sources of cobalt. In fact, $[Co_2(CO)_8]$ is systematically generated as an intermediate in the equilibrium (Eq. (2.3)) with $[Co(H)(CO)_4]$ and $[Co(H)(CO)_3]$, as observed by high-pressure IR and NMR spectroscopies [60, 72].

The tetra-coordinated $[Co(H)(CO)_{n+1}(L)_{2-n}]$ (**1**) is the active species (with $n = 0$–2 and L = monophosphine, or L_2 = diphosphine, as recently reported by Chirik and coworkers with the $(R,R)^{iPr}$DuPhos ligand [73]). Complex **2**, a bipyramidal trigonal cobalt(I), results from the coordination of the alkene in one of the equatorial positions. The hydride ligand occupies an axial position (Scheme 2.2). The migratory insertion of the alkene leads to two alkyl species, the linear (**3**) and branched (not shown) isomers. The *l* isomer is the major intermediate when the R group is electron donating [54]. As discussed earlier (Chart 2.1), this *l*:*b* selectivity can be improved with the design of sterically hindered and basic bicyclic monophosphine ligands. The acyl cobalt complex **4** is then obtained by the coordination of CO followed by a migratory insertion. Recent density-functional theory (DFT) calculations and predictions of reaction paths confirm that this migratory insertion step is rate-determining with an activation energy of 10–16 kcal mol^{-1} [69, 71, 74].

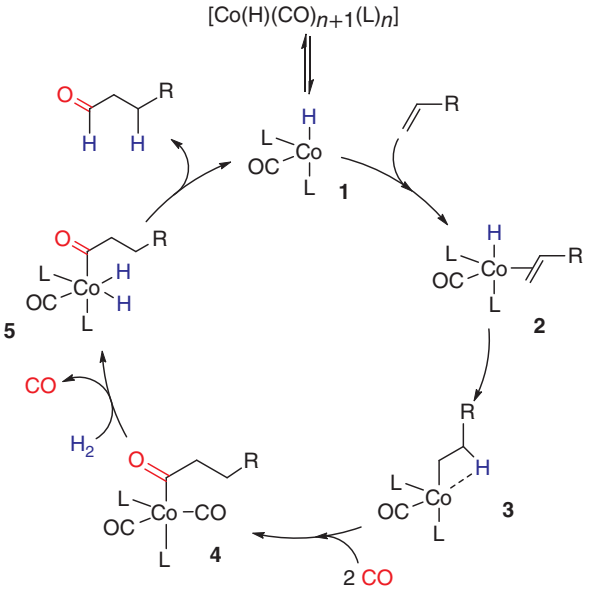

Scheme 2.2 Simplified mechanism of the cobalt-mediated hydroformylation of a monosubstituted terminal alkene from the active species **1** (only the linear isomer has been represented).

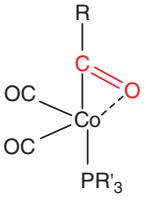

Figure 2.1 η^2-acyl structure of the unsaturated $[Co(COR)(CO)_2(PR'_3)]$ species.

An analogous acyl $[Co[C(O)R](CO)_3(N_2)]$ complex has been characterized under N_2 and low H_2 partial pressure [75]. Similarly, various $[Co[C(O)R](CO)_3(L)]$ (L = monophosphine) have been isolated and shown to be active in the catalytic reaction. A kinetic investigation of the stoichiometric hydrogenolysis of acyl $[Co(COR)(CO)_3L]$ complexes (L = monophosphine) by high-pressure infrared spectroscopy has shown that the dissociation of a CO ligand precedes the oxidative addition of H_2. DFT analysis of the $[Co(COR)(CO)_2L]$ intermediate is consistent with an η^2-COR ligand (Figure 2.1) rather than the possible agostic C–H interaction of the R group [71, 76, 77].

Finally, after oxidative addition of H_2, the dihydride cobalt(III) complex **5** is formed. Reductive elimination of the aldehyde regenerates **1**, the active species.

Interestingly, complex **1** is also able to competitively isomerize internal alkenes to yield significant quantities of terminal alkene by a succession of migratory insertion/β-H elimination sequences.

In contrast to the Co(I)/Co(III) catalytic systems described above, Stanley's catalyst [61] appears to involve Co(II) complexes. Most catalytic steps are

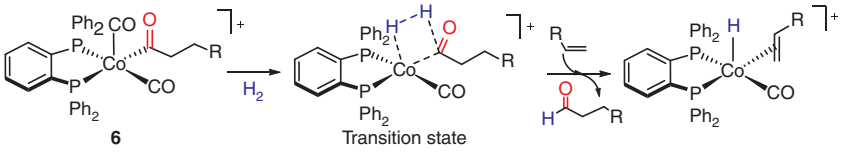

Scheme 2.3 Key steps of the H_2 activation in the hydrogenolysis of the acyl intermediate **6**.

similar, except for the H_2 activation. In short, the $[Co(H)(CO)(dppBz)]^+$ complex (with dppBz = 1,2-bis(diphenylphosphino)benzene) is converted into $[Co(H)(CO)_2(dppBz)]^+$ and $[Co(H)(CO)_3(dppBz)]^+$. Then, coordination of the alkene ($RCH{=}CH_2$) yields a $19e^-$ intermediate $[Co(H)(CO)_2(RCH{=}CH_2)(dppBz)]^+$. The following hydride transfer generates the alkyl species followed by the formation of the $17e^-$ acyl intermediate **6**. The activation of dihydrogen is in effect not an oxidative addition on the Co(II) metal center, but an η^2 interaction of H_2 with the Co and CO acyl atoms as shown in Scheme 2.3.

In industrial hydroformylation processes, to convert C_5–C_{14} alkenes (175 °C, 290–300 bar), the many different possible products have to be separated from the cobalt catalyst. This was usually done by evaporation of the volatiles, including small amounts of cobalt carbonyls [78]. The removal of the cobalt was also carried out chemically, mainly through the more recent ExxonMobil process by conversion of the $[Co_2(CO)_8]/[Co(H)(CO)_4]$ mixture into the water-soluble $Na[Co(CO)_4]$, providing a cobalt-free organic phase [47, 54, 79]. The addition of sulfuric acid to the aqueous phase under CO/H_2 pressure regenerates the $[Co(H)(CO)_4]$ complex that is then extracted under an alkene stream.

Another efficient industrial process for propene and other light alkenes (C_2–C_5) utilizes the $[Rh(H)(CO)(TPPTS)_3]$ complex with the water-soluble tris(*p*-sulfonatophenyl)phosphine ligand (TPPTS) (Scheme 2.4). The water solubility of the alkenes is sufficient to carry out the hydroformylation reaction in a biphasic medium, which also facilitates the catalyst recovery and recycling. This biphasic approach was also explored with the $[Co_2(CO)_8]$/TPPTS system in the

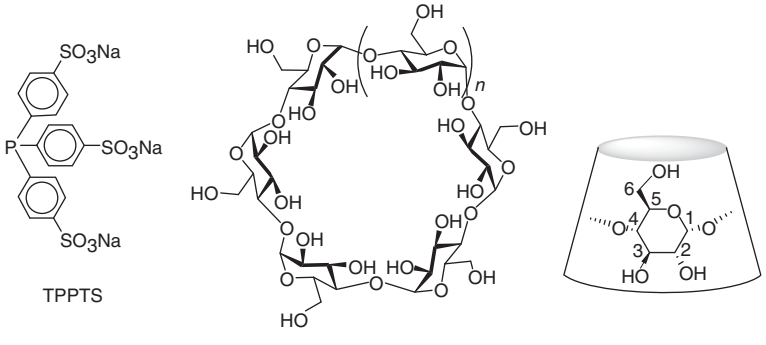

Scheme 2.4 Tris(*p*-sulfonatophenyl)phosphine (TPPTS) ligand and α-cyclodextrin ($n = 1$), β-cyclodextrin ($n = 2$), and γ-cyclodextrin ($n = 3$) and their cone geometry.

case of pent-2-ene that led to 70% of hexanal, due to the isomerization of the internal C=C double bond [80]. Other strategies to facilitate the alkene/catalyst contact have been proposed from the modification of the TPPTS ligand [81] to the utilization of the thermoregulated phase-transfer catalysis promoted by the $Ph_2P(CH_2CH_2OMe)_{16}Me$ ligand [82, 83] and even non-phosphorus-containing ligands [84].

A modification of the catalytic system was introduced by the utilization of surfactants. For example, the conversion of oct-1-ene and dec-1-ene in the presence of $CoCl_2(TPPTS)_2$/CTAB (CTAB: cetyltrimethylammonium bromide) furnished the aldehydes in 90–95% yield with a *l*:*b* selectivity of 2.3 [85]. Cobalt $[Co(H)(CO)(TPPTS)_2]$ active species can also be encapsulated into methylated β-cyclodextrin (Scheme 2.4). The conversion of oct-1-ene at 100 °C and 80 bar reaches 98% yielding the C_9 aldehyde (96%) with a *l*:*b* ratio of 1.3 [86]. Moreover, an unexpected selectivity for the branched aldehydes (80–90% selectivity) in metal–organic framework (MOF) was recently reported [87]. The high concentrations of reactants in the MOF's micropores are proposed as an explanation for the observed selectivity.

In addition to the previous biphasic media, other reaction solvents have been investigated. Supercritical carbon dioxide ($scCO_2$) is a powerful alternative medium to classical solvents with $[Co_2(CO)_6[P(3\text{-}FC_6H_4)_3]_2]$ being easily separated from the reaction mixture and recycled several times [88, 89]. Ionic liquids (ILs) have also been shown to be competent reaction medium [90]. $[Co_2(CO)_8]$ in the presence of pyridine [91, 92], 2-methoxypyridine [93], and *N*-methylguanidine [94, 95] was shown to produce active catalytic systems in IL.

Most hydroformylations of high-value-added organic molecules utilize Rh catalysts, and nowadays very few catalytic transformations use cobalt complexes. Hydroformylation of (−)-α-pinene in the presence of an unmodified Co catalyst led to (−)-2-formylbornane [96]. The hydroformylation of camphene has also been reported [97]. Lastly, the reactivity of epoxy-alkenes **7** under CO/H_2 conditions is noteworthy (Scheme 2.5). Indeed, a mixture of linear and branched aldehydes (*l*:*b* 54 : 46) is obtained with a 99% selectivity (98% conversion), the epoxide remaining intact even though the reaction is carried out in toluene at 100 °C and under 80 bar of CO/H_2 [98].

The hydroformylation of epoxides had indeed been described earlier [99, 100] (Scheme 2.6).

The active species $[CoH(CO)_4]$ protonates the epoxide **8** that then undergoes a nucleophilic attack by $[Co(CO)_4]^-$ to provide the complex **10** (Scheme 2.7) After CO migratory insertion, the acylcobalt species **11** undergoes an oxidative addition in

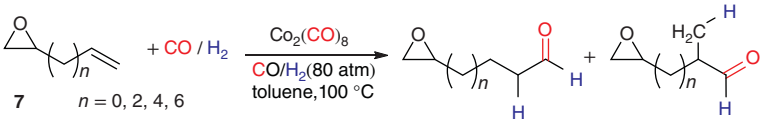

Scheme 2.5 Selective hydroformylation reaction of epoxy-alkenes **7**.

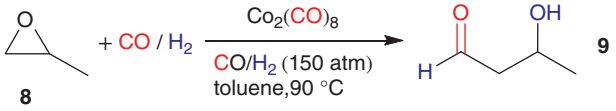

Scheme 2.6 Hydroformylation of propylene oxide **8**.

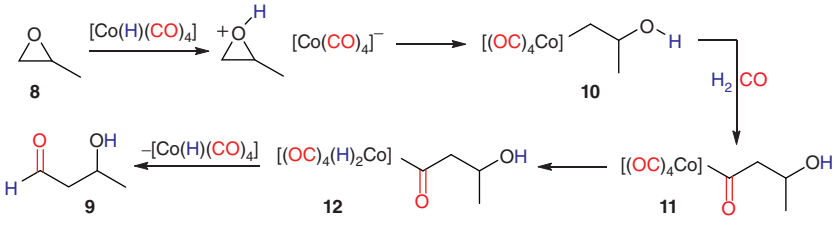

Scheme 2.7 Proposed mechanism for the hydroformylation of **8**.

the presence of H_2 to produce **12**. The reductive elimination from **12** produces **9** and regenerates $[CoH(CO)_4]$.

Modest conversions (13%) of **8** were obtained when the cobalt catalyst was modified by phobane-based diphosphines. Further improvement (40% conversion) could be achieved with additives such as $Ca(OAc)_2$ or $Eu(OAc)_3$ [101].

From a total of 12 million of t/y [102], the two cobalt oxo processes still account for 2.5×10^6 t/y production [103] and are mainly devoted to higher alkenes, whereas rhodium has replaced cobalt for propene, butene, and pentene in the Union Carbide, Mitsubishi, and Rhône-Poulenc/Ruhrchemie (now Oxea) processes. The limited scope of cobalt catalysts in fine organic chemistry is due to the important development of Rh and Pt catalysts. However, the recent demonstration of the high catalytic activity of Co(II) species in the hydroformylation reaction could potentially find applications in regioselective and enantioselective transformations.

2.4 Carbonylation of Alkynes by the Pauson–Khand [2+2+1] Reaction

The Pauson–Khand reaction is a powerful chemical transformation that allows the formation of cyclopentenones via the formation of three C—C bonds. The stoichiometric reaction of norbornadiene and an acetylenic compound $R_1C{\equiv}CR_2$ complexed to the $[Co_2(CO)_6]$ framework was studied by Pauson and Khand [104–106]. It was shown to generate the cyclopentenone carbonyl[2.2.1]hept-2-ene in addition to the cyclopentadienylcobaltdicarbonyl, presumably arising from the retro Diels–Alder reaction of norbornadiene. Since then, the scope of this reaction has been largely extended and performed under catalytic conditions [107, 108]. This annulation reaction involving three reactants is color-coded throughout this chapter, as shown in Scheme 2.8.

An initial mechanism was proposed by Magnus and Principe [109] and Schore and coworker [110]. The complexation of the acetylenic moiety as an initial step leads to

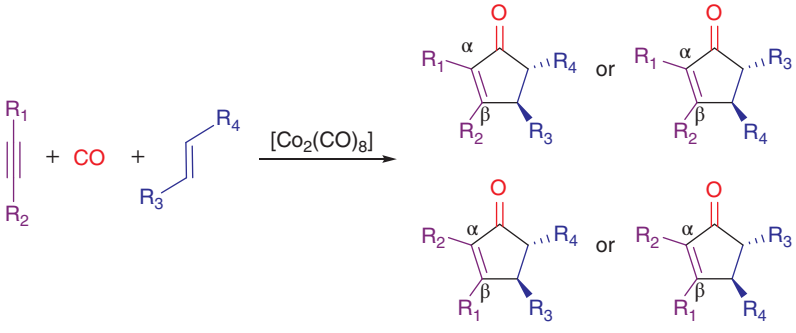

Scheme 2.8 Synthesis of cyclopentenones via [2+2+1] cycloaddition of an alkyne, an alkene, and carbon monoxide.

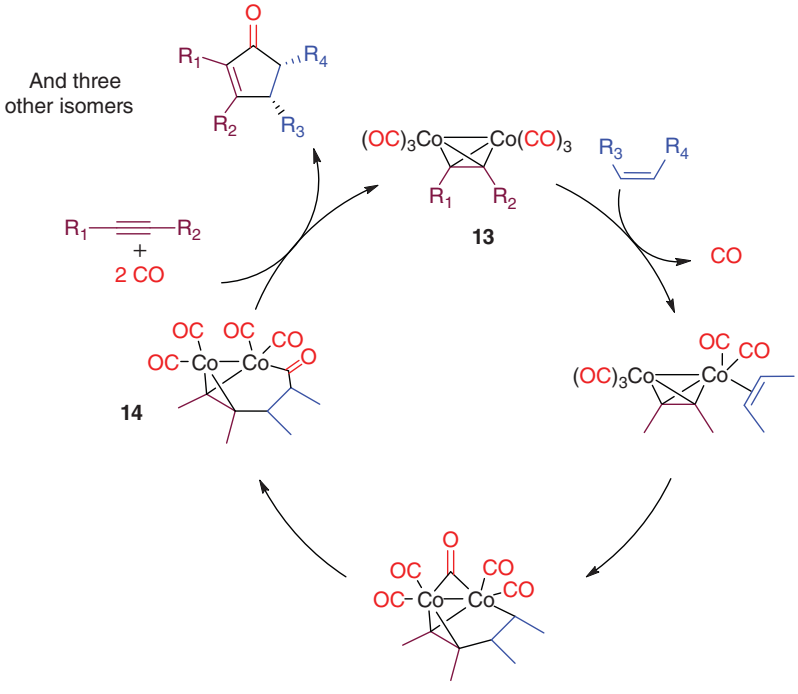

Scheme 2.9 Simplified catalytic cycle of the Pauson–Khand reaction.

the known and generally isolable complex $[Co_2(CO)_6(R_1C{\equiv}CR_2)]$ **13**. This complex undergoes then the formation of a cobaltocycle after ligand exchange between CO and an alkene. The migratory insertion of CO into a Co—C bond leads to the acyl complex **14**. Subsequent reductive elimination produces the cyclopentenone and under CO regenerates **13** (Scheme 2.9).

This mechanism was further investigated by Nakamura and Yamanaka by DFT calculations [111]. The migratory insertion into the Co—C(sp^2) is favored over the insertion into the Co—C(sp) bond. Additionally, the second cobalt atom is not an

inert spectator and was described as an electron reservoir, regulating the electron density on the other cobalt center along the catalytic cycle. More recently, Gimbert and coworkers [112] have proposed that after the cobaltocycle formation, the CO ligand involved in the migratory insertion step originates from the other cobalt metal atom. The transfer occurs through the formation of a bridging CO ligand. Based on mass spectrometry results and DFT calculations, the coordination of an external ^{13}CO was shown to occur after the migratory insertion step. A simplified catalytic cycle proposed by Gimbert is represented in Scheme 2.9. The cobaltocycle formation is proposed as the rate-determining step.

Microwave activation of the Pauson–Khand reaction was also analyzed *in situ* and *in silico* [113]. The rapid heating of the reaction mixture was shown to be effective for the catalytic reaction. The computational approach is consistent with Gimbert's mechanism.

Pauson, Magnus, and Schore were the first to report on the regioselectivity of the Pauson–Khand reaction [107–110]. Coordination of the alkene on the $[Co_2(CO)_6(R_1C{\equiv}CR_2)]$ complex yields a cobalt complex, which is ready to undergo a cyclometalation. This key step governs not only the regioselectivity but also the enantio- or diastereoselectivity of the annulation reaction. The regioselectivity of the transformation was correlated to the nature of the substituents on the alkene and alkyne. Generally, with internal alkynes, electron-withdrawing groups are introduced at the C_β position of the cyclopentenone, whereas electron-releasing groups are usually C_α directing. More recently, a detailed study has shown that the natural bond order (NBO) charges in the transition state correlate with the regioselectivity. In addition, weak interactions such as H-bonding and steric constraints can govern the outcome of the reaction [114]. Concerning the coordination of the alkenes, steric interactions appear to play a significant role on the orientation relative to the alkyne [115].

In the intramolecular version of the Pauson–Khand reaction, the regioselectivity is controlled by the enyne substrate. To obtain the desired product, a careful analysis of the coordination modes must be carried out, taking into account steric effects and tether length (Scheme 2.10, NMO: *N*-methylmorpholine *N*-oxide) [116].

This reaction is a powerful tool to generate stereogenic carbons in the cyclometalation step. The "$Co_2(CO)_6$" moiety is achiral, and therefore the reaction's diastereoselectivity is substrate-controlled. The diastereoselective synthesis of **16** starting from siloxy-tethered 1,7-enynes (**15**) is a recent example (Scheme 2.11). The diastereoselectivity was controlled by the stereocenter in the propargylic position with diastereoisomeric ratios of up to 20 : 1. Additionally, an enantiomeric ratio of 98.5 : 1.5 was reported. The products synthesized on multigram scales were reported as useful scaffolds for stereochemical diversity [117].

Since the first reports of enantioselective catalytic Pauson–Khand reactions [118–120], Riera and coworkers have explored the utilization of chiral diphosphine ligands in the dinuclear cobalt coordination sphere [121]. Coordination of (*S*,*S*)-QuinoxP* (**17**, Scheme 2.12) occurs on one of the two cobalt metal centers and produces an active catalyst with modest enantioselectivities. The modest asymmetric transfer is likely the result of the norbornadiene coordination on the other

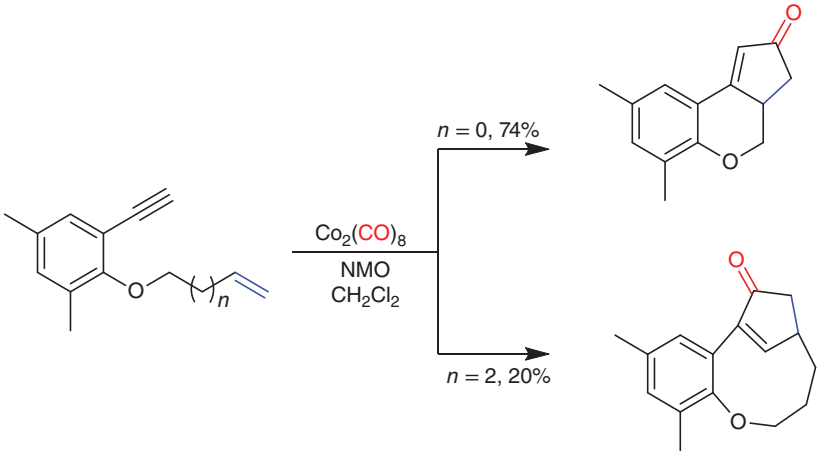

Scheme 2.10 Effects of the tether length on the intramolecular Pauson–Khand annulation reaction. Source: Modified from Lovely et al. [116].

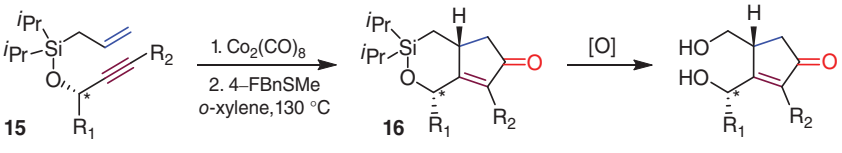

Scheme 2.11 Intramolecular diastereo- and enantioselective Pauson–Khand annulation reaction.

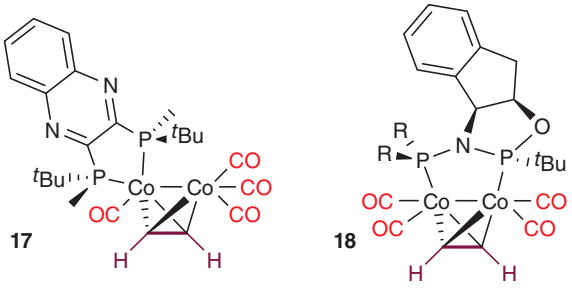

Scheme 2.12 QuinoxP* and ThaxPhos alkyne complexes.

"$Co(CO)_3$" moiety. On the contrary, the ThaxPhos ligand (**18**, Scheme 2.12) was shown to bridge both cobalt nuclei and induce good-to-excellent enantioselectivities. However, the catalysis was limited to silylalkyne substrates [122].

Furthermore, many studies have shown the sensitivity of the transformation to the reaction conditions. Numerous catalytic systems with different types of additives and promoters have thus been developed [123]. The following two significant examples illustrate these catalytic systems and their application to synthetic

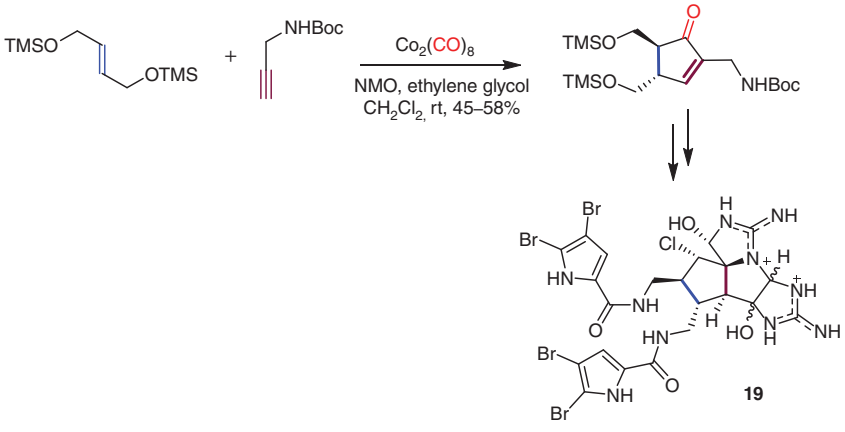

Scheme 2.13 Synthesis of a key intermediate of **19** via an intermolecular Pauson–Khand reaction.

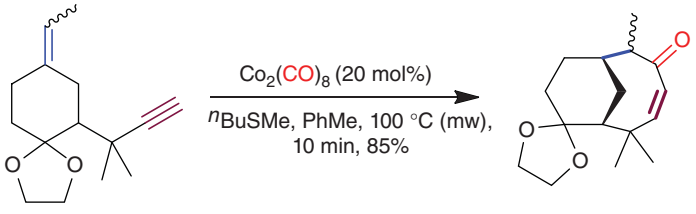

Scheme 2.14 Catalytic Pauson–Khand reaction in the absence of external CO, promoted by microwave heating.

organic chemistry. Baran and coworkers have developed the specific utilization of *N*-methylmorpholine-*N*-oxide (NMO)/ethylene glycol as additives [124]. NMO promotes the formation of a vacant coordination site, which is presumably stabilized by ethylene glycol [125]. Thus the authors prepared on a gram scale axinellamine A (**19**, Scheme 2.13, $CF_3CO_2^-$ counter ions not shown) in 12 steps instead of the 20 steps (1%) previously required.

The second example simultaneously uses *n*-BuSMe as an additive and microwave activation [126]. In this particular case, the reaction proceeds without an external source of CO, which was provided by $[Co_2(CO)_8]$ (Scheme 2.14).

The cobalt-mediated Pauson–Khand reaction is largely utilized in the total synthesis of biologically active natural and unnatural products. The intramolecular version of this reaction has been utilized in a key step in the synthesis of **20** [127] and **21** [128, 129] (Scheme 2.15, with TMTU = tetramethylthiourea). For simplicity, the scheme depicts only the starting enyne, the resulting cyclopentenone intermediate, and the target product.

Even though other metals catalyze the Pauson–Khand transformation, cobalt catalysis still plays a central role in this annulation reaction. A well-suited enyne

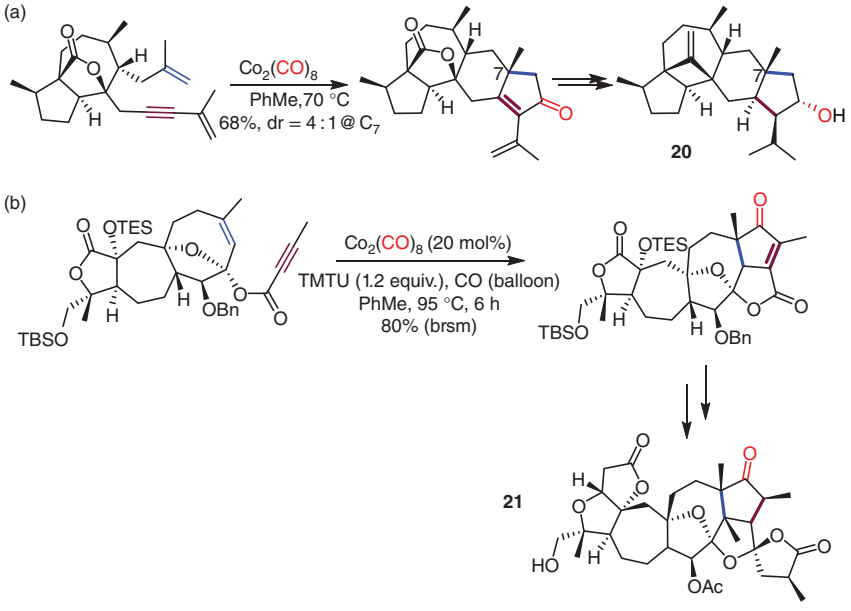

Scheme 2.15 Applications of the Pauson–Khand reaction in the elaboration of key intermediates in the total syntheses of (a) **20** and (b) **21**.

substrate can usually be found through a careful retrosynthetic analysis. In its intramolecular version, the present reaction leads to the desired target. The intermolecular Pauson–Khand is more difficult to control. However, Baran et al. have established that this transformation can be practical in gram-scale total synthesis, even in the initial step. The scope can still be broaden by further specific developments, such as more effective promoters and better stabilizing additives. Finally, the search for novel enantiopure ligands, as pioneered by Verdaguer and Riera, should prove fruitful in catalytic enantioselective Pauson–Khand reactions.

2.5 Carbonylation of Methanol

As mentioned in the introduction, Reppe and coworkers developed the cobalt-catalyzed carbonylation of methanol. Even though yields in acetic acid (16%) and methyl acetate (54%) are more modest than those using nickel (87% and 6%, respectively) [15], industrial developments focused on cobalt due to the high volatility and toxicity of $[Ni(CO)_4]$ [130]. Under harsh operating conditions (250 °C and 680 bar) [12], the selectivity to acetic acid is 90% based on methanol and 70% based on CO, mainly due to the WGS reaction (Eq. (2.1)) [15, 16]. The CoI_2 salt reacts with carbon monoxide to produce the dicobalt octacarbonyl $[Co_2(CO)_8]$ precursor, and then the hydrido cobalt tetracarbonyl $[Co(H)(CO)_4]$ is formed, according to Eqs. (2.4) and (2.5) [131, 132]. The $[Co(H)(CO)_4]$ is a strong acid in

protic solvents, leading to H^+ and $[Co(CO)_4]^-$, which are also catalytically active:

$$2\,CoI_2 + 2\,H_2O + 10\,CO \longrightarrow Co_2(CO)_8 + 4HI + 2\,CO_2 \quad (2.4)$$

$$Co_2(CO)_8 + H_2O + CO \longrightarrow 2\,[Co(H)(CO)_4] + CO_2 \quad (2.5)$$

The cobalt hydride species, $[Co(H)(CO)_4]$, and methyl iodide, resulting from the reaction of HI with methanol, react to produce $[Co(CH_3)(CO)_4]$ and HI. The CO migratory insertion (rate-determining step) provides the acetyl species $[Co(COCH_3)(CO)_3]$ and, under CO pressure, $[Co(COCH_3)(CO)_4]$. In the last catalytic step, water reacts with the latter species to regenerate $[Co(H)(CO)_4]$ and produce CH_3COOH [132, 133]. In addition, the cobalt complex $[Co(CO)_4]^-$ [134–136], which results from the disproportionation of $[Co_2(CO)_8]$ or the ionization of $[Co(H)(CO)_4]$, reacts with CH_3I to give $[Co(CH_3)(CO)_4]$ and I^-. Prior to the coordination of the fourth CO ligand, the intermediate resulting from the migratory insertion has been trapped with the addition of bis(triphenylphosphine)iminium iodide ([PPN]I). The product, $[PPN]^+[I–Co(COCH_3)(CO)_3]^-$, has been isolated and fully characterized [137]. Further, the role of the anionic Co^I complex is supported by the accelerating effect of pyridine (around 400-fold), which forms the $[C_5H_5NCOCH_3]^+[Co(CO)_4]^-$ intermediate [138], as revealed by an fourier-transform infrared spectroscopy (FTIR) study. Finally, hydrolysis of $[Co(COCH_3)(CO)_4]$ regenerates $[Co(CO)_4]^-H^+$ and CH_3COOH [16].

In addition to phosphine ligands, iodide sources, starting from magnesium carbonyl cobaltate, and the addition of a palladium or a platinum co-catalyst [139, 140] led to significant improvements of the reaction conditions, particularly the pressure (200 bar). However, the gain was not sufficient with regard to the rhodium catalyst that currently operates. More recently, the $[(\eta^5\text{-}C_5Me_5)Co(CO)_2]/PEt_3/H_2O/MeI$ system was shown to be active at 100 bar and 120–140 °C with a catalytic activity in acetic acid/methyl acetate. The observed rate is 1.5 times greater than the rate with rhodium (turnover frequency 314 h^{-1} compared with 188 h^{-1}) even if the concentration of cobalt is 30 times that of rhodium [141, 142]. Whereas $[PMeEt_3]I$ is expected to form in the medium, a free phosphine ligand is also present in the solution, and the complex $[ICo(CO)_2(PEt_3)_2]$ has been isolated and fully characterized after catalysis. However, the analogous complex $[ICo(CO)_2(PMe_2Ph)_2]$ has a modest activity [142]. Bi- to quadridentate 1,3-dioxolane and 1,4-dioxane phosphine ligands have also been investigated [143]. In combination with CoI_2, these diphosphine ligands led to methanol conversions of 95% and selectivity to methyl acetate and acetic acid of 33% and 60%, respectively, at 160 °C and under 200 bar. Efficient cobalt complexes could thus appear in the near future to compete with the present rhodium catalysts. In this context, Co has been deposed on zeolites that allows the carbonylation of methanol at 180 °C and 700 bar with a conversion of 73% in 42 hours into 43% methyl acetate, 10.6% acetic acid, and 17.3% dimethyl ether in the presence of halide promoters [144].

The Co-catalyzed direct carbonylation reaction is essentially devoted to the carbonylation of methanol. It has not found broader applications to secondary and tertiary alcohols.

2.6 Carbonylation of Heterocycles

Carbonylation of heterocycles has been well reviewed [145, 146]. We will present the main results related to this functionalization for cyclic ethers and their corresponding N- and S-containing congeners and oxazolines.

$[Co_2(CO)_8]$ was found to promote the stoichiometric carbonylation of epoxides into the corresponding β-lactones under harsh conditions. These heterocycles are usually difficult to prepare by conventional organic methods and are of particular interest in fine chemistry [145, 147]. Alper and coworkers found that in the presence of $BF_3{\cdot}Et_2O$ or $B(C_6F_5)_3$ Lewis acids, the $[PPN][Co(CO)_4]$ complex catalyzes the carbonylation of epoxides in high yields and with good selectivity (Scheme 2.16) [148].

Coates and his research group then used cationic Lewis acids such as $[(\eta^5\text{-}C_5H_5)_2Ti(THF)_2]^+$ or $[(salph)Al(THF)_2]^+$ (with salph = *N*,*N*′-bis(3,5-di-*tert*-butylsalicylidene)phenylenediamine) as co-catalysts to operate under milder conditions (60 °C and 60 bar) [149]. Following this initial report, they performed a detailed mechanistic investigation on the monosubstituted 1,2-epoxybutane carbonylation reaction. The coordination of the epoxide to the aluminum-based Lewis acid ($[LA]^+$) (Scheme 2.17) facilitates the nucleophilic attack of the anionic $[Co(CO)_4]^-$ via an S_N2 mechanism. The resulting alkyl species undergoes then a migratory CO insertion to yield **22** after CO coordination. Complex **22** was determined to be the resting state of the catalyst. In THF, the formation of the β-lactone from **22** is rate-determining and followed in the last step by the regeneration of the active species $[Co(CO)_4]^-$ [150, 151].

In the case of 2,2-disubstituted epoxides, the rate-determining step is the nucleophilic attack of $[Co(CO)_4]^-$ on carbon 1, provided that a weakly coordinating solvent is utilized. Contrary to THF, sterically hindered solvents, such as 2,5-dimethyltetrahydrofuran, have been shown to facilitate the coordination of the epoxide on the Lewis acid $[LA]^+$. The catalytic cycle is then similar to the one described above, and the β,β-disubstituted β-lactone is the major product [152].

In addition, the carbonylation of 1,2-disubstituted epoxides produces the corresponding (α,β)-β-lactones. The *cis*-epoxides (**23**) lead to the *trans*-β-lactones (**24**), whereas the *trans*-epoxides (**25**) produce the *cis*-β-lactones (**26**, Scheme 2.18).

Coates and coworkers have developed specific aluminum-based Lewis acids for the carbonylation of *cis*- and *trans*-epoxides, with, respectively, $[\mathbf{27}]^+[Co(CO)_4]^-$ (with Ar = *p*-chlorophenyl) and $[\mathbf{28}]^+[Co(CO)_4]^-$ (Scheme 2.18) [153]. This reaction has also been extended to a double carbonylation reaction under 58 atm in 1,4-dioxane. The second carbonylation occurs on the β-lactones to yield succinic anhydrides (**31**, Scheme 2.19). The reaction was carried out on a large scope of alkyl-

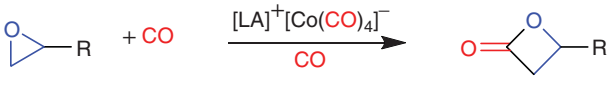

Scheme 2.16 Carbonylation of epoxides catalyzed by $[Co(CO)_4]^-$ and assisted by a cationic Lewis acid $[LA]^+$. Source: Modified from Lee et al. [148].

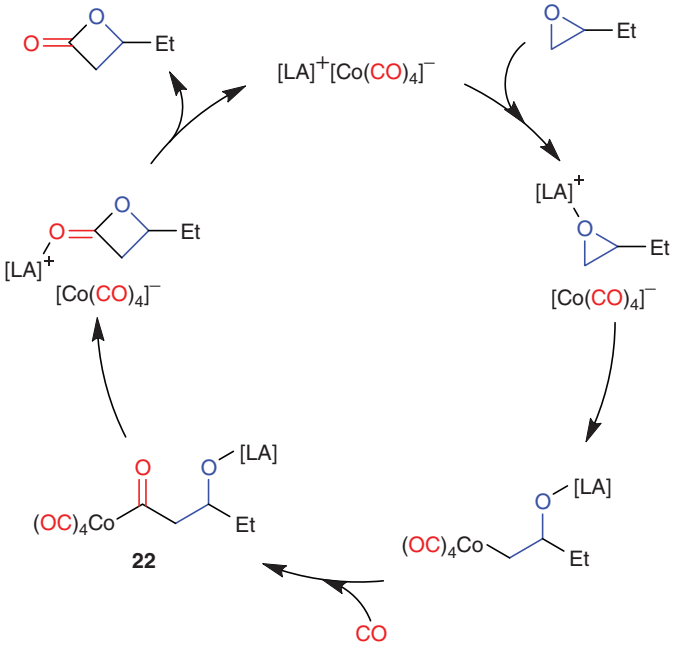

Scheme 2.17 Main steps of epoxides carbonylation reactions catalyzed by $[LA]^+[Co(CO)_4]^-$.

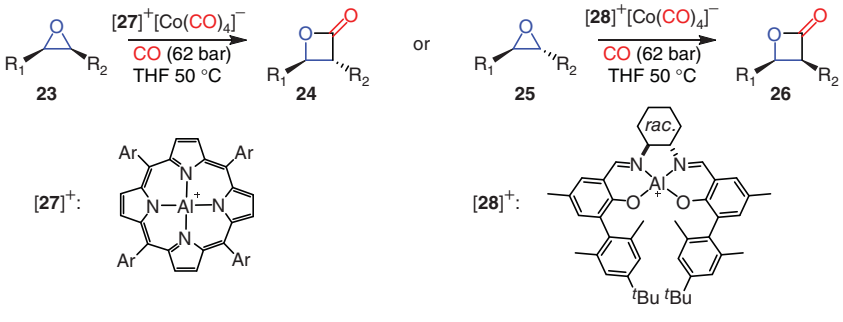

Scheme 2.18 Regioselective carbonylation of 1,2-disubstituted epoxides.

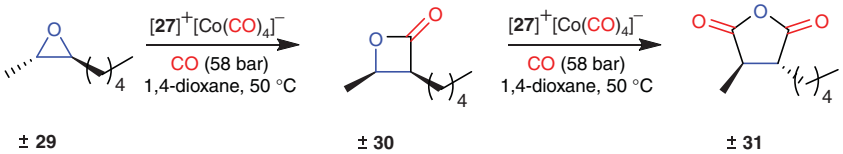

Scheme 2.19 Double carbonylation reaction of racemic epoxide **29** into **31**.

or aryl-monosubstituted epoxides with excellent yields of succinic anhydrides. The reaction was also shown to be dia- and enantioselective when 1,2-disubstituted epoxides were employed. The two carbonylation steps result in two inversions of a stereogenic carbon atom, thus retaining *in fine* its configuration [154]. *In situ* generated catalysts using $[Co_2(CO)_8]$ and aluminum phtalocyanines can easily generate the active species. Thus, operating at 75 °C and 40 bar CO in THF, conversions as high as 95% of propylene oxide with a selectivity in methylsuccinic anhydride of 98% were obtained, opening the way to low-cost and stable catalysts for the double carbonylation of epoxides [155, 156].

It can be mentioned that in the reaction in the presence of CH_3I and CTAB on styrene oxide, a phase transfer leads to the double carbonylation into the enol tautomer of 4,5-dihydro-4-phenylfuran-2,3-dione for which the $[Co(COCH_3)(CO)_4]$ species is formed [157].

Interestingly, the regiodivergent nucleophilic attack of the $[Co(CO)_4]^-$ on racemic *cis*-epoxides, such as **32** and **33**, was observed in the presence of the enantiopure Lewis acid $[\mathbf{36}]^+$ (Scheme 2.20). This transformation was shown to be a competent approach to enantioenriched *trans*-β-lactones, such as **34** and **35** [158].

This regioselective catalytic pathway was successfully used to synthesize (−)-tetrahydrolipstatin (**39**) from enantiomerically pure (*S*)-1-((*2S*,*3R*)-3-hexyloxiran-2-yl)tridecan-2-ol (**37**), after protection of the alcohol function with *N*-formyl-L-leucine Scheme 2.21). This stereoselective carbonylation allowed the synthesis of **39** in 10 steps from **38** with an overall yield of 31%. Interestingly, the other enantiomerically pure *cis*-epoxides have been utilized in the synthesis of the corresponding *trans*-β-lactones [159].

The cobalt-catalyzed carbonylation of epoxides can also be utilized to synthesize enantiopure β-hydroxy esters or amides in the presence of an appropriate nucleophile [160–163]. This strategy provides an alternative to the aldol reaction for the synthesis of *syn*- and *anti*-β-hydroxy esters. In addition, under hydroformylation reaction conditions, epoxides have been converted into β-hydroxy aldehydes [164]. When oxetanes are utilized in the presence of $Co_2(CO)_8$, the reaction is more sluggish [165]. The transformation was optimized by the addition of silanes [166–168] or silylamines [169] to ring-open oxetane, tetrahydrofuran, and 1,3-dioxolane.

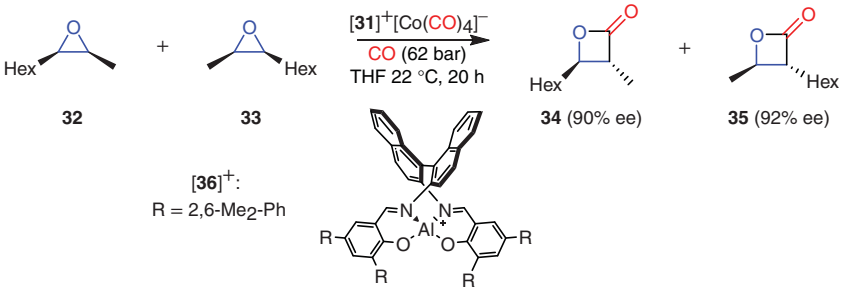

Scheme 2.20 Regiodivergent carbonylation of *cis*-1,2-disubstituted epoxides **32** and **33** yielding enantioenriched *trans*-β-lactones **34** and **35**.

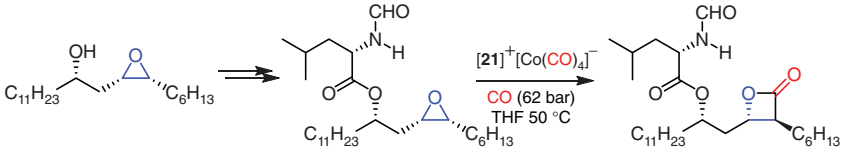

Scheme 2.21 Late-stage carbonylation reaction in the total synthesis of (–)-tetrahydrolipstatin.

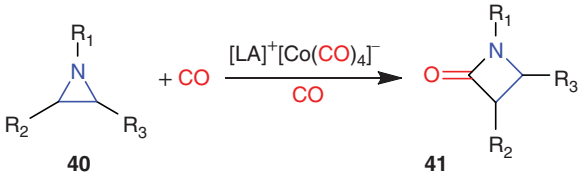

Scheme 2.22 Carbonylation of aziridines catalyzed by $[Co(CO)_4]^-$ assisted by a cationic Lewis acid $[LA]^+$. Sources: Mahadevan et al. [149], Davoli et al. [170].

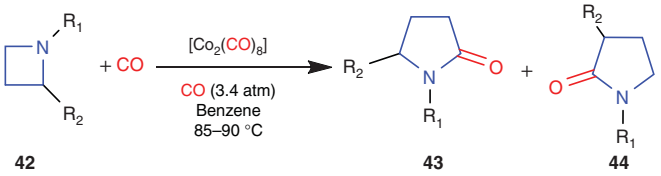

Scheme 2.23 Synthesis of pyrrolidinones **43** and **44** from azetidine and CO.

Under similar reaction conditions, $[LA]^+[Co(CO)_4]^-$ complexes have been utilized to carbonylate aziridines (**40**) to yield β-lactams (**41**), and various substituents are tolerated [149, 170] (Scheme 2.22). Additionally, the CO insertion at the less sterically hindered suggests a nucleophilic attack of the $[Co(CO)_4]^-$ comparable with what is observed for the epoxides.

Similar reactions with only $[Co_2(CO)_8]$/CO were carried out to transform aziridinones into azetidine-2,4-diones [171] and diaziridines into 1,3-diazetidinones [172].

The carbonylation of azetidines was also investigated by Alper and coworkers The reaction was shown to form pyrrolidinones **43** and **44** from alkyl substituted azetidines (**42**) in the presence of $[Co_2(CO)_8]$/CO (3.4 bar, Scheme 2.23). The reaction was also carried out with 2-vinylazetidines to produce tetrahydroazepinones [173].

The cobalt-catalyzed carbonylation of thiiranes has also been described by Alper and coworkers under phase-transfer conditions and in the presence of MeI (Scheme 2.24) [174].

The cobalt-catalyzed carbonylation of saturated heterocycles has also found applications in the synthesis of polymers. For example, propylene oxide and CO allow access to poly(hydroxyalkanoate) (Scheme 2.25) [175–179]. The $[Co_2(CO)_8]$/3-hydroxypyridine has been shown to be a competent catalytic system for the alternating copolymerization of epoxides and CO. The polymerization was also extended

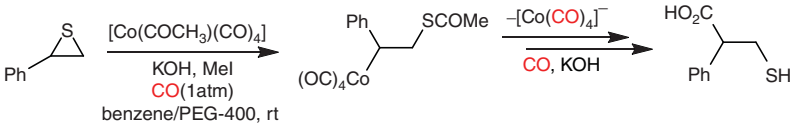

Scheme 2.24 Cobalt-catalyzed carbonylation of 2-phenylthiirane in the presence of CO, KOH, and benzene/PEG-400. Source: Modified from Calet et al. [174].

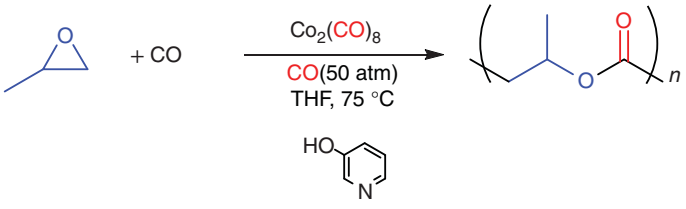

Scheme 2.25 Alternating copolymerization of propylene oxide and CO catalyzed by $[Co_2(CO)_8]$/3-hydroxypyridine. Sources: Dunn and Coates [175], Allmendinger et al. [176], Takeuchi et al. [177], Nakano et al. [178], Liu and Jia [179].

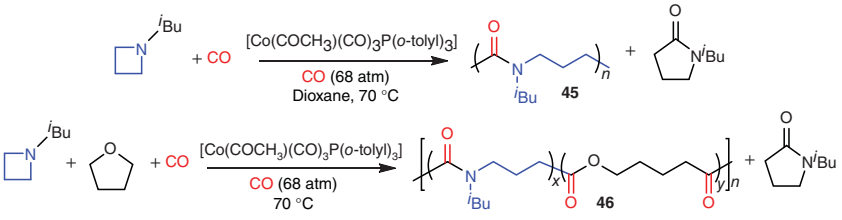

Scheme 2.26 Copolymerization of azetidine and CO in 1,4-dioxane or THF. Sources: Liu and Jia [179], Chai et al. [188].

to enantiomerically pure epoxides to produce isotactic poly(β-hydroxybutyrates) [180]. The analogous copolymerization of aziridines and CO [181–183] was also examined as a route for the synthesis of poly-β-peptoids [184–187].

More recently, *N*-alkyl azetidines were copolymerized with CO to synthesize poly(amide-*co*-amine) (**45**) with $[Co(COCH_3)(CO)_3P(o\text{-tolyl})_3]$ as a catalyst (Scheme 2.26) [188, 189]. The analogous polymerization of epoxides and aziridines catalyzed by the same catalyst was also reported. However, in addition to the desired poly(amide-*block*-ester)s (**46**), significant quantities of polyesters arising exclusively from the polymerization of CO and the epoxides were produced [179].

Beyond saturated heterocycles, the carbonylation reaction can be applied to oxazolidines **47** as reported by Coates and coworkers. The $[Co(SiPh_3)(CO)_4]$ complex in the presence of benzyl alcohol generates the $[Co(CO)_4]^-$ active species. The amide **48** is obtained after protonation and nucleophilic attack of $[Co(CO)_4]^-$. The mechanism then follows the already described carbonylation and ring-closure steps to provide the dihydro-oxazinone **49** (Scheme 2.27) [190].

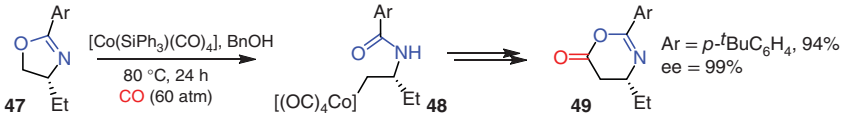

Scheme 2.27 Cobalt-catalyzed carbonylation reaction of oxazolidines **47** in the presence of CO. Source: Modified from Byrne et al. [190].

Scheme 2.28 Carbonylation of alky- and aryl-substituted oxazolines under hydroformylation reaction conditions. Source: Modified from Laitar et al. [191].

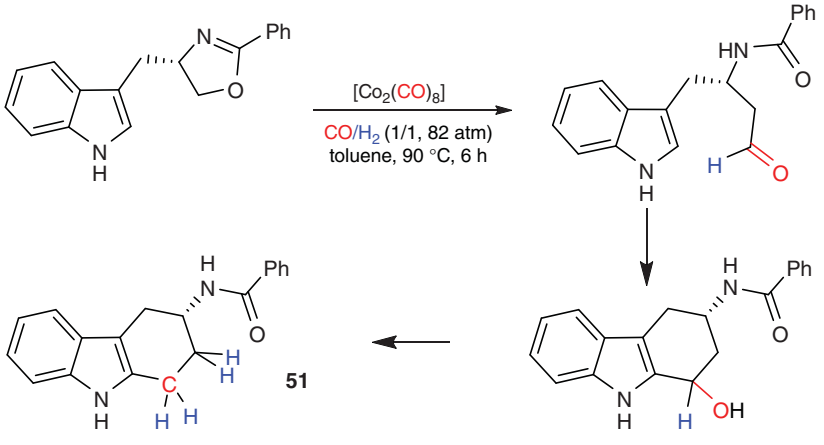

Scheme 2.29 Synthesis of **51** under hydroformylation reaction conditions.

Amino alcohols derived from α-amino acids, protected as oxazolidines, can thus undergo a one-carbon homologation to produce dihydro-oxazinones, which can easily be hydrolyzed into β-amino acids. In addition, in the presence of dihydrogen, the carbonylation reaction ends with the formation of β-amidoaldehydes (**50**) in good yields and excellent enantioselectivities (Scheme 2.28) [191].

In the presence of a nucleophile within the product, the aldehyde can further react to produce polycyclic compounds such as Ampakines and their derivatives [192]. Similarly, this strategy was utilized by Coates and coworkers to synthesize compound **51** (Scheme 2.29) structurally related to pharmaceuticals such as Ramatroban and Frovatriptan [191].

Applications of such catalytic carbonylations in viable industrial processes can only be envisaged if the cobalt complex can be easily recycled. As recent reports show, research groups have started to propose cobalt-supported catalysts for a more

facile recovery. The strategy here is to immobilize the Lewis acid $[LA]^+$ through its supporting ligands and to rely on the ion pairing to retain $[Co(CO)_4]^-$ in the coordination sphere [193–197]. These early results show that a real interest in these reactions exists, which should fuel the research of novel systems for the carbonylation reaction of heterocycles.

2.7 Carbonylation of Alkyl and Aryl Halides

In 1963, Heck and Breslow observed that $Na[Co(CO)_4]$ catalyzes at 35 °C the formation of phenylacetanilide ($PhCH_2CONHPh$) from benzyl chloride, CO, and aniline [198]. Alper and des Abbayes [199], as well as Cassar and Foà [200], reported that, in the presence of an ammonium salt and NaOH, the phase-transfer-catalyzed carbonylation of benzyl chloride or bromide at atmospheric pressure gives phenylacetic acid in high yields. In the organic phase, the $[NBu_4][Co(CO)_4]$ and $PhCH_2Br$ produce $[NBu_4]Br$ and $[Co(CH_2Ph)(CO)_4]$, which then undergo a migratory CO insertion, followed by a hydrolysis step to yield the product [201]. It is also possible to form *in situ* aryl iodides from benzyl alcohol by the addition of sodium iodide/ethyl polyphosphate [202]. More recently, a facile access to phenyl acetic acids **52** was disclosed starting from benzyl chlorides in the presence of $CoCl_2$ and 2-(1*H*-benzimidazol-2-yl)benzoic acid **53** under phase-transfer conditions (Scheme 2.30). The catalytic phase was recycled four times. Additionally, when the substrate carried two benzylic chloride groups, both were carbonylated [203].

The carbonylation of aryl halides into the corresponding acids or esters proceeds under CO (1 atm) at 25 °C in the presence of an alkylcobalt carbonyl complex (**54**) in high yields (Scheme 2.31) [204]. The reaction could also be carried out on heterocycles such as furans, thiophenes, and pyridines. More recently, Boyarskii et al. reported the utilization an epoxide to produce a metallolactone anionic cobalt complex to catalyze the same reaction [205, 206].

Cobalt-catalyzed carbonylations of halides often result in mixtures of mono- and dicarbonylated alkyl [199, 207–212] and aryl [204, 213–215] products. This has prompted the development of reaction conditions under which dicarbonylation products could be selectively obtained. This double carbonylation reaction has been reviewed [156].

Foà and coworkers demonstrated that $[Co_2(CO)_8]$ in the presence of CH_3I and $Ca(OH)_2$ can favor the dicarbonylation of alkyl and aryl chlorides and bromides at

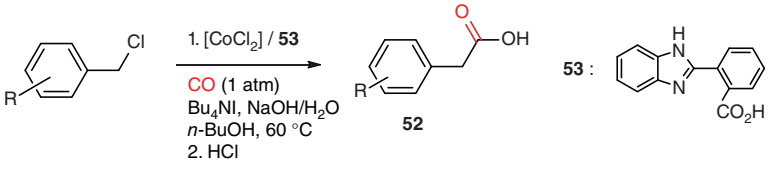

Scheme 2.30 Synthesis of phenyl and phenyl-substituted acetic acids under phase-transfer-catalyzed carbonylation.

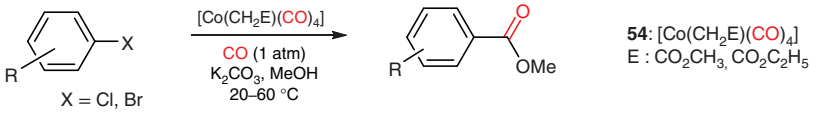

Scheme 2.31 Monocarbonylation of aryl halides into the corresponding aryl methyl esters with the most active catalysts. Source: Modified from Foà et al. [204].

25 °C and 1 bar of CO [213]. Mortreux and coworkers also reported the carbonylation of (1-bromoethyl)benzene under similar conditions to yield benzylpyruvic acid [210]. The addition of a phosphine ligand, particularly the water-soluble TPPTS, did not improve the double vs. the monocarbonylation reaction [216]. Such system was also applied in dioxane/water solvents to naphthalene bromides [215]. A photostimulation can be performed to doubly carbonylate *o*-dihalogenated benzene into $Ar(COOH)_2$ or *o*-halogenated benzoic acids into $C_6H_4(COOH)$(*o*-COCOOH) or phthalonic acid [214].

The mono- and dicarbonylation of alkyl and aryl halides are carried out in complex mixtures. The mechanisms are not fully characterized, but are considered to generally involve a neutral or anionic Co(I) complex. Cobalt complexes have found applications in the carbonylation of halogenated alkyl and aryl substrates under very mild conditions. The large scope of the transformation thus facilitates the access to functionalized organic products even on large scale.

2.8 C–H Bond Carbonylations

Using the Schiff base **55**, Murahashi reported the first cobalt-catalyzed C–H carbonylation reaction under harsh conditions (Scheme 2.32). The cyclisation product **56** was obtained in 80% yield. This reaction was also extended to the Schiff bases derived from *p*-hydroxybenzaldehyde, 1-naphtaldehyde, and 2-naphtaldehyde to produce the corresponding products in 70–96% yield [217]. This CO annulation reaction was also shown to proceed with the diazobenzene [218].

Almost 60 years later, Daugulis and coworkers discovered the cobalt-catalyzed C–H carbonylation of benzamides **57** (Scheme 2.33, Y = CO). The reaction was carried out in trifluoroethanol in the presence of sodium pivalate and $Mn(OAc)_3/O_2$, as oxidant at atmospheric pressure of CO. The phthalimide products were obtained in good yields ranging from 60% to 91% [219].

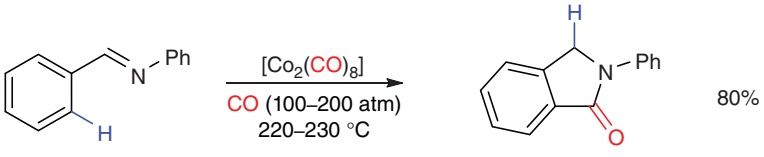

55 56

Scheme 2.32 Cobalt-catalyzed carbonylation of Schiff base **55**.

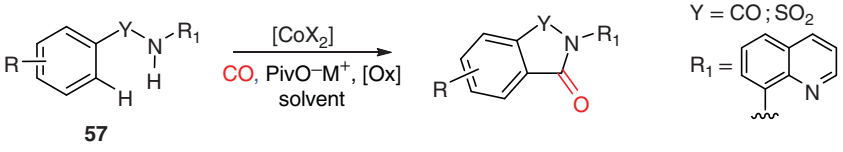

Scheme 2.33 Cobalt-catalyzed C–H carbonylation of benzamides **57**.

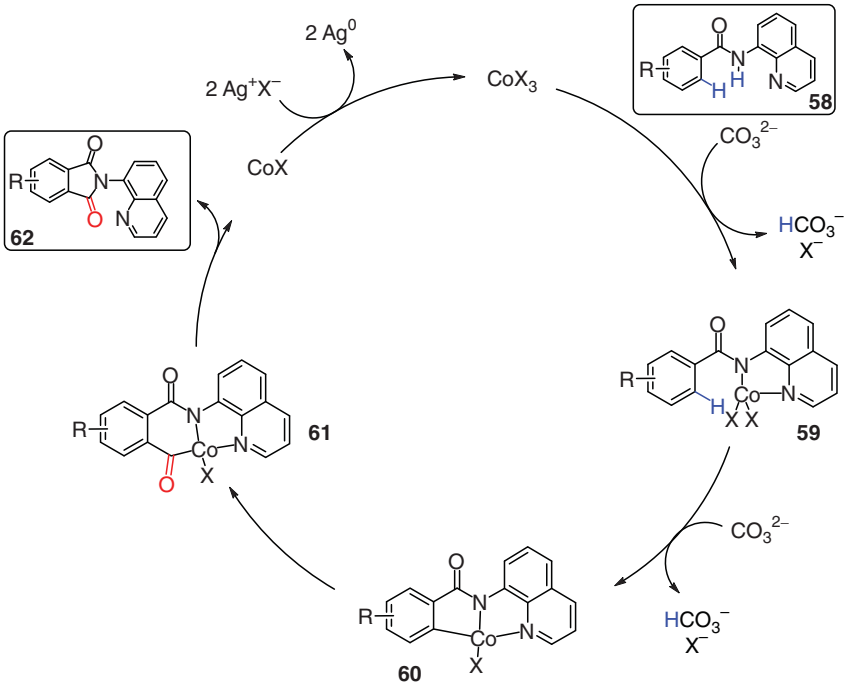

Scheme 2.34 Proposed catalytic cycle for the oxidative N–H and C–H activation followed by CO annulation reaction.

The $Mn(OAc)_3/O_2$ oxidant could be replaced by Ag_2CO_3 or electrochemical oxidative conditions [220]. In addition, the scope of this reaction was further explored with CO surrogates such as diisopropyl azodicarboxylate (DIAD) [221] or CO_2 [222]. The organic scaffold was also modified to sulfonamides (Scheme 2.33, Y = $-SO_{2-}$,) to produce the corresponding products in good yields (55–73%) [222, 223].

The proposed mechanism (Scheme 2.34) involves Co(I) and Co(III) intermediates. Coordination of the deprotonated 8-aminoquinoline substrate **58**, yielding **59**, is followed by a C–H activation that produces **60**. This compound contains two metal–ligand sigma bonds in addition to the quinoline coordination. CO migratory insertion and reductive elimination from **61** yield the phthalimides **62** and a Co(I) complex. Finally, the active species is regenerated via silver-mediated oxidation. The reaction was also carried out with other directing groups such as in **63** [224, 225], **64** [226, 227], **65** [228], and **66** [229] (Chart 2.2).

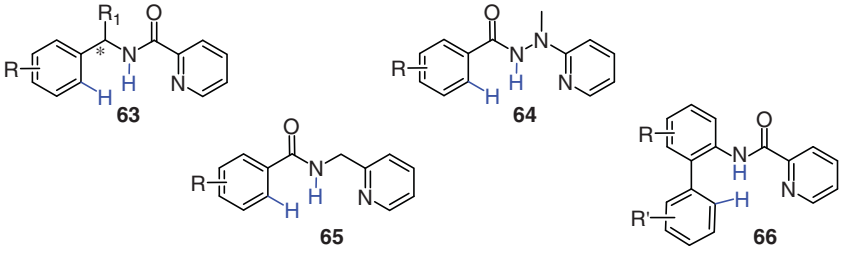

Chart 2.2 General substrate scope of the CO annulation reaction with different directing groups formed by the N–H function.

The reaction was also applied to vinyl phenols to yield coumarin derivatives [230]. In addition, the reaction was extended to C(sp^3)—H bond with the same directing 8-quinoline group [222, 231–233]. The reactions proceeded in moderate-to-good yields with numerous functional groups, which were tolerated at the α position.

The development of cobalt-catalyzed C–H functionalization is regaining interest. This ligand-based transformation requires the assistance of a directing group. The coordination of the amine–amide chelate produces a pincer complex, which can undergo a one-carbon homologation. Understanding of the mechanistic details should provide a rational basis for further optimization of the organic transformation. This approach should prove fruitful in the development of cost effective catalysis to produce organic compound of high added value.

2.9 Miscellaneous Co-Catalyzed Carbonylations

Cobalt-catalyzed carbonylation reactions have also involved to a lesser extent isocyanate and imine functions. In particular, the cobalt-catalyzed carbonylative cyclization of isocyanates and epoxides has been reported [234]. The complex $[LA]^+[Co(CO)_4]^-$, in the presence of isocyanates **67**, epoxide **68**, and CO_2 catalyzes the formation of 1,3-oxazinane-2,4-diones **69** (Scheme 2.35; $[LA]^+ = [Al(salph)(THF)_2]^+$ and salph = *N*,*N*′-*o*-phenylenebis(3,5-di-*tert*-butylsalicylideneimine). Diverse aryl and alkyl isocyanates were shown to yield the corresponding products with moderate-to-excellent yields (46–97%), particularly with electron-poor aryl isocyanates. Product **69** is proposed to form from complex **22** (Scheme 2.17) that is then intercepted by the electrophilic isocyanates.

Similar results were obtained with imines and epoxides [235]. Complex $[Co_2(CO)_8]$/LiCl, in the presence of epoxide **8**, imine **70**, and CO, catalyzes the formation of 1,3-oxazinan-4-ones **71** (Scheme 2.36).

The reaction could be carried out with aromatic imines and methyl-substituted epoxides in good-to-excellent yields (50–98%). When more sterically hindered epoxides were utilized, the reaction did not proceed. In fact, in the absence of epoxides, CO and imines **72** polymerize in the presence of $[Co(PhCH_2CO)(CO)_4]$ to form polypeptides **73** (Scheme 2.37).

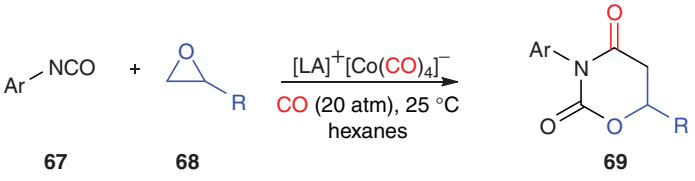

67 68 69

Scheme 2.35 Cobalt-catalyzed cyclization of CO, isocyanates **67**, and epoxides **68**.

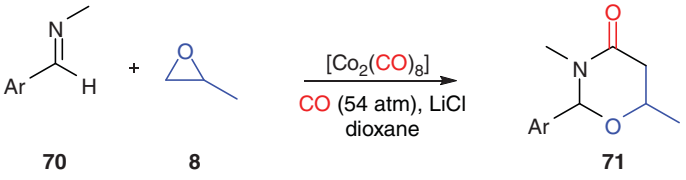

70 8 71

Scheme 2.36 Cobalt-catalyzed cyclization of CO, imine **70**, and epoxide **8**.

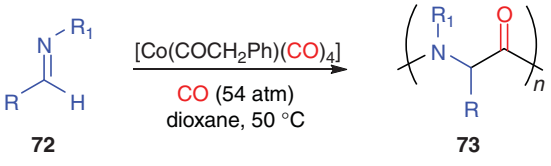

72 73

Scheme 2.37 Cobalt-catalyzed copolymerization of imines and CO into polypeptides.

2.10 Summary and Conclusions

Cobalt-catalyzed carbonylation reactions have regain interest in the past few years. Cobalt catalysts, initially developed in the hydroformylation reactions, are still operating in the transformation of heavy alkenes. However, recent discoveries using unusual Co(II) complexes have open the way to extend the alkenes scope to produce aldehydes.

Similarly, cobalt was also initially utilized in the development of the Pauson–Khand reaction, which remains an important and powerful transformation in the synthetic chemist toolbox. The cobalt catalysis has been further developed to many functionalizations, such as the formation of lactones from epoxides. Even more recently, cobalt catalysis has gained interest in the field of C–X and C–H carbonylation. It has been utilized in organic transformation to synthesize sophisticated organic frameworks. Due to the progress of coordination and computational chemistry, it can be expected that cobalt will gain a central role in the development of highly efficient catalysts. In particular, the activation of CO and its surrogates under mild conditions should be a research field fertile in results for fine chemistry.

References

1 Sabatier, P. and Senderens, J.-B. (1902). *C.R. Hebd. Séances Acad. Sci.* 134: 514–516.
2 Fischer, F. and Tropsch, H. (1925). Hydrocarbons. German Patent DE484337.
3 Roelen, O. (1938). Chemische Verwertungsgesellschaft Oberhausen MBH. German Patent DE484337.
4 Roelen, O. (1938). Production of oxygenated carbon compounds. US Patent US2327066.
5 Roelen, O. (Ruhrchemie AG). (1938). Composés oxygénés du carbone. French Patent FR860289.
6 Underwood, A.J.V. (1940). *Ind. Eng. Chem.* 32: 449–454.
7 Roelen, O. (1978). *Petrochemie* 31: 524–529.
8 Niu, C., Xia, M., Chen, C. et al. (2020). *Appl. Catal., A* 601: 117630.
9 Rahmati, M., Safdari, M.-S., Fletcher, T.H. et al. (2020). *Chem. Rev.* 120: 4455–4533.
10 Adeleke, A.A., Liu, X., Lu, X. et al. (2020). *Rev. Chem. Eng.* 36: 437–457.
11 BASF. (1913). Verfahren zur Darstellung von Kohlenwasserstoffen und deren Derivaten. German Patent DE293787.
12 Reppe, W., Kröper, H., and Pistor, H.-J. (Farben, I.G.). (1941). German Patent DE763693.
13 Mullen, A. (1980). Carbonylations catalyzed by metal carbonyls – Reppe reactions. In: *New Syntheses with Carbon Monoxide* (ed. J. Falbe), 243–308. Berlin, Germany: Springer-Verlag.
14 Arpe, H.J. (2010). *Industrial Organic Chemistry*, 5e. Weinheim, Germany: Wiley-VCH Verlag GmbH & Co.
15 Reppe, W., Kröper, H., von Kutepow, N., and Pistor, H.J. (1953). *Justus Liebigs Ann. Chem.* 582: 72–86.
16 Steinhoff, B.A. and Zoeller, J.R. (2018). Carbonylation of methanol and its derivatives to acetic acid and acetic anhydride. In: *Applied Homogeneous Catalysis with Organometallic Compounds*, 3e, vol. 1 (eds. B. Cornils, W.A. Herrmann, M. Beller and R. Paciello), 93–118. Weinheim, Germany: Wiley-VCH Verlag GmbH & Co.
17 Zweig, J.E., Kim, D.E., and Newhouse, T.R. (2017). *Chem. Rev.* 117: 11680–11752.
18 Peng, J.-B., Wu, F.-P., and Wu, X.-F. (2019). *Chem. Rev.* 119: 2090–2127.
19 Fischer, F. and Tropsch, H. (1926). *Brennstoff-Chem.* 7: 97–104.
20 Tropsch, H. (1924). *Brennstoff-Chem.* 5: 97–102.
21 Fischer, F. (1925). *Ind. Eng. Chem.* 17: 574–576.
22 Mondal, P., Dang, G.S., and Garg, M.O. (2011). *Fuel Process. Technol.* 92: 1395–1410.
23 Higman, C. and Tam, S. (2014). *Chem. Rev.* 114: 1673–1708.

24 Reimert, R., Marschner, F., Renner, H.-J. et al. (2011). *Gas Production, 2. Processes, Ullmann's Encyclopedia of Industrial Chemistry*, 7e, vol. 16, 423–482. Weinheim, Germany: Wiley-VCH Verlag GmbH & Co.

25 Zhao, X., Joseph, B., Kuhn, J., and Ozcan, S. *iScience* 23: 2020, 101082.

26 Jacobs, G. and Davis, B.H. (2016). Reactor approaches for Fischer–Tropsch synthesis. In: *Multiphase Catalytic Reactors* (eds. Z.I. Onsan and A.K. Avci), 269–294. Wiley.

27 Börner, A. and Franke, R. (2016). Syngas and alternative syngas source. In: *Hydroformylation, Fundamentals, Processes, and Applications in Organic Synthesis*, 267–283. Weinheim, Germany: Wiley-VCH.

28 Cornils, B. (2018). Applied homogeneous catalysis with organometallic compounds. In: *Applied Homogeneous Catalysis with Organometallic Compounds*, 3e, vol. 1 (eds. B. Cornils, W.A. Herrmann, M. Beller and R. Paciello), 23–90. Weinheim, Germany: Wiley-VCH Verlag GmbH & Co.

29 Morimoto, T. and Kakiuchi, K. (2004). *Angew. Chem. Int. Ed.* 43: 5580–5588.

30 Wu, L., Liu, Q., Jackstell, R., and Beller, M. (2014). *Angew. Chem. Int. Ed.* 53: 6310–6320.

31 Morimoto, T., Yamasaki, K., Hirano, A. et al. (2009). *Org. Lett.* 11: 1777–1780.

32 Natte, K., Dumrath, A., Neumann, H., and Beller, M. (2014). *Angew. Chem. Int. Ed.* 53: 10090–10094.

33 Cheng, K., Kang, J., King, D.L. et al. (2017). *Adv. Catal.* 60: 25–208.

34 Cao, J., Zheng, Z.-J., Xu, Z., and Xu, L.-W. (2017). *Coord. Chem. Rev.* 336: 43–53.

35 Liu, Q., Yuan, K., Arockiam, P.-B. et al. (2015). *Angew. Chem. Int. Ed.* 54: 4493–4497.

36 Gautam, P. and Bhanage, B.M. (2015). *Catal. Sci. Technol.* 5: 4663–4702.

37 Konishi, H. (2018). *Chem. Pharm. Bull.* 66: 1–19.

38 Konishi, H. and Manabe, K. (2019). *Tetrahedron Lett.* 60: 151147.

39 Chen, Z., Wang, L.C., and Wu, X.-F. (2020). *Chem. Commun.* 56: 6016–6030.

40 Wannberg, J. and Larhed, M. (2003). *J. Org. Chem.* 68: 5750–5753.

41 Hermange, P., Lindhardt, A.T., Taaning, R.H. et al. (2011). *J. Am. Chem. Soc.* 133: 6061–6071.

42 Nielsen, D.U., Neumann, K.T., Lindhardt, A.T., and Skrydstrup, T. (2018). *J. Labelled Compd. Radiopharm.* 61: 949–987.

43 Ravn, A.K., Johansen, M.B., and Skrydstrup, T. (2020). *ChemPlusChem* 85 (7): 1529–1533.

44 Yabe, T. and Sekine, Y. (2018). *Fuel Process. Technol.* 181: 187–198.

45 Chen, S., Zaffran, J., and Yang, B. (2020). *Appl. Catal., B* 118859: 270.

46 Xie, S., Zhang, Q., Liu, G., and Wang, Y. (2016). *Chem. Commun.* 52: 35–59.

47 Cornils, B. (1980). Hydroformylation. Oxo synthesis, Roelen reaction, reactivity and structure: concepts in organic chemistry. In: *New Syntheses with Carbon Monoxide* (ed. J. Falbe), 1–225. Berlin, Germany: Springer-Verlag.

48 van Leeuwen, P.W.N.M. (2004). Cobalt catalysed hydroformylation. In: *Homogeneous Catalysis: Understanding the Art*, 125–138. Berlin, Germany: Springer.

49 Wiese, K.-D. and Obst, D. (2006). *Top. Organomet. Chem.* 18: 1–33.

50 Hebrard, F. and Kalck, P. (2009). *Chem. Rev.* 109: 4272–4282.

51 Bohnen, H.-W. and Cornils, B. (2002). *Adv. Catal.* 47: 1–64.
52 Franke, R., Selent, D., and Börner, A. (2012). *Chem. Rev.* 112: 5675–5732.
53 Hibbel, J., Wiebus, E., and Cornils, B. (2013). *Chem. Ing. Tech.* 85: 853–1871.
54 Börner, A. and Franke, R. (2016). *Hydroformylation: Fundamentals, Processes and Applications in Organic Synthesis*, Vols. 1 and 2. Weinheim, Germany: Wiley-VCH Verlag GmbH & Co.
55 Mason, R.F. and van Winkle J.L. (Shell Oil Co.). (1965). Bicyclic heterocyclic sec- and tert-phosphines. US Patent US3400163, issued September 1968.
56 van Winkle, J.L., Lorenzo, S., Morris, R.C., and Mason, R.F. (Shell Oil Co.). (1965). Single stage hydroformylation of olefins to alcohols. US Patent US3420898.
57 Bungu, P.N. and Otto, S. (2007). *Dalton Trans.*: 2876–2884.
58 Eberhard, M.R., Carrington-Smith, E., Drent, E.E. et al. (2005). *Adv. Synth. Catal.* 34: 1345–1348.
59 Steynberg, J.P., Govender, K., and Steynberg, P.J. (Sasol Technology). (2000). Production of oxygenated products. International Patent Application WO200214248.
60 Polas, A., Wilton-Ely, J.D.E.T., Slawin, A.M.Z. et al. (2003). *Dalton Trans.* 24: 4669–4677.
61 Hood, D.M., Johnson, R.A., Carpenter, A.E. et al. (2020). *Science* 367: 542–548.
62 Tudor, R. and Ashley, M. (2007). *Platinum Met. Rev.* 51: 116–126.
63 Tudor, R. and Ashley, M. (2007). *Platinum Met. Rev.* 51: 164–171.
64 Tudor, R. and Shah, A. (2017). *Johnson Matthey Technol. Rev.* 61: 246–256.
65 Heck, R.F. and Breslow, D.S. (1961). *J. Am. Chem. Soc.* 83: 4023–4027.
66 Rush, L.E., Pringle, P.G., and Harvey, J.N. (2014). *Angew. Chem. Int. Ed.* 53: 8672–8676.
67 Habershon, S. (2016). *J. Chem. Theory Comput.* 12: 1786–1798.
68 Sameera, W.M.C., Maeda, S., and Morokuma, K. (2016). *Acc. Chem. Res.* 49: 763–773.
69 Kim, Y., Kim, J.W., Kim, Z., and Kim, W.Y. (2018). *Chem. Sci.* 9: 825–835.
70 Szlapa, E.N. and Harvey, J.N. (2018). *Chem. Eur. J.* 24: 17096–17104.
71 Li, P., Shen, C., Min, J. et al. (2020). *Catal. Sci. Technol.* 10: 2994–3007.
72 Crause, C., Bennie, L., Damoense, L. et al. (2003). *Dalton Trans.*: 2036–2042.
73 MacNeil, C.S., Mendelsohn, L.N., Zhong, H. et al. (2020). *Angew. Chem. Int. Ed.* 59: 8912–8916.
74 Varela, J.A., Vazquez, S.A., and Martinez-Nunez, E. (2017). *Chem. Sci.* 8: 3843–3851.
75 Bianchi, M., Frediani, P., Piacenti, F. et al. (2002). *Eur. J. Inorg. Chem.*: 1155–1161.
76 Bungu, P.N. and Otto, S. (2011). *Dalton Trans.* 40: 9238–9249.
77 Birbeck, J.M., Haynes, A., Adams, H. et al. (2012). *ACS Catal.* 2: 2512–2523.
78 Van Driessche, E.T.A., Garton, R.D., and Caers, R.F. (2013). PCT/EP09/05995 to ExxonMobil (19 August 2009). US Patent granted on 28 July 2011.
79 Beller, M., Cornils, B., Frohning, C.D., and Kohlpaintner, C.W. (1995). *J. Mol. Catal. A: Chem.* 104: 17–85.

80 Beller, M. and Krauter, J.G.E. (1999). *J. Mol. Catal. A: Chem.* 143: 31–39.

81 Hanson, B.E., Ding, H., and Kohlpaintner, C.W. (1998). *Catal. Today* 42: 421–429.

82 Wu, D., Zhang, J., Wang, Y. et al. (2012). *Appl. Organomet. Chem.* 26: 718–721.

83 Wu, D., Wang, Y., Li, G. et al. (2014). *Catal. Commun.* 44: 54–56.

84 Matsinha, L.C., Siangwata, S., Smith, G.S., and Makhubela, B.C.E. (2019). *Catal. Rev. Sci. Eng.* 61: 111–133.

85 Dabbawala, A.A., Parmar, D.U., Bajaj, H.C., and Jasra, R.V. (2008). *J. Mol. Catal. A: Chem.* 282: 99–106.

86 Dabbawala, A.A., Parmar, J.N., Jasra, R.V. et al. (2009). *Catal. Commun.* 10: 1808–1812.

87 Bauer, G., Ongari, D., Tiana, D. et al. (2020). *Nat. Commun.* 11: 1059–1067.

88 Patcas, F., Maniut, C., Ionescu, C. et al. (2007). *Appl. Catal., B* 70: 630–636.

89 Olmos, A., Asensio, G., and Perez, P.J. (2016). *ACS Catal.* 6: 4265–4280.

90 Magna, L., Olivier-Bourbigou, H., Saussine, L., and Kruger-Tissot, V. (2003). Hydroformylation process using a cobalt catalyst in a non- aqueous ionic liquid with catalyst recycle. European Patent Application EP 1352889 A1 (20031015).

91 Magna, L., Harry, S., Proriol, D. et al. (2007). *Oil Gas Sci. Technol.* 62: 775–780.

92 Hebrard, F., Kalck, P., Saussine, L. et al. (2007). *Dalton Trans.*: 190–191.

93 Magna, L., Harry, S., Faraj, A., and Olivier-Bourbigou, H. (2013). *Oil Gas Sci. Technol.* 68: 415–428.

94 Olivier-Bourbigou, H., Magna, L., and Morvan, D. (2010). *Appl. Catal., A* 373: 1–56.

95 Dengler, J.E., Doroodian, A., and Rieger, B. (2011). *J. Organomet. Chem.* 696: 3831–3835.

96 Himmele, W. and Siegel, H. (1976). *Tetrahedron Lett.* 12: 907–910.

97 LoCicero, J.C. and Johnson, R.T. (1952). *J. Am. Chem. Soc.* 74: 2094–2097.

98 Botteghi, C., Marchetti, M., Paganelli, S., and Scognamillo, S. (2002). *J. Mol. Catal. A: Chem.* 179: 79–86.

99 Yokokawa, C., Watanabe, Y., and Takegami, Y. (1964). *Bull. Chem. Soc. Jpn.* 37: 677–679.

100 Takegami, Y., Yokokawa, C., and Watanabe, Y. (1064). *Bull. Chem. Soc. Jpn.* 37: 935–940.

101 Takahashi, K. and Nozaki, K. (2014). Hydroformylation of epoxides. In: *Science of Synthesis, C-1 Building Blocks in Organic Synthesis* (ed. van Leeuwen) Thieme, 207–217.

102 Bahrmann, H., Bach, H., and Frey, G.D. Oxo synthesis. In: *Ullmann's Encyclopedia of Industrial Chemistry*, 7e, vol. 2013, 1–8. Wiley-VCH Verlag GmbH & Co.

103 Beller, M. (2012). Carbonylation reactions. In: *Catalysis, from Principles to Applications* (eds. M. Beller, A. Renken and R. van Santen), 233–249. Weinheim: Wiley-VCH.

104 Khand, I.U., Knox, G.R., Pauson, P.L., and Watts, W.E. (1973). *J. Chem. Soc., Perkin Trans. 1*: 975–977.

105 Pauson, P.L., Khand, I.U., Knox, G.R., and Watts, W.E. (1971). *J. Chem. Soc. D*: 36.

106 Khand, I.U., Knox, G.R., Pauson, P.L. et al. (1973). *J. Chem. Soc., Perkin Trans. 1*: 977–981.

107 Pauson, P.L. (1985). *Tetrahedron* 41: 5855–5860.

108 Rautenstrauch, V., Megard, P., Conesa, J., and Kuester, W. (1990). *Angew. Chem. Int. Ed.* 29: 1413–1416.

109 Magnus, P. and Principe, L.M. (1985). *Tetrahedron Lett.* 26: 4851–4854.

110 La Belle, B.E., Knudsen, M.J., Olmstead, M.M. et al. (1985). *J. Org. Chem.* 50: 5215–5222.

111 Yamanaka, M. and Nakamura, E. (2001). *J. Am. Chem. Soc.* 123: 1703–1708.

112 Lesage, D., Milet, A., Memboeuf, A. et al. (2014). *Angew. Chem. Int. Ed.* 53: 1939–1942.

113 Rodriguez, M.A. and Prieto, P. (2016). *Tetrahedron* 72: 7443–7448.

114 Fager-Jokela, E., Muuronen, M., Khaizourane, H. et al. (2014). *J. Org. Chem.* 79: 10999–11010.

115 Billington, D.C. and Pauson, P.L. (1982). *Organometallics* 1: 1560–1561.

116 Lovely, C.J., Seshadri, H., Wayland, B.R., and Cordes, A.W. (2001). *Org. Lett.* 3: 2607–2610.

117 Gallagher, A.G., Tian, H., Torres-Herrera, O.A. et al. (2019). *Org. Lett.* 21: 8646–8651.

118 Hiroi, K., Watanabe, T., Kawagishi, R., and Ikuko, A. (2000). *Tetrahedron Lett.* 41: 891–895.

119 Hiroi, K., Watanabe, T., Kawagishi, R., and Abe, I. (2000). *Tetrahedron: Asymmetry* 11: 797–808.

120 Sturla, S. and Buchwald, S.L. (2002). *J. Org. Chem.* 67: 3398–3403.

121 Garçon, M., Cabre, A., Verdaguer, X., and Riera, A. (2017). *Organometallics* 36: 1056–1065.

122 Orgué, S., Leon, T., Riera, A., and Verdaguer, X. (2015). *Org. Lett.* 17: 250–253.

123 Lindsay, D.M. and Kerr, W.J. Recent advances in the Pauson–Khand reaction. In: *Cobalt Catalysis in Organic Synthesis: Methods and Reactions*, 1e, vol. 2020 (eds. M. Hapke and G. Hilt), 259–285. Wiley-VCH.

124 Su, S., Rodriguez, R.A., and Baran, P.S. (2011). *J. Am. Chem. Soc.* 133: 13922–13925.

125 Cabré, A., Verdaguer, X., and Riera, A. (2017). *Synthesis* 49: 3945–3951.

126 Kerr, W.J., McLaughlin, M., Paterson, L.C., and Pearson, C.M. (2018). *Tetrahedron* 74: 5062–5068.

127 Zhao, N., Yin, S., Xie, S. et al. (2018). *Angew. Chem. Int. Ed.* 57: 3386–3390.

128 Liu, D.-D., Sun, T.-W., Wang, K.-Y. et al. (2017). *J. Am. Chem. Soc.* 139: 5732–5735.

129 Zhu, L., Wang, Z., Liu, S. et al. (2019). *Chin. Chem. Lett.* 30: 889–894.

130 Le Berre, C., Serp, P., Kalck, P., and Torrence, G.P. (2014). Acetic acid. In: *Ullmann's Encyclopedia of Industrial Chemistry* (ed. B. Elvers), 1–34. Wiley-VCH Verlag GmbH & Co.

131 von Kutepow, N., Himmele, W., and Hohenschutz, H. (1965). *Chem. Ing. Tech.* 37: 383–388.

132 Hohenschutz, H., von Kutepow, N., and Himmele, W. (1966). *Hydrocarbon Process.* 45: 141–144.

133 Forster, D. and Singleton, T.C. (1982). *J. Mol. Catal.* 17: 299–314.

134 Mizoroki, T. and Nakayama, M. (1968). *Bull. Chem. Soc. Jpn.* 41: 1628–1633.

135 Mizoroki, T., Matsumoto, T., and Ozaki, A. (1979). *Bull. Chem. Soc. Jpn.* 52: 479–482.

136 Mirbach, M.F. and Mirbach, M.J. (1985). *J. Mol. Catal.* 32: 59–75.

137 Röper, M., Schieren, M., and Heaton, B.T. (1986). *J. Organomet. Chem.* 299: 131–136.

138 Imyanitov, N.S., Bogoradovskaya, N.M., and Semenova, T.A. (1978). *Kinet. Catal. (translation of Kinetika i Kataliz)* 19: 573–579.

139 von Kutepow, N. and Müller, F. J. (BASF). Production of acetic acid or mixtures of the same with methyl acetate. (1973). DE Patent 2303271.

140 Nozaki, K. (Shell Oil). (1973). Production of carboxylic acids and esters. US Patent 3,856,856.

141 Ditzel, E.J., Poole, A.D., Cole-Hamilton, D.J., and Marr, A.C. (BP Chemicals). (1999) Process for the carbonylation of an alcohol and/or reactive derivative thereof. EP 1043300.

142 Marr, A.C., Ditzel, E.J., Benyei, A.C. et al. (1999). *Chem. Commun.*: 1379–1380.

143 Lindner, E., Reber, J.-P., and Wegner, P. (1988). *Z. Naturforsch., B* 43: 1268–1270.

144 Hölderich, W., Fouquet, G., Harder, W., and Cäsar, F. (BASF). (1987). Verfahren zur Herstellung von Essigsaüre, Methylacetat und/oder Dimethylether. DE 3606169.

145 Huang, C.-Y. and Doyle, A.G. (2014). *Chem. Rev.* 114: 8153–8198.

146 Li, Y., Hu, Y., and Wu, X.-F. (2018). *Chem. Soc. Rev.* 47: 172–194.

147 Khumtaveeporn, K. and Alper, H. (1995). *Acc. Chem. Res.* 28: 414–422.

148 Lee, J.T., Thomas, P.J., and Alper, H. (2001). *J. Org. Chem.* 66: 5424–5426.

149 Mahadevan, V., Getzler, Y.D.Y.L., and Coates, G.W. (2002). *Angew. Chem. Int. Ed.* 41: 2781–2784.

150 Church, T.L., Getzler, Y.D.Y.L., and Coates, G.W. (2006). *J. Am. Chem. Soc.* 128: 10125–10133.

151 Allmendinger, M., Zintl, M., Eberhardt, R. et al. (2004). *J. Organomet. Chem.* 689: 971–979.

152 Hubbell, A.K., La Pointe, A.M., Lamb, J.R., and Coates, G.W. (2019). *J. Am. Chem. Soc.* 141: 2474–2480.

153 Mulzer, M., Whiting, B.T., and Coates, G.W. (2013). *J. Am. Chem. Soc.* 135: 10930–10933.

154 Rowley, J.M., Lobkovsky, E.B., and Coates, G.W. (2007). *J. Am. Chem. Soc.* 129: 4948–4496.

155 Jiang, J., Rajendiran S., and Yoon, S. (2019). *Asian J. Org. Chem.* 8: 151–154.

156 Das, D. and Bhanage, B.M. (2020). *Adv. Synth. Catal.* 362: 3022–3058.

157 Alper, H., Arzoumanian, H., Petrignani, J.-F., and Saldana-Maldonado, M. (1985). *J. Chem. Soc., Chem. Commun.* (6): 340–341.

158 Mulzer, M., Ellis, W.C., Lobkovsky, E.B., and Coates, G.W. (2014). *Chem. Sci.* 5: 1928–1933.

159 Mulzer, M., Tiegs, B.J., Wang, Y. et al. (2014). *J. Am. Chem. Soc.* 136: 10814–10820.
160 Hinterding, K. and Jacobsen, E.N. (1999). *J. Org. Chem.* 64: 2164–2165.
161 Goodman, S.N. and Jacobsen, E.N. (2002). *Angew. Chem. Int. Ed.* 41: 4703–4705.
162 Liu, J., Wu, H., Xu, L. et al. (2007). *J. Mol. Catal. A: Chem.* 269: 97–103.
163 Xu, J.-X. and Wu, X.-F. (2019). *J. Org. Chem.* 84: 9907–9912.
164 Nakano, K., Katayama, M., Ishihara, S. et al. (2004). *Synlett*: 1367–1370.
165 Wang, M.D., Calet, S., and Alper, H. (1989). *J. Org. Chem.* 54: 20–21.
166 Kang, K.T. and Weber, W.P. (1985). *Tetrahedron Lett.* 26: 5733–5734.
167 Murai, T., Furuta, K., Kato, S. et al. (1986). *J. Organomet. Chem.* 30: 249–254.
168 Murai, T., Yasui, E., Kato, S. et al. (1989). *J. Am. Chem. Soc.* 111: 7938–7946.
169 Tsuji, Y., Kobayashi, M., Okuda, F., and Watanabe, Y. (1989). *J. Chem. Soc., Chem. Commun.*: 1253–1254.
170 Davoli, P., Moretti, I., Prati, F., and Alper, H. (1999). *J. Org. Chem.* 64: 518–521.
171 Roberto, D. and Alper, H. (1984). *Organometallics* 3: 1767–1769.
172 Komatsu, M., Tamabuchi, S., Minakata, S., and Ohshirob, Y. (1999). *Heterocycles* 50: 67–70.
173 Roberto, D. and Alper, H. (1989). *J. Am. Chem. Soc.* 111: 7539–7543.
174 Calet, S., Alper, H., Petrignani, J.-F., and Arzoumanian, H. (1987). *Organometallics* 6: 1625–1628.
175 Dunn, E.W. and Coates, G.W. (2010). *J. Am. Chem. Soc.* 132: 11412–11413.
176 Allmendinger, M., Eberhardt, R., Luinstra, G.A., and Rieger, B. (2002). *J. Am. Chem. Soc.* 124: 5646–5647.
177 Takeuchi, D., Sakaguchi, Y., and Osakada, K. (2002). *J. Polym. Sci., Part A: Polym. Chem.* 40: 4530–4537.
178 Nakano, K., Fumitaka, K., and Nozaki, K. (2004). *J. Polym. Sci., Part A: Polym. Chem.* 42: 4666–4670.
179 Liu, G. and Jia, L. (2004). *J. Am. Chem. Soc.* 126: 14716–14717.
180 Allmendinger, M., Eberhardt, R., Luinstra, G.A., and Rieger, B. (2003). *Macromol. Chem. Phys.* 204: 564–569.
181 Jia, L., Ding, E., and Anderson, W.R. (2001). *Chem. Commun.* (16): 1436–1437.
182 Zhao, J., Ding, E., Allgeier, A.M., and Jia, L. (2003). *J. Polym. Sci., Part A: Polym. Chem.* 41: 376–385.
183 Tanaka, S.-i., Hoh, H., Akahane, Y. et al. (2007). *J. Organomet. Chem.* 692: 26–35.
184 Jia, L., Sun, H., Shay, J.T. et al. (2002). *J. Am. Chem. Soc.* 124: 7282–7283.
185 Darensbourg, D.J., Phelps, A.L., Le Gall, N., and Jia, L. (2004). *J. Am. Chem. Soc.* 126: 13808–13815.
186 Lin, S.-H., Yu, X.-F., Tu, Y.-F. et al. (2010). *Chem. Commun.* 46: 4273–4275.
187 Lin, S., Zhang, B., Skoumal, M.J. et al. (2011). *Biomacromolecules* 12: 2573–2582.
188 Chai, J., Liu, G., Chaicharoen, K. et al. (2008). *Macromolecules* 41: 8980–8985.
189 Liu, G. and Jia, L. (2006). *Angew. Chem. Int. Ed.* 45: 129–131.
190 Byrne, C.M., Church, T.L., Kramer, J.W., and Coates, G.W. (2008). *Angew. Chem. Int. Ed.* 47: 3979–3983.

191 Laitar, D.S., Kramer, J.W., Whiting, B.T. et al. (2009). *Chem. Commun.*: 5704–5706.

192 Mulzer, M. and Coates, G.W. (2011). *Org. Lett.* 13: 1426–1428.

193 Park, H.D., Dinca, M., and Roman-Leshkov, Y. (2017). *ACS Cent. Sci.* 3: 444–448.

194 Park, H.D., Dinca, M., and Roman-Leshkov, Y. (2018). *J. Am. Chem. Soc.* 140: 10669–10672.

195 Jiang, J. and Yoon, S. (2019). *J. Mater. Chem. A* 7: 6120–6125.

196 Ganesan, V. and Yoon, S. (2019). *ACS Appl. Mater. Interfaces* 11: 18609–18616.

197 Ganesan, V. and Yoon, S. (2020). *Inorg. Chem.* 59: 2881–2889.

198 Heck, R.F. and Breslow, D.S. (1963). *J. Am. Chem. Soc.* 85: 2779–2782.

199 Alper, H. and Des Abbayes, H. (1977). *J. Organomet. Chem.* 134: C11–C14.

200 Cassar, L. and Foà, M. (1977). *J. Organomet. Chem.* 134: C15–C16.

201 Des Abbayes, H. and Buloup, A.J. (1980). *Organomet. Chem.* 198: C36–C38.

202 Imamoto, T., Kusumoto, T., and Yokoyama, M. (1982). *Bull. Chem. Soc. Jpn.* 55: 643–644.

203 She, M.-Y., Xiao, D.-W., Yin, B. et al. (2013). *Tetrahedron* 69: 7264–7268.

204 Foà, M., Francalanci, F., Bencini, E., and Gardano, A. (1985). *J. Organomet. Chem.* 285: 293–303.

205 Khaibulova, T.S., Boyarskaya, A., Larionov, E., and Boyarskiy, V.P. (2014). *Molecules* 19: 5876–5897.

206 Boyarskii, V.P., Duka, G.G., Boyarskaya, I.A., and Russian, J. (2009). *Gen. Chem.* 79: 2449–2451.

207 Francalanci, F. and Foà, M. (1982). *J. Organomet. Chem.* 232: 59–70.

208 Francalanci, F., Gardano, A., Abis, L. et al. (1983). *J. Organomet. Chem.* 243: 87–94.

209 Monflier, E., Pellegrini, S., Mortreux, A., and Petit, F. (1991). *Tetrahedron Lett.* 32: 4703–4704.

210 Monflier, E., Mortreux, A., and Petit, F. (1993). *Appl. Catal., A* 102: 53–67.

211 Des Abbayes, H. and Buloup, A. (1978). *J. Chem. Soc., Chem. Commun.*: 1090–1091.

212 Li, G.-X., Li, L., Huang, H.-M., and Cai, H.-Q. (2003). *J. Mol. Catal. A: Chem.* 193: 97–102.

213 Francalanci, F., Bencini, E., Gardano, A. et al. (1986). *J. Organomet. Chem.* 301: C27.

214 Kashimura, T., Kudo, K., Mori, S., and Sugita, N. (1986). *Chem. Lett.* (4): 483–486.

215 Miura, M., Akase, F., and Nomura, M. (1987). *J. Org. Chem.* 52: 2623–2325.

216 Monflier, E. and Mortreux, A. (1994). *J. Mol. Catal.* 88: 295–300.

217 Murahashi, S. (1955). *J. Am. Chem. Soc.* 77: 6403–6404.

218 Murahashi, S. and Horiie, S. (1956). *J. Am. Chem. Soc.* 78: 4816–4817.

219 Grigorjeva, L. and Daugulis, O. (2014). *Org. Lett.* 16: 4688–4690.

220 Zeng, L., Li, H., Tang, S. et al. (2018). *ACS Catal.* 8: 5448–5453.

221 Ni, J., Li, J., Fan, Z., and Zhang, A. (2016). *Org. Lett.* 18: 5960–5963.

222 Barsu, N., Kalsi, D., and Sundararaju, B. (2018). *Catal. Sci. Technol.* 8: 5963–5969.

223 Nguyen, T.T., Grigorjeva, L., and Daugulis, O. (2017). *Chem. Commun.* 53: 5136–5138.

224 Ling, F., Ai, C., Lv, Y., and Zhong, W. (2017). *Adv. Synth. Catal.* 359: 3707–3712.

225 Lukasevics, L., Cizikovs, A., and Grigorjeva, L. (2020). *Org. Lett.* 22: 2720–2723.

226 Qiu, S., Zhai, S., Wang, H. et al. (2018). *Adv. Synth. Catal.* 360: 3271–3276.

227 Sau, S.C., Mei, R., Struwe, J., and Ackermann, L. (2019). *ChemSusChem* 12: 3023–3027.

228 Fu, L.-Y., Ying, J., and Wu, X.-F. (2019). *J. Org. Chem.* 84: 12648–12655.

229 Ling, F., Zhang, C., Ai, C. et al. (2018). *J. Org. Chem.* 83: 5698–5706.

230 Liu, X.-G., Zhang, S.-S., Jiang, C.-Y. et al. (2015). *Org. Lett.* 17: 5404–5407.

231 Barsu, N., Bolli, S.K., and Sundararaju, B. (2017). *Chem. Sci.* 8: 2431–2435.

232 Williamson, P., Galvan, A., and Gaunt, M.J. (2017). *Chem. Sci.* 8: 2588–2591.

233 Zeng, L., Tang, S., Wang, D. et al. (2017). *Org. Lett.* 19: 2170–2173.

234 Church, T.L., Byrne, C.M., Lobkovsky, E.B., and Coates, G.W. (2007). *J. Am. Chem. Soc.* 129: 8156–8162.

235 Zhang, Y., Ji, J., Zhang, X. et al. (2014). *Org. Lett.* 16: 2130–2133.

3

Nickel-Catalyzed Carbonylations

Debarati Das and Bhalchandra M. Bhanage

Institute of Chemical Technology, Department of Chemistry, Nathalal Parekh Marg, Mumbai 400019, India

3.1 Introduction

Nickel means "bad partner (boy)" in the German language. In the sixteenth century, miners serendipitously discovered this element from a reddish ore of what they thought to be copper. That piece of "enchanted rock," nickeline (nickel arsenide now) had a new element nickel (Ni) that later impacted the academic and industrial catalyses. Later, in 1754, it was isolated in pure form by Cronstedt [1]. After a further hundred years and more, in 1890s, Mond discovered the first carbonyl nickel complex, $Ni(CO)_4$, which widened the path of advancement in organonickel chemistry, and it was described as "Mond gave wings to a metal" [2]. However, the recognition of CO was limited to an odorless, colorless, flammable, toxic gas.

Ni is the only metal that reacts with CO at room temperature and at atmospheric pressure of gaseous CO. Although the water-shift reaction inaugurated CO chemistry, its systematic exploration started after the Mond process. In 1906, Sabatier pioneered the Ni-catalyzed hydrogenation of CO to methane and was awarded Nobel Prize in Chemistry in 1912 [3]. This reaction purifies the stream of hydrogen gas from CO in the industrial production of ammonia. Further, Wilke first studied the structure and reactivity of $Ni(COD)_2$ (COD = 1,5-cyclooctadiene) and explored the olefin oligomerization reactions [4]. $Ni(CO)_4$ was considered as a carbonylative catalyst by Reppe at BASF [5], but it required very high pressures (350–600 bar) and high temperatures even for moderate rates to convert acetylene, CO, and water to acrylic acid [5c, e, 6]. Since $Ni(CO)_4$ is highly toxic, its commercial application as a catalyst has diminished with time. Moreover, the high affinity between CO and Ni(0) forms fully coordinated $Ni(CO)_4$, which eventually prohibits the oxidative addition of the C—X bond to the metallic center and also the migratory insertion of CO. Hence, the rational selection of ligand and optimum pressure of CO are two key ingredients for a successful Ni-catalyzed carbonylation using $Ni(CO)_4$ as catalyst.

In general, the term carbonylation includes a large number of closely related reactions wherein CO is incorporated into a substrate as C1 source. Mainly, unsaturated

Carbon Monoxide in Organic Synthesis: Carbonylation Chemistry,
First Edition. Edited by Bartolo Gabriele.

compounds such as alkenes or alkynes and activated alkyl- and aryl-X compounds (X = OH, halide) act as substrates to give carbonyl compounds of industrial interest. The most prominent example of such of industrial reaction is carbonylation of methanol to yield acetic acid. It was widely used until and unless comparatively cheap feedstock had replaced it.

The judicious choice of both the transition-metal catalyst and the reaction conditions form the basis of the catalytic carbonylation. In this context, the first-row transition metals have acted as efficient alternatives to the second- and third-row metals in many organic reactions, owing to stable different oxidation states. However, nickel and palladium reside to the same group in the periodic table and can possess oxidation numbers of 0 and +2. So, oxidative addition, transmetalation, and reductive elimination can be expected from Ni, too. The main challenge of carbonylations lies on the strong affinity between Ni-species and π-acidic CO to easily form nickel complexes, $Ni(CO)_4$ and/or $Ni(CO)_3L$, which eventually decrease the electron density of the Ni center and produce undesirable unreactive species for the catalytic cycle. In this context, the use of CO surrogates controls the kinetics of unreactive carbonyl nickel species and helps the reaction to completion. On the other hand, tailoring of ligands associated with metal also ensures selectivity and controls activity of that particular catalyst. Among the popular Ni-catalysts, homogeneous catalysts, like Ni-halides and Ni-chelates, are prominent, whereas NiO nanoparticles as heterogeneous catalysts also give a good competition in terms of reusability and efficacy for carbonylation. Ni has also acted as co-catalyst or promoters for some carbonylations. In this chapter, we will discuss about the advancement of Ni-catalysts for last 10 years in carbonylations.

3.2 Nickel Halides in Carbonylation Reaction

Nickel is most explored as nickel halides for various carbonylation reactions. Notably, nickel catalysts have been used as efficient carbonylative catalysts in the last decade. Initial reports of N-halides involved drastic reaction conditions, so tuning of catalytic systems is advisable.

Methanol carbonylation is one of the most important and oldest reactions that have been industrialized. The vapor-phase carbonylation of methanol is more promising with less corrosion and easy separation of product and catalyst in contrast to conventional methods. Modern research focuses on the study of Ni-based catalysts for the vapor-phase carbonylation of methanol [7–9]. In this context, a direct vapor-phase methanol carbonylation was reported with $NiCl_2$–$CuCl_2$/HMOR catalysts, devoid of any methyl iodide promoter (responsible for corrosion) [10]. The optimum composition of the composite catalyst was achieved with 5 wt% $NiCl_2$ and 15 wt% $CuCl_2$, which resulted in a methanol conversion of 84.2% and carbonylation selectivity of 73.5% at $P = 1.5$ MPa and $T = 623$ K (Table 3.1). Interestingly, the microporous material mordenite or H-mordenite (HMOR) is known for its hydrothermal stability, shape selectivity, strong acidity, and mass transfer ability. The higher pressure favored acetic acid formation, as attaining 1.5 MPa the

Table 3.1 Methanol carbonylation with different loading of catalysts.

Catalysts	Methanol conversion (%)	Selectivity (%)					AC + MA yield (%)
		DME	AC	MA	AC + MA	HC	
20% $CuCl_2$/HMOR	84.3	50.2	26.2	13.1	39.3	10.5	33.1
5% $NiCl_2$–15% $CuCl_2$/HMOR	84.2	13.2	48.4	25.1	73.5	13.3	61.9
15% $NiCl_2$–5% $CuCl_2$/HMOR	81.1	41.7	29.2	22.1	51.3	7.0	41.6
20% $NiCl_2$/HMOR	87.9	30.7	11.5	47.8	59.3	10.0	52.1

AC, acetic acid; MA, methyl acetate; DME, dimethyl ether; HC, hydrocarbon.
Conditions: $P = 1.5$ MPa, $T = 623$ K, $n(CO)/n(CH_3OH) = 13$.

conversion of methanol increased from 71.8% to 84.2% and the selectivity of acetic acid and methyl acetate (MA) increased effectively from 29.3% to 73.5%. Similarly, at higher temperature such as 623 K, the selectivities to activated carbon (AC) and MA increased to 48.4% and 25.1%, respectively.

The activation of simple C—N bonds in organic compounds represents a major challenge for researchers [11]. The most direct and accessible pathway for valuable amides is achieved by carbonylation on activated C—N bond [12]. In this context, a new method was developed with nickel-catalyzed direct carbonylation of benzyl amines via C—N bond activation [13]. This rapid and simple method proceeded by formation of an amine–I_2 charge-transfer complex, which activated the inert C—N bond via oxidative addition to Ni(0). Incidentally, charge-transfer complexes polarize chemical bonds, reforming the redox potential and thus weakening the chemical bonds. Iodine can act as good electron acceptor and is popular for forming charge-transfer (CT) complexes with amines [14]. The approach is to cleave the C—N bond of tertiary amines for making the room for CO insertion by catalytic carbonylation reaction with catalytic amount of iodine and $NiCl_2$ to synthesize amides (Scheme 3.1).

The initially formed amine–I_2 charge-transfer complex **1** can undergo oxidative addition with an active catalytic center Ni(0) to give a Ni(I) complex **2** via a radical pathway (Scheme 3.2). The migratory insertion of CO along with the release of I_2 due

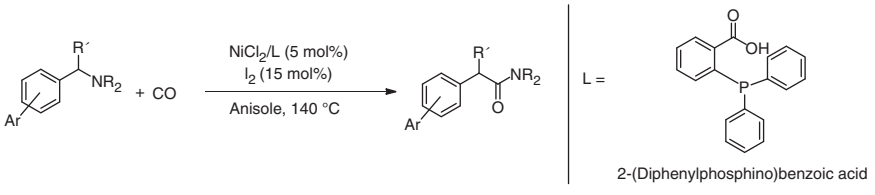

Scheme 3.1 Amide synthesis.

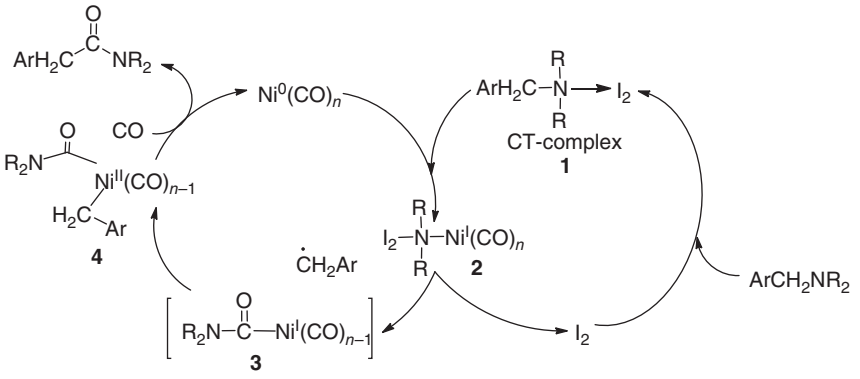

Scheme 3.2 Plausible reaction mechanism of amide formation.

to the lower electron density of the amide moiety can form acylnickel(I) species **3**. Further, the intermediate **3** can undergo the oxidative addition of the benzylic radical with formation of the acylnickel(II) species **4** that can further undergo reductive elimination to obtain the desired amide with regeneration of the active Ni(0) catalyst.

Difluoroalkyl ketones are important building blocks for the preparation of several fluorinated compounds, but their synthetic approaches are limited and complicated [15]. Zhang and coworkers proposed the first example of nickel-catalyzed carbonylation of difluoroalkyl halides with arylboronic acids using $NiCl_2$·dimethyl ether (DME) as catalyst under mild conditions to provide difluoroalkyl ketones through a cost-effective approach (Scheme 3.3) [16]. The reaction can be performed with *gem*-difluoropropargyl bromide and several arylboronic acids under 1 atm of CO with high functional group tolerance and moderate-to-high yields (45–82%). Moreover, several heteroaromatic rings, such as pyridine, carbazole, and dibenzo[*b,d*]thiophene-containing boronic acids, were found to be compatible with the reaction conditions (38–66%).

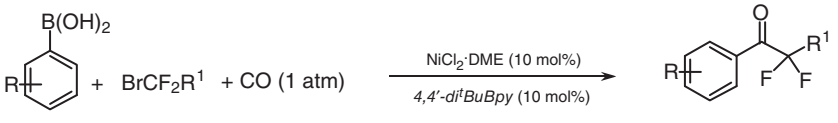

Scheme 3.3 Synthetic protocol of difluoroalkyl ketones. Source: Modified from Zhao et al. [16].

Compared with aliphatic *gem*-difluoropropargyl bromides, the aromatic counter parts gave poor yield probably due to significant defluorination side reactions, whereas unactivated difluoroalkyl bromides did not produce the desired products. Furthermore, these reaction conditions could be applied for the late-stage synthesis of difluoroactivated bioactive molecules especially for ketone-based peptides in the synthesis of anti-HIV agents. The reaction proceeded with a transmetalation of $[Ni^{II}(L_n)X_2]$ with the aryl boronic acid to produce an aryl nickel(II) complex $[ArNi^{II}(L_n)X]$ **5** followed by CO insertion to generate the arylacyl nickel(II) complex $[Ar(CO)Ni^{II}(L_n)\text{-}X]$ **6** (Scheme 3.4). Complex **6** further reacts with difluoroalkyl

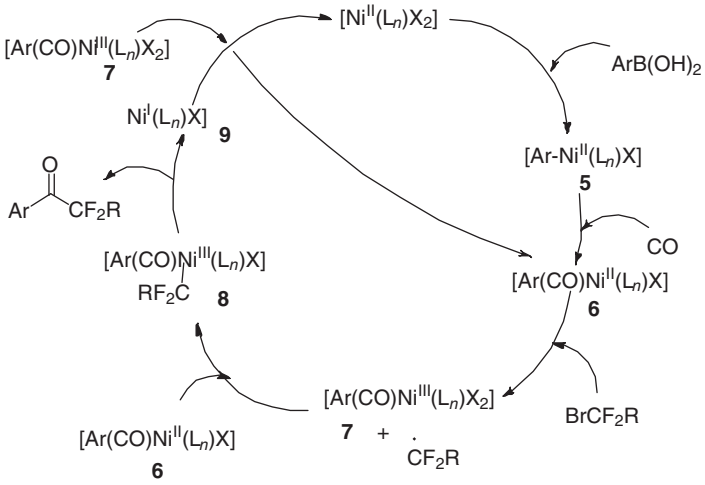

Scheme 3.4 Radical mechanism pathway for the synthesis of difluoroalkyl ketones.

bromide to afford a difluoroalkyl radical species along with a nickel(III) complex $[Ar(CO)Ni^{III}(L_n)X_2]$ **7**. The difluoroalkyl radical is then trapped by another **6** to furnish the key intermediate $[Ar(CO)Ni^{III}(L_n)CF_2R(X)]$ **8**, which can undergo reductive elimination to give the difluoroalkyl ketone along with nickel(I) complex $[Ni^{I}(L_n)X]$ **9**. In the end, a comproportionation reaction can occur between **9** and **7** to form nickel(II) catalyst $[Ni^{II}(L_n)X_2]$ and **6**. The versatility of this procedure is demonstrated by the synthesis of novel difluoroalkyl ketones containing a C≡C bond that can further serve as suitable building blocks for many bioactive fluorinated compounds.

In a related study, an example of the economical nickel-catalyzed carbonylation of secondary alkyltrifluoromethyl halides with arylboronic acids under atmospheric CO has been reported [17]. Interestingly, secondary benzyl bromides and difluoromethylated, trifluoromethylated, and difluoroacetylated secondary alkyl iodides were found to be reactive in this straightforward reaction conditions to furnish alkyl ketones, including some of great significance in medicinal chemistry. Analogous carbonylation reaction of secondary aliphatic electrophiles and CO with the well-studied palladium catalysts, for synthesizing alkyl ketones, still remains difficult to realize because of the competition between the unfavorable β-H elimination and the desired reductive elimination process [18]. The main challenges of Ni-catalyzed carbonylation of secondary trifluoromethylated aliphatic electrophiles under atmospheric CO are to limit the generation of unreactive carbonyl nickel species under CO atmosphere (Scheme 3.5) and to avoid the β-fluoride elimination of trifluoromethylated secondary alkyl iodides that is typically noticed in transition-metal-catalyzed reactions (Scheme 3.5). The electronic nature of the arylboronic acids did not impact on the reaction output (60–80% yields). This method showed good functional group tolerance associated with wide substrate scope. Notably, this nickel-catalyzed carbonylation reaction methodology can be beneficial for pharmaceutical industry, as reactions of anti-histaminergic drug

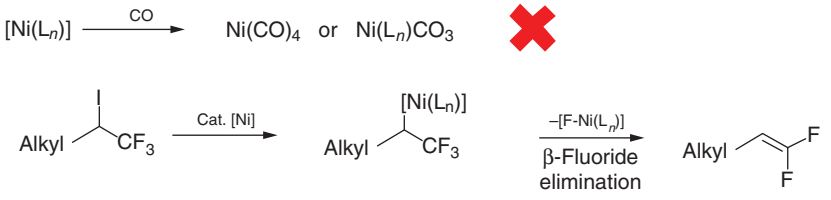

Scheme 3.5 Undesired processes in Ni-catalyzed carbonylative coupling of secondary alkyl-trifluoromethyl halides with arylboronic acids.

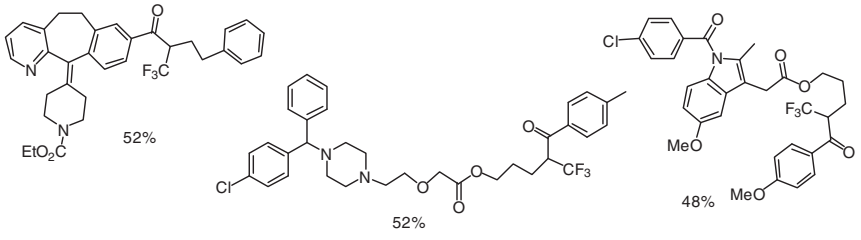

Figure 3.1 Pharmaceutical drugs obtained by Ni-catalyzed carbonylative coupling of secondary alkyl-trifluoromethyl halides with arylboronic acids.

loratadine-derived arylboronic acid with trifluoromethylated secondary alkyl iodide partner, or for cetirizine and inomelactin containing aliphatic electrophiles- all responded in this method (Figure 3.1).

3.3 Ni-Chelates as Precatalysts

Activation of C—H bonds represents a fascinating and promising strategy for the syntheses of valued products. Compared with the well-studied C(sp^2)–H activation, C(sp^3)–H activation began only recently because of inert nature of most alkanes and the poor selectivity [19]. A $Ni(acac)_2$-catalyzed aminocarbonylation by activating unreactive alkanes and formanilides under CO atmosphere has been demonstrated to achieve moderate-to-excellent yields of amides (Scheme 3.6) [20]. Notably, formanilides served as an efficient amine source, owing to the unusual deformylation of imide intermediates. Several formanilides were examined with cyclohexane to afford corresponding amides in good yields (81–90%). *N*-Pyridylformamide was also found to be reactive with a 38% yield of the product.

The proposed reaction mechanism follows a radical pathway initiated by homolytic cleavage of peroxide (di-*tert*-butylperoxide [DTBP]) with the aid of

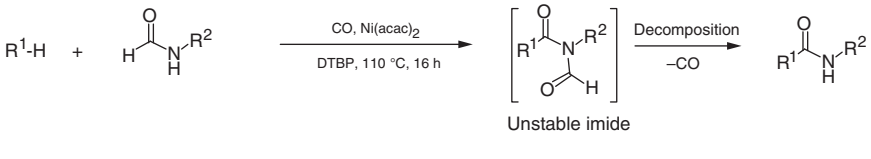

Scheme 3.6 Amide synthesis (acac, acetylacetonate; DTBP, di-*tert*-butylperoxide). Source: Modified from Han et al. [20].

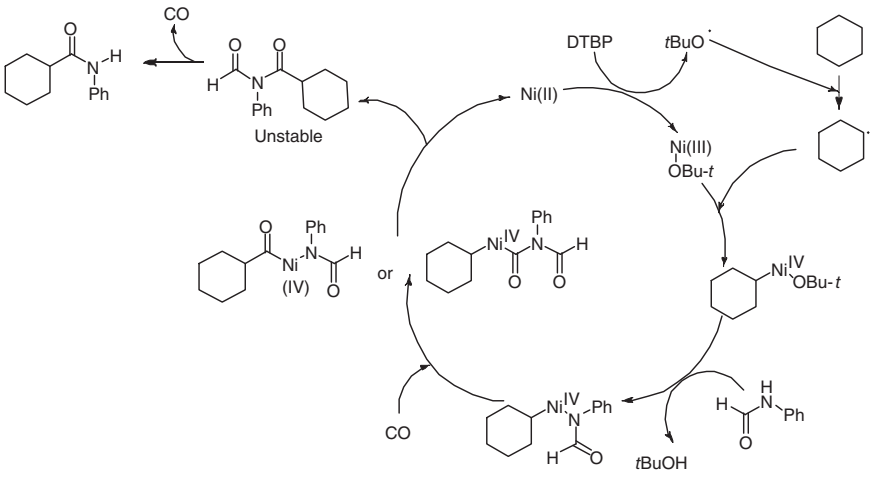

Scheme 3.7 Mechanism of amide synthesis.

Ni(II) catalyst to provide the ^{t}BuO radical and a Ni(III) species (Scheme 3.7). This radical subsequently abstracts hydrogen from cyclohexane(alkane) to give the cyclohexyl radical and *tert*-butanol. The newly formed cyclohexyl radical can undergo oxidative addition to Ni(III) species to produce a nickel(IV) species. The reaction between formanilide and Ni(IV) species with elimination of *tert*-butanol gives an amido-Ni(IV) intermediate by an H-transfer process. The CO insertion may result in the formation of two isomeric Ni(IV) species, which then undergo reductive elimination to yield an unstable intermediate with regeneration of the Ni(II) catalyst. Eventually, decarbonylation of that unstable species produces the desired amide. This reaction protocol ensures straight functionalization of alkanes to furnish amides in high yields with the use of an inexpensive nickel-based catalyst.

Compared with palladium catalysts, nickel catalysts are known to decrease the reactivity in carbonylation reactions [21], which may allow C–H functionalization together with carbonylation. Isoindolinones constitute the core unit of several natural products and other pharmaceutics [22]. In this context, a tandem nickel-catalyzed carbonylation has been reported by Arndtsen and coworkers in which *N*-acyl iminium chloride salts were formed under atmospheric CO using Ni(1,5-cyclooctadiene)$_2$ as catalyst. A further cyclization have resulted desired isoindolinones (Scheme 3.8) [23].

As observed by Watson and coworkers, the nickel catalyst can play the role of a Lewis acid and may facilitate C—H bond functionalization [24]. From the proposed

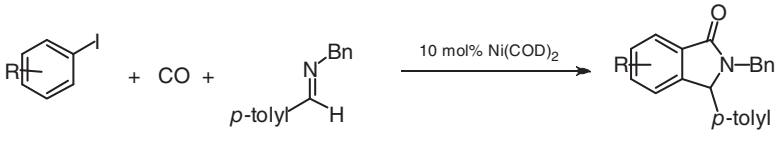

Scheme 3.8 Schematic representation of synthesis of isoindolinones. Source: Modified from Tjutrins et al. [23].

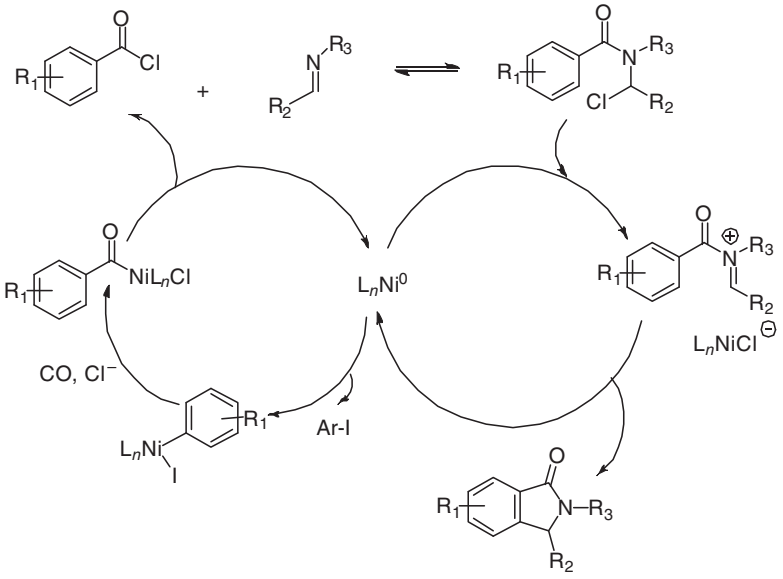

Scheme 3.9 The role of nickel catalyst as a Lewis acid and for C–H bond functionalization.

mechanism, it is evidenced that the nickel catalyst behaved as the Lewis acid and promoted cyclization (Scheme 3.9). Apart from *N*-acyl iminium chloride, more electrophilic iodide or triflate salts also responded in similar way. Both electron-deficient (50–80%) and electron-rich (74%) *p*-substituted aryl iodides delivered products in good yields, whereas symmetrically dimethyl-substituted aryl iodides gave 55% yield. In the case of *meta*-substitution, a mixture of isomeric products (42% + 22%) was obtained while *o*-substituted aryl iodides remained inactive.

The relevance of radical carbonylation along with limitations has also been discussed in ^{11}C-labeling chemistry [25]. However, the method was not applied in positron emission tomography (PET) tracer development before 2016. Notably, PET is a powerful clinical tool to detect diseases at early stages and to follow up the progress of treatment and also helps to analyze the mechanism of action and therapeutic and toxic effects of a drug molecule in the drug development process [26]. In 2016, it was demonstrated that a $Ni(COD)_2$ catalyst may promote the carbonylative cross-coupling of alkyl iodides containing β-hydrogen by using [^{11}C]CO under atmospheric pressure in the presence of bathophenanthroline in *tert*-butanol as the solvent at 100 °C [27]. The reaction led to a trapping efficiency (TE) and radiochemical yield (RCY) of 89% and 72%, respectively (Scheme 3.10).

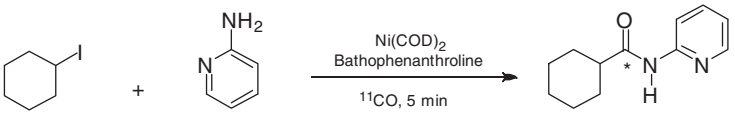

Scheme 3.10 Carbonylative cross-coupling in the presence of $Ni(COD)_2$ catalyst and bathophenanthroline ligand and bathophenanthroline ligand.

The protocol was found to be also useful for the syntheses of five ([^{11}C] carbonyl) amides with appreciable TE and RCY of 70–90% and 33–57%, respectively. The precatalyst $Ni(COD)_2$ together with the supporting ligand bathophenanthroline forms the best reagent pair to achieve the highest RCY of the product.

The enantioselective synthesis of γ-lactam motifs is obtained by transition-metal-catalyzed reactions either by an enantioselective C–H functionalization [28] or the addition of nucleophilic α-carbon atoms to η^1-allene or η^3-π-allyl ligands [29]. In 2017, Ogoshi and coworkers adapted catalytic carbonylation as an atom-economical pathway for the synthesis of polycyclic γ-lactams from ene-imine systems [30]. This reaction involves an efficient regeneration of the catalytically active nickel(0) species from nickel carbonyl complex $[Ni(CO)_3L]$ in the presence of gaseous CO. The $Ni(COD)_2/PCy_3$-catalyzed carbonylative cycloaddition of the 1,5-ene-imines produced various tricyclic γ-lactams with excellent yields (83–99%) under the optimized reaction conditions (Scheme 3.11).

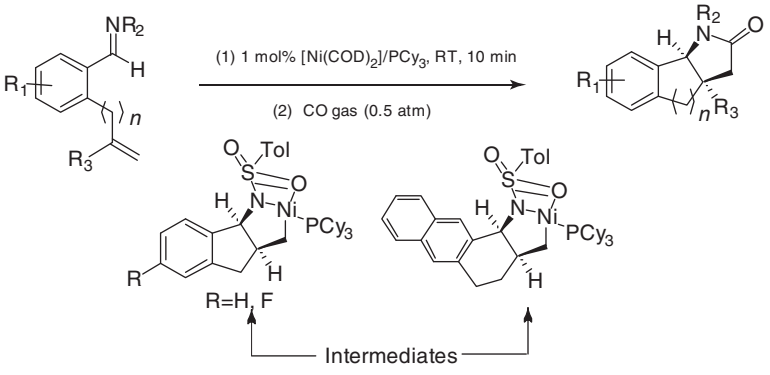

Scheme 3.11 $Ni(COD)_2/PCy_3$-catalyzed carbonylative cycloaddition of the 1,5-ene-imines.

Recently, the $Ni(COD)_2$-catalyzed asymmetric [2+2+1] carbonylative cycloaddition methodology was explored in detail to furnish enantio-enriched tricyclic γ-lactams **11** from 1,5- and 1,6-ene-imines **10** (Scheme 3.12) [31]. Furthermore, the protocol was employed to synthesize various enantiopure *N*-heterocycles, from tricyclic γ-lactams including enantiopure strigolactam GR-24. This asymmetric [2+2+1] carbonylative cycloaddition of 1,5- and 1,6-ene-imines in the presence of

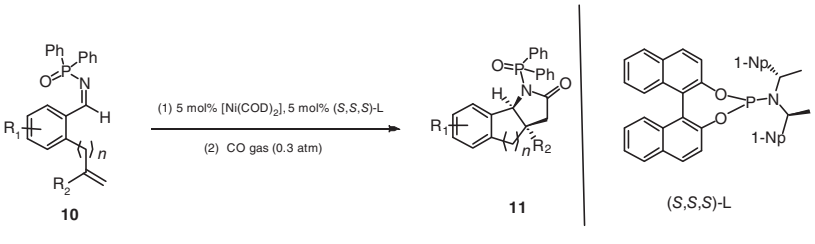

Scheme 3.12 [2+2+1] Carbonylative asymmetric cycloaddition. Source: Modified from Ashida et al. [31].

nickel(0)/(*S*,*S*,*S*)-L-catalyst resulted exclusively in single diastereomers from 12 substrates out of 16 substrates studied.

Introducing electron-donating group (4-MeO) in the *N*-diphenylphosphinoyl group resulted in 44% yield and 89% ee, while the 4-CF_3-C_6H_4 groups displayed decrease of the enantioselectivity (88% yield, 68% ee). From the above results, it can be established that the coordination abilities of the N-substituents make a substantial contribution toward the stabilization of the hetero-nickelacycle intermediates. In the course of the reaction, it can be explained that the coordination of ene-imine **10** to Ni(0)/(*S*,*S*,*S*)-L results in a (η^2:η^2 − 1)Ni(L) complex, which remains in equilibrium with nickel carbonyl species such as $Ni(CO)_2(L)_2$ (**12**) and $Ni(CO)_3(L)$ (**13**) in the presence of CO. The oxidative cyclization then produces a hetero-nickelacycle **14** in a diastereoselective manner. The CO insertion of this hetero-nickelacycle followed by reductive elimination should overcome isomerization (to transform into another nickelacycle) to afford the product **11** in an enantioselective manner (Scheme 3.13).

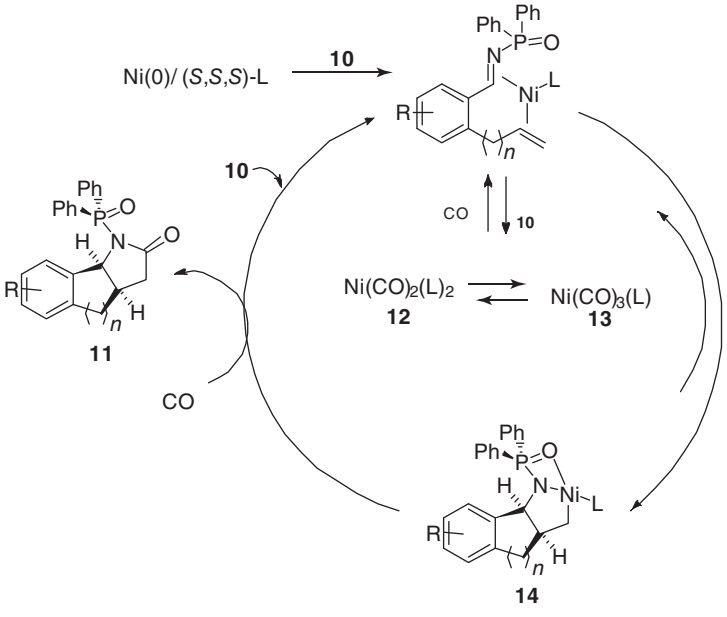

Scheme 3.13 Mechanism of [2+2+1] carbonylative cycloaddition.

3.4 Nanoparticles as Active Catalysts

As discussed earlier, nickel and palladium both reside in the same group in the periodic table and can attain oxidation numbers of 0 and +2. Moreover, nickel is earth abundant, less toxic, and cost effective compared with palladium. These properties make nickel a potential candidate for transition-metal-catalyzed cross-coupling reactions including the carbonylative Suzuki reaction. In 2014, the

first nickel-catalyzed carbonylative Suzuki reaction of arylboronic acids with aryl iodides was reported under atmospheric pressure of carbon monoxide and in a green solvent, poly(ethyleneglycol), which is attractive for industrial applications [32]. In addition to that, this protocol is devoid of any ligand, shows good selectivity, and involves easy *in situ* generation of nickel nanoparticle as active catalyst. Both the electron-poor and -rich aryl iodides could be successfully used in this carbonylative coupling with 70–91% yields (Scheme 3.14).

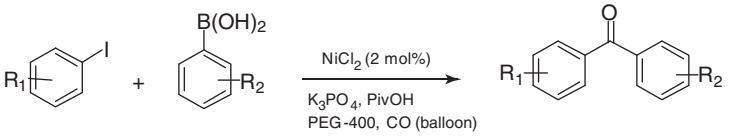

Scheme 3.14 Suzuki carbonylation by *in situ* generated nanocatalyst.

Furthermore, double carbonylation of 1,4-diiodobenzene resulted in a 60% yield of the desired product that serves as an important synthetic precursor. Control experiments confirmed that novel *in situ* generated nickel nanoparticles possessed a higher activity than the conventionally synthesized nickel nanoparticles as this process omits probability of aggregation. Furthermore, this catalytic system could be recycled up to five times.

The chemistry of acetylene is incomplete without Reppe carbonylation [5]. Though several modern reactions have flourished for the synthesis of acrylic acid, the contribution of Reppe carbonylation can never be forgotten. Several homogeneous nickel catalysts were explored as effective carbonylation reaction in literature [33]. NiO/Bi_2O_3 composite oxide (synthesized by precipitation/calcination route), a new reusable heterogeneous catalyst, was reported for Reppe carbonylation to produce acrylic acid (Scheme 3.15) [34]. Here, the addition of Bi_2O_3 to the catalyst has influenced the physical and chemical properties of NiO and also enhanced stability of smaller nanoparticles. The larger specific surface area of this oxide composite also contributed to catalytic activity of this composite. The 11.1 wt% of Bi_2O_3 in the catalyst was found to be optimum and exhibited higher activity compared with pure phase.

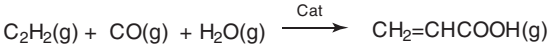

Scheme 3.15 Catalytic carbonylation of acetylene. Source: Modified from Lin et al. [34].

Another example of Reppe carbonylation was explored in the presence of supported NiO nanoparticle [35]. From a series of nickel-loaded catalysts, 2D-layered clay mineral vermiculite (2D-VT) (natural VT [composition: 38.76% SiO_2, 24.05% MgO, 20.04% Al_2O_3, 6.22% K_2O, 4.93% Fe_2O_3, 3.03% CaO, 2.02% Na_2O, and 0.94% TiO_2] is treated with H_2O_2) serves as a good carrier among others, like NaY (SiO_2/Al_2O_3 = 5.4), HY (SiO_2/Al_2O_3 = 5.2), MCM-41, and talcum powder (TP). The calcined nickel-supported expanded NiO/2D-VT showed appreciable catalytic performance and resulted in the highest yield (83.1%). During the reaction, the 2D-layered structure of vermiculite (VT) could supply hydroxyl groups present in

middle layer to active metal oxide, NiO, to form hydrogen carboxyl group, and the thermal stability of VT limited the formation of carbon deposits in the NiO/2D-VT catalyst. The NiO/2D-VT catalyst presented less carbon deposits and remained active for more cycles (up to 6 cycles) compared with others. The loss of NiO on the VT layers caused decrease in reactivity in the cycles. The carbonylation reaction of acetylene usually held as batch reaction at a high-temperature and high-pressure reactor (500 ml) made of 316 stainless steel equipped with stirring and sampling devices and safety measures.

It was later found that the microwave (MW) radiation calcined catalyst (MW-NiO/2D-VT) displayed a better catalytic performance than the muffle furnace (MF) calcination catalyst (MF-NiO/2D-VT) on account of the faster rate of heating, short baking time, stability, and the immediate formation of nano-NiO particles with uniform dispersion and better dispersibility as agglomeration is reduced [36]. Further, theoretical calculation revealed a lower apparent activation energy for the catalyst.

3.5 Dinickel Complexes as Catalysts

The dinickel complexes as catalysts have been explored for Pauson–Khand reaction using $M_x(CO)_y$ (M = Fe, Mn, Cr, Mo; *x* and y variables) reagents as an alternative CO sources [37]. During the investigation it was observed that various $M_x(CO)_y$ species formed adducts with the dinickel catalyst [NDI]Ni_2 (NDI = naphthyridine diimine) but could not generate CO equivalents nor avoided undesired leaching of Ni from the chelating ligand. These observations have influenced further to investigate the efficacy of isolable $Ni_2M(CO)_x$ complexes for this [2+2+1] carbonylation reaction. Interestingly, the Ni_2Fe species **15**, which is formed in the presence of $Fe(CO)_5$, participated, with five available CO equivalents, in carbonylation of enyne (5.0 equiv) at 80 °C. The Pauson–Khand reaction product **16** was obtained in 70% yield. Similarly, the reaction with norbornadiene (5.0 equiv) afforded the corresponding carbonylated product **17** in a slightly lower yield of 50% (Scheme 3.16).

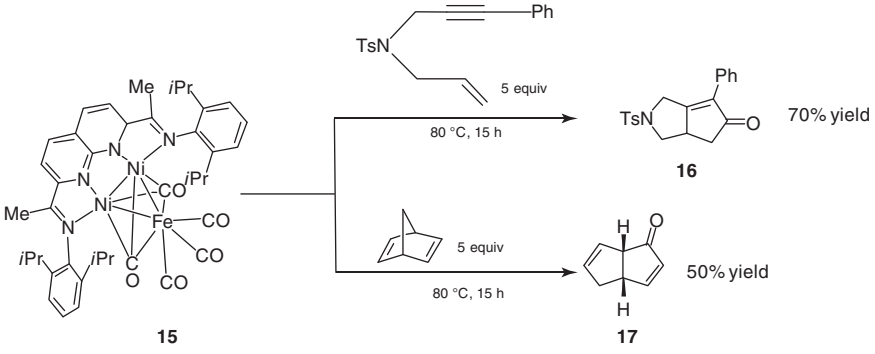

Scheme 3.16 Stoichiometric Pauson–Khand and norbornadiene carbonylation reactions using an isolable heterotrinuclear $Ni_2Fe(CO)_5$ complex.

3.6 Ni/AC as a Promising Heterogeneous Catalyst

An interesting heterogeneous catalytic system in carbonylation reactions is Ni/activated carbon (Ni/AC) that is advantageous in terms of cost and product separation. However, its application has been restricted to academia only due to low stability, aggregation, and leaching of metal and generation of plenty of side products that eventually deactivate the catalytic system. Several studies by Fujimoto et al. have established that the electron transfer between activated carbon and nickel plays a crucial role in the reaction along with the non-dissociative and multiplicative adsorption of CO on Ni/AC catalyst [38], whereas another report has showed an important redox cycle of nickel and activated carbon [38c]. Furthermore, it is well known that oxygen-containing groups influence the electronic property of carbon material support and hence can affect catalytic reactions. In 2014, vapor-phase ethanol carbonylation was reported in the presence of Ni/C catalyst using several active carbon carriers [39]. Active carriers such as wood charcoal, shell charcoal, coconut shell charcoal, and bamboo charcoal along with $Ni(OAc)_2$ as precursor were considered for the synthesis of Ni/C catalytic systems by equivalent-volume impregnation method. Several techniques, such as N_2-adsorption, X-ray photoelectron spectroscopy, IR, and SEM, were used to investigate the structural properties of carbon carriers. The carbonylation reaction of ethanol gave propionic acid and ethyl propionate in the presence of CO and EtI (Scheme 3.17). The activity of Ni/C catalyst synthesized by wood charcoal carriers was the highest as the conversion of ethanol and yield of propionic acid were 67.62% and 65.48%, respectively, while the catalyst with bamboo charcoal resulted in lowest yield of 58.78% and 35.15% selectivities. The other two catalysts showed moderate yields and selectivities. The greater activity of that catalyst can be accounted for its structural analysis. The maximum specific surface area of wood activated carbons, plenty of micro-hole structure, availability of middle-pore structure, and much oxygen functional groups on the surface, particularly the number of surface carboxyl groups, contributed to the high activity.

Scheme 3.17 Ethanol carbonylation.

Further, the significance of oxygen-containing groups on the initial activity and stability of Ni/AC catalyst have been explored to study the methanol vapor-phase carbonylation to get methyl acetate and acetic acid as the main products, whereas methane and DME are obtained as the by-products [40]. The mechanism explained that, activated charcoal assisted the reduction of oxidized nickel in the redox cycle (Scheme 3.18). Further, the oxygen containing groups (electron-withdrawing) suppress the electron mobility of the AC, hence catalyst with high oxygen content exhibited low initial activity. A new instrument named Micro-Fluidized Bed Reactor Analyst-Particle (MFBRA-P) has been developed, which can sample out catalyst particles online during a reaction without extra turbulence to the reaction. The

$CH_3I + Ni^0 \longrightarrow CH_3–Ni^{2+}–I$ (1)

[Oxidative addition of CH_3I to the catalyst surface]

$CH_3–Ni^{2+}–I + CO \longrightarrow CH_3CO–Ni^{2+}–I$ (2)

[Insertion of CO into the methyl–metal bond]

$CH_3CO–Ni^{2+}–I + CH_3OH \longrightarrow CH_3COOCH_3 + Ni^0 + HI$

[Reductive elimination of the products]

$HI + CH_3OH \longrightarrow CH_3I + H_2O$ (3)

Scheme 3.18 Vapor-phase carbonylation of methanol. Source: Modified from Pang et al. [40].

study has shown that the deactivation of the Ni/AC catalyst can be accounted for the accumulation of oxygen-containing carbonaceous deposits. The catalyst that has electron-withdrawing groups (more oxygen-containing groups) can show lower initial activity for methanol carbonylation reaction as it suppresses the redox cycle of nickel. On the other hand, high initial content of oxygen-containing groups can quench the adsorption of oxygen-containing carbonaceous deposits during the reaction. Thus, the oxygen content was relatively stable, resulting in better catalytic stability. Furthermore, the MFBRA-P instrument helped to analyze the deactivation behavior.

3.7 Use of CO Surrogates with Nickel Catalysts

As discussed earlier, the use of CO surrogates can avoid the need for handling of toxic gas and maintaining optimum CO concentration, thus favoring operationally simpler protocols. So, the use of surrogates can be important in both academia and industry.

3.7.1 Metal Carbonyls as CO Surrogates

The carbonylative syntheses of ketones using $Ni(CO)_4$ with electrophiles involve intermediate acylnickel(II) complexes, but this practice is limited due to toxicity concerns and availability [41]. It also involves generation of unreactive nickel species that hampers the catalytic cycle. In this context, role of CO surrogates in carbonylation reactions is evident. Adapting Ni-catalyzed cross-electrophile coupling (XEC) with electrochemical reduction (using Ni/Fe sacrificial anode) aryl iodides and benzyl chlorides could be coupled using $Fe(CO)_5$ as CO source. The reactivity of intermediate acylnickel(II) complexes was studied toward aryl, alkyl, and benzylic electrophiles and a cross-selective carbonylative coupling of unactivated primary alkyl bromides with aryl halides to form aryl alkyl ketones (Scheme 3.19) [42].

However, the addition of Zn flakes impacted less, and several aryl bromides were coupled with primary alkyl bromides by this process. The thermal

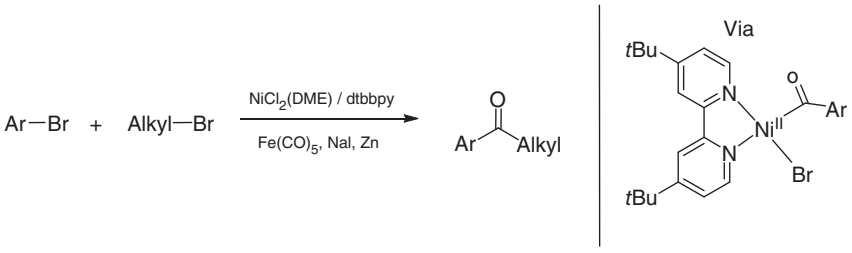

Scheme 3.19 Cross-electrophile coupling by Ni catalyst (dtbbpy, 4,4′-di-*tert*-butyl-2,2′-bipyridine). Source: Modified from Wotal et al. [42].

disproportionation of aryol nickel complexes (II) might have formed diaryl ketones, whereas the deficiency of CO in the reaction mixture triggered non-carbonylated products.

Benzophenones were synthesized by a new nickel-catalyzed carbonylative homocoupling of aryl iodides with molybdenum carbonyl as the co-catalyst and solid CO source [43]. Both electron-rich and electron-deficient iodobenzenes could be used in this protocol and provided diaryl ketones in 57–93% yields. Moreover, the synergetic effect of both nickel and molybdenum has turned out to be decisive for this transformation.

The synthesis of unsymmetrical diaryl ketones was achieved by coupling of aryl iodides with Ph_3SnCl or Ph_3SnOEt under phosphine-free condition using $Cr(CO)_6$ as an easy handling reliable solid source of carbon monoxide at atmospheric pressure in the presence of $NiBr_2$ precatalyst [44]. This carbonylative Stille coupling methodology provided various unsymmetrical ketones in good yields from both electron-rich and electron-deficient aryl iodides. However, 4-nitrophenyl iodide gave several by-products as the nitro group underwent reduction. Sterically hindered iodobenzenes were also reactive in this methodology.

The authors further extended their studies, employing cheap and easily available $NiCl_2$ catalytic system for the efficient alkoxycarbonylation, thiocarbonylation (Scheme 3.20), and amidocarbonylation reactions of various aryl iodides in the presence of $Cr(CO)_6$ as the solid source of CO at atmospheric pressure [45]. However, 1,4-diiodobenzene produced the monocarbonylated product with 90% yield even in the presence of 2 equiv of $Cr(CO)_6$ in thiocarbonylation reaction but underwent double alkoxycarbonylation and double amidocarbonylation with 78% and 83% yields, respectively. A variety of aryl iodides tolerated this mild reaction conditions with good yields. Furthermore, when alcohols were used as nucleophile, no competing O-arylation side reactions were observed. However, this protocol was not suitable for bromobenzenes, as well as aromatic amines and thiols as nucleophiles. The proposed mechanism proceeded through the formation of Ni(0) active catalyst that subsequently reacted with aryl iodides and CO to give the final products.

This solid reliable CO source, $Cr(CO)_6$, was further used for coupling of aryl boronic acids with several aromatic and aliphatic amines and also primary and

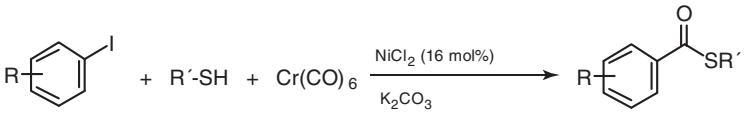

Mechanism:

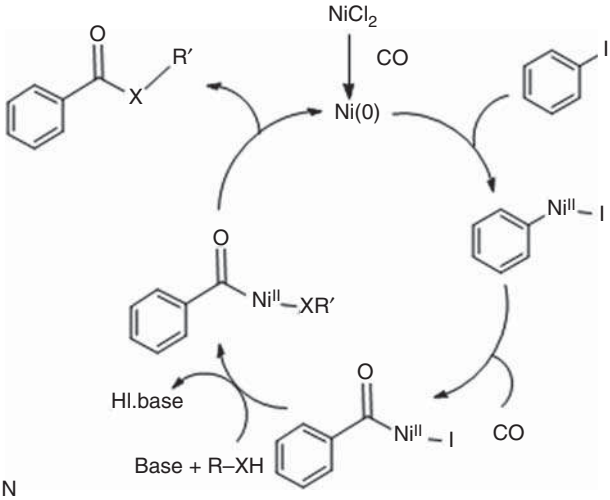

X: S, O, N
R′: aliphatic, aromatic

Scheme 3.20 Thiocarbonylation reaction and general mechanism of alkoxy, amino and thiocarbonylation.

secondary alcohols to generate amides and esters, respectively, under air without applying additional external oxidant and using $NiCl_2$(dmg)/4,4′-bipy as catalytic system (Figure 3.2) [46]. Apart from metal carbonyl, $CHCl_3$ was also used as CO source in combination of CuI/1,10-phenanthroline catalyst. However, $Cr(CO)_6$ was more efficient than $CHCl_3$. The primary alcohols responded in faster rates toward arylboronic acid derivatives in comparison with phenols and the secondary ones. Selectivity was observed for benzyl amine and aniline. Sterically hindered substrates gave the desired products with lower yields. These protocols were effectively applied in large scales that made them suitable for industrial applications.

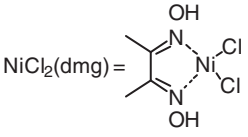

Figure 3.2 $NiCl_2$(dmg) catalyst (dmg, dimethylgloxime).

The nickel-catalyzed carbonylative homologation of aryl iodides was explored with $Mo(CO)_6$ as potential CO source and silane as the deoxygenation reagent to benzylate various indoles (Scheme 3.21) [47]. During the course of reaction, the ketone **18** is reduced by silane to give the alcohol or its silyl ether **20** (Scheme 3.22). However, another path for the formation of **20** is possible through aldehyde **19** intermediate. Subsequently, the final product **17** is obtained by hydrogenation of **20**

by silane (Scheme 3.22). Notably, molybdenum hexacarbonyl played dual role in this transformation as CO source and as catalyst for the deoxygenation process.

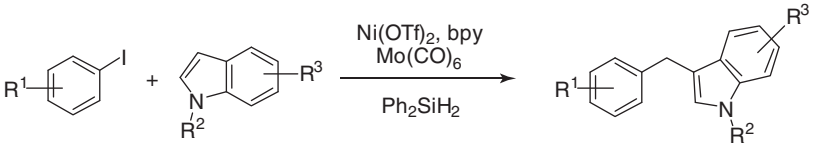

Scheme 3.21 $Ni(OTf)_2$-mediated carbonylation. Source: Peng et al. [47]. Licensed under CCBY 4.0.

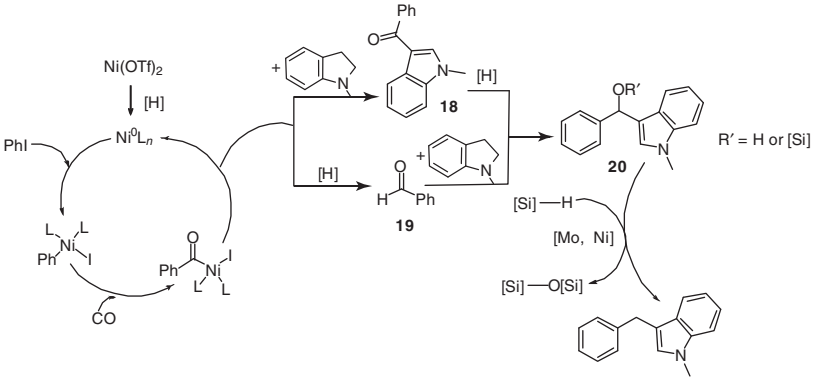

Scheme 3.22 Mechanism for the carbonylation of aryl iodides with indole derivatives.

$Mo(CO)_6$ was further utilized as the solid CO source to activate both cyclic and acyclic ethers in atom-economical way to provide functionalized alkyl iodides in moderate to excellent yields (Scheme 3.23) [48]. Under the standard protocol, both electron-deficient (42–93%) and electron-rich (49–93%) iodobenzenes provided the corresponding iodoesters. On the other hand, steric effects guided the selectivity toward *m*- and *p*-substituted products (66–88%) over the *o*-substituted ones (51%, but 70% yield obtained at 130 °C). Symmetrical cyclic ethers like tetrahydropyran and oxetane responded well with moderate yields, whereas unsymmetrical cyclic ethers produced mixtures of products. However, aryl bromides and chlorides were found unresponsive in this protocol. Mechanistically, the acyl nickel complex **21** can be coordinated by THF (ether substrate) and thus activating the oxygen and the adjacent carbon **22**. Subsequently, the cleavage of the C—O bond can give intermediate **23** that finally undergoes reductive elimination to produce **24** with regeneration of Ni(0) (Scheme 3.23).

3.7.2 Formates as CO Surrogates

Several α,β-unsaturated γ-lactams were synthesized by the $Ni(COD)_2$-catalyzed [2+2+1] carbonylative cycloaddition of imines and alkynes with phenyl formate as CO surrogate [49]. The role of phenyl formate is decisive to maintain an

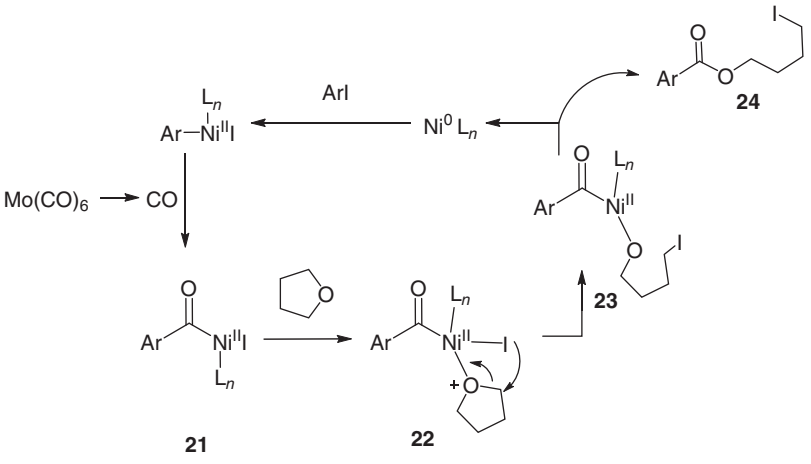

Scheme 3.23 Synthesis of alkyl iodides with cyclic ether THF. Source: Modified from Peng et al. [48].

optimum concentration of *in situ* CO to react with hetero-nickelacycle intermediate, without quenching the catalytic activity of the Ni(0) complex. Several aryl- and alkyl-substituted symmetrical alkynes produced the lactams in 46–76% (Scheme 3.24).

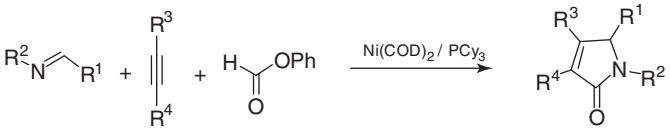

Scheme 3.24 Use of formate as CO source for carbonylation.

Ethyl chloroformate can also serve as a safe CO source for $NiBr_2$·diglyme-catalyzed reductive carbonylation coupling of several alkyl halides to synthesize a wide range of both symmetric and asymmetric dialkyl ketones in moderate-to-good yields [50]. This protocol is advantageous because of mild reaction conditions and various functional group tolerances. Further, double carbonylation can be attained with 1,6-diiodohexane (42% yield), and also the derivatization of a natural product, dihydrocholesterol, could be realized in 70% yield. The reaction proceeded through a radical pathway involving a Ni(0)/Ni(I)/Ni(II)/Ni(III) cycle (Scheme 3.25).

The same catalytic precursor ($NiBr_2$·diglyme) along with dimethylformamide (DMF) as the convenient CO source could be used for the carbonylative homocoupling of several aryl boronic acids to synthesize diaryl ketones [51]. Both electron-donating and electron-withdrawing groups were tolerated in this transformation and resulted good-to-excellent yields (52–92%). In the catalytic cycle, DMF can act as a reducing agent to reduce Ni(II) to Ni(0) that can subsequently bind to C—H bond of DMF.

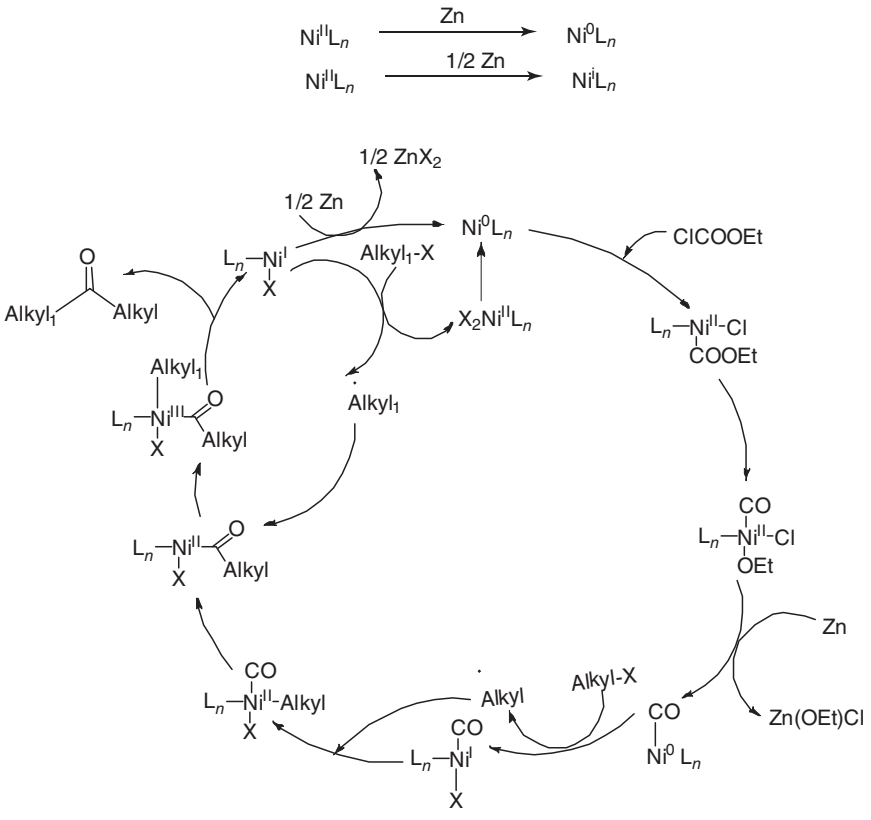

Scheme 3.25 $NiBr_2$·diglyme-catalyzed carbonylation to obtain dialkyl ketones using ethyl chloroformate as CO source.

3.7.3 Acid or Acid Chlorides as CO Surrogates

A nickel-dppb-catalyzed carbonylative Sonogashira cross-coupling reaction was employed to synthesize various α,β-alkynyl ketones taking oxalic acid (in DMF) as the *ex situ* solid CO source in a double-vial (DV) system (DV system helped to prevent excess CO exposure of the catalytic system) [52]. The Ni-dppb complex was found to be highly selective under moisture conditions and also played a prominent role in inhibiting the formation of byproducts. As shown in Scheme 3.26, the oxonium ion can attack intermediate **25** followed by intermolecular hydride shift of **26** to release an unexpected product, 1,3-diketone as enols.

Acid chlorides or anhydrides were used as acylating agents in the Ni-catalyzed ($NiCl_2$·dme) 1,2-iminoacylation of oxime ester-tethered alkenes to produce a variety of substituted pyrrolines (Scheme 3.27). This methodology avoids the use of CO gas, pre-generated organometallics, and strong basic additives [53].

The role of pincer ligands is evident in catalytic chemistry. The chelating effect of pincer ligands ensures stability and controls the addition of incoming groups. In this context, significant work by Skrydstrup and coworkers has to be mentioned [54].

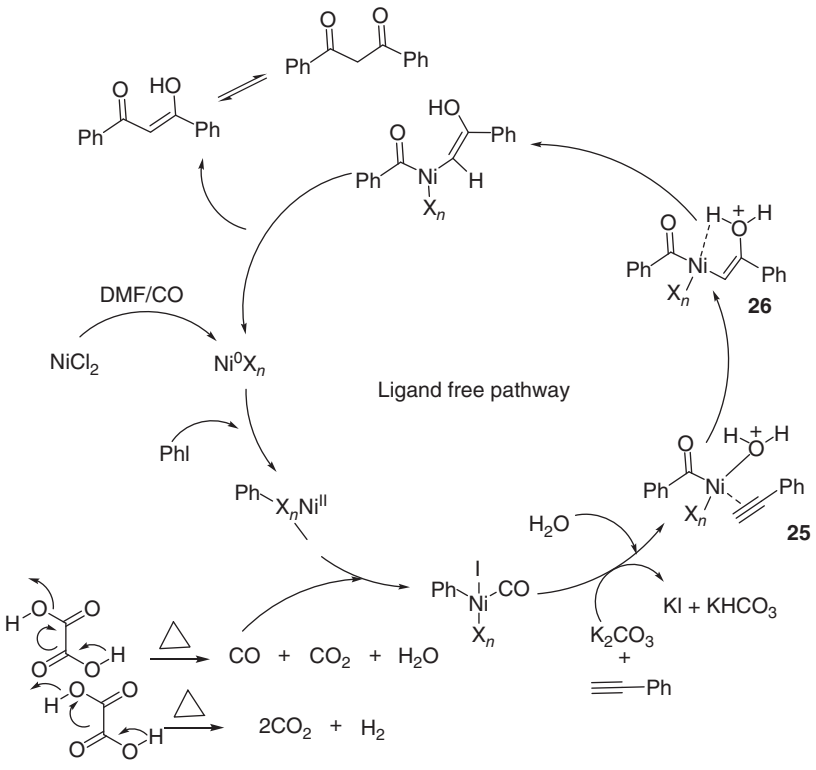

Scheme 3.26 Ligand-free pathway for carbonylative Sonogashira reaction (dppb, 1,4-bis(diphenylphosphino)butane).

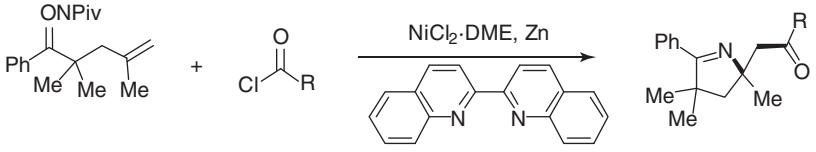

Scheme 3.27 1,2-Iminoacylation of oxime ester-tethered alkenes.

They examined a set of nickel(II) pincer complex for the successful carbonylative Negishi coupling between benzyl bromides with alkyl zinc reagents under CO atmosphere by applying their two-chamber technology. These coupling reactions provided an easy synthesis of sp^3-derived building blocks, which are more difficult in analogous palladium-catalyzed carbonylations because of the competitive β-hydride elimination from palladium alkyl complexes. The study investigated a set of nickel(II) pincer complexes (**27**–**35**) (Scheme 3.28) that were analyzed with ^1H and ^{13}C NMR spectroscopies.

Among all the Ni-NN_2 pincer complexes tested, **29** efficiently produced a stable acyl species as confirmed by NMR studies. This *in situ* generated acyl species reacted with benzyl bromide to provide benzyl alkyl ketone as the major species with 40% yield. The carbonylative coupling between BnBr and *n*Pr-ZnBr was examined by

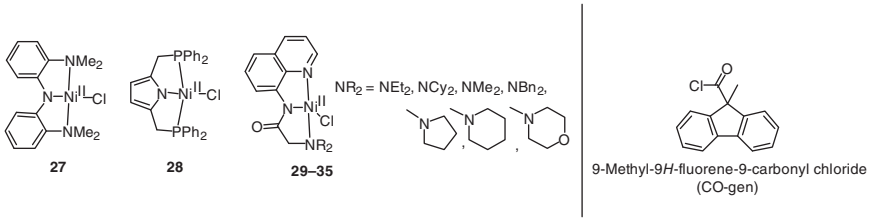

27 28 29–35

Scheme 3.28 Pincer ligands used for carbonylative Negishi coupling. CO gas was released from 9-methyl-9*H*-fluorene-9-carbonyl chloride (COgen). Source: Refs. [27–38].

engaging a two-chamber setup for controlled release of CO gas from a solid source, thus limiting the overexposure of the catalytic system. The reaction with **29** (5 mol%) and 1.5 equiv of CO at 50 °C with stirring for five hours in a solvent combination of butyronitrile and THF formed **36** with 13% yield together with byproducts **37**, **38**, and **39** (13 : 38 : 10 : 3% yields) while with THF only afforded trace amounts of the desired product (2 : 17 : 29 : 13% yields) (Scheme 3.29). To minimize the undesired reactions, a stock solution of benzyl bromide was added by a syringe to a stirred solution of **29** and *n*Pr-ZnBr over two hours, and **36** was formed in a 40% yield along with diminished yields of side products (40 : 1 : 1 : 4).

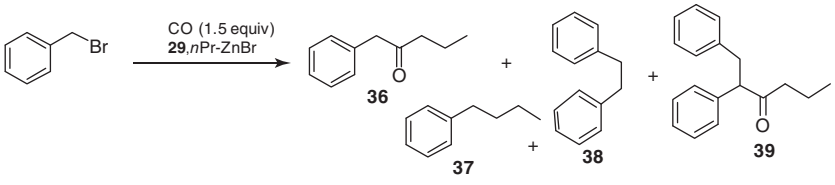

Scheme 3.29 Ni-pincer-mediated carbonylation of benzyl bromide.

The catalytic cycle is initiated by transmetalation of the starting Ni(II) complex **40** to produce a Ni(II) alkyl complex **41** (Scheme 3.30). Further CO insertion can lead to the Ni(II) acyl complex **42**. Single-electron transfer from this species to the electrophile formed the Ni(III) complex **43** and a benzylic radical. A second Ni(II) acyl species (**42**) and benzylic radical can further couple to form Ni(III) acyl alkyl complex **44**. Further, **44** can undergo reductive elimination to give the product and the Ni(I) species **45**. Comproportionation with **43** can regenerate the two Ni(II) complexes **40** and **42** that subsequently keep the catalytic cycle alive. Notably, the system is found to be sensitive to high concentrations CO as it can react with Ni(I) and Ni(III) intermediates to form some inactive off-cycle species. In contrast, if the partial pressure of CO was too low, direct alkylation was favored.

Interestingly, by the double chamber method, the nickel pincer **31** complex could be used for carbonylation of α-bromonitriles and alkyl zinc reagents in the presence of COgen (Scheme 3.31) to access β-ketonitriles in good yields that cannot be obtained by Pd-catalyzed carbonylations [55]. Furthermore, this methodology is more efficient than the conventional acylation of metalated nitrile in terms of functional group tolerance. The reaction takes place through a radical-based mechanism and a $Ni^{I}/Ni^{II}/Ni^{III}$ catalytic cycle (Scheme 3.32).

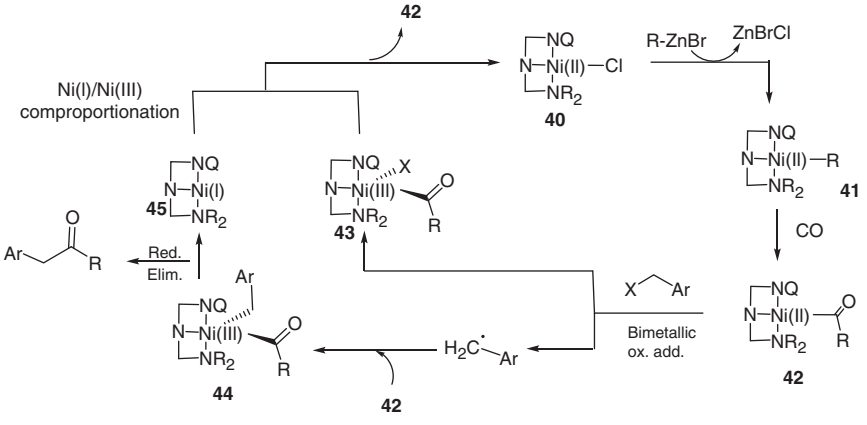

Scheme 3.30 Mechanism of carbonylative Negishi coupling.

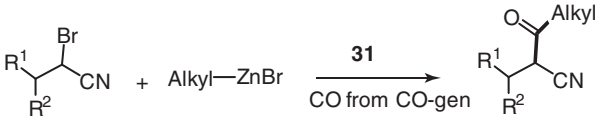

Scheme 3.31 Carbonylation of α-bromonitriles and alkyl zinc reagents in the presence of COgen.

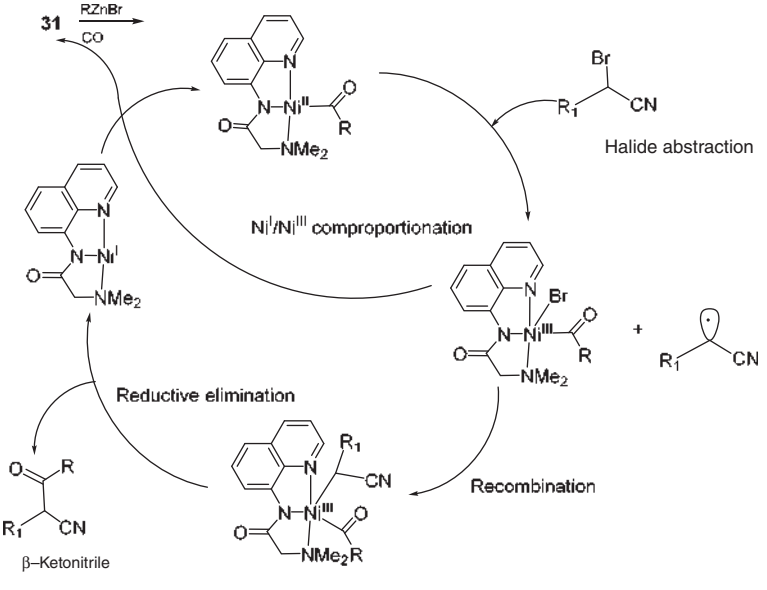

Scheme 3.32 Synthesis of β-ketonitriles.

3.8 Other Prominent Roles of Nickel in Carbonylation

Apart from above-mentioned catalytic carbonylations, Ni was shown to participate along with other metals to play either co-catalyst or promoter. Furthermore, several unconventional Ni catalysts also have given good yields for carbonylations. A Ni-catalyzed carbonylation has been shown to couple allyl halides and acetylenes for cyclopentane annulation with controlled stereochemistry and high yield (Scheme 3.33) [56]. In this reaction, Fe plays important roles as reluctant for Ni(II) halide and forms polynuclear species with nickel to help in the electron transfer reaction (Scheme 3.33).

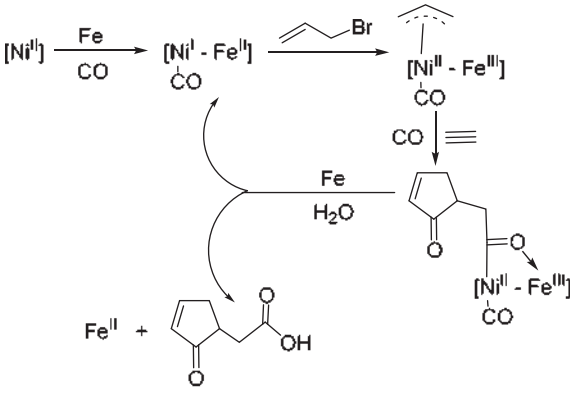

Scheme 3.33 Proposed mechanism of formation cyclopentanone derivatives. Source: Modified from Del Moral et al. [56].

Nickel was used as promoter for magnetic iron oxide catalyst to synthesize N-substituted carbamates with 90–98% isolated yields from various amines utilizing alkyl carbamates as carbonyl source (Scheme 3.34) [57]. The results indicate the presence of a delicate synergistic effect between Ni and Fe species in the catalytic cycle. Furthermore, the catalyst could be recovered based on the magnetic property of the catalyst and remained active up to five runs. However, steric hindrance and nucleophilicity influence further alcoholysis of the urea intermediate. The mechanism is suggested to consist in two possible steps: one is direct deamination of alkyl carbamate with amine, and another proceeds through the formation of a substituted urea intermediate, followed by alcoholysis to get the N-substituted carbamate.

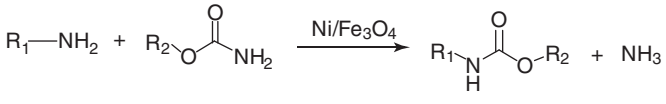

Scheme 3.34 Ni/Fe_3O_4-catalyzed indirect carbonylation. Source: Modified from Shang et al. [57].

Another interesting bimetallic catalytic system is Ni–Cu, which was used for the direct aerobic carbonylation of aromatic sp^2 and unactivated sp^3 C—H bonds of

amides [58]. This reaction is characterized by high regioselectivity and good functional group compatibility and also used DMF as CO source (Scheme 3.35). In the course of reaction, the synergistic effect of Ni and Cu was evident. The C–H activation of the amide is initiated by nickel species to prepare a nucleophile while the copper species helps DMF to procure the electrophile. A nickel complex **48** is formed from the reaction of Ni(II) species and amide **46** that can give cyclometalation via either sp^2 (reversible) or sp^3 C—H bond activation (irreversible) to provide **49**. On the other hand, an *N*-methyl-*N*-methylene-methane aminium species **50** is formed *in situ* from DMF by decarbonylation, nucleophilic addition, and elimination process under oxygen atmosphere with the assistance of copper. Further, a sequence of nucleophilic addition, oxidation, intramolecular nucleophilic addition, and hydrolysis provided the final product **47**.

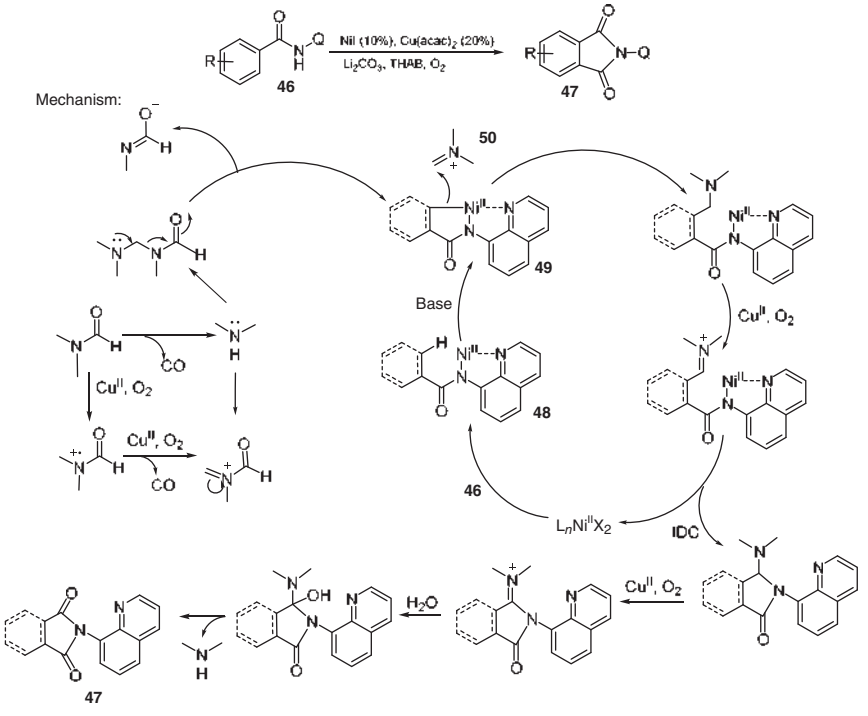

IDC: intramolecular dehydrogenative cyclization

Scheme 3.35 Indirect carbonylative cycloaddition of unactivated amides (here, THAB, tetraheptylammonium bromide; Q, 8-quinolinyl).

$Ni(NO_3)_2 \cdot 6H_2O$ has been established as an efficient catalyst under a nitrogen atmosphere and microwave irradiation for the transformation of arylboronic acids to α,β-unsaturated carbonyl compounds [59]. This ligand-free method provided 1,4-adducts from several chalcones and cinnamates in moderate-to-excellent yields within 5–30 minutes (Scheme 3.36). The catalytic cycle is initiated by the formation

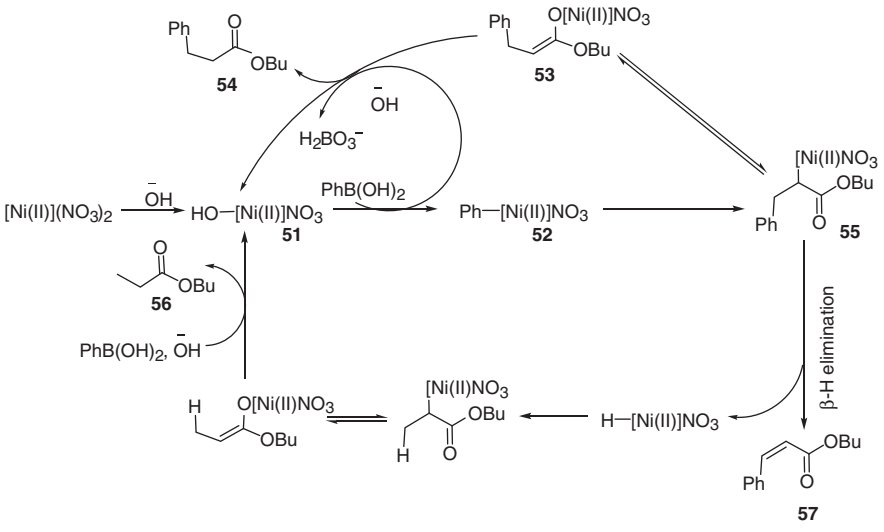

Scheme 3.36 Microwave-assisted indirect carbonylation of arylboronic acids to α,β-unsaturated carbonyl compounds.

of HO-[Ni(II)]NO_3 species **51** that is generated by the attack of a strong base on coordinated nitrate of Ni$(NO_3)_2$. Transmetalation of **51** and phenylboronic acid provides intermediate **52**. After the reaction with acrylate, subsequent rearrangement formed the O-bound nickel enolate **53**. The 1,4-addition product **54** is obtained from **53** with the help of phenylboronic acid and KOH, and the catalyst species is regenerated. Further, β-H elimination of intermediate **55** can assist the formation of ketone **56** and Heck-type product **57** (Scheme 3.36).

A novel green synthetic approach for carbonylative Suzuki reaction has been reported by utilizing Pd nanoparticle supported on a Ni(II) pyrazolate metal–organic framework (MOF) as highly efficient and reusable heterogeneous catalyst at 10 bar of CO (Scheme 3.37). The impregnation of the [Ni(H_2BDP-$SO_3)_2$] system with a methanolic solution of [$PdCl_2(CH_3CN)_2$] at room temperature assisted the formation of Pd@[Ni(H_2BDP-$SO_3)_2$] containing both Pd^{2+} ions and Pd NPs embedded in the MOF material [60].

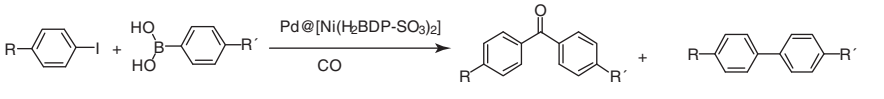

Scheme 3.37 Carbonylative Suzuki reaction. Diaryl is obtained only at 5 bar and using CO balloon (Ni-MOF, [Ni(2,5-di(1*H*-pyrazol-4-yl)benzenesulfonate)$_2$]).

Besides MOFs, three Ni zeolites, Ni-ZSM-5 (SiO_2/Al_2O_3 = 50), Ni-IM-5 (SiO_2/Al_2O_3 = 48), and Ni-MCM-41 [61], have been explored as highly efficient heterogeneous catalysts for the carbonylation of acetylene with carbon monoxide and water to provide acrylic acid [62]. The interplay of acid sites and

nickel sites determined the catalytic activity (as represented by TOF_{cat}). Among them, the mesoporous material Ni-MCM-41 showed the highest TOF_{cat} (of 70.60 g acrylic acid per g cat. per h), and Ni-IM-5 the greatest TOF_{Ni} (5108 g acrylic acid per g Ni per h). Characterizations by various techniques revealed that nickel existed as Ni^{2+}, and topology or pore architecture did not influence the catalytic activity. Furthermore, stability and reusability (four times for Ni-MC-M41 and two times for others) were additional advantages.

In 2018, exploration of zwitterionic Ni^{II}-acyl complexes as carbonylative catalysts has paved the way to novel catalyst synthesis for carbonylative polymerization (COPs) of cyclic ethers (Scheme 3.38) [63]. The cationic charge at the Ni^{II} center ensured the electrophilicity to the Ni–acyl bond for the reaction with cyclic ethers to generate an acyl-cyclic ether oxonium intermediate, whereas the ligand-centered anionic charge helped in the ion pairing of the Ni(0) nucleophile and oxonium cation. Comparatively more nucleophilic THF initiates the reaction by interacting with acyl group that eventually undergoes exchange with EO to generate a reactive species for ring-opening reaction with free THF (Scheme 3.38). Moreover, the propagating chain end of the tertiary oxonium can undergo several THF and EO enchainments (**58** → **59**) until and unless nucleophilic addition of the Ni(0) counteranion to the THF oxonium regenerated a Ni—C σ bond (**59** → **60**). The zwitterionic Ni–acyl species is reformed by CO coordination.

Terminal alkynes and substituted aryl and heteroaryl iodides could be used as substrates for palladium/phosphine ligand-free carbonylative Sonogashira reaction in the presence of $Ni(OAc)_2$ as catalyst (Ni(0) as active catalyst) to obtain various aryl α,β-alkynyl ketones and flavones in good-to-excellent yields (65–88% and 42–85%, respectively) (Scheme 3.39) [64].The mechanism of this phosphine free carbonylative Sonogashira reaction was initiated by formation of Ni(0) from $Ni(OAc)_2$ by CO.

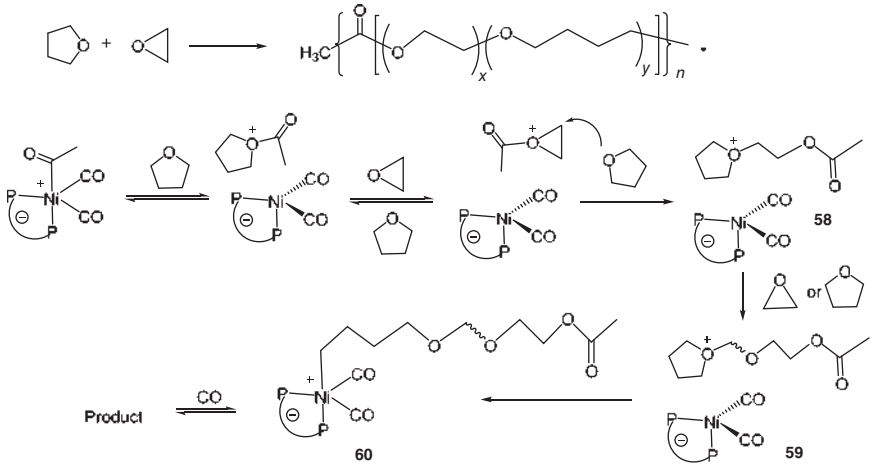

Scheme 3.38 Carbonylative polymerization of THF and EO. Here, THF also act as co-catalyst. Source: Modified from Dai et al. [63].

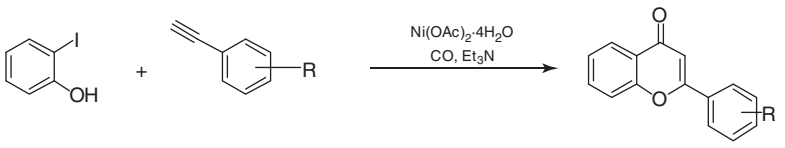

Mechanism:

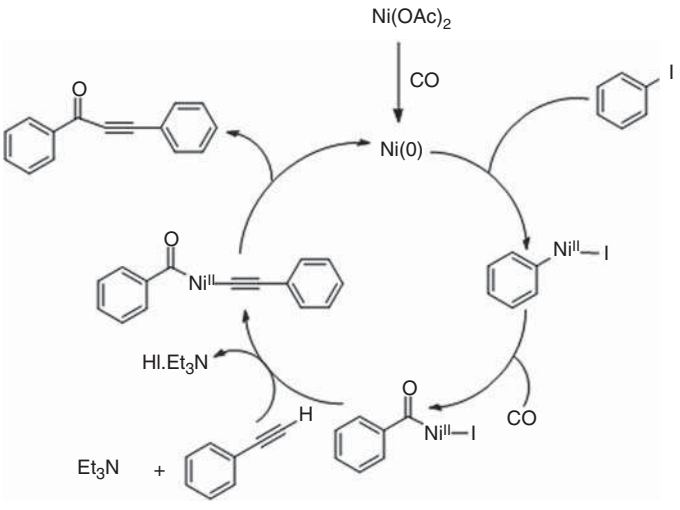

Scheme 3.39 Synthetic scope of flavones using the carbonylative Sonogashira reaction. Source: Modified from Charugandla et al. [64].

The oxidative addition of aryl iodide, followed by CO insertion and finally anion exchange with acytelene nucleophile generated ynone compound.

3.9 Conclusion and Future Outlook

In this chapter, we have discussed about modern Ni-metal-mediated carbonylations that facilitate mild reaction conditions and tolerance of functional groups. The most important problem related to transition-metal-catalyzed organic catalysis is the high cost and recyclability of the catalyst. Thus, design and syntheses of new, cheap, and reusable catalytic systems are a dynamic part of research in catalytic chemistry both in academia and industry. The cost of nickel in its elemental form is roughly 2000 times lower than palladium and 10 000 times lower than platinum on a mole-for-mole basis [3]. Furthermore, in contrast to the other popular catalysts, such as Pd, which is governed by Pd(0)/Pd(II) cycle and mostly non-radical pathways, the easy accessibility of Ni(I) and Ni(III) oxidation states apart from common Ni(0) and Ni(II) favors variety of reaction pathways. Those transformations can be based on Ni(0)/Ni(II), Ni(I)/Ni(III), Ni(0)/Ni(II)/Ni(I), etc. Ni belongs to the first row of transition metal series, so it possesses a small atomic radius that enables it to form shorter bonds with ligands. Furthermore, Ni can easily donate d-electrons to π-acceptors, and β-hydride elimination tends to be slower with nickel as confirmed

by several studies. Another concern regarding carbonylation in both industry and academia is efficient handling of the CO gas and a large-scale synthesis. Several acids, acid chlorides, and metal carbonyls can be used as CO surrogates that not only generate CO *in situ* but also help maintain optimum CO concentration. Many organic transformations mentioned above have been explored in large scales for industrial purposes. The most common Ni(0) catalyst, $Ni(COD)_2$, requires the use of glove box and drastic reaction conditions. These catalysts are further substituted with easily available nickel halides or even heterogeneous catalysts to produce products with equal efficiency. The recyclability of those catalysts is additional advantages. We hope that this chapter on Ni-catalyzed carbonylation will gain its recognition in the research of inexpensive catalyst developments and that Ni catalysis will evolve in the future for its advancement both in academia and industry.

References

1 Keim, W. (1990). *Angew. Chem. Int. Ed. Engl.* 29: 235–244.
2 Mond, L., Langer, C., and Quincke, F. (1890). *J. Chem. Soc. Trans.* 57: 749–753.
3 Tasker, S., Standley, E., and Jamison, T. (2014). *Nature* 509: 299–309.
4 Wilke, G. (1988). *Angew. Chem. Int. Ed. Engl.* 27: 185–206.
5 (a) Reppe, W., Kroper, H., Kutepow, N., and Pistor, H. (1953). *Liebigs Ann. Chem.* 582: 72–86. (b) Reppe, W., Kroper, H., Pistor, H., and Weissbarth, O. (1953). *Liebigs Ann. Chem.* 582: 87–116. (c) Reppe, W., Friederich, H., von Kutepow, N., and Morsch, W. (1956). US 2,729,651 (BASF); (d) Reppe, W., von Kutepow, N., and Bille, H. (1961). US 3,014,962 (BASF); (e) Thomas, E.B. and Alcock, E.H. (1953). US 2,650,245 (British Celanese Ltd); (f) Reppe, J.W. (1949). *Acetylene Chemistry*, 171. New York, NY: A. Meyer and Co.
6 (a) Forster, D. (1977). *Ann. N.Y. Acad. Sci.* 295: 79–82. (b) Hagemeyer, H.J. Jr., (1956). US 2,739,169 (Eastman Kodak).
7 Liu, T.C. and Chiu, S.J. (1994). *Appl. Catal.* 117: 17–27.
8 Merenov, A.S. and Abraham, M.A. (1998). *Catal. Today* 40: 397–404.
9 Merenov, A.S., Nelson, A., and Abraham, M.A. (2000). *Catal. Today* 55: 91–101.
10 Wang, H.X., Guo, W.W., and Zhu, L.J. (2013). *Appl. Mech. Mater.* 316–317: 983–986.
11 (a) Lawrence, S.A. (2004). *Amines: Synthesis, Properties and Applications*. Cambridge: Cambridge University Press. (b) Hili, R. and Yudin, A.K. (2006). *Nat. Chem. Biol.* 2: 284–287. (c) Ricci, A. (2007). *Amino Group Chemistry: From Synthesis to the Life Sciences*. Weinheim: Wiley-VCH.
12 (a) Khumtaveeporn, K. and Alper, H. (1995). *Acc. Chem. Res.* 28: 414–422. (b) Ouyang, K., Hao, W., Zhang, W.-X., and Xi, Z. (2015). *Chem. Rev.* 115: 12045–12090. (c) Huang, C.-Y. and Doyle, A.G. (2014). *Chem. Rev.* 114: 8153–8198. (d) Wang, Q., Su, Y., Li, L., and Huang, H. (2016). *Chem. Soc. Rev.* 45: 1257–1272.
13 Yu, H., Gao, B., Hu, B., and Huang, H. (2017). *Org. Lett.* 19: 3520–3523.

14 (a) Nagakura, S. (1958). *J. Am. Chem. Soc.* 80: 520–524. (b) Halpern, A.M. and Weiss, K. (1968). *J. Am. Chem. Soc.* 90: 6297–6302. (c) Pierre, J.-L., Handel, H., Labbé, P., and Le Goaller, R. (1980). *J. Am. Chem. Soc.* 102: 6574–6575. (d) Stenzel, V., Jeske, J., du Mont, W.-W., and Jones, P.G. (1995). *Inorg. Chem.* 34: 5166–5170. (e) Rouhollahi, A. and Shamsipur, M. (1999). *Anal. Chem.* 71: 1350–1353.

15 (a) Zhao, H.-Y., Feng, Z., Luo, Z., and Zhang, X. (2016). *Angew. Chem. Int. Ed.* 55: 10401–10405. (b) Andersen, T.L., Frederiksen, M.W., Domino, K., and Skrydstrup, T. (2016). *Angew. Chem. Int. Ed.* 55: 10396–10400. (c) Pattison, G. (2018). *Eur. J. Org. Chem.* 2018: 3520–3540. (d) Yin, H., Kumke, J.J., Domino, K., and Skrydstrup, T. (2018). *ACS Catal.* 8: 3853–3858.

16 Zhao, H.-Y., Gao, X., Zhang, S., and Zhang, X. (2019). *Org. Lett.* 21: 1031–1036.

17 Cheng, R., Zhao, H.-Y., Zhang, S., and Zhang, X. (2020). *ACS Catal.* 10: 36–42.

18 (a) Wu, X.-F., Neumann, H., and Beller, M. (2013). *Chem. Rev.* 113: 1–35. (b) Sheffy, F.K. and Stille, J.K. (1983). *J. Am. Chem. Soc.* 105: 7173–7175. (c) Grigg, R. and Mutton, S.P. (2010). *Tetrahedron* 66: 5515–5548. (d) Nagahara, K., Ryu, I., Komatsu, M., and Sonoda, N. (1997). *J. Am. Chem. Soc.* 119: 5465–5466. (e) Bissember, A.C., Levina, A., and Fu, G.C. (2012). *J. Am. Chem. Soc.* 134: 14232–14237.

19 (a) Jazzar, R., Hitce, J., Renaudat, A. et al. (2010). *Chem. Eur. J.* 16 (9): 2654–2672. (b) Li, H., Li, B.-J., and Shi, Z.-J. (2011). *Catal. Sci. Technol.* 1 (2): 191–206. (c) He, J., Wasa, M., Chan, K.S.L. et al. (2017). *Chem. Rev.* 117 (13): 8754–8786.

20 Han, Z., Chaowei, D., Lice, L. et al. (2018). *Tetrahedron* 74: 3712–3718.

21 (a) Tamaru, Y. (2005). Carbonylation and decarbonylation. In: *Modern Organonickel Chemistry*, 224–239. Weinheim, Germany: Wiley-VCH. (b) Kubiak, C.P. (1995). Nickel, palladium, and platinum. In: *Comprehensive Organometallic Chemistry II* (eds. G. Wilkinson, E.W. Abel and G.A. Stone), 1–27. Oxford, UK: Elsevier.

22 For examples, see:(a)Riedinger, C., Endicott, J.A., Kemp, S.J. et al. (2008). *J. Am. Chem. Soc.* 130: 16038–16044. (b) Luzzio, F.A., Mayorov, A.V., Ng, S.S.W. et al. (2003). *J. Med. Chem.* 46: 3793–3799. (c) Zhang, L., Chen, X., Liu, J. et al. (2012). *Eur. J. Med. Chem.* 58: 624–639. (d) Guillaumel, J., Léonce, S., Pierré, A. et al. (2006). *Eur. J. Med. Chem.* 41: 379–386. (e) Hardcastle, I.R., Valeur, E., Watson, A. et al. (2011). *Med. Chem.* 54: 1233–1243.

23 Tjutrins, J., Shao, J.L., Yempally, V. et al. (2015). *Organometallics* 34: 1802–1805.

24 Shacklady-McAtee, D.M., Dasgupta, S., and Watson, M.P. (2011). *Org. Lett.* 13: 3490–3493.

25 (a) Itsenko, O. and Långström, B. (2005). *J. Org. Chem.* 70: 2244–2249. (b) Itsenko, O., Kihlberg, T., and Långström, B. (2006). *Nat. Protoc.* 1: 798–802. (c) Itsenko, O., Kihlberg, T., and Långström, B. (2004). *J. Org. Chem.* 69: 4356–4360.

26 (a) Talbot, P.S. and Laruelle, M. (2002). *Eur. Neuropsychopharmacol.* 12: 503–511. (b) Cherry, S.R. (2001). *J. Clin. Pharmacol.* 41: 482–491. (c) Fowler, J.S., Volkow, N.D., Wang, G.-J. et al. (1999). *J. Nucl. Med.* 40: 1154–1163.

27 Rahman, O., Långström, B., and Halldin, C. (2016). *ChemistrySelect* 1: 2498–2501.

28 (a) Park, Y. and Chang, S. (2019). *Nat. Catal.* 2: 219–227. (b) Xing, Q., Chan, C.-M., Yeung, Y.-W., and Yu, W.-Y. (2019). *J. Am. Chem. Soc.* 141: 3849–3853. (c) Gois, P.M.P., Candeias, N.R., and Afonso, C.A.M. (2005). *J. Mol. Catal. A: Chem.* 227: 17–24. (d) Pedroni, J. and Cramer, N. (2015). *Angew. Chem. Int. Ed.* 54: 11826–11829.

29 (a) González, A.Z., Benitez, D., Tkatchouk, E. et al. (2011). *J. Am. Chem. Soc.* 133: 5500–5507. (b) Bantreil, X., Prestat, G., Madec, D. et al. (2009). *Synlett* 2009: 1441–1444. (c) Bantreil, X., Prestat, G., Moreno, A. et al. (2011). *Chem. Eur. J.* 17: 2885–2896.

30 Hoshimoto, Y., Ashida, K., Sasaoka, Y. et al. (2017). *Angew. Chem. Int. Ed.* 56: 8206–8210.

31 Ashida, K., Hoshimoto, Y., Tohnai, N. et al. (2020). *J. Am. Chem. Soc.* 142: 1594–1602.

32 Zhong, Y., Gong, X., Zhu, X. et al. (2014). *RSC Adv.* 4: 63216–63220.

33 (a) Szmant, H.H. (1989). *Organic Building Blocks of the Chemical Industry*. New York: Wiley, Chapter 4. (b) Kiss, G. (2001). *Chem. Rev.* 101 (11): 3435–3456.

34 Lin, T.J., Xie, H., Meng, X., and Shi, L. (2015). *Catal. Commun.* 68: 88–92.

35 Hu, G., Guo, D., Shang, H. et al. (2020). *Catal. Lett.* 150: 674–682.

36 Hu, G., Guo, D., Shang, H. et al. (2020). *ChemistrySelect* 5: 2940–2948.

37 Adolph, C.M., Lee, S.A., Zeller, M., and Uyeda, C. (2019). *Tetrahedron* 75: 3336–3340.

38 (a) Fujimoto, K., Shikada, T., Omata, K., and Tominaga, H. (1982). *Ind. Eng. Chem. Prod. Res. Dev.* 21: 429–432. (b) Omata, K., Fujimoto, K., Shikada, T., and Tominaga, H. (1988). *Ind. Eng. Chem. Res.* 27: 2211–2213. (c) Yagita, H. and Fujimoto, K. (1991). *J. Mol. Catal.* 69: 191–197.

39 Song, J., Wang, L., Song, G., and Wang, J. (2014). *J. Chem. Pharm. Res.* 6 (1): 628–633.

40 Pang, F., Song, F., Zhang, Q. et al. (2016). *Chem. Eng. J.* 293: 129–138.

41 (a) Chiusoli, G.P. and Cassar, L. (1967). *Angew. Chem. Int. Ed. Engl.* 6: 124–133. (b) Rhee, I., Ryang, M., Watanabe, T. et al. (1977). *Synthesis* 1977: 776–777. (c) Semmelhack, M.F. (1972). *Org. React.* 19: 115–198.

42 Wotal, A.C., Ribson, R.D., and Weix, D.J. (2014). *Organometallics* 33: 5874–5881.

43 Peng, J.-B., Wu, F.-P., Li, D. et al. (2018). *J. Org. Chem.* 83: 6788–6792.

44 Iranpoor, N., Firouzabadi, H., and Etemadi-Davan, E. (2015). *J. Organomet. Chem.* 794: 282–287.

45 Iranpoor, N., Firouzabadi, H., Etemadi-Davan, E. et al. (2015). *New J. Chem.* 39: 6445–6452.

46 Etemadi-Davan, E., Iranpoor, N., and Arshad, P. (2018). *Asian J. Org. Chem.* 7: 683–687.

47 Peng, J.-B., Wu, F.-P., Qi, X. et al. (2018). *Commun. Chem.* 1: 87–93.

48 Peng, J.-B., Wu, F.-P., Xu, C. et al. (2018). *iScience* 8: 175–182.

49 Hoshimoto, Y., Ohata, T., Sasaoka, Y. et al. (2014). *J. Am. Chem. Soc.* 136: 15877–15880.

50 Shi, R. and Hu, X. (2019). *Angew. Chem. Int. Ed.* 58: 7454–7458.

51 Li, Y., Tu, D.-H., Wang, B. et al. (2017). *Org. Chem. Front.* 4: 569–572.

52 Shaifali, Ram, S., Thakur, V., and Das, P. (2019). *Org. Biomol. Chem.* 17: 7036–7041.

53 Wang, L. and Wang, C. (2018). *Org. Chem. Front.* 5: 3476–3482.

54 Andersen, T.L., Donslund, A.S., Neumann, K.T., and Skrydstrup, T. (2018). *Angew. Chem. Int. Ed.* 57: 800–804.

55 Donslund, A.S., Neumann, K.T., Corneliussen, N.P. et al. (2019). *Chem. Eur. J.* 25: 9856–9860.

56 del Moral, D., Ricart, S., and Moretó, J.M. (2010). *Chem. Eur. J.* 16: 9193–9202.

57 Shang, J., Guo, X., Shi, F. et al. (2011). *J. Catal.* 279: 328–336.

58 Wu, X., Zhao, Y., and Ge, H. (2015). *J. Am. Chem. Soc.* 137: 4924–4927.

59 Chen, W., Sun, L., Huang, X. et al. (2015). *Adv. Synth. Catal.* 357: 1474–1482.

60 Augustyniak, A.W., Zawartka, W., Navarro, J.A.R., and Trzeciak, A.M. (2016). *Dalton Trans.* 45: 13525–13531.

61 Zhao, X.S., Lu, G.Q., and Millar, G.J. (1996). *Ind. Eng. Chem. Res.* 35: 2075–2090.

62 Xie, H., Lin, T., Shi, L., and Meng, X. (2016). *RSC Adv.* 6: 97285–97292.

63 Dai, Y., He, S., Peng, B. et al. (2018). *Angew. Chem. Int. Ed.* 57: 14111–14115.

64 Charugandla, R., Vangala, M.S., Chidara, S., and Korupolu, R.B. (2018). *Tetrahedron Lett.* 59: 3283–3287.

4

Carbonylations Catalyzed by Other First Row Transition-Metal Catalysts (Manganese, Iron, Copper)

Chong-Liang Li, Hai Wang and Xiao-Feng Wu

Leibniz-Institut für Katalyse e.V. an der Universität Rostock (LIKAT), Albert-Einstein-Straße 29a, 18059 Rostock, Germany

4.1 Introduction

Carbonylation is currently considered one of the most powerful procedures for the synthesis of carbonyl-containing organic compounds. However, concerning the catalysts applied, noble metals, such as palladium, ruthenium, and rhodium, are more intensively studied. Concerning the high costs of the noble metals, the relatively cheap first-row transition metal catalysts attract more attention. The catalysts are abundant and less environmentally toxic. In this chapter, the achievements of using manganese, iron, and copper as the catalysts in carbonylation reactions have been summarized and discussed. The contents are cataloged by the types of products produced.

4.2 Synthesis of Ketones

Transition metal-catalyzed carbonylative Stille/Suzuki reaction, which employs aryl halides and organostannanes/organoboronic acids as reactants, has long been widely used to prepare valuable aryl ketones. Through the palladium catalysis platform, Kang et al. reported that the use of hypervalent iodine compounds in place of aryl halides was successful. In 1996, they reported a copper-catalyzed carbonylative transformation of organostannanes and organoboranes with hypervalent iodonium salts under mild conditions [1]. By employing CuI as the catalyst, both organostannanes and organoboranes reacted with diaryliodonium salts under carbon monoxide atmospheric pressure. They delivered the corresponding aryl ketones with good to excellent yields (Scheme 4.1). However, only limited examples were reported, and electron-withdrawing substituted substrates were not reported.

In 2014, Han and coworkers developed a nanocopper-catalyzed carbonylative Suzuki reaction of aryl halides with organoboronic acids [2]. In the absence of ligands, this practical and recyclable transformation affords good to excellent yields

Carbon Monoxide in Organic Synthesis: Carbonylation Chemistry,
First Edition. Edited by Bartolo Gabriele.

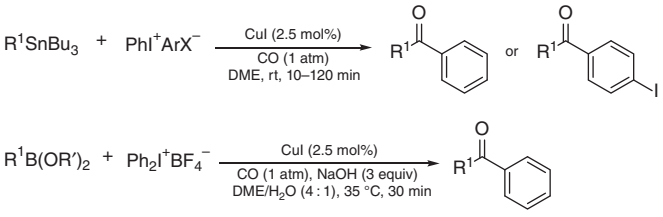

Scheme 4.1 CuI-catalyzed carbonylative cross-coupling of organostannanes and organoboranes with hypervalent iodine compounds.

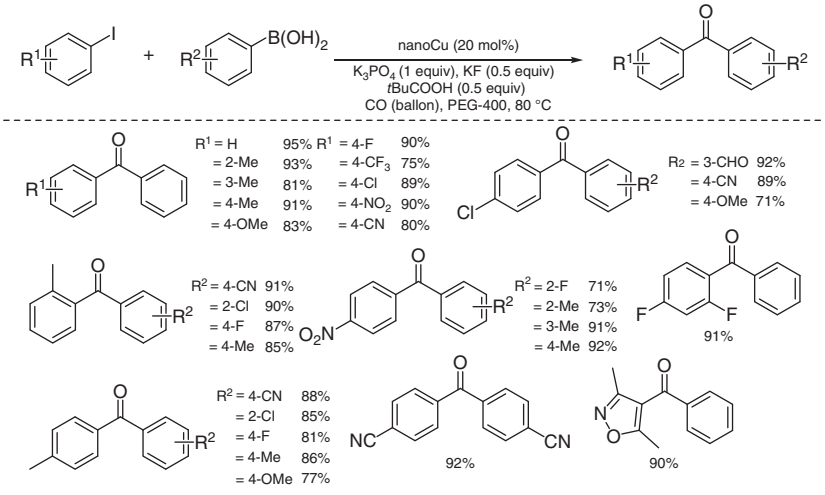

Scheme 4.2 NanoCu-catalyzed carbonylative Suzuki coupling of aryl iodides with arylboronic acids.

of the desired ketones under ambient carbon monoxide pressure in poly(ethylene glycol) at 80 °C (Scheme 4.2). It is worth noting that pivalic acid could effectively suppress the formation of the direct cross-coupling biaryl products.

Recently, Mankad and coworkers reported a copper–carbene/manganese–carbonyl bimetallic system able to catalyze the carbonylative Suzuki–Miyaura reaction of arylboronic esters and alkyl halides, providing a general platform to catalytically access a variety of ketone products (Scheme 4.3) [3]. This co-catalysts system operates under mild conditions (low carbon monoxide pressure and reaction temperature) and exhibits as a complementary tool to the existing carbonylation platform. The hypothetical mechanism for this transformation consists of a manganese catalyzed Heck–Breslow cycle for alkyl halide carbonylation and a copper-catalyzed cycle that generates catalytic quantities of an arylcopper species from a mild arylboronic ester nucleophile. The two metallic catalysis cycles finally intersect with a heterobimetallic, product-releasing C–C coupling step.

The hypothesized mechanism for this copper/manganese-catalyzed Suzuki–Miyaura-type carbonylation is depicted in Figure 4.1. As said above, it consists of a manganese catalyzed Heck–Breslow carbonylation cycle of alkyl halides and a

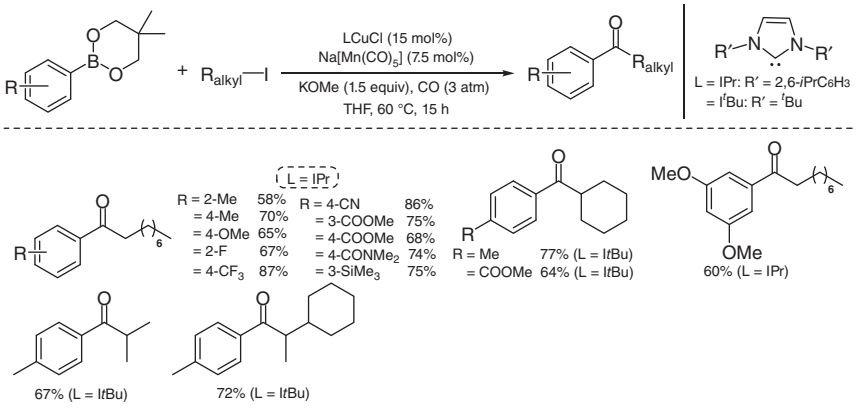

Scheme 4.3 Cu/Mn bimetallic catalysis of carbonylative Suzuki–Miyaura reaction. Source: Modified from Pye et al. [3].

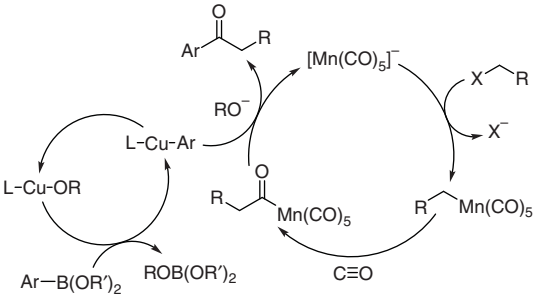

Figure 4.1 Copper/manganese bimetallic-catalyzed mechanism for the carbonylative Suzuki–Miyaura reaction.

copper-catalyzed cycle that generates catalytic quantities of an arylcopper species. The two transition-metal catalytic cycles intersect at a stage when an arylcopper nucleophile interacts with an acyl-metal electrophile.

The sluggish nature of slow oxidative addition step under carbonylative conditions and fast β-hydride elimination has limited palladium capacity to facilitate alkyl electrophile coupling protocols. To overcome this problem, Mankad and coworkers developed a copper-catalyzed radical hydrocarbonylative cross-coupling reaction of alkynes with alkyl iodides to synthesize unsymmetrical dialkyl ketones (Scheme 4.4) [4]. Using IPrCuCl (10 mol%) as the catalyst, carbonylative transformations of various alkyl terminal alkynes with alkyl iodides proceeded smoothly under low pressure of carbon monoxide (6 atm) and using polymethylhydrosiloxane (PHMS) (6.0 equiv) as the reductive reagent. The authors proposed two tandem copper-catalyzed pathways: (i) hydrocarbonylative coupling of the alkyne and the alkyl iodide and (ii) reducing the unsaturated intermediate to the saturated ketone product.

In 2008, Bhanage and coworkers first developed a $Cu(TMHD)_2$ (TMHD: 2,2,6,6-tetramethyl-3,5-heptanedionate) catalyzed, palladium-free carbonylative Sonogashira coupling reaction of alkynes with aryl iodides (Scheme 4.5) [5]. Using $Cu(TMHD)_2$ (5 mol%) as the catalyst, toluene as solvent, and Et_3N (3.0 equiv) as a

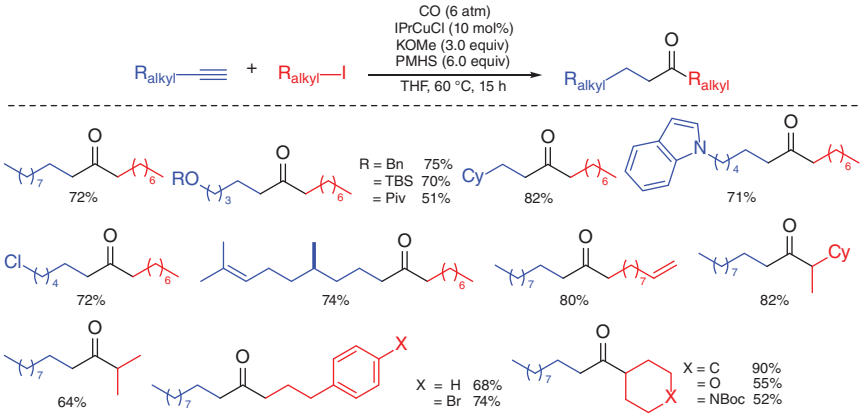

Scheme 4.4 IPrCuCl-catalyzed hydrocarbonylative C—C coupling of terminal alkynes with alkyl iodides. Source: Modified from Cheng and Mankad [4].

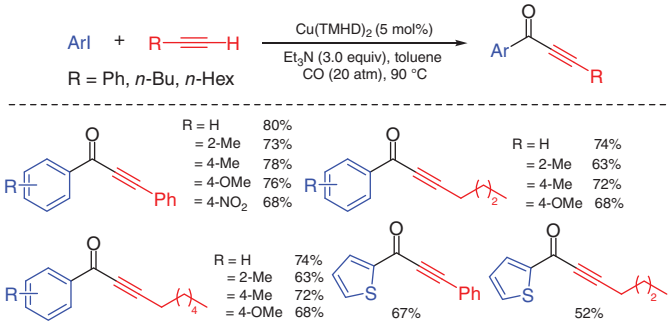

Scheme 4.5 $Cu(TMHD)_2$-catalyzed carbonylative Sonogashira coupling reaction of alkynes with aryl iodides. Source: Modified from Tambade et al. [5].

base, the carbonylative Sonogashira coupling reaction of aliphatic/aromatic alkynes with electron-donating and electron-withdrawing aryl iodides proceeded smoothly. It gave the corresponding alkynones in good yields.

In 2014, Han and coworker developed an iron-catalyzed carbonylative Suzuki reaction of aryl iodides (Scheme 4.6a) [6]. Using the combination of $FeCl_2$ (4 mol%) and $FeCl_3$ (6 mol%) as the catalyst system, carbonylative Suzuki reactions of various aryl iodides with arylboronic acids proceeded smoothly under atmospheric pressure carbon monoxide using PEG-400 as a green solvent. A range of functional groups, such as hydroxyl, chloro, bromo, and nitrile, were compatible with the reactions. Variously substituted diaryl ketones were obtained in good yields. In 2016, they reported another general iron-catalyzed carbonylative Suzuki–Miyaura reaction (Scheme 4.6b) [7]. Employing $FeCl_2$ as the precatalyst and stoichiometric $CHCl_3$ as the CO source, a broad range of synthetically useful biaryl ketones were synthesized in good to excellent yields. Both aryltrifluoroborates and arylboronic acids were found to be suitable for this reaction. The addition of strongly basic hydroxide played a critical role in the hydrolysis of $CHCl_3$ to release CO. This protocol provides an

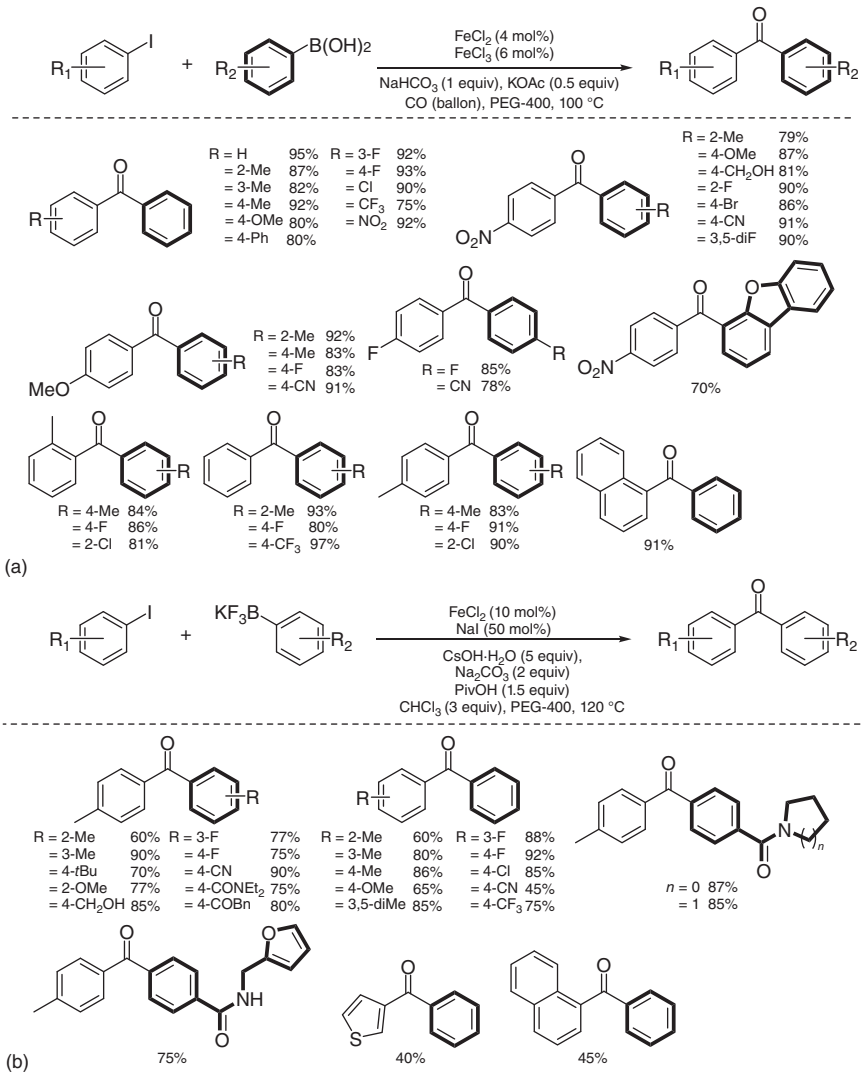

Scheme 4.6 Iron-catalyzed carbonylative Suzuki reactions. Source: Modified from Zhong et al. and Zhao et al. [6, 7].

alternative for effective ^{13}C labeling by using the commercially available ^{13}C-labeled $CHCl_3$.

In 2019, Wu and coworkers developed a carbonylative protocol to introduce an alkyl–acyl group into heteroarenes from cyclobutanone oximes, which is an efficient complement to the classic Friedel–Crafts acylation reaction. In the presence of $Fe(OTf)_2$ as the catalyst, this transformation proceeds via intermolecular alkyl-acylation of different heteroarenes. A broad range of alkyl heteroaryl ketones is synthesized with excellent functional group tolerance with good chemoselectivity (Scheme 4.7) [8].

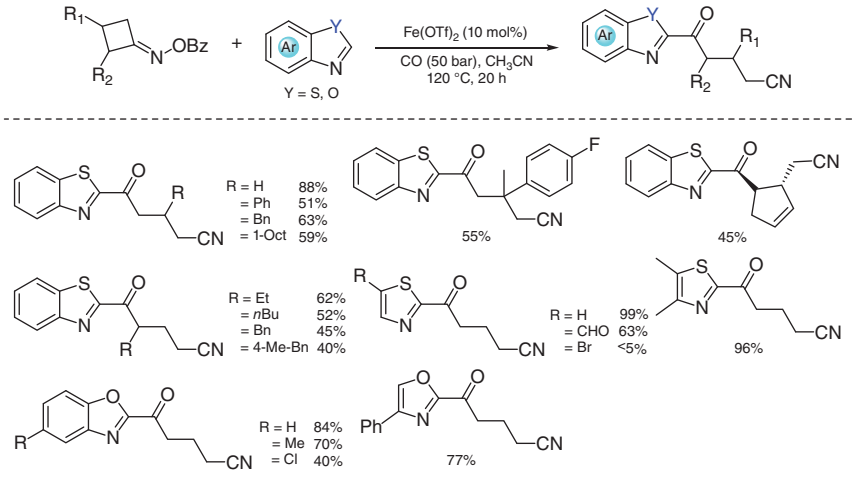

Scheme 4.7 $Fe(OTf)_2$-catalyzed carbonylative alkyl-acylation of heteroarenes. Source: Modified from Yin et al. [8].

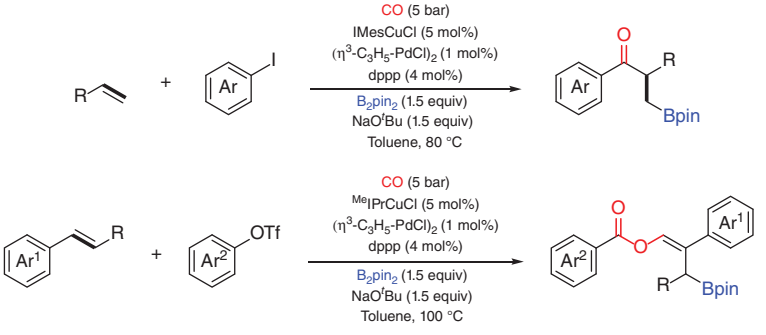

Scheme 4.8 (NHC)Cu(I)/Pd(II)-catalyzed four-component borocarbonylation of vinylarenes. Source: Modified from Wu et al. [9].

Recently, Wu and coworkers also disclosed a novel (NHC)copper(I)/palladium-catalyzed, four-component borocarbonylation of vinylarenes to synthesize β-boryl ketones and vinyl esters (Scheme 4.8) [9]. With this combination of copper and palladium catalytic system, vinylarenes, aryl halides/triflates, B_2Pin_2, and carbon monoxide were converted into the desired products in good to excellent yields. Aryl triflates and aryl iodides were applied as the starting materials for synthesizing β-boryl ketones and β-boryl vinyl esters (which inserted 2 equiv of carbon monoxide), respectively.

A detailed copper/palladium catalytic mechanism, which consists of two individual catalytic cycles, is outlined in Figure 4.2. In the copper catalytic cycle, activation of the copper catalyst L′CuCl with a strong base delivers the active catalytic species L′CuOtBu. This would then be captured by B_2pin_2 to form L′Cu-Bpin. Subsequently, borocupration of the styrene substrates affords the alkyl–copper intermediate species **I**. A CO insertion event of **I** delivers an acyl–copper intermediate **II**, which tautomerizes to the vinyl alkoxide copper complexes **III**. At this stage,

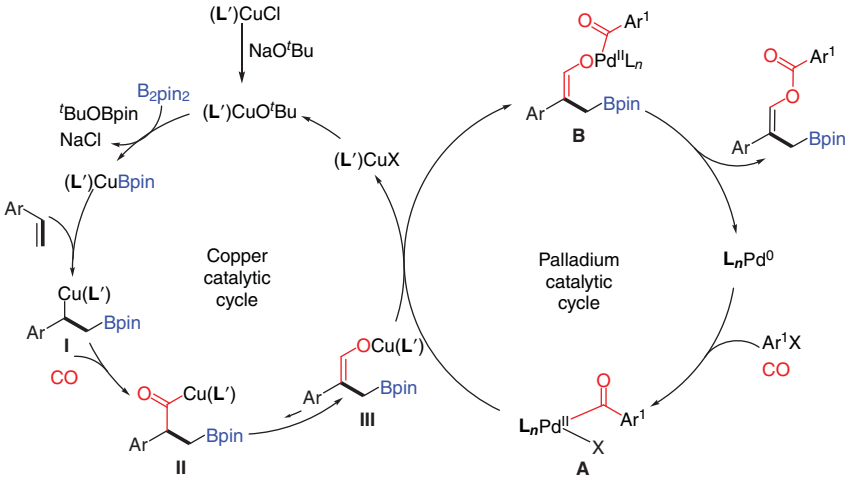

Figure 4.2 Proposed mechanism for the Cu/Pd-catalyzed borocarbonylation of vinylarenes.

the copper and palladium catalytic cycles begin to intersect via the transmetalation of **III** with acyl palladium species **A** (generated via CO insertion of Ar^1X to $L_nPd(0)$), thus leading to acyl–Pd–oxygen intermediate species **B**. The desired β-boryl vinyl esters are obtained after a reductive elimination step of **B** with regeneration of $L_nPd(0)$ to close the palladium catalytic cycle.

In 2020, the Wu group developed a copper-catalyzed regioselective borocarbonylation of β-boryl ketones from unactivated alkenes with readily available alkyl halides (Scheme 4.9) [10]. A broad range of β-boryl ketone derivatives was prepared in moderate to excellent yields with complete regioselectivity.

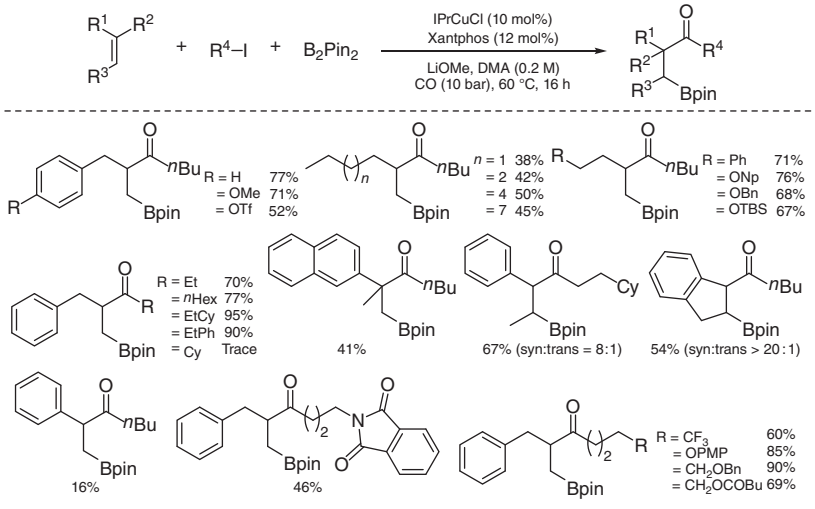

Scheme 4.9 IPrCuCl-catalyzed borocarbonylation of unactivated alkenes with alkyl halides. Source: Modified from Wu et al. [10].

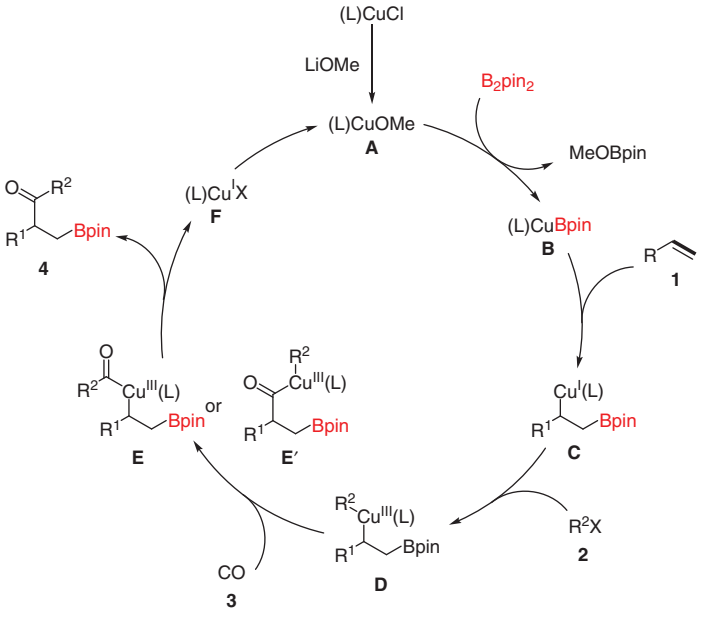

Figure 4.3 Proposed mechanism for the IPrCuCl-catalyzed borocarbonylation of unactivated alkenes with alkyl halides.

A detailed description of a plausible catalytic cycle for this transformation is presented in Figure 4.3. Firstly, reaction of IPrCuCl with base (LiOMe) and ligand gives the active copper-complex (L)CuOMe (**A**). Then, **A** reacts with B_2pin_2 to afford copper-boryl species (L)CuBpin (**B**). Subsequently, **B** inserts into the C=C bond of olefin (**1**) to obtain borylcuprated intermediate **C**, which reacts with the alkyl halide to generate copper(III) complex **D** via a radical intermediate and under the assistance of Xantphos ligand. Then, CO coordinates to copper catalyst and inserts into the C(sp^3)—Cu(III) bond to form the intermediate complexes **E** or **E′**. Then, the desired final product **4** is formed after a reductive elimination step with simultaneous regeneration of the (L)Cu(I)X species (**F**) for the next catalytic cycle.

4.3 Synthesis of Esters

In 2018, the Wu group discovered a copper/iron co-catalyzed alkoxycarbonylation of unactivated alkyl bromides (Scheme 4.10) [11]. In the presence of the co-catalysis system, various alkyl bromides were transformed into the corresponding aliphatic esters in good to excellent yields under 40 bar of carbon monoxide atmosphere. Mechanistic studies supported that this co-catalytic system overcomes the traditional copper oxidative addition problem and β-hydrogen elimination with an alkyl radical-capture mechanism. The alkyl radical is generated through a halogen abstraction.

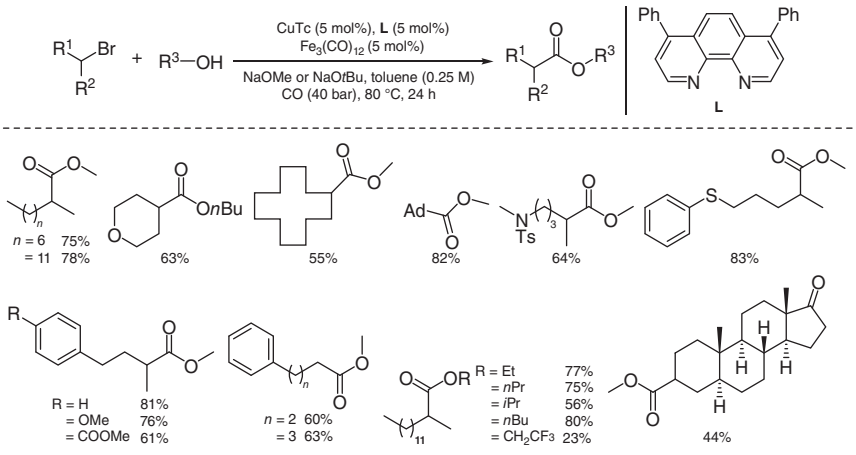

Scheme 4.10 CuTc/$Fe_3(CO)_{12}$-catalyzed alkoxycarbonylation of unactivated alkyl bromides. Source: Li and Wu [11].

Directing-group-assisted carbonylative C—H activation has been substantially investigated for its high regioselectivity. The direct carbonylation of unactivated C(sp^3)—H bonds is considered one of the most attractive areas. In 2017, Wu and coworkers first reported a novel $CuCl_2$-catalyzed alkoxycarbonylation of alkanes with alcohols through direct activation of C(sp^3)—H bond of alkanes (Scheme 4.11a) [12]. This carbonylative process was found able to give moderate to good yields of various aliphatic esters. With the employment of copper(I)/1,10-phen catalysis system, the same group then firstly developed an aminocarbonylation reaction from alkanes and primary amines via C(sp^3)—H bond activation. (Scheme 4.11b) [13].

With copper(I) as the catalyst, Wu and coworkers reported a four-component carbonylative reaction of bulk industrial aliphatic alkenes, alcohols, and acetonitrile (Scheme 4.12) [14]. This protocol requires a 4,4′,4″-tri-*tert*-butyl-2,2′:6′,2″-terpyridine (10 mol%) and *n*-$BuPAd_2$ (5 mol%) ligands system, which efficiently improved the reaction reactivity and chemoselectivity.

In 2016, Alexanian and coworkers reported a manganese-catalyzed carbonylative difunctionalization of alkenes. They use primary and secondary alkyl iodides in reactions with a diverse array of cyclic and acyclic substrates (Scheme 4.13) [15]. It exhibits a broad scope in carbocycle and heterocycle synthesis, with the potential for good diastereocontrol levels in the carboacylation process.

The Wu group recently reported a novel iron-catalyzed carbonylative cyclization to synthesize various functionalized pyrroline esters from γ,δ-unsaturated aromatic oxime esters and alcohols (Scheme 4.14) [16]. The reaction preceded with $Fe(acac)_3$ (5 mol%) as the catalyst and 1,10-phen·HCl·$2H_2O$ (10 mol%) as the efficient *N*-bidentate ligand. Various substituted γ,δ-unsaturated aromatic oxime esters were successfully converted to the pyrroline esters in good yields.

In 2019, the Wu group reported a novel manganese(III)-catalyzed carbonylation of aryl-substituted cyclobutanols for synthesizing ring-opening esters (Scheme 4.15)

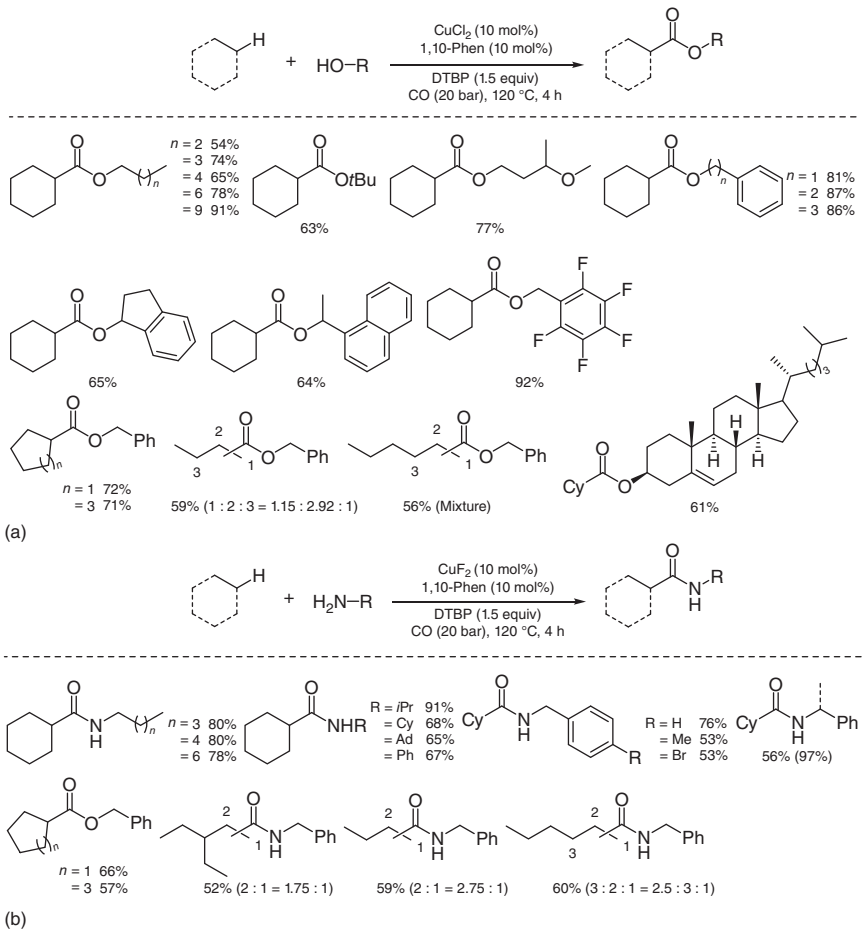

Scheme 4.11 Cu(I)-catalyzed carbonylation of alkanes with alcohol and amine nucleophiles. Source: Modified from Li et al. [12, 13].

[17]. Easily synthesized cyclobutanols and broadly available alcohols were treated with $Mn(OAc)_3 \cdot H_2O$ (20 mol%), bipy (30 mol%), and PIDA (phenyliodine(III) diacetate, 2.5 equiv) to produce the desired esters.

A plausible mechanism for this manganese-catalyzed carbonylation is shown in Figure 4.4. Initially, the phenyliodine(III) diacetate oxidizes the catalyst **A** and, together with aryl-substituted cyclobutanol **1**, deliver the manganese intermediate complex **B**. Subsequently, a cyclobutyloxy-radical **Int-1** was released through a single-electron transfer (SET) process, which undergoes a "radical clock"-type ring-opening tautomerization, leading to a key alkyl radical **Int-2**. It is almost concurrently presumed that the acyl radical **C** is formed under high CO pressure (60 bar). It can coordinate to the manganese center to generate manganese intermediate complex **D**. An X ligand exchange leads to an Mn(V) complex **E**, giving the final ester product **4** after a reductive elimination step.

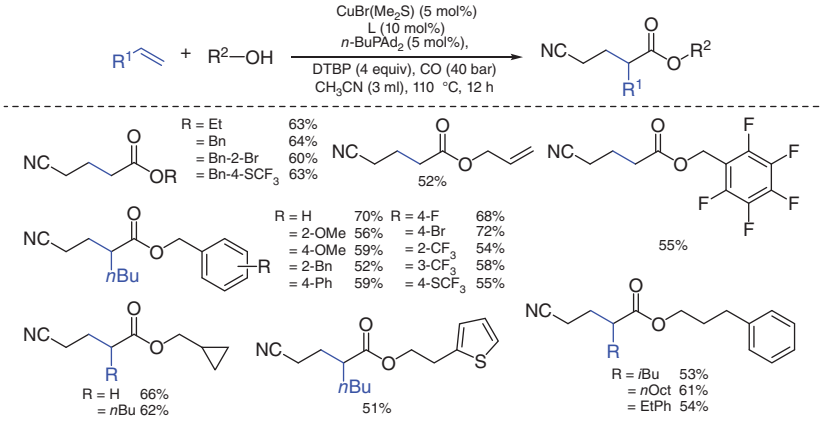

Scheme 4.12 $CuBr(Me_2S)$-catalyzed carbonylative four-component reaction of ethene and aliphatic olefins. Source: Modified from Li et al. [14].

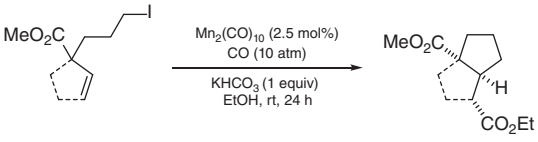

Scheme 4.13 $Mn_2(CO)_{10}$-catalyzed carboacylation of alkenes with alkyl iodides. Source: Modified from McMahon et al. [15].

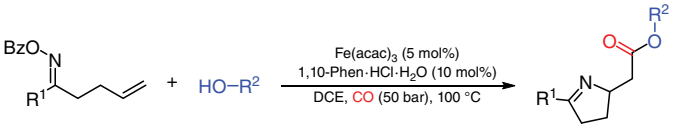

Scheme 4.14 $Fe(acac)_3$-catalyzed carbonylative cyclization of γ,δ-unsaturated aromatic oxime esters. Source: Modified from Zhang et al. [16].

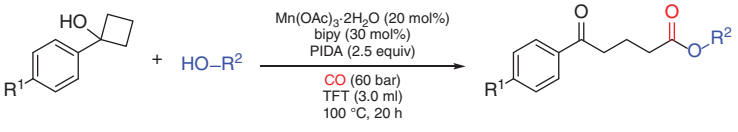

Scheme 4.15 $Mn(OAc)_3 \cdot H_2O$-catalyzed ring-opening carbonylation of aryl cyclobutanols. Source: Modified from Meyer et al. [17].

In 2020, Wu and coworkers disclosed a novel copper(II)-catalyzed carbonylation of *N*-fluoro-sulfonamides to synthesize β-homoproline derivatives, which are important motifs in many valuable functionalized pharmaceuticals and natural molecules (Scheme 4.16) [18]. *N*-Fluoro-sulfonamides and easily available alcohols were treated with $Cu(OTf)_2$, *N*-bidentate ligand, and Li_2CO_3 under 50 bar of CO

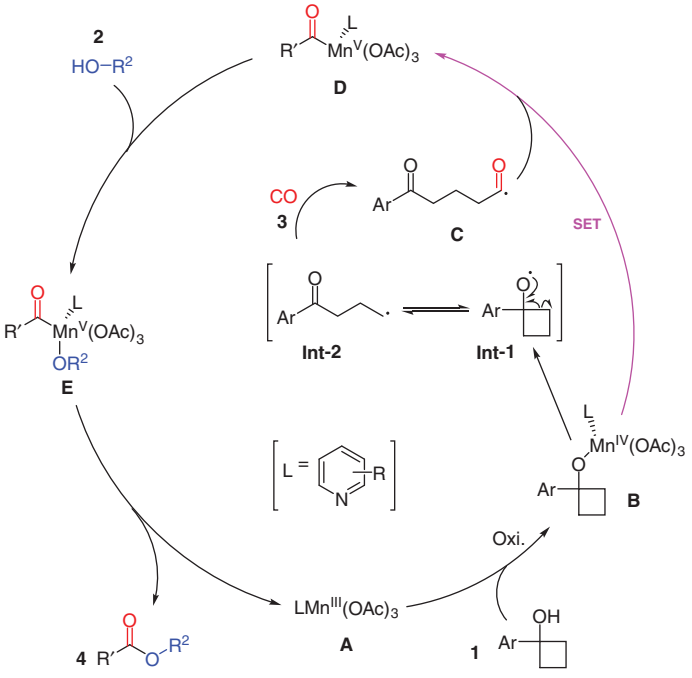

Figure 4.4 Plausible mechanism for the Mn-catalyzed ring-opening carbonylation of aryl cyclobutanols.

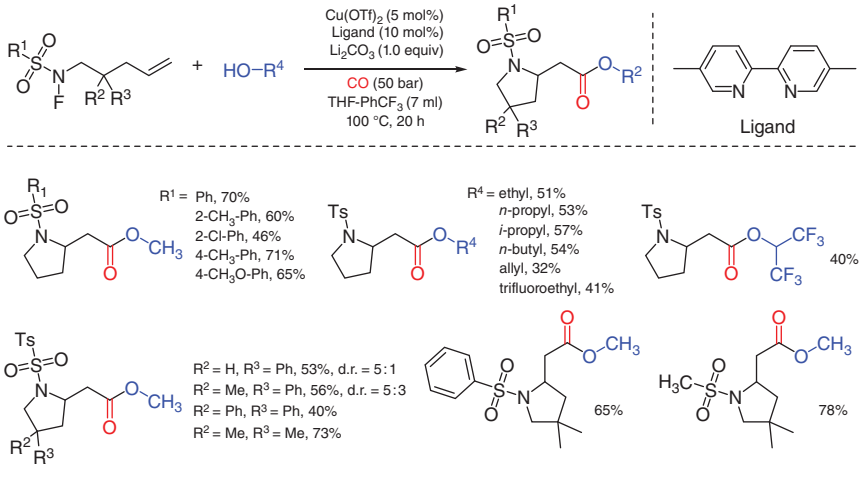

Scheme 4.16 $Cu(OTf)_2$-catalyzed carbonylation of *N*-fluoro-sulfonamides to synthesize β-homoprolines. Source: Modified from Zhang et al. [18].

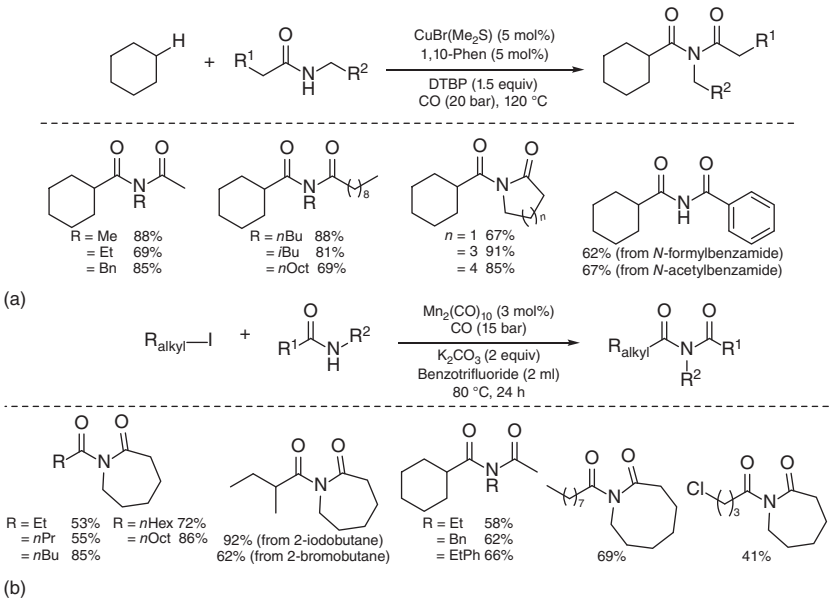

Scheme 4.17 Cu or Mn-catalyzed carbonylative coupling of alkyl iodides with amides. Source: Modified from Li et al. [19, 20].

atmosphere to produce the desired products. A mixture of solvents (THF and $PhCF_3$) plays an important role in this transformation.

4.4 Synthesis of Amides

In 2016, the Wu group explored a CuBr(Me_2S)-catalyzed carbonylation reaction of cycloalkanes with weak nucleophilic amides (Scheme 4.17a) [19]. Since the amides were comparatively sluggish toward the oxidants, this finding turns out to be a complementary approach to existing aminocarbonylation platforms. A series of imides were synthesized in good yields selectively at the tertiary C—H bond. However, a mixture of different products was obtained when an open-chain alkane was used in this reaction. In 2017, the same group first reported a manganese-catalyzed carbonylation reaction of alkyl iodides with amides, which allowed the preparation of various imides in moderate to good yields (Scheme 4.17b) [20]. Control experiments and electron paramagnetic resonance (EPR) spectroscopy studies confirmed the radical nature of this new process. This procedure is expected to complement the current methods for carbonylation reactions in organic synthesis.

A possible reaction mechanism of this copper-catalyzed carbonylation is proposed in Figure 4.5. The generation of a well-known *tert*-butoxy radical from copper(I)-catalyzed or thermal homolytic cleavage of the peroxide would and its reaction with cyclohexane substrate would lead to radical intermediate **A**. A sequential oxidation of the copper(I) species delivers a copper(III)–cyclohexane

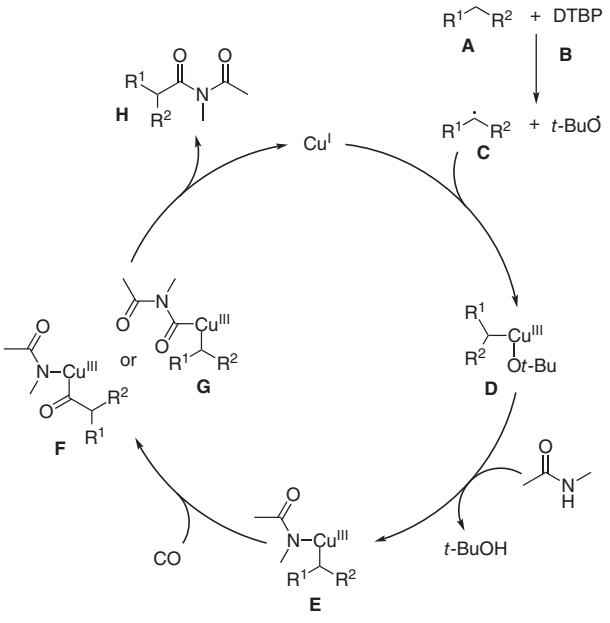

Figure 4.5 Plausible mechanism for the Cu-catalyzed carbonylative coupling of alkyl iodides with amides.

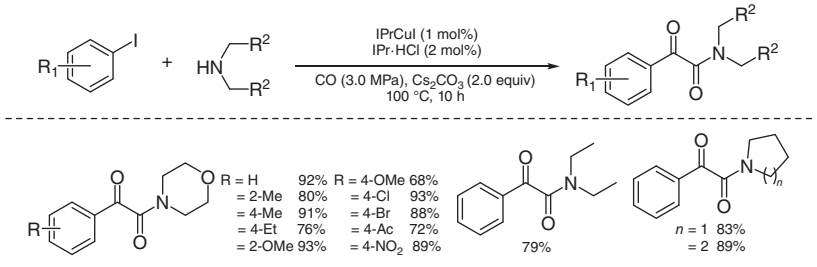

Scheme 4.18 IPrCuI/NHC-catalyzed double carbonylation reaction.

intermediate complex **B**. Then, **B** reacts with the amide to yield C–Cu(III)–N intermediate complexes **C**. Subsequent CO insertion forms intermediates **D** or **E**, which then afford the final carbonylation product **F** after reductive elimination. Moreover, the active CuI catalytic species is regenerated for the next catalytic cycle.

Using a copper-complex combined with an *N*-heterocyclic carbene precursor, Xia and coworkers reported a double carbonylation of aryl iodides with secondary amines in 2009 (Scheme 4.18) [21]. This *N*-heterocyclic carbene (NHC)-CuX-based catalysis system is efficient, as a range of α-keto amides were obtained in good yields and with high selectivity.

The first catalytic carbonylation process with iron as the catalyst was reported by Beller and coworkers in 2009 [22]. In the presence of catalytic quantities of $Fe(CO)_5$ or $Fe_3(CO)_{12}$, a series of substituted *trans*-3,4-disubstituted succinimides

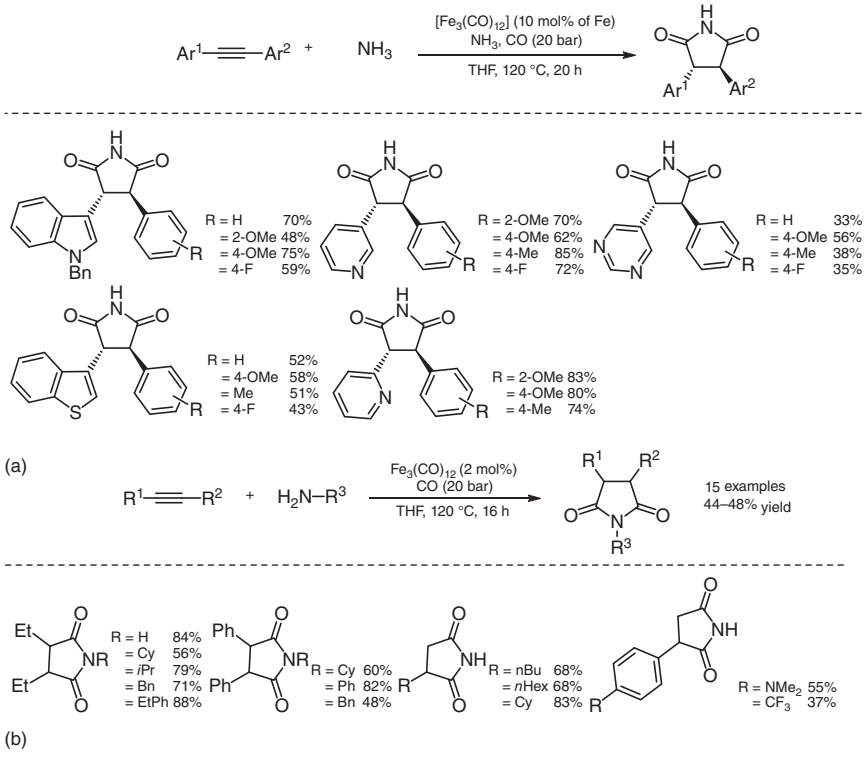

Scheme 4.19 $Fe_3(CO)_{12}$-catalyzed carbonylation for the synthesis of succinimides. Source: Modified from Prateeptongkum et al. [23].

were successfully synthesized from the reaction of alkynes with amine nucleophiles (Scheme 4.19) [23]. Both internal and terminal alkynes were transformed to succinimide derivatives in moderate to good yields. The pressure of CO is critical in this transformation.

In 2011, Petricci and coworkers reported a microwave-assisted aminocarbonylation of ynamides by using catalytic $Fe_3(CO)_{12}$ with low pressures of carbon monoxide (Scheme 4.20) [24].

Using $[Fe_3CO_{12}]$ as the catalyst, Beller and coworkers first developed a selective aminocarbonylation of terminal alkynes to synthesize acryl- and cinnamides in 2011 (Scheme 4.21) [25]. A wide variety of cinnamides and acrylamides were obtained smoothly in moderate to excellent yields under 10 bar carbon monoxide pressure. Additionally, this protocol provides an alternative strategy for the functionalization of alkynes to substituted acrylic acid derivatives.

Based on previous stoichiometric iron-reagents participated carbonylation literatures and their studies, two independent reaction pathways were proposed, as shown in Figure 4.6. For the right catalytic cycle, succinimide formation would proceed by a concerted double insertion of CO. For the left catalytic cycle, the [FeH] complex (an iron hydride carbonyl cluster) reacts with alkyne and CO, which would generate an iron intermediate complex. Then, the addition of an amine to the iron carbonyl

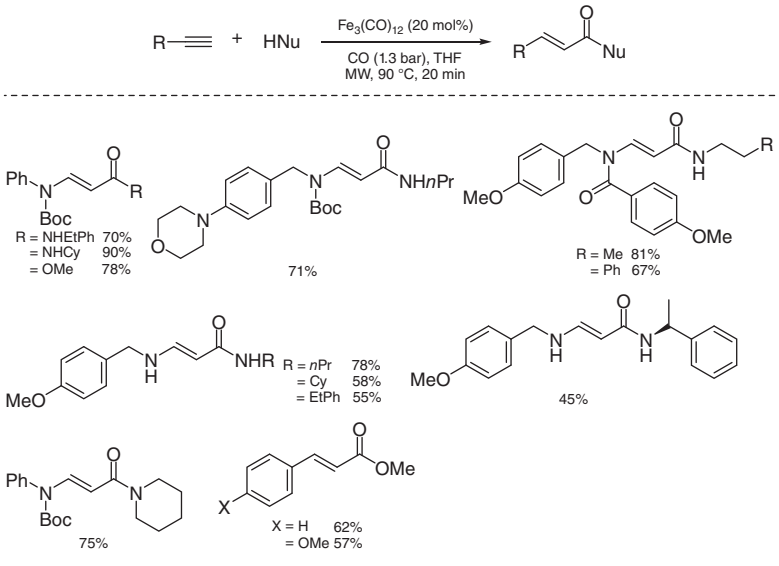

Scheme 4.20 Microwave-assisted aminocarbonylation of ynamides. Source: Modified from Pizzetti et al. [24].

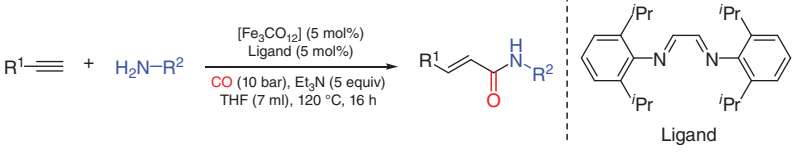

Scheme 4.21 $[Fe_3CO_{12}]$-catalyzed carbonylation of terminal alkynes. Source: Modified from Driller et al. [25].

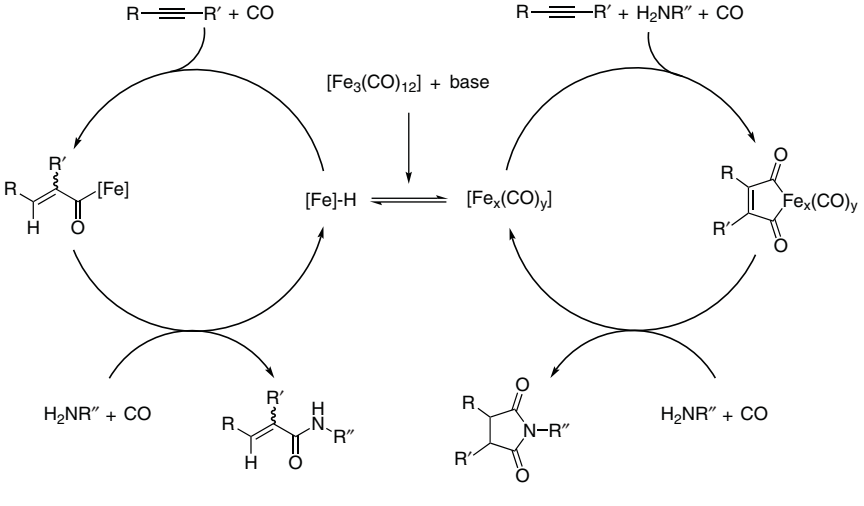

Figure 4.6 Plausible mechanism for the iron-catalyzed carbonylation of alkynes.

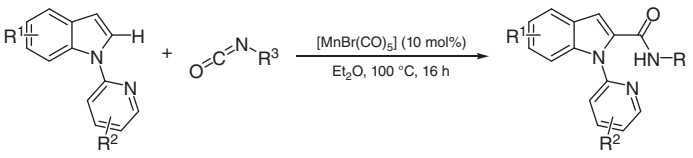

Scheme 4.22 $MnBr(CO)_5$-catalyzed C–H aminocarbonylation of heteroarenes.

complexes could easily form $[HNEt_3][HFe_3(CO)_{11}]$. Additionally, their studies also suggest that the precatalyst $[HNEt_3][HFe_3(CO)_{11}]$ delivers similar yields and selectivities as iron carbonyl species, such as $[Fe(CO)_5]$, $[Fe_2(CO)_9]$, and $[Fe_3(CO)_{12}]$. Thus, the formation of an acylcarbonyliron complex occurs, which upon attack by amine leads to acrylamide products with the regeneration of the iron complex. Interestingly, the carbonylative regioselectivity of alkynes in this protocol contrasts with previously reported palladium-catalyzed Markovnikov regioselectivity.

In 2015, the Ackermann group developed a novel manganese(I)-catalyzed aminocarbonylation of C—H bonds of heteroarenes [26]. Using 10 mol% of $MnBr(CO)_5$ as the catalyst, aminocarbonylative C–H activation reactions of various removable 2-pyridyl-directed indoles with alkyl isocyanates proceeded smoothly with moderate to excellent yields (Scheme 4.22). This transformation has a broad substrate scope, and even sterically bulky alky isocyanates were applied successfully in this process.

Mechanistically, the detailed experimental studies revealed that an organometallic C–H manganesation step and a rate-determining migratory insertion were involved in this process (Figure 4.7). Specifically, the manganese(I) complex **A** could be coordinated by a 2-pyridyl-indole substrate and then produce the manganese(I) complex **B**. A fast and reversible C–H manganesation process could then occur with elimination of HBr to generate a cyclometalated complex **C**. A coordination step of alkyl isocyanates to **C** to produce an isocyanate-manganese complex **D** was followed by CO insertion to generate manganese complex **E**. Finally, the desired product was obtained by a proto-demetalation step with regeneration of the catalytically active manganese(I) complex **A**.

Using $Cu(OAc)_2$ as catalyst and Ag_2CO_3 as the oxidant, the Ge and Li group developed a copper site-selective carbonylation of $C(sp^2)$—H bonds with nitromethane (Scheme 4.23) [27]. This work was based on the Daugulis seminal study, which first introduced 8-aminoquinoline as the directing group in a palladium-catalyzed $C(sp^2)/C(sp^2)$–H functionalization. This protocol is characterized by moderate to excellent regioselectivity and good functional tolerance under an 8-aminoquinoline structure. Their mechanistic studies suggest that the $C(sp^2)$—H bond cleavage is an irreversible, rather than a rate-determining step.

In 2017, Wu and coworkers reported a copper-catalyzed carbonylative cross-coupling of arylboronic acids with *N*-chloroamines to synthesize aryl amides (Scheme 4.24) [28]. With copper(I) oxide as the catalyst, various desired amide compounds produced moderate to good yields. Functional groups such as iodide and alkene are tolerated.

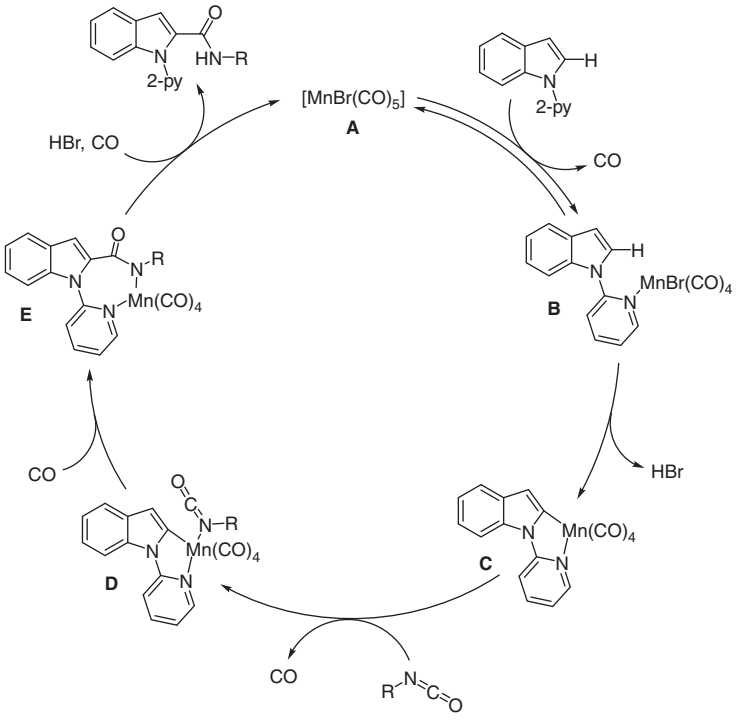

Figure 4.7 Proposed mechanism for the manganese(I)-catalyzed C–H aminocarbonylation of heteroarenes.

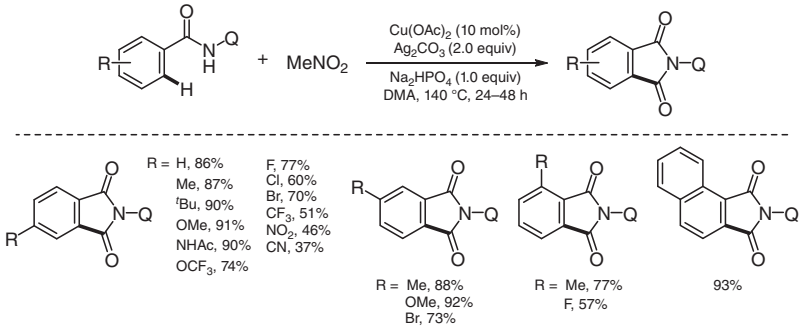

Scheme 4.23 $Cu(OAc)_2$-catalyzed carbonylation of $C(sp^2)$—H bonds with $MeNO_2$. Source: Modified from Wu et al. [27].

In 2019, Wu and coworkers reported a copper(II)-catalyzed aminocarbonylation procedure for the transformations of remote $C(sp^3)$—H bonds in *N*-fluoro-sulfonamides (Scheme 4.25) [29]. This reaction involves three main steps: (i) amidyl radical generation, (ii) 1,5-HAT (hydrogen atom transfer) process, and (iii) radical carbonylation reactions. Also, this reaction yielded various δ-lactam products in high yields and good regioselectivity. More interestingly, this

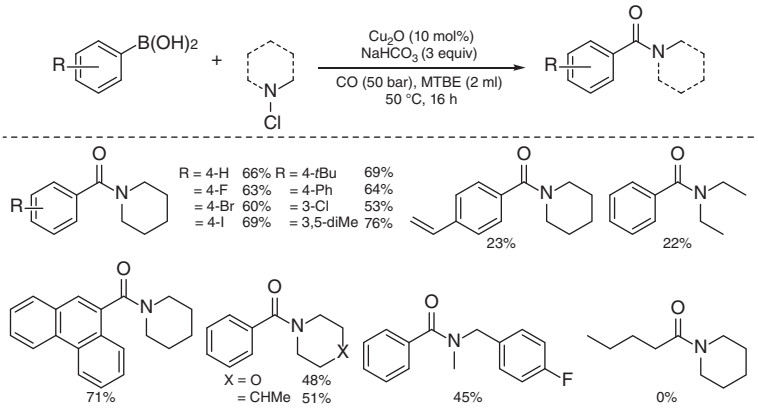

Scheme 4.24 Cu_2O-catalyzed aminocarbonylation of arylboronic acids with *N*-chloroamines. Source: Modified from Yin et al. [28].

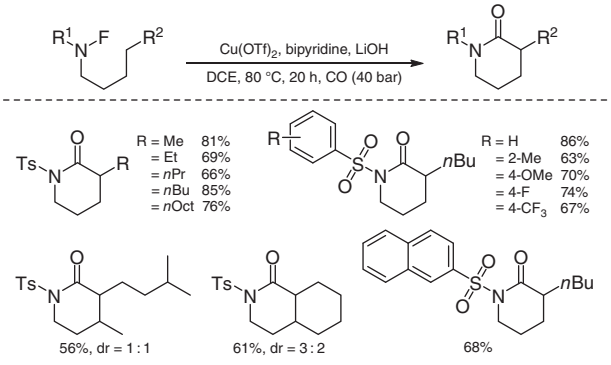

Scheme 4.25 $Cu(OTf)_2$-catalyzed intermolecular aminocarbonylation of remote $C(sp^3)$—H bonds in *N*-fluoro-sulfonamides. Source: Modified from Yin et al. [29].

methodology can also be successfully applied to modify *N*-fluorocarboxamides and the late-stage functionalization of medicine celecoxib-based derivatives.

In 2017, Wu and coworkers reported an example of copper(II)-catalyzed carbonylative acetylation of amines (Scheme 4.26) [30]. With peroxide as the oxidant and the methyl source with a copper catalyst under CO pressure, good yields of *N*-acetyl amides could be obtained.

Recently, Cantat and coworkers first reported iron-catalyzed carbonylation of C—N bonds in *tert*-amines (Scheme 4.27) [31]. With the use of low-valent iron catalysts, amides could be obtained from both aromatic and aliphatic amines. Interestingly, the inorganic Lewis acid, especially $AlCl_3$ and $Nd(OTf)_3$, could significantly facilitate the transformation, enabling the carbonylation reaction to undergo a relatively low CO atmosphere pressure.

Mechanistically, alkylation of $K_2[Fe(CO)_4]$ (Collman's reagent) with iodomethane, which is in equilibrium with the amine reagent, affords the anionic alkyl species

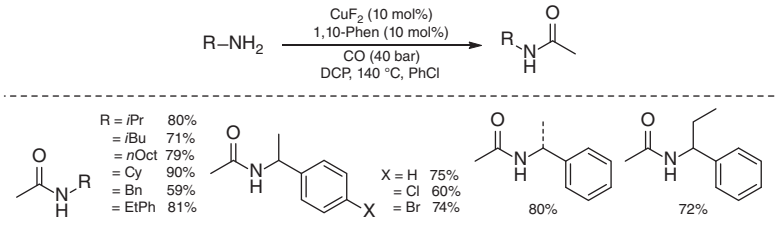

Scheme 4.26 CuF_2-catalyzed carbonylative acetylation of amines. Source: Modified from Li et al. [30].

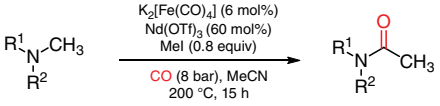

Scheme 4.27 $K_2[Fe(CO)_4]$-catalyzed carbonylation of tertiary amines. Source: Modified from Allah et al. [31].

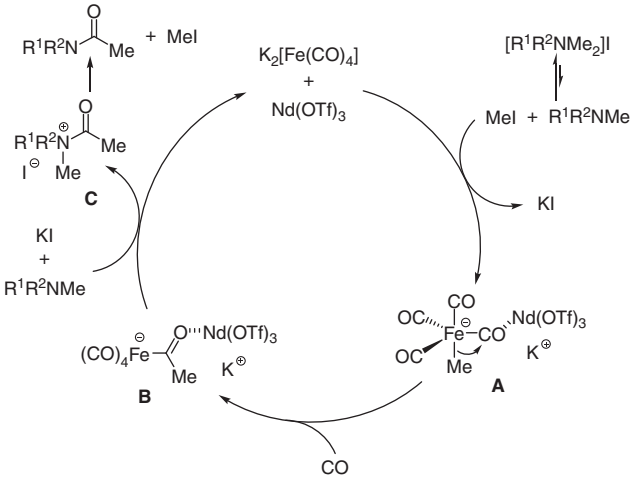

Figure 4.8 Proposed mechanism for the $[Fe(CO)_4]$-catalyzed carbonylation of tertiary amines.

$K[Fe(CH_3)(CO)_4]$ **A** (Figure 4.8). Subsequently, the Lewis acid co-catalyst coordination facilitates a CO migratory insertion to generate the acylferrate intermediate **B**. Nucleophilic addition of the free amine on the acyl ligand forms, after the elimination step, the quaternarized amide product **C**, which leads to the amide product by iodide attack regenerating iodomethane. It should be noted that this mechanism circumvents the problematic activation of the stable C—N bond. The generation of an electrophilic acyl moiety and its reaction with the amine reagent is the key step in this process. The C—C bond between the alkyl residue and CO is formed before the C—N bond cleavage.

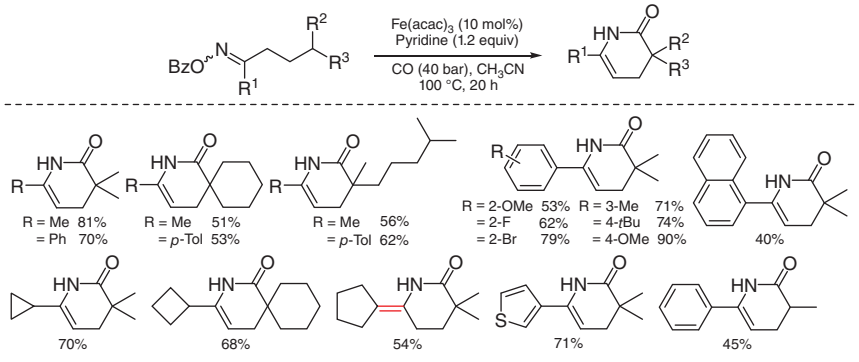

Scheme 4.28 $Fe(acac)_3$-catalyzed intramolecular aminocarbonylation of oxime esters. Source: Modified from Yin et al. [32].

In 2019, the Wu group developed an iron-catalyzed approach for the intramolecular carbonylation of a tertiary carbon radical, generated from a 1,5-hydrogen atom transfer of various oxime esters captured by CO gas smoothly. Numerous six-membered lactams were chemo-selectively constructed in high yields excellent chemo-selectivities (Scheme 4.28) [32].

The Mankad group recently disclosed a novel synergistic copper-catalyzed reductive aminocarbonylation to synthesize amides directly from alkyl iodides and readily available nitroarenes (Scheme 4.29) [33]. By employing $PhSiH_3$ as a hydrogen source, a range of substituted aryl nitroarenes reacted with alkyl iodides and converted into the corresponding amides in moderate to good yields. It should be mentioned that the copper catalyst plays a dual role in this transformation: (i) carbonylation of alkyl iodides and (ii) reduction of nitroarenes. It provides a powerful, practical, and supplementary methodology to amides synthesis in the organic community.

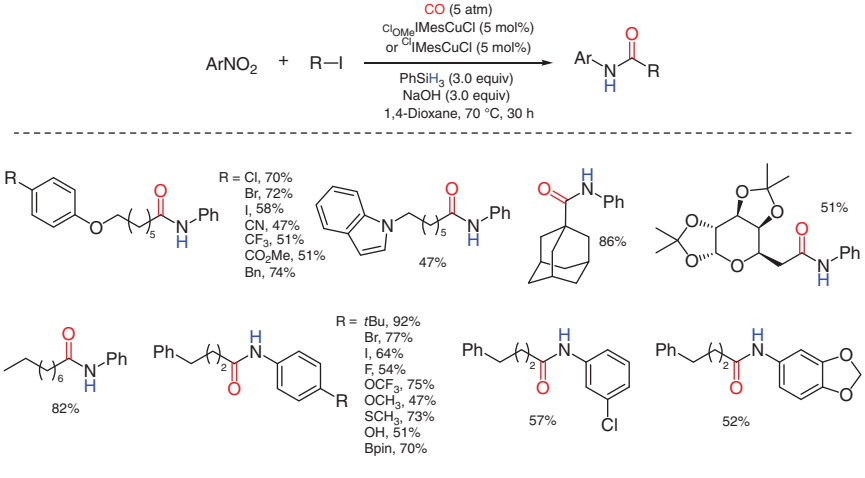

Scheme 4.29 Synergistic copper-catalyzed reductive aminocarbonylation of nitroarenes. Source: Modified from Zhao et al. [33].

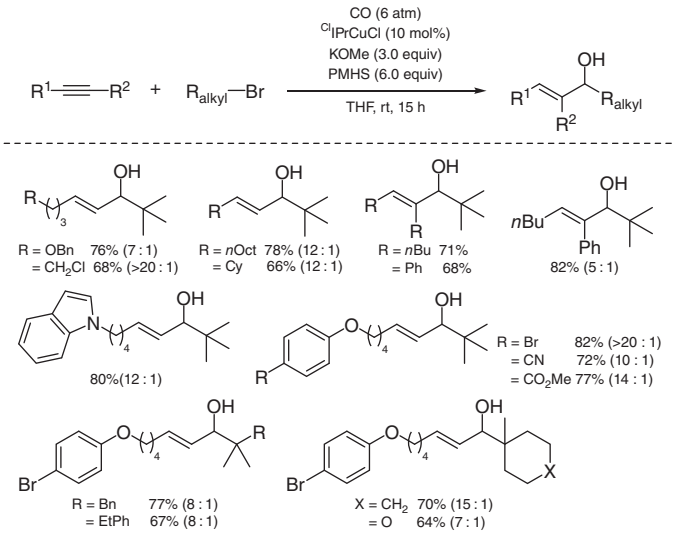

Scheme 4.30 Synthesis of allylic alcohols via ^{Cl}IPrCuCl-catalyzed hydrocarbonylative coupling of alkynes with alkyl halides. Source: Modified from Cheng et al. [34].

4.5 Synthesis of Other Products

In 2018, the Mankad group developed a modular procedure to synthesize allylic alcohols from tertiary, secondary, and primary alkyl halides and alkynes via a copper(I)-catalyzed hydrocarbonylative coupling and 1,2-reduction tandem sequence. The reaction tolerates various functional groups under mild reaction conditions, affording the corresponding allylic alcohols in good yield and excellent selectivity. The use of tertiary alkyl halides enables the synthesis of various allylic alcohols bearing α-quaternary carbon centers, which are still challenging using the previous catalytic methods (Scheme 4.30) [34].

In 2018, the Mankad group developed a copper-catalyzed four-component coupling reaction of alkynes, alkyl halides, B_2pin_2, and CO to synthesize β-borylated tetrasubstituted enones, and it provides a unique umpolung of the α,β-unsaturated ketone moiety (Scheme 4.31) [35]. The utility of this method was demonstrated by the various transformations of the corresponding reduced oxaborole. Moreover, the Suzuki–Miyaura coupling of α-boryl-tetrasubstituted enones with an aryl halide enabled the synthesis of an all-carbon tetrasubstituted enone, which is still challenging to construct using existing methods.

A proposed mechanism of this four-component borocarbonylative coupling reaction is outlined in Figure 4.9. Initially, in the presence of strong base and B_2pin_2, the active copper complexes LCu-Bpin reacts with alkyne substrate and affords the β-boroalkenylcopper(I) complex **A**. Instead of oxidative addition of the alkyl halide to **A** to give the carboboration product **G** via intermediate **F**, an alkyl radical $R^3\bullet$ is generated from the reaction of **A** and the alkyl halide (path a). This radical species then undergoes carbonylation to give the acyl radical species **C**, which reacts with

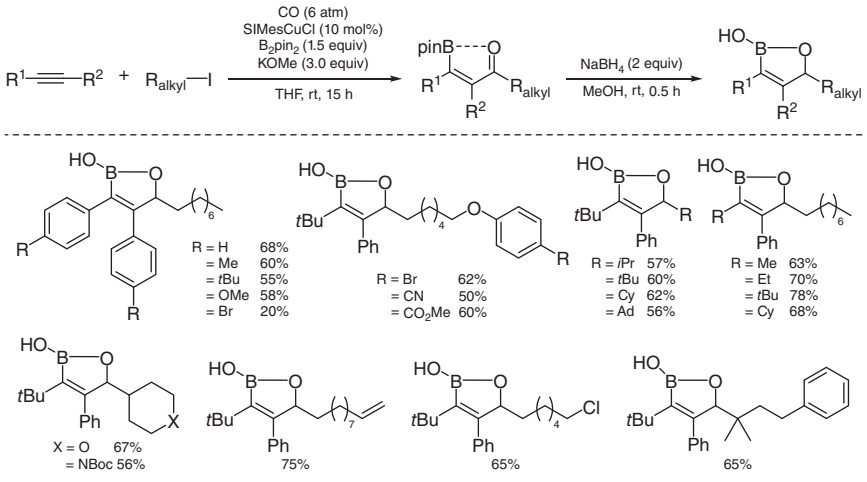

Scheme 4.31 (NHC)CuCl-catalyzed borocarbonylative coupling of internal alkynes with unactivated alkyl halides. Source: Modified from Cheng et al. [35].

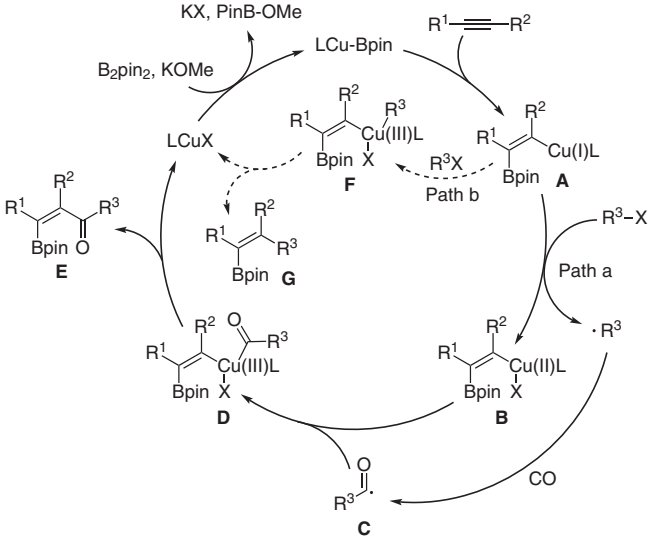

Figure 4.9 Proposed mechanism for the borocarbonylative coupling of alkynes with alkyl halides.

the copper(II) complex **B** to form the copper(III) intermediate **D**. Finally, reductive elimination affords the β-borylated tetrasubstituted enone **E**. The authors supposed that the corresponding highly-substituted products **E** would be sufficiently inert to avoid further borylation under their reaction conditions.

In the same year, the same group developed an (NHC)copper(I)-catalyzed carbonylative hydroxymethylation reaction of primary, secondary, and tertiary alkyl iodides to construct one-carbon-extended primary alcohols under mild conditions

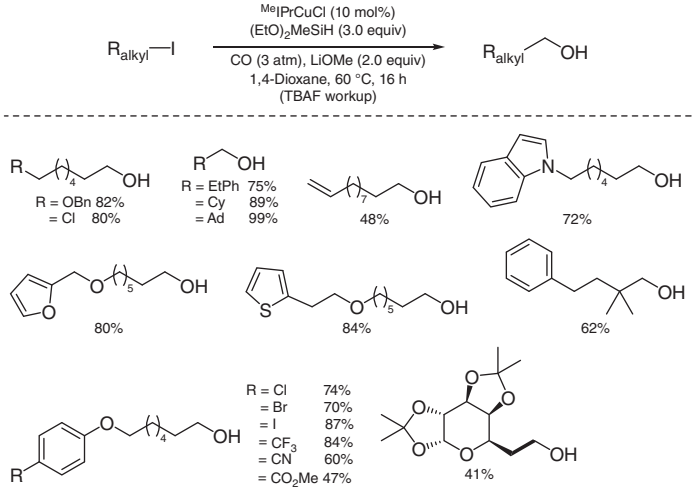

Scheme 4.32 ^{Me}IPrCuCl-catalyzed carbonylative hydroxymethylation of unactivated alkyl iodides. Source: Modified from Zhao et al. [36].

(Scheme 4.32) [36]. This protocol is compatible with various functional groups and heterocycles.

A plausible mechanism of this copper-catalyzed hydroxymethylation is shown in Figure 4.10. An alkyl radical initiates this transformation, which results from a radical initiator generated from the hydrosilane and metal alkoxide. After that, an atom-transfer carbonylative reaction would afford acyl iodide **B**, through the formation of acyl radical intermediate species **A**. Subsequently, a nucleophilic substitution process occurs between **B** and a copper hydride to deliver alkyl aldehyde **C**. Concurrently, **C** undergoes a copper hydride catalyzed reduction to deliver alkoxide intermediate complex **D**, which furnishes the final silyl-protected alcohol **E**. It should be

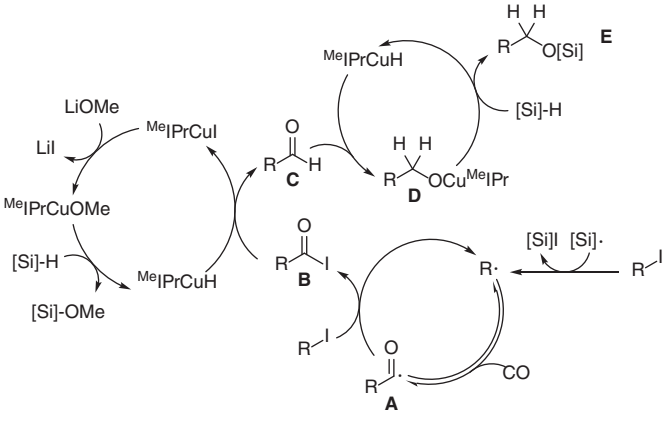

Figure 4.10 Proposed mechanism for the ^{Me}IPrCuCl-catalyzed carbonylative hydroxymethylation of unactivated alkyl iodides.

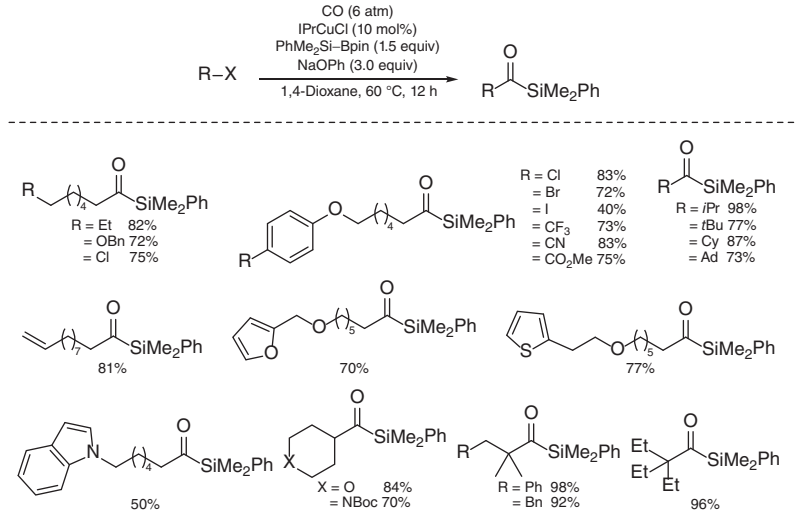

Scheme 4.33 IPrCuCl-catalyzed carbonylative silylation of alkyl halides. Source: Modified from Cheng et al. [37].

mentioned that the well-known β-hydride elimination is avoided due to the absence of metal-alkyl intermediates in this catalytic cycle.

More recently, they reported a copper(I)-catalyzed carbonylative silylation of unactivated alkyl halides, enabling an efficient synthesis of alkyl-substituted acylsilanes in high yields (Scheme 4.33) [37]. A variety of functional groups are tolerated under the mild reaction conditions, and primary, secondary, and tertiary alkyl halides are all applicable. This method's practical utility has been demonstrated in the synthesis of acylsilanes bearing different silyl groups and *in situ* reduction of a product to the corresponding α-hydroxylsilane in one pot. Mechanistic experiments indicate that a silylcopper intermediate activates alkyl halides by SET to form alkyl radical intermediates. The carbon–halogen bond cleavage is not involved in the rate-determining step. Also, the formed acylsilanes can be further reduced *in situ* by adding a hydrosilane reagent.

Based on the previous study, the same authors reported a novel copper(I)-catalyzed synthesis of stereodefined cyclopropyl bis(boronates) from alkenes using CO as the C1 source (Scheme 4.34) [38]. In this process, various aliphatic alkenes were transformed into the desired bis(boronate ester)-substituted cyclopropanes in moderate to excellent yields. Given the potential utility of cyclopropyl boronates, the synthetic transformations of the resulting cyclopropyl bis(boronates) demonstrate

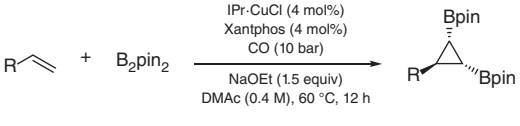

Scheme 4.34 IPr·CuCl-catalyzed synthesis of stereodefined cyclopropyl bis(boronates). Source: Modified from Wu et al. [38].

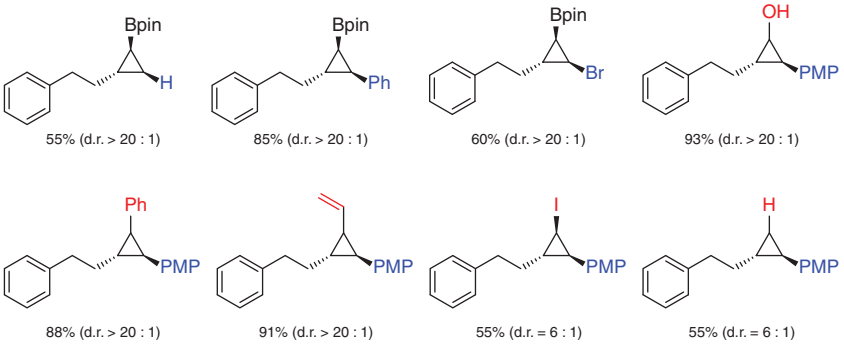

Figure 4.11 Derivatization of the B−C bond of cyclopropyl bis(boronates) (PMP = 4-MeO−C_6H_4−).

the great importance for the organic synthesis community (Figure 4.11). Interestingly, good to excellent stereoselectivity was observed in these functionalized cyclopropane compounds.

A possible reaction pathway is proposed in Figure 4.12. Initially, the active LCu(I)Bpin complex **A** is formed with the strong organic base. Then, two catalytic pathways based on this LCu(I)Bpin complex **A** begin. In catalytic cycle **I**, CO reacts with **A** through an insertion step, producing LCu(C=O)Bpin intermediate **G**. Then, the bis(boryl) ketone intermediate is eliminated after reaction with

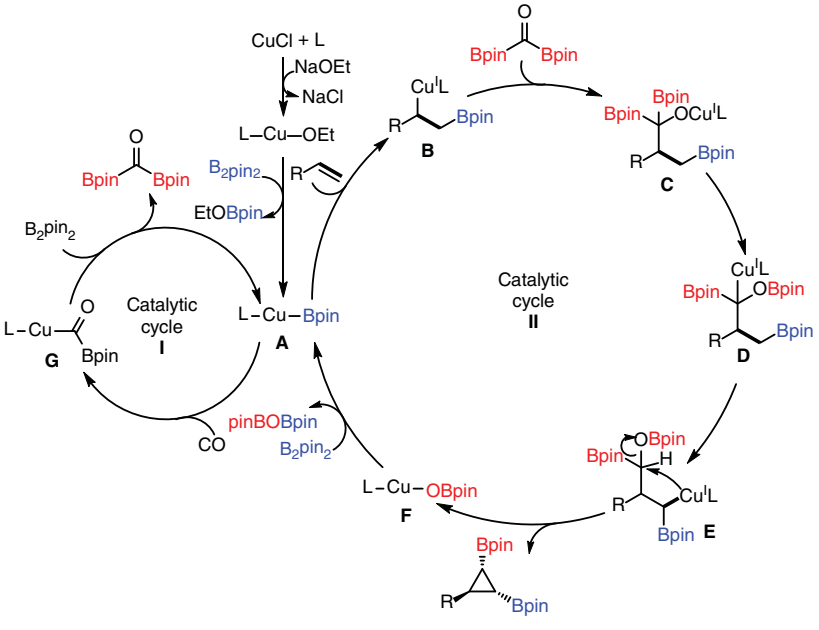

Figure 4.12 Plausible reaction mechanism for the IPr·CuCl-catalyzed synthesis of cyclopropyl bis(boronates).

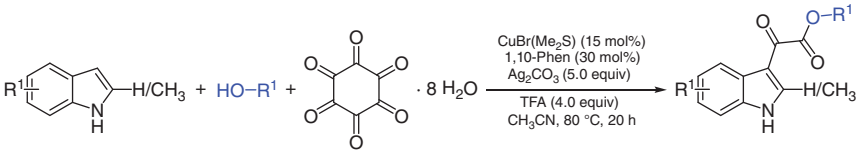

Scheme 4.35 $CuBr(Me_2S)$-catalyzed carbonylation of indoles with hexaketocyclohexane. Source: Modified from Wang et al. [39].

B_2pin_2. In the catalytic cycle **II**, an alkene substrate coordinates and inserts into the Cu—B bond of complex **A** to give an alkylcopper intermediate **B**. Afterward, the *in situ*-produced bis(boryl) ketone intermediate reacts with alkylcopper intermediate **B** to give copper complex **C**, which generates copper intermediate **D** after an intramolecular rearrangement. Then, intermediate **E** is formed after a 1,3-copper shift, which eliminates cyclopropyl boronate as the final product and generates the LCu(I)OBpin complex **F**. Finally, the LCuOBpin complex **F** reacts with B_2pin_2 to give **A** thus closing the catalytic cycle.

In 2018, Wu and coworkers developed a novel copper(I)-catalyzed carbonylative protocol of indoles using hexaketocyclohexane as an efficient double carbonyl source (Scheme 4.35) [39]. Using $CuBr(Me_2S)$ (15 mol%) as the catalyst, 1,10-phen (30 mol%) as the ligand, and hexaketocyclohexane, this double carbonylative methodology avoids harsh conditions (especially a high pressure of CO gas) and is applicable to various substrates.

In 2017, Liu and coworkers demonstrated a direct double carbonylation for the synthesis of isatins from primary and secondary anilines (Scheme 4.36) [40]. This transformation generates isatin derivatives in moderate yields using glyoxal as a double carbonyl source and Cs_2CO_3 (1.3 equiv) as the source.

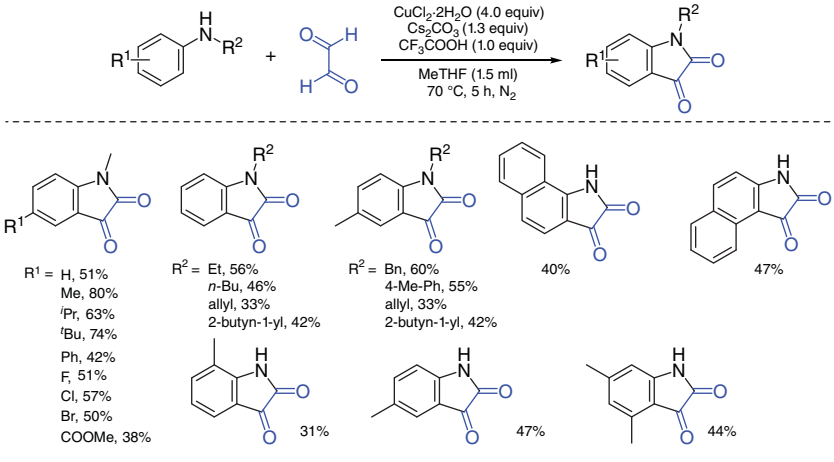

Scheme 4.36 $CuCl_2 \cdot 2H_2O$-promoted double carbonylation. Source: Modified from Kuan et al. [40].

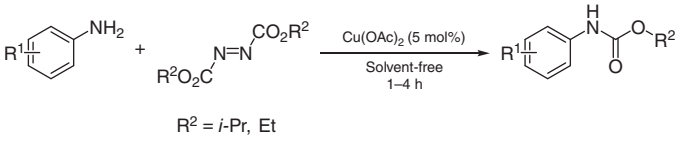

Scheme 4.37 $Cu(OAc)_2$-catalyzed carbonylation to synthesize carbamates.

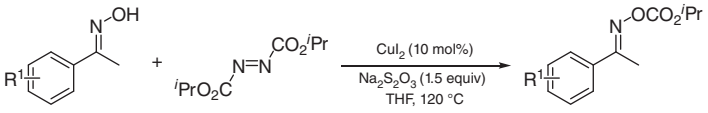

Scheme 4.38 CuI_2-catalyzed carbonylation reaction to synthesize oxime carbonates.
Source: Modified from Usman et al. [42].

In 2016, the Guan group developed a copper(II)-catalyzed carbonylation for the synthesis of carbamate derivatives from readily available anilines and DIAD (diisopropyl azodicarboxylate) as the carbonyl source [41]. This process involves both N—H bond cleavage and N—C bond formation and is carried out under solvent-free conditions (Scheme 4.37). A wide variety of arylcarbamates were synthesized in moderate to good yields.

Based on the previous study, the same group reported a novel copper(II)-catalyzed reaction of oximes for the synthesis of oxime carbonate derivatives using DIAD as the carbonyl source (Scheme 4.38) [42]. With the employment of CuI_2 (10 mol%) as the catalyst and $Na_2S_2O_3$ (1.5 equiv) as the additive, which might facilitate the C—N bond cleavage of DIAD under solvent conditions, this convenient protocol extends the scope of carbonates for the organic synthesis community.

4.6 Summary and Conclusions

In summary, the main achievements on using manganese, iron, and copper as the catalysts in carbonylative transformations have been summarized and discussed. The advantages of those catalysts are their low costs and low toxicity. However, concerning their catalytic reactivity, it was proven to be unique in some cases and needs to be further explored.

References

1 Kang, S.K., Yamaguchi, T., Kim, T.H., and Ho, P.S. (1996). *J. Org. Chem.* 61: 9082–9083.
2 Cheng, L., Zhong, Y., Ni, Z. et al. (2014). *RSC Adv.* 4: 44312–44316.
3 Pye, D.R., Cheng, L.-J., and Mankad, N.P. (2017). *Chem. Sci.* 8: 4750–4755.
4 Cheng, L.-J. and Mankad, N.P. (2017). *J. Am. Chem. Soc.* 139: 10200–10203.
5 Tambade, P.J., Patil, Y.P., Nandurkar, N.S., and Bhanage, B.M. (2008). *Synlett*: 886–888.

6 Zhong, Y. and Han, W. (2014). *Chem. Commun.* 50: 3874–3877.
7 Zhao, H., Du, H., Yuan, X. et al. (2016). *Green Chem.* 18: 5782–5787.
8 Yin, Z., Zhang, Z., Soulé, J.-F. et al. (2019). *J. Catal.* 372: 272–276.
9 Yuan, Y., Wu, F.P., Xu, J.X., and Wu, X.-F. (2020). *Angew. Chem. Int. Ed.* https://doi.org/10.1002/anie.202006427.
10 Wu, F.-P., Yuan, Y., Schunemann, C. et al. (2020). *Angew. Chem. Int. Ed.* 59: 10451–10455.
11 Li, Y.H. and Wu, X.-F. (2018). *Commun. Chem.* 1: 39.
12 Li, Y., Wang, C., Zhu, F. et al. (2017). *ChemSusChem* 10: 1341–1345.
13 Li, Y., Zhu, F., Wang, Z., and Wu, X.-F. (2016). *ACS Catal.* 6: 5561–5564.
14 Li, Y., Zhu, F., Wang, Z., and Wu, X.-F. (2018). *Chem. Commun.* 54: 1984–1987.
15 McMahon, C.M., Renn, M.S., and Alexanian, E.J. (2016). *Org. Lett.* 18: 4148–4150.
16 Zhang, Y., Yin, Z., Wang, H., and Wu, X.-F. (2020). *Chem. Commun.* 56: 7045–7048.
17 Meyer, T., Yin, Z., and Wu, X.-F. (2019). *Tetrahedron Lett.* 60: 864–867.
18 Zhang, Y., Yin, Z., and Wu, X.-F. (2020). *Org. Lett.* 22: 1889–1893.
19 Li, Y., Dong, K., Zhu, F. et al. (2016). *Angew. Chem. Int. Ed.* 55: 7227–7230.
20 Li, Y., Zhu, F., Wang, Z. et al. (2017). *ChemCatChem* 9: 915–919.
21 Liu, J., Zhang, R., Wang, S. et al. (2009). *Org. Lett.* 11: 1321–1324.
22 Driller, K.M., Klein, H., Jackstell, R., and Beller, M. (2009). *Angew. Chem. Int. Ed.* 48: 6041–6044.
23 Prateeptongkum, S., Driller, K.M., Jackstell, R. et al. (2010). *Chem. Eur. J.* 16: 9606–9615.
24 Pizzetti, M., Russo, A., and Petricci, E. (2011). *Chem. Eur. J.* 17: 4523–4528.
25 Driller, K.M., Prateeptongkum, S., Jackstell, R., and Beller, M. (2011). *Angew. Chem. Int. Ed.* 50: 537–541.
26 Liu, W., Bang, J., Zhang, Y., and Ackermann, L. (2015). *Angew. Chem. Int. Ed.* 54: 14137–14140.
27 Wu, X., Miao, J., Li, Y. et al. (2016). *Chem. Sci.* 7: 5260–5264.
28 Yin, Z., Wang, Z., Li, W., and Wu, X.-F. (2017). *Eur. J. Org. Chem.* 2017: 1769–1772.
29 Yin, Z., Zhang, Y., Zhang, S., and Wu, X.-F. (2019). *J. Catal.* 377: 507–510.
30 Li, Y., Wang, C., Zhu, F. et al. (2017). *Chem. Commun.* 53: 142–144.
31 Allah, T.N., Savourey, S., Berthet, J.C. et al. (2019). *Angew. Chem. Int. Ed.* 58: 10884–10887.
32 Yin, Z., Zhang, Z., Zhang, Y. et al. (2019). *Chem. Commun.* 55: 4655–4658.
33 Zhao, S. and Mankad, N.P. (2019). *Org. Lett.* 21: 10106–10110.
34 Cheng, L.-J., Islam, S.M., and Mankad, N.P. (2018). *J. Am. Chem. Soc.* 140: 1159–1164.
35 Cheng, L.-J. and Mankad, N.P. (2018). *Angew. Chem. Int. Ed.* 57: 10328–10332.
36 Zhao, S. and Mankad, N.P. (2018). *Angew. Chem. Int. Ed.* 57: 5867–5870.
37 Cheng, L.-J. and Mankad, N.P. (2020). *J. Am. Chem. Soc.* 142: 80–84.
38 Wu, F.P., Luo, X., Radius, U. et al. (2020). *J. Am. Chem. Soc.* 142: 14074–14079.
39 Wang, Z., Yin, Z., and Wu, X.-F. (2018). *Chem. Commun.* 54: 4798–4801.

40 Kuan, S.H.C., Sun, W., Wang, L. et al. (2017). *Adv. Synth. Catal.* 359: 3484–3489.
41 Usman, M., Ren, Z.-H., Wang, Y.-Y., and Guan, Z.-H. (2016). *RSC Adv.* 6: 107542–107546.
42 Usman, M., Ren, Z.-H., Wang, Y.-Y., and Guan, Z.-H. (2017). *Org. Biomol. Chem.* 15: 1091–1095.

Part II

Carbonylations Promoted by Second Row Transition Metal Catalysts

5

Ruthenium-Catalyzed Carbonylations

Helfried Neumann and Rajenahally V. Jagadeesh

Leibniz-Institut für Katalyse e. V. (LIKAT Rostock), Albert-Einstein-Str. 29a, Rostock, D-18059, Germany

5.1 Introduction

Many ruthenium-catalyzed carbonylations make use of $Ru_3(CO)_{12}$ cluster as potential catalyst without ligand or sometimes together with coordinating P or N ligands. In some reactions, the three-membered cluster remains intact, and the carbonylation occurs on the cluster, while in other reactions, the $Ru_3(CO)_{12}$ cluster cleaves to the mono-ruthenium species $Ru(CO)_5$. These versatilities of ruthenium catalysts result in the ability to activate many different reactions. For example, ruthenium catalyzes well-known industrially important reactions such as typical hydroformylations and alkoxycarbonylations as well as cyclization reactions and direct CH carbonylations. Clearly, rhodium- and palladium-based catalysts are superior compared with ruthenium in the hydroformylation and alkoxycarbonylation reaction, respectively. However, for CH activation of arenes with nitrogen-containing auxiliary groups, ruthenium is considered to be the most efficient catalyst. In addition, ruthenium is also used in the heterogeneous catalysis often in combination with other metals, for example, in the Fischer–Tropsch synthesis (FTS) or in the refinement of syngas to oxo products. Because of this large range of catalytical possibilities, the mechanism of ruthenium catalyzed reactions is often complex and not fully understood yet. Moreover, the oxidation states of ruthenium are in the range of −2 to +8, which makes mechanistical studies more difficult than in the case of group 10 metals (Ni, Pd, Pt) that exist mainly in oxidation states +2 and 0. Here, elementary steps, like oxidative addition, β-hydride elimination, and reductive elimination, are well understood. In addition, the tendency of ruthenium to form the cluster is another problem to predict the mechanism. However, there is a large potential of improving and finding ruthenium-catalyzed reactions, especially when ligands are taken into account for designing new catalysts. More precise studies about the active ruthenium species and knowledge about the decomposition of the cluster are necessary to find more active ruthenium catalysts. In this chapter, the "classical" CH carbonylation of arenes and the Pauson–Khand reaction (PKR) as a milestone in the transition

Carbon Monoxide in Organic Synthesis: Carbonylation Chemistry,
First Edition. Edited by Bartolo Gabriele.

metal chemistry are described [1]. In addition, more recent progress achieved in Ru-catalyzed alkoxycarbonylation and hydroformylation as well as hydrogenation of CO and CO_2 is summarized.

5.2 CH Activation of Nitrogen-Containing Arene Derivatives

Ruthenium-catalyzed CH activation of arenes is an interesting modern field of research because the reaction is 100% atom economic and no production of waste occurs in contrast to aryl halides, where, for example, in coupling reactions 1 equiv base is necessary to regenerate the catalyst. The term CH activation means a reaction that causes C—H bond cleavage by a metal giving an oxidative addition product [2]. In 1993, Murai et al. published a seminal article [3] in which acetophenone and related compounds were alkylated by olefins using 2 mol% of the mononuclear catalyst $RuH_2(CO)(P(C_6H_5)_3)_3$. By refluxing in toluene, the ruthenium complex could insert regioselectively into the *o*-CH bond of acetophenone forming a five-membered metalacycle. The latter, after insertion of an olefin and reductive elimination, released *o*-alkylated acetophenone. Accidently, in the same year, Moore et al. published the other seminal publication [4] concerning CH activation, which is with a certain degree complementary to the first one. Here, pyridine, also used as solvent, was acylated at the C-2 position at 150 °C with 10 bar CO and an olefin. While Murai's reaction proceeded mainly with ketones or esters and was catalyzed by mononuclear $RuH_2(CO)(P(C_6H_5)_3)_3$ complex, Moore's reaction worked only with nitrogen-containing arenes in the presence of a small amount (0.04 mol%) of trinuclear catalyst $Ru_3(CO)_{12}$ and CO. Without CO, no reaction took place even at 180 °C. The olefins could not have β-hydrogen atoms in Murai's reaction for good results, but in Moore's reaction, *n*-alkenes, cyclohexene, and styrenes were tolerated. The reaction mechanism is not fully clarified, but it is generally accepted that the first elementary step is the oxidative addition of pyridine at the expense of two coordinated CO forming complex **A**. Complex **A** (Scheme 5.1) can be obtained by reacting $Ru_3(CO)_{12}$ and pyridine in boiling hexane. This gives a red-orange solid in excellent yield, thus showing that the Ru cluster is conserved [5]. Next, an olefin inserts in the Ru—H bond giving linear and branched (not shown) alkyl complex **B**. In principle, CO can insert in either alkyl–Ru (**C1**) bond or pyridyl–Ru bond (**C2**), and finally the reductive elimination yields isomeric mixtures of linear and branched (not shown) ketones. Since the reaction is first order in pyridine, it is assumed that the Ru cluster survives the catalytic cycle.

Taking up this idea, Murai and coworkers investigated the acylation of 1,2-dimethylimidazole using 2 mol% $Ru_3(CO)_{12}$ with 20 bar CO. In line with the observation of Moore, an acylation at the 4-position of imidazole was exclusively achieved and produced, with 1-hexene, linear (*l*) and branched (*b*) products in 94 : 6 ratio, and 65% yield, but no product in 5-position was observed [6]. The reaction worked well with other olefins such as R = Ph 74%, (*l*:*b*,75 : 25), 2-MeC_6H_4 77% (93 : 7), *t*-Bu 88% (99 : 1), $SiMe_3$ 66% (99 : 1), CH_2SiMe_3 61% (94 : 6), and CH_2CN 42% (87 : 13) (Scheme 5.2).

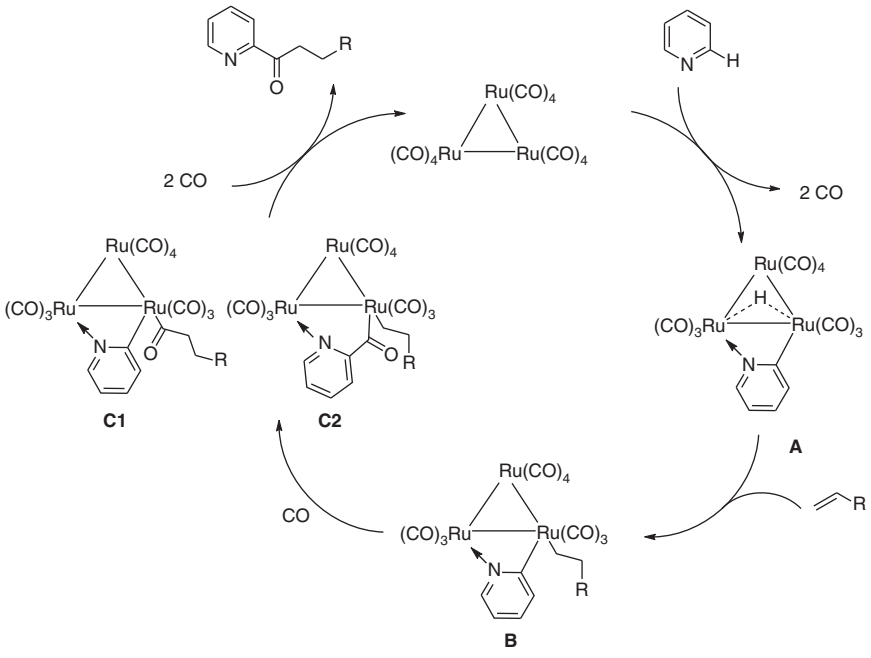

Scheme 5.1 The reaction mechanism for the acylation of pyridine.

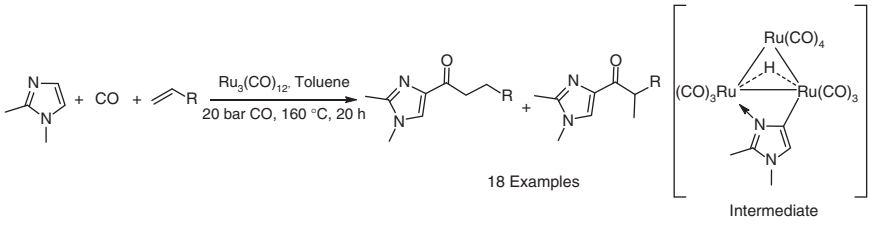

Scheme 5.2 Acylation of 1,2-dimethylimidazole.

The advantage of this type of CH activation is the high regioselectivity depending on the location of the substitutes, which can influence the direction of the acylation. For instance, 1-methyl benzimidazole gives an acylation at C-2 (Scheme 5.3a) [7]. The corresponding intermediate as orange-red crystals could be also obtained by refluxing $Ru_3(CO)_{12}$ and benzimidazole in benzene [8] showing that the nitrogen lone pair is essential for coordination to ruthenium. However, when the 2-position is blocked by a methyl group, then the ruthenium attacks at the 4-position, and CH activation occurs on this position (Scheme 5.3b).

Sterically hindrance by R_1 = *i*-Pr resulted in the decrease of yield to 8%, and an electron-withdrawing acetyl group R_2 = Ac suppressed the product formation completely. Clearly, the insertion of the ruthenium cluster into the CH bond is sensitive to electronic and steric effects. Based on this observation, it is evident that a reduced basicity of the coordinating nitrogen hampers the reaction. For example, 1,2-dimethyl benzimidazole is much more basic (p*K*'s = 6.19 of its conjugated

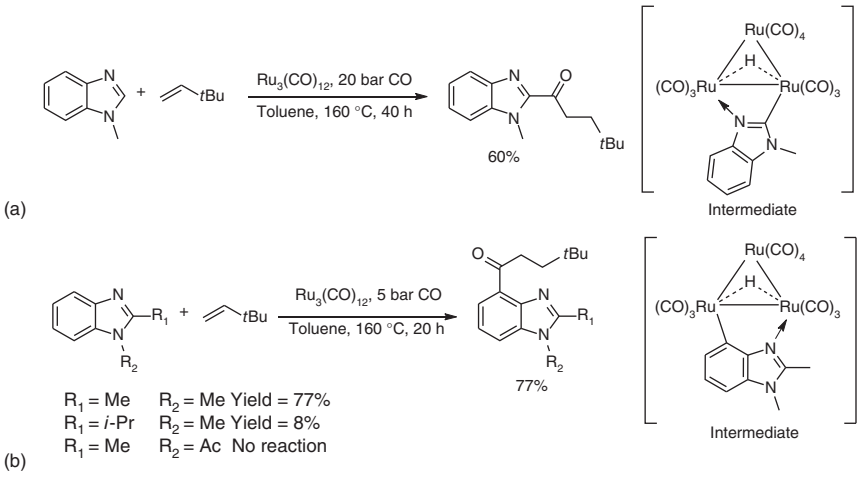

Scheme 5.3 (a) Acylation occurs only on the 2-position of imidazole. (b) Acylation occurs only on the annealed ring, when the 2-position is blocked. Source: Modified from Fukuyama et al. [7].

acid) and more reactive than 2-methylbenzoxazole, which has a lower basicity (p*K*'s = 0.99 of its conjugated acid). Moreover, in the latter case, no reaction is observed. Interestingly, there are substrates in which CH activation has two possibilities and mixtures of acylated product can be achieved. Generally, the more electron-rich CH bond is always favored to the activation toward to the electron poor one [9]. For example, Murai carried out an interesting competition experiment with 1-methyl-2-phenylimidazole (Scheme 5.4a) [10]. Here, CH activation can happen both at the C-4 position of the imidazole ring, as described above, and in the *ortho* position of the phenyl ring. Since the imidazole ring is more electron rich than the phenyl ring, the oxidative addition of ruthenium cluster is favored, giving 79% yield of the corresponding product. The phenyl unit is less electron rich and only 12% of acetylated product is obtained.

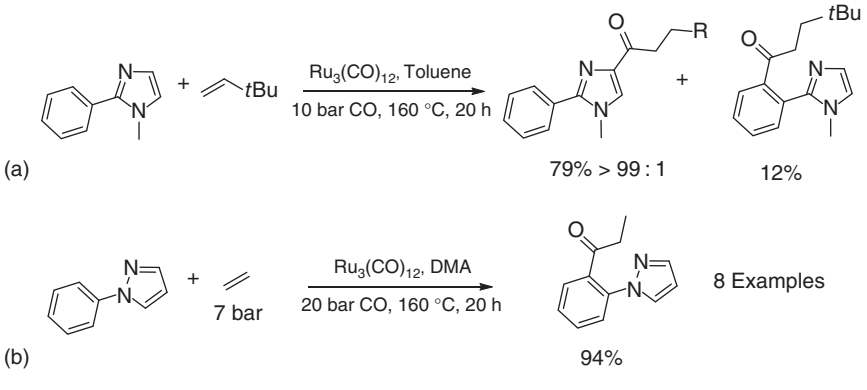

Scheme 5.4 (a) Electron-rich 1-methyl-2-phenylimidazole is mainly acylated at the C-4 position of the imidazole ring. (b) Electron-poor 1-phenyl-1*H*-pyrazole is acylated at the *ortho* position of the phenyl ring. Source: Modified from Chatani et al. [10].

By contrast, a similar experiment with 2-phenyl-1*H*-pyrazole gives exclusively acylation product at the *ortho* position of the phenyl ring (Scheme 5.4b) since the more electron-rich phenyl ring compared with pyrazole favors the CH activation. This behavior is in line with a higher yield of electron-rich phenyl rings bearing OMe and Me (87%), while the withdrawing CF_3 group reduces the yields to 40% [11]. The idea of substituting a benzene ring by an electron poor heteroaromatic compound turned out to be a very successful approach. The heteroaromatic unit can be considered as an untouched directing group.

In this regard, Murai and coworkers investigated the ruthenium-catalyzed carbonylation of 2-phenylpyridine [12]. As shown in Scheme 5.5a, the pyridyl ring is not acylated, because it is electron poor, but the *ortho* position the phenyl ring is acylated on both sites depending on the reaction time. It is believed that a ruthenium mononuclear intermediate is responsible for the oxidative addition in the first elementary step in contrast to the α-acylation of pyridine in the Moore's reaction, where the triruthenium cluster remains intact [13]. To overcome the selectivity problem, a methyl group either *ortho* to the pyridyl ring or *ortho* to the phenyl ring introduced in the 2-phenylpyridine scaffold gives consistent products (Scheme 5.5b). In example c (Scheme 5.5), the necessary coordination of the nitrogen to the ruthenium center is not possible for a second acylation because of the hindered rotation. Another approach to improve the selectivity is to make the pyridyl ring more electron poor by introducing *m*-CF_3 or *m*-ester groups, so a second acylation is completely suppressed. The use of olefin is limited to ethylene that gives 51% acylated product in the reaction (Scheme 5.5a), while only 30% of product is formed with

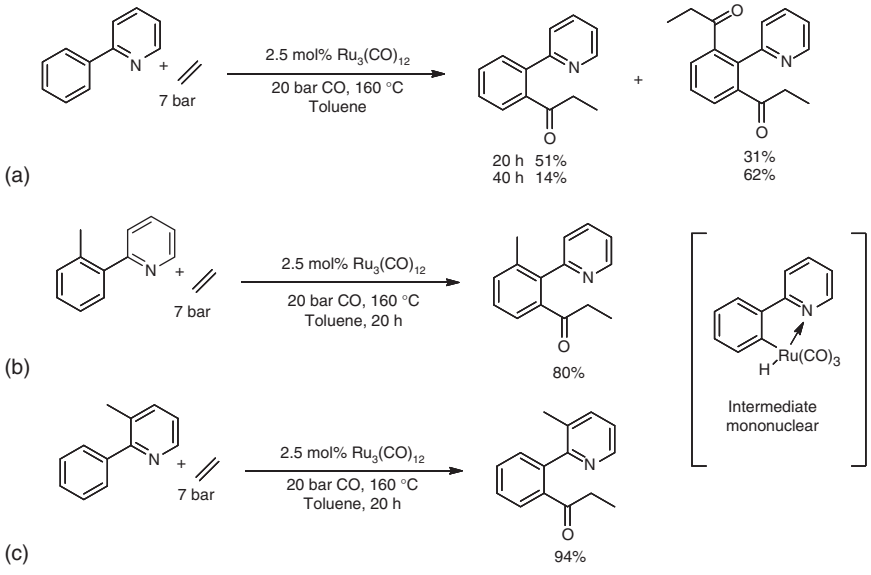

Scheme 5.5 (a) Acylation can occur on each *ortho* position of the phenyl ring. (b) When one *ortho* position is blocked, only the left position can be acylated. (c) A blocked β-position gives rise to mono-acylation of the phenyl ring in *ortho* position.

3,3-dimethyl-1-butene. Olefins such as cyclohexene, allyltrimethylsilane, styrene, methyl methacrylate, vinyl acetate, triethoxyvinylsilane, and isopropenyltrimethylsilane are not reactive in this reaction. However, in the case of styrene, a different synthetic protocol makes the reaction possible (Scheme 5.6) [14]. Using $[Ru(cod)Cl_2]$ polymer as catalyst, the acylation with different styrene derivatives is working, but interestingly only water as solvent is successful in this reaction.

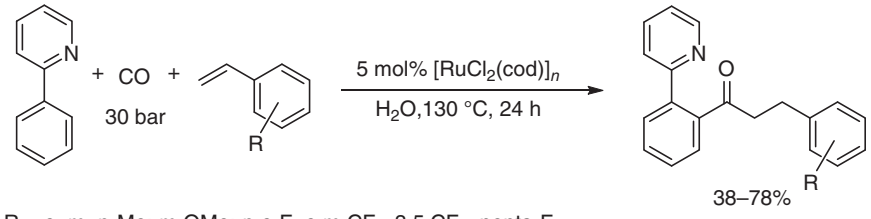

R = *o*, *m*, *p*-Me; *m*-OMe; *p*,*o*-F, *o*,*m*-CF_3, 3,5,CF_3, penta-F

Scheme 5.6 Hydroaroylation of styrene using water as solvent. Source: Modified from Tlili et al. [14].

This concept of the *ortho* CH activation of benzene was further developed and expanded to other directing groups bearing a nitrogen in the arene core. For example, using triazole as directing group, different substituted phenyl triazole derivatives can be acylated according to the reaction pattern mentioned above with 4 mol% $Ru_3(CO)_{12}$, 7 bar ethylene, and 10 bar CO at 160 °C [15].

A drawback of the pyridyl as directing group is the difficulty to remove it after the carbonylation. Therefore, especially useful are such compounds with removable directing groups. Murai and coworkers allowed to react *o*-methylbenzaldehyde with *tert*-butyl amine to obtain the corresponding imine and then carried out the ruthenium-catalyzed acylation with ethylene. Indeed, the imine was cleaved, and an intramolecular ring closure to indenones was achieved [16] (Scheme 5.7).

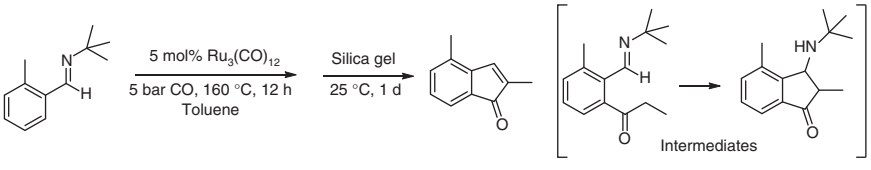

Scheme 5.7 Removing the directing group under ring closure to indenones. Source: Modified from Fukuyama et al. [16].

The most useful substrates are 2-phenyloxazolines derivatives [17] because they have a removable directing group and can be easily synthesized either classically from benzoic acid and 2-amino-2-methyl-1-propanol [18] or through a palladium-catalyzed direct coupling reaction as reported by Ackermann et al. [19]. After the CH activation and acylation, the oxazoline group can be removed either by hydrolysis in sulfuric acid or in a 2-step procedure using MeI, followed by treatment with a 20% NaOH/MeOH solution [20] (Scheme 5.8).

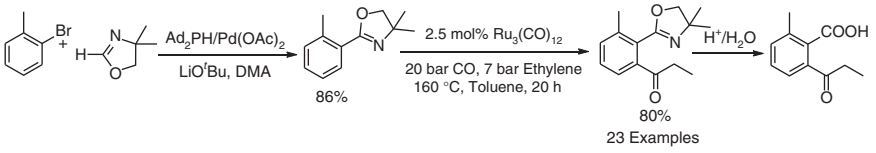

Scheme 5.8 The protecting and deprotecting concept for the 2-phenyloxazolines in the acylation reaction. Source: Modified from Ie et al. [17] and Ackermann et al. [19].

The ruthenium-catalyzed carbonylation of 2-(*o*-methylphenyl)oxazolines works substantially with ethylene and propene to give a mixture of linear and branched isomers (40 hours, 22%, 51 : 49). Unfortunately, the reaction of 1-hexene, *tert*-butylethylene, vinylcyclohexane, isoprene, 1,5-hexadiene, cyclohexene, 1,5-cyclooctadiene, styrene, methyl acrylate, vinyl acetate, allyltrimethylsilane, and triethoxyvinylsilane are not successful. Following the general trend, the electron-poor phenyl groups gave lower yields, but they are more selective than electron-rich phenyl groups. For example, when the phenyl group is substituted by *m*-OMe, even double acylation can be observed while electron-withdrawing groups (CF_3, Br, CN, etc.) give monoacylation. In the case of an *o*-cyano group, the electron density is so low that no reaction is observed. The reaction mechanism is not clarified, but it is believed that the active species has a mononuclear ruthenium center. Wu and coworkers demonstrated that, in place of a CH activation, ruthenium can activate *N*,*N*-dimethyl-2-pyridinylaniline for a carbonylative Suzuki coupling to yield aryl ketones (Scheme 5.9) [21].

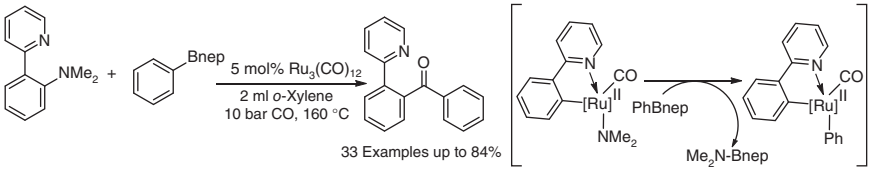

Scheme 5.9 Carbonylative Suzuki coupling of *N*,*N*-dimethyl-2-pyridinylaniline. Source: Modified from Xu et al. [21].

Undoubtedly, $Ru_3(CO)_{12}$ is the main catalyst in the CH activation of arenes assisted by a heteroarene containing nitrogen in either α or β and γ position. However, employing 1-methyl-4-(2-pyridinyl)piperazine (Scheme 5.10a) as substrate, only $Rh_4(CO)_{12}$ and not $Ru_3(CO)_{12}$ works in the acylation reaction. In the first step, the oxidative addition in the sp^3-hybridized CH bond takes place, but, before CO inserts in the ethyl-rhodium complex, β-hydride elimination takes place to yield an enamine and ethane as a side product. The next CH activation of the enamine gives rise to the final acylated product [22]. When 2-pyridyl enamine is used as substrate bearing sp^2-hybridized carbon atoms, again the $Ru_3(CO)_{12}$ complex is active and gives acylated products in high yield (Scheme 5.10b). Moreover, 2-pyridyl enamine substrates tolerate different olefins such as styrene, 3,3-dimethyl-1-butene, and acrylic ester [23].

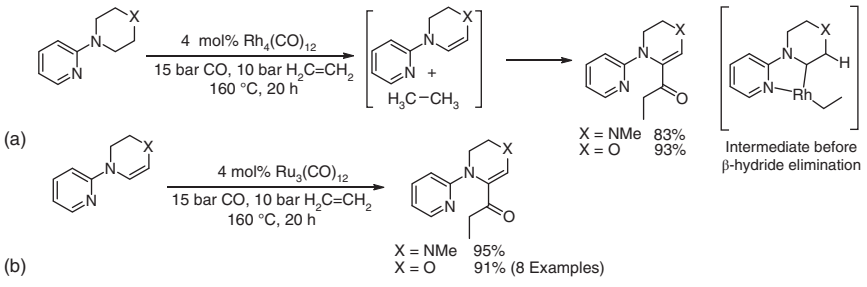

Scheme 5.10 (a) $Rh_4(CO)_{12}$ activates the sp^3-hybridized carbon atoms of piperazine and morpholine residues. (b) $Ru_3(CO)_{12}$ activates only sp^2-hybridized carbon atoms of enamine and enol in the piperazine and morpholine units.

However, Chatani and coworkers showed that a more complicated chelating 2-picolylamide structure can proceed via CH activation even at a sp^3-hybridized carbon [24]. As shown in Scheme 5.11a, a ruthenium species activates the NH bond of the amide and ethylene inserts into the Ru—H bond to give ethyl ruthenium species **a**. The crucial step here is the CH activation of the *tert*-butyl group (R = Me) with releasing of ethane, with formation of intermediate **b**. In this case, ethylene is not the reactant but is a sacrificial molecule. CO insertion and reductive elimination gives *N*-(2-picolyl) succinimide derivatives. The long reaction time (five days) in this case revealed that the activation of sp^3-hybridized CH bond is more challenging and difficult to realize.

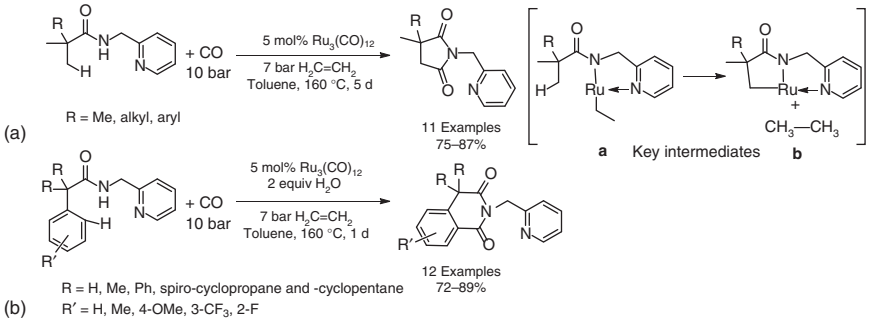

Scheme 5.11 (a) $Ru_3(CO)_{12}$ activates the sp^3-hybridized CH bond of the *tert*-butyl group (R = Me) via ethylene as sacrificial reagent. (b) $Ru_3(CO)_{12}$ activates the sp^2-hybridized CH bond of phenyl via ethylene as sacrificial reagent.

This synthesis concept can be applied to *N*-(2-picolyl)benzylamides [25] as shown in Scheme 5.11b. Again, ethylene is not a reactant, but a sacrificial molecule, and no reaction occurs in the absence of ethylene. The CH activation takes place on the benzyl ring in *o*-position, resulting in isoquinoline-1,3(2*H*,4*H*)-dione products.

5.3 Ruthenium-Catalyzed Carbonylations of Olefins and Nitroarenes

The rhodium-catalyzed hydroformylation of olefins to aldehydes, the palladium-catalyzed alkoxycarbonylation of olefins to esters, and the synthesis of isocyanates using phosgene and anilines are among the most important big-scale processes in the industry. However, there are many approaches that have been developed to replace these established methods by ruthenium-catalyzed procedures.

5.3.1 Ruthenium-Catalyzed Hydroformylations

It is always a milestone when an established industrial process is replaced by another more efficient one. A prominent example is the cobalt-catalyzed hydroformylation of olefins, which is replaced by the more selective and efficient, but much more expensive, rhodium-based systems.

Not surprisingly, Wilkinson et al., who provoked the deep change in the hydroformylation of olefins by using $[RhCl(PPh_3)_3]$ complexes (55 °C, >90 bar H_2/CO) instead of cobalt-based catalysts, also tested for the first time the similar ruthenium complexes $Ru(CO)_3(PPh_3)_2$ [26]. However, it was realized that the reaction needed drastic conditions (100 °C, 100 bar H_2/CO) while the catalytic activity was only moderate. Nevertheless, ruthenium-catalyzed hydroformylation would be an interesting alternative to the established rhodium-catalyzed process because ruthenium is less expensive than rhodium by a factor of 30.

Although there is progress in the ruthenium-catalyzed hydroformylation, still the rhodium system is more efficient by 1–2 orders of magnitude. A direct comparability of a typically rhodium-catalyzed hydroformylation of 10-undecenitrile using phosphinite BiPhePhos with the analogous ruthenium system (Scheme 5.12) shows that, in the case of rhodium, TOF of 4800 h^{-1} is reached, while for the ruthenium system, the TOF is only 120–420 h^{-1} [27]. Nozaki and coworkers carried out a comprehensive study of the $Cp^*Ru(acac)_2$/Xantphos system in the hydroformylation of propylene and 1-decene (Scheme 5.13). Although the TOF of 0.5 h^{-1} is very low, the active species Cp*RuH/Xantphos has been isolated via reduction of the corresponding chloride complex, giving rise to the possibility to investigate the mechanism [28].

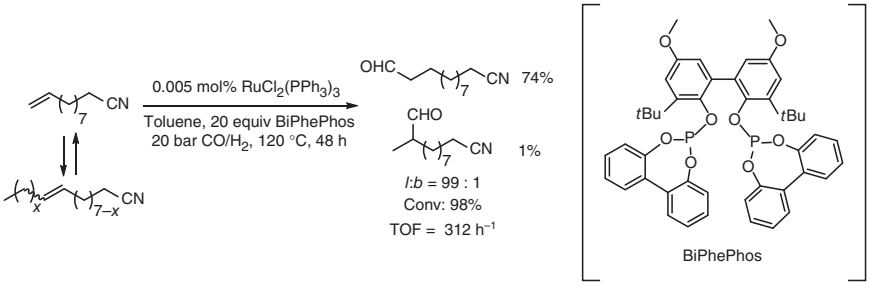

Scheme 5.12 Hydroformylation of 10-undecenitrile.

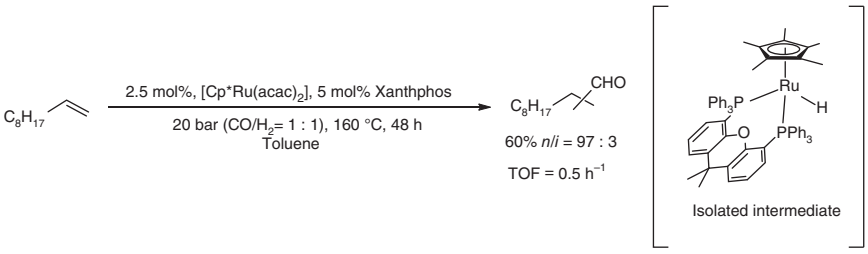

Scheme 5.13 Cp*RuH/Xantphos-catalyzed hydroformylation of 1-decene.

In the hydroformylation reaction, very often alcohols are formed as byproducts by *in situ* hydrogenation of aldehydes. Especially ruthenium complexes are known to be good hydrogenation catalysts, which tend to have this behavior. Beller and coworkers demonstrated that even linear alcohols can be formed with high regioselectivity in a tandem hydroformylation/reduction sequence using $Ru_3(CO)_{12}$ and 2-(dicyclohexylphosphino)-1-(2-methoxyphenyl)-1*H*-imidazole (**L1**) ligand as catalyst system (Scheme 5.14a) [29]. This catalytic system active for both hydroformylation and hydrogenation can also be applied in the hydroaminomethylation (Scheme 5.14b) [30]. However, the reaction needs to be stopped at the stage of aldehyde by reducing the partial pressure of hydrogen and then proceeding the reaction in polycarbonate under milder conditions (Scheme 5.14c) [31]. As a representative example, when 1-octene is subjected to the reaction conditions, a 79% yield of aldehyde with a high *n*/*iso* selectivity of 95 : 5 and TOF of 800 h^{-1} is achieved. Mechanistic spectroscopic/DFT studies show that the [$Ru(CO)_4$**L1**] is the dominant species during the hydroformylation [32].

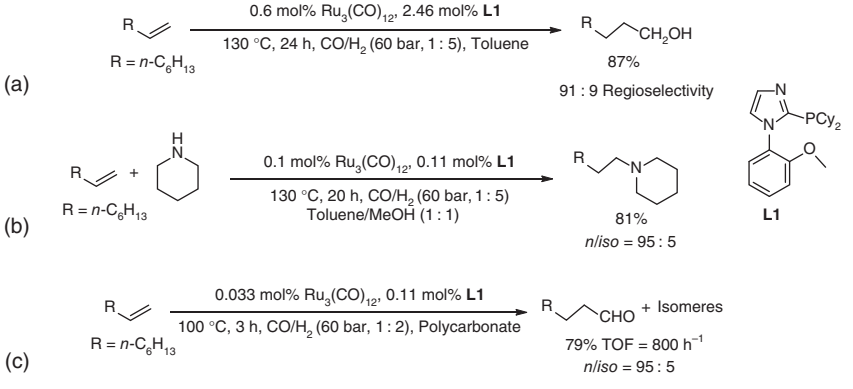

Scheme 5.14 One catalyst system ($Ru_3(CO)_{12}$/**L1**) can give either (a) linear alcohols. Source: Wu et al. [29a] and Fleischer et al. [29b], (b) secondary amines. Source: Wu et al. [30a] and Wu et al. [30b], or (c) linear aldehydes depending on the conditions. Source: Modified from Fleischer et al. [29b].

The superior activity of the $Ru_3(CO)_{12}$/**L1** catalytic system for hydroformylation prompted Behr and coworkers to set up a continuous operating miniplant for the hydroformylation of 1-octene [33]. The isolation of the product is performed

by phase separation between the nonpolar product phase and the polar catalyst *N,N*-dimethylformamide (DMF) phase. A *n*-regioselectivity of 94 : 6, a TOF of 41 h^{-1}, and a space-time of 63 kg/m^3 on a timescale of 90 hours has been achieved. The crucial influence of the ligand on the hydroformylation and the advances made in this area can be seen when looking back in 1996. Mitsudo and coworkers use 1,10-phenanthroline/$Ru_3(CO)_{12}$ system for the hydroformylation of 1-octene, propylene, and ethylene (Scheme 5.15).

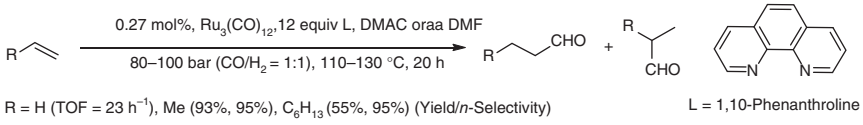

Scheme 5.15 Hydroformylation with $Ru_3(CO)_{12}$/1,10-phenanthroline

Although the yield and *n*-regioselectivity with propylene is high, still the yield in the case of 1-octene is less and only up to 55% with 95% selectivity. The TOFs in the case of propylene and 1-octene are 17 and 10 h^{-1}, respectively. However, the more reactive ethylene gives a TOF of 23 h^{-1} [34]. Like famous Moore's CH activation of pyridine, in which $Ru_3(CO)_{12}$ cluster remains unaffected (see Scheme 5.1), Süssfink and coworkers reported [$NEt_4HRu_3(CO)_{11}$] cluster as the catalyst for the hydroformylation of propylene [35]. As shown in Scheme 5.16, the addition of propylene and insertion of CO take place onto $[HRu_3(CO)_{11}]^-$ hydrido cluster without cleavage. Finally, the addition of hydrogen regenerates the catalyst by releasing butanal.

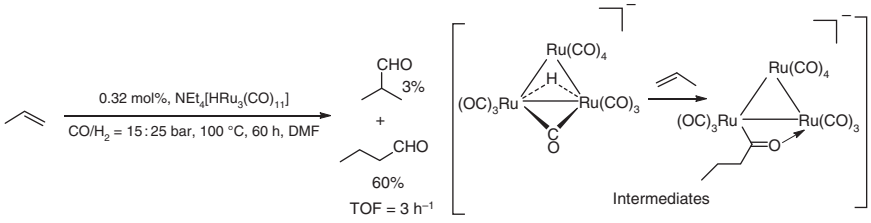

Scheme 5.16 Hydroformylation using $[HRu_3(CO)_{11}]^-$ as catalyst.

Due to its ionic structure, the catalyst can be separated from the reaction solution and reused several times without loss of activity. Khan and coworkers reported another approach such as the Rhône–Poulenc-Process in which the hydroformylation occurs in the water phase using Ru/EDTA (ethylenediaminetetraacetic acid) catalyst (Scheme 5.17).

The authors synthesized a water-soluble K[Ru(III)EDTA(H_2O)] complex, which successfully hydroformylates 1-octene exclusively to give linear nonanal [36] with TOF of 12 h^{-1}. During the reaction, the Ru(III)EDTA complex remains intact, and the elementary steps occur on the axial position of the complex. Similar to the hydroformylation–amination (Scheme 5.14b), Börner and coworkers investigated a tandem hydroformylation–acetalization reaction in which the ruthenium catalyst

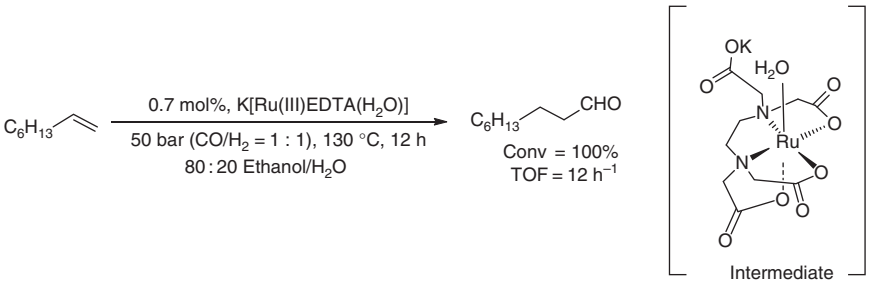

Scheme 5.17 Hydroformylation of 1-octene using K[Ru(III)EDTA(H_2O)].

is immobilized in the ionic liquid phase [BMIM]BF_4, to give, with diols, linear and branched acetals in good yield [37] (Scheme 5.18).

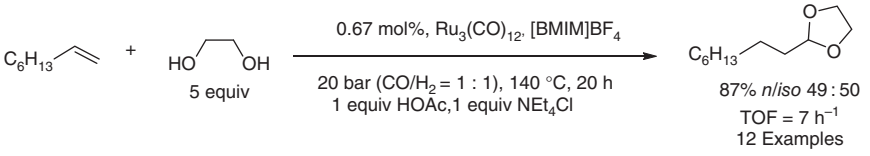

Scheme 5.18 Tandem hydroformylation–acetylation reaction to acetals. Source: Modified from Norinder et al. [37].

Ruthenium-catalyzed hydroformylation can also be carried out with a mixture of CO_2/H_2. Sasaki and coworker used 40 bar CO_2 as carbonylation agent with 40 bar hydrogen and 2 mol% $Ru_4H_4(CO)_{12}$/LiCl as catalyst in *N*-methyl-2-pyrrolidone (NMP) for a tandem hydroformylation/reduction sequence to afford cyclohexylmethanol starting from cyclohexene [38].

5.3.2 Ruthenium-Catalyzed Alkoxycarbonylation of Olefins

Palladium is certainly the most active metal in the alkoxycarbonylation of olefins, among which the methoxycarbonylation of ethylene constitutes the most prominent example reaching TOF of up to 44 000 h^{-1} [39]. There are also ruthenium catalysts, which show activity in the alkoxycarbonylation. Beller and coworkers screened a catalytic system consisting of 1 mol% $Ru_3(CO)_{12}$ and 200 mol% [BMIM]Cl for the alkoxycarbonylation of cyclic olefins (Scheme 5.19) [40]. Linear olefins are also working, but with poor *n*/*i* selectivity. The good solubility of transition metals in the

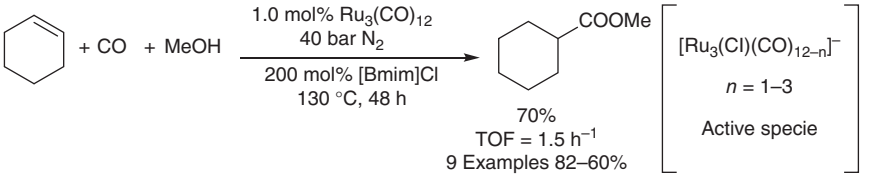

Scheme 5.19 Alkoxycarbonylation of cyclic olefins. Source: Modified from Wu et al. [40].

ionic liquid gives the advantage of reusing the catalyst. The catalyst can be recycled up to three times with moderate loss of activity.

Most likely, the chloride in [BMIM]Cl is responsible for the generation of the active specie $[Ru_3(Cl)(CO)_{12}-n]$ $(n = 1-3)$ and finally for cleaving the Ru cluster to give the mononuclear ruthenium center. Halides are known to cleave $Ru_3(CO)_{12}$ to $Ru(CO)_5$ [41]. Keim and coworkers report about the methoxycarbonylation of olefins in which the CO source is methanol [42] (Scheme 5.20). Interestingly, the ruthenium catalyst dehydrogenates methanol to give CO and hydrogen (via formaldehyde) and then catalyzes the methoxycarbonylation. In this case, methanol is used as solvent, CO source, and one of reactants (methyl source) for forming the methyl ester.

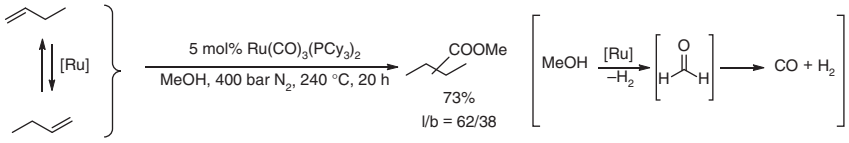

Scheme 5.20 Methoxycarbonylation of 1-butene using methanol as CO source. Source: Modified from Behr et al. [42].

The hydrogen is necessary to form a Ru–H species, which adds to the double bond giving a butylruthenium complex. CO insertion and methanolysis of the acyl complex yields the product. Taking the stoichiometry into account, Keim and coworker tested methyl formate as CO surrogate in the methoxycarbonylation of ethylene. A relatively high catalyst loading of 20 mol% $Ru_3(CO)_{12}$ is necessary to give methyl propionate in 92% yield at 230 °C [43]. The group of Mortreux and coworkers developed this idea further and applied methyl formate in combination with 0.04 mol% $[RuCl_2(CO)_3]_2$ and 0.08 mol% Et_4NI as a promoter in the methoxycarbonylation of ethylene and achieved high TOFs of 1500 h^{-1} (Scheme 5.21) [44]. The mechanism involves a direct activation of methyl formate rather than decomposition to CO and methanol.

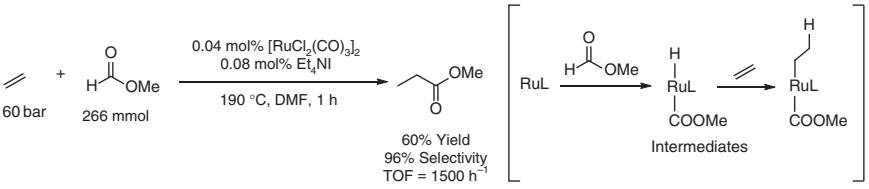

Scheme 5.21 Methyoxycarbonylation of ethylene with methyl formate using $[RuCl_2(CO)_3]_2$ and Et_4NI as catalyst. Source: Modified from Legrand et al. [44].

Another promoter recognized as active for the methoxycarbonylation of ethylene is bis(triphenylphosphine)iminium chloride ([PPN]Cl). With $Ru_3(CO)_{12}$, this promoter forms labile cluster of the types $[PPN][Ru_3(\mu\text{-}Cl)(CO)_9]$ and $[PPN]_2[Ru_4(\mu\text{-}Cl)_2(CO)_{11}]$ (Scheme 5.22) [45]. Using this catalytic system, 99% yield of methyl propionate with 99% selectivity and TOF of 28 h^{-1} is achieved. More

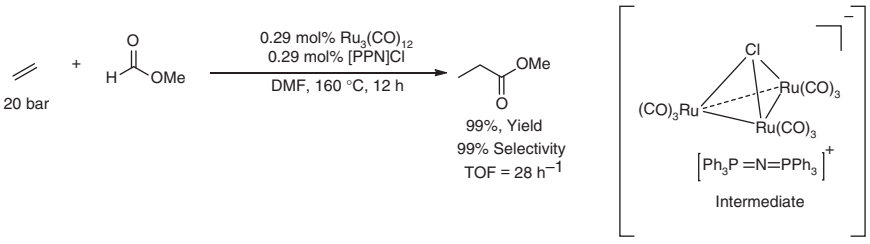

Scheme 5.22 Methyoxycarbonylation of ethylene with methyl formate using $Ru_3(CO)_{12}$ and [PPN]Cl as catalyst. Source: Modified from Lavigne amd Lugan [45].

detailed studies show that the cluster $[PPN]Ru(CO)_3Cl_3$ synthesized from $RuCl_3$, CO, and [PPN]Cl gives TOF = 170 h^{-1} [46].

A Chinese group combined the two promoters [PPN]Cl and Et_4NI with $RuCl_3$ to obtain an efficient catalytic system, which gave a TOF of 146 h^{-1} [47]. A more industrial alternative using $RuCl_3$/NaI catalyst system gives similar results. A very green and sustainable method for the alkoxycarbonyaltion of olefins exploits the use of carbon dioxide, which is reduced *in situ* to either CO or methyl formate (Scheme 5.23) [48]. Competitive experiments show that most likely CO_2 is reduced to CO, which is responsible for the carbonylation.

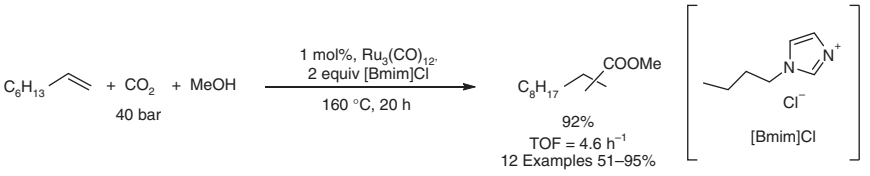

Scheme 5.23 Methoxycarbonylation with carbon dioxide. Source: Modified from Wu et al. [48].

Linear olefins (with poor regioselectivity) and cyclic olefins have been alkoxycarbonylated in good yield. Another way to synthesize esters from olefins is to use paraformaldehyde as CO source (Scheme 5.24). As an example, the $Ru_3(CO)_{12}/PCy_3$ catalytic system in the presence of two equivalents BMIMCl converts cyclic olefins and styrenes to the corresponding esters using paraformaldehyde. In the case of 1-octene, 74% of yield with 51 : 40 regioselectivity is achieved. Labeling experiments with ^{13}C MeOH show clearly that the CO does not derive from methanol but comes from paraformaldehyde. Due to the use of BMIMCl as ionic liquid, the catalyst can be recycled up to four times [49].

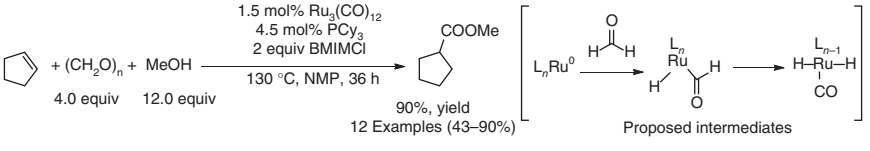

Scheme 5.24 Paraformaldehyde as CO surrogate in the methoxycarbonylation of olefins.

5.3.3 Carbonylation of Nitroarenes

Isocyanates, especially diisocyanates, are basic starting materials for the synthesis of polyurethanes, which are important industrial products used for thermoplastic foams, elastomers, and agrochemicals. Classically, isocyanates are synthesized in two steps from nitrobenzenes, which are reduced to anilines first and finally converted to isocyanates by reaction with phosgene. Although the reaction with phosgene is selective and gives high yields, 2 equiv of HCl waste are formed that must be separated from overstoichiometrically phosgene by an expensive cooling technology. A more interesting method is the metal-catalyzed carbonylation of nitrobenzene to urethane in the presence of ethanol or methanol. At 250–285 °C, the urethane releases ethanol by forming isocyanate (Scheme 5.25). Many catalytic systems based on Pd, Pt, Rh, Ru, Se, Ni, and Cu are showing activities, but the phosgene route is still the dominant procedure in the industry.

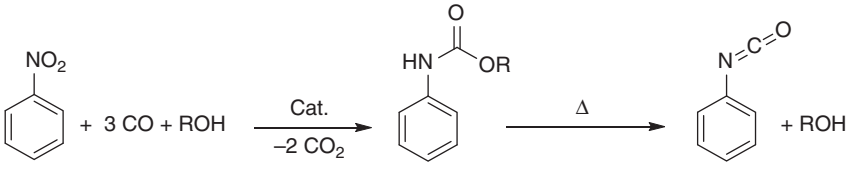

Scheme 5.25 Metal-catalyzed carbonylation of nitrobenzene to carbamate.

A pilot process developed by Mitsubishi Chemical uses SeO_2 as catalyst in this reaction, but selenium is too toxic for setting up a plant and contaminates the products. Another pilot process by Asahi Chemical company performed the synthesis of carbamates via oxidative carbonylation of anilines in the presence of MeOH using Pd/I^- as catalyst [50]. The most promising system for the synthesis of carbamates is the palladium-catalyzed carbonylation of nitrobenzene because high activity without corrosion makes this catalyst system attractive for an industrial process (Scheme 5.26a) [51]. In the presence of *p*-TsOH, only 0.045 mol% $Pd(OAc)_2$

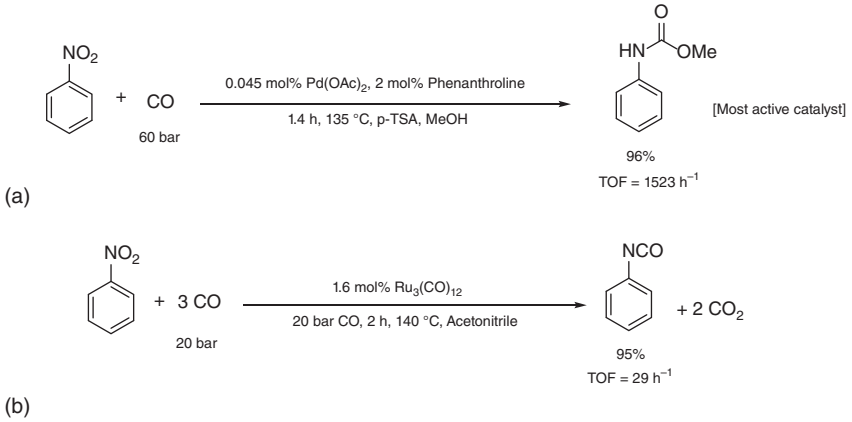

Scheme 5.26 (a) Synthesis of carbamate via palladium-catalyzed carbonylation of nitrobenzene. Source: Cenini and Ragaini [51]. (b) $Ru_3(CO)_{12}$-catalyzed carbonylation of nitrobenzene to phenylisocyanate. Source: Modified from Basu et al. [52].

and 2 mol% phenanthroline as ligand are needed to obtain 96% yield of carbamate. The reaction proceeds at 60 bar of CO at 135 °C in MeOH with a TOF of 1523 h^{-1} [53]. Ruthenium-catalyzed reactions do not reach this activity, but a direct synthesis from nitrobenzene to phenylisocyanate has been realized using 1.6 mol% $Ru_3(CO)_{12}$ at 20 bar CO and 140 °C to give 95% of product (Scheme 5.26b) [52].

One of the best investigated and explored catalysts for reductive carbonylation of nitroarenes to urethanes is the $Ru(CO)_3$DPPE complex **A** shown in Scheme 5.27 [54]. Nitroarenes combined with one aliquot of aniline are carbonylated in the presence of methanol and 1.2 mol% $Ru(CO)_3$DPPE at 68 bar CO at 160 °C to give 88% of urethane. The reaction is completed after 1.5 hours and achieves 49 h^{-1} of TOF. Complex **A** transfers one electron from the outer sphere to the nitroarene, and after the radicals collapse, the $Ru(CO)_2(DPPE)\mu_2$-ArNO complex **B** is formed with the release of CO_2 [55].

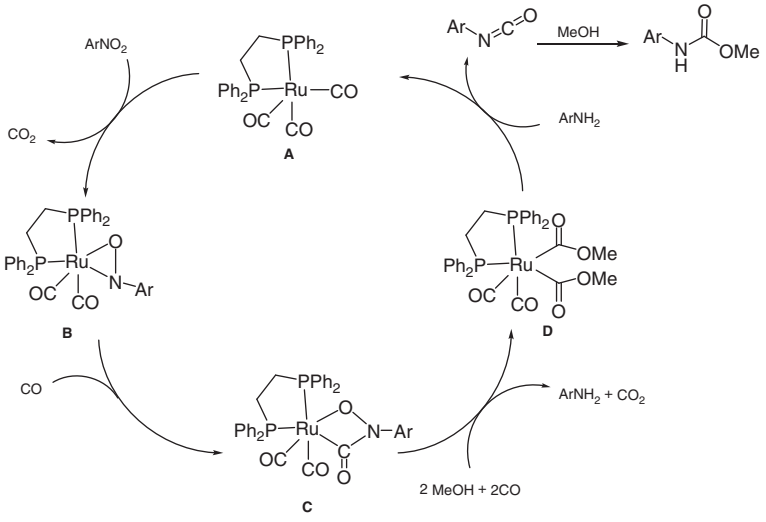

Scheme 5.27 Reaction mechanism of nitroarene carbonylation to carbamate. Sources: Cenini and Ragani [54].

With 5-chloro-2-nitrobenzotrifluoride as substrate, the X-ray structure of complex **B** (Scheme 5.27) was obtained, showing that electron-withdrawing groups stabilize complex **B**. In the presence of CO, complex **B** is immediately carbonylated to complex **C**, which was characterized by NMR and X-ray structure for Ar = *o*-tolyl [56]. Complex **C** reacts with MeOH and CO to form complex **D** by releasing aniline [57]. Aniline displaces a methoxy group in complex **D** and decomposes the complex to form isocyanate, which reacts further to give the carbamate.

The other efficient ruthenium catalyst (TOF = 62 h^{-1}) for the carbonylation of nitrobenzene utilizes 1 mol% $Ru_3(CO)_{12}$ and 7 equiv $[NEt_4]Cl$, which gives 93% urethane at 170 °C and 60 bar CO in 1.5 hours. Different nitroarenes substituted with Me, CF_3, CO_2Me, and Cl groups are tolerated (73–88%) [58]. Mechanistically, it is

believed that mono- (Scheme 5.28a) or bis-arylimido-capped clusters are intermediates in this reaction [60]. The structures of mono- [61] and bis-arylimido-capped clusters [62] were confirmed by single-crystal diffraction.

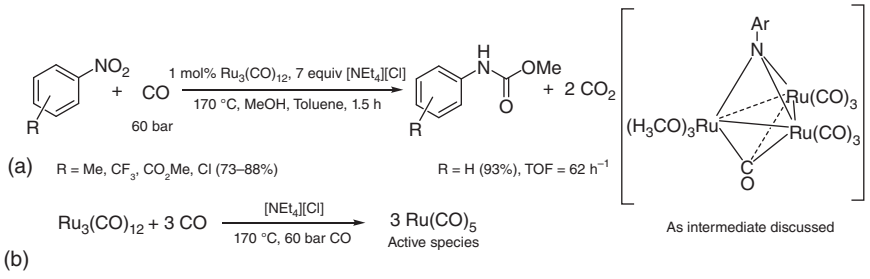

Scheme 5.28 (a) An arylimido-capped clusters as intermediate is proposed for the carbonylation of nitrobenzene. (b) Alternatively, $Ru(CO)_5$ as catalytical active species is responsible for the carbonylation of nitrobenzene. Source: Modified from Ragaini et al. [59].

However, under the conditions described by Cenini and coworker, high-pressure infrared (IR) *in situ* spectroscopy demonstrated that the active species is mainly $Ru(CO)_5$. Here, the role of chloride stemming from $[NEt_4][Cl]$ salt is important in promoting both the cleavage of the ruthenium cluster and the reaction with nitrobenzene via $Ru(CO)_4Cl^-$ as a probable intermediate (Scheme 5.28b) [59]. Analogous to carbamates, the preparation of ureas can be achieved by ruthenium-catalyzed carbonylation of nitrobenzene and aniline (Scheme 5.29). An efficient catalyst (TOFs up to 65 h^{-1}) for this reaction is the Merrifield-anchored 2-(2-pyridyl)benzimidazole polymeric Ru-Py-Mer catalyst, which allows up to six times recycling without significant loss of product yield [63].

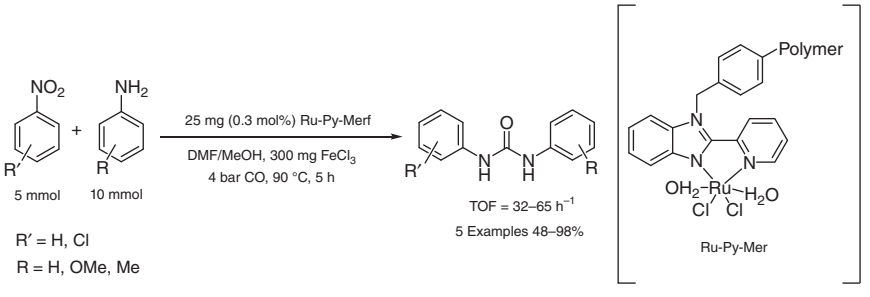

Scheme 5.29 Synthesis of unsymmetrical urea from anilines and nitrobenzenes.

Different symmetrically substituted ureas are prepared in >90% yield. A similar polymer-supported ruthenium(II) catalyst, $[Ru(PSimd)(CO)_2Cl_2]$, based on Merrifield-anchored imidazole ligands, also gives good results with good recovery [64]. Diphenylurea is also obtained via oxidative carbonylation of aniline using $Bu_4N(Ru(CO)_3I)$ complex under 38 bar CO and 3 bar O_2 (67% yield, Scheme 5.30) [65].

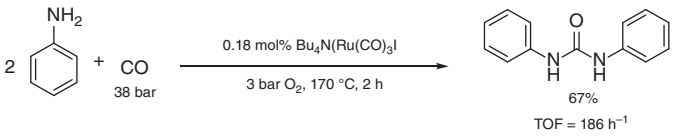

Scheme 5.30 Oxidative carbonylation of aniline to diphenylurea. Source: Modified from Mulla et al. [65].

5.4 Ruthenium-Catalyzed Carbonylation of Amines and Alcohols

The ruthenium-catalyzed carbonylation of piperidine to *N*-formylpiperidine is a very good method, but harsh conditions are required [66]. The reaction is carried out under neat conditions with 0.16 mol% $RuCl_3$ and 100 bar CO at 180 °C. Also, other cyclic amines such as pyrrolidine and morpholine are successfully carbonylated. In this reaction, the imine shown in Scheme 5.31a is considered to be the key intermediate. A metal-free catalyzed process is also possible (Scheme 5.31b) [67].

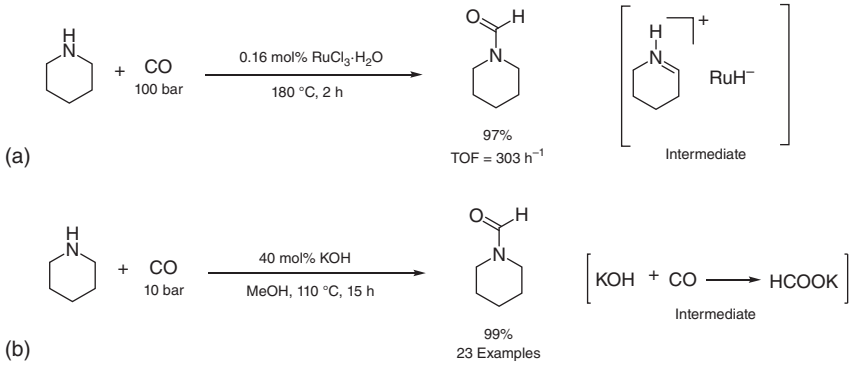

Scheme 5.31 (a) Ruthenium-catalyzed carbonylation of piperidine. Source: Modified from Jenner et al. [66]. (b) Metal-free carbonylation of piperidine. Source: Modified from Li [67].

The use of methanol as solvent allows to carbonylate linear dialkyl amines in good yields and selectivities, but harsh conditions are still necessary (450 bar CO, 200 °C) [68]. Milder conditions for the carbonylation of octylamine and benzylamine are possible using 0.17 mol% $Ru_3(CO)_{12}$ catalyst and running the reaction in benzene at 120 °C and 40 bar CO [69]. Interestingly, *in situ* high-pressure IR spectroscopy shows that, during the carbonylation of piperidine, the $Ru_3(CO)_{12}$ catalyst is decomposed to $Ru(CO)_5$ after a few hours of reaction under 10 bar of CO at 60 °C, which indicates that the active species is probably $Ru(CO)_5$ [70].

Similar to the formylation of amines, alcohols can be carbonylated in a ruthenium-catalyzed reaction to obtain alkyl formates. As an example, $Ru_3(CO)_{12}$ catalyzes the formylation of primary alcohols in pyridine as the solvent to give formates with high selectivity but in moderate yields (Scheme 5.32a) [71]. Alternatively, primary alcohols can be carbonylated to esters and acids in moderate yields, but harsh conditions are required too (Scheme 5.32b) [72].

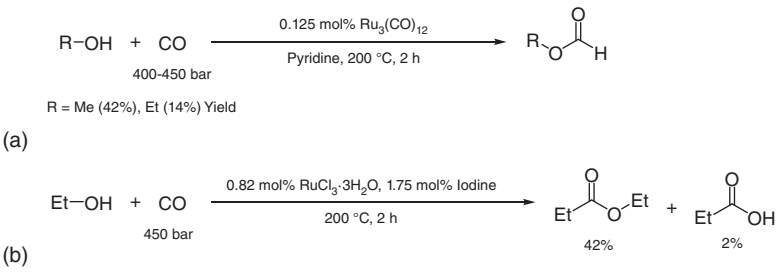

Scheme 5.32 (a) Carbonylation of alcohols to formates. (b) Carbonylation of alcohols to esters and acids. Source: Modified from Jenner and Bitsi. [71].

5.5 Ruthenium-Catalyzed Cyclocarbonylations

The Pauson-Khand reaction (PKR) belongs to a widespread class of cyclization reaction that combines a (hetero) double bound, an alkyne or alkene, and CO to give cyclopenta(e)nones, lactones, and lactames. This reaction offers a lot of possibilities for the design of new drugs and the synthesis of natural compounds.

The ruthenium-catalyzed PKR was discovered by Mitsudo et al. in 1997. They investigated the oxidative addition induced by a [2+2] cycloaddition of norbornene with an alkyne, which gives rise to the formation of a ruthenacyclopentene as a key intermediate. Also, they hypothesized that an insertion of CO in such a ruthenacyclo-pentene would allow for a [2+2+1] PKR for the preparation of cyclopentenones (Scheme 5.33a) [73]. The intramolecular version of this PKR (with 2 mol% $Ru_3(CO)_{12}$ and 15 bar of CO in *N,N*-dimethylacetamide (DMAC)), applied to 1,6-enyne derivatives, produced the corresponding cyclopentenones (Scheme 5.33b).

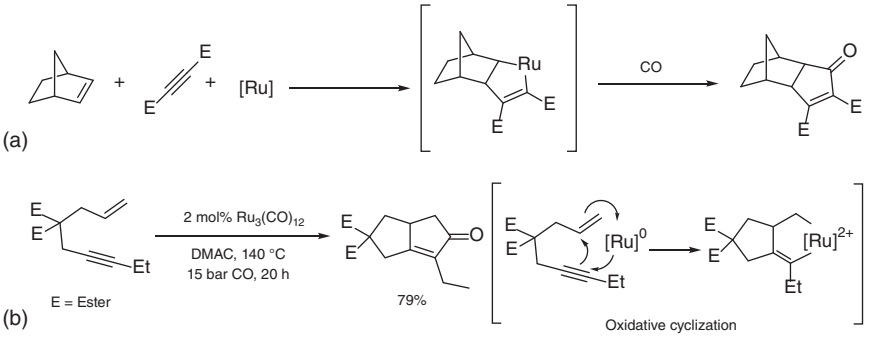

Scheme 5.33 (a) Hypothesized [2+2+1] intermolecular Pauson-Khand reaction. (b) Implemented [2+2+1] intra molecular Pauson-Khand reaction. Source: Modified from Kondo et al. [73].

Independently, in the same year, Murai et al. published a similar synthetic protocol using 2 mol% $Ru_3(CO)_{12}$ and 10 bar CO in dioxane as the solvent. Murai used also other 1,6-enyne derivatives connected with oxygen and NTs groups

instead of the maloneic unit. Because of the chelating behavior of 1,6-enynes, the intramolecular PKR is favored over the intermolecular one, which remained a challenge for a long time. However, significant progress has been accomplished not by finding a new catalyst, which is still 5 mol% $Ru_3(CO)_{12}$, but by applying dimethyl(2-pyridyl)(vinyl)silane as the olefinic component [74]. As shown in Scheme 5.34a, the dimethyl(2-pyridyl)(vinyl)silane agent acts as a chelating ligand coordinating the Ru center in a certain direction, which is important for the regioselective outcome.

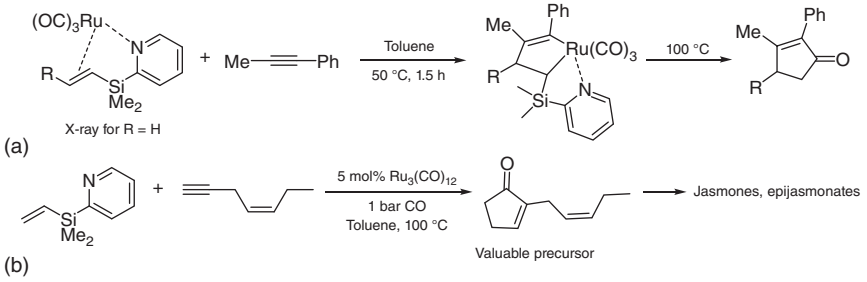

Scheme 5.34 (a) Intermolecular [2+2+1] Pauson-Khand reaction with a removable auxiliary group. (b) A useful example for the intermolecular [2+2+1] Pauson-Khand reaction with a removable auxiliary group.

It should be noted that this behavior is different from a conventionally PKR in which the alkyne first coordinates to the metal since alkynes are stronger donors. After oxidative cyclization with an alkyne and CO insertion, the 2-pyridylsilane group can be removed by desilylation. This is a most valuable step to access natural products and drug precursors (Scheme 5.34b). Later on, Murai and coworkers showed that the intramolecular [2+2+1] PKR can be easily extended to hetero double bonds using either yne-aldehyde or yne-imine each with three carbon tethers. With a similar synthetic protocol using $Ru_3(CO)_{12}$ as catalyst, the preparation of α,β-unsaturated lactones (Scheme 5.35a) [75] and α,β-unsaturated lactams was achieved (Scheme 5.35b) [76].

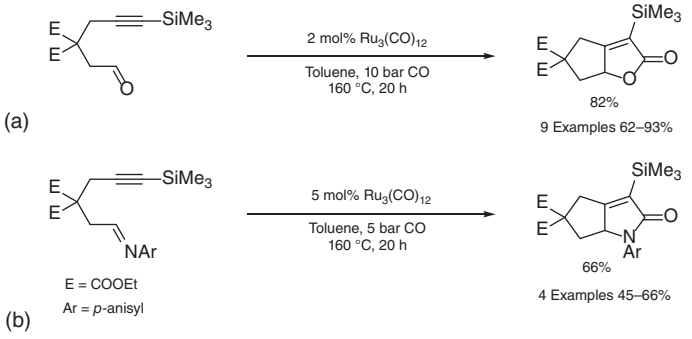

Scheme 5.35 (a) Hetero [2+2+1] Pauson-Khand reactions giving lactones. Source: Modified from Chatani et al. [75]. (b) Hetero [2+2+1] Pauson-Khand reactions giving lactams. Source: Modified from Chatani et al. [76].

It is a general idea to activate both $Ru_3(CO)_{12}$ and the substrate by a nitrogen-containing auxiliary arene in proximity to the reacting group often realized by a pyridyl unit. For example, in the hetero [2+2+1] PKR in which the alkyne part is replaced by an alkene, only activated ketones bearing a 2-pyridyl unit in α-position are suitable substrates, leading to γ-lactones (Scheme 5.36a). Via O and N coordination, an activated cyclic ruthenium complex is formed, which can react with ethylene and CO to generate probably a six-membered ruthenacycle, which furnishes γ-lactones as final products after reductive elimination. Murai and coworkers demonstrated that other ketones, such as acetyl pyrazine, acetyl thiazol, and acetyl oxazole possessing a sp^2 nitrogen in β-position, give excellent yields of the corresponding lactones [77]. The reaction also works with an α-ketoester, when the auxiliary is a carbonyl group, taking over the function of the pyridyl moiety (Scheme 5.36b) [78].

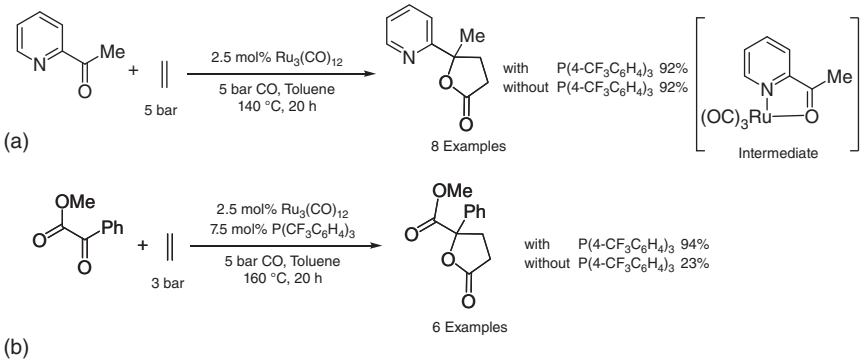

Scheme 5.36 (a) 2-Pyridyl ketone. Source: Modified from Tobisu et al. [78] and (b) α-ketoester in the [2+2+1] hetero Pauson-Khand reaction for γ-lactones syntheses. Source: Modified from Chatani et al. [78].

Interestingly, catalyst precursor, $Ru_3(CO)_{12}$ itself, is active in PKRs without the requirement of any phosphine ligands. However, in the case of α-ketoesters, the addition of 7.5 mol% weak basic ligand $P(4\text{-}CF_3C_6H_4)_3$ increases the γ-lactone yield up to 94%. By contrast, when no ligand or the more basic $P(4\text{-}OMeC_6H_4)_3$ ligand are used, only 23% and 59% yields are achieved, respectively.

Inspired by the [2+2+1] hetero-PKR for the preparation of γ-lactones, Snapper and coworkers carried out a tandem olefin metathetic hetero-Pauson–Khand sequence

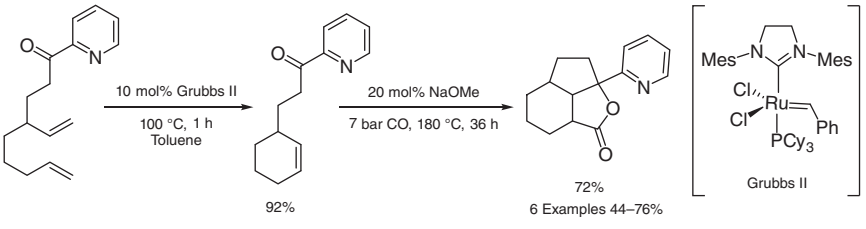

Scheme 5.37 Ring-closing metathesis and subsequent hetero-Pauson–Khand reaction. Source: Modified from Finnegan and Snapper [79].

to synthesize polycyclic lactones in one pot (Scheme 5.37) [79]. For this purpose, a special aroyl pyridine was synthesized in three steps from a suitable diene precursor. The metathesis proceeds with 10 mol% Grubbs II catalyst at elevated temperature to give 92% of the metathesis product. A temperature of 100 °C is necessary to avoid blocking the catalyst by coordination with the pyridine.

Before the subsequent hetero-PKR can take place, the catalyst must be reduced by adding 20 mol% of NaOMe. Finally, with 7 bar CO at 180 °C, the polycyclic γ-lactone is obtained in 72% yield. The concept of hetero-PKR can also be applied to iminopyridines or 1,2-iminoester, which react to give lactams (Scheme 5.38a) [80], and in analogous fashion, a [2+2+1] cycloaddition allows the reaction of ketimines to give spiro-lactams (Scheme 5.38b) [81].

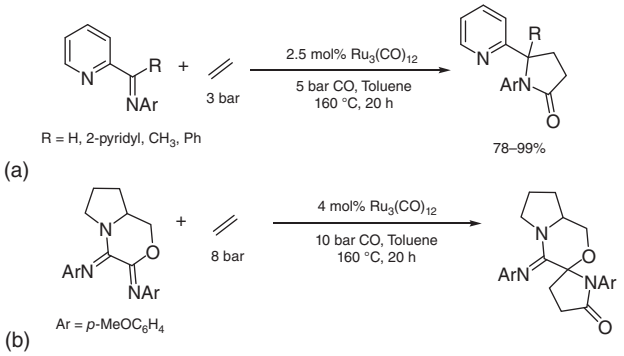

Scheme 5.38 [2+2+1] Hetero Pauson-Khand reaction with (a) iminopyridines and (b) ketimines giving lactams. Source: (a) Modified from Chatani et al. [80]. (b) Modified from Göbel and Imhof [81].

α,β-Unsaturated imines are candidates for the [4+1] cyclization in a hetero-PKR. The nitrogen of imine anchors a "$Ru(CO)_4$" species, and the resulting ruthenacycle gives, after insertion of CO and isomerization, γ-lactams in high yield (Scheme 5.39) [82].

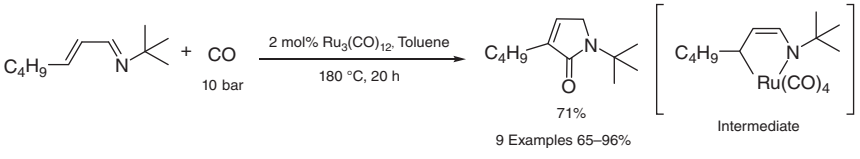

Scheme 5.39 [4+1] Hetero-Pauson–Khand reaction with imines. Source: Modified from Morimoto et al. [82].

The $Ru_3(CO)_{12}$-catalyzed [2+2+1+1] cyclization of acetylene with CO (120 bar) and H_2 (10 bar) gives hydroquinone (59%) at 200 °C. This is an industrially driven chemistry using basic chemicals. Similar approaches were carried out by Reppe et al. using $[Fe(NH_3)_6][Co(CO)_4]_2$ and $[Co(NH_3)_6][Co(CO)_4]_2$ catalysts to produce 35–50% of hydroquinone [83]. Interestingly, Murai et al. developed a hydroquinone synthesis with alkyl-substituted acetylenes and norbornene as the only working olefin, using 2 mol% $Ru_3(CO)_{12}$ as catalyst (Scheme 5.40a) [84].

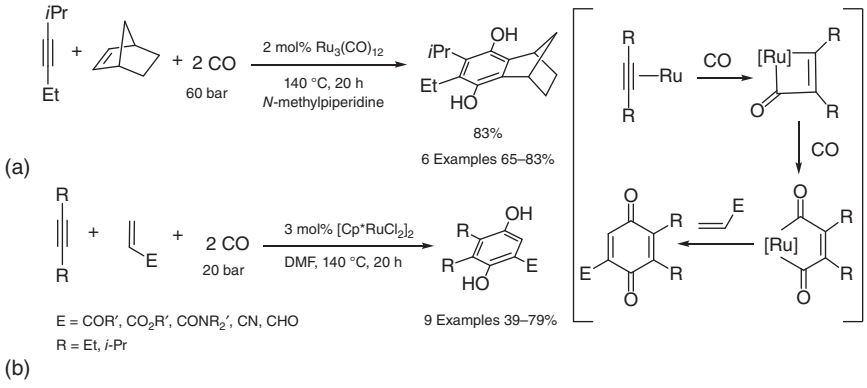

Scheme 5.40 (a) [2+2+1+1] Cycloaddition of alkynes, norbornene and CO for the synthesis of hydroquinones. Source: Modified from Suzuki et al. [84]. (b) [2+2+1+1] Cycloaddition of alkynes, acrylates or α, β-unsaturated olefins and CO for the synthesis of hydroquinones. Source: Modified from Fukuyama et al. [85].

Later on, the scope was expanded by employing 3 mol% $[Cp^*RuCl_2]_2$, which also tolerated both acrylates and α,β-unsaturated olefins (Scheme 5.40b) [85]. By DFT calculations, Murai's [2+2+1+1] cyclization assumes that ruthenacyclobutenone formation is the first elementary step in the reaction path, leading to the hydroquinone formation [86].

The α,β-unsaturated γ-lactone motif, which occurs frequently in natural products, is accessible by carbonylative cyclization of allenyl alcohols [87]. The reaction proceeds in dioxane at 100 °C with 10 bar CO, 1 mol% $Ru_3(CO)_{12}$, and 1.5 equiv NEt_3 and tolerates alkyl and phenyl substituents (Scheme 5.41a). With homoallenyl alcohols ($n = 2$), six-membered δ-lactones can also be prepared. An analogous reaction with α- NH-tosylate (NHT) group in place of hydroxy converts allenyl (homo) sulfonamides to α,β-unsaturated γ-lactams or δ-lactams, respectively, under similar conditions (dioxane, 20 bar CO, NEt_3, 100 °C) [89].

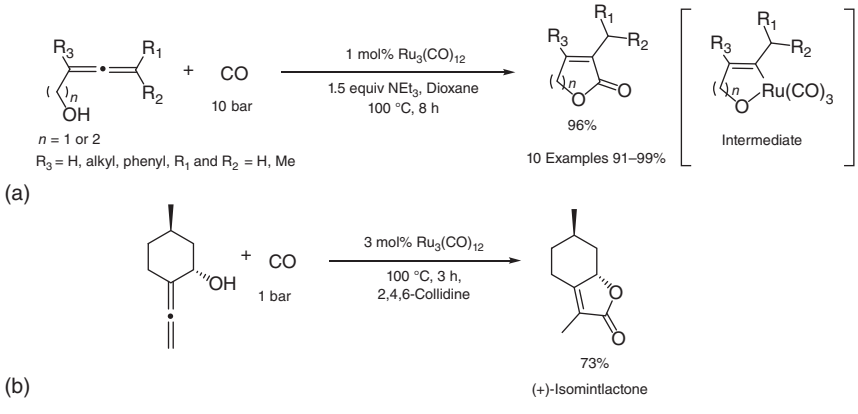

Scheme 5.41 (a) Carbonylative cyclization of allenyl alcohols to α,β-unsaturated γ-lactones. Source: Yoneda et al. [87]. (b) Synthesis of the natural product (+)-isomintlactone. Source: Modified from Tsubuki et al. [88].

In a modification of this synthetic protocol, 2-ethenylidene 5-methyl cyclohexanol is cyclized to the natural product (+)-isomintlactone with retention of the chiral center by running the reaction in 2,4,6-collidine at 1 bar CO and 100 °C (Scheme 5.41b) [88].

5.6 Ruthenium-Catalyzed Reactions Using Syngas

5.6.1 Fischer–Tropsch Synthesis

The FTS is a chemical process that transforms solid coal to a liquid fuel. In a highly endothermic reaction ($\Delta H = +119$ kJ/mol), coal and water react to give syngas (H_2/CO), which are converted in a very exothermic reductive oligomerization process over heterogeneous catalysts to a mixture of liquid or solid hydrocarbons. Instead of coal, also biomaterials can used as a feedstock. The initial step in the formation of these products is the cleavage of adsorbed CO. The nascent carbon is hydrogenated to CH and CH_3 species, which serve as monomer and chain initiator. By insertion of CH_2 in an absorbed alkyl group, chain propagation occurs. This progress is terminated either by β-hydride elimination, giving linear olefins; otherwise paraffins are produced by addition of hydrogen to alkyl species. The chain length depends on the catalyst and conditions. Ruthenium is known to be a very efficient catalyst, giving even long-chain alkanes with molecular weight of up to 1 000 000 at 150–100 bar and 100–180 °C. This polymer has similar properties to Zieglers-type low-pressure polyethylene (Scheme 5.42a) [90]. By contrast, at low pressure (10 bar) and at 220–340 °C, the ruthenium catalyst produces only methane (Scheme 5.42b).

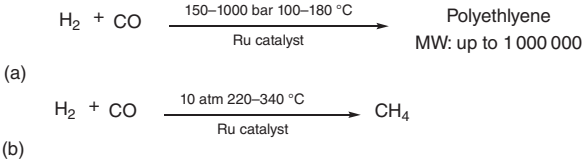

Scheme 5.42 Ruthenium-catalyzed Fischer–Tropsch synthesis using (a) high pressure gives polyethylene and using (b) low pressure gives methane. Source: Keim [90].

Many FTS studies about heterogeneous ruthenium catalyst have been carried out. Hensen and coworkers investigated Ru nanoparticles in aqueous-phase FTS modified by organic capping agents such as trimethyl(tetradecyl)ammonium bromide (TTAB), polyvinylpyrrolidone (PVP), and sodium 3-mercapto-1-propanesulfonate (SMPS). Organic capping agents control the growth of nanoparticles and agglomeration during the synthesis. The activity increases in the order Ru–SMPS < Ru–PVP < Ru–TTAB [91]. In another study, the particle size of Ru nanoparticles supported on carbon nanotubes (CNTs) ranging from 2.3 to 9.2 nm is investigated in the FTS. The TOF reaches a maximum with increasing the mean size of Ru particles from 2.3 to 6.3 nm [92]. A Ru-SiO_2 catalyst with uniform

structure is synthesized by the alkoxide method [93] and used in the FTS under reaction conditions of 503 K, 10 bar H_2, and 20 bar CO. The catalysts show high activity for the preparation of olefin/paraffin mixtures, with suppression of CH_4 and CO_2 [94]. Usually, ruthenium catalysts give high-molecular-weight polymers, but Aika and Takeishi showed that a Raney ruthenium catalyst pretreated with a mixed gas of water and helium is able to hydrogenate CO to methanol. In the Sabatier reaction, which converts CO_2 and hydrogen to methane, the same catalyst is more active by 3 orders of magnitude than the supported ruthenium catalysts because Raney ruthenium possesses more active sites [95]. Madon and Iglesia performed experiments with large and small particle size of Ru/TiO_2 pellets, which plays a role in the selectivity of FTS. In the Ru/TiO_2 pores, a concentration gradient of H_2 and CO leads to lighter and more paraffinic hydrocarbons, since hydrocarbons cover with increasing reaction time the active centers [96]. The influence of metal dispersion and support (SiO_2, Al_2O_3, TiO_2) on FTS has been studied for ruthenium and cobalt. The site-time yields are in the case of Ru catalyst similar, but with Co the synthesis rates are proportional to the metal dispersion and independent on the metal oxide support [97].

In the course of finding more environmentally friendly conditions, light can be exploited to realize a photocatalytic FTS. Ruthenium nanostructures dispersed on graphene are suitable to catalyze FTS using a 300 W Xe lamp at 150 °C with 20 bar H_2 and 10 bar CO [98]. A TOF of 14.4 h^{-1} is achieved (Scheme 5.43).

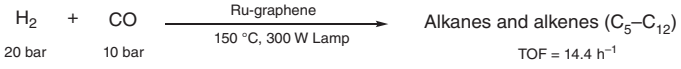

Scheme 5.43 Light-induced FTS.

In a theoretical DFT contribution, Aleix Comas-Vives explored the first principles of bond breaking mechanism in the case of ruthenium catalysts, which is easier to calculate than their industrial Fe and Co counterparts. Ruthenium catalysts are considered as the most active FTS catalyst with regard to high-molecular-weight hydrocarbons [99]. As mentioned above, FTS is an exothermic reaction, and the mechanistic multistep CO activation is compared with the direct mechanism (Scheme 5.44).

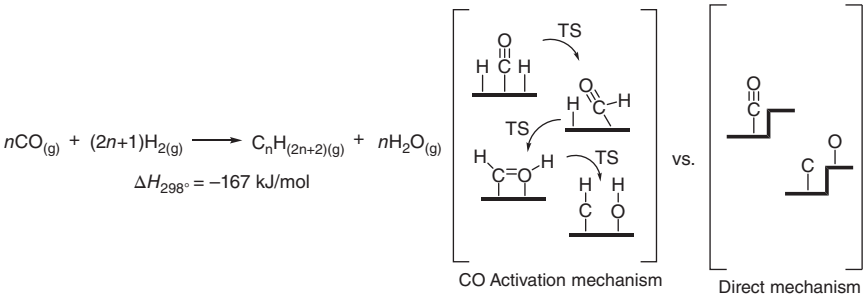

Scheme 5.44 Model of CO activation on the ruthenium nanoparticles.

5.6.2 Synthesis of Oxo Products from Syngas

The most important reaction of syngas is the industrial methanol production using heterogeneous catalysts. Modified oxide systems based on $ZnO–Cr_2O_3$ (300 bar, 350 °C) and later $CuO–ZnO/Al_2O_3$ (50–80 bar, 250 °C) are efficient catalytic systems. Dombek showed that also $Ru_3(CO)_{12}$ catalyst can convert syngas to methanol in a homogeneous reaction. The addition of KI promotes the methanol formation by increasing the TOF to 14 times. Also, minor amounts of ethylene glycol and ethanol are formed (Scheme 5.45a).

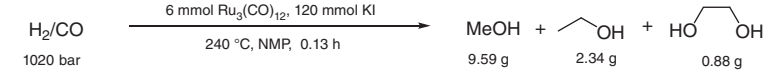

(a)

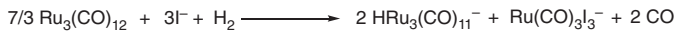

(b)

Scheme 5.45 (a) Iodide-promoted synthesis of methanol with syngas. (b) Formation of Ru intermediates occurring in reaction (a). Source: Modified from Dombek [100].

After the reaction, $HRu_3(CO)_{11}^-$ and $Ru(CO)_3I_3^-$ complexes were analyzed in the reaction mixture and could also be isolated according to reaction (b) in Scheme 5.45 [100]. Interestingly each complex alone has no activity in the carbonylation of hydrogen, but a combination of 2 : 1 as occurs in reaction (b) presents the optimum catalytic performance [101].

Knifton studied the syngas reaction with the goal of preparing ethylene glycol (Scheme 5.46a). Since the thermodynamic data are unfavorable, they investigated the reaction in the presence of acetic acid to obtain ethylene glycol diacetate by a thermodynamically more favored process.

(a)

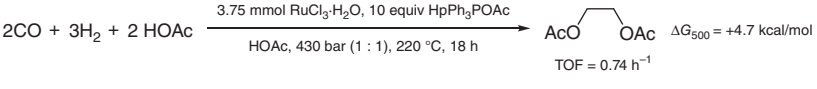

(b)

Scheme 5.46 (a) The reaction Gibbs energy for the formation of ethylene glycol is high (+15.8 kcal/mol). (b) The reaction Gibbs energy of for the formation of ethylene glycol diacetate is low (+4.7 kcal/mol). Source: (b) Modified from Knifton [102].

After a screening of reaction parameters, the best catalytic conditions were obtained with $RuCl_3$ and heptyltriphenylphosphonium acetate at 430 bar CO/H_2 and 220 °C, giving a TOF of 0.74 h^{-1} (Scheme 5.46b) [102]. In another study, Knifton converted syngas to acetic acid using a bimetallic heterogeneous Ru–Co–I catalyst by carrying out the reaction in low-melting tetrabutylphosphonium bromide (Scheme 5.47) [103]. $Ru(CO)_3I_3$ is the dominant specie in the formation of

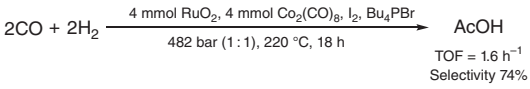

Scheme 5.47 Synthesis of acetic acid with a bimetallic Ru/Co catalyst. Source: Modified from Knifton [103].

methanol. The iodide anion is responsible for the conversion of methanol to methyl iodide, which is then carbonylated to acetic acid by the cobalt co-catalyst. The last step reminds the well-known Monsanto process, where methanol is carbonylated to acetic acid in an iodide-promoted reaction.

A comparative study between $Ru_3(CO)_{12}$ and RuO_2 catalyst about the syngas reaction to alcohols showed that both catalysts give methanol, ethanol, and propanol as main product, but in the case of RuO_2, higher alcohols (from butanol to hexanol) are formed. Labeling experiments with $^{13}CH_3OH$ and ^{13}CO indicated that the higher olefins are formed by a chain grow mechanism on the ruthenium center (Scheme 5.48b) while methanol and ethanol formations proceed via an intermolecular hydride transfer mechanism (Scheme 5.48a) [104].

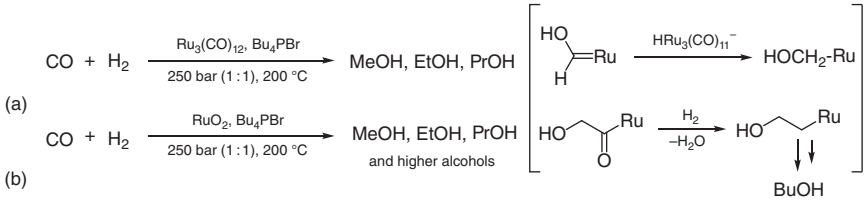

Scheme 5.48 (a) $Ru_3(CO)_{12}$-catalyzed reaction of syngas to lower alcohols (C_1 to C_3). (b) RuO_3-catalyzed reaction of syngas to higher alcohols. Source: Modified from Blank et al. [104].

Starting directly from methanol and syngas, Liu and coworker developed a homologation reaction to ethanol using a rhodium/ruthenium bimetallic catalyst system. This group investigated the effects of lithium salts, methyl iodine addition, syngas ratio, temperature, and pressure. The strongest influence on TOF is given by the temperature, leading to an increase of the TOF from 50.6 to 178 h^{-1} by rising the temperature from 110 to 140 °C (Scheme 5.49a) [106]. The rhodium metal catalyzes the carbonylation of methanol to acetaldehyde via carbonylation of MeI, while ruthenium, known as a good hydrogenation catalyst, reduces acetaldehyde to ethanol.

Instead of mixing a ruthenium and rhodium precursor, Hidasi et al. prepared a tetrahedral $NEt_4[RuCo_3(CO)_{12}]$ cluster from $RuCl_3{\cdot}H_2O$ and $Na[Co(CO)_4]$ and employed the catalyst in the homologation reaction of methanol promoted by MeI. The reaction proceeds at 78 bar H_2 and 39 bar CO with a selectivity of 65% to give 16% ethanol (Scheme 5.49b) [105].

Another important refinement of methanol is the production of dimethoxymethane (OME1) with syngas. OME1 is, on one hand, an environmental fuel, because of its low vapor pressure, high viscosity, high oxygen content, and high

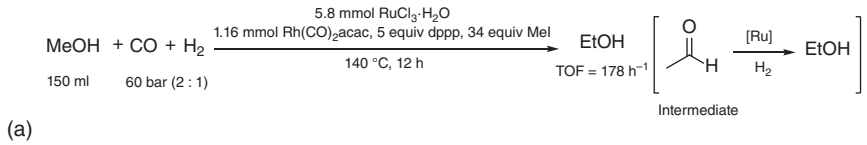

(a)

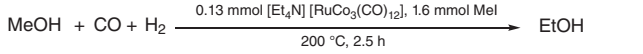

(b)

Scheme 5.49 (a) Homologation reaction from methanol to ethanol using Rh/Ru bimetallic catalyst. (b) Homologation reaction from methanol to ethanol using a $[RuCo_3(CO)_{12}]^-$ cluster. Source: (b) Modified from Hidai et al. [105].

cetane number and, on the other hand, a good solvent, because of its low toxicity and good solvent properties. Tanksale and coworkers reported about a one-pot, two-step process using a Ru–Ni catalyst supported on zeolite beta (beta polymorph A [BEA]) converting syngas to formaldehyde, which reacts with methanol in a classical acetal reaction to give OME1 (Scheme 5.50) [107].

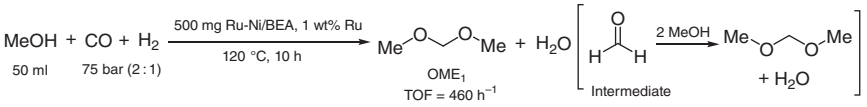

Scheme 5.50 One-pot reaction of MeOH and syngas leading to dimethoxymethane OME1. Source: Modified from Ahmad et al. [107].

5.7 Synthesis of Oxo Products from H_2 and CO_2

The exothermic water–gas shift reaction (WGSR), which converts CO and water to H_2 and CO_2, is an important industrially used reaction for hydrogen production, which is taken for Haber–Bosch process and refineries. The endothermic reverse WGSR ($\Delta H°_{298} = +41$ kJ/mol) is the basis of using CO_2 in carbonylation reactions, since CO_2 is converted to CO and water, and becomes possible at high temperatures. For example, Yasuda et al. reported on a ruthenium catalyst using a supported ionic liquid phase (SILP) consisting of $[RuCl_2(CO)_3]_2$ and 1-butyl-3-methylimidazolium chloride as ionic liquid to give TOF of 24 h^{-1} in the reverse WGSR, carried out at 170 °C (Scheme 5.51a) [108].

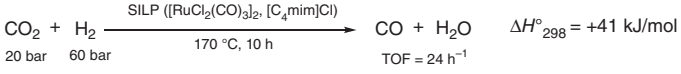

(a)

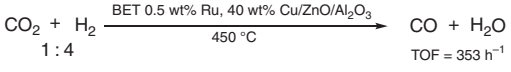

(b)

Scheme 5.51 (a) The endothermic reverse water gas shift reaction in supported ionic liquid-phase (SILP). Source: Modified from Yasuda et al. [108]. (b) The endothermic reverse water gas shift reaction in a continuous process. Source: Modified from Zhuanga et al. [109].

Much more efficient and selective is the reverse WGSR, when CO_2 and H_2 is running in a continuous process over a 0.5 wt% ruthenium-promoted $Cu/ZnO/Al_2O_3$ catalyst at 450 °C. TOF of 353 h^{-1} is obtained (Scheme 5.51b) [109].

Based on the reverse WGSR, a methanol homologation with CO_2 and hydrogen for ethanol production has been realized by a catalytic system consisting of $[RuCl_2(CO)_3]_2/Co_4(CO)_{12}$ at 160 °C. Here, the ruthenium catalyst acts to ensure the formation of CO from CO_2 according to the WGSR. CO and MeOH reacts via methyl iodide in a cobalt-catalyzed reaction to give acetaldehyde, which is then hydrogenated by ruthenium to ethanol (Scheme 5.52) [110]. The catalytic system is reusable up to five times.

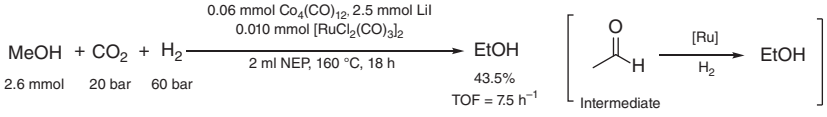

Scheme 5.52 Homologation of methanol to ethanol using CO_2 and H_2. Source: Modified from Wang et al. [110].

Because of environmental considerations, the refinement of CO_2 with H_2 to fuels and oxo products has become an increasingly important issue. Besides the reverse WGSR in which CO_2 is converted to CO, it is well known that CO_2 can also be converted with hydrogen to formic acid, which can react with methanol to yield methyl formate. Klankermayer and coworkers applied this reaction for the preparation of OME1 products. At 20 bar CO_2 and 60 bar H_2 and in the presence of MeOH, OME1 is achieved with a TOF of 12 h^{-1} under mild conditions (80 °C). The triphos-based ruthenium catalyst [Ru(triphos)(tmm)] (triphos = 1,1,1-tris(diphenylphosphinomethyl)ethane, tmm = trimethylenemethane) allows hydride transfer to CO_2 while $Al(OTf)_3$ acts as Lewis acidic co-catalyst for the protonolysis steps (Scheme 5.53a). Label experiments with $^{13}CO_2$ show that the methylene group in OME1 derives exclusively from the employed CO_2 (Scheme 5.53b) [111].

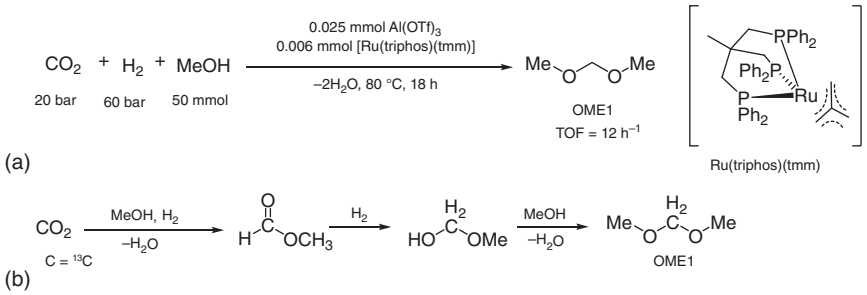

Scheme 5.53 (a) Synthesis of dimethoxymethane OME1 from CO_2, H_2, and MeOH. (b) Label experiments with $^{13}CO_2$. Source: Modified from Thenert et al. [111].

5.8 Conclusions

Each metal has often a domain for a certain reaction, where it is better than the other metals. For example, rhodium is superior for hydroformylation and hydrogenation, and palladium is superior in coupling chemistry and in the alkoxycarbonylation. Also, ruthenium is superior in metathesis reaction using Grubbs catalyst and hydrogen autotransfer reactions using pincer complexes. In carbonylation reactions, ruthenium is superior in PKRs and carbonylative CH activation. However, ruthenium is not superior in carbonylation reactions of olefins compared with other existing processes. Nevertheless, since the ruthenium chemistry is very versatile and often undiscovered, many surprising results including efficient carbonylation catalysts can be expected in the future. There is huge potential to tune catalysts by addition of suitable ligands. Many reactions are carried out with $Ru_3(CO)_{12}$ as catalyst precursor without any directing ligands, but some carbonylation reactions show the of positive influence ligands. For example, this is true in the 2-(dicyclohexylphosphino)-1-(2-methoxyphenyl)-*1H*-imidazole ligand in the hydroformylation or the $Ru(CO)_3$DPPE complex in the carbonylation of nitroarenes. A ligand-promoted catalyzed reaction has the additional advantage that mechanistic studies are easier to perform because the ligand can be considered as a probe indicating what is taking place in the reaction. It is not an accident that the studies on the carbonylation of nitroarenes are carried out with the $Ru(CO)_3$DPPE complex. Similar to the expanding field of defined ruthenium complexes with pincer ligands in the hydrogenation autotransfer reactions, it is conceivable that defined highly active ruthenium complexes will be synthesized in the future for carbonylation reactions, too.

References

1 For a good review see also:Chatani, N. (2004). *Top. Organomet. Chem.* 11: 173–195.
2 Yamamoto, A. (1986). *Organotransition Metal Chemistry*, 229. New York/Chichester/Brisbane/Toronto/Singapore: Wiley.
3 Murai, S., Kakiuchi, F., Sekine, S. et al. (1993). *Nature* 366: 529–531.
4 Moore, E.J., Pretzer, W.R., O'Connell, T.J. et al. (1992). *J. Am. Chem. Soc.* 114: 5888–5890.
5 (a) Bruce, M.I., Humphrey, M.G., Wallis, R.C. et al. (1986). *J. Organomet. Chem.* 314: 311–322. (b) Fish, R.H., Kim, T.-J., Stewart, J.L. et al. (1986). *Organometallics* 5: 2193–2198. (c) Chen, D., Li, Y., Wang, B. et al. (2006). *Organometallics* 25: 307–310.
6 Chatani, N., Fukuyama, T., Kakiuchi, F., and Murai, S. (1996). *J. Am. Chem. Soc.* 118: 493–494.
7 Fukuyama, T., Chatani, N., Tatsumi, J. et al. (1998). *J. Am. Chem. Soc.* 120: 11522–11523.
8 Cabeza, J.A. and Oro, L.A. (1988). *J. Chem. Soc., Dalton Trans.*: 1437–1444.

9 This behavior is also observed in other reactions. For example, fluorination of arenes with perfluoroalkyl halides is easier with electron rich than with electron poor arenes. See:Zhang, S., Rotta-Loria, N., Weniger, F. et al. (2019). *Chem. Commun.* 55: 6723–6726.

10 Chatani, N., Fukuyama, T., Tatamidani, H. et al. (2000). *J. Org. Chem.* 65: 4039–4047.

11 Asaumi, T., Chatani, N., Matsuo, T. et al. (2003). *J. Org. Chem.* 68: 7538–7540.

12 Chatani, N., Ie, Y., Kakiuchi, F., and Murai, S. (1997). *J. Org. Chem.* 62: 2604–2610.

13 In the literature (Cambridge Crystallographic Data Centre) there is no example for a triruthenium complex with 2-phenylpyridine or similar compounds as a ligand. But there are examples with 2-phenylpyridine coordinated twice to a single ruthenium center.(a)Chen, D., Zhang, X., Xu, S. et al. (2010). *Organometallics* 29: 3418–3430. (b) Fan, Z., Ni, J., and Zhang, A. (2016). *J. Am. Chem. Soc.* 138: 8470–8475.

14 Tlili, A., Schranck, J., Pospech, J. et al. (2014). *ChemCatChem* 6: 1562–1566.

15 Haito, A., Yamaguchi, M., and Chatani, N. (2018). *Asian J. Org. Chem.* 7: 1315–1318.

16 Fukuyama, T., Chatani, N., Kakiuchi, F., and Murai, S. (1997). *J. Org. Chem.* 62: 5647–5650.

17 Ie, Y., Chatani, N., Ogo, T. et al. (2000). *J. Org. Chem.* 65: 1475–1488.

18 Meyers, A.I., Temple, D.L., Haidukewych, D., and Mihelich, E.D. (1974). *J. Org. Chem.* 39: 2787–2793.

19 Ackermann, L., Barfüsser, S., Kornhaass, C., and Kapdi, A.R. (2011). *Org. Lett.* 13: 3082–3085.

20 Gutierrez, D.A., Lee, W.-C.C., Shen, Y., and Li, J.J. (2016). *Tetrahedron Lett.* 57: 5372–5376.

21 Xu, J.-X., Zhao, F., Yuan, Y., and Wu, X.-F. (2020). *Org. Lett.* 22: 2756–2760.

22 Ishii, Y., Chatani, N., Kakiuchi, F., and Murai, S. (1997). *Organometallics* 16: 3615–3622.

23 Chatani, N., Ishii, Y., Ie, Y. et al. (1998). *J. Org. Chem.* 63: 5129–5136.

24 Hasegawa, N., Shibata, K., Charra, V. et al. (2013). *Tetrahedron* 69: 4466–4472.

25 Shibata, K., Hasegawa, N., Fukumoto, Y., and Chatani, N. (2012). *ChemCatChem* 4: 1733–1736.

26 Evans, D., Osborn, J.A., Jardine, F.H., and Wilkinson, G. (1965). *Nature* 208: 1203–1204.

27 Le Goanvic, L., Couturier, J.-L., Dubois, J.-L., and Carpentier, J.-F. (2016). *J. Mol. Catal. A: Chem.* 417: 116–121.

28 Takahashi, K., Yamashita, M., Tanaka, Y., and Nozaki, K. (2012). *Angew. Chem. Int. Ed.* 51: 4383–4387.

29 (a) Wu, L., Fleischer, I., Jackstell, R. et al. (2013). *J. Am. Chem. Soc.* 135: 14306–14312. (b) Fleischer, I., Wu, L., Profir, I. et al. (2013). *Chem. Eur. J.* 19: 10589–10594.

30 (a) Wu, L., Fleischer, I., Jackstell, R., and Beller, M. (2013). *J. Am. Chem. Soc.* 135: 3989–3996. (b) Wu, L., Fleischer, I., Zhang, M. et al. (2014). *ChemSusChem* 7: 3260–3263.

31 Fleischer, I., Wu, L., Profir, I. et al. (2013). *Chem. Eur. J.* 19: 10589–10594.

32 Kubis, C., Profir, I., Fleischer, I. et al. (2016). *Chem. Eur. J.* 22: 2746–2757.

33 Kämper, A., Kucmierczyk, P., Seidensticker, T. et al. (2016). *Catal. Sci. Technol.* 6: 8072–8079.

34 Mitsudo, T., Suzuki, N., Kondo, T., and Watanabe, Y. (1996). *J. Mol. Catal. A: Chem.* 109: 219–225.

35 Süssfink, G. (1980). *J. Organomet. Chem.* 193: C20–C22.

36 Khan, M.M.T., Halligudi, S.B., and Abdi, S.H.R. (1988). *J. Mol. Catal.* 48: 313–317.

37 Norinder, J., Rodrigues, C., and Börner, A. (2014). *J. Mol. Catal. A: Chem.* 391: 139–143.

38 Tominaga, K. and Sasaki, Y. (2000). *Catal. Commun.* 1: 1–3.

39 Dong, K., Fang, X., Gülak, S. et al. (2017). *Nat. Commun.* 8: 14117–14123.

40 Wu, L., Liu, Q., Jackstell, R., and Beller, M. (2015). *Org. Chem. Front.* 2: 771–774.

41 Dombek, B.D. (1983). *J. Organomet. Chem.* 250: 467–483.

42 Behr, A., Kanne, U., and Keim, W. (1986). *J. Mol. Catal.* 35: 19–28.

43 Keim, W. and Becker, J. (1988). *J. Mol. Catal.* 44: 197–200.

44 Legrand, C., Castanet, Y., Mortreux, A., and Petit, F. (1994). *J. Chem. Soc., Chem. Commun.*: 1173–1174.

45 Lavigne, G. and Lugan, N. (1992). *J. Am. Chem. Soc.* 114: 10669–10670.

46 Lugan, N., Lavigne, G., Soulié, J.M. et al. (1995). *Organometallics* 14: 1712–1731.

47 Li, Y.-R., Xu, Z.-N., Bai, B. et al. (2019). *Chin. J. Chem.* 37: 769–774.

48 Wu, L., Liu, Q., Fleischer, I. et al. (2014). *Nat. Commun.* 5: 3091–3096.

49 Liu, Q., Wu, L., Jackstell, R., Beller, M. (2014). *ChemCatChem* 6: 2805–2809.

50 Arpe, H.J. (2007). *Industrielle Organischen Chemie*, Sechste Vollständig überarbeitete Auflage, 424. Weinheim: Wiley-VCH.

51 Cenini, S. and Ragaini, F. (1997). *Catalysis by Metal Complexes, Catalytic Reductive Carbonylation of Organic Nitro Compounds*, 80–87. Dordrecht: Springer Science+Business Media, B.V.

52 Basu, A., Bhaduri, S., and Khwaja, L.H. (1987). *J. Organomet. Chem.* 319: C28–C30.

53 (a) Drent, E. (1990). *Pure Appl. Chem.* 62: 661–669. (b) Ragaini, F., Cognolato, C., Gasperini, M., and Cenini, S. (2003). *Angew. Chem. Int. Ed.* 42: 2886–2889.

54 Cenini, S. and Ragani, F. (1997). *Catalysis by Metal Complexes Vol 20, Catalytic Reductive Carbonylation of Organic Nitro Compounds*, 109 and 280. Springer-Science+Business Media, B.V.

55 Skoog, S.J., Campbell, J.P., and Gladfelter, W.L. (1994). *Organometallics* 13: 4137–4139.

56 Gargulak, J.D., Noirot, M.D., and Gladfelter, W.L. (1991). *J. Am. Chem. Soc.* 113: 1054–1055.

57 Gargulak, J.D. and Gladfelter, W.L. (1994). *Organometallics* 13: 698–705.

58 Cenini, S., Crotti, C., Pizzotti, M., and Porta, F. (1988). *J. Org. Chem.* 53: 1243–1250.

59 Ragaini, F. and Cenini, S. (2000). *J. Mol. Catal. A: Chem.* 161: 31–38.

60 (a) Han, S.H., Song, J.S., Macklin, P.D. et al. (1989). *Organometallics* 8: 2127–2138. (b) Bhaduri, S., Khwaja, H., Sapre, N. et al. (1990). *J. Chem. Soc., Dalton Trans.*: 1313–1321.

61 (a) Bhaduri, S., Gopalkrishnan, K.S., Sheldrick, G.M. et al. (1983). *J. Chem. Soc., Dalton Trans.*: 2339–2341. (b) Formally speaking, the nitrene in the cluster contributes 4 electrons and can replace 2 CO.

62 Crotti, C. and Cenini, S. (1991). *J. Mol. Catal.* 70: 175–187.

63 Dey, T.K., Ghosh, K., Basu, P. et al. (2018). *New J. Chem.* 42: 9168–9176.

64 Islam, S.M., Ghosh, K., Roy, A.S. et al. (2014). *J. Organomet. Chem.* 772–773: 152–160.

65 Mulla, S.A.R., Gupte, S.P., and Chaudhari, R.V. (1991). *J. Mol. Catal.* 67: L7–L10.

66 Jenner, G., Bitsi, G., and Schleifer, E. (1987). *J. Mol. Catal.* 39: 233–236.

67 Li, W. and Wu, X.-F. (2015). *Chem. Eur. J.* 21: 14943–14948.

68 Bitsi, G. and Penner, G. (1987). *J. Organomet. Chem.* 330: 429–435.

69 Tsuji, Y., Ohsumi, T., Kondo, T., and Watanabe, Y. (1986). *J. Organomet. Chem.* 309: 333–344.

70 Liu, G., Hakimifard, M., and Garland, M. (2001). *J. Mol. Catal. A: Chem.* 168: 33–37.

71 Jenner, G. and Bitsi, G. (1987). *J. Mol. Catal.* 40: 71–82.

72 Jenner, G. and Bitsi, G. (1988). *J. Mol. Catal.* 45: 235–246.

73 Kondo, T., Suzuki, N., Okada, T., and Mitsudo, T. (1997). *J. Am. Chem. Soc.* 119: 6187–6188.

74 Itami, K., Mitsudo, K., and Yoshida, J. (2002). *Angew. Chem. Int. Ed.* 41: 3481–3484.

75 Chatani, N., Morimoto, T., Fukumoto, Y., and Murai, S. (1998). *J. Am. Chem. Soc.* 120: 5335–5336.

76 Chatani, N., Morimoto, T., Kamitani, A. et al. (1999). *J. Organomet. Chem.* 579: 177–181.

77 Tobisu, M., Chatani, N., Asaumi, T. et al. (2000). *J. Am. Chem. Soc.* 122: 12663–12674.

78 Chatani, N., Tobisu, M., Asaumi, T. et al. (1999). *J. Am. Chem. Soc.* 121: 7160–7161.

79 Finnegan, D.F. and Snapper, M.L. (2011). *J. Org. Chem.* 76: 3644–3653.

80 Chatani, N., Tobisu, M., Asaumi, T., and Murai, S. (2000). *Synthesis* 7: 925–928.

81 Göbel, A. and Imhof, W. (2001). *Chem. Commun.*: 593–594.

82 Morimoto, T., Chatani, N., and Murai, S. (1999). *J. Am. Chem. Soc.* 121: 1758–1759.

83 (a) Pino, P., Braca, G., and Sbrana, G. (1964) Verfahren zur Herstellung von Hydrochinon. German Patent 1251329; (b) Reppe, W., Kutepow, N.v., and Magin, A. (1969). *Angew. Chem. Int. Ed.* 8: 727–733.

84 Suzuki, N., Kondo, T., and Mitsudo, T. (1998). *Organometallics* 17: 766–769.

85 Fukuyama, T., Yamaura, R., Higashibeppu, Y. et al. (2005). *Org. Lett.* 7: 5781–5783.

86 Wang, C. and Wu, Y.-D. (2008). *Organometallics* 27: 6152–6162.

87 Yoneda, E., Kaneko, T., Zhang, S.-W. et al. (2000). *Org. Lett.* 2: 441–443.

88 Tsubuki, M., Takahashi, K., and Honda, T. (2009). *J. Org. Chem.* 74: 1422–1425.

89 Kang, S.K., Kim, K.J., Yu, C.M. et al. (2001). *Org. Lett.* 3: 2851–2853.

90 Keim, W. (ed.) (1983). *Catalysis in C1 Chemistry*, 42. Dordrecht: D. Reidel Publishing Company.

91 Quek, X.-Y., Pestman, R., van Santen, R.A., and Hensen, E.J.M. (2013). *ChemCatChem* 5: 3148–3155.

92 Kang, J., Deng, W., Zhang, Q., and Wang, Y. (2013). *J. Energy Chem.* 22: 321–328.

93 In the alkoxid method a ruthenium precursor for example ruthenium acetylacetonate is dissolved in ethylenglycole and ethanol. The addition of orthosilicate forms a homogeneous solution, which is hydrolysed at 353K by water/ethanol giving a transparent glassy gel. The obtained gel is dried and calcinated for 15h at 823 K giving 2–20% Ru-SiO_2.

94 Okabe, K., Takahara, I., Inaba, M. et al. (2007). *J. Jpn. Pet. Inst.* 50: 65–68.

95 Aika, K. and Takeishi, K. (1995). *Appl. Catal., A* 133: 31–45.

96 Madon, R.J. and Iglesia, E. (1994). *J. Catal.* 133: 31–45.

97 Iglesia, E., Soled, S.L., and Fiato, R.A. (1992). *J. Catal.* 137: 2121–2224.

98 Guo, X.-N., Jiao, Z.-F., Jin, G.-Q., and Guo, X.-Y. (2015). *ACS Catal.* 5: 3836–3840.

99 Foppa, L., Iannuzzi, M., Coperet, C., and Comas-Vives, A. (2018). *ACS Catal.* 8: 6983–6992.

100 Dombek, B.D. (1981). *J. Am. Chem. Soc.* 103: 6508–6510.

101 Dombek, B.D. (1989). *J. Organomet. Chem.* 372: 151–161.

102 Knifton, J.F. (1982). *J. Catal.* 76: 101–111.

103 Knifton, J.F. (1985). *J. Catal.* 96: 439–453.

104 Blank, J.H., Hembre, R., Ponasikb, J., and Cole-Hamilton, D.J. (2014). *Catal. Sci. Technol.* 4: 218–223.

105 Hidai, M., Orisaku, M., Ue, M. et al. (1983). *Organometallics* 2: 292–298.

106 Chen, Y. and Liu, D. (2018). *Fuel Process. Technol.* 171: 301–307.

107 Ahmad, W., Chan, F.L., Chaffee, A.L. et al. (2020). *ACS Sustainable Chem. Eng.* 8: 2081–2092.

108 Yasuda, T., Uchiage, E., Fujitani, T. et al. (2018). *Appl. Catal.* 232: 299–305.

109 Zhuanga, Y., Curriea, R., McAuleyb, K.B., and Simakov, D.S.A. (2019). *Appl. Catal., A* 575: 74–86.

110 Wang, Y., Zhang, J., Qian, Q. et al. (2019). *Green Chem.* 21: 589.

111 Thenert, K., Beydoun, K., Wiesenthal, J. et al. (2016). *Angew. Chem. Int. Ed.* 55: 12266–12269.

6

Rhodium-Catalyzed Carbonylations

Oreste Piccolo[1] *and Stefano Paganelli*[2]

[1] *Studio di Consulenza Scientifica (SCSOP), Via Bornò 5, 23896 Sirtori (LC), Italy*
[2] *Università Ca' Foscari Venezia, Dipartimento di Scienze Molecolari e Nanosistemi, Via Torino 155, 30172 Venezia Mestre (VE), Italy*

6.1 Introduction

Carbonylation reactions represent a very useful tool for the production of value-added bulk and fine chemicals [1].

A range of carboxylic acids, esters, aldehydes, and amides can be easily prepared by metal-catalyzed carbonylations. Representative examples of this technology are the production of acetic acid, mostly produced via carbonylation of methanol (Rh-based Monsanto or Ir-based Cativa process) [2], and the production of methyl propionate, a key intermediate for polymethacrylates, produced on the scale of >300 000 t/yr by methoxycarbonylation of ethylene [3]. Hydroformylation process or "oxo synthesis" is another relevant process that produces aldehydes starting from olefins and synthesis gas [4].

Among all the transition metals, palladium-based catalysts are largely employed in carbonylative couplings [5]. Iridium, rhodium, and ruthenium play an important role in these processes. However, despite industrial applications, iridium catalysts remain undeveloped in carbonylation reactions [6 and loc. cit.], and the capability of rhodium and ruthenium is much less discovered than Pd in this area. Only limited reviews on Ru- and Rh-catalyzed carbonylations have been reported so far [7]. Due to the high price and limited availability of precious metal-based catalysts, cheaper metals like cobalt or iron have been used too, but their scope is still limited [8]. In particular, rhodium cost could represent a serious drawback, especially on an industrial scale, but its high activity, selectivity, and possibility to recover and recycle it make rhodium the metal of choice for important industrial processes [2]. Despite the differences in catalysts, substrates, and nucleophiles, the reaction starts with the corresponding metal-hydride species, formed by the reaction of the precatalyst with acid additives (TsOH, HBF_4, etc.), followed by coordination and insertion of the unsaturated substrate. A further insertion of carbon monoxide leads to the acyl metal complex that undergoes to the attack of the nucleophile with regeneration of the metal hydride [9]. This important technology suffers from a serious drawback,

Carbon Monoxide in Organic Synthesis: Carbonylation Chemistry,
First Edition. Edited by Bartolo Gabriele.

namely, the use of CO, a toxic reagent that is also difficult to transport in bulk. In this view, many efforts have been done to perform carbonylations by using new carbonyl sources [3], for instance, carbon dioxide [10], methanol [11], and even biomass [12].

In 1938, hydroformylation was discovered by the German chemist Otto Roelen at Ruhrchemie during his investigation on the Fischer–Tropsch reaction catalyzed by a mixture containing cobalt, thorium, and magnesium oxide. Subsequently, it was understood that $HCo(CO)_4$ was the active species, and at the end of the 1960s, most of the hydroformylation plants used cobalt-based catalysts and operated at a pressure between 200 and 450 bar and at a temperature between 140 and 180 °C [4]. However, starting from the 1960s, also rhodium complexes began to be investigated as catalysts, and Wilkinson demonstrated that arylphosphines, besides the alkylphosphines, ligands of choice for cobalt, could be used as ligands for rhodium [13]. Despite the rapid development of rhodium-catalyzed hydroformylation, it took 10 years before the first process was launched on the market (Celanese 1974). Union Carbide (1976) and Mitsubishi Chemical Corporation (1978) were the first companies to use a low-pressure oxo (LPO) process using triphenylphosphine (TPP) as ligand [4]. Rhodium complexes are the most efficient catalysts for hydroformylation reactions in terms of both activity and selectivity [4], and since the mid-1970s, the rhodium catalysts began to replace the cobalt-based catalytic systems for propene and butene hydroformylation. Also, other metals, cheaper than rhodium, were used as hydroformylation catalytic precursors and, even if less active and selective than rhodium catalysts, showed good performances [4]. The most interesting results were obtained by using metals as platinum, ruthenium, and iridium.

In the late 1960s, the platinum-catalyzed hydroformylation of alkenes was described, and since then an extensive research was carried out by using different phosphorus ligands [14 and loc. cit.]. The most outstanding results were obtained in the enantioselective hydroformylation (EHF), catalyzed by Pt/Sn systems, for the synthesis of natural products and for the preparation of building blocks for fine chemicals [14 and loc. cit., 15]. Despite the interesting results obtained, platinum-based catalytic systems never came to a real application as they could not compete with the much more active and selective Rh catalysts.

Ruthenium was also tested as a cheaper alternative metal for hydroformylation in the 1960s, but its activity was too lower compared with rhodium [16 and loc. cit.]. Beller and coworkers developed the first and general ruthenium-based catalytic system for hydroformylation [17]. High regioselectivities of >95% and yields of c. 80% for linear aldehydes were successfully achieved with imidazole-substituted phosphine ligands [16 and loc. cit.]. Very recently, ruthenium was applied in the hydroformylation of 1-octene in a continuously operated miniplant. Noteworthy, the oxo-products were extracted in iso-octane while the catalyst is retained in a polar dimethylformamide (DMF) phase [16 and loc. cit.].

Regarding iridium, it was not extensively employed in hydroformylation reactions because of the competing hydrogenation activity of iridium complexes under hydroformylation conditions. However, iridium/phosphine complexes showed a good activity in the hydroformylation of olefins under mild conditions, being competing hydrogenation side reactions suppressed [6]. Recently, the

iridium/phosphine-catalyzed hydroformylation of 1-octene was carried out in a continuous plant, showing favorable long-term catalyst activity and stability, affording conversion, and aldehyde chemoselectivity rates of approximately 85% [18].

6.2 Hydroformylation

Hydroformylation is one of the most important homogeneous catalyzed industrial processes, and, nowadays, about 12 million tons per year of aldehydes are produced [4]. Rhodium phosphine-based catalytic systems represent the most used catalysts for hydroformylation reaction (Scheme 6.1).

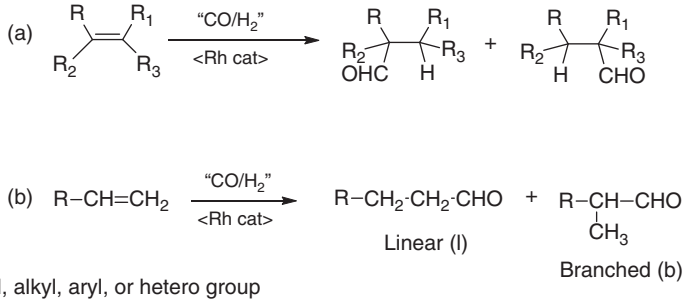

Scheme 6.1 (a) General hydroformylation reaction and (b) hydroformylation of α-olefins.

Ligands strongly influence the selectivity and activity of rhodium catalysts; therefore, modified phosphino and phosphito ligands have been extensively investigated as they can modify the electronic and steric effects around the metal, thus affecting the rate and chemo- and regioselectivity of the reaction [19–21]. At the end of 1960s, Heck proposed a mechanism commonly accepted [22], corresponding to the so-called dissociative mechanism of Wilkinson and coworkers [13], but many efforts have been directed to understand kinetics and mechanism of the rhodium-catalyzed hydroformylation reaction as these reactions are sensitive to the experimental conditions employed. For the Rh/PPh_3 system, the starting complex is $HRh(CO)(PPh_3)_3$, and the kinetic data reveal a first-order dependence with respect to olefin and rhodium concentration and zero order on hydrogen partial pressure. These data support the hypothesis that the slow step of the catalytic cycle is either the coordination of the substrate to rhodium or the migratory insertion of the alkene into the Rh—H bond. It has not been established experimentally whether alkene complexation is reversible or not, but experiments carried out with deuterated substrates suggested that both alkene coordination and insertion into the Rh—H bond can be reversible at low pressure. However, experimental data obtained employing the same catalytic system, but at different reaction conditions, claimed that the oxidative addition of hydrogen was the rate-determining step as an acceleration of the hydroformylation rate was observed upon increasing the H_2 pressure. Even today, the study of the kinetic and the reaction mechanism is of

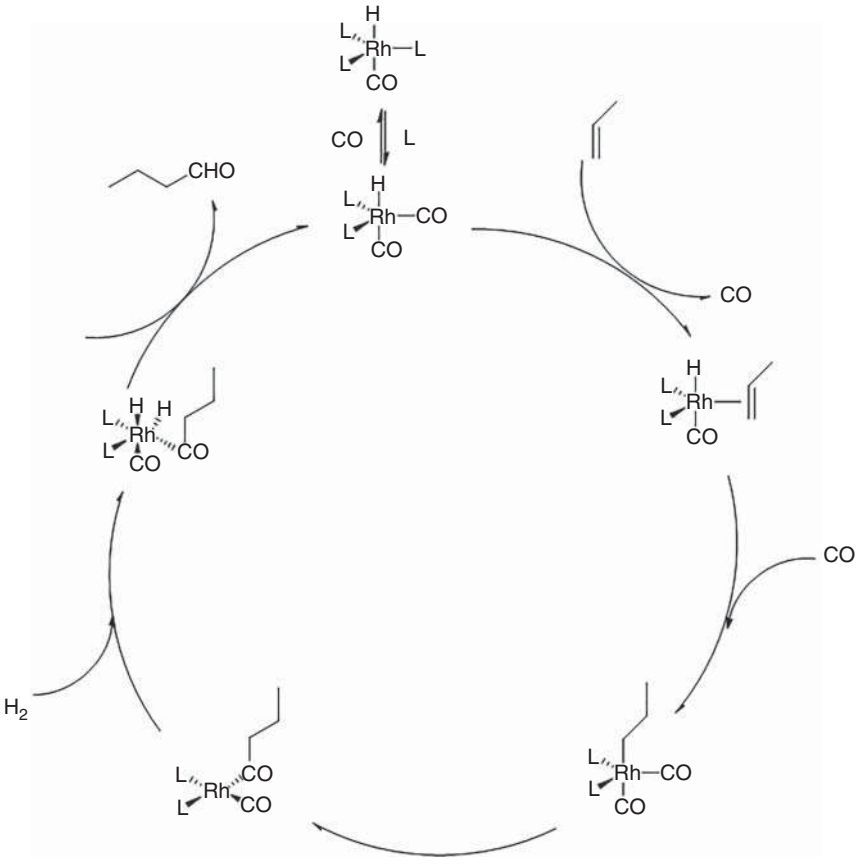

Figure 6.1 Catalytic cycle for rhodium-catalyzed propene hydroformylation. Sources: Bernales and Froese [23], Kläh and Garland [24], Fourmy et al. [25], Gellrich et al. [26], Kégl [27], Zhang et al. [28], Bondžić et al. [29], Kharat et al. [30], Jover and Maseras [31], Dingwall et al. [32], Wildt et al. [33], Jiao et al. [34], Brezny and Landis [35], Jörke et al. [36], Vilches-Herrera et al. [37], Eshon et al. [38], Van Leeuwen et al. [39], Bai et al. [40], Bai et al. [41], Shin et al. [42], Breckwoldt et al. [43], Breckwoldt et al. [44], Kloß et al. [45], Brezny and Landis [46], Yu et al. [47] and Wang et al. [48].

great interest, stimulating a passionate research as attested by the numerous articles appeared in the recent literature (Figure 6.1) [23–48].

6.2.1 Catalyst Recovery

The recovery and recycling of the catalyst is the main drawback of the homogeneous hydroformylation process. Many efforts have been done in the past decade for developing a more efficient catalytic system for rhodium-catalyzed hydroformylation, not only in terms of activity but also in the design of an easy recoverable catalytic system. Multiphase system, as the aqueous biphase oxo-process discussed below, normally requires post-reaction separation, not always easy to perform, with the risk of losing products and/or catalyst. Further technical problems are present for a multiphase process when a continuous equipment is used. Therefore, catalyst

immobilization is still the mainstream in the research of continuous hydroformylation, even if it may be useful for a batch-mode process, too. Leaching, the major problem for immobilized catalysts, can be prevented by using novel strategies such as the molecular weight enlargement (MWE) plus nanofiltration. Several reports have also demonstrated the long-term effectiveness of polymer, silica, or ionic liquid (IL)-bound rhodium catalysts with low leaching. However, in all cases, cost is another crucial factor to be considered for an industrial process. The strategies involving ionic liquids as film on a silica support or just as solvent (in combination with the use of $scCO_2$) are very expensive. However, further improvements are expected to overcome these challenges to achieve more sustainable technologies for the development of industrially applicable continuous hydroformylation processes [49]. Reviews on different strategies for heterogenization of rhodium-based hydroformylation catalysts were published in these last years [50, 51]. In most cases, heterogenized homogeneous catalysts gave very good results. For instance, $HRh(CO)(PPh_3)_3$-encapsulated hexagonal mesoporous silica (HMS) was found to be an efficient heterogeneous catalyst for the selective hydroformylation of 2,3-dihydrofuran (2,3-DHF) and 2,5-DHF. The Rh complex encapsulated *in situ* into the organic phase of template inside the pores of HMS was found to act as nanophase reactors. The catalyst was separated by simple filtration, washed with warm water, and effectively recycled for six times [52]. The heterogeneous catalyst was also employed in the hydroformylation of styrene affording complete substrate conversion and up to 88.9% formation of the iso-aldehyde [53].

2-(Diphenylphosphino)ethyltriethoxysilane (DPPES) was anchored on silica surface by a grafting method to produce a bonded phosphine ($SiO_2(PPh_2)$). The supported $SiO_2(PPh_2)$/Rh catalyst, formed *in situ* from $SiO_2(PPh_2)$ and $Rh(acac)(CO)_2$, was used as catalyst in 1-octene hydroformylation, showing very high conversion and selectivity (98.4% and 95.3%, respectively). The reaction activity remained practically unchanged after four recycles, and the rhodium content leaching in organic phase was less than 0.1% [54]. Rhodium(I) complexes based on TPP and water-soluble tris(*m*-sulfonatophenyl)phosphine trisodium salt (TPPTS, Figure 6.2) were anchored on mesoporous silica (MCM-41 and SBA-15) and used as catalysts in the hydroformylation of 1-octene. High activities and regioselectivities toward *n*-nonanal (80–90%) were obtained for the immobilized catalysts. The catalysts could be reused several times without loss of activity or selectivity under identical reaction conditions [55]. Activated carbon with nanoporous structure, prepared from mango seed shell, was used as support to impregnate the active hydroformylation rhodium complexes $HRh(CO)(PPh_3)_3$ and $Rh(acac)(CO)_2$. These supported catalysts were employed in the hydroformylation of olefins as 1-hexene, 1-octene, and styrene, showing excellent selectivity for aldehydes (~99%), good stability, and recyclability up to four cycles [56].

More recently, regioselectivity in olefin hydroformylation was controlled by building a microenvironment around Rh clusters that mimic the Rh phosphine molecular complex. Rh and K species are simultaneously enveloped by S-1 zeolites, and the *in situ* doped K species, which build a steric hindrance microenvironment on the surfaces of Rh clusters, facilitates the formation of linear aldehyde. As a

matter of fact, the regioselectivity in propylene hydroformylation was enhanced from 46% to 83%, with TOF as high as 7328 h^{-1} [57].

Porous organic ligand (POL)-supported catalysts are new heterogeneous catalysts, and a series of porous polymers containing diphosphine groups was synthesized through polymerizing the vinyl-functionalized diphosphine monomers. The Rh/POL-dppe catalysts were very active and selective in the hydroformylation of olefins, probably due to the extremely high ligand concentration (the ratio of dppe to Rh in the Rh/POL-dppe catalyst is about 10) and to the mobility of dppe ligands in the framework in the swollen state. They were also easily separated from the reaction system and recycled without losing any activity and selectivity [58]. A new porous organic polymer (POP) was synthesized through copolymerization of divinyl-functionalized phosphoramidite ligand and trivinyl-functionalized triphenylphosphane. The rhodium-loaded polymeric material was successfully used as a heterogeneous catalyst in hydroformylation of terminal and internal olefins, affording high linear-to-branched aldehyde ratios and excellent turnover number (TON) values. Remarkably, the heterogeneous catalyst was also reused for 10 cycles in 1-hexene hydroformylation without losing activity and selectivity [59]. Also, the heterogeneous catalyst (Rh/POL-BINAPa and PPh_3) exhibited good performances in the hydroformylation of various symmetrical and unsymmetrical alkynes to afford the corresponding α,β-unsaturated aldehydes with high selectivity, activity, and recyclability [60]. A new POP with large surface area and hierarchical pores, obtained via copolymerization of bivinyl-functionalized pyrrole-based biphosphoramidite with styrene under solvothermal conditions, has been used as a solid support and ligand for Rh-catalyzed solvent-free higher olefins hydroformylation. The catalyst showed a very high regioselectivity toward the linear aldehydes. Moreover, it could be easily recovered and used in successive experiments with good maintenance of both catalytic activity and regioselectivity [61]. Very recently, a new hyperbranched poly(arylene oxindole) (HBPAO) derivative charged with Nixantphos, a xanthene-based phosphine ligand able to immobilize rhodium, was prepared and employed in the microwave-assisted hydroformylation of olefins. All the substrates, included styrene derivatives, selectively afforded the desired linear aldehydes, thus indicating a reverse regioselectivity with respect to the homogeneous reaction. This behavior can be attributed to the unique dendritic nature of the support, resulting in a positive dendritic effect. Furthermore, the catalytic system was successfully recovered and reused without any decrease in conversion or selectivity [62]. A thermoregulated phase-separable Rh nanocatalyst was applied in the hydroformylation of styrene and exhibited excellent catalytic performances. The biphase system, constituted by the quaternary ammonium-based ionic liquid *N*,*N*-dimethyl-*N*-(2-(2-methoxyethoxy)ethyl)-*N*-(2-(2-octyloxyethoxy)ethyl) ammonium methanesulfonate and cyclohexane, allowed the easy separation of the catalyst from products. In addition, it could be reused for 20 recycles without evident loss in catalytic activity and aldehyde yield [63].

The rhodium-catalyzed hydroformylation of alkenes has been performed under biphasic conditions using combinations of α-cyclodextrin (α-CD) and poloxamines (Tetronics®). Thermoresponsive hydrogels containing the Rh catalyst were formed,

and the presence of α-CD was crucial to provoke the decantation of the multiphasic system once the reaction was complete [64].

Homogeneous catalysts have been heterogenized by using colloidal particles that covalently bind ligands. In particular, functionalized polymer particles with trimethylammonium moieties, dispersed in water, with a hydrophobic core and a hydrophilic shell, have been synthesized by emulsion polymerization. The colloidal dispersions have been applied as phase transfer agents in the multiphasic rhodium-catalyzed hydroformylation of 1-octene. The polymer particles were proven to act as carriers for the water-soluble hydroformylation catalyst due to the electrostatic interaction between the functionalized particles bearing ammonium groups and the sulfonated ligands of the catalyst. The particles were stable under the hydroformylation conditions, and the aqueous catalyst phase could be recycled three times [65].

A new bio-generated phosphine-free rhodium-based system embedded in a peculiar polysaccharide matrix (Rh-EPS) was obtained and purified from cultures of bacterial cells of *Klebsiella oxytoca* DSM 29614. Rh-EPS was used as catalyst in the aqueous biphasic hydroformylation of some aliphatic and aromatic olefins, showing good activity and recyclability. Noteworthy, the catalytic system, though not soluble in water but only suspended in it, was active exclusively in the presence of water [66]. More recently, the low metal content 0.18% Rh/Al_2O_3 was prepared and fully characterized. The activity of this catalytic system was tested in the hydroformylation of styrene and of two different isomeric olefins ((*E*)-2-ethyl-5-(prop-1-en-1-yl)thiophene and 2-allyl-5-ethylthiophene), precursors of a fragrance with a fresh, green floral smell, reminiscenting of lily of the valley. This heterogeneous catalyst was easy to recover and possibly to recycle [67]. Very interestingly, atomically dispersed, supported Rh catalysts were synthesized on MgO and CeO_2. The MgO-supported rhodium catalyst was found to be barely active for the liquid-phase hydroformylation of styrene, while Rh_1/CeO_2 was found to be highly active, showing a performance comparable with the molecular catalyst $HRh(CO)(PPh_3)_3$ [68].

Ionic liquid-based and supported ionic liquid phases (SILPs) have been extensively used in hydroformylation. These systems allow an easy recovery and recycle of the catalyst, reducing catalyst leaching during product separation. High catalytic activities and good regioselectivity could be obtained depending on the properties of ligands [69]. Recently, a class of room-temperature phosphine-functionalized polyether guanidinium ionic liquids (RTP-PolyGILs), synthesized by ion exchange reaction of TPPTS with PolyGILs, were used in the Rh-catalyzed hydroformylation of 1-octene. Working with only catalytic amounts of RTP-PolyGILs, very high TOF, total turnover number (TTON), and good aldehyde selectivity were achieved, and Rh leaching was only 0.07–0.3 ppm. Noteworthy, these RTP-PolyGILs acted not only as ligands to bind metal catalysts but also as catalyst carriers, and their structures affected the activity, selectivity, and stability of the Rh catalysts [70]. 1-Octene was also hydroformylated using a new type of 1-polyethylene glycol monomethyl ether-3-methyl imidazole rhodium ionic liquid catalyst. At the best, octene conversion reached about 90%, and the yield of nonylaldehyde was >70%.

This new ionic liquid catalyst had the characteristics of "high-temperature homogeneous catalysis, low-temperature phase separation," thus allowing the recovery and recycle of the catalyst [71]. 1-Butene hydroformylation, in the presence of Rh diphosphite-modified SILP catalysts, has been investigated, and the product distribution between *n*-pentanal, *n*-butane, and 2-butene was strongly dependent on the inlet composition of 1-butene, hydrogen, and carbon monoxide. The isomerization and hydrogenation side reactions were very probably due to the H_2 oxidative addition as the initial step of the catalytic cycle [72]. A ionic liquid (IL)-in-oil Pickering emulsion system was employed for the heterogeneous hydroformylation of 1-dodecene with Rh-sulfoxantphos as the catalyst and surface-modified dendritic mesoporous silica nanospheres (DMSN) as the stabilizer to afford linear-to-branched aldehyde (*l*/*b*) ratio of 98/2, chemoselectivity of 94%, and TOF of 413 h^{-1}. The high efficiency of IL-in-oil Pickering emulsion has been attributed to the increased interface area and unique properties of ILs. Moreover, solid stabilizers with large and open pore channels could greatly increase the reaction rate of Pickering emulsion systems by accelerating the diffusion rate. Furthermore, the recyclability was good, and no leaching of Rh species was observed [73]. Very recently, the SILP catalyst consisting of a Rh/BiPhePhos complex dissolved in 1-ethyl-3-methylimidazolium bis(trifluoromethylsulfonyl)imide and immobilized on a mesoporous silicon carbide monolith was used in the continuous gas-phase hydroformylation of but-1-ene. The resulting monolith was catalytically active and selective toward linear aldehyde formation [74].

Besides ionic liquids, other solvents have been largely employed with the aim to carry out the hydroformylation process in a multiphase system as $scCO_2$ [75] and perfluorinated solvents [76], thus allowing an easy recovery of the homogeneous catalyst.

The biphasic hydroformylation of 1-dodecene, catalyzed by Rh/PPh_3 or Rh/BiPhePhos, has been studied by using decane and propylene carbonate as polar catalyst solvent, but a lower yield (52%) was obtained with respect to the single phase reaction (only decane as the solvent). The process was performed also in continuous, but a relatively high rhodium leaching between 5 and 54 ppm Rh was found unsuitable for a technical process. More promising was the use of organophilic nanosolvent filtration (ONS) that led to a catalyst concentration <1 ppm Rh in the apolar product phase [77]. Long-chain alkenes have been efficiently hydroformylated in polyethylene glycol (PEG-200), an environmentally benign solvent, in the presence of rhodium catalysts modified with the water-soluble phosphines BISBIS (sodium salt of sulfonated 2,2′-bis(diphenylphosphinomethyl)-1,1′-biphenyl) or TPPTS. Phase separation and recycling of PEG-200 and catalyst were achieved, and the leaching of rhodium into product phase was less than 0.06 wt% of the initial amount [78].

6.2.2 Aqueous Biphase Hydroformylation

An important strategy to carry out hydroformylation reactions in industrially feasible protocols is the aqueous biphasic hydroformylation of alkenes that has

Figure 6.2 TPPTS.

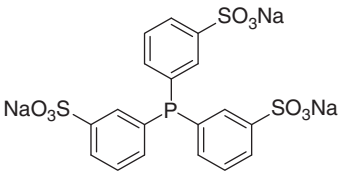

Figure 6.3 Aqueous biphase hydroformylation.

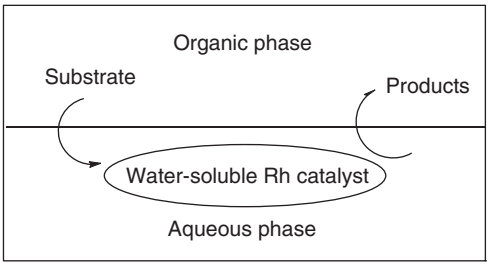

been industrially operative since 1984 using RuhrChemie/Rhône-Poulenc process [79–82]. Low-molecular-weight olefins, such as propene and butene, were hydroformylated using a water-soluble Rh(I)/TPPTS catalytic system (where TPPTS = tris(*m*-sulfonatophenyl)phosphine trisodium salt) (Figure 6.2).

In this reaction, Rh/TPPTS is embedded in the aqueous phase while the substrate and products are in the organic phase. However, using suitable conditions, the hydroformylation occurs in the mixture interphase. At the end of reaction, phase separation permits to separate products and to recover the catalyst in the aqueous phase that may be recycled (Figure 6.3).

A review on aqueous biphase hydroformylation illustrating strategies and new trends for this reaction was recently published [83 and loc. cit.]. Here, the most significant papers between 2015 and 2020, according to our personal point of view, are discussed. Water-soluble sulfonated triarylphosphines continue to be used, often in combination with ionic or nonionic surfactants, polyhydroxy compounds such as cyclodextrins (CDs), and small amounts of miscible or partially miscible solvents, or working under microemulsion conditions to facilitate reaction with long-chain hydrophobic olefins.

As matter of fact, surfactants that increase the solubility between the two nonmiscible liquid phases can promote the hydroformylation of long-chain olefins as 1-dodecene. By using a nonionic surfactant, it was possible to carry out the reaction in a continuously operated miniplant with TON of ~200 h^{-1} and high selectivity of 98 : 2 to the desired linear aldehyde. The organic components in the product phase amounted to values between 95 and 99 wt% and 99.99% of the rhodium catalyst remained in the aqueous phase [84]. The addition of small amounts of the cationic surfactant cetyltrimethylammonium bromide (CTAB) also significantly accelerated the aqueous biphase hydroformylation of bio-renewable substrates available from natural essential oils as eugenol, estragole, and safrole. However, at high concentrations, the surfactant unfavorably affected the hydroformylation selectivity [85]. A similar strategy was used on some acyclic terpenic compounds, i.e. β-citronellene,

linalol, and nerolidol, which were hydroformylated in a water/toluene biphasic system by using a rhodium/water-soluble phosphine catalytic system in the presence of cetyltrimethylammonium chloride (CTAC) to afford several fragrance compounds, with pleasant sweet floral and woody scents, in high yields [86].

A great challenge in aqueous biphasic catalysis is to overcome mass transfer limitations to convert hydrophobic organic molecules using water-soluble organometallic catalysts. In this contest, CD derivatives are considered as very effective tools as they favor contacts between substrate-containing organic phase and catalyst-containing aqueous phase, resulting in a significant improvement of the catalytic performance [87]. For instance, triglycerides were hydroformylated in aqueous medium through the formation of supramolecular complexes resulting from the inclusion of the alkenyl chains of triglycerides into the cavity of modified CDs. This system was efficiently applied to commercial oils [88]. A water-soluble β-CD-based phosphane consisting of a 3,3′-disulfonatodiphenyl phosphane connected to the primary face of β-CD by a dimethyleneamino spacer was used in the Rh-catalyzed hydroformylation of higher olefins. The catalytic system proved to be far more successful and efficient than a system consisting of supramolecularly interacting phosphanes and CDs [89]. Very recently, amphiphilic oleic succinyl-cyclodextrins (OS-CDs), synthesized from oleic acid derivatives and maleic anhydride, increased the catalytic activity of rhodium during the hydroformylation of water-insoluble olefins, such as 1-decene and 1-hexadecene, by promoting mass transfer. However, chemoselectivity was rather weak, due the isomerization of the substrate's double bond [90]. Randomly methylated CDs, in combination with sulfonated naphthylphosphanes, were successfully used in the aqueous biphasic Rh-catalyzed hydroformylation of 1-decene [91]. More recently, randomly methylated β-CD was applied as the mass transfer agent in a continuous process of Rh-catalyzed hydroformylation of 1-decene. It was shown that the process could be successfully operated under the steady state for over 200 hours with chemoselectivity of >97% toward the desired aldehyde product. Moreover, very low Rh leaching (total of 0.59%) was observed over the entire period of 200 hours [92]. Eugenol was hydroformylated in an aqueous medium in the presence of Rh/TPPTS and different modified CDs showing high selectivity toward the linear aldehydes (87%). The catalytic system was recycled up to four consecutive experiments without loss in its catalytic activity and selectivity [93].

As alternative to CDs, some modified pillar5arenes were applied in aqueous biphase Rh-catalyzed hydroformylation of terminal alkenes. The main advantage of modified pillar5arenes over CDs lies in their ability to reduce the surface tension, recognize the substrate, and, above all, prevent interaction with ligands, stabilizing the organometallic species in water. Chemoselectivity was not very high (aldehyde selectivity up to 92%), probably due to the substrate isomerization, but the proportion of linear and branched aldehydes was high (l/b up to 4.1). Moreover, the pillar5arene-based catalytic system was reusable over five consecutive catalytic runs [94]. As an alternative to CDs, polyols were used, and the Rh/TPPTS-catalyzed aqueous biphase hydroformylation of 1-octene in acid medium afforded acetals of the initially formed aldehydes. Noteworthy, a minor additive (2 wt%) of the

obtained acetal mixture improves the lubricating properties of diesel fuel by 30% and markedly reduces gum formation during combustion [95].

Methyl oleate was hydroformylated in aqueous media by using the water-soluble Rh/NaTPPTS catalyst dissolved in a mixture of water and 2-propanol, thus avoiding the use of any surfactant, CD, or other phase transfer agents. Excellent chemoselectivity (>96%) and regioselectivity (>98%) to the desired branched aldehyde products were achieved. Beneficially, a pure nonpolar aldehyde product phase was obtained after the reaction, containing only low amounts of 2-propanol (<2%) and keeping catalyst leaching very low (<0.5%). The catalyst/ligand system remained stable for 10 recycling cycles reaching accumulated TONs of up to 20 000 [96].

Technical grade methyl 10-undecenoate was hydroformylated to methyl 11-formylundecanoate (76%) in the presence of a rhodium catalytic precursor and the water-soluble ligand sulfoxantphos, using 1-butanol as cosolvent. In batch experiments, 5% of the rhodium leached in the organic product phase due to the relatively high miscibility of water in the organic 1-butanol phase. A detailed phase investigation under reaction conditions was made for the development of a highly efficient process for the formation of bifunctional molecules, useful for new polymers, starting from technical grade methyl 10-undecenoate obtained from castor oil [97]. Very recently, the reaction performance of the aqueous biphasic hydroformylation of methyl 10-undecenoate and methyl oleate was significantly improved by the use of a jet loop reactor, thus allowing a reduced loading of the cosolvent 1-butanol or the increasing loading of the substrate methyl oleate from 6 to 30 wt% [98].

The use of a jet loop reactor on miniplant scale had been already reported in the hydroformylation of 1-octene in the biphasic aqueous system, without any additive, in the presence of TPPTS, showing advantages in terms of productivity and catalytic activity. When the bidentate ligand sulfoxantphos was used, regioselectivity increased up to linear-to-branched aldehyde (l/b) ratio = 53, but catalytic activity was reduced [99]. Other phosphine ligands were also used. The hydroformylation of 1-butene catalyzed by $Rh(acac)(CO)_2$ with an excess of *N*-pyrrolylphosphine and PPh_3 ligands at 50–80 °C and 4–10 bar of syngas in toluene and in a toluene/water mixture was investigated. Regioselectivity toward the linear aldehyde increased by adding water to the reaction mixture. Water can facilitate the formation of the catalytically active rhodium hydride. Moreover, water interacts with the hydrido-olefin rhodium intermediate facilitating the formation of the linear alkyl complex in the migratory insertion step, thus favoring the linear aldehyde formation [100]. Similar results were reported in another paper [101]. The role and relevance of water was observed also on the catalytic activity of $Rh(acac)(CO)_2$ in combination with zwitterionic hydrophilic phosphines [102]. The hydroformylation of diolefins, alkynes, and unsaturated alcohols was investigated in "on-water" reactions, in the absence of any organic solvent, by using the catalytic systems Rh/PAA (water soluble) with an excess of the hydrophobic phosphine PPh_3. Very high regioselectivity toward the linear aldehyde was observed, probably due to the aggregation of hydrophobic PPh_3 molecules around the active rhodium center that facilitates the formation of linear alkyl and acyl intermediates, leading to linear aldehydes [103]. Amphiphilic

phosphine-functionalized nanogel particles were used as ligands for the biphasic rhodium-catalyzed hydroformylation of 1-octene. Even if the phosphine ligands are embedded within a cross-linked structure, metal coordination is fast and catalytic activity good [104]. Micelle-like polymer particles have been applied as phase transfer agents in aqueous multiphasic hydroformylation reactions of long chain alkenes catalyzed by rhodium catalytic precursors in the presence of water-soluble sulfonated phosphines. For instance, 1-octene was hydroformylated with a substrate to catalyst ratio of 80 000, achieving a TOF of more than 3000 h^{-1}. The aqueous catalyst phase was used in four consecutive experiments without significant loss of activity [105]. The aqueous biphasic hydroformylation of 1-octene was successfully performed by using TPP-functionalized core cross-linked micelles as nanoreactors and $[Rh(acac)(CO)_2]$ as catalyst precursor. Selectivity was better than that of the homogeneous reaction catalyzed by the Rh/PPh_3 system, with minor isomerization and linear-to-branched aldehyde ratios (l/b) between 3 and 6. Rh leaching, only few ppm, appeared related to a particle aggregation phenomenon probably through particle cross-linking [106]. Very recently, a Nixantphos-functionalized styrene has been developed and incorporated as a comonomer in the CCM synthesis. The application of the Nixantphos@CCM polymer as nanoreactor to the aqueous biphasic hydroformylation of 1-octene produced *n*-nonanal with excellent regioselectivity but only with a moderate activity, which may be attributed to mass transport limitation [107].

Emulsions, which are composed of microdroplet or nanodroplet suspensions in an immiscible fluid, have attracted much research attention for biphasic catalysis. Among various types of emulsions, solid colloidal particle-stabilized microdroplets are especially fascinating because of their stability and easier separation process. Nanoscale droplets of aqueous phase homogeneous catalyst Rh/TPPTS could be formed by encapsulation method and used for biphasic hydroformylation of long-chain alkenes. Due to the small droplet sizes, the organic–aqueous interface area could be greatly enhanced, yielding improved catalytic activity and aldehyde selectivity [108]. Microemulsion systems using $Rh(acac)(CO)_2$/sulfoxantphos catalyst system were applied in the hydroformylation of 1-dodecene. The reaction rate was dependent on syngas pressure, indicating an inhibition of the reaction, most probably due to the high partial pressure of CO [109]. Long-chain olefins were hydroformylated in a microemulsion system, and surfactants played a fundamental role determining the stability of the microemulsion and the local concentrations at the oil–water interface [110]. The hydroformylation of long-chain alkenes in microemulsions on a larger scale was carried out in a miniplant. In addition, during a 200 hours' miniplant operation, a stable aldehyde yield of 21% was obtained, and the catalyst loss in the product phase was below 0.1 ppm [111].

Phosphines with a strong π-acceptor character containing sulfonic and trifluoromethyl groups are more inert toward oxidation than classical sulfonated phosphines and were used as ligands in the biphasic hydroformylation of vinyl acetate and allyl cyanide with an increase of reaction rate up to four times compared with the results obtained with the non-trifluoromethylated phosphines [112].

Besides phosphines, also water-soluble nonphosphine ligands (in combination with Rh(I) precursors) were successfully employed in the aqueous biphasic

hydroformylation. This is an emerging trend for this reaction [83 and loc. cit.]. These catalysts precursors have demonstrated good activity and aldehyde selectivity in hydroformylation reactions. However, the regioselectivity is often poor. High conversions and good aldehyde chemoselectivities were observed also with each recycle. In this contest, Rh(DHTANa), a water-soluble catalyst easily obtained by mixing in water the catalytic precursor $[Rh(COD)Cl]_2$ and the dihydrothioctic acid sodium salt (DHTANa), was active in the biphase hydroformylation of styrene, producing exclusively the two corresponding aldehydes, with 80–86% selectivity toward the branched aldehyde 2-phenylpropanal [113]. Water-soluble rhodium complexes obtained via reaction of $[Rh(COD)(MeCN)_2]BF_4$ with sulfonated α-diimine ligands were employed in the aqueous biphasic hydroformylation of 1-octene, obtaining high conversions and regioselectivity. The catalysts were reused over four consecutive catalytic runs without significant loss in catalytic activity [114]. A series of water-soluble Rh(I) mononuclear complexes of general formula [Rh(sulfsal-X-R)(COD)] (sulfsal = sulfonated salicylaldimine; COD = cyclooctadiene; where R = H, Cl, CH_3 and X = H, *t*-Bu) have been synthesized and used as catalyst precursors in the aqueous biphasic hydroformylation of 1-octene without addition of any phase transfer agents, co-solvents, or hydrophobic ligands. Very interestingly, it was observed that a combination of homogeneous catalysis and catalysis mediated by nanoparticles was taking place in these systems [115]. Hydroformylation of styrene and 1-hexene was catalyzed by $[RhCl(COD)]_2$ in combination with a water-soluble sulfonated pyridyl-triazolyl *N*,*N*-bidentate ligand showing good catalytic activity and complete chemoselectivity. The aqueous catalytic phase was recycled four times, and it was shown that after the first catalytic run, rhodium was present in the aqueous phase in nanoparticle form [116].

6.2.3 Enantioselective Hydroformylation

Enantioselective hydroformylation (EHF) might represent one of the most efficient routes for the preparation of nonracemic aldehydes from alkenes in the presence of syngas in a perfect atom-economic way. However, the practical application remains still a challenge, and the goal to design a universal and economic catalyst seems too far to be reached even if the academic research is active in this field. In addition, numerous applications in the synthesis of important nonracemic intermediates for the preparation of pharmaceuticals and other fine chemicals have been described (Scheme 6.2).

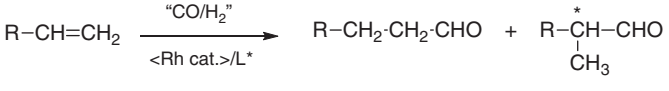

R = alkyl or aryl group
L* = chiral nonracemic ligand

Scheme 6.2 Enantioselective hydroformylation (EHF).

In a review of 2018, the problems and perspectives of EHF were discussed. According to the authors, there are many impediments to scalable applications: (i) relatively low diversity of chiral nonracemic ligands that provide effective rates and selectivities, (ii) limited exploration of substrate scope, (iii) limited mechanistic understanding of the factors that control reaction selectivity and rate, and (iv) few demonstrations of efficient flow reactor processes [117]. Although the selectivity in EHF can be controlled to some extent by the reaction conditions and substrates, it is mainly determined by the nature of the nonracemic ligands used (Figure 6.4).

The choice of the optimal ligand changes from case to case, but encouraging results have been obtained during the past decade with the introduction of ligands such as bisdiazaphos, Ph-BPE, Yanphos, some P-chirogenic ligands, and many others [118]. For instance, a rhodium complex, in conjunction with commercially available Ph-BPE ligand, catalyzed the EHF of 1-alkenes, affording good branched-to-linear (*b*/*l*) aldehyde ratios (up to 15/1) and very high enantioselectivity (up to 98 : 2 enantiomeric excess [ee]) [119]. The Rh-catalyzed EHF of vinyl arenes in the presence of different phospholane–phosphoramidite ligands containing four elements of chirality gave enantioselectivities up to 79% ee [120]. An accessible protocol for the EHF of vinylarenes, using formaldehyde as a substitute for syngas, was reported. The regioselectivity (*b*/*l* up to 96/4) and enantioselectivity (up to 95% ee) were obtained using Ph-BPE as a ligand [121]. α,ω-Bisphosphite ligands, which incorporate a polyether motif as regulation site, were able to increase the enantioselectivity in the rhodium-catalyzed EHF of different substrates. As a matter of fact, small amounts of polyether-binder RAs (RA = regulation agent) were shown to regulate the activity of the catalysts, obtaining up to 82% ee. Computational studies suggested that the increase in enantioselectivity provided by the RAs arises from adaptation of the P—Rh—P bond angle (β) to the particular requirements of the substrate [122]. Yanphos and bisdiazaphospholate ligands gave interesting results in the production of intermediates for pharmaceuticals and fine chemicals, even if not on a commercial scale, due to several technical

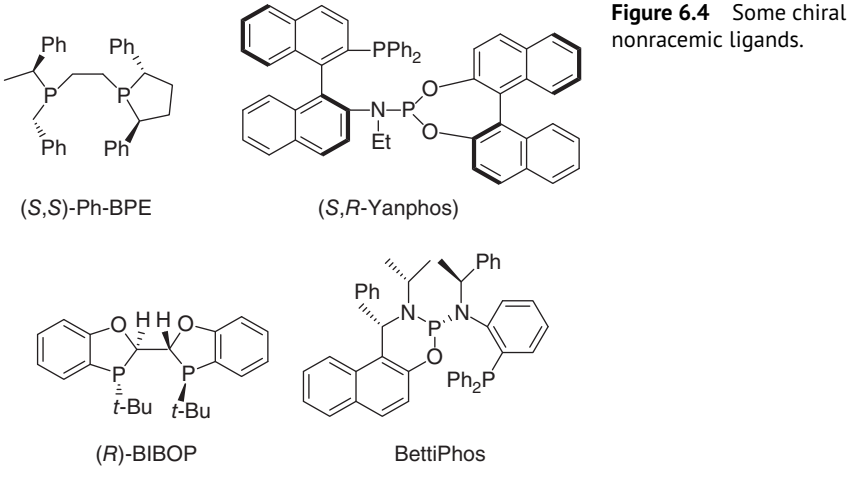

Figure 6.4 Some chiral nonracemic ligands.

challenges [123, 124]. [Rh(acac)$(CO)_2$], in combination with (*S*,*R*)-*N*-Bn-Yanphos, catalyzed the hydroformylation of methyl cyclopent-3-enecarboxylate to the corresponding cyclopentane carboxaldehyde with 91% conversion, 91% ee, and 95 : 5 diastereoselectivities [125]. Very recently, the rhodium-catalyzed enantioselective anti-Markovnikov hydroformylation of α-substituted acrylates/acrylamides has been described. By employing the Rh/(*S*,*S*)-DTBM-Yanphos complex, a series of β-chiral linear aldehydes were obtained in high yields (up to 94% yield) and high enantioselectivities (up to 96% ee) [126].

Excellent conversions (>99%), enantioselectivities (up to 95 : 5 ee), and *b*/*l* of up to 400 were achieved in the rhodium-catalyzed EHF of various terminal olefins in the presence of air-stable and tunable chiral bis-dihydrobenzo oxaphosphole ligands (BIBOPs) [127]. Very high regioselectivities ($b/l > 1000$) and excellent enantioselectivities up to 97% ee were achieved in the rhodium-catalyzed EHF of vinyl esters and vinyl amides by using hybrid bidentate phosphine-phosphorodiamidite ligands based on a chiral Betti base backbone and diphenylphosphinoaniline derivatives (BettiPhos), having a stereogenic P atom at the phosphorodiamidite moiety [128]. Chiral tetrasubstituted aldehydes with 85% ee were obtained by hydroformylation of 1,1′-disubstituted acrylates catalyzed by nonracemic bisdiazaphospholane (BDP)- and bisphospholanoethane-ligated rhodium complexes [38]. The hydroformylation on the β position of a heteroatom such as oxygen or nitrogen atom is not easy to accomplish, but recently, chiral β-aldehydesilanes, useful synthetic intermediates for bioactive molecules and natural products, were prepared with excellent enantioselectivities (up to 97% ee) and regioselectivities (β/α up to >99) by hydroformylation of *Z*-alkenylsilanes. DFT calculations, carried out for Rh/Yanphos-catalyzed EHF, suggested that the silicon group can activate the substrate and is critical for the regioselectivity [129]. Very useful compounds are 3,4-dihydroisocoumarins and their derivatives as key intermediates for the synthesis of biologically active molecules. For instance, 4-methyl-3,4-dihydroisocoumarin was prepared in a 95.1 : 4.9 enantiomeric ratio by EHF of ethyl 2-vinylbenzoate followed by *in situ* lactonization during the reduction process in the presence of Rh/BIBOP type ligands as catalytic system [130]. Also, valuable lactones, lactams, furanidines, and pyrrolidines could be obtained by EHF of allylic alcohols and amines. Recently, Rh-catalyzed highly enantioselective anti-Markovnikov hydroformylation of 1,1-disubstituted allylic alcohols and amines has been performed with up to 90% yield and 93% ee by using a Rh/chiral hybrid phosphorus ligand catalytic system [131].

Related to the problem of cost of the ligands, a possibility could be offered by the use of immobilized catalysts. Recently, norbornene has been enantioselectively hydroformylated in the presence of Rh/C1-symmetrical diphosphite ligands containing furanose backbone. The *exo*-norbornane carboxaldehyde was exclusively produced with ee up to 71%. The ligands were modified with a pyrene moiety to accomplish their immobilization onto carbon materials, and the corresponding Rh complexes were immobilized onto multiwalled carbon nanotubes (MWCNTs), reduced graphene oxide (rGO), and carbon beads (CBs). The novel catalytic systems were tested in the EHF of norbornene providing similar performances in terms of

both activity and selectivity compared with the non-immobilized systems, but it was not possible to recycle the catalyst because of rhodium leaching, working in a batch mode. However, when used under continuous flow mode, these catalysts revealed to be robust and provided even higher ee than the corresponding homogeneous systems [132]. Very interesting was also the study on the EHF of styrene and 2-vinyl-6-methoxynaphthalene, catalyzed by rhodium(bisdiazaphospholane) (BDP) complexes, carried out also in a continuous reactor system consisting of 20 vertical bubble flow pipes in series [133, 134]. Significantly, this study demonstrated that (i) careful attention to the flow reactor can result in good gas–liquid mass transport for a reaction that is sensitive to partial pressures of gaseous reagents, (ii) operando high-pressure NMR in benchmarking catalytic rates and selectivities is very useful for optimization of flow reactors, and (iii) application of EHF could be performed safely and effectively in a pharmaceutical environment.

6.2.4 Tandem Hydroformylation

A large number of new examples involving tandem and one-pot sequences under hydroformylation conditions have been developed after the review in 2015, where they are summarized in five important tandem categories such as hydroformylation–hydrogenation, hydroformylation with additional C—C bond formations, hydroformylation–elimination reactions, hydroformylation in the presence of *N*-nucleophiles, and hydroformylation–acetalization [135].

Some relevant contributions are here reported, especially related to hydroformylation–isomerization and hydroformylation–hydrogenation to obtain alcohols or amines, but not exclusively (Scheme 6.3).

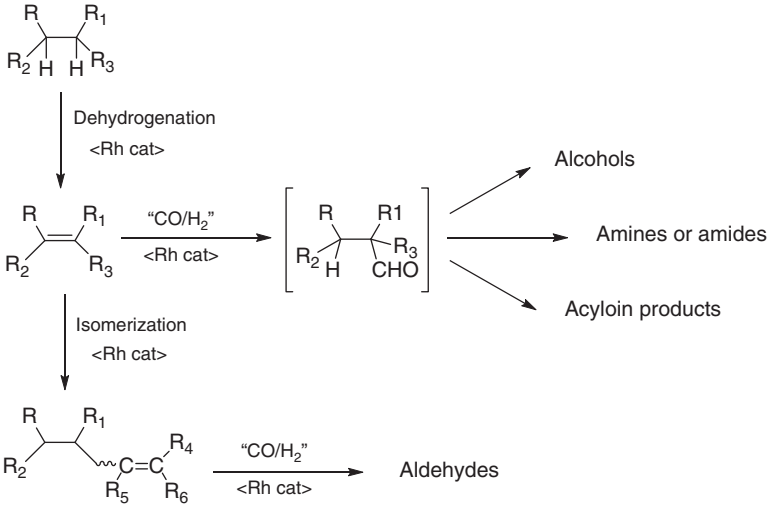

R–R_6 = H, alkyl, aryl, or hetero group

Scheme 6.3 Main examples of tandem reactions.

The hydroformylation–isomerization of 10-undecenitrile and related functionalized unsaturated fatty substrates, useful to produce bifunctional compounds, was carried out in the presence of rhodium/BiPhePhos or the corresponding iridium catalyst, affording the linear aldehyde in high selectivity (ratio *l*/*b* aldehydes = 99/1). Rh species had the best $TOF_{HF} = 3320\ h^{-1}$ and a better recyclability, but Ir species allowed slightly better control of the distribution of the internal isomers. The formation of internal olefin isomers with Rh catalyst was studied in detail [136, 137]. Highly selective tandem isomerization–hydroformylation reactions allowed to convert mixtures of *n*-decenes with internal double bond position to the desired terminal aldehyde undecanal in the presence of the Rh/BiPhePhos catalyst. The reaction was deeply investigated experimentally and by theoretical modeling, and it was found that the tandem reaction showed completely opposite dependencies regarding temperature and synthesis gas pressure compared with the conventional hydroformylation of 1-decene [138]. Rh/bis(phosphite) ligand complex catalyzed the isomerizing hydroformylation not only of short-chain internal olefins such as *cis*-2-octene but also of highly challenging long-chain plant oil-derived internal olefins such as methyl oleate. The isomerization was favored at higher temperatures, and the terminal formylation was favored at lower syngas pressures [139]. The tandem isomerization hydroformylation of the long-chain fatty oleonitrile was catalyzed by $Rh(acac)(CO)_2$/BiPhePhos system. The higher ratio linear-to-branched aldehyde (58/42) was obtained at 120 °C and 10 bar CO/H_2 (1 : 1) with a 0.5 mol% catalyst load and a low ligand excess (2 equiv vs. Rh). Chemoselectivity, at the best, was 60% because of concomitant hydrogenation reaction [140]. The synthesis of adipaldehyde through isomerization–hydroformylation of butadiene catalyzed by the (DIOP)Rh system was studied. The thermodynamically favored intermediate, pent-2-enal, was however formed and was the source of by-products. The amount of pent-4-enal was actually low, but its hydroformylation was more rapid and afforded adipaldehyde. So, a suitable isomerization catalyst, which could shift the equilibrium between pent-2-enal and pent-4-enal toward the latter compound, was necessary to increase the amount of adipaldehyde [141]. The rhodium-catalyzed isomerizing hydroformylation was also applied to the cashew nutshell liquid (CNSL), a nonedible plant sourced oil that is readily available on a large scale from agricultural resources. The best results were obtained in the presence of the rhodium complex 1,2-bis((di-*tert*-butylphosphanyl)methyl)benzene (BDTBPMB), affording a linear selectivity up to 74% [142].

Besides olefins, also alkanes, the main constituents of petroleum, are attractive feedstocks for producing value-added chemicals. A molecular dual-catalyst system for production of linear aldehydes from *n*-alkanes has been described; the process consisted of alkane dehydrogenation over a heterogeneous Cr/Al_2O_3 catalyst followed by direct gas-phase hydroformylation using advanced SILP Rh catalysis. The latter step made use of rhodium complexes modified with the diphosphite ligands such as BiPhePhos to efficiently convert the butane/butene mixture from the dehydrogenation step into aldehydes [143]. More recently, a system consisting of a pincer iridium catalyst for transfer dehydrogenation of the alkane, using *t*-butylethylene or ethylene as a hydrogen acceptor, and, sequentially, a rhodium

catalyst for olefin isomerization–hydroformylation with syngas, has shown high regioselectivity for linear aldehydes [144]. In the same work the authors obtained also linear alkyl amines from alkanes using the same catalytic system [144].

Very recently, the rhodium-catalyzed hydroformylation of 1-arylbutadienes derived from lignocellulosic bioresources has been carried out in toluene and green solvents. Depending on the nature of the diphosphine ligand, consecutive C=C double bond isomerization and hydrogenation took place, resulting in a useful tandem process, thus producing conjugated enals or saturated aldehydes in good to excellent selectivity [145].

The production of alcohols, which has a great industrial importance for fine and commodities companies, was recently reviewed. One strategy uses a tandem hydroformylation–hydrogenation reaction ("hydrohydroxymethylation") with a single catalyst, while others, where the hydroformylation step was still involved, utilize two different catalysts or also include, before the hydrogenation step, an intermediate aldol condensation [146]. The rhodium-catalyzed hydrohydroxymethylation is of great importance especially for higher-value products. Chemoselectivity could be optimized through modification with organic ligands, preferably nitrogen and phosphorus ligands. Besides syngas, other sources for syngas or CO, such as paraformaldehyde or CO_2, were also used to produce alcohols with the assistance of rhodium catalysts [146]. The hydrohydroxymethylation of dicyclopentadiene, with formation of the corresponding diols, was catalyzed by a phosphine-free rhodium catalyst such as $[Rh(octanoate)_2]_2$ in combination with triethylamine to give a 79% yield of the desired diol under mild reaction conditions (Scheme 6.4).

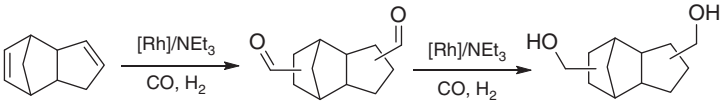

Scheme 6.4 Hydrohydroxymethylation of dicyclopentadiene.

Moreover, the Rh/amine catalyst complex was recycled by a simple water extraction of the diol product and used in three recycling runs [147].

The same tandem reaction allowed also to obtain trihydroxylated triglycerides; tertiary amines were employed as well in this case to coordinate Rh. The Rh/amine catalyst proved to be active both in the hydroformylation of the carbon–carbon double bond and in the reduction of the resulting aldehydes into alcohols [148].

The one-pot hydroaminomethylation (HAM) of alkenes is a tandem reaction that involves three successive steps: hydroformylation of the alkene into the corresponding aldehyde followed by its condensation with a N–H function and the catalyzed hydrogenation of the imine/enamine intermediate into the corresponding saturated amine. The nature of the metal catalyst and of ligands, temperature, CO/H_2 partial pressures, and solvent are essential in terms of activity and selectivity. Phosphine ligand-modified rhodium complexes generally displayed better activity and regioselectivity in both hydroformylation and hydrogenation steps. Apart from the

phosphorus ligands, carbene and nitrogen-containing ligands were also developed and showed good activity due to the promotion of the hydrogenation step. The rate of the hydroformylation step needs to be faster than that of the hydrogenation step. The separation of the catalyst from the organic products by biphasic or (semi-)heterogenized systems and its recycling have been demonstrated in many cases. The HAM reaction was reviewed [149, 150]. The HAM has been recently employed to prepare amines from estragole with di-*n*-butylamine. Rhodium(I) catalysts modified with phosphines, phosphites, and phospholes were employed, and phosphole-promoted systems showed the best performance, being more selective in the hydroformylation step and more efficient in the reductive amination one [151]. The HAM of aniline and its derivatives with heterocyclic and/or cyclic olefins were successfully carried out in the presence of $[Rh(cod)_2]BF_4/PPh_3$ at syngas pressure of 4 MPa ($H_2/CO = 3:1$), 100 °C, 20 hours, without any additive. The conversion of aniline reached >99% and the yield, for example, of an important intermediate, *N*-[(tetrahydrofuran-3-yl)methyl]aniline, was up to 99% (Scheme 6.5) [152].

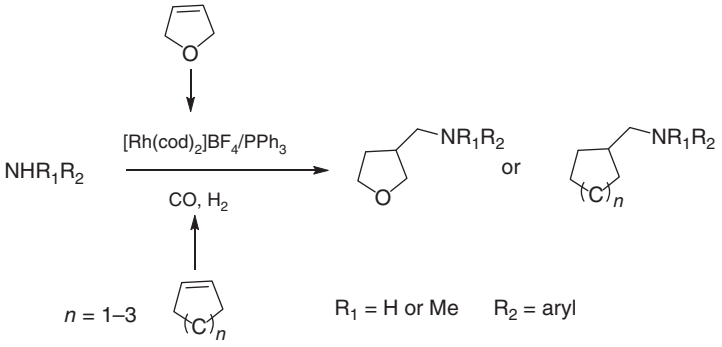

Scheme 6.5 Synthesis of *N*-arylated amines by hydroaminomethylation. Source: Modified from Wang and Zheng [152].

Amines with potential bioactivity were obtained by HAM of bio-renewable alkenes, i.e. estragole, limonene, camphene, and β-pinene, in the presence of di-*n*-butylamine, morpholine, 4-methylpiperidine, or 1,2,3,4-tetrahydroisoquinoline. Very interestingly, the reaction could be carried out in greener solvents (as *p*-cymene, anisole, and, in particular, ethanol) than the conventionally used solvents [153]. Novel cationic Rh(I) imino-pyridine complexes were employed as catalyst precursors in the HAM of 1-octene with both primary (aniline and benzylamine) and secondary amines (piperidine). It was found that the basicity of the amine impacts on the rate of the reaction. The more basic the amine, the faster the reaction, and the higher the yield of the targeted *N*-alkylated amines. The HAM of 1-octene with primary amines was successfully performed without the formation of tertiary amines except when the reaction was performed over extended reaction times [154]. It was possible to carry out the HAM of different α-olefins with a wide range of alkyl, aryl, and heteroarylamines that do not react under more conventional conditions with a single catalyst by using two distinct mutually compatible catalysts. The hydroformylation step was catalyzed by a rhodium diphosphine complex while

the reductive amination, which was conducted as a transfer hydrogenation with aqueous, buffered sodium formate as the reducing agent, was catalyzed by a cyclometalated iridium complex [155]. The bis-HAM of linear aliphatic 1-alkenes was successfully performed with high yields and selectivities toward linear products by using piperazine as the diamine component. For instance, 1-octene gave the corresponding bis-alkylated product in 80% yield with a linear selectivity of 77% in the presence of [Rh]/BiPhePhos catalyst system. Many other olefins, such as branched 1-alkenes, internal alkenes, styrene, cycloalkenes and olefins with alcohol and ester groups, were successfully transformed into the corresponding bis-HAM products with moderate-to-excellent yields and linearities. Especially, the possibility to elegantly link two ester or alcohol functionalities via a piperazine ring under the formation of linear α,ω-bifunctional components opened up a new tandem catalytic methodology for the atom-economic formation of potential polyester monomers [156]. The HAM process could be conveniently performed also in aqueous biphase system as previously described. As an alternative strategy to HAM, primary diamines could be obtained from olefins and ammonia by metal-catalyzed hydroformylation, hydrogenation, and direct amination using two different catalysts. For example, the rhodium-catalyzed hydrohydroxymethylation step converted non-conjugated dienes into the intermediate diols, and then ammonia was added in a ruthenium-catalyzed amination step to obtain primary diamines [157]. Tertiary amine derivatives were prepared by HAM reactions catalyzed by Rh(I)/xantphos (hydroformylation of *n*-alkyl olefins), by Rh(I)/bulky arylphosphite systems (hydroformylation of steroid internal double bonds) or by Rh(I)/TPP (hydroformylation of the vinyl-aromatic indole derivative) [158]. In the same paper, a sequential hydroformylation/Strecker reaction, to prepare new α-amino acids, was studied [158].

Less common but equally important tandem reactions involving hydroformylation are now illustrated.

A very interesting reaction is the tandem hydroformylation/acyloin reaction, which leads directly to acyloins from olefins. Excellent overall reaction selectivities up to >99% with excellent yields up to 96% for the desired intermediate *n*-aldehydes and very good yields up to 79% for the final acyloin products were obtained (Scheme 6.6) [159].

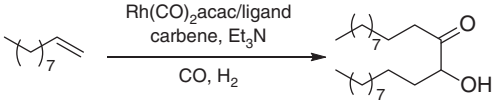

Scheme 6.6 Example of tandem hydroformylation/acyloin reaction. Source: Modified from Ostrowski et al. [159].

Also, cashew nut sulfonamides could be prepared by a highly selective domino hydroformylation–reductive sulfonamidation reaction of olefins in the presence of a specific rhodium phosphine catalyst system [160].

The hydroformylation of unsaturated esters as acrylates was combined with a Michael reaction in tandem or one-pot fashion. The reaction furnished functionalized compounds with a quaternary carbon atom, useful intermediates in the synthesis of more complex compounds (Scheme 6.7) [161].

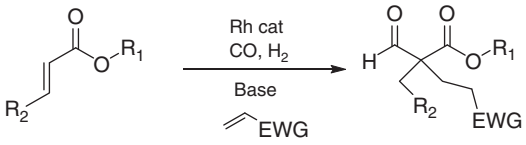

R_1 = alkyl
R_2 = H or alkyl
EWG = electron-with drawing group

Scheme 6.7 Tandem hydroformylation/Michael reaction of acrylates. Source: Modified from Quintero-Duque and Fleischer [161].

The alkyne-mediated rhodium-catalyzed hydroformylation/double-cyclization domino reaction of 3-butenamides allowed to synthesize indolizidines, quinolizidines, 1-azabicyclo[5.3.0]decanes, and 1-azabicyclo[5.4.0]undecanes, useful intermediates for biologically active compounds [162].

1,5-Dimethylhexahydro-1*H*-inden-4(2*H*)-one was efficiently obtained from (*R*)-carvone by using homogeneous Rh/dppp catalyst and pyridinium *p*-toluenesulfonate (PPTS) as a mild acidic co-catalyst. The catalytic system proceeded through one-pot (*R*)-carvone hydroformylation, intramolecular keto-aldol condensation, and hydrogenation reactions, sequentially. The use of PPTS as a co-catalyst accelerated the intramolecular keto-aldol condensation without any unusual effect on Rh/dppp catalyst [163]. Finally, as relevant example of possible synergies between chemo- and bio-catalysis, a tandem hydroformylation/chemoenzymatic reaction has been explored to produce aliphatic nitriles by using a cyanide-free approach. The protocol, starting from *n*-alkenes to obtain nitriles without the need of purification of intermediates, followed these three steps: hydroformylation, aldoxime formation, and transformation of the aldoxime into final target products, after removal of traces of hydroxylamine as an enzyme-deactivating component, through dehydration by means of aldoxime dehydratases (Scheme 6.8) [164].

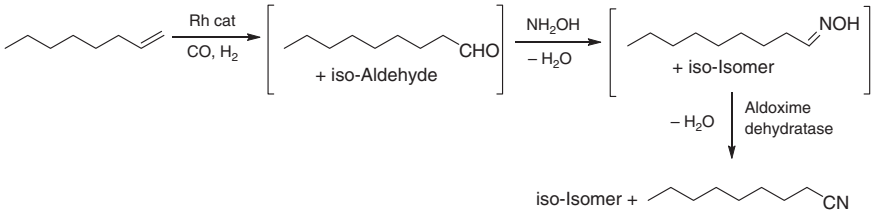

Scheme 6.8 Nonanenitrile synthesis by tandem hydroformylation/chemoenzymatic reaction. Source: Modified from Plass et al. [164].

6.2.5 Syngas Surrogates

Not only carbon monoxide is an unsafe gas, but also the employment of pressurized CO can require considerable investment costs, thus limiting its use in the industry. CO-free hydroformylations are therefore desirable in the view of a

more sustainable process; moreover, some carbon monoxide surrogates are easily transportable and available from waste biomass (e.g. formaldehyde, methanol, oxalates, formates, etc.). In this contest, the use of formaldehyde as a surrogate for both CO and hydrogen is highly appealing and has been the topic of research for some time [165–168]. For instance, the linear-selective hydroformylation of vinyl heteroarenes has been performed by using formaldehyde as syngas substitute. Yields up to 84% and high regioselectivity (linear-to-branched aldehyde of up to 93/7) were achieved when BIPHEP and Nixantphos were simultaneously employed as ligands [169]. The oxo process, catalyzed by $[Rh(COD)Cl]_2$, in combination with the two above phosphane ligands (BIBHEP and Nixantphos), was a key step in the synthesis of 7-methoxycryptopleurine, an anti-inflammatory and antiviral drug with cytotoxicity against different human cancer cell lines. The hydroformylation reaction, carried out at 90 °C by using formaldehyde as syngas surrogate, afforded regioselectively the linear aldehyde in good yield [170]. Again, formaldehyde was used as surrogate of syngas in the hydroformylation of 1-hexene catalyzed by $[Rh(\kappa^2\text{-P,P-dppe})_2]$acac (dppe: 1,2-bis(diphenylphosphino)ethane). It was hypothesized a catalytic cycle that firstly involves the reversible oxidative addition of formaldehyde to the catalytic precursor to yield the intermediate $[Rh(H)(CHO)(\kappa^2\text{-P,P-dppe})_2]^+$, followed by the insertion of the olefin into the Rh—H bond, and the cycle is completed by the reductive elimination of the aldehyde to regenerate the catalytic precursor and restart the cycle [171]. As already reported in Section 6.2.3 on enantioselective hydroformylation, formaldehyde, as a syngas substitute, was also employed with success in the enantioselective hydroformylation of vinylarenes [121]. Noteworthy, the rhodium complex was able to catalyze both the decarbonylative degradation of formaldehyde to CO and H_2 and the subsequent hydroformylation reaction [103]. It was possible to carry out also an enantioselective transfer hydroformylation (ETHF) by using paraformaldehyde as syngas substitute. The reaction, catalyzed by $[Rh(acac)(CO)_2]$ modified with 1,2-bis[(2*S*,5*S*)-2,5-diphenylphospholano]ethane(1,5-cyclooctadiene) (Ph-BPE), afforded high selectivities, TOFs, and enantioselectivity of up to 96% ee [172]. A following protocol was developed by the same authors, in which a catalyst for formaldehyde decomposition to CO and H_2 was combined with the catalyst of choice for the subsequent EHF. This enabled ETHF reactions that were problematic to be significantly improved and permitted the application to many intermediates of biologically active molecules [165].

Not only formaldehyde but also different molecules as formates, alcohols, aldehydes, CO_2, etc. can be used as surrogates. For instance, a variety of primary alcohols have been used for the *ex situ* delivery of carbon monoxide and molecular hydrogen in a two-chamber reactor. The gaseous mixture was liberated in one chamber by an iridium-catalyzed dehydrogenative decarbonylation of the alcohol and then consumed in the other chamber in a rhodium-catalyzed hydroformylation of olefins. Hexane-1,6-diol was found to be the optimum alcohol for both reactions, affording aldehydes with moderate-to-excellent yields [166]. A mixture of methyl formate and water was used as an alternative syngas source for hydroformylation of

unsaturated compounds in the presence of rhodium catalysts modified with phosphine ligands. Under reaction conditions, methyl formate decomposes producing methanol and carbon monoxide. The water–gas shift reaction (WGSR) takes place under the same conditions, resulting in carbon dioxide and hydrogen generation. Interestingly, methanol, hydrogen, and CO_2 formed could be isolated and used for the synthesis of methyl formate, an initial source for gas production [173]. The gaseous mixture CO_2/H_2 was used also in the hydroformylation of aryl iodides and bromides catalyzed by RhI_3/PPh_3 and Ac_2O/Et_3N. The reaction proceeded through three cascade steps, involving HCOOH formation, CO release, and formylation of aryl halides [168].

Recently, a syngas-free rhodium-catalyzed hydroformylation of alkynes was performed via formyl and hydride transfer from an alkyl aldehyde. Noteworthy, the hydroformylation of alkynes is one of the most efficient methods to obtain α,β-unsaturated aldehydes. However, the regioselectivity is difficult to control and the formation of byproducts such as hydrogenated products of alkynes and saturated aldehydes is poorly suppressed. The use of an inexpensive and easy-to-handle alkyl aldehyde as *n*-butyraldehyde or *n*-propionaldehyde and of a commercially available catalyst and ligand allowed to transform a broad range of internal alkynes into versatile stereodefined α,β-unsaturated aldehydes with excellent chemo-, regio-, and stereoselectivities [174].

Very interestingly, also CO_2 and poly(methylhydrosiloxane) (PMHS), two nontoxic and inexpensive chemical waste products, were used as the carbonyl source and hydrogen in the hydroformylation of olefins catalyzed by an efficient rhodium phosphoramidite catalytic system. Most likely, the reaction proceeded through a one-pot tandem sequence of PMHS-mediated CO_2 reduction to CO followed by a conventional rhodium-catalyzed hydroformylation with CO/H_2 [167].

6.3 Carbonylation

Rh-catalyzed carbonylation reactions are of fundamental importance for the industrial production of many bulk and fine chemicals [1], and one of the most significant examples is represented by the production of acetic acid (Scheme 6.9a) [175]. In the catalytic cycle (Scheme 6.9a), oxidative addition of methyl iodide to *cis*-$[Rh(CO)_2I_2]^-$ gives an octahedral Rh(III) methyl complex that undergoes rapid methyl migration to give an acetyl complex. Coordination of CO, reductive elimination and hydrolysis of acetyl iodide affords acetic acid. An alternative to sequential reductive elimination and hydrolysis of acetyl iodide is direct reaction of water with a rhodium acetyl complex to give acetic acid. Starting from the first methanol to acetic acid carbonylation process (BASF 1960), more convenient processes have been developed. Several efforts have already been done in the laboratory-scale process to develop more advantageous homogeneous or heterogeneous catalysts. For instance, homogeneous $[Rh(CO)_2Cl(P\text{-}O)]$ and $[Rh(CO)Cl(P\text{-}O)_2]$ (P-O = 2-$Ph_2PC_6H_4COOCH_3$) showed efficient catalytic activity with high TON [176]. However, even if homogeneous methanol carbonylation is

one of the main processes to produce acetic acid, it suffers from complex separation operations. Heterogenization process is a key route to solve this issue, but less activity, poor selectivity, and instability are commonly the key problems for heterogeneous carbonylation catalysts. Many efforts have been done to develop new heterogeneous catalytic systems, which were reviewed very recently [177]. In particular, new Rh carbonylation centers supported on POPs were developed, and the single-site Rh supported on POPs by chemical bonds could enhance the carbonylation stability [177]. Also, iodide immobilization or iodide-free technics such Rh-acid bifunctional catalysts and zeolites are important for the development of an ecofriendly process, but carbonylation activity is low [177]. Based on Rh/ZSM-5 as the typical catalyst, an inorganic/organic composite catalyst could be designed, aiming at lowering the reaction energy barrier and enhancing carbonylation activity via the adjustment of acid zeolites component and the change of Rh structure by the modification of ligand monomer [177]. The CT-ACETICA™ process employs resin-supported rhodium catalysts and is an efficient example of immobilization of homogeneous catalytic systems. Many studies have shown that using montmorillonites, mordenites, or zeolites as catalyst or catalyst supports, relatively high productivities and selectivities in acetic acid can be achieved [175]. Very interestingly, heterogeneous vapor-phase methanol carbonylation was catalyzed by the *in situ* generated $[Rh(CO)I_3]^{2-}$ species ionically immobilized onto the cationic framework of porous ionic polymers (PIPs) in the form of $[P]^+$–$[Rh(CO)I_3]^{2-}$–$[P]^+$, showing unprecedented activity and superb long-term stability. The newly arising PIPs materials with ionic framework, with respect to the well-known vinyl-polymerized POPs, were superior analogues due to the dual- or multi-ionically bound interactions between metals and PIPs [178]. Acetic acid and *N*,*N*-dimethylacetamide were also obtained by carbonylation of methyl iodide and trimethylamine in 1-methyl-2-pyrrolidone in a process catalyzed by $[Rh(CO)_2I_2]^-$ in the presence of calcium oxide and water (Scheme 6.9b). Practically, there were two carbonylation routes of trimethylamine and methyl iodide, and the carbonylation rate of trimethylamine was faster than that of methyl iodide. $[Rh(CO)_2I_2]^-$ in the presence of trimethylamine was reused 25 times (6.9) [179].

Other carboxylic acids may be obtained, too. In this contest, vapor-phase ethanol carbonylation, a potential route to valuable C_3 products, was catalyzed by Rh supported on porous Cs-exchanged heteropolyacid $Cs_3PW_{12}O_{40,}$ with ethyl iodide as a co-catalyst. Propionate selectivity reached 96% at 170 °C with added H_2O. Slow deactivation through formation of Rh nanoparticles was observed [180]. Vapor-phase EtOH carbonylation to propionates has been performed also with Rh/zeolite $Na_{13}X$ and EtI. In the absence of Rh, only products from dehydration of EtOH were formed. CO was found to have an inhibitory impact on EtOH conversion, presumably caused by reversible coordination and formation of an inactive Rh complex. The working catalyst was proposed to be a mixture of an active anionic Rh(I)I supported at an exchange site on the zeolite (~80%) and an inactive Rh(III) species (~20%) [181]. An air- and moisture-stable polystyrene-supported Rh(I) complex was used also in the carbonylation of glycerol in acetic acid medium at 30 atm of carbon monoxide. In the presence of HI, glycerol was converted to isopropyl iodide and allyl iodide, and

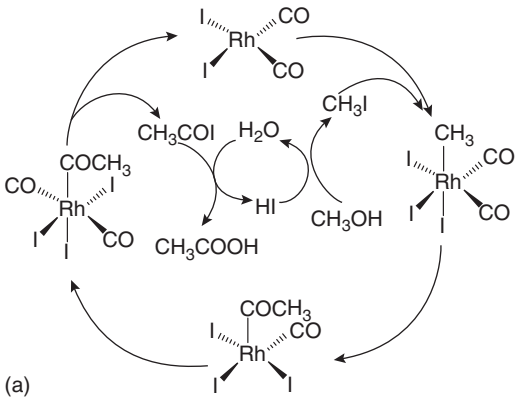

$$N(CH_3)_3 + CH_3I \xrightarrow[CO]{[Rh(CO)_2I_2]^-} H_3C{-}\overset{\overset{O}{\|}}{C}{-}N(CH_3)_2 + H_3C{-}\overset{\overset{O}{\|}}{C}{-}OH$$

(b)

Scheme 6.9 (a) Reaction mechanism for methanol carbonylation; (b) Carbonylation of methyl iodide and trimethylamine. Source: Modified from Hong [179].

butyric and iso-butyric acids were formed from these intermediates. The catalyst was reused for six consecutive cycles with consistent catalytic activity [182].

Carbonylation of methyl acetate to acetic anhydride, a product widely employed in the chemical and pharmaceutical industry, was studied to determine the suitable reaction conditions. A rhodium iodine system was used as catalyst, and working at 150 °C and 5 MPa pressure, 92% conversion and almost 100% selectivity were achieved [183].

Very recently, carbonylative dimerization of butyl acrylate with $[RhCp^*Cl_2]_2$ as the catalyst and Ac-Gly-OH (*N*-acetyldiglycine) as the acidic additive has been described. Under the best conditions, ($[RhCp^*Cl_2]_2$ (1 mol%), $AgSbF_6$ (4 mol%), H_2O (1.0 equiv), and Ac-Gly-OH (2.0 equiv) in HFIP (hexafluoroisopropanol) (1 mL) under CO (5 bar) and N_2 (5 bar) for 24 hours), dibutyl (*E*)-4-oxohept-2-enedioate, and dibutyl 4-oxoheptanedioate were successfully synthesized (Scheme 6.10a) [184]. Carbonylative dimerization had been previously investigated and a possible reaction mechanism was hypothesized for the Pd-catalyzed dimerization of styrene in the presence of CO. In the first step, formation of the active palladium hydride complex should occur followed by coordination and insertion of the alkene. Subsequent insertion of CO into the palladium alkyl bond forms the corresponding palladium acyl complex. Then, coordination and reaction with a second alkene molecule takes place. Finally, the terminal product is formed by β-hydride elimination to generate the active palladium hydride complex for the next catalytic cycle (Scheme 6.10b) [185].

Carbonylation is also a powerful tool to prepare amides. For instance, hydroamidation of olefins with aliphatic amines was carried out by using a ligand- and

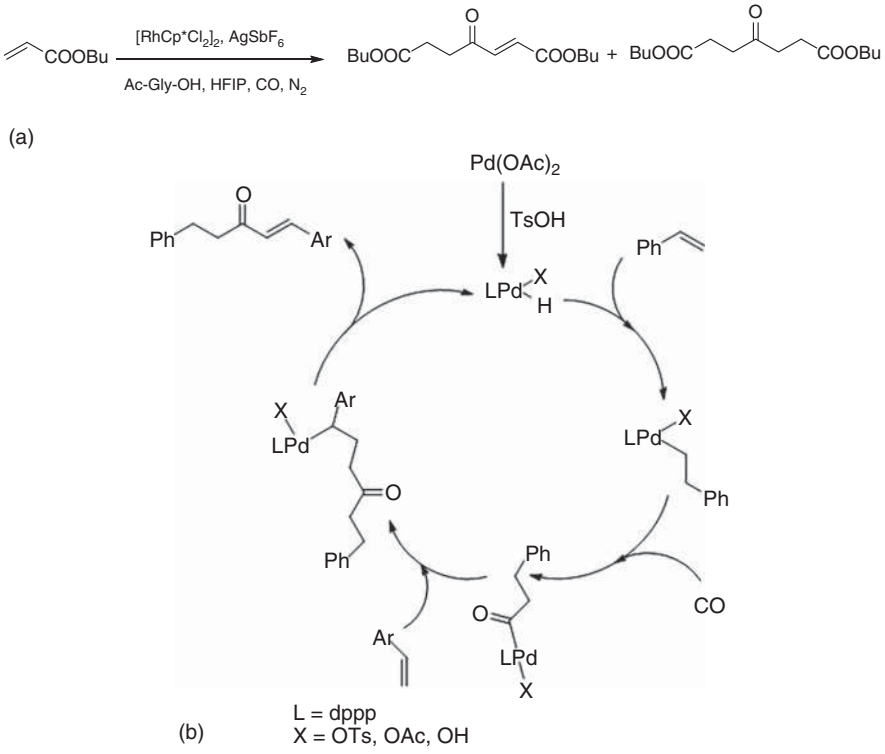

Scheme 6.10 (a) Carbonylative dimerization of butyl acrylate. Source: Modified from Wang and Wu [184]. (b) Palladium-catalyzed carbonilative dimerization of styrene. Source: Modified from Wu, Neumann and Beller [247].

additive-free rhodium catalyst as $RhCl_3 \cdot 3H_2O$. *N*-Alkyl amides were selectively formed also in the presence of aryl amines and alcohols. Preliminary mechanistic studies revealed the formation of [Rh(I)-H] complex as active species and the aminolysis of the rhodium-acyl complex as the crucial reaction step [186]. Under heating conditions [Rh(I)−H] species is formed from the Rh precursor in the presence of amines and CO. Then, insertion of the double bond of olefins into the Rh−H bond leads to alkyl Rh species. Subsequent insertion of CO generates the acyl Rh(I) species. Nucleophilic addition of the amine to the rhodium-acyl complexes produces the desired amide products with regeneration of the Rh(I)−H complex (Scheme 6.11). Hydroamidation of cyclopentadiene and dicyclopentadiene with pyrrolidine led to the formation of the corresponding mono- and diamides in a single step. The best result was obtained by using $[Rh(COD)Cl]_2$, without any additional ligands, as catalyst, affording 82% of the monoamide of dicyclopentadiene with a high TOF and over 90% selectivity within one hour [187].

The carbonylation of a series of primary and secondary aliphatic amines to form amides with TON up to 224 was accomplished using porphyrin rhodium(II) metalloradical. CO was converted to the active acyl-like metalloradical, $[(por)Rh(CO)]^{\cdot}$ (por = porphyrin), and a study on the reactivity of $[(por)Rh(CO)]^{\cdot}$ and other

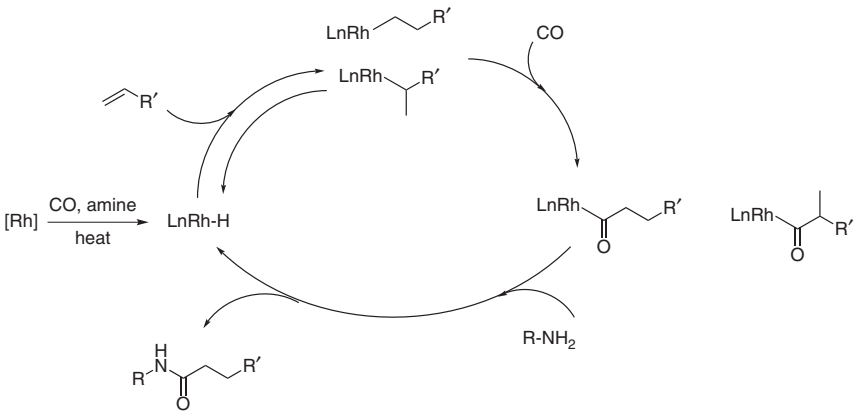

Scheme 6.11 Hydroamidation of olefins.

rhodium porphyrin compounds, such as (por)-RhCHO and (por)RhC(O)NHnPr, was conducted experimentally and computationally [188]. Recently, a novel rhodium-catalyzed three-component reaction to synthesize amides from organic azides, carbon monoxide, and (hetero)arenes via nitrene intermediates and direct C–H functionalization was described. Noteworthy, the reaction proceeded in an intermolecular fashion with N_2 as the only by-product, and mechanistic studies showed that the amides were formed via a key Rh-nitrene intermediate [189].

Catalytic carbonylation of unsaturated compounds is known since Reppe's experiments, and the carbonylation of alkynes represents a valuable synthetic route to obtain unsaturated acid derivatives and different heterocycles, useful for the synthesis of fine chemicals and pharmaceuticals. Compared with palladium, only few reports on rhodium-catalyzed alkoxycarbonylation of alkynes have been published. For instance, the Rh-catalyzed carbonylation of diphenylacetylene in ethanol gave 5-ethoxy-(5*H*)-furan-2-one as the main product [190]. Various internal alkynes were converted to the corresponding 1,4-dicarboxylate esters in moderate-to-good yields by using $Rh_4(CO)_{12}$ as catalyst. A selective monocarbonylation was achieved by Artok and coworkers, who employed $[RhCl(cod)]_2$ to convert internal alkynes to unsaturated esters in good yields [191]. On the other hand, 1,6-enynes with electron-deficient double bond underwent a carbonylative cyclization under the same conditions [8 and loc. cit.] (Scheme 6.12). The [2 +2 + 2 + 1] cycloaddition of disubstituted alkynes proceeds via the formation of a five-membered rhodacycle, followed by chelation of the alkene and insertion of the double bond so forming the fused [5-7-5] intermediate **A**. Coordination of CO and its insertion gives eight-membered rhodacycles **B** and **C**, which by reductive elimination affords the cycloheptadienone **D** (Scheme 6.12b).

Maleimide derivatives were produced by rhodium-catalyzed carbonylative annulation of anilines with internal alkynes. By using acetylacetone as the ligand for rhodium, various polysubstituted maleimides were isolated in high yields. However, aliphatic amines could not be used here instead of anilines. It was proposed that the real rhodium catalyst is generated from the precursor in the

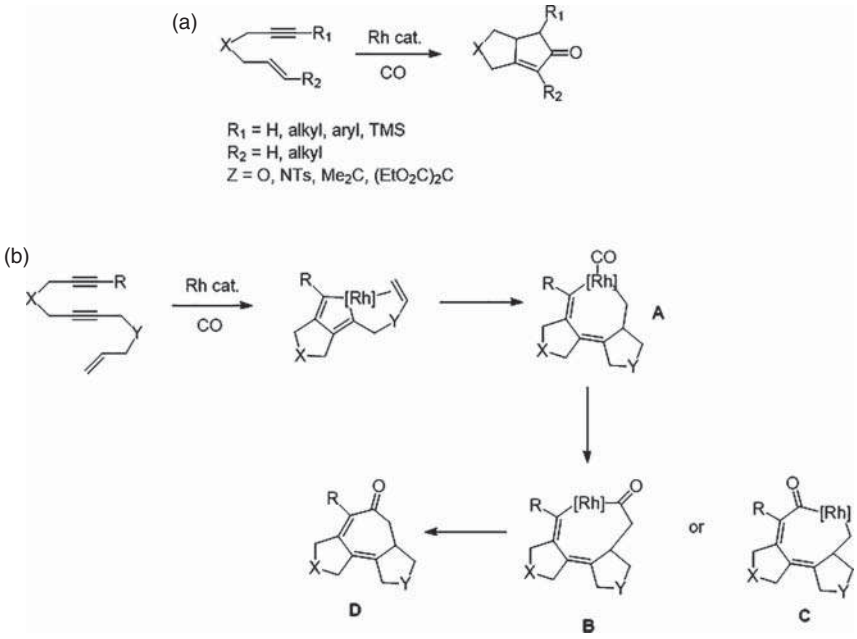

Scheme 6.12 (a) Synthesis of cyclopentenones from 1,6- and 1,7-enynes and CO. Source: Modified from Quintero-Duque et al. [8]. (b) Reaction mechanism for the formation of cycloheptadienones from ene-diynes. Source: Modified from Blond [192].

presence of the ligand and CO. Then, by reaction with aniline, a three-membered rhodium cycle is formed. This one, subsequently reacts with the internal alkyne to give the desired five-membered cycle. A six-membered cycle, as one of the key intermediates, is formed after insertion of another molecule of CO. Finally, the final maleimide is eliminated through reductive elimination to complete the catalytic cycle (Scheme 6.13) [193].

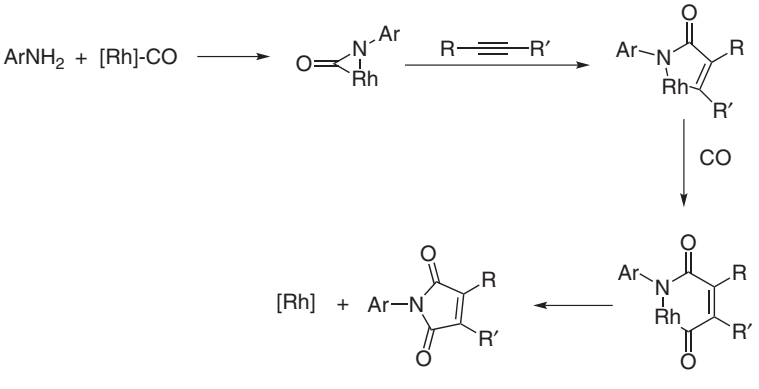

Scheme 6.13 Rhodium-catalyzed carbonilative annulation of aniline.

Other heterocycle ring systems can be obtained by carbonylation process. β-Lactams, a class of potent antibiotics, are valuable building blocks for the construction of diverse nitrogen-containing structures. A convenient route to access this interesting scaffold is the carbonylation of aziridines, in which carbon monoxide is inserted into one of the ring carbon–nitrogen bonds. First, there is coordination of the arene ring of aziridines to rhodium, followed by oxidative addition of rhodium(I) to the more substituted aziridine carbon-nitrogen bond. Subsequent ligand migration from the N-Rh bond to a carbonyl carbon may form five-membered complexes. Carbonylation and subsequent reductive elimination, with or without the participation of another molecule of aziridine, would then afford 3-aryl-β-lactams (Scheme 6.14). A comprehensive overview of aziridine-to-azetidin-2-one carbonylation studies was reported (Scheme 6.14) [194].

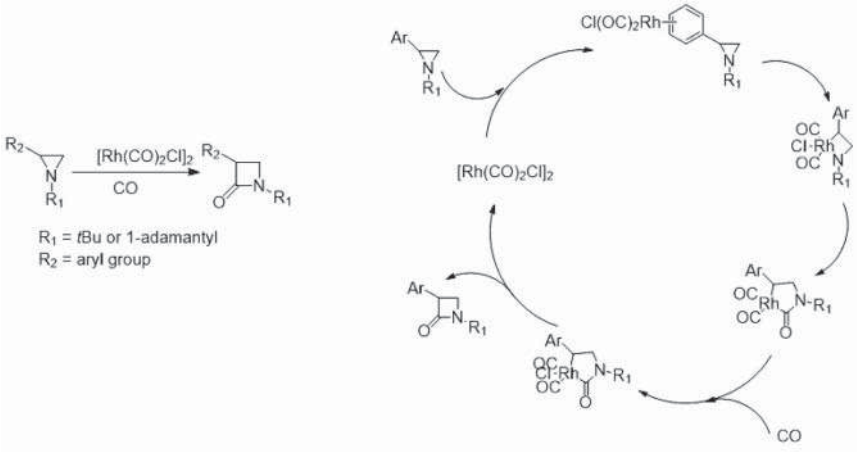

Scheme 6.14 Carbonylation of aziridines and postulated reaction mechanism. Source: Modified from Piens and D'hooghe [194].

Rh-catalyzed carbonylative C—C bond activation of cyclopropanes gave access to a wide range of complex heterocyclic compounds. Synthetic methodologies and key mechanistic features were reviewed. Noteworthy, it was found that N-based directing groups are effective at controlling the regioselectivity of C—C bond activation during the formation of rhodacyclopentanone intermediates [195]. 6*H*-Isoindolo[2,1-*a*]indol-6-ones was synthesized by rhodium-catalyzed NH-indole-directed C–H carbonylation of 2-arylindoles at atmospheric pressure of carbon monoxide. Mechanistic studies suggest the formation of five-membered rhodacycle species in the catalytic cycle [196]. Highly substituted indoles were prepared by carbonylative benzannulation of pyrrolyl propargylic esters. The dearomative benzannulation strategy could be extended to the synthesis of other heterocycles such as benzofurans, benzothiophenes, carbazoles, dibenzofurans [197], and several highly substituted benzofuran-containing natural products (Scheme 6.15) [198]. When the propargylic ester (**A**) was used as the starting material, DFT calculations indicated a metal-mediated 1,2-migration of (**A**), followed by the formation of a

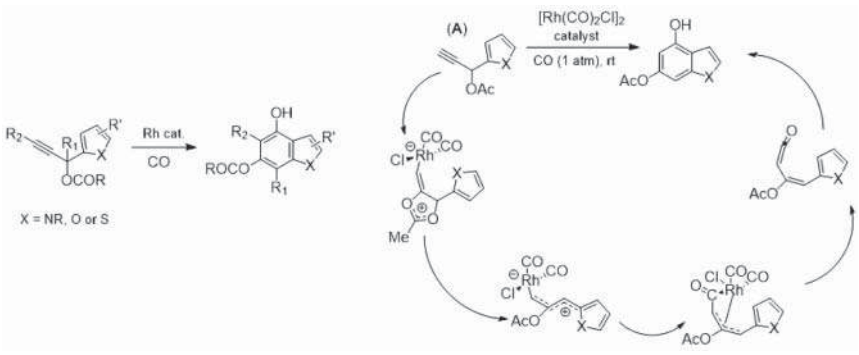

Scheme 6.15 Benzannulation for the synthesis of different heterocycles and proposed reaction mechanism for the benzannulation of the propargylic ester (**A**). Source: Modified from Liu et al. [198].

zwitterion intermediate, a metallocycle and a ketene intermediate, to give the target product by a 6π-electrocyclization and aromatization (Scheme 6.15) [198].

Indole-2-carboxylic esters were obtained by $RhCl_3 \cdot 3H_2O$-catalyzed carbonylation of indoles with alcohols. $RhCl_3 \cdot 3H_2O$ was employed for the first time in the direct carbonylation of aromatic C—H bonds with CO, and this catalyst could be applied to synthesize pyrrole-2-carboxylic esters and indole δ-lactone moiety [199]. The coordination of the substrate to Rh(III) catalyst gives a five-membered rhodacycle. Then, migratory insertion of CO into the Rh—C bond and coordination of alcohol via ligand exchange gives the intermediate A. The reaction product is finally formed by reductive elimination. Also, a mechanism involving coordination of CO and alcohol, followed by migratory insertion of CO, can not be excluded (Scheme 6.16).

In the last years, ethanol-fuel blends have attracted much interest because of a better fuel combustion efficiency and a reduction of particulate and CO emission. In this view, the methanol reductive carbonylation to ethanol is very attracting due to the fewer steps involved compared with the direct syngas conversion. As a matter of fact, the methanol reductive carbonylation to ethanol was accomplished by using diphosphine ligand-modified Rh-based catalysts. Ligands have a crucial effect toward TOF and selectivity. The diphosphine ligand with the appropriate number of methylene groups between two phosphorus atoms could improve the catalytic activity. The steric congestion around the empty coordination site in the Rh diphosphine complexes favored the reaction of rhodium with H_2, thus promoting ethanol/acetaldehyde formation [200].

Recently, a catalytic system consisting of rhodium, ruthenium, dppp, and methyl iodide was investigated for reductive carbonylation of methanol to ethanol at 6.0 MPa and 120 °C. The rhodium catalyst was found to catalyze methanol reductive carbonylation for acetaldehyde formation, and ruthenium catalyst was responsible to catalyze hydrogenation of acetaldehyde to ethanol. Raising Ru/Rh ratio and reaction temperature, acetaldehyde hydrogenation to ethanol was favored. High H_2/CO and dppp/Rh ratio could suppress the acetic acid formation [201].

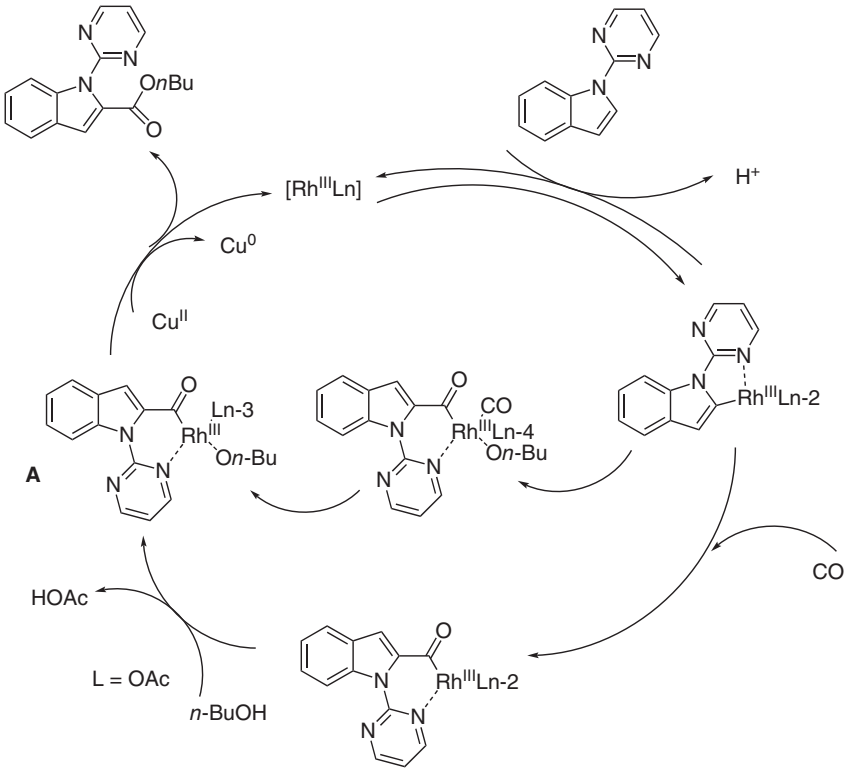

Scheme 6.16 Possible reaction mechanism for $RhCl_3$-catalyzed alkoxycarbonylation.

Status and prospects in higher alcohols synthesis from syngas and, in future, from CO_2 was recently reviewed. This protocol would comprise a more environmentally friendly, versatile, and economical alternative to the present methods [202].

Interestingly, $RhCl_3 \cdot 3H_2O$, in the presence of PPh_3 as ligand and Et_3N as the base, catalyzed the reductive carbonylation of aryl iodides to aryl aldehydes with CO and H_2 under relatively mild conditions (90 °C, 10 bar syngas). In a proposed reaction mechanism, $RhCl_3 \cdot 3H_2O$ reacts with PPh_3 to form $Rh(PPh_3)_3Cl$, followed by an oxidative addition to the aryl iodide, so producing the corresponding arylrhodium complex. Then, the coordination and insertion of CO leads to the formation of a benzoylrhodium complex. Next, metathesis with H_2 affords the aldehyde product. The base, Et_3N neutralizes the proton in the rhodium hydroiodide complex and regenerates the active Rh species (Scheme 6.17). A scaled-up experiment indicated that the catalytic method could find valuable applications in industrial productions [203]. Also, carbonylative cycloaddition revealed to be a very efficient technology. In fact, cycloaddition reactions have proven to be quite efficient methods for the synthesis of highly functionalized medium-sized carbo- and heterocycles, useful intermediates for the synthesis of natural molecules. Many polyunsaturated compounds, i.e. enynes, ene-diynes, allenynes, allenenes, bisallenes, trisallenenes, and vinylcyclopropanes, reacted in this process and represented a fascinating class

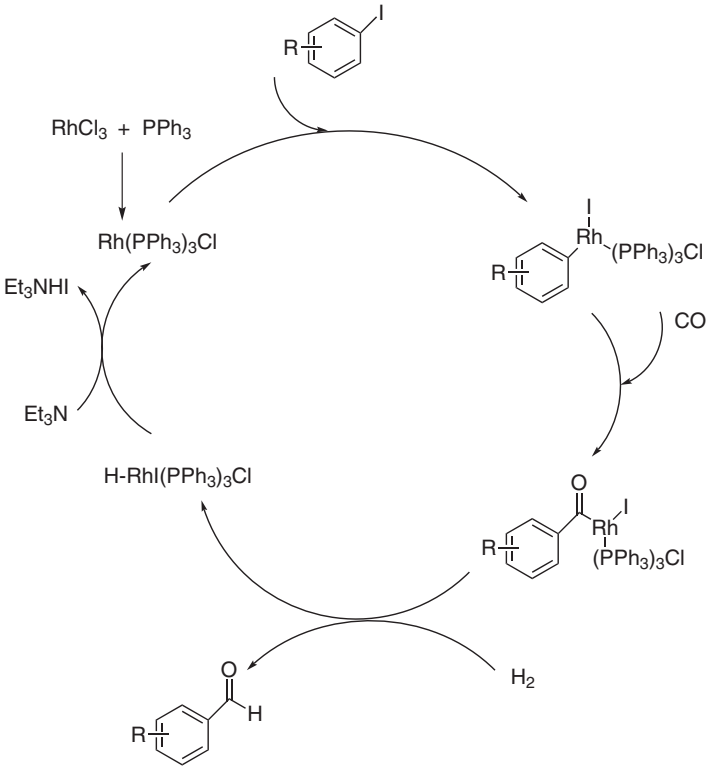

Scheme 6.17 Reductive carbonylation of aryliodides.

of substrates in carbonylative cycloaddition. The use of carbonylative cycloaddition for the synthesis of the most challenging ring sizes, i.e. seven-, eight-, and nine-membered rings, was recently reviewed (Scheme 6.18) [204, 205].

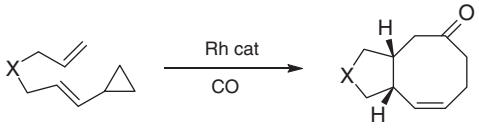

X = NTs, O, $C(CO_2Me)_2$

Scheme 6.18 Carbonylative cycloaddition reaction. Source: Salacz et al. [204] and Wang et al. [205].

Rh-catalyzed benzo/[7+1] cycloaddition of cyclopropyl-benzocyclobutenes (CP-BCBs) and CO to benzocyclooctenones has been described. This is the first example of transition-metal-catalyzed cycloaddition of benzocyclobutenes for the synthesis of eight-membered carbocycles fused with aryl rings. The reaction involves a thermal electrocyclic ring opening of the four-membered ring in CP-BCB and a Rh-catalyzed C–C cleavage of the cyclopropane ring [206] (Scheme 6.19). Under thermal conditions, ring opening of the benzocyclobutene

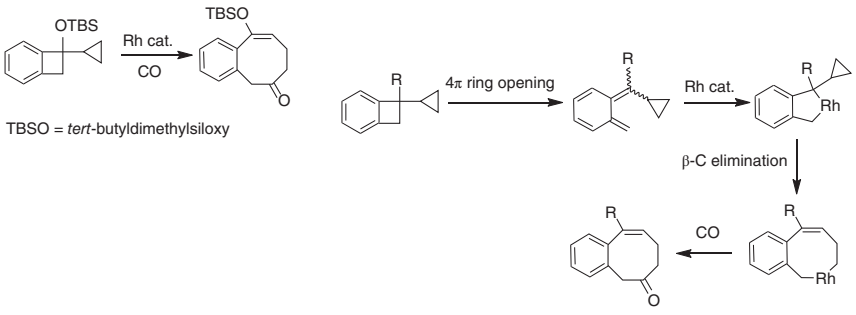

Scheme 6.19 Example of benzo/[7+1] cycloaddition of cyclopropyl-benzocyclobutenes and CO to benzocyclooctenones and proposed reaction mechanism. Source: Modified from Fu et al. [206].

ring in cyclopropyl-benzocyclobutene (CP-BCB) would generate a butadienylcyclopropane (BDCP) intermediate, which then undergoes the rhodium-catalyzed [7 + 1] cycloaddition to furnish the benzocyclooctenone product.

A catalytic oxidative cyclocarbonylation of ketimines to provide 3-methyleneisoindolin-1-ones was accomplished through a rhodium-catalyzed C—H bond activation, in which two C—H bonds were successfully cleaved. This transformation represents a useful method for the preparation of 3-methyleneisoindolin-1-ones that are of interest in synthetic organic chemistry [207]. Two postulated pathways were proposed to account for this Rh-catalyzed C–H bond activation/cyclocarbonylation of ketimine and the catalytic cycle was likely initiated by the removal of chloride of $[Cp^*RhCl_2]_2$ promoted by Ag^+ to generate an active species (Scheme 6.20) [207].

As already described for the hydroformylation reaction, many attempts have been performed in the use of CO surrogates [3]. After the review by Beller and collaborators [3], this area has attracted further significant interest.

A successful example of a CO gas-free carbonylation reaction using aldehydes as a carbonyl source was described. In this context, the CO gas-free cyclocarbonylation reaction of haloarenes, having a carbon nucleophile, was performed using aldehydes as a carbonyl source. The reaction was catalyzed by a Rh(I)/Pd(0) hybrid catalytic system, and two discrete complexes, Rh(I) and Pd(0), were responsible for the decarbonylative degradation of aldehydes and the introduction of the resulting carbonyl moiety via the CO-relay from Rh(I) or Pd(0), respectively. Noteworthy, these two catalysts functioned cooperatively without interfering with each other (Scheme 6.21) [208].

Furfural, as a carbonyl source, was used in the synthesis of fluoren-9-ones by Rh-catalyzed intramolecular C–H/C–I carbonylative coupling of 2-iodobiphenyls. It was demonstrated that the rate-determining step was not a C—H bond cleavage but the oxidative addition of the C—I bond to a Rh(I) center [209]. Again, furfural was employed in the rhodium(I)-catalyzed carbonylative annulation of α,α-dimethyl-(2-bromoaryl)methanols with internal alkynes to form indenones. Just the generation of the carbonyl source via the decarbonylation of furfural was

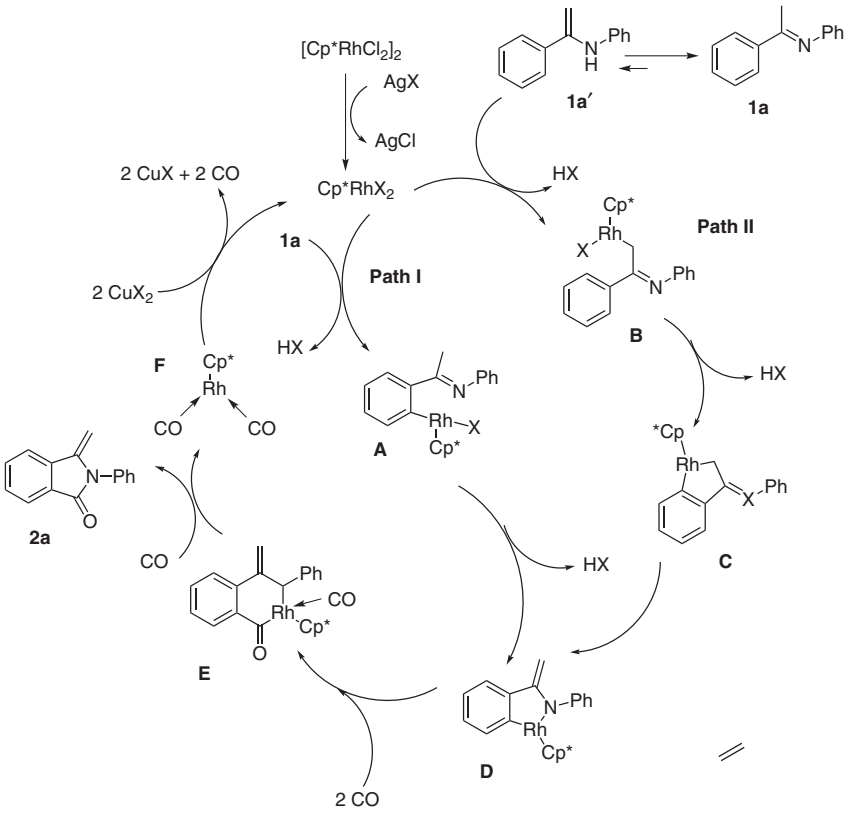

Scheme 6.20 Reaction mechanism for oxidative cyclocarbonylation of ketimines.

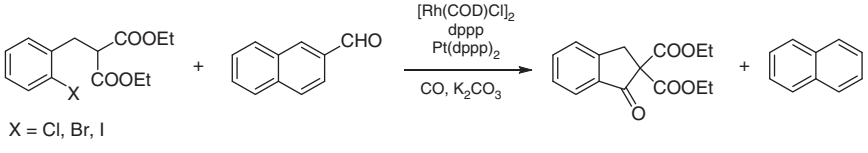

Scheme 6.21 CO gas-free cyclocarbonylation reaction of haloarenes. Source: Modified from Morimoto et al. [208].

the key to the success of this reaction [210]. Furfural was utilized as the CO precursor in the rhodium-catalyzed carbonylative C—N bond cleavage of tertiary amines to afford a variety of tertiary amides in moderate-to-excellent yields [211]. Besides furfural, hydroxymethyl furfural (HMF), a renewable resource, played a dual role as both CO surrogate and reaction reagent in a rhodium-catalyzed carbonylative reaction for the synthesis of furfuryl esters. For instance, iodobenzene and HMF were chosen as model substrates, with $Rh(cod)_2BF_4$ as the catalyst and DPPP as the ligand, in the presence of Na_2CO_3 as the base and 4 Å MS (SiO_2 powder) as the additive in 2-methyltetrahydrofuran at 125 °C for 24 hours (Scheme 6.22) [211].

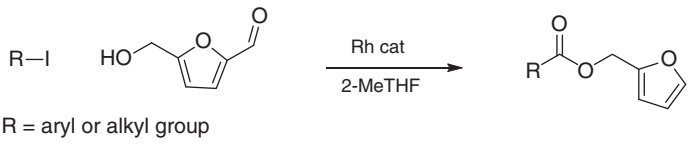

Scheme 6.22 Hydroxymethyl furfural as CO surrogate and reagent in the carbonylative reaction for the synthesis of furfuryl esters. Source: Modified from Qi et al. [211].

Also, paraformaldehyde can be used as surrogate of CO. In this context, the rhodium-catalyzed carbonylation of (2-pyridylmethylene)cyclobutanes to afford five-membered ring ketones could be performed using paraformaldehyde as the CO source [212].

An alternative strategy in the carbonylation process was represented by CO_2 reduction to CO, combined with carbonylation with CO generated *ex situ*. As such, CO_2 has been efficiently reduced to CO by triphenysilane using CsF in a sealed two-chamber reactor. Subsequently, rhodium(I)-mediated Pauson–Khand-type reaction proceeded smoothly to yield amides, alkynones, and bicyclic cyclopentenones, respectively [213]. Recently, the first efficient amino group-assisted C–H carboxylation with CO_2 under redox neutral conditions, utilizing a Rh(I)/phosphine ligand catalytic system, was described. This reaction was compatible with a broad range of substrates, including challenging electron-deficient heteroarenes. Preliminary mechanistic studies revealed a reversible oxidative addition to a Rh(I) species followed by the reductive elimination of HX to generate a rhodacycle, which undergoes reversible nucleophilic carboxylation with CO_2 to form a rhodium carboxylate. Final, lactamization of this carboxylate assisted by *t*-BuOK gave the target product and regenerated the Rh(I) catalyst (Scheme 6.23) [214].

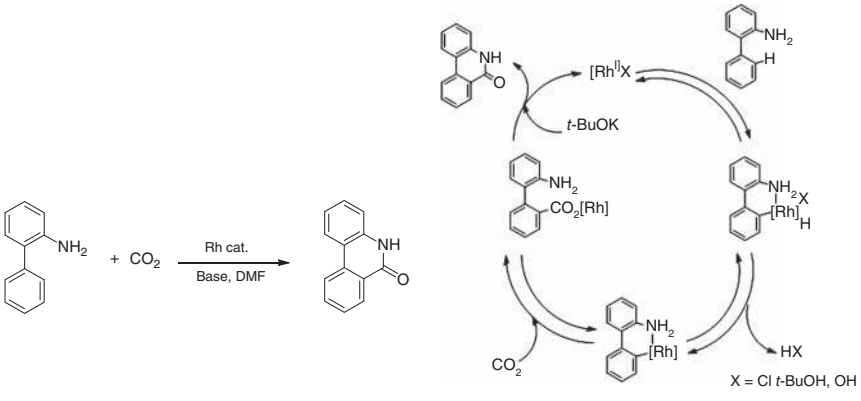

Scheme 6.23 C–H carboxylation of 2-phenylaniline with CO_2 and reaction mechanism. Source: Modified from Gao et al. [214].

Very recently, the Rh(I)-catalyzed regioselective arylcarboxylation of electron-deficient acrylamides with arylboronic acids under atmospheric pressure of CO_2 has been carried out for the first time, thus affording a series of malonate derivatives, valuable building blocks in organic syntheses [215].

6.4 Some Relevant Patents and Patent Applications (2015–2020)

The industrial activity to improve reaction processes involving hydroformylation or carbonylation reactions, to find more efficient catalysts and greener and more sustainable protocols, remains very active. Some selected patents or patent applications in the last five years are here summarized and divided in three groups.

6.4.1 Hydroformylation

$Rh(acac)(CO)_2$ and some phospholane phosphite ligands are highly isoselective catalysts for alkyl alkene hydroformylation to branched aldehydes [216, 217]. Methods of producing dialdehyde compounds, such as 3-methylglutaraldehyde or nonanedial, were disclosed using the same Rh precursor and a bisphosphite ligand [218, 219]. The preparation of 3-aryl-propanals with a peculiar catalyst was claimed in two Chinese patent applications [220, 221]. A quite complex protocol was very recently described as a method for producing aldehydes by hydroformylation of olefins finalized to recovery and reuse of a Rh catalyst [222]. The use of a tertiary phosphine as antioxidant to protect a bidentate phosphite used as ligand of a Rh complex to produce with high selectivity valeraldehyde (l/b ratio = 37) was asserted [223]. Also, a method for aldehydes production by hydroformylation of olefins, in the presence of solubilized rhodium–phosphorous complex, was patented [224]. A simple and peculiar equipment, employed in a hydroformylation process, resulting in improved heavies removal, reduced exposure of the catalyst to elevated temperature, and lower rates of catalyst degradation, was described [225]. A process that ensures a relatively high conversion rate of vinyl acetate at relatively mild reaction conditions and improves the selectivity to 3-acetoxypropanal was claimed [226]. Another reaction devoted to the synthesis of functionalized aldehydes, such as 3-(perfluoroalkyl)propanals, was improved [227]. A hydroformylation method with improved catalyst stability at reaction conditions was reported; a specific α,β-unsaturated carbonyl compound was incorporated during the hydroformylation reaction to increase the reaction yield and inhibit the decomposition of ligand and catalyst [228]. Processes for preparation of bicyclic aldehyde compounds and the corresponding amine and isocyanate compounds were described [229]. A more sustainable protocol, working under milder conditions and lower organopolyphosphite ligand/catalytic metal ratio, was stated for hydroformylation processes [230]. A heterogeneous catalyst for the hydroformylation of olefins and/or alkynes in the gas phase with a mixture of hydrogen and carbon monoxide was reported [231]. A method for preparation of aldehyde by hydroformylation of DHF was patented in China [232]. An efficient process for the catalytic production of unsaturated aldehydes from olefins, through the collaboration between academia and industry, was achieved; a specific role to the outcome of the process was played by a co-catalyst selected from a weak organic acid and an organic amine [233]. The synthesis of 3-methylcrotonaldehyde is disclosed in a process comprising a hydroformylation reaction of epoxy isobutane with carbon monoxide and hydrogen in the presence

of rhodium catalyst; analogously, citral and vitamins A and E may be prepared in high yield under mild conditions [234]. The multistep protocol to synthetize a bifunctional 9(10)-hydroxymethyl tetracyclo[6.2.1.1.0]dodecane-4-carboxylic acid ester, useful monomer for the preparation of polyesters, was claimed. Also, a rhodium-catalyzed hydroformylation was followed by a hydrogenation in the presence of a cobalt sponge, while the polymerization was catalyzed by tetra-Bu titanate [235]. Finally, a method for producing 1,3-propanediol, other useful monomer for polyesters, characterized by the hydroformylation of vinyl acetate, was patented in China [236].

6.4.2 Preparation of Acetic Acid and Similar Compounds and Derivatives

Oxidative coupling catalysts and different methods for producing acetic acid from methane, carbon monoxide, and oxygen, under mild conditions, were recently claimed [237]. A few processes for preparing acetic acid and other alkanoic acids were described [238–240]. In addition, carbon nitride heterogeneous catalyst, containing rhodium, was prepared and used to produce acetic acid by a carbonylation reaction between methanol and carbon monoxide. The catalyst exhibited excellent long-term stability and activity by being capable of overcoming the disadvantages of the method using a conventional homogeneous catalyst and minimizing the phenomenon of rhodium leaching [241]. The stabilization of catalysts for the synthesis of acetic acid and amides was also the topic of a patent and related applications [242, 243]; an imidazolium cation as a iodide salt or methyl iodide and trimethylamine were claimed as stabilizers. A catalyst on a solid support, characterized by the presence of pyridine or imidazole derivatives, Rh species and alkali metal such Li, was reported as efficient promoter for carbonylation processes [244]. One-step methods for preparing methyl acetate and some alkenoates were described in a Chinese patent and patent applications [245–247]. Only two documents claimed the preparation methods of synthesis of primary amides from olefins, carbon monoxide and ammonia gas [248] or amides from carbonyl compounds [249].

6.4.3 Alcohols

An interesting one-step process for preparing polyols via rhodium-catalyzed hydrohydroxymethylation of fatty acid esters, obtained from vegetable oils, in the presence of carbon monoxide, hydrogen, tertiary amine, and CD-based auto-emulsifying system, was recently described [250].

6.5 Summary and Conclusions

Carbonylation reactions represent a clean and atom-economic way to produce both bulk and fine chemicals. Most of the processes use rhodium, iridium, and palladium-based catalysts, which show the highest activities and selectivities;

however, their cost represents a serious drawback, especially on an industrial scale. In this view, the separation of the catalyst from the reaction products is still challenging, and many efforts have been done to recover and recycle the precious metals. To overcome the problems connected to the traditional distillation, an energy-intensive process that can provoke the thermal decomposition of products and/or catalyst, biphasic catalysis, and heterogenization of homogeneous catalysts have been developed and successfully employed also on industrial scale, as demonstrated by the aqueous biphase hydroformylation process discovered at RuhrChemie/Rôhne-Poulenc [79–82]. Much work is still in progress to design new more and more active catalysts capable to work in biphase systems, and further work needs to be carried out to establish long-term stability of these catalysts. Moreover, also metal-supported heterogeneous catalysts are arousing the interest of the researchers as evidenced by recent papers. To develop more economically sustainable processes, catalysts based on cheaper metals like ruthenium, iron, and so on have been applied. However, currently, these catalytic systems never came to a real application.

Nowadays, the real thorn in the side of carbonylation reactions is the use of carbon monoxide, which is a cheaper and abundantly available feedstock but also dangerous. In fact, there are increasingly restrictive regulations, also concerning its transportation. Moreover, pressurized CO can require considerable investment costs, thus limiting its use in the industry; therefore a very challenging research is in progress to use carbon monoxide surrogates, easily transportable and available also from waste biomass (e.g. formaldehyde, methanol, oxalates, formates, etc.). Noteworthy, most of the processes recently patented that use CO belong to Chinese companies; this may be due not only to the well-documented and extensive activity of the Chinese scientific community but, probably, also to less restrictions regarding the use and transport of carbon monoxide in China.

References

1 Kelkar, A.A. (2016). Carbonylations and hydroformylations for fine chemicals. In: *Industrial Catalytic Processes for Fine and Specialty Chemicals* (eds. S.S. Joshi and V.V. Ranade), 663–692. Amsterdam, The Netherlands: Elsevier.

2 Beller, M. and Wu, X.-F. (2013). *Transition Metal Catalyzed Carbonylation Reactions: Carbonylative Activation of C–X Bonds*. Berlin, Germany: Springer-Verlag.

3 Wu, L., Liu, Q., Jackstell, R., and Beller, M. (2014). *Angew. Chem. Int. Ed.* 53: 6310–6320.

4 (a) van Leeuwen, P.W.N.M., Casey, C.P., and Whiteker, G.T. (2000). *Rhodium Catalyzed Hydroformylation* (eds. P.W.N.M. van Leeuwen and C. Claver). Dordrecht, Germany: Kluwer. (b) van Leeuwen, P.W.N.M. (ed.) (2004). *Homogeneous Catalysis: Understanding the Art*. Dordrecht, Germany: Kluwer Academic Publishers. (c) Franke, R., Selent, D., and Börner, A. (2012). *Chem. Rev.* 112: 5675–5732. (d) Börner, A. and Franke, R. (eds.) (2016). *Hydroformylation:*

Fundamental, Processes, and Applications in Organic Synthesis. Weinheim, Germany: Wiley-VCH.

5 Wu, X.-F. and Neumann, H. (2012). *ChemCatChem* 4: 447–458. and loc. cit.

6 Piras, I., Jennerjahn, R., Jackstell, R. et al. (2011). *Angew. Chem. Int. Ed.* 50: 280–284.

7 (a) Chatani, N. (2004). *Top. Organomet. Chem.* 11: 173–195. (b) Chatani, N. and Murai, S. (1996). *Synlett*: 414–424.

8 Quintero-Duque, S., Dyballa, K.M., and Fleischer, I. (2015). *Tetrahedron Lett.* 56: 2634–2650.

9 Wu, X.-F., Fang, X., Wu, L. et al. (2014). *Acc. Chem. Res.* 47: 1041–1053 and loc. cit.

10 (a) Tsuchiya, K., Huang, J.-D., and Tominaga, K.-I. (2013). *ACS Catal.* 3: 2865–2868. (b) Tominaga, K.-I. (2006). *Catal. Today* 115: 70–72.

11 Jo, E.-A., Lee, J.-H., and Jun, C.-H. (2008). *Chem. Commun.*: 5779–5781.

12 Verendel, J.J., Nordlund, M., and Andersson, P.G. (2013). *ChemSusChem* 6: 426–429.

13 (a) Young, J.F., Osborn, J.A., Jardine, F.A., and Wilkinson, G. (1965). *Chem. Commun.*: 131–132. (b) Evans, D., Osborn, J.A., and Wilkinson, G. (1968). *J. Chem. Soc. A*: 3133–3142. (c) Evans, D., Yagupsky, G., and Wilkinson, G. (1968). *J. Chem. Soc. A*: 2660–2665.

14 van Duren, R., van der Vlugt, J.I., Kooijman, H. et al. (2007). *Dalton Trans.*: 1053–1059.

15 Pongrácz, P., Kollár, L., and Mika, L.T. (2016). *Green Chem.* 18: 842–847.

16 Kämper, A., Kucmierczyk, P., Seidensticker, T. et al. (2016). *Catal. Sci. Technol.* 6: 8072–8079.

17 Fleischer, I., Wu, L., Profir, I. et al. (2013). *Chem. Eur. J.* 19: 10589–10594.

18 Kamper, A., Warrelmann, S.J., Reiswich, K. et al. (2016). *Chem. Eng. Sci.* 144: 364–371.

19 (a) Casey, C.P., Whiteker, G.T., Melville, M.G. et al. (1992). *J. Am. Chem. Soc.* 114: 5535–5543. (b) Kamer, P.C.J., van Leeuwen, P.W.N.M., and Reek, J.N.H. (2001). *Acc. Chem. Res.* 34: 895–904. (c) Cobley, C.J., Froese, R.D.J., Klosin, J. et al. (2007). *Organometallics* 26: 2986–2999.

20 Diebolt, O., Tricas, H., Freixa, Z., and van Leeuwen, P.W.N.M. (2013). *ACS Catal.* 3: 128–137.

21 Watkins, A.L. and Landis, C.R. (2010). *J. Am. Chem. Soc.* 132: 10306–10317.

22 Heck, R.F. (1969). *Acc. Chem. Res.* 2: 10–16.

23 Bernales, V. and Froese, R.D. (2019). *J. Comput. Chem.* 40: 342–348.

24 Klähn, M. and Garland, M.V. (2015). *ACS Catal.* 5: 2301–2316.

25 Fourmy, K., Nguyen, D.H., Dechy-Cabaret, O., and Gouygou, M. (2015). *Catal. Sci. Technol.* 5: 4289–4323.

26 Gellrich, U., Koslowski, T., and Breit, B. (2015). *Catal. Sci. Technol.* 5: 129–133.

27 Kégl, T. (2015). *RSC Adv.* 5: 4304–4327.

28 Zhang, B., Jiao, H., Michalik, D. et al. (2016). *ACS Catal.* 6: 7554–7565.

29 Bondžić, B.P., Rominger, F., and Hofmann, P. (2016). *J. Mol. Catal. A: Chem.* 423: 472–477.

30 Kharat, A.N., Kouchi, F.R., and Jahromi, B.T. (2016). *J. Coord. Chem.* 69: 12–19.

31 Jover, J. and Maseras, F. (2016). QM/MM calculations on selectivity in homogeneous catalysis. In: *Computational Studies in Organometallic Chemistry*, vol. 167 (eds. S.A. Macgregor and O. Eisenstein), 59–79. Berlin, Germany: Springer-Verlag.

32 Dingwall, P., Fuentes, J.A., Crawford, L. et al. (2017). *J. Am. Chem. Soc.* 139: 15921–15932.

33 Wildt, J., Brezny, A.C., and Landis, C.R. (2017). *Organometallics* 36: 3142–3151.

34 Jiao, Y., Serrano Torne, M., Gracia, J. et al. (2017). *Catal. Sci. Technol.* 7: 1404–1414.

35 Brezny, A.C. and Landis, C.R. (2017). *J. Am. Chem. Soc.* 139: 2778–2785.

36 Jörke, A., Seidel-Morgenstern, A., and Hamel, C. (2017). *J. Mol. Catal. A: Chem.* 426: 10–14.

37 Vilches-Herrera, M., Concha-Puelles, M., Carvajal, N. et al. (2018). *Catal. Commun.* 116: 62–66.

38 Eshon, J., Foarta, F., Landis, C.R., and Schomaker, J.M. (2018). *J. Org. Chem.* 83: 10207–10220.

39 van Leeuwen, P.W.N.M. and Kamer, P.C.J. (2018). *Catal. Sci. Technol.* 8: 26–113.

40 Bai, S.-T., Sinha, V., Kluwer, A.M. et al. (2019). *ChemCatChem* 11: 5322–5329.

41 Bai, S.-T., Sinha, V., Kluwer, A.M. et al. (2019). *Chem. Sci.* 10: 7389–7398.

42 Shin, T., Kim, H., Kim, S. et al. (2019). *Org. Lett.* 21: 5789–5792.

43 Breckwoldt, N.C.C., Goosen, N.J., Vosloo, H.C.M., and Van der Gryp, P. (2019). *React. Chem. Eng.* 4: 695–704.

44 Breckwoldt, N.C.C., Smith, G.S., Van der Gryp, P., and Goosen, N.J. (2019). *React. Kinet. Mech. Catal.* 128: 333–347.

45 Kloß, S., Selent, D., Spannenberg, A. et al. (2019). *Catalysts* 9: 1036.

46 Brezny, A.C. and Landis, C.R. (2019). *ACS Catal.* 9: 2501–2513.

47 Yu, S.-m., Snavely, W.K., Chaudhari, R.V., and Subramaniam, B. (2020). *Mol. Catal.* 484: 110721–110726.

48 Wang, S., Zhang, J., Peng, F. et al. (2020). *Ind. Eng. Chem. Res.* 59: 88–98.

49 Wang, X. (2015). *J. Flow Chem.* 5: 125–132.

50 Li, C., Wang, W., Yan, L., and Ding, Y. (2018). *Front. Chem. Sci. Eng.* 12: 113–123.

51 Hanf, S., Rupflin, L.A., Gläser, R., and Schunk, S.A. (2020). *Catalysts* 10: 510.

52 Khokhar, M.D., Shukla, R.S., and Jasra, R.V. (2015). *J. Mol. Catal. A: Chem.* 400: 1–6.

53 Khokhar, M.D., Shukla, R.S., and Jasra, R.V. (2015). *React. Kinet. Mech. Catal.* 114: 265–277.

54 Zhang, X.-Y., Zheng, C.-Y., Zheng, X.-L. et al. (2015). *Acta Phys. Chim. Sin.* 31: 738–742.

55 Vunain, E., Ncube, P., Jalama, K., and Meijboom, R. (2018). *J. Porous Mater.* 25: 303–320.

56 Ganga, V.S.R., Dabbawala, A.A., Munusamy, K. et al. (2016). *Catal. Commun.* 84: 21–24.

57 Zhang, J., Sun, P., Gao, G. et al. (2020). *J. Catal.* 387: 196–206.

58 Sun, Q., Dai, Z., Liu, X. et al. (2015). *J. Am. Chem. Soc.* 137: 5204–5209.

59 Jia, X., Liang, Z., Chen, J. et al. (2019). *Org. Lett.* 21: 2147–2150.

60 Liang, Z., Chen, J., Chen, X. et al. (2019). *Chem. Commun.* 55: 13721–13724.

61 Wanga, Z. and Yang, Y. (2020). *RSC Adv.* 10: 29263–29267.

62 Verheyen, T., Santillo, N., Marinelli, D. et al. (2019). *ACS Appl. Polym. Mater.* 1: 1496–1504.

63 Xue, X., Song, Y., Xu, Y., and Wang, Y. (2018). *New J. Chem.* 42: 6640–6643.

64 Chevry, M., Vanbésien, T., Menuel, S. et al. (2017). *Catal. Sci. Technol.* 7: 114–123.

65 Peral, D., Stehl, D., Bibouche, B. et al. (2018). *J. Colloid Interface Sci.* 513: 638–646.

66 Paganelli, S., Piccolo, O., Baldi, F. et al. (2015). *Catal. Commun.* 71: 32–36.

67 Paganelli, S., Tassini, R., Rathod, V.D. et al. (2021). *Catal. Lett.* 151: 1508–1521.

68 Amsler, J., Sarma, B.B., Agostini, G. et al. (2020). *J. Am. Chem. Soc.* 142: 5087–5096.

69 Rieger, B., Plikhta, A., and Castillo-Molina, D.A. (2014). Ionic liquids in transition metal-catalyzed hydroformylation reactions. In: *Ionic Liquids (ILs) in Organometallic Catalysis* (eds. J. Dupont and L. Kollar), 95–144. Berlin, Germany: Springer-Verlag.

70 Jin, X., Feng, J., Ma, Q. et al. (2019). *Green Chem.* 21: 3267–3275.

71 Song, Y.N., Lv, Z.G., and Guo, Z.M. (2019). *IOP Conf. Ser.: Mater. Sci. Eng.* 490: 022075.

72 Walter, S., Spohr, H., Franke, R. et al. (2017). *ACS Catal.* 7: 1035–1044.

73 Tao, L., Zhong, M., Chen, J. et al. (2018). *Green Chem.* 20: 188–196.

74 Logemann, M., Marinkovic, J.M., Schörner, M. et al. (2020). *Green Chem.* 22: 5691–5700.

75 Olmos, A., Asensio, G., and Pérez, P.J. (2016). *ACS Catal.* 6: 4265–4280.

76 Law, C.-k.E. and Horváth, I.T. (2016). *Org. Chem. Front.* 3: 1048–1062.

77 Zagajewski, M., Dreimann, J., Thönes, M., and Behr, A. (2016). *Chem. Eng. Process. Process Intensif.* 99: 115–123.

78 Zhao, Y., Liu, Y., Wei, J. et al. (2018). *Catal. Lett.* 148: 438–442.

79 Kuntz, E.G. (1987). *Chem. Tech.* 17: 570–575.

80 Cornils, B. and Kuntz, E.G. (1995). *J. Organomet. Chem.* 502: 177–186.

81 Cornils, B. (1998). *Org. Process Res. Dev.* 2: 121–127.

82 (a) Kuntz, E. (1976) Aldehyde prepn. by olefin hydroformylation in liquid phase - using catalyst system contg. sulphonated aryl phosphine and rhodium. (Rhône-Poulenc Ind.). Fr.Pat. 2314910. (b) Kuntz, E. (1976) Verfahren zur herstellung von aldehyden. (Rhône-Poulenc Ind.). DE 2627354.

83 Matsinha, L.C., Siangwata, S., Smith, G.S., and Makhubela, B.C.E. (2019). *Catal. Rev. Sci. Eng.* 61: 111–133.

84 Pogrzeba, T., Müller, D., Hamerla, T. et al. (2015). *Ind. Eng. Chem. Res.* 54: 11953–11960.

85 Baricelli, P.J., Rodriguez, M., Melean, L.G. et al. (2015). *Appl. Catal., A* 490: 163–169.

86 Vieira, C.G., de Freitas, M.C., de Oliveira, K.C.B. et al. (2015). *Catal. Sci. Technol.* 5: 960–966.

87 Hapiot, F., Menuel, S., Bricout, H. et al. (2015). *Appl. Organomet. Chem.* 29: 580–587.

88 Vanbésien, T., Sayede, A., Monflier, E., and Hapiot, F. (2016). *Catal. Sci. Technol.* 6: 3064–3073.

89 Leblond, J., Potier, J., Menuel, S. et al. (2017). *Catal. Sci. Technol.* 7: 3823–3830.

90 Cocq, A., Bricout, H., Djedaïni-Pilard, F. et al. (2020). *Catalysts* 10: 56.

91 Elarda, M., Denis, J., Ferreira, M. et al. (2015). *Catal. Today* 247: 47–54.

92 Künnemann, K.U., Schurm, L., Lange, D. et al. (2020). *Green Chem.* 22: 3809–3819.

93 Jagtapa, S.A., Monflier, E., Ponchel, A., and Bhanage, B.M. (2017). *Mol. Catal.* 436: 157–163.

94 Benatmane, M., Cousin, K., Laggoune, N. et al. (2018). *ChemCatChem* 10: 5306–5313.

95 Gorbunov, D.N., Egazaryants, S.V., Kardasheva, Yu.S. et al. (2015). *Russ. Chem. Bull.* 64: 943–947.

96 Herrmann, N., Bianga, J., Gaide, T. et al. (2019). *Green Chem.* 21: 6738–6745.

97 Bianga, J., Herrmann, N., Schurm, L. et al. (2020). *Eur. J. Lipid Sci. Technol.* 122: 1900317.

98 Herrmann, N., Bianga, J., Palten, M. et al. (2020). *Eur. J. Lipid Sci. Technol.* 122: 1900166.

99 Warmeling, H., Janz, D., Peters, M., and Vorholt, A.J. (2017). *Chem. Eng. J.* 330: 585–595.

100 Alsalahi, W., Grzybek, R., and Trzeciak, A.M. (2017). *Catal. Sci. Technol.* 7: 3097–3103.

101 Mieczyńska, E., Grzybek, R., and Trzeciak, A.M. (2018). *ChemCatChem* 10: 305–310.

102 Chen, S.-J., Li, Y.-Q., Wang, P. et al. (2015). *J. Mol. Catal. A: Chem.* 407: 212–220.

103 Alsalahi, W. and Trzeciak, A.M. (2016). *J. Mol. Catal. A: Chem.* 423: 41–48.

104 Lobry, E., Cardozo, A.F., Barthe, L. et al. (2016). *J. Catal.* 342: 164–172.

105 Bibouche, B., Peral, D., Stehl, D. et al. (2018). *RSC Adv.* 8: 23332–23338.

106 Cardozo, A.F., Julcour, C., Barthe, L. et al. (2015). *J. Catal.* 324: 1–8.

107 Joumaa, A., Gayet, F., Garcia-Suarez, E.J. et al. (2020). *Polymers* 12: 1107.

108 Zhang, X., Wei, J., and Xiaoming Zhang, X. (2019). *New J. Chem.* 43: 14134–14138.

109 Pogrzeba, T., Illner, M., Schmidt, M. et al. (2019). *Ind. Eng. Chem. Res.* 58: 4443–4453.

110 Pogrzeba, T., Schmidt, M., Milojevic, N. et al. (2017). *Ind. Eng. Chem. Res.* 56: 9934–9941.

111 Illner, M., Müller, D., Esche, E. et al. (2016). *Ind. Eng. Chem. Res.* 55: 8616–8626.

112 Peral, P., Herrera, D., Real, J. et al. (2016). *Catal. Sci. Technol.* 6: 800–808.

113 Paganelli, S., Piccolo, O., Pontini, P. et al. (2015). *Catal. Today* 247: 64–69.

114 Omosun, N.N. and Smith, G.S. (2019). *Eur. J. Inorg. Chem.*: 2558–2564.
115 Matsinha, L.C., Mapolie, S.F., and Smith, G.S. (2015). *Dalton Trans.* 44: 1240–1248.
116 Scrivanti, A., Beghetto, V., Alam, Md.M. et al. (2017). *Inorg. Chim. Acta* 455: 613–617.
117 Brezny, A.C. and Landis, C.R. (2018). *Acc. Chem. Res.* 51: 2344–2354.
118 Deng, Y., Wang, H., Sun, Y., and Wang, X. (2015). *ACS Catal.* 5: 6828–6837.
119 Yu, Z., Eno, M.S., Annis, A.H., and Morken, J.P. (2015). *Org. Lett.* 17: 3264–3267.
120 Hammerer, T., Leitner, W., and Franciò, G. (2015). *ChemCatChem* 7: 1583–1592.
121 Morimoto, T., Fujii, T., Miyoshi, K. et al. (2015). *Org. Biomol. Chem.* 13: 4632–4636.
122 Mon, I., Bauzá, A., Frontera, A., and Rovira, L. (2015). *Chem. Eur. J.* 21: 11417–11426.
123 Chen, C., Dong, X.-Q., and Zhang, X. (2016). *Chem. Rec.* 16: 2674–2686.
124 Chen, C., Jin, S., Zhang, Z. et al. (2016). *J. Am. Chem. Soc.* 138: 9017–9020.
125 You, C., Wei, B., Li, X. et al. (2016). *Angew. Chem. Int. Ed.* 55: 6511–6514.
126 Li, S., Li, Z., You, C. et al. (2020). *Org. Lett.* 22: 1108–1112.
127 Tan, R., Zheng, X., Qu, B. et al. (2016). *Org. Lett.* 18: 3346–3349.
128 Schmitz, C., Holthusen, K., Leitner, W., and Franciò, G. (2016). *ACS Catal.* 6: 1584–1589.
129 You, C., Li, X., Yang, Y. et al. (2018). *Nat. Commun.* 9: 2045.
130 Qu, B., Tan, R., Herling, M.R. et al. (2019). *J. Org. Chem.* 84: 4915–4920.
131 You, C., Li, S., Li, X. et al. (2019). *ACS Catal.* 9: 8529–8533.
132 Cunillera, A., Blanco, C., Gual, A. et al. (2019). *ChemCatChem* 11: 2195–2205.
133 Johnson, M.D., May, S.A., Calvin, J.R. et al. (2016). *Org. Process Res. Dev.* 20: 888–900.
134 Abrams, M.L., Buser, J.Y., Calvin, J.R. et al. (2016). *Org. Process Res. Dev.* 20: 901–910.
135 Bondžić, B.P. (2015). *J. Mol. Catal.* 408: 310–334.
136 Ternel, J., Couturier, J.-L., Dubois, J.-L., and Carpentier, J.-F. (2015). *ChemCatChem* 7: 513–520.
137 Le Goanvic, L., Couturier, J.-L., Dubois, J.-L., and Carpentier, J.-F. (2018). *Catalysts* 8: 148.
138 Jörke, A., Gaide, T., Behr, A. et al. (2017). *Chem. Eng. J.* 313: 382–397.
139 Pandey, S. and Chikkali, S.H. (2015). *ChemCatChem* 7: 3468–3471.
140 Le Goanvic, L., Ternel, J., Couturier, J.-L. et al. (2018). *Catalysts* 8: 21.
141 Maji, T., Mendis, C.H., Thompson, W.H., and Tunge, J.A. (2016). *J. Mol. Catal. A: Chem.* 424: 145–152.
142 Pandey, S., Shinde, D.R., and Chikkali, S.H. (2017). *ChemCatChem* 9: 3997–4004.
143 Walter, S., Haumann, M., Wasserscheid, P. et al. (2015). *AIChE J.* 61: 893–897.
144 Tang, X., Jia, X., and Huang, Z. (2018). *J. Am. Chem. Soc.* 140: 4157–4163.
145 Vieira, G.M., Granato, A.V., Gusevskaya, E.V. et al. (2020). *Appl. Catal., A* 598: 117583.

146 Morales Torres, G., Frauenlob, R., Franke, R., and Börner, A. (2015). *Catal. Sci. Technol.* 5: 34–54.
147 Fuchs, S., Lichte, D., Dittmar, M. et al. (2017). *ChemCatChem* 9: 1436–1441.
148 Vanbésien, T., Monflier, E., and Hapiot, F. (2016). *Green Chem.* 18: 6687–6694.
149 Chen, C., Dong, X.-Q., and Zhang, X. (2016). *Org. Chem. Front.* 3: 1359–1370.
150 Kalck, P. and Urrutigoïty, M. (2018). *Chem. Rev.* 118: 3833–3861.
151 Oliveira, K.C.B., Carvalho, S.N., Duarte, M.F. et al. (2015). *Appl. Catal., A* 497: 10–16.
152 Zheng, Z. and Wang, L. (2019). *Synthesis* 51: 1585–1594.
153 de Oliveira Dias, A., Gutiérrez, M.G.P., Villarreal, J.A.A. et al. (2019). *Appl. Catal., A* 574: 97–104.
154 October, J. and Mapolie, S.F. (2020). *Catal. Lett.* 150: 998–1010.
155 Hanna, S., Holder, J.C., and Hartwig, J.F. (2019). *Angew. Chem. Int. Ed.* 58: 3368–3372.
156 Seidensticker, T., Vosberg, J.M., Osrowski, K.A., and Vorholt, A.J. (2016). *Adv. Synth. Catal.* 358: 610–621.
157 Fuchs, S., Lichte, D., Jolmes, T. et al. (2018). *ChemCatChem* 10: 4126–4133.
158 Almeida, A.R., Carrilho, R.M.B., Peixoto, A.F. et al. (2017). *Tetrahedron* 73: 2389–2395.
159 Ostrowski, K.A., Faßbach, T.A., Vogelsang, D., and Vorholt, A.J. (2015). *ChemCatChem* 7: 2607–2613.
160 Dong, K., Fang, X., Jackstell, R., and Beller, M. (2015). *Chem. Commun.* 51: 5059–5062.
161 Quintero-Duque, S. and Fleischer, I. (2017). *Synthesis* 49: 925–932.
162 Tsai, J.-C., Lin, Y.-H., Chen, G.-T. et al. (2018). *Chem. Asian J.* 13: 3190–3197.
163 Bhagade, S.S. and Bhanage, B.M. (2018). *Catal. Commun.* 112: 21–25.
164 Plass, C., Hinzmann, A., Terhorst, M. et al. (2019). *ACS Catal.* 9: 5198–5203.
165 Pittaway, R., Dingwall, P., Fuentes, J.A., and Clarke, M.L. (2019). *Adv. Synth. Catal.* 361: 4334–4341.
166 Christensen, S.H., Olsen, E.P.K., Rosenbaum, J., and Madsen, R. (2015). *Org. Biomol. Chem.* 13: 938–945.
167 Ren, X., Zheng, Z., Zhang, L. et al. (2017). *Angew. Chem. Int. Ed.* 56: 310–313.
168 Liu, Z., Yang, Z., Yu, B. et al. (2018). *Org. Lett.* 20: 5130–5134.
169 Pan, J., Morimoto, T., Kobayashi, H. et al. (2019). *Hetorocycles* 98: 519–533.
170 Anton-Torrecillas, C., Bosque, I., Gonzalez-Gomez, J.C. et al. (2015). *J. Org. Chem.* 80: 1284–1290.
171 Rosales, M., Pérez, H., Arrieta, F. et al. (2016). *J. Mol. Catal. A: Chem.* 421: 122–130.
172 Fuentes, J.A., Pittaway, R., and Clarke, M.L. (2015). *Chem. Eur. J.* 21: 10645–10649.
173 Gorbunov, D., Nenasheva, M., Terenina, M. et al. (2020). *ChemistrySelect* 5: 6407–6414.
174 Tan, G., Wu, Y., Shi, Y., and You, J. (2019). *Angew. Chem. Int. Ed.* 58: 7440–7444.
175 Kalck, P., Le Berre, C., and Serp, P. (2020). *Coord. Chem. Rev.* 402: 213078.
176 Dutta, D.K. (2018). *J. Indian Chem. Soc.* 95: 879–892.

177 Ren, Z., Lyu, Y., Song, X., and Ding, Y. (2020). *Appl. Catal., A* 595: 117488.
178 Ren, Z., Lyu, Y., Song, X. et al. (2019). *Adv. Mater.* 31: 1904976.
179 Hong, J.-H. (2015). *Catalysts* 5: 1969–1982.
180 Yacob, S., Park, S., Kilos, B.A. et al. (2015). *J. Catal.* 325: 1–8.
181 Yacob, S., Kilos, B.A., Barton, D.G., and Notestein, J.M. (2016). *Appl. Catal., A* 520: 122–131.
182 Molla, R.A., Ghosh, K., Roy, A.S., and Islam, S.M. (2015). *J. Mol. Catal. A: Chem.* 396: 268–274.
183 Wang, B., Geù, B., Zhu, J., and Wang, L. (2018). *Chin. J. Chem. Eng.* 26: 1937–1942.
184 Wang, H. and Wu, X.-F. (2020). *J. Organomet. Chem.* 910: 121134.
185 Wu, X.-F., Neumannn, H., Beller, M. (2012). *Chem. Asian J*., **7**: 1199–1202.
186 Dong, K., Fang, X., Jackstell, R. et al. (2015). *J. Am. Chem. Soc.* 137: 6053–6058.
187 Behr, A., Levikov, D., and Nürenberg, E. (2015). *Catal. Sci. Technol.* 5: 2783–2787.
188 Zhang, J., Zhang, W., Xu, M. et al. (2018). *J. Am. Chem. Soc.* 140: 6656–6660.
189 Yuan, S.-W., Han, H., Li, Y.-L. et al. (2019). *Angew. Chem. Int. Ed.* 131: 8979–8984.
190 Mise, T., Hong, P., Yamazaki, H. (1983). *J. Org. Chem*., **48**: 238–242.
191 Artok, L., Kuş, M., Aksın-Artok, Ö., Dege, F.N., Özkılınç, F.Y. (2009). *Tetrahedron*, **65**: 9125–9133.
192 Sabacz, L., Girard, N., Sufferet, J., Blond, G.(2018). *Monatsh Chem*., **149**: 671–686.
193 Zhu, F., Li, Y., Wang, Z., and Wu, X.-F. (2016). *ChemCatChem* 8: 3710–3713.
194 Piens, N. and D'hooghe, M. (2017). *Eur. J. Org. Chem.* 2017: 5943–5960.
195 Dalling, A.G. and Bower, J.F. (2018). *Chimia* 72: 595–600.
196 Huang, Q., Han, Q., Fu, S. et al. (2016). *J. Org. Chem.* 8: 12135–12142.
197 Li, X., Xie, H., Fu, X. et al. (2016). *Chem. Eur. J.* 22: 10410–10414.
198 Liu, J.-t., Wang, H.-y., Xi, B.-m. et al. (2017). *Adv. Synth. Catal.* 359: 693–697.
199 Zhao, K., Du, R., Wang, B. et al. (2019). *ACS Catal.* 9: 5545–5551.
200 Chen, Y., Liu, D., and Yu, Y. (2017). *RSC Adv.* 7: 49875–49882.
201 Chen, Y. and Liu, D. (2018). *Fuel Process. Technol.* 171: 301–307.
202 Luk, H.T., Mondelli, C., Curulla Ferré, D. et al. (2017). *Chem. Soc. Rev.* 46: 1358–1426.
203 Liu, Z., Wang, P., Yan, Z. et al. (2020). *Beilstein J. Org. Chem.* 16: 645–656.
204 Salacz, L., Girard, N., Suffert, J., and Blond, G. (2018). *Monatsh. Chem.* 149: 671–686.
205 Wang, Y. and Yu, Z.-X. (2015). *Acc. Chem. Res.* 48: 2288–2296.
206 Fu, X.-F., Xiang, Y., and Yu, Z.-X. (2015). *Chem. Eur. J.* 21: 4242–4246.
207 Gao, B., Liu, S., Lan, Y., and Huang, H. (2016). *Organometallics* 35: 1480–1487.
208 Morimoto, T., Yamashita, M., Tomiie, A. et al. (2020). *Chem. Asian J.* 15: 473–477.
209 Furusawa, T., Morimoto, T., Nishiyama, Y. et al. (2016). *Chem. Asian J.* 11: 2312–2315.
210 Furusawa, T., Tanimoto, H., Nishiyama, Y. et al. (2017). *Chem. Lett.* 46: 926–929.

211 Qi, X., Zhou, R., Ai, H.-J., and Wu, X.-F. (2020). *J. Catal.* 381: 215–221.

212 Matsuda, T., Fukuhara, K., Yonekubo, N., and Oyama, S. (2017). *Chem. Lett.* 46: 1721–1723.

213 Lang, X.-D. and He, L.-N. (2018). *ChemSusChem* 11: 2062–2067.

214 Gao, Y., Cai, Z., Li, S., and Li, G. (2019). *Org. Lett.* 21: 3663–3669.

215 Cai, L., Fu, L., Zhou, C. et al. (2020). *Green Chem.* 22: 7328–7332.

216 Iu, L., Clarke, M., Fontenot, K.J., and Janka, M.E. (2018) Highly isoselective catalyst for alkene hydroformylation. US10144751 (Eastman Chem CO.).

217 Iu, L., Clarke, M., and Janka, M.E. (2019) Highly isoselective catalyst for alkene hydroformylation. US10183961 (Eastman Chem CO.).

218 Tsuruta, T., Minamoto, N., and Omatsu, T. (2019) Method of producing dialdehyde compound. US10479750 (Kuraray CO.).

219 Yoshikawa, T. and Tsuji, T. (2016) Method for producing dialdehyde. US9464018 (Kuraray CO.).

220 Liu, Z., Liu, X., Yu, Q., and Zhu, J. (2018) Preparation method for m-trifluoromethylphenol benzenepropanal. CN109096070 A (China Petrol. & Chem Corp.).

221 Liu, Z., Liu, X., Liu, X., and Wang, Y. (2018) Preparing method for 3-benzenepropanal. CN109096071 A (China Petrol. & Chem Corp.).

222 Satou, T. and Tanaka, Y. (2019) Method for producing aldehyde and method for producing alcohol. WO2019098242 A1 (Mitsubishi Chem Corp.).

223 Munslow, I. and Kangas, M. (2018) Carbonylation process and ligand composition comprising a bidentate phosphite ligand and a tertiary phosphine anti-oxidant. WO2018147793 A1 (Perstorp AB).

224 Smith, G.L. and Simpson, K. (2019) Process for producing aldehydes. US10351503 (Dow Tech. Inv. LLC).

225 Miller, G.A., Biedenstein, V.L., Shahatul, M., et al. (2019) Hydroformylation process. US9868686 (Dow Tech. Inv. LLC).

226 Xu, X., Zhang, M., Liu, H., et al. (2019) Method for hydroformylating vinyl acetate. CN106565484 (China Petrol. & Chem Corp.).

227 Yamakawa, A., Otsuka, Y., and Kobayashi, O. (2017) 3-(perfluoroalkyl)propanal production method. JP6211897 (Tosoh F. Tech. Inc.).

228 Ko, D.-H., Eom, S.-S., Hong, M.-H., et al. (2014) Hydroformylation method having improved catalyst stability in reaction. US8884071 (LG Chemical Ltd).

229 Tokunaga, K., Kakinuma, N., and Kuma, S. (2016) Preparation method of aldehyde compound with limited amount of acrylonitrile. US9487475 (Mitsui Chem. Inc.).

230 Brammer, M.A., Watson, R.B., and Watkins, A.L. (2017) Catalyst preparation process. US9539566 (Dow Tech. Inv. LLC).

231 Schunk, S.A., Lejkowski, M., Titlbach, S., et al. (2017) Method for the hydroformylation of olefins and/or alkynes in the gas phase with a mixture of hydrogen and carbon monoxide in the presence of heterogeneous catalyst. EP3130399 A1 (BASF SE).

232 Li, Y., Lai, C., Gao, S., et al. (2018) Method of preparing aldehyde by hydroformylation of dihydrofuran. CN106432142 (Shanghai Huayi CO Ltd.).

233 Beller, M., Jackstell, R., and Fang, X. (2016) Process for the catalytic production of unsaturated aldehydes. US9238607 (Evonik Ind. AG).

234 He, Y., Dong, L., Qiao, X., et al. (2018) Synthetic method of 3-methylcrotonaldehyde. CN108047013 A (Wanhua Chem. Group CO Ltd).

235 Watanabe, T., Motoi, T., and Yoshimura, Y. (2019) Bifunctional compound having norbornane skeleton and production method therefor. US10246404 (Mitsubishi Gas Chem. CO).

236 Zha, X. and Yang, Y. (2017) Method for producing 1,3-propylene glycol through hydroformylation of vinyl acetate. CN105585437 (China Petrol. & Chem Corp.).

237 Tao, F., Huang, W., Tang, Y., and Li, Y. (2019) Catalysts and methods for producing acetic acid from methane, carbon monoxide, and oxygen. WO2019191053 A (Univ. Kansas & Univ. Notre Dame du Lac).

238 Shimizu, M. (2019) Methods for producing acetic acid. JP6569019 (Daicel Corp.).

239 Li, Y., Gao, S., Lai, C., et al. (2019) Method for producing alkanoic acid. CN110124755 A (Shanghai Huayi CO Ltd.).

240 Zhu, G., Wang, Z., Hu, Z., et al. (2019) Technology for synthesizing acetic acid. CN109232223 A (Jiangsu Sopo Group CO Ltd. & Jiangsu Sopo Eng.Tech. CO Ltd.).

241 Bae, J.U., Chang, T.S., Kim, B.S., et al. (2018) Carbon nitride heterogeneous catalyst containing rhodium, method for preparing the same, and method for preparing acetic acid using the same. US10124321 (Korea Res. Inst. Chem. Tech.).

242 Le Berre, C.M., Nguyen, D.H., Serp, P.G., et al. (2017) Production of acetic acid with enhanced catalyst stability. US9598342 (Celanese Int. Corp.).

243 Hong, J.H. (2017) Stabilization of catalyst for acetic acid preparation, and method for preparing amide of anhydrous tertiary amine. WO2017078507 A.

244 Zhu, Z.G., Tustin, G.C., Zoeller, J.R., et al. (2016) Carbonylation catalyst and processing using same. US9387469 (Eastman Chem. CO).

245 Zhang, H., Mao, Z., Jia, H., et al. (2019) Method for preparing methyl acetate by using methanol through one-step method. CN107892648 (Southwest Res. & Design Inst. Chem. Ind.).

246 Liu, X., Liu, Z., Liu, G., and Wang, Y. (2018) Synthesis method for 2-crotonate. CN109096109 A (China Petrol. & Chem Corp.).

247 Liu, X., Liu, Z., and Yu, Q. (2018) Synthesis method for 4,4,4-trifluorocrotonates. CN109096108 A (China Petrol. & Chem Corp.).

248 Liu, Y., Wang, P., Liu, H., et al. (2018) Method for preparing primary amide from olefin, carbon monoxide and ammonia gas. CN107935878 A (Univ. East China Normal).

249 Kolesnikov, P.N., Chusov, D.A., Afanas'ev, O.I., and Maleev, V.I. (2017) Method of amides obtaining from carbonyl compounds. RU2620269 C1 (A N Nesmeyanov Inst, Organoel. Compounds Russian Acad. of Sciences).

250 Hapiot, F., Monflier, E., and Vanbesien, T. (2018) Process for preparing polyols. US10138200 (Pivert Sas).

7

Palladium(0)-Catalyzed Carbonylations

Jianming Liu[1], Chengtao Yue[2] and Fuwei Li[2]

[1]Collaborative Innovation Center of Henan Province for Green Manufacturing of Fine Chemicals, Key Laboratory of Green Chemical Media and Reactions, Ministry of Education, School of Chemistry and Chemical Engineering, Henan Normal University, Xinxiang, Henan 453007, PR China
[2]State Key Laboratory for Oxo Synthesis and Selective Oxidation, Suzhou Research Institute of LICP, Lanzhou Institute of Chemical Physics (LICP), Chinese Academy of Sciences, Lanzhou 730000, China

7.1 Introduction

The transition metal-catalyzed carbonylative reactions have greatly enriched the routes for the preparation of carbonyl compounds [1–4]. Mainly, the palladium(0)-catalyzed carbonylation of different substrates using cheap carbon monoxide (CO) as a carbonyl source has received considerable attention due to its wide application in the high-efficient production of carbonyl derivatives [5–8]. With Pd(0) catalysts, this synthetic approach consists of the following three steps: oxidative addition of palladium(0) to the C—X bond of substrates, followed by insertion of CO into the C—Pd bond of the above intermediate and reductive displacement to produce the desired carbonyl compounds (Scheme 7.1). Based on this approach, which can also occur intramolecularly, different carbonyl compounds such as esters, amides, ketones, and α,β-alkynyl ketone have been synthesized from aryl halides, alkenes, alkynes, esters, and aziridines. Moreover, by combining carbonylation with cyclization or cross-coupling reaction, many meaningful carbonyl compounds such as spirooxindoles, β-lactams, vinylallenyl esters, quinazolinones, and flavones have been successfully fabricated in a one-pot synthesis. This chapter summarized the main achievements in palladium(0)-catalyzed carbonylative synthesis of esters, amide, ketones, α,β-alkynyl ketones, and other important carbonyl derivatives.

Carbon Monoxide in Organic Synthesis: Carbonylation Chemistry,
First Edition. Edited by Bartolo Gabriele.

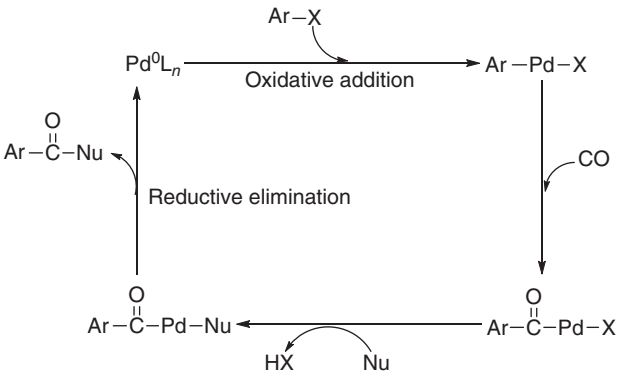

Scheme 7.1 Typical mechanism for palladium(0)-catalyzed carbonylation reactions(unreactive ligands on palladium are not shown in intermediate formulae for clarity).

7.2 Palladium(0)-Catalyzed Carbonylative Synthesis of Ester Derivatives

7.2.1 Palladium(0)-Catalyzed Carbonylative Synthesis of Ester Derivatives from Aryl Halides

2-Substituted-4*H*-3,1-benzoxazin-4-ones are widely found in natural products and pharmaceuticals. They have attracted great attention in producing heterocyclic compounds and bioactive benzoxazines [9]. In 1996, Cacchi, Marinelli, and coworker developed a valuable synthetic route to 2-substituted-4*H*-3,1-benzoxazin-4-ones from *N*-(2-iodophenyl) substituted amides through palladium-catalyzed intramolecular cyclocarbonylation, with the oxygen of the amido group serving as internal nucleophile (Scheme 7.2) [10]. This transformation produced the 2-substituted-4*H*-3,1-benzoxazin-4-ones in moderate to good yields.

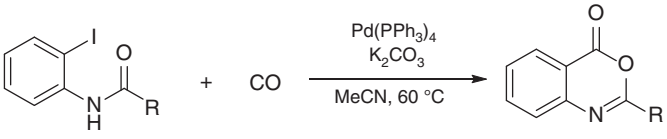

R = Me (5 h, 60%); Et (21 h, 35%); Ph (12 h, 92%)

Scheme 7.2 Palladium-catalyzed carbonylative synthesis of 2-substituted-4*H*-3, 1-benzoxazin-4-ones. Source: Cacchi et al. [10].

In 2009, Willis and coworkers reported the synthesis of isocoumarins via palladium-catalyzed intramolecular cyclocarbonylation of α-(*o*-haloaryl)-substituted ketones (Scheme 7.3) [11]. Isocoumarins were obtained in good yields under balloon pressure of CO, the enolate oxygen acting as the intramolecular nucleophile. Both cyclic and acyclic ketones were suitable for this reaction, affording the corresponding isocoumarins in high yields. This useful strategy was successfully applied to furnish the synthesis of the natural product thunberginol **A**.

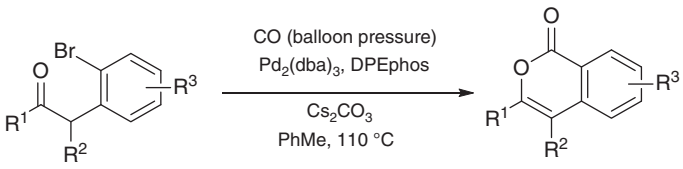

Scheme 7.3 Palladium-catalyzed carbonylative synthesis of isocoumarins. Source: Tadd et al. [11].

As shown in Scheme 7.4, the starting α-(*o*-haloaryl)-substituted ketone, prepared via α-arylation of 3,4-dimethoxyacetophenone with aryl iodide, could readily deliver the thunberginol **A** in good yield via an intramolecular cyclocarbonylation of aryl ketone and subsequent deprotection of methyl ethers using BBr_3.

Compared to the molecular Pd(0) complexes, palladium-on-carbon (Pd/C) could advance the carbonylative reactions toward more sustainable conditions due to its facile reusability. In 2010, Petricci and coworkers successfully used Pd/C as the heterogeneous catalyst for carbonylation of aryl halides (Scheme 7.5) [12]. Different nucleophiles, such as amines, primary and secondary alcohols, could be coupled well with aryl halides via the carbonylation reaction to synthesize the carbonyl compounds under microwave irradiation. This catalytic system could be applied to the cyclocarbonylation of *o*-iodoaniline with acyl chlorides to generate benzoxazinones under microwave-assisted conditions, and the Pd/C catalyst was found to retain its high efficiency after two cycles.

Interestingly, Larock and coworker reported a one-pot multicomponent synthetic route to prepare highly substituted lactone- and ester-containing furans through palladium-catalyzed intramolecular cyclocarbonylation or intermolecular alkoxycarbonylation (Scheme 7.6) [13]. In this contribution, the key intermediates hydroxyl-containing 3-iodofurans were contained by an iodocyclization reaction. These iodine-containing furans could then successfully be converted into lactone- and ester-containing furans through the organopalladium carbonylation chemistry. This strategy opened up a new route toward a highly efficient generation of the heterocyclic compounds under mild conditions.

In 2015, Jun and coworkers described the Pd/C-catalyzed carbonylative esterification of less active aryl chlorides with primary alcohols in the absence of CO (Schemes 7.7 and 7.8) [14]. Here, the primary alcohols functioned as both the coupling partner and the carbonyl source. Initially, the oxidation of alcohol generated the aldehyde, and the oxidative dehydroxymethylation of the aldehyde produced alkane and Pd(0)CO via the cleavage of the C—C bond. Then the oxidation addition of Pd(0)CO to the aryl chloride delivered the acylpalladium intermediate, and reduction elimination of acylpalladium intermediate with alcohol gave the corresponding ester (Scheme 7.8). This synthetic approach tolerated various aryl chlorides and primary alcohols, providing the desired esters in good to excellent yields.

In 2018, Ogawa and coworker described a palladium-catalyzed double carbonylative cyclization of benzoins for the construction of bis-ester-bridged stilbenes containing a pyrano[3,2-*b*]pyran-2,6-dione (PPD) core from aldehydes (Scheme 7.9) [15]. These bis-ester-bridged stilbenes displayed two reversible reductions at low potentials, owing to the fused tetracyclic π-systems.

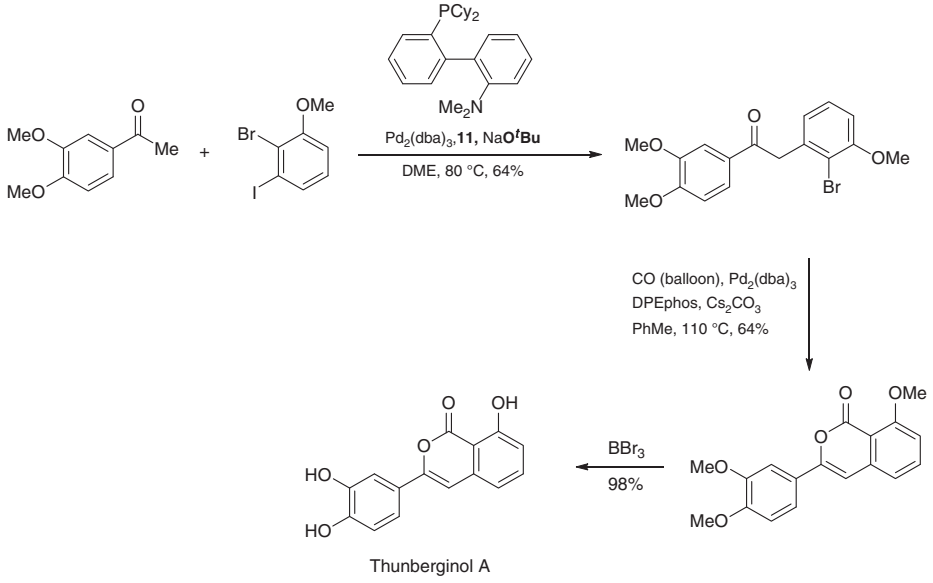

Scheme 7.4 Synthesis of thunberginol **A**.

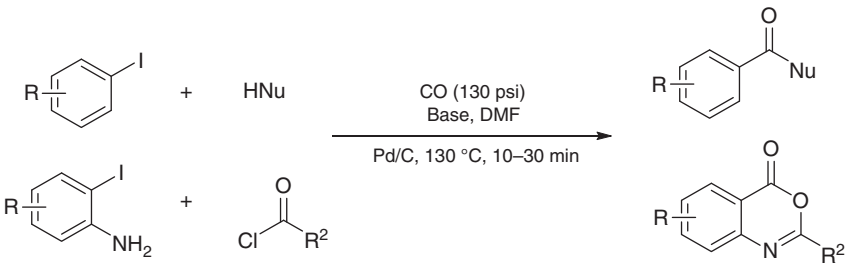

Scheme 7.5 Palladium-catalyzed carbonylation of aryl halides. Source: Salvadori et al. [12].

In 2019, Zhu and coworkers reported a palladium-catalyzed enantioselective Heck/carbonylative lactonization and lactamization sequence to prepare all-carbon spirooxindole compounds from non-oxindole-based materials (Scheme 7.10) [16]. This process went smoothly to deliver various spirooxindole γ- and δ-lactones/lactams through the enantioselective Heck/carbonylative lactonization and lactamization. Importantly, by introducing more stereogenic centers around the chiral quaternary spiro-carbon center, this efficient approach could be applied to synthesize the natural product coixspirolactam, which is an effective prostaglandin D2 receptor (CRTH2) antagonist (Scheme 7.11).

Recently, Wu and coworkers described a new procedure for the preparation of 2-aminobenzoxazinones from 1-azido-2-iodobenzenes and amines via palladium-catalyzed intramolecular cyclocarbonylation (Scheme 7.12) [17]. 2-Aminobenzoxazinone derivatives were obtained in excellent yields under the catalysis of Pd/C upon using CO as a carbonyl source. Mechanistic investigations demonstrated that the reaction occurred through four steps: (i) Oxidative addition of 1-azido-2-iodobenzene to Pd(0) and insertion of CO generated acylpalladium intermediate **I**; (ii) The interaction between the azide group and CO delivered acylpalladium intermediate **II** containing the isocyanate group; (iii) Nucleophilic attack of the amine to isocyanate group formed intermediate **III**; (iv) Reductive elimination gave the final product and regenerated the Pd(0) (Scheme 7.13). With this method, a bioactive 2-aminobenzoxazine was obtained in good yield (Scheme 7.14).

7.2.2 Palladium(0)-Catalyzed Carbonylative Synthesis of Ester Derivatives from Alkynes

In 1997, Alper and coworker reported the carbonylative synthesis of 2(5*H*)-furanones from substituted alkynols using Pd_2dba_3/phosphines as the catalyst system in the presence of H_2 and CO (Scheme 7.15) [18]. It was found that cyclocarbonylation of conjugated ene-ynols containing alkyl, phenyl, and vinyl groups proceeded well to provide the corresponding 3-alkenyl-2(5*H*)-furanones in good yields. Mechanistic studies indicated that the initial insertion of Pd(0) into the C—O bond of the alkynol generated alkynyl palladium, and itsrearrangement led to the formation of an allenylpalladium intermediate which further underwent carbonylation and cyclization to produce 2(5H)-furanone. This approach provided a new synthetic route to the natural product thunberginol.

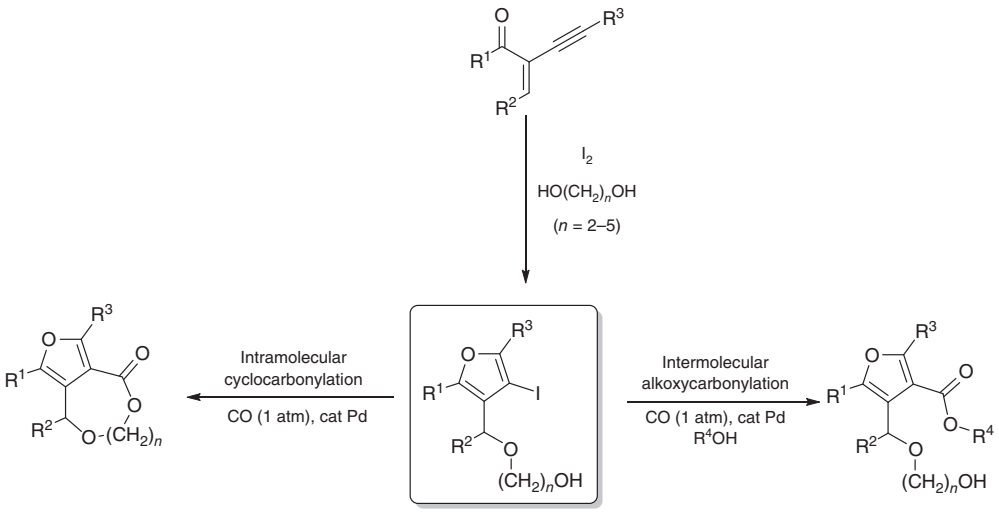

R^3 = Ph, 4-$MeOC_6H_4$, 3-$MeOC_6H_4$, 4-$Me_2NC_6H_4$, 4-NCC_6H_4, 3-thiophenyl, 1-cyclohexenyl, etc.
R^4OH = HOH, MeOH, $HO(CH_2)_nOH$ (n = 2–5), PhOH, BnOH, ROH (R = alkyl), etc.

Scheme 7.6 Palladium-catalyzed intramolecular cyclocarbonylation and intermolecular alkoxycarbonylation. Source: Cho and Larock [13].

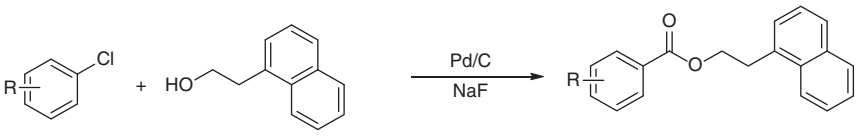

Scheme 7.7 Alkoxycarbonylation of aryl chlorides with primary alcohols. Source: Modified from Park et al. [14].

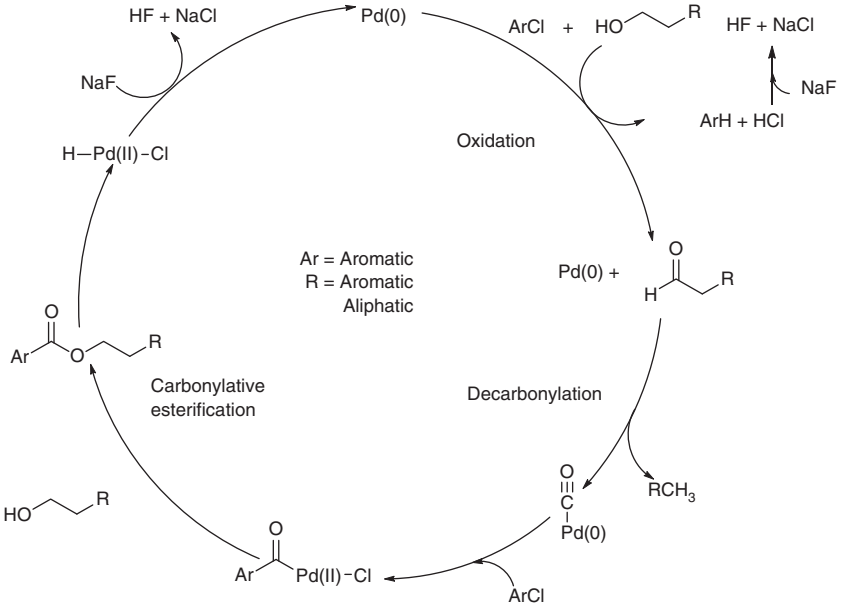

Scheme 7.8 Plausible mechanism of alkoxycarbonylation of aryl chlorides with primary alcohols. Source: Park et al. [14].

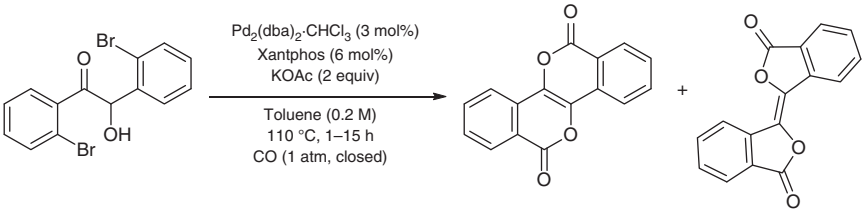

Scheme 7.9 Palladium-catalyzed double carbonylative cyclization of benzoins. Source: Modified from Tani and Ogawa [15].

In 2011, Artok and coworkers developed a Pd(0)-catalyzed carbonylation of (*Z*)-2-en-4-yn carbonates for the construction of vinylallenyl esters in the presence of a balloon pressure of CO (Scheme 7.16) [19]. A range of (*Z*)-2-en-4-yn carbonates were investigated in different alcohols, generating the vinylallenyl esters with an exclusively *E*-configuration and in high yields. Control experiments disclosed that the cooperative coordination of palladium with both alkynyl and carbonate moieties triggered the decarboxylation of the carbonate and then caused the carbonylative

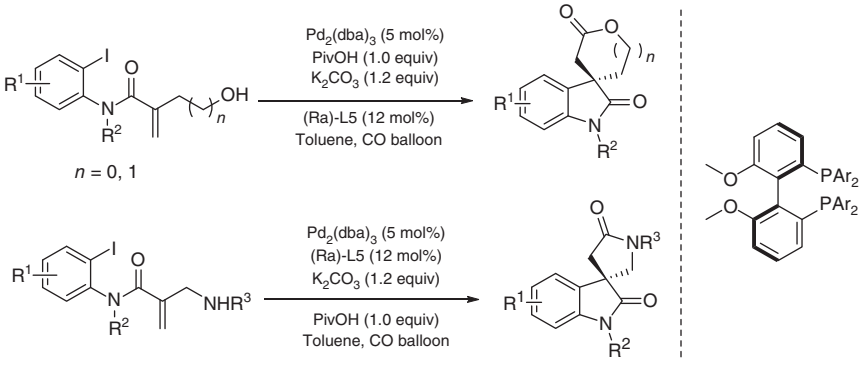

Scheme 7.10 Palladium-catalyzed enantioselective carbonylative Heck cyclization. Source: Modified from Hu et al. [16].

transformation. Moreover, carbonylation of *Z*-conjugated enyne reagents with a leaving group in the allylic position also preceded well to deliver the desired esters.

In 2013, an efficient route for constructing nonracemic 2,3-allenoates from the enantioenriched secondary propargylic mesylates was developed by Ma and coworker (Scheme 7.17) [20]. This reaction proceeded via palladium(0) bis(dibenzylideneacetone)/(*S*)-5,5′-bis(diphenylphosphino)-4,4′-bibenzodioxole [(*S*)-SEGPHOS]-catalyzed alkoxycarbonylation of propargylic mesylates, which selectively generated the desired 2,3-allenoates with excellent yields.

Subsequently, Ma and coworkers further described the enantiospecific synthesis of nonracemic 2,4-disubstituted 2,3-allenoates using the inexpensive commercially available non-chiral bisdiphenylphosphinophenylether (DPEphos) (Scheme 7.18) [21]. This catalytic system was capable of catalyzing the carbonylation of various nonracemic non-terminal propargylic mesylates to generate the corresponding 2,4-disubstituted 2,3-allenoates. Notably, the gram-scale synthesis of an optically active 2,3-allenoate was accomplished, affording the desired product with 90% yield and 96% ee using 1 mol% $Pd(dba)_2$ and DPEphos (Scheme 7.19). Control experiments demonstrated that the matched coordination of Pd with DPEphos afforded a relatively stable planar allenylic Pd(II) complex, which functioned as the key intermediate in this chirality transfer process. A very fast alkoxycarbonylation with CO and BnOH effectively prevented racemization.

In 2015, an efficient Pd(0)-catalyzed thiolative lactonization of internal alkynes containing a hydroxyl group was achieved by Ogawa and coworkers (Scheme 7.20) [22]. Various internal alkynes bearing a hydroxy group, such as homopropargyl alcohol derivatives, were compatible with thiolative carbonylation, generating the corresponding thio group bearing-lactones in good yields. Control experiments disclosed that the insertion of CO into the palladium alkoxide complex formed by ligand exchange between palladium sulfide complex and acetylenic alcohol is the key for the thiolative lactonization. This reaction overcame the challenge of the carbonylative addition of organic disulfides to internal alkynes.

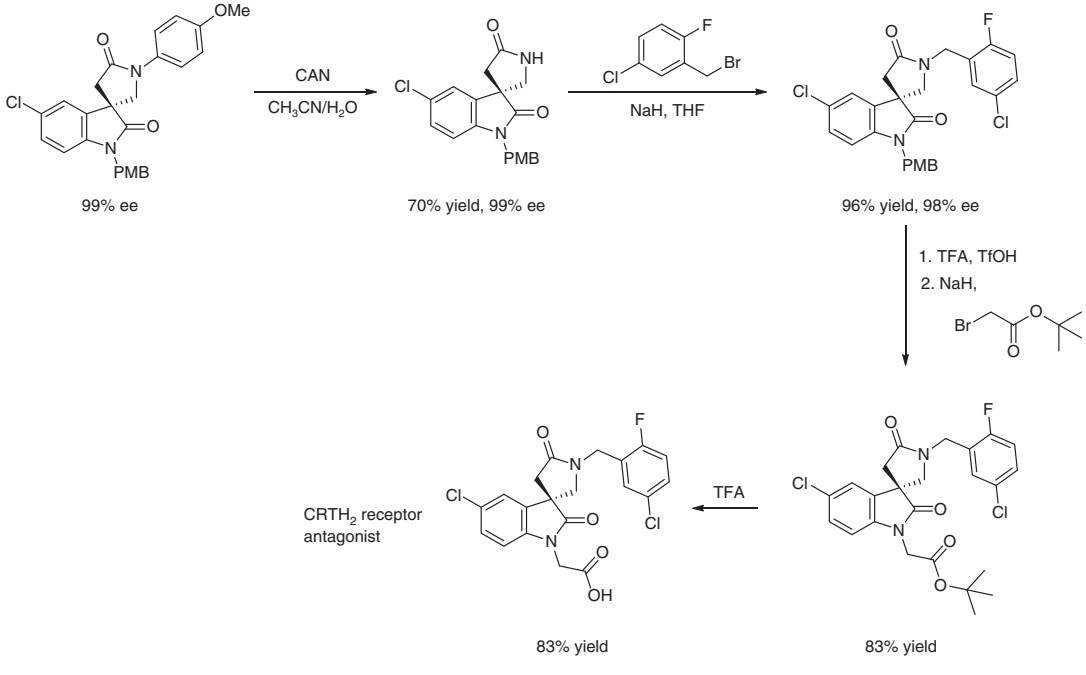

Scheme 7.11 Synthesis of CRTH2 receptor antagonist.

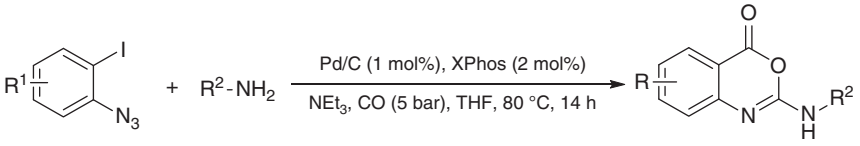

Scheme 7.12 Palladium-catalyzed carbonylation of 1-azido-2-iodobenzenes with amines. Source: Zhang et al. [17].

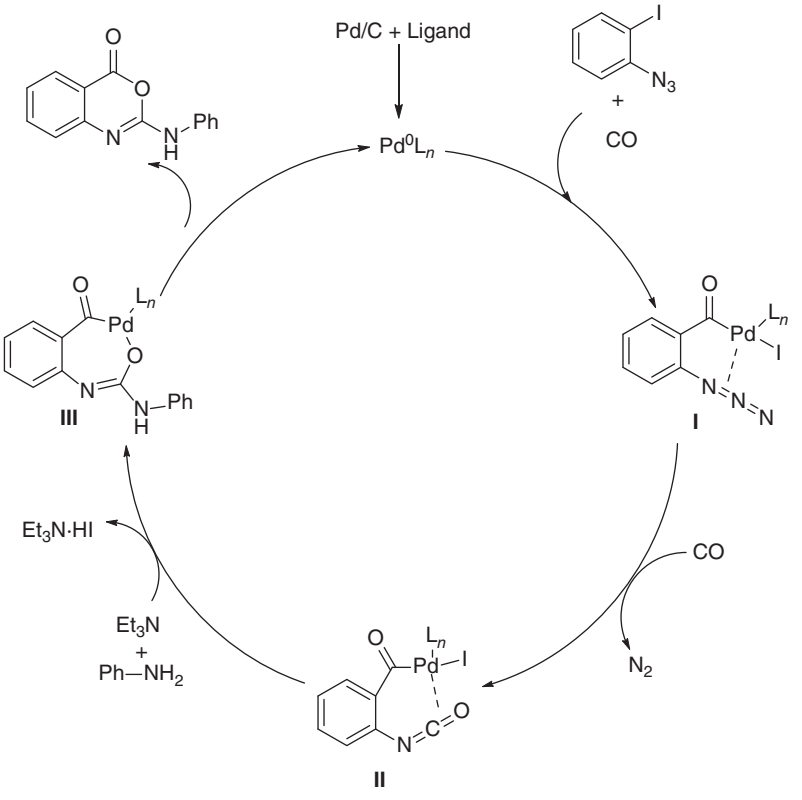

Scheme 7.13 Proposed reaction mechanism for carbonylation of 1-azido-2-iodobenzene with amine.

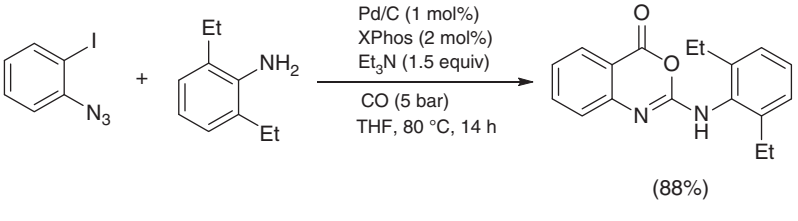

Scheme 7.14 Synthesis of a bioactive 2-aminobenzoxazine derivative.

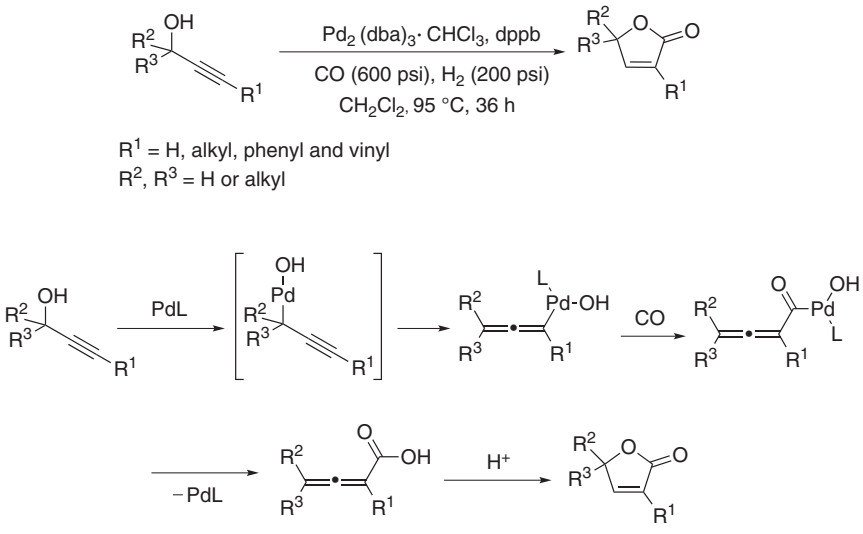

Scheme 7.15 $Pd_2(dba)_3$ catalyzed carbonylative synthesis of 2(5*H*)-furanones. Source: Yu and Alper [18].

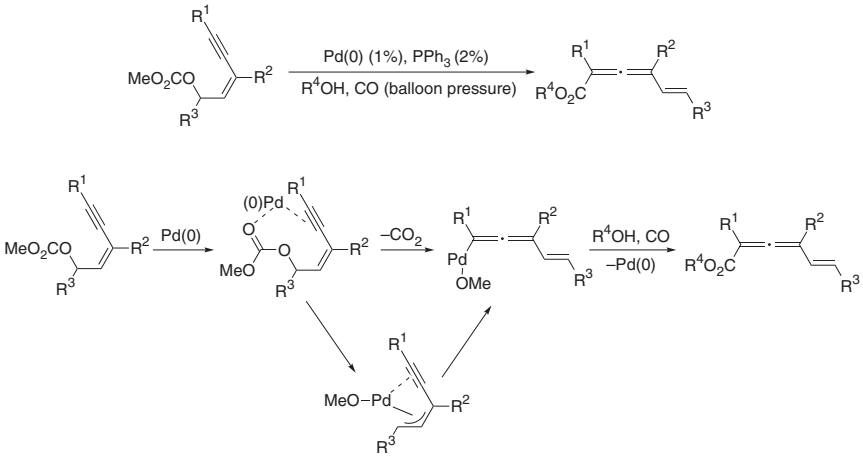

Scheme 7.16 Pd(0)-catalyzed carbonylation of (*Z*)-2-en-4-yn carbonates. Source: Akpınar et al. [19].

Carbon monoxide and styrene could be easily obtained by a Pd/C-catalyzed C—C bond cleavage of cinnamaldehyde derivatives. Thus, cinnamaldehyde could be used as the CO carrier for the carbonylation of aromatic iodides with alcohols and amines. In 2017, Sajiki and coworkers reported a Pd/C-catalyzed efficient carbonylative synthesis of lactones and 1,2-diarylethenes via decarbonylation of cinnamaldehyde and carbonylation of aromatic iodides with alcohols and amines (Scheme 7.21) [23]. This reaction was accomplished by using an H-shaped pressure-tight glass-sealed tube.

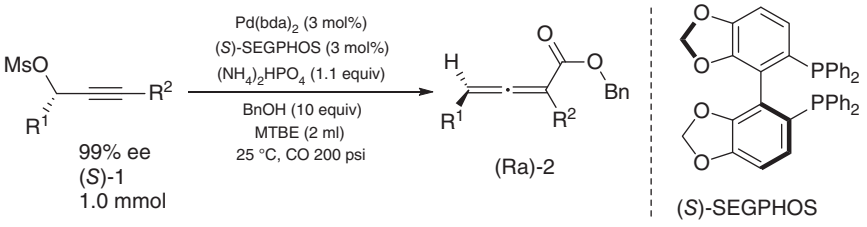

Scheme 7.17 Pd(0)-catalyzed alkoxycarbonylation of propargylic mesylates. Source: Modified from Wang and Ma [20].

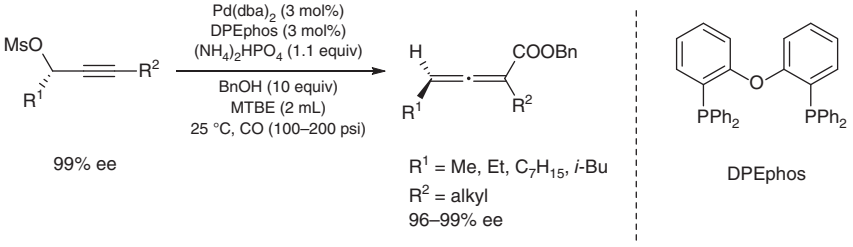

Scheme 7.18 Palladium-catalyzed enantiospecific carbonylative procedure for the synthesis of nonracemic 2,4-disubstituted 2,3-allenoates. Source: Wang et al. [21].

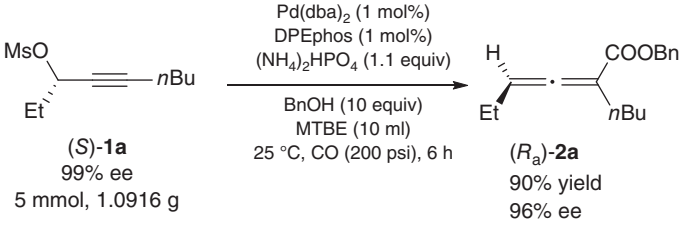

Scheme 7.19 Gram-scale enantiospecific synthesis of a nonracemic 2,3-allenoate.

7.2.3 Palladium(0)-Catalyzed Carbonylative Synthesis of Ester Derivatives Using Benzyl Amines

Wu and coworkers recently developed a new route to synthesize methyl 2-arylacetates via palladium-catalyzed direct carbonylative transformation of benzyl amines (Scheme 7.22) [24]. This reaction was proposed to be initiated by the oxidative addition of Pd(0) to the C—N bond of benzyl amines. Various primary, secondary, and tertiary benzyl amines were tolerated, producing the corresponding methyl 2-arylacetates in good to excellent yields in the absence of other additives. Notably, the methylphenidate (which is known as a marketing drug for attention deficit hyperactivity disorder [ADHD] and narcolepsy), could also be synthesized in good yield with the above method (Scheme 7.23).

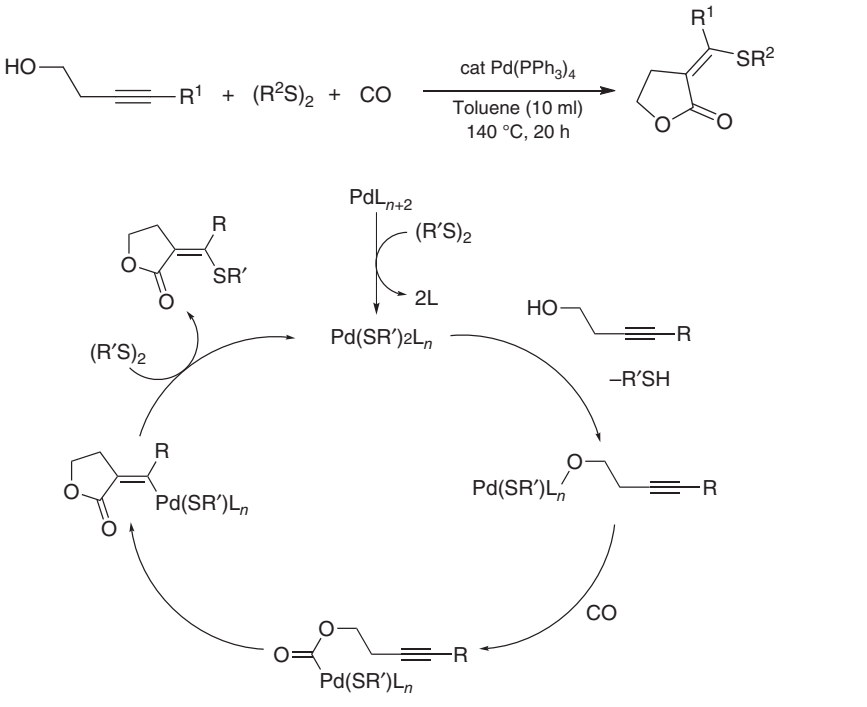

Scheme 7.20 Pd(0)-catalyzed thiolative lactonization of internal alkynes. Source: Higashimae et al. [22].

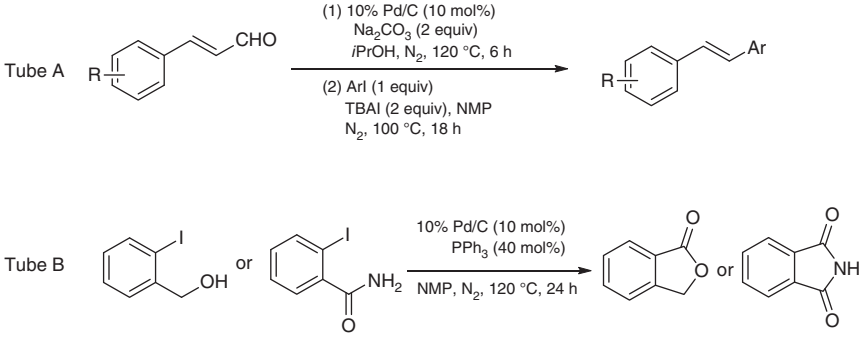

Scheme 7.21 Pd/C-catalyzed carbonylation with cinnamaldehydes as CO carrier. Source: Hattori et al. [23].

7.3 Palladium(0)-Catalyzed Carbonylative Synthesis of Amide Derivatives

7.3.1 Palladium(0)-Catalyzed Carbonylative Synthesis of β-Lactams

β-Lactams are important synthetic building blocks for the production of heterocyclic compounds [25–27]. Hence, great efforts have been devoted to developing new

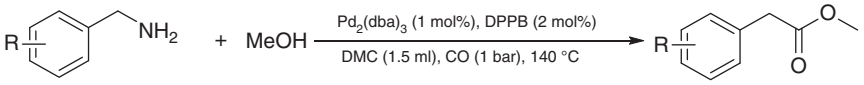

Scheme 7.22 Palladium-catalyzed carbonylative transformation of benzylamines. Source: Li et al. [24].

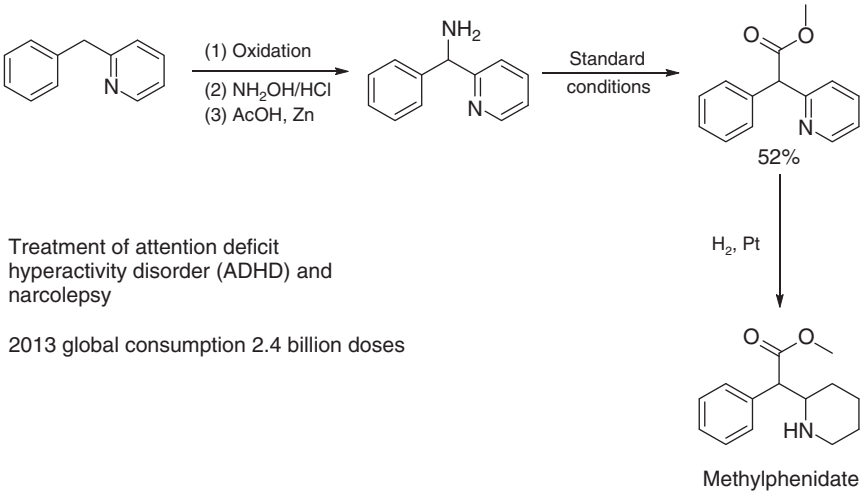

Scheme 7.23 Synthesis of methylphenidate.

and efficient synthetic routes to construct β-lactams. Alper and Perera established the palladium-catalyzed direct carbonylative synthesis of β-lactams from azirines (Scheme 7.24) [27]. Mechanistic studies indicated that azirine first underwent an oxidative addition with Pd(0) to give a π-allyl Pd intermediate which functioned as a nucleophile to attack a second azirine to produce a bicyclic system containing the aziridine moiety, and carbonylation of the aziridine moiety in this bicyclic system further delivered the β-lactam".

In 1993, the palladium-catalyzed carbonylation of allyl diethyl phosphate with imines to construct lactam compounds was achieved by Torii et al. (Scheme 7.25) [28]. The reaction proceeded smoothly to afford a wide range of 3-alkenyl-β-lactams, providing a new route for constructing β-lactams.

In 2010, Aggarwal and coworkers developed a simple and efficient protocol to synthesize β-lactams and δ-lactams via the palladium-catalyzed carbonylation of vinyl aziridines (Scheme 7.26) [29]. Lactams were readily obtained in moderate to excellent yields under the catalysis of $Pd_2(dba)_3/PPh_3$. The reaction could selectively deliver the *trans*- or *cis*-β-lactam or even the δ-lactam derivatives by adjusting the reaction parameters (including Pd catalysts, CO pressure, and reaction temperature) *trans*. Mechanism investigation indicated that the Pd(0)-mediated isomerization of intermediate π-allyl Pd complexes followed by carbonylation and ring closure selectively delivered the trans-isomer (β-lactam).

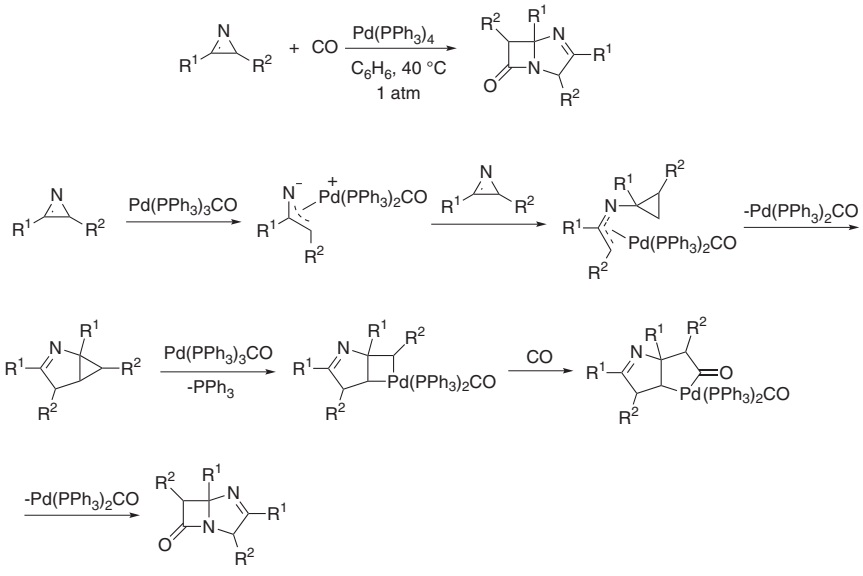

Scheme 7.24 Palladium-catalyzed carbonylation of azirines. Source: Modified from Alper and Perera [27].

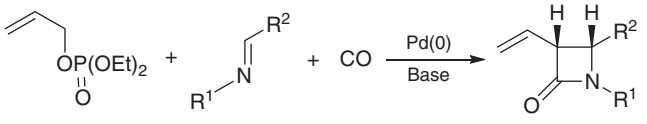

Scheme 7.25 Palladium-catalyzed carbonylation of allyl diethyl phosphate with imines. Source: Modified from Torii et al. [28].

In 2016, Arndtsen, Bengali, and coworkers reported a Pd(0)-catalyzed multicomponent method for the construction of β-lactams from aryl halides, imines, and CO (Scheme 7.27) [30]. This reaction proceeded via two tandem catalytic carbonylation reactions using $Pd(P^tBu)_3$ as the catalyst and tetrabutylammonium chloride as an additive. This provided a diverse range of polysubstituted β-lactams in good yields. Control experiments indicated that the *in situ*-formed acid chloride via carbonylation of aryl halide was a key intermediate for this transformation. The use of a sterically encumbered P^tBu_3 promoted the reductive elimination of this intermediate from the acylpalladium species. This approach provided a versatile platform for the multicomponent synthesis of novel spirocyclic β-lactams.

7.3.2 Palladium(0)-Catalyzed Carbonylative Synthesis of Five, Six, Seven-Membered Cyclic Amides

In 1989, Mori, Shibasaki, and coworkers reported the synthesis of lactams via a tandem carbonylation/nitrogenation reaction using *o*-halophenyl alkyl ketones and titanium-isocyanate complex as reactants (Scheme 7.28) [31]. This transformation

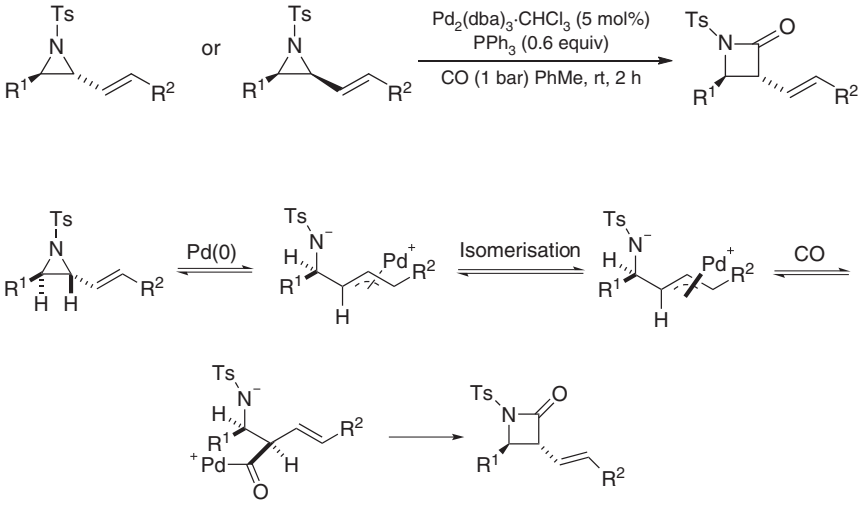

Scheme 7.26 Palladium-catalyzed carbonylation of vinyl aziridines. Source: Modified from Fontana et al. [29].

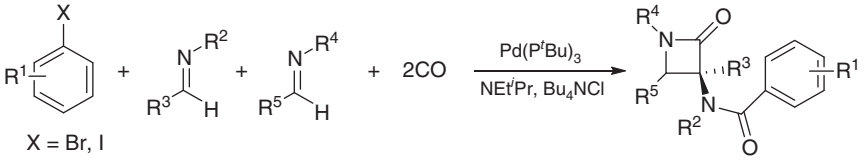

Scheme 7.27 The one-pot multicomponent synthesis of β-lactams. Source: Modified from Torres et al. [30].

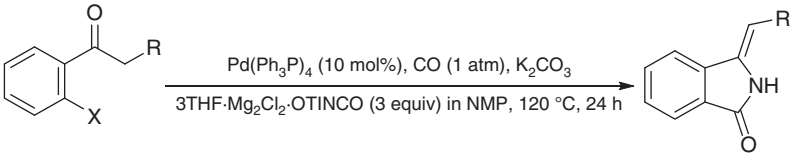

Scheme 7.28 The synthesis of lactams via a tandem carbonylation/nitrogenation reaction. Source: Modified from Uozumi et al. [31].

firstly involved a palladium-catalyzed cyclocarbonylation of *o*-halophenyl alkyl ketones to form an enol lactone intermediate and then produced the desired amides by nitrogenation of enol lactones.

In 1990, Ferraccioli and coworkers reported the synthesis of 2,3,4,5-tetrahydro-1*H*-2,4-benzodiazepine-1,3-dione derivatives via palladium-catalyzed intramolecular cyclocarbonylation of 1-butyl-1-(2-iodobenzyl)-3-phenylurea (Scheme 7.29) [32]. It was found that the product selectivity was highly dependent on the polarity of the solvents, and the use of a polar solvent such as *N,N*-dimethylformamide (DMF) could effectively stabilize the desired seven-membered ring from rearrangement and ring contraction.

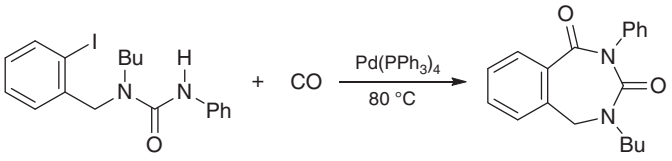

Scheme 7.29 Palladium-catalyzed intramolecular cyclization of 1-butyl-1-(2-iodobenzyl)-3-phenylurea. Source: Modified from Bocelli et al. [32].

Palladium-catalyzed intermolecular aminocarbonylation/intramolecular amidation cascade sequences for the production of 2-quinolones from 2-(2-haloalkenyl)aryl halide substrates was achieved by Willis and coworkers (Scheme 7.30) [33]. This reaction tolerated a variety of 2-(2-haloalkenyl)aryl halides and *N*-nucleophiles, affording a wide range of 2-quinolones. Moreover, this amination/carbonylation sequence could be accomplished by delaying the carbon monoxide introduction, delivering the isoquinolone product.

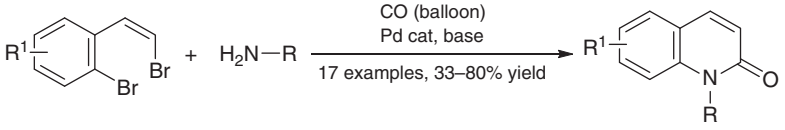

Scheme 7.30 Palladium-catalyzed intermolecular aminocarbonylation/intramolecular amidation. Source: Tadd et al. [33].

The carbonylation of carbenes has been an effective route for synthesizing carbonyl compounds [34, 35]. Recently, Wang and coworkers described the Pd-catalyzed carbonylation of α-diazo carbonyl compounds or *N*-tosylhydrazones with CO to produce amides (Scheme 7.31) [36]. It was found that ketene intermediates were initially generated from α-diazocarbonyl compounds or *N*-tosylhydrazone salts upon heating the reaction mixture in the presence of Pd(0) catalyst under CO atmosphere. This was followed by nucleophilic attack by alcohols, amines, or imines to give the desired ketone and β-lactam in good yields with excellent *trans*-diastereoselectivity. Density functional theory (DFT) calculations suggested that Pd-catalyst participated in the [2+2] cycloaddition process and affected the

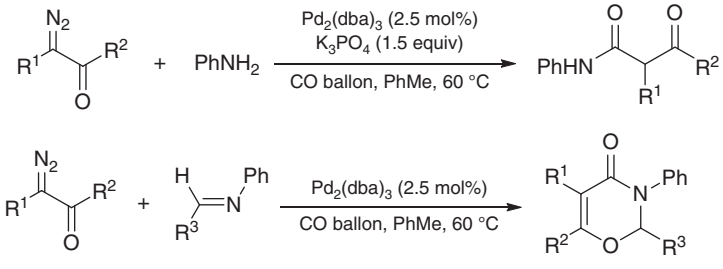

Scheme 7.31 Pd-catalyzed carbonylation of α-diazo carbonyl compounds or *N*-tosylhydrazone. Source: Modified from Zhang et al. [36].

diastereoselectivity of the β-lactam products by assisting isomerization of the additional intermediate. Alternatively, the acylketenes were formed via the Pd-catalyzed carbonylation of *R*-diazoketones, coupled with imines to undergo a formal [4+2] cycloaddition, leading to the 1,3-dioxin-4-one derivatives.

In 2020, Huang and coworkers further established a palladium-catalyzed carbonylative cyclization strategy to produce quinazolinones from azaarenes or imines based on the difunctionalization of the C=N bond (Scheme 7.32) [37]. The trapping of the acylpalladium species by the C=N bond of azaarenes or imines successfully delivered the corresponding quinazolinone derivatives.

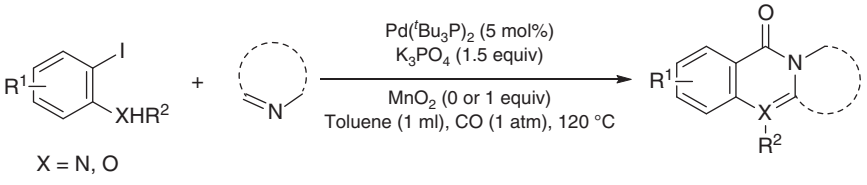

Scheme 7.32 Palladium-catalyzed carbonylative cyclization reaction leading to quinazolinones. Source: Zhou et al. [37].

7.3.3 Palladium(0)-Catalyzed Carbonylative Synthesis of Benzamide Derivatives

Recently, the catalytic aminocarbonylation of phenols for the construction of benzamides was achieved by Beller and coworkers (Scheme 7.33) [38]. Nonaflates, generated from the reaction between perfluoro butanesulfonylfluoride and phenol, were the key intermediates that initiated the carbonylation process via oxidative addition to Pd(0) (Scheme 7.34). With this method, various phenols could be transformed into the desired benzamides in good to excellent yields.

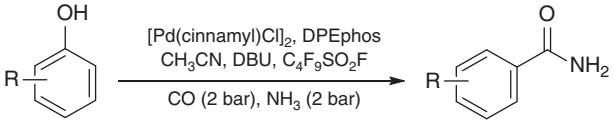

Scheme 7.33 Palladium-catalyzed aminocarbonylation of phenols. Source: Wu et al. [38].

In 2016, Sekar and coworkers reported the construction of *N*-aroyl sulfoximines via Pd/C catalyzed sulfoximinocarbonylation of aryl halides with NH-sulfoximines (Scheme 7.35) [39]. Both aryl iodides and aryl bromides could be effectively transformed into the corresponding *N*-aroyl sulfoximines in good to excellent yields. Moreover, the catalyst could be reused five times without loss of activity.

Notably, Arndtsen and coworkers used electrophilic aroyl-DMAP salts **1**, formed *in situ* by palladium-catalyzed carbonylative coupling of aryl chlorides with 4-dimethylaminopyridine (DMAP), as acyl-transfer reagents to give amides and esters (Scheme 7.36). [40] This reaction proceeded well to afford the desired amides and esters with good functional group compatibility. The proposed reaction

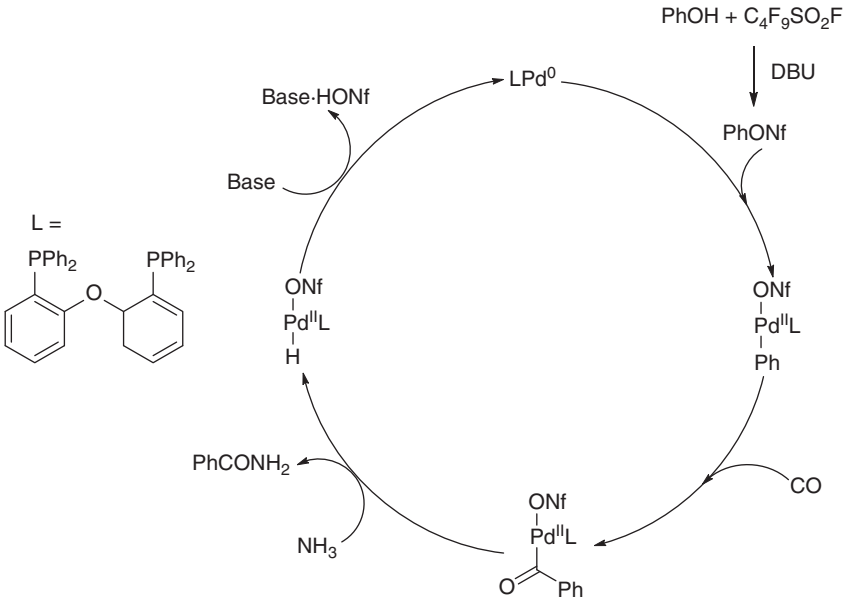

Scheme 7.34 Proposed mechanism for aminocarbonylation of phenols.

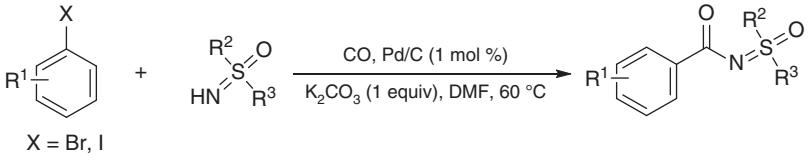

Scheme 7.35 Pd/C catalyzed sulfoximinocarbonylation of aryl halides with NH-sulfoximines. Source: Bala et al. [39].

mechanism is as follows: First, Pd(0) complex underwent the oxidative addition with aryl chloride; Second, the insertion of CO into the C—Pd bond of the above intermediate generated compound **2**. Third, ligand exchange between Cl anion and DMAP led to the intermediate **3**; Last, reductive elimination of intermediate **3** gave the aroyl-DMAP salts **1**, which were readily reacted with nucleophiles to furnish the final products (Scheme 7.37). Importantly, increasing the ligand steric hindrance favored the reductive elimination of **1** from intermediate **3**.

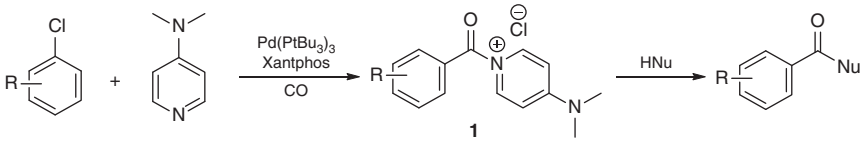

Scheme 7.36 Palladium-catalyzed carbonylative coupling of aryl chloride with 4-dimethylaminopyridine. Source: Lagueux-Tremblay et al. [40].

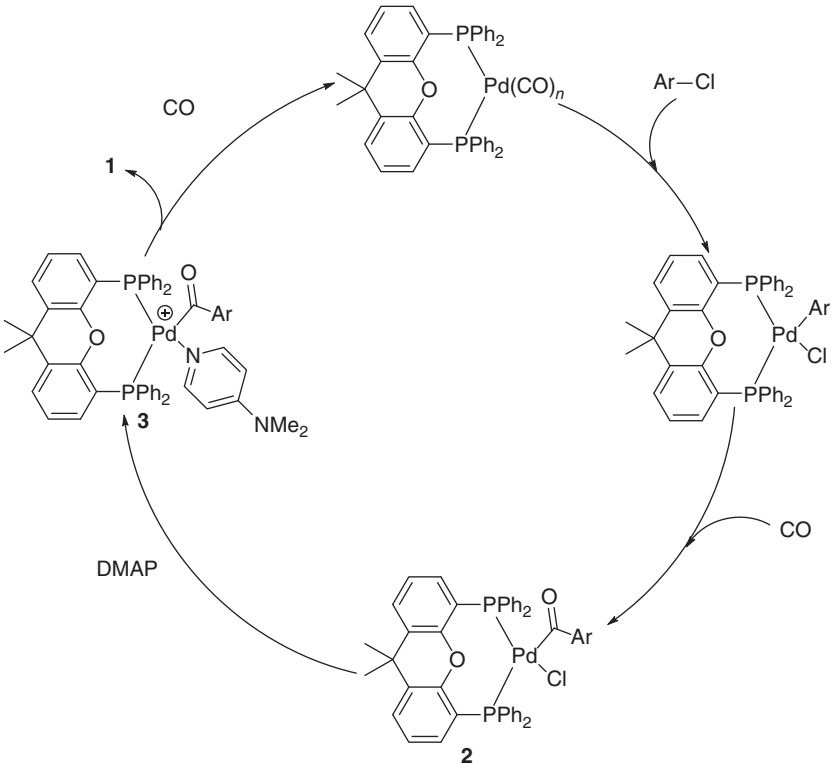

Scheme 7.37 Plausible mechanism for palladium-catalyzed carbonylative coupling of aryl chlorides with 4-dimethylaminopyridine.

Pd/C-catalyzed carbonylative transformation of aryl azides with α-carbonyl sulfoxonium ylides to synthesize α-carbonyl-α′-amide sulfoxonium ylides was accomplished by Wu and coworkers in 2020 (Scheme 7.38) [41]. The reaction generated useful α-carbonyl-α′-amide sulfoxonium ylides in good yields and in gram-scale. Moreover, the obtained α-carbonyl-α′-amide sulfoxonium ylide could be further transformed into the 1,3-dicarbonyl compound with excellent yield.

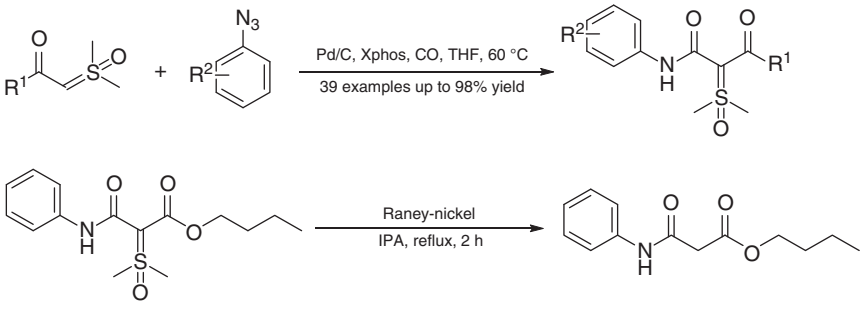

Scheme 7.38 Pd/C-catalyzed carbonylative transformation of aryl azides with α-carbonyl sulfoxonium ylides. Source: Yuan et al. [41].

7.4 Palladium(0)-Catalyzed Carbonylative Synthesis of Ketone Derivatives

7.4.1 Palladium(0)-Catalyzed Carbonylative Synthesis of Ketone Derivatives from Aryl Halides

In 2001, Kang and coworkers developed a palladium(0)-catalyzed carbonylation-coupling-*endo*-cyclization strategy to synthesize functional pyrrolidine- or piperidine-substituted enones from α-allenic sulfonamides and aryl iodides (Scheme 7.39) [43]. In this reaction, oxidative addition of ArI to Pd(0) and CO insertion firstly led to the formation of acylpalladium intermediate. This was followed by the insertion of allene into the acylpalladium afforded π-allylpalladium complex, which subsequently underwent *endo*-cyclization and reductive elimination to give the desired product (Scheme 7.40).

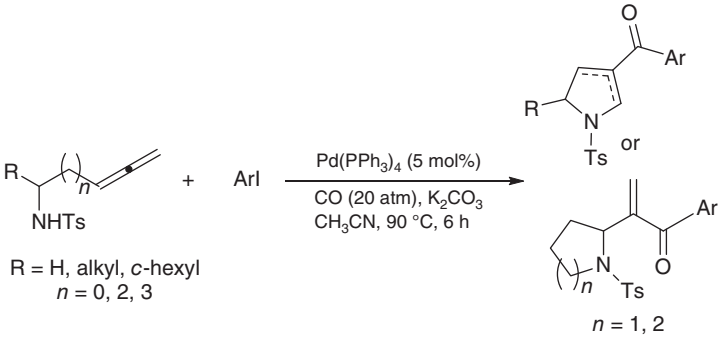

Scheme 7.39 Pd(0)-catalyzed carbonylation-coupling-*endo*-cyclization of α-allenic sulfonamides and aryl iodides. Source: Modified from Park and Lee [42].

In 2002, Larock and coworker reported the synthesis of 3-substituted 4-aroylisoquinolines form *N*-*tert*-butyl-2-(1-alkynyl)benzaldimines and aryl halides via a $Pd(PPh)_4$-catalyzed carbonylative cyclization process (Scheme 7.41) [44]. This reaction successfully produced various isoquinoline products containing an aryl, alkyl, or vinylic group at C-3 and an aroyl group at C-4 of the isoquinoline ring. Mechanistic investigations demonstrated that the triple bond was activated by coordination to the acylpalladium intermediate, facilitating the nucleophilic attack by the nitrogen atom of the imine and then resulted in intermediate **C** (Scheme 7.42). After reductive elimination, 3-substituted 4-aroylisoquinoline was obtained by the cleavage of the *tert*-butyl group from the nitrogen in the presence of a base. Subsequently, with this method, the same group reported the carbonylative cyclization of *N*-*tert*-butyl-(1-alkynyl)benzaldimines [45].

In 2002, Cacchi and coworkers described the synthesis of 6-trifluoromethyl-12-acylindolo[1,2-*c*]quinazolines from readily available bis(*o*-trifluoroacetamidophenyl) acetylene, aryl iodides and vinyl triflates via a combined carbonylation and cyclization route (Scheme 7.43) [46]. Control experiments indicated that this reaction

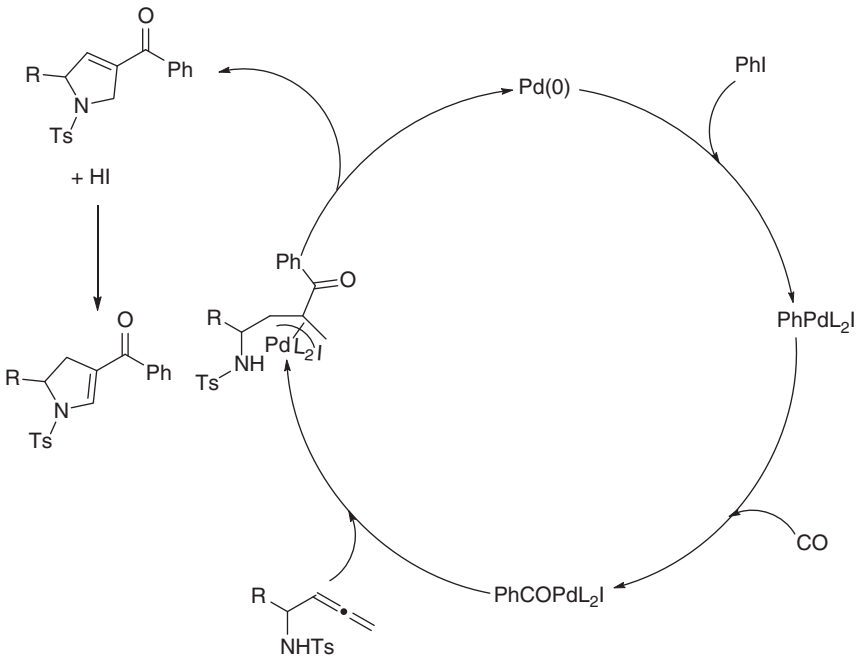

Scheme 7.40 Proposed mechanism for carbonylation-coupling *endo*-cyclization of α-allenic sulfonamides and aryl iodides.

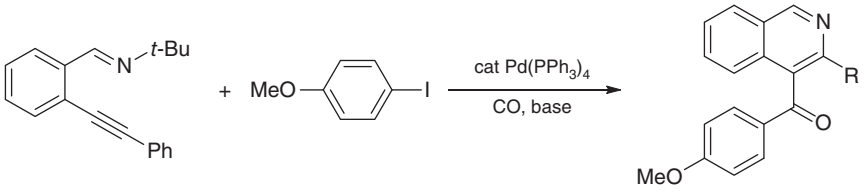

Scheme 7.41 Pd(0)-catalyzed carbonylative cyclization of *N*-*tert*-butyl-2-(1-alkynyl) benzaldimine and aryl halide. Source: Dai et al. [44].

proceeded by forming a 3-acyl-2-(*o*-trifluoroacetamidophenyl)indole intermediate, which underwent cyclization to produce the indoloquinazolines. This methodology tolerated various functional groups, providing an effective way to obtain various 12-acylindolo[1,2-*c*]quinazolines.

In 2012, Lee and coworker reported the synthesis of benzoylacetonitrile derivatives via a palladium(0)-catalyzed carbonylation of aryl iodides with trimethylsilylacetonitrile (Scheme 7.44) [42]. Mechanistic investigations indicated that the transmetalation of acylpalladium intermediate with trimethylsilylacetonitrile in the presence of ZnF_2 and $CuBr_2$ was involved in the catalytic cycle (Scheme 7.45). This reaction is an example of carbonylative cross-coupling process and provided a broad scope and good yields of benzoylacetonitrile derivatives without any additional ligands.

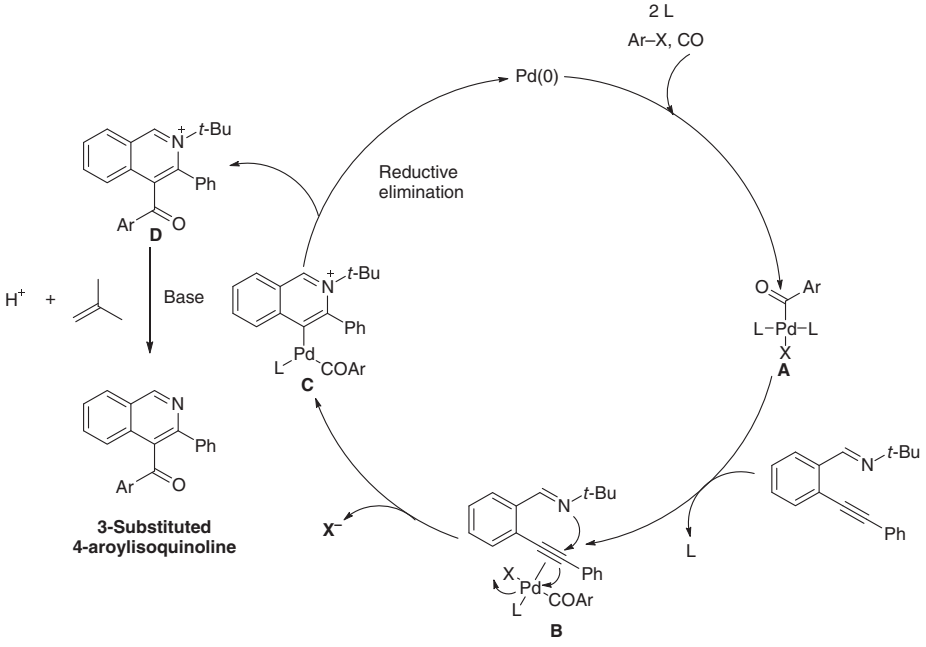

Scheme 7.42 Proposed mechanism for carbonylative cyclization leading to 3-substituted 4-aroylisoquinolines.

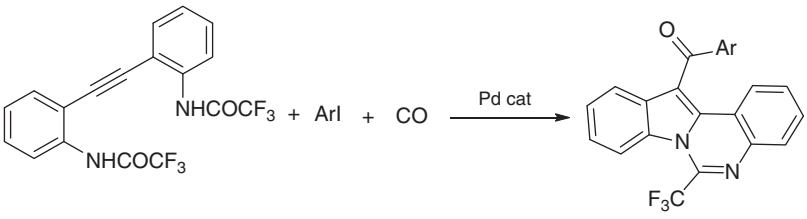

Scheme 7.43 A straightforward route to 12-acylindolo[1,2-*c*]quinazolines. Source: Battistuzzi et al. [46].

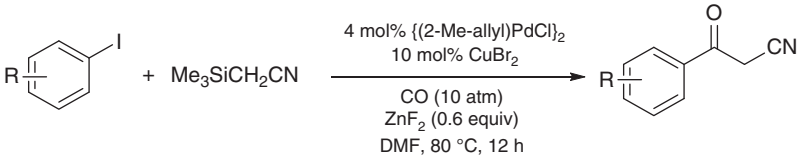

Scheme 7.44 Palladium(0)-catalyzed carbonylation of aryl iodides with trimethylsilylacetonitrile. Source: Park and Lee [42].

In 2017, Bhanage and coworkers reported the synthesis of biaryl ketones via Pd/C-catalyzed carbonylative Suzuki–Miyaura cross-coupling of aryl iodides with arylboronic acids upon using *N*-formylsaccharin as a CO surrogate (Scheme 7.46) [47]. Carbonylations of various aryl iodides with arylboronic acids in the presence of *in-situ* formed *CO* efficiently delivered the corresponding biaryl ketones in good to excellent yields. (Scheme 7.46) [47]. The Pd/C catalyst could be reused five times without appreciable loss of the activity.

The transition metal-catalyzed direct carbonylation of unfunctionalized aromatics to form valuable ketones is an important challenge due to the relative inertness of the C—H bond. In 2018, Arndtsen and coworkers established a new approach to achieving the carbonylation at a C—H bond via tandem carbonylation and acylation reaction (Scheme 7.47) [48]. Mechanistic studies disclosed that the C–H carbonylation took place via acylation of unfunctionalized aromatics by the *in-situ* formed aroyl triflate electrophile from carbonylation of aryl halides. This approach opened up a new way to furnish the intermolecular arene C–H carbonylation with electrophilic substitution chemistry, providing the targeted ketones with low palladium loadings from available aryl iodides, CO, and arenes.

Recently, Goggiamani and coworkers developed a palladium(0)-catalyzed carbonylative cyclization of *N*-(2-iodoaryl)enaminones to synthesize 2-substituted 3-aroylquinolin-4(1*H*)-ones (Scheme 7.48) [49]. This reaction is an example of intramolecular carbonylative Heck coupling, and takes place through the mechanism shown in Scheme 7.48. 2-Substituted-3-aroylquinolin-4(1*H*)ones could be obtained by omitting the isolation of *N*-(2-iodoaryl)enaminone intermediates from 2-iodoanilines and α,β-ynones via an efficient carbonylation-intramolecular cyclization cascade mode, and the reaction showed good tolerance toward ether, keto, cyano, ester, and chlorine group. Notably, the prepared 2-substituted 3-aroylquinolin-4(1*H*)-ones were proved to be efficient in inhibiting the Hedgehog

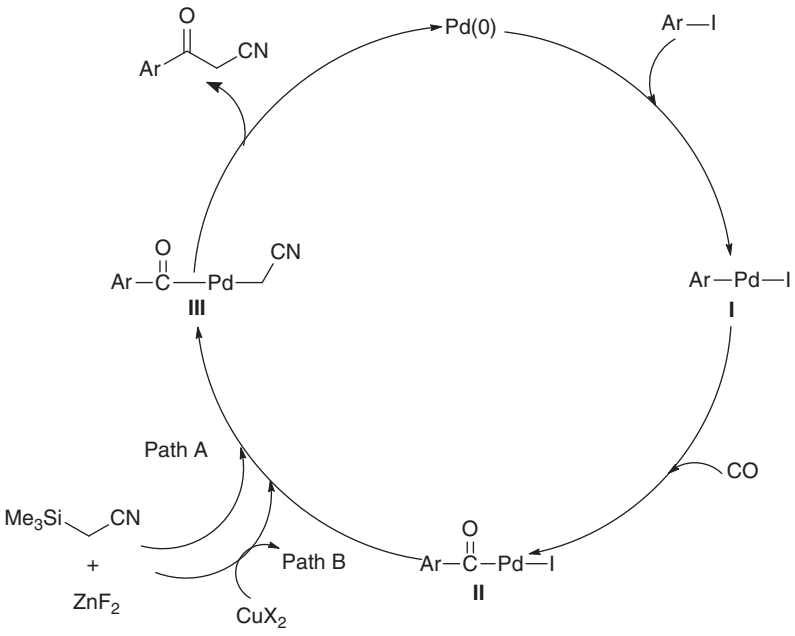

Scheme 7.45 Proposed mechanism for carbonylation of aryl iodides with trimethylsilylacetonitrile.

pathway through direct antagonism of the wild-type and drug-resistant form of the Smoothened receptor.

In 2018, Lei et al. described an efficient procedure for constructing flavones through Pd/C-catalyzed carbonylation of aryl halides with 2-hydroxyacetophenones (Scheme 7.49) [50]. Various aryl halides and 2-hydroxyacetophenones were effectively transformed into the desired flavones in good to excellent yields under the balloon pressure of CO. Here, phenoxycarbonylation of aryl halides with 2-hydroxyacetophenone firstly resulted in the formation of 2-acetylphenyl benzoate intermediate. The acetyl group's enolate was then formed, which attacked the ester's carbonyl to give the hemiacetal intermediate. Dehydration of the latter finally produced the target flavone.

A general and convenient palladium(0)-catalyzed cascade carbonylation procedure for the construction of β-substituted γ,δ-unsaturated ketones was accomplished by Wu and coworker in 2019 (Scheme 7.50) [51]. The reaction tolerated a variety of functional groups, affording the desired ketones in good to excellent yields. Notably, the addition of zinc salt could induce the transmetalation between the aluminum reagent and zinc salt, which promoted the subsequent carbonylation process.

In 2019, the same group reported a palladium-catalyzed cyclocarbonylation strategy for the construction of benzosilinones from (2-iodophenyl)hydrosilanes and terminal alkynes (Scheme 7.51) [52]. The process is an example of carbonylative Sonogashira coupling, followed by cyclization. The reaction proceeded smoothly to afford various benzosilinones in good to excellent yields. Mechanistic investigations

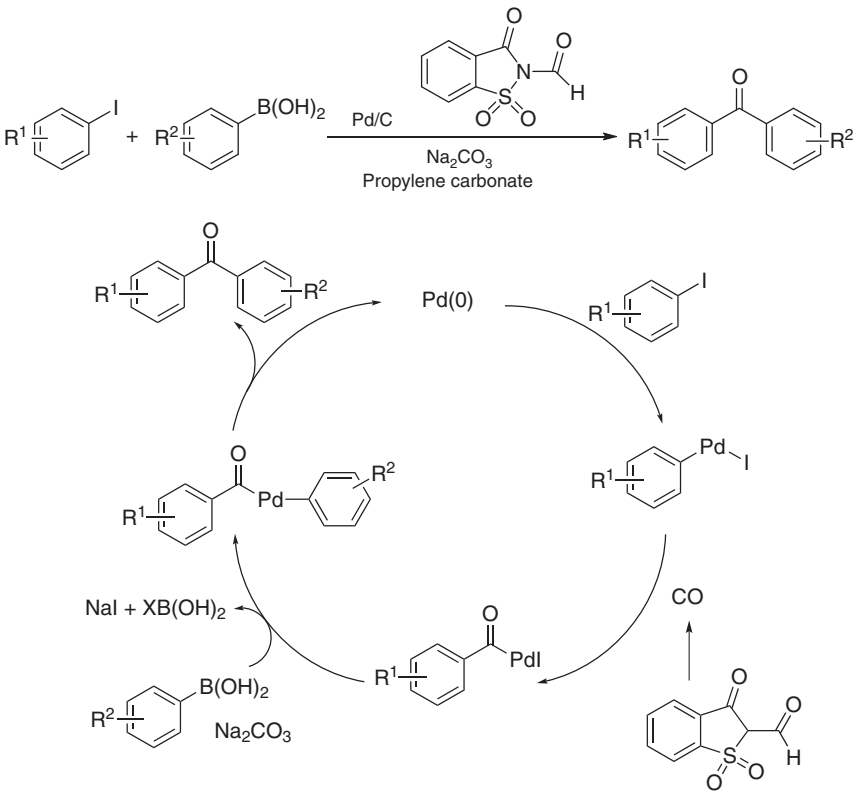

Scheme 7.46 Pd/C-catalyzed carbonylative Suzuki–Miyaura cross-coupling. Source: Modified from Gautam et al. [47].

indicated that (2-iodophenyl)hydrosilanes firstly gave oxidative addition to Pd(0) to give **A** followed by CO insertion to produce acylpalladium intermediate **B**. Reaction with terminal alkyne in the presence of the base DABCO took place to give intermediate **C** which corresponded to the carbonylative Sonogashira cross-coupling product. Intramolecular hydrosilylation of alkynone **C** finally delivered the corresponding benzosilinones (Scheme 7.52).

Transition metal-catalyzed carbonylative Heck reactions have been developed as efficient approaches for constructing carbonyl compounds. However, the development of asymmetric carbonylative Heck reaction approaches to fabricate functional molecules containing both a chiral center and a carbonyl group is still challenging. In 2020, Yao, Lin, and coworkers described the synthesis of chiral bicyclo[3.2.1]octanes via palladium-catalyzed enantioselective tandem Heck/carbonylation desymmetrization of cyclopentenes (Scheme 7.53) [53]. This approach offered an effective way to obtain multifunctional chiral bicyclo[3.2.1]octanes with one all-carbon quaternary and two tertiary carbon stereogenic centers in high diastereo- and enantioselectivities, which opened a new route in the asymmetric synthesis of carbonyl-containing chiral molecules.

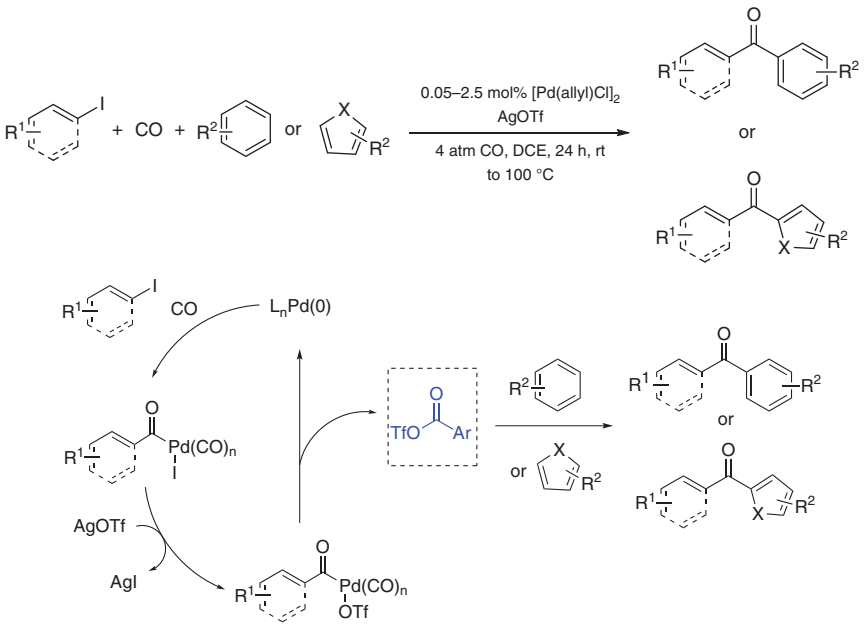

Scheme 7.47 Palladium-catalyzed intermolecular arene C–H carbonylation. Source: Kinney et al. [48].

7.4.2 Palladium(0)-Catalyzed Carbonylative Synthesis of Ketone Derivatives from Other Substrates

A palladium-catalyzed intramolecular carbonylative Heck-type reaction of unactivated alkyl iodides was accomplished by Alexanian and coworker in 2010 (Scheme 7.54) [54]. This reaction tolerated various important functional groups, affording a variety of synthetically valuable monocyclic and bicyclic enones in good yields. Importantly, palladium(0) could efficiently react with alkyl iodides via S_N2 and single-electron pathways. This mode of alkyl halide activation could be applied in the discovery of other synthetic transformations.

7.5 Palladium(0)-Catalyzed Carbonylative Synthesis of α,β-Alkynyl Ketones Derivatives

The prevalence of α,β-alkynyl ketones in many biologically active molecules has motivated new synthetic routes to these ketones. A promising way to construct these compounds is the Pd-catalyzed carbonylative coupling reaction of aryl iodides with terminal alkynes (carbonylative Sonogashira coupling). In 2008, Xia and coworkers developed a Pd/C-catalyzed carbonylative Sonogashira coupling reaction of aryl iodides with terminal alkynes to synthesize α,β-alkynyl ketones (Scheme 7.55) [55]. This method successfully produced a series of α,β-alkynyl ketones in good yields, and the Pd/C catalysts could be reused five times without loss of activity.

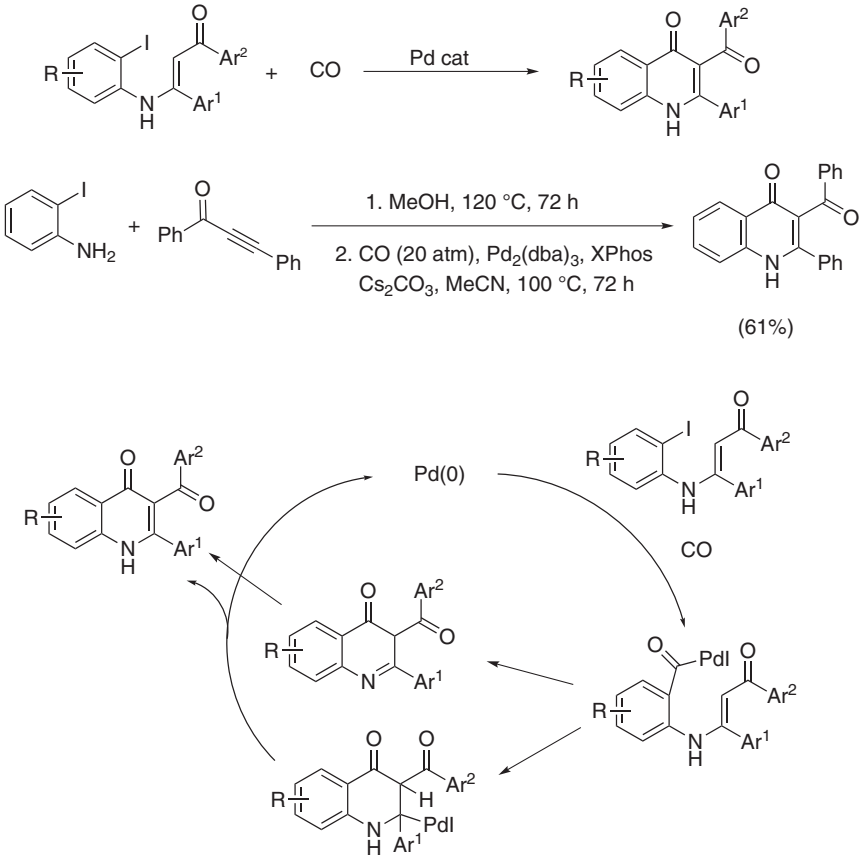

Scheme 7.48 Palladium-catalyzed carbonylative cyclization of *N*-(2-iodoaryl)enaminone. Source: Modified from Alfonsi et al. [49].

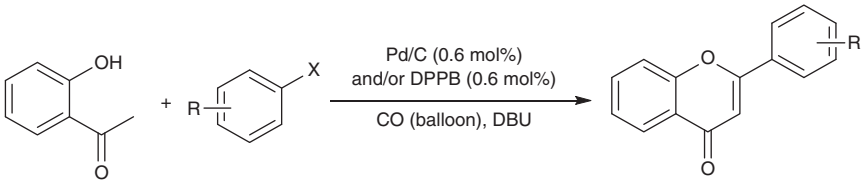

Scheme 7.49 Pd/C-catalyzed carbonylation of aryl halides with 2-hydroxyacetophenone. Source: Lei et al. [50].

Subsequently, Xia, Sun, and coworkers further developed a magnetically separable Pd/Fe_3O_4 catalyst for the carbonylative Sonogashira coupling reaction of aryl iodides with terminal alkynes (Scheme 7.56) [56]. Owing to the superparamagnetic behavior of Fe_3O_4, the Pd/Fe_3O_4 catalyst was easily separated from the reaction mixture, and its catalytic efficiency remained unaltered even after seven cycles.

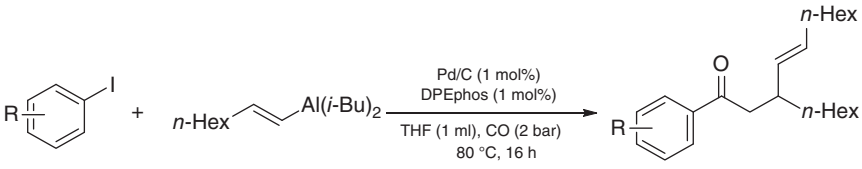

Scheme 7.50 Palladium(0)-catalyzed cascade carbonylation leading to β-substituted γ,δ-unsaturated ketones. Source: Chen and Wu [51].

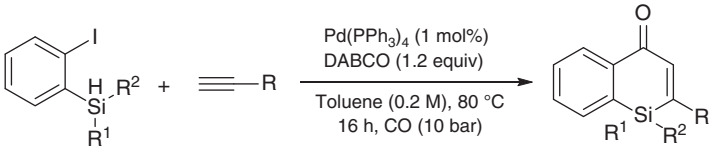

Scheme 7.51 Palladium-catalyzed cyclocarbonylation of (2-iodophenyl)hydrosilanes with a terminal alkynes. Source: Chen and Wu [52].

Regarding heterogeneous Pd-catalyzed carbonylation reactions, Li and coworkers developed a novel porous N-doped carbon-supported Pd nanoparticle catalyst (Pd@CN) for domino carbonylative synthesis of pyrazole derivatives from aryl iodides, terminal alkynes, and hydrazines (Scheme 7.57) [57]. This catalyst was prepared via direct carbonization of palladium-N-heterocyclic carbene coordination polymer (P-Pd-NHC) (Scheme 7.58). The obtained Pd@CN showed higher activity than the molecular $PdCl_2(PPh_3)_2$ complex catalyst in this domino reaction, and the catalyst displayed good stability in the reusability test.

7.6 Palladium(0)-Catalyzed Carbonylative Synthesis of Other Carbonyl Compounds

In 2005, Alper and Xiao established the first example of a Pd-catalyzed dithiocarbonylation reaction employing thiols and propargylic mesylates as substrates (Scheme 7.59) [58]. This transformation provided the desired dithioesters in good to excellent yields with high stereoselectivities. Mechanistic investigations indicated that the propargylic mesylates first gave oxidative addition to Pd(0) to form allenylpalladium intermediate, subsequently transformed into a thiopalladium intermediate by ligand exchange with thiols, and the following CO insertion and reductive elimination delivered an allenyl thioester that readily took a second carbonylation process. This methodology provided an elegant route for the construction of dithioesters.

In 2006, Alper and coworkers described the synthesis of thioester-containing six-membered ring lactones via palladium-catalyzed double carbonylation and cyclization reaction of enynols with thiols (Scheme 7.60) [59]. Enynols underwent a sequential carbonylation–cyclization–carbonylation process to deliver the desired lactones (Scheme 7.61). First, oxidative addition of the O—H bond of enynols to

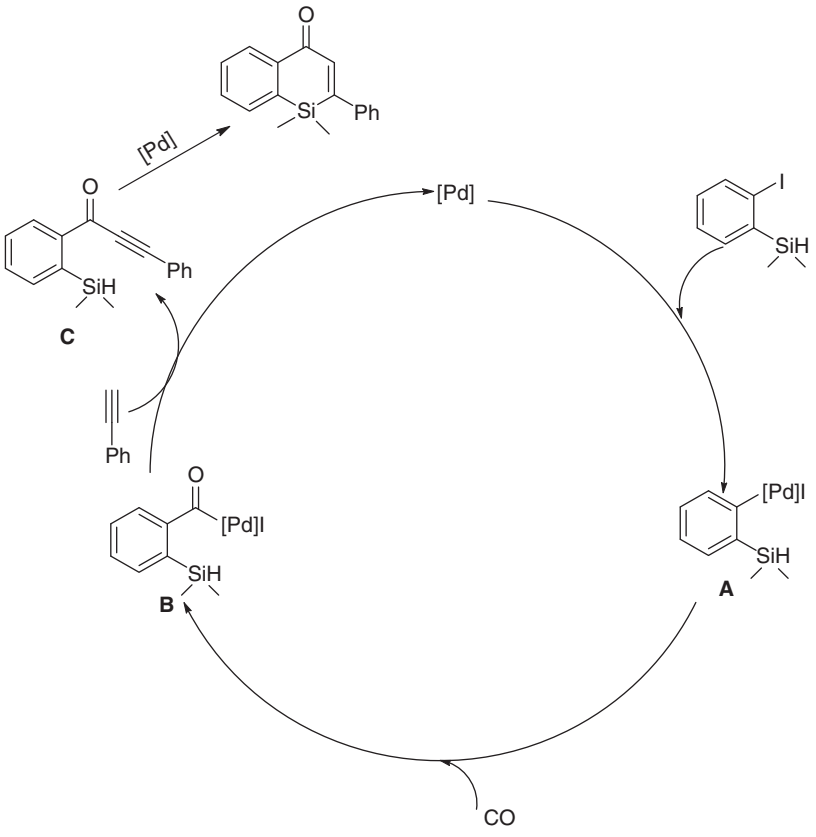

Scheme 7.52 Proposed reaction mechanism for the synthesis of benzosilinones by carbonylative Sonogashira coupling followed by intramolecular hydrosilylation.

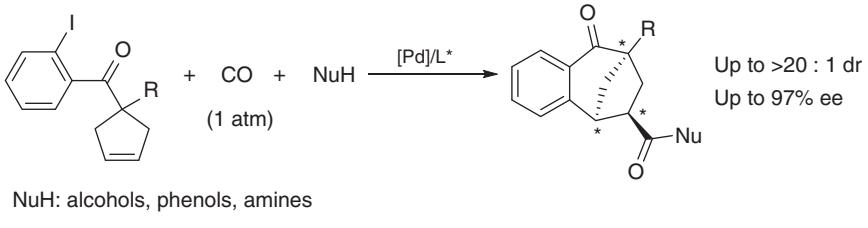

Scheme 7.53 Palladium-catalyzed tandem enantioselective Heck/carbonylation desymmetrization of cyclopentenes. Source: Yuan et al. [53].

Pd(0) generated intermediate **I**, following which insertion of CO into the Pd—O bond afforded intermediate **II** (path a). After an intramolecular hydropalladation, reductive elimination of the resultant intermediate **III** delivered intermediate **IV**. Alternatively, Pd(0) could also undergo oxidative addition by the thiol, producing intermediate **V**, and it could react with enynols to give intermediate **IV**

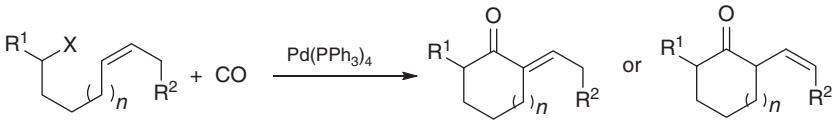

Scheme 7.54 Palladium-catalyzed Heck-type carbonylation of alkyl iodides. Source: Bloome and Alexanian [54].

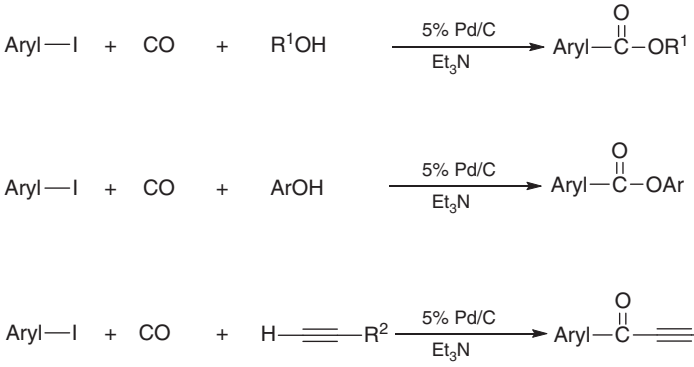

Scheme 7.55 Pd/C-catalyzed carbonylative reactions of aryl iodide to give esters and α,β-alkynyl ketones. Source: Liu et al. [55].

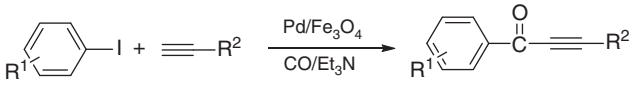

Scheme 7.56 Pd/Fe_3O_4 catalyzed carbonylative Sonogashira coupling of aryl iodides with a terminal alkynes. Source: Liu et al. [56].

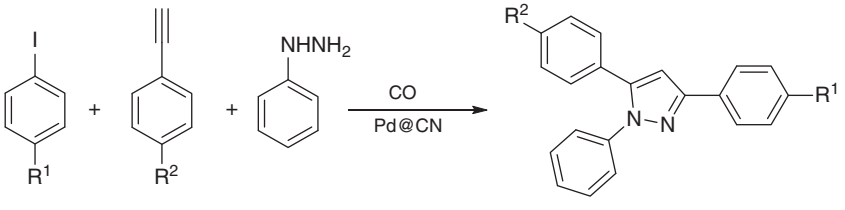

Scheme 7.57 Carbonylative cascade reaction catalyzed by Pd@CN leading to pyrazole derivatives.

via a sequential hydropalladation–carbonylation process involving intermediates **VI**, **VII**, and **VIII** (path b). Finally, intermediate **IV** underwent a second hydropalladation–carbonylation process to furnish the final lactone products.

In 2018, Lee, Kim, and coworkers reported the palladium-catalyzed carbonylation of aryl iodides with thioacetates for the construction of thioesters (Scheme 7.62) [60]. This reaction displayed broad substrate scope and excellent functional group compatibility. Mechanistic studies demonstrated that a thiol was generated from the

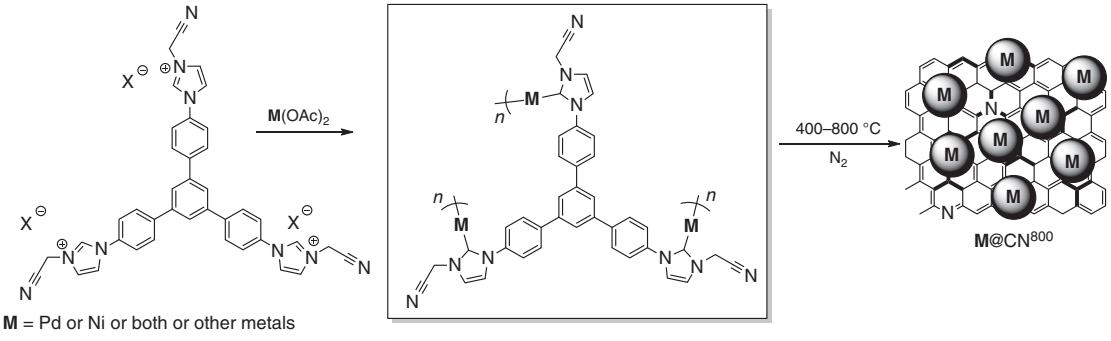

Scheme 7.58 Synthesis of P-M-NHC and M@CN. Source: Modified from Li et al. [57].

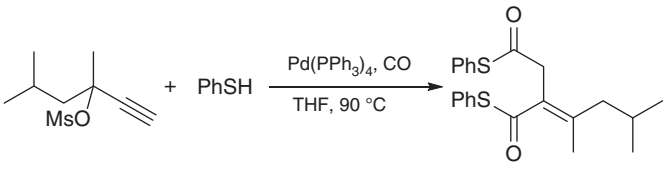

Scheme 7.59 Pd(0)-catalyzed dithiocarbonylation. Source: Xiao and Alper [58].

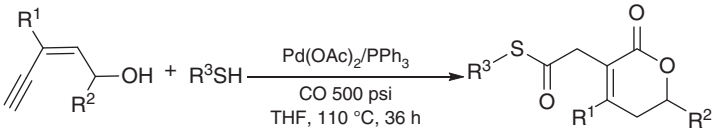

Scheme 7.60 Palladium-catalyzed double carbonylation and cyclization reaction of enynols with thiols. Source: Cao et al. [59].

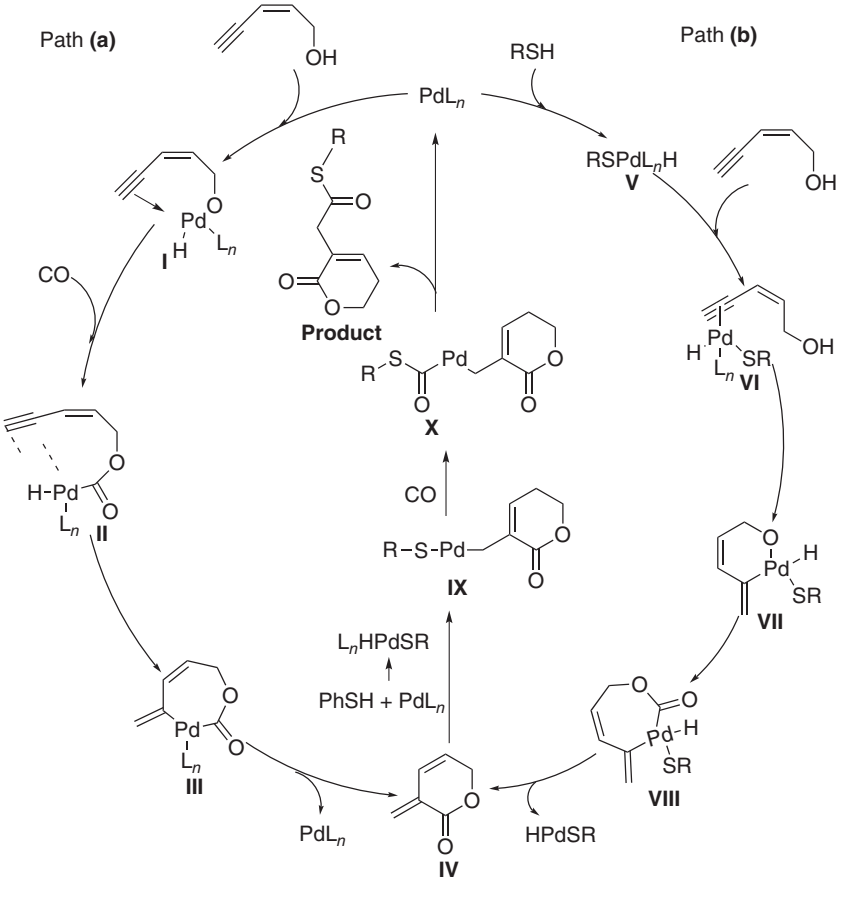

Scheme 7.61 Possible mechanism.

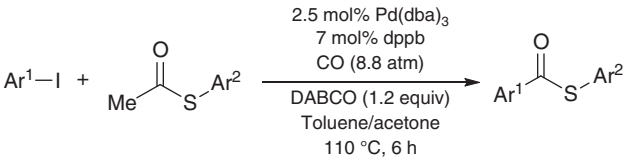

Scheme 7.62 Palladium-catalyzed carbonylation of thioacetates and aryl iodides. Source: Modified from Kim et al. [60].

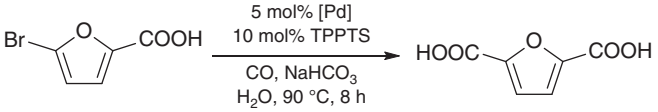

Scheme 7.63 Palladium-catalyzed carbonylation of 5-bromo-furoic acid to construct 2,5-furandicarboxylic acid (FDCA).

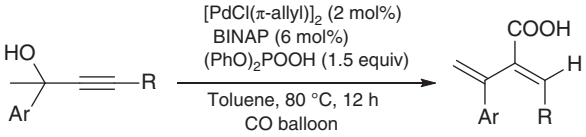

Scheme 7.64 Regioselective dehydrative hydroxycarbonylation of propargylic alcohol. Source: Yuan et al. [62].

reaction with thioacetate and base. The thiol reacted with acylpalladium intermediate to give palladium sulfide intermediate in the presence of a base, and reductive elimination of this intermediate furnished the final product.

In 2018, a new route to synthesize 2,5-furandicarboxylic acid (FDCA) from 5-bromo-furoic acid was established by Yin's group [61]. Here, 5-bromo-furoic acid could be effectively converted to FDCA via Pd-catalyzed carbonylation of the C—Br bond in an aqueous solution (Scheme 7.63). Control experiments indicated that FDCA was observed as the dominant product under low pH conditions. This strategy offered an alternative route for the synthesis of FDCA originating from C5 based bulk biomass, which could replace *p*-phthalic acid as a starting material in the polymer industry.

In 2019, Ma and coworkers reported 1,3-alkadien-2-yl carboxylic acids from propargylic alcohols via Pd-catalyzed regioselective dehydrative hydroxycarbonylation (Scheme 7.64) [62]. Mechanistic studies demonstrated that propargylic alcohols were first transformed into conjugated 1,3-enynes with the aid of $(PhO)_2POOH$. The sequential hydropalladation and carbonylation furnished the desired product. This reaction could be conducted on a gram scale, affording the corresponding 1,3-alkadien-2-yl carboxylic acid in good yield.

Recently, Gabriele and coworkers described the palladium-catalyzed carbonylation of 2-(propynylthio)benzimidazoles for the synthesis of 2-methyl-1-thia-4a, 9-diazafluoren-4-ones (Scheme 7.65) [63]. The substrates bearing an internal triple bond were well tolerated, leading to the desired products in good yields. This process underwent the palladium-promoted propargyl-allene rearrangement to generate a

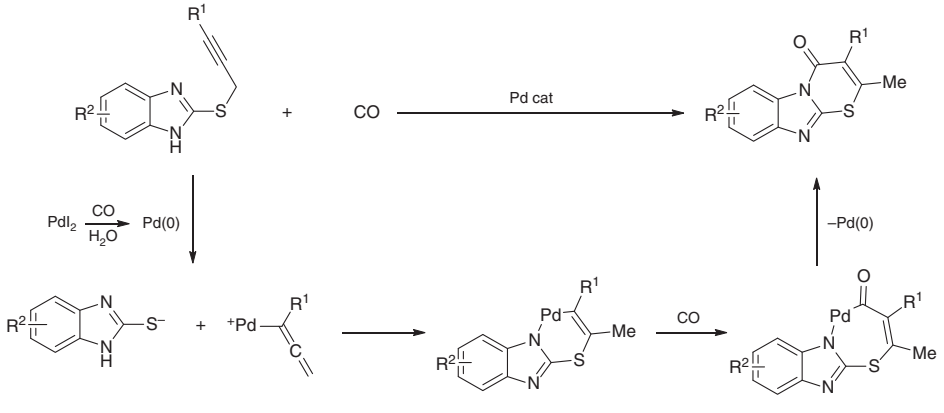

Scheme 7.65 Palladium-catalyzed cyclocarbonylation to access thiadiazafluorenone. Source: Veltri et al. [63].

thiolate and an allenylpalladium intermediate, which underwent thiolate addition to the central allenic carbon and cyclocarbonylation.

7.7 Summary and Conclusions

This chapter summarizes the recent achievements in the Pd(0)-catalyzed carbonylative synthesis of carbonyl compounds. Various carbonyl formation reactions, such as carbonylation of amines, alcohols, thiols, aryl halides, alkynes and allenes, and cyclocarbonylations, were accomplished under the catalysis of Pd(0) catalysts. Both homogeneous Pd complex systems and supported Pd systems functioned well in catalyzing these reactions. The heterogeneous Pd catalysts could advance the carbonylative reactions toward more sustainable conditions due to the easy separation and reuse of the catalyst. It is our conviction that Pd(0)-catalyzed carbonylative reaction in the future could overcome the following challenges: (i) Carbonylation of unactivated C—H bonds; (ii) Low catalyst loading; (iii) Bimetallic co-catalysis.

References

1 Wu, X.-F., Fang, X., Wu, L. et al. (2014). *Acc. Chem. Res.* 47: 1041–1053.
2 Wu, X.-F., Neumann, H., and Beller, M. (2011). *Chem. Soc. Rev.* 40: 4986–5009.
3 Wu, X.-F., Neumann, H., and Beller, M. (2013). *Chem. Rev.* 113: PR1–PR40.
4 Ryu, I. and Sonoda, N. (1996). *Angew. Chem.* 108: 1140–1157.
5 Liu, Q., Zhang, H., and Lei, A. (2011). *Angew. Chem. Int. Ed.* 50: 10788–10799.
6 Sumino, S., Fusano, A., Fukuyama, T., and Ryu, I. (2014). *Acc. Chem. Res.* 47: 1041–1053.
7 Zhu, C., Liu, J., Li, M.-B., and Bäckvall, J.-E. (2020). *Chem. Soc. Rev.* 49: 341–353.
8 Grigg, R. and Mutton, S.P. (2010). *Tetrahedron* 66: 5515–5548.
9 Krantz, A., Spencer, R.W., Tam, T.F. et al. (1990). *J. Med. Chem.* 33: 464–479.
10 Cacchi, S., Fabrizi, G., and Marinelli, F. (1996). *Synlett* 10: 997–998.
11 Tadd, A.C., Fielding, M.R., and Willis, M.C. (2009). *Chem. Commun.* 44: 6744–6746.
12 Salvadori, J., Balducci, E., Zaza, S. et al. (2010). *J. Org. Chem.* 75: 1841–1847.
13 Cho, C.-H. and Larock, R.C. (2011). *ACS Comb. Sci.* 13: 272–279.
14 Park, H.-S., Kim, D.-S., and Jun, C.-H. (2015). *ACS Catal.* 5: 397–401.
15 Tani, Y. and Ogawa, T. (2018). *Org. Lett.* 20: 7442–7446.
16 Hu, H., Teng, F., Liu, J. et al. (2019). *Angew. Chem. Int. Ed.* 58: 9225–9229.
17 Zhang, Y., Yin, Z., Wang, H., and Wu, X.-F. (2019). *Org. Lett.* 21: 3242–3246.
18 Yu, W.-Y. and Alper, H. (1997). *J. Org. Chem.* 62: 5684–5687.
19 Akpınar, G.E., Kus, M., Ucuncu, M. et al. (2011). *Org. Lett.* 13: 748–751.
20 Wang, Y. and Ma, S. (2013). *Adv. Synth. Catal.* 355: 741–750.
21 Wang, Y., Zhang, W., and Ma, S. (2014). *Org. Chem. Front.* 1: 807–811.
22 Higashimae, S., Tamai, T., Nomoto, A., and Ogawa, A. (2015). *J. Org. Chem.* 80: 7126–7133.

23 Hattori, T., Ueda, S., Takakura, R. et al. (2017). *Chem. Eur. J.* 23: 8196–8202.
24 Li, Y., Wang, Z., and Wu, X.-F. (2018). *ACS Catal.* 8: 738–741.
25 Bose, A.K., Kapur, J.C., Fahey, J.L., and Manhas, M.S. (1973). *J. Org. Chem.* 38: 3438–3439.
26 Howarth, T.T., Brown, A.G., and King, T.J. (1976). *J. Chem. Soc., Chem. Commun.*: 266–267.
27 Alper, H. and Perera, C.P. (1981). *J. Am. Chem. Soc.* 103: 1289–1291.
28 Torii, S., Okumoto, H., Sadakane, M. et al. (1993). *Tetrahedron Lett.* 34: 6553–6556.
29 Fontana, F., Tron, G.C., Barbero, N. et al. (2010). *Chem. Commun.* 46: 267–269.
30 Torres, G.M., Macias, M.D.L.H., Quesnel, J.S. et al. (2016). *J. Org. Chem.* 81: 12106–12115.
31 Uozumi, Y., Kawasaki, N., Mori, E. et al. (1989). *J. Am. Chem. Soc.* 111: 3725–3727.
32 Bocelli, G., Catellani, M., Cugini, F., and Ferraccioli, R. (1990). *Tetrahedron Lett.* 40: 2623–2624.
33 Tadd, A.C., Matsuno, A., Fielding, M.R., and Willis, M.C. (2009). *Org. Lett.* 11: 583–586.
34 Hegedus, L.S. (1997). *Tetrahedron* 53: 4105–4128.
35 de Meijere, A., Schirmer, H., and Duetsch, M. (2000). *Angew. Chem. Int. Ed.* 39: 3964–4002.
36 Zhang, Z., Liu, Y., Ling, L. et al. (2011). *J. Am. Chem. Soc.* 133: 4330–4341.
37 Zhou, X., Ding, Y., and Huang, H. (2020). *Chem. Asian J.* 15: 1678–1682.
38 Wu, X.-F., Neumann, H., and Beller, M. (2012). *Chem. Eur. J.* 18: 419–422.
39 Bala, B.D., Sharma, N., and Sekar, G. (2016). *RSC Adv.* 6: 97152–97159.
40 Lagueux-Tremblay, P.-L., Fabrikant, A., and Arndtsen, B.A. (2018). *ACS Catal.* 8: 5350–5354.
41 Yuan, Y., Chen, B., Zhang, Y., and Wu, X.-F. (2020). *J. Org. Chem.* 85: 5733–5740.
42 Park, A. and Lee, S. (2012). *Org. Lett.* 14: 1118–1121.
43 Kang, S.-K. and Kim, K.-J. (2001). *Org. Lett.* 3: 511–514.
44 Dai, G. and Larock, R.C. (2002). *J. Org. Chem.* 67: 7042–7047.
45 Dai, G. and Larock, R.C. (2002). *Org. Lett.* 4: 193–196.
46 Battistuzzi, G., Cacchi, S., Fabrizi, G. et al. (2002). *Org. Lett.* 4: 1355–1358.
47 Gautam, P., Gupta, R., and Bhanage, B.M. (2017). *Eur. J. Org. Chem.* 24: 3431–3437.
48 Kinney, R.G., Tjutrins, J., Torres, G.M. et al. (2018). *Nat. Chem.* 10: 193–199.
49 Alfonsi, R., Botta, B., Cacchi, S. et al. (2017). *J. Med. Chem.* 60: 1469–1477.
50 Lei, Y., Li, Z., Wan, Y. et al. (2018). *Appl. Organomet. Chem.* 32: 4163–4169.
51 Chen, B. and Wu, X.-F. (2019). *Org. Lett.* 21: 7624–7629.
52 Chen, B. and Wu, X.-F. (2019). *Adv. Synth. Catal.* 361: 3441–3445.
53 Yuan, Z., Zeng, Y., Feng, Z. et al. (2020). *Nat. Commun.* 11: 2544–2551.
54 Bloome, K.S. and Alexanian, E.J. (2010). *J. Am. Chem. Soc.* 132: 12823–12825.
55 Liu, J., Chen, J., and Xia, C. (2008). *J. Catal.* 253: 50–56.
56 Liu, J., Peng, X., Sun, W. et al. (2008). *Org. Lett.* 10: 3933–3936.
57 Li, Z., Liu, J., Huang, Z. et al. (2013). *ACS Catal.* 3: 839–845.

58 Xiao, W.-J. and Alper, H. (2005). *J. Org. Chem.* 70: 1802–1807.
59 Cao, H., Xiao, W.-J., and Alper, H. (2006). *Adv. Synth. Catal.* 348: 1807–1812.
60 Kim, M., Yu, S., Kim, J., and Lee, S. (2018). *Org. Chem. Front.* 5: 2447–2452.
61 Zhang, S., Shen, G., Deng, Y. et al. (2018). *ACS Sustainable Chem. Eng.* 6: 13192–13198.
62 Yuan, Y., Jia, M., Zhang, W., and Ma, S. (2019). *Chem. Commun.* 55: 7938–7941.
63 Veltri, L., Amuso, R., Cuocci, C. et al. (2019). *J. Org. Chem.* 84: 8743–8749.

8

Palladium(II)-Catalyzed Carbonylations

Bartolo Gabriele[1], Nicola Della Ca'[2], Raffaella Mancuso[1], Lucia Veltri[1] and Ida Ziccarelli[1]

[1] University of Calabria, Laboratory of Industrial and Synthetic Organic Chemistry (LISOC), Department of Chemistry and Chemical Technologies, Arcavacata di Rende, Via Pietro Bucci 12/C, 87036, Italy
[2] Università di Parma, Department of Chemistry, Life Sciences and Environmental Sustainability, Parco Area delle Scienze 17/A, Parma 43124, Italy

8.1 Introduction

The reactivity of Pd(II) species in carbonylation reactions is quite different from that showed by Pd(0). A first major difference concerns the high stability of Pd(II) toward oxidation to Pd(IV), which clearly hinders the possibility for a catalytic cycle starting with oxidative addition and terminating with reductive elimination, analogous to that, very common, involving the oxidative addition to Pd(0) seen in Chapter 7. On the other hand, Pd(II) is much more electrophilic than Pd(0), so it is able to attack with an electrophilic mechanism several different organic substrates, including alkanes, aromatic rings, carbon–carbon multiple bonds, alcohols, phenols, and amines. These attacks result in carbon, oxygen, or nitrogen palladation, as shown in Scheme 8.1. The ensuing organopalladium(II) complexes are then able to undergo, after CO coordination, migratory insertion of carbon monoxide to yield the corresponding acyl-, alkoxycarbonyl-, or carbamoylpalladium intermediates. The precise fate of these organocarbonylpalladium(II) intermediates clearly depends on the nature of the organic substrate, the possible presence of coreagent(s), and reaction conditions. In any case, they then tend to evolve toward the formation of the final carbonylated organic product with either (i) the direct regeneration of the Pd(II) species that initiated the process or (ii) the formation of a reduced Pd(0) species (Scheme 8.2). In the first case, a catalytic cycle is directly attained (Scheme 8.2a), while, in the second case (Scheme 8.2b), the presence in the reaction mixture of a suitable oxidizing agent, able to reconvert Pd(0) to Pd(II) (Scheme 8.2c), is needed to achieve a catalytic process. Since palladium is a noble metal, route (b) followed by reoxidation (c), which corresponds to a so-called oxidative carbonylation, is a common pathway followed under Pd(II) catalysis, so it is not surprising that most of the examples reported in the literature of oxidative carbonylations are based on Pd(II)-catalyzed processes [1].

Carbon Monoxide in Organic Synthesis: Carbonylation Chemistry,
First Edition. Edited by Bartolo Gabriele.

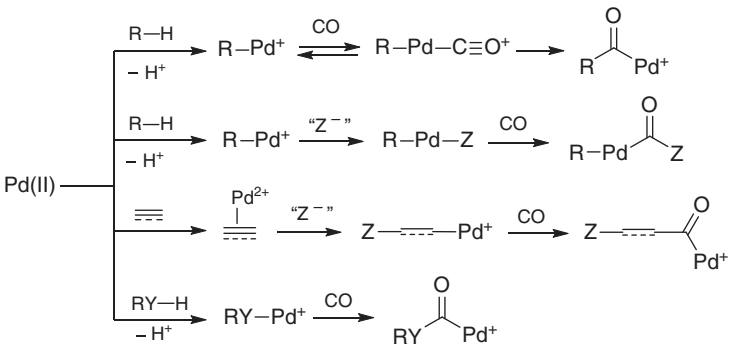

Scheme 8.1 Activation of different organic substrates by Pd(II) in carbonylation reactions (R = alkyl, aryl; "Z^-" represents a generic nucleophile or ligand able to bond to carbon; Y = O, NR. Additional ligands on palladium are not shown for clarity).

Organocarbonylpalladium(II) complex ⟶ Carbonylated product + Pd(II) (a)

Organocarbonylpalladium(II) complex ⟶ Carbonylated product + Pd(0) (b)

Pd(0) + Oxidant ⟶ Pd(II) + Reduced oxidant (c)

Scheme 8.2 Formation of carbonylated products from the organocarbonylpalladium(II) intermediates formed as shown in Scheme 8.1. (a) Pd(II) is directly regenerated; (b) Pd(II) is reduced to Pd(0); and (c) Pd(0) obtained from reaction (b) is reoxidized back to Pd(II) by the action of an external oxidant. The combination of processes (b) and (c) corresponds to a catalytic oxidative carbonylation.

8.2 Palladium(II)-Catalyzed Carbonylation of Alkanes and Saturated C–H Bonds

Under suitable conditions, simple alkanes may undergo Pd(II)-promoted C–H activation followed by carbonylation. Pioneering studies in this field were carried out by Fujiwara who, in 1989, reported the transformation of cyclohexane into cyclohexanecarboxylic acid (195% yield based on palladium). The process was initially performed in a TFA–cyclohexane–MeOH mixture (TFA = trifluoroacetic acid) at 80 °C under 30 atm of CO in the presence of $Pd(OAc)_2$ as catalyst and $K_2S_2O_8$ as external oxidant [2]. The turnover number (TON) of the reaction could be improved from 1.95 to ca. 205 (with a product yield of 8.8% based on starting cyclohexane) by adding $Cu(OAc)_2$ as co-catalyst (50 equiv with respect to Pd), which likely promoted Pd(0) reoxidation (Scheme 8.3a; in this and the following schemes of this chapter, unreactive ligands are omitted for clarity) [3]. The reaction was believed to occur through electrophilic palladation followed by CO migratory insertion, reductive elimination to give an anhydride, and exchange with R′OH (R′ = Ac or CF_3CO), as shown in Scheme 8.3b. Later on, the method was extended to substituted cyclohexanes and adamantane, and it was found to be both regioselective (C–H order of

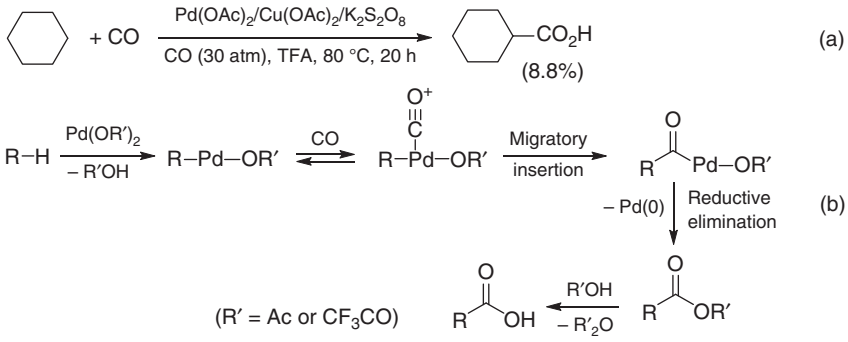

Scheme 8.3 Pd(II)-catalyzed oxidative carbonylation of cyclohexane to cyclohexanecarboxylic acid (a) and proposed reaction mechanism (b) for the oxidative carbonylation of alkanes. Sources: Fujiwara et al. [2], Nakata et al. [3], Satoh et al. [4].

reactivity: tertiary > secondary > primary) and stereoselective (as the main products presented the carboxylic group at the equatorial positions) [4].

Particularly from an industrial point of view, the most important alkane carbonylation involves the direct conversion of methane into acetic acid. Fujiwara's group showed that their method could also be employed for realizing this transformation, using either $Pd(OCOEt)_2$ and/or $CuSO_4$ as catalyst with $K_2S_2O_8$ as oxidant [5] or $Pd(OAc)_2/CuCl_2$ with O_2 as oxidant [6], as exemplified in Scheme 8.4 [5]. When applied to propane, the carbonylation afforded a mixture of butyric and isobutyric acids [5]. The activity shown by copper even in the absence of palladium suggested the involvement of a different mechanism with respect to direct electrophilic activation, so the authors proposed a radical process, at least in the presence of the Pd–Cu bimetallic system [5, 7]. More recently, the formal oxidative coupling between two molecules of methane to give acetic acid was reported, and it was demonstrated that, under the reaction conditions, one of the methane molecules is actually converted into carbon monoxide, which then carbonylates methane to acetic acid [8].

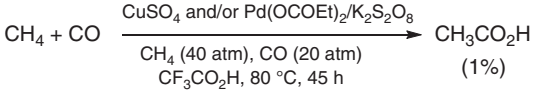

Scheme 8.4 Cu or Cu/Pd-catalyzed oxidative carbonylation of methane to acetic acid. Source: Nishiguchi et al. [5].

Pd(II)-catalyzed oxidative alkoxycarbonylation of alkanes to alkylcarboxylic esters can also be accomplished when working in the presence of an alcohol as external nucleophile. Recently, an efficient method for realizing this process has been reported and applied to a variety of alkanes with product yields up to 94% using $PdCl_2$ as catalyst in the presence of PPh_3 as ligand and di-*tert*-butylperoxide (DTBP) as external oxidant. This reaction also worked nicely for ethane, producing, with benzyl alcohol, benzyl propanoate in 61% yield (Scheme 8.5a). As expected, mixtures of products were formed starting from substrates bearing different C–H sites [9]. Based

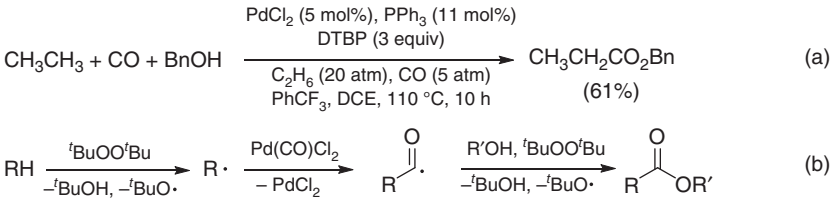

Scheme 8.5 $PdCl_2$-catalyzed oxidative alkoxycarbonylation of ethane to benzyl propionate (a) and proposed reaction mechanism (b). Source: Modified from Lu et al. [9].

on experimental evidences, a radical mechanism, involving the formation of an acyl radical as key intermediate, has been proposed (Scheme 8.5b) [9]. Aminocarbonylation, resulting from the use of an amine as the external nucleophile, is also possible, with formation of amides, again through a radical mechanism [10].

A radical mechanism was also suggested for the selective alkoxy- and aminocarbonylation of benzylic C—H bonds to give substituted 2-arylacetic esters [11] and amides [12], respectively. On the other hand, the allylic carbonylation of alkenes occurred through the formation of a π-allylpalladium intermediate from allylic palladation, followed by alkoxycarbonylation at the less hindered position to give β,γ-unsaturated esters (Scheme 8.6) [13].

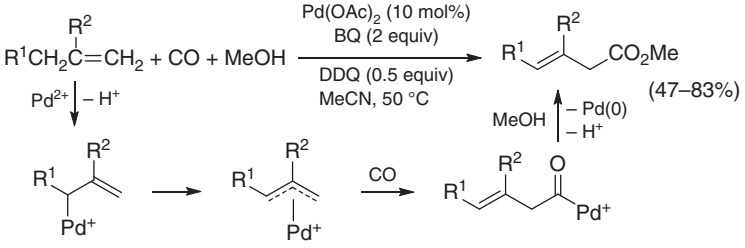

Scheme 8.6 Pd(II)-catalyzed oxidative allylic carbonylation of alkenes (BQ = benzoquinone; DDQ = 2,3-dichloro-5,6-dicyano-1,4-benzoquinone). Source: Modified from Chen et al. [13].

The presence of a suitably placed functional group (FG) able to coordinate to Pd(II) may direct the C(sp^3)–H palladation in a specific position and thus allow a selective carbonylation reaction. This is well exemplified by the oxidative alkoxycarbonylation of *N*-(2-(6-(propoxymethyl)pyridin-2-yl)ethyl)acetamides, which proceeds through the formation of a palladacycle from C–H activation followed by CO insertion to give an acylpalladacycle intermediate (Scheme 8.7) [14]. The latter then undergoes nucleophilic displacement by an external alcohol (via either nucleophilic attack to the carbonyl followed by palladium elimination or by attack to palladium followed by reductive elimination) to give the final product and Pd(0), which is reoxidized to Pd(II) by the action of Ag(I) [14].

The FG directing the C(sp^3)–H palladation may also act as intramolecular nucleophile, with formation of heterocyclic derivatives [15–26], as exemplified in Scheme 8.8 for the formation of β- and γ-lactams from suitably substituted amines

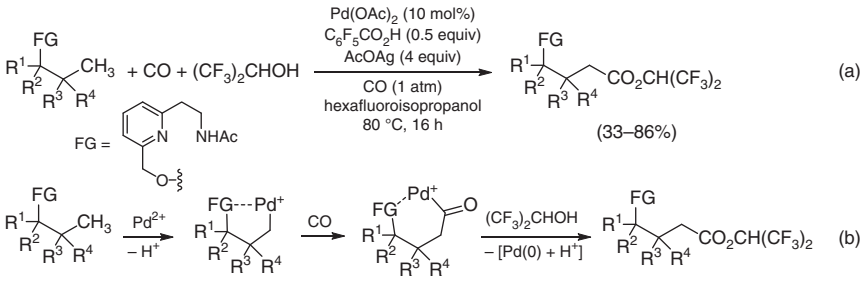

Scheme 8.7 Pd(II)-catalyzed oxidative alkoxycarbonylation of a substrate bearing a suitably placed functional group (FG) able to direct the C(sp^3)–H palladation in a specific position (a) and proposed reaction mechanism (b). Source: Modified from Tanaka et al. [14].

[16] and amides [18], respectively. Either C(sp^3)–H palladation followed by CO insertion and intramolecular nucleophilic displacement or FG palladation followed by CO insertion, C(sp^3)–H palladation, and reductive elimination may take place in these reactions [15–26].

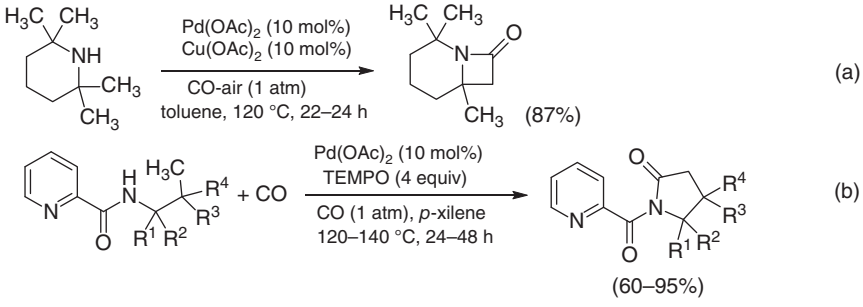

Scheme 8.8 Pd(II)-catalyzed oxidative cyclocarbonylation of suitably substituted amine and amide derivatives with C(sp^3)–H activation, leading to β-lactams (a) [16] and γ-lactams (b) [18]. Source: Modified from McNally et al. [16], (b) Wang et al. [18].

8.3 Palladium(II)-Catalyzed Carbonylation of Arenes and Heteroarenes

The C(sp^2)—H bond of an aromatic or heteroaromatic ring can be activated by Pd(II), resulting in aromatic palladation, through different kinds of mechanistic pathways, including S_EAr (electrophilic aromatic substitution), concerted metalation–deprotonation (CMD), or even (although less frequently observed) a radical mechanism. In the presence of CO and under suitable conditions, the aryl-palladium(II) intermediate may then evolve toward the formation of a carbonylated product. Since the 1980s, following the pioneering works by the Fujiwara's group and Arzoumadinis and Rauch, significant progress has been realized in this field, with applications, in particular, to the synthesis of heterocyclic derivatives.

The original work of Fujiwara involved the use of simple arenes and heteroarenes, such as benzene, toluene, anisole, chlorobenzene, furan, and thiophene.

The carbonylation was carried out using the substrate as the reaction solvent with $Pd(OAc)_2$ as the catalyst at 100 °C for 20 hours under 15 atm of CO, in the absence of external oxidant, so palladium black was recovered at the end of the process. The isolated yields of the corresponding (hetero)arylcarboxylic acids ranged from 14% to 48% based on palladium (Scheme 8.9) [27]. The relative reactivity and the selective formation of the *para* and *ortho* products from anisole and toluene were in agreement with a mechanism starting with S_EAr palladation, which then evolved in a similar manner as that shown in Scheme 8.3b for alkanes with R = Ar and R′ = Ac [27]. Interestingly, the same authors found that, using 1,2-dibromoethane as additive, carboxylic anhydrides could be obtained instead of acids [28].

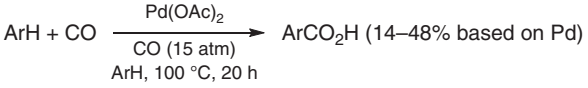

Scheme 8.9 Stoichiometric Pd(II)-mediated carbonylation of arenes and heteroarenes to arylcarboxylic acids (ArH = benzene, toluene, anisole, *p*-chlorobenzene, furan, thiophene). Source: Modified from Fujiwara et al. [27].

On the other hand, Arzoumadinis and Rauch found that benzene could be converted into a mixture of benzophenone and anthraquinone (Scheme 8.10a) and benzophenone into anthraquinone (Scheme 8.10b) by $PdCl_2$-mediated stoichiometric carbonylations carried out under rather harsh conditions (68 atm of CO, 218 °C for four hours in the presence of $FeCl_3$, for the carbonylation of benzene; 38 atm of CO, 190 °C for 0.5 hours in the presence of $CuCl_2$, for the carbonylation of benzophenone) [29]. The process leading to benzophenone started with aromatic palladation

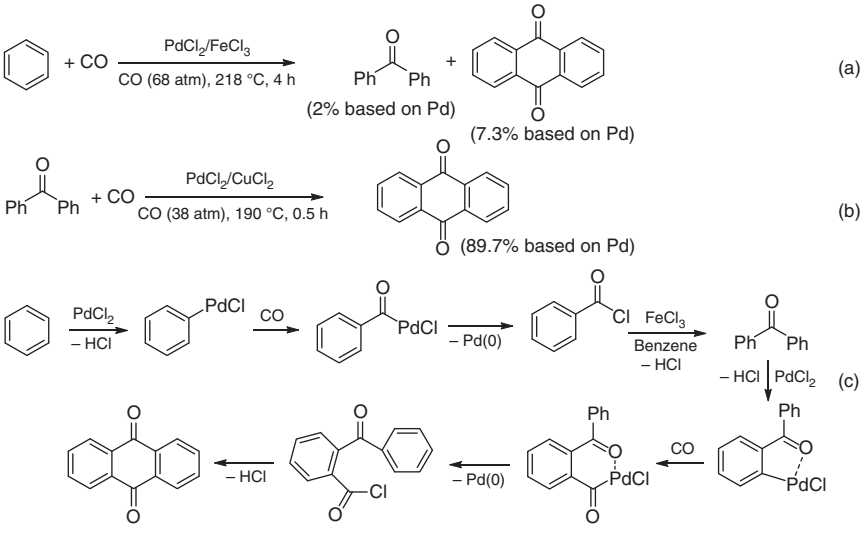

Scheme 8.10 Carbonylation of benzene to benzophenone and of benzophenone to anthraquinone. Source: Modified from Arzoumadinis and Rauch [29].

followed by CO insertion and reductive elimination to give benzoyl chloride, from which benzophenone was formed by Friedel–Crafts acylation. Benzophenone subsequent cyclocarbonylation exemplifies the importance of a suitably placed functional group to regioselectively direct the C(sp^2)–H activation in a specific position. In fact, *ortho*-palladation of benzophenone was favored by the carbonyl coordination to the metal center to give an intermediate that then evolved through CO insertion, reductive elimination, and intramolecular Friedel–Crafts acylation (Scheme 8.10c) [29].

Later on, suitable conditions were elaborated to carry out (hetero)arene carbonylation to carboxylic acids or anhydrides sub-stoichiometrically or catalytically in the presence of a suitable oxidant (such as O_2, peroxides, $K_2S_2O_8$ in TFA, $Na_2S_2O_8$, MnO_2, K_2MnO_4, Cu(II), and benzoquinone [BQ]) [1, 30–41].

Alkoxycarbonylation is also possible, when using an alcohol as external nucleophile. Scheme 8.11 shows as example the oxidative alkoxycarbonylation of indoles occurring regioselectively by S_EAr palladation at the more reactive β-position [42, 43]. In a similar manner as in the Wacker process, the Pd(0) formed at the end of the carbonylation shown in Scheme 8.11 was reoxidized back to Pd(II) by the action of Cu(II), which was reduced to Cu(I) and reoxidized in its turn by the action of oxygen (from air) [42].

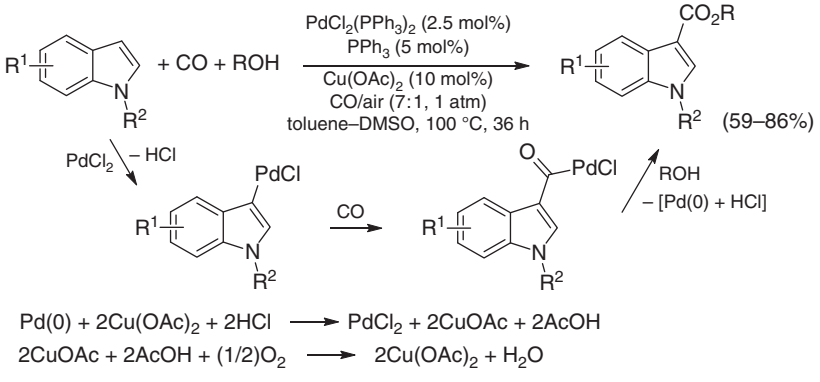

Scheme 8.11 Pd(II)-catalyzed oxidative alkoxycarbonylation of indoles at the β-position. Source: Modifed from Zhang et al. [42].

As we have already seen for C(sp^3)–H activation, a suitably placed functional group able to coordinate to Pd(II) may direct the aromatic C(sp^2)–H palladation in a specific position and thus allow a selective carbonylation reaction [44–55], *ortho* activation being, of course, the most common case (Scheme 8.12). For example, 2-phenoxypyridines were converted into alkyl 2-(pyridin-2-yloxy)benzoates (or the corresponding free phenols) using 10 mol% of $Pd(OAc)_2$ and AgTFA as the oxidant under 1 atm of a 4 : 1 mixture of CO–O_2 at 100 °C (Scheme 8.13) [50]. Note that, however, these conditions fall within the explosion limits for a CO–O_2 mixture [1].

Of particular interest is the possibility of intramolecular nucleophilic displacement with formation of carbonylated heterocycles. This takes place when the FG directing aromatic palladation may also act as internal nucleophile (NuH),

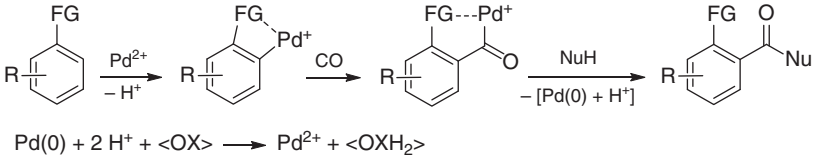

Scheme 8.12 Pd(II)-catalyzed oxidative *ortho*-carbonylation of functionalized arenes (FG = functional group able to coordinate Pd(II)).

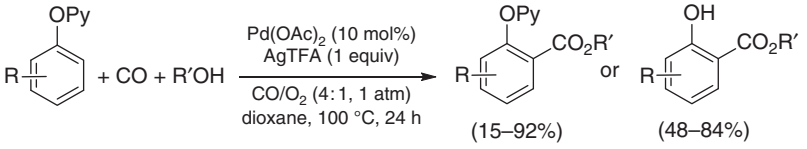

Scheme 8.13 Pd(II)-catalyzed oxidative *ortho*-alkoxycarbonylation of 2-phenoxypyridines [50]. Note that the reaction conditions ($CO-O_2$ 4 : 1, 100 °C) fall within the explosion limits for $CO-O_2$ mixtures [1]. Sources: Liu et al. [50], Bartish and Drissel [1].

possibly through the formation of a palladacycle followed by reductive elimination (Scheme 8.14a). In some cases, the process may start with Nu palladation, which is followed by CO insertion, intramolecular aromatic palladation, and reductive elimination (Scheme 8.14b). Numerous examples of these kinds of reactivities have been reported in the literature [56–96]; Scheme 8.15 shows, in particular, the synthesis of pyrroloquinazolinediones from indoline derivatives [77].

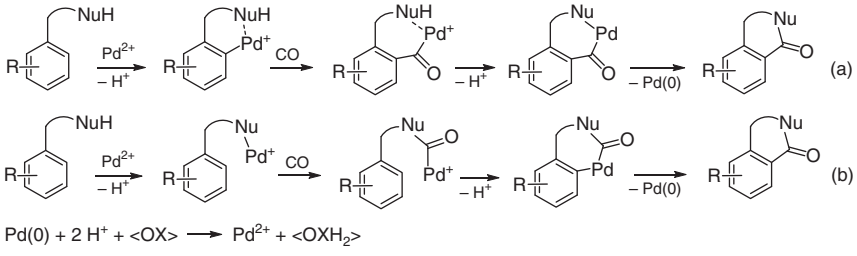

Scheme 8.14 Pd(II)-catalyzed oxidative *ortho*-carbonylation of aromatic derivatives functionalized with a nucleophilic group by intramolecular nucleophilic displacement (a) or intramolecular $C(sp^2)-H$ palladation (b).

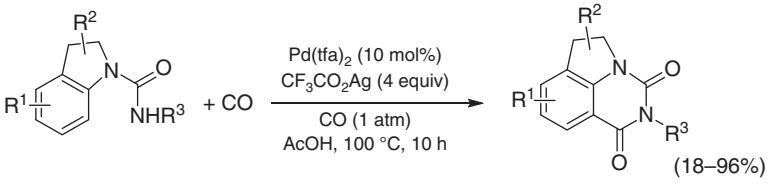

Scheme 8.15 Synthesis of pyrroloquinazolinedione derivatives by Pd(II)-catalyzed oxidative carbonylation of indoline-1-carboxamides. Source: Wang et al. [77].

Sequential double CO insertion [97] and double aromatic palladation [98–100] are also possible, as exemplified in Schemes 8.16a [97] and 8.16b [98], respectively. In some cases, the intramolecular insertion of an unsaturated compound (olefin, alkyne, or aryne) besides CO may take place [101–106], as exemplified in Scheme 8.16c [101].

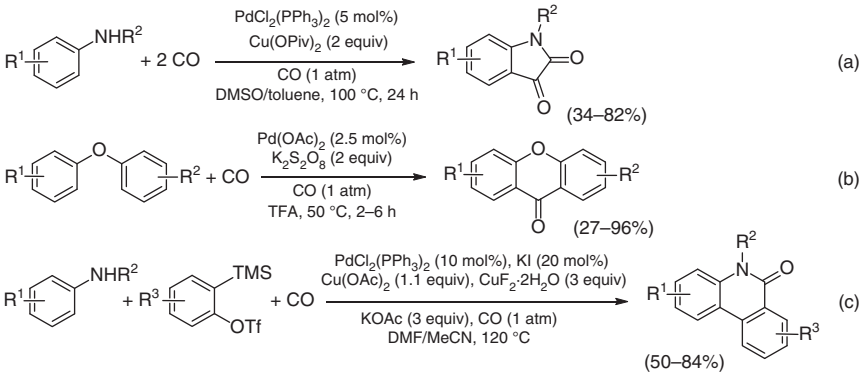

Scheme 8.16 Pd(II)-catalyzed oxidative carbonylation of suitably functionalized aromatic derivatives with (a) double CO insertion [97], (b) double C(sp^2)–H activation [98], and (c) aryne and CO insertion [101]. Source: (a) Li et al. [97], (b) Modified from Zhang et al. [98], (c) Modified from Feng et al. [101].

8.4 Palladium(II)-Catalyzed Carbonylation of Alkenes

8.4.1 Palladium(II)-Catalyzed Carbonylation of Unfunctionalized Alkenes, Dienes, and Allenes

Unfunctionalized olefins can undergo different types of carbonylation reactions under the promotion of Pd(II), owing to the possibility of simultaneous coordination of both the π-olefinic bond and carbon monoxide to Pd(II).

A first possibility consists in the oxidative monoalkoxycarbonylation with C(sp^2)–H activation. This is a very important process, since it may allow to synthesize α,β-unsaturated esters from α-olefins (Scheme 8.17a) and so may also be of industrial interest for the direct production of cinnamyl esters (Scheme 8.17a, R = Ar), which are valuable fragrance and pharmacologically active compounds [107]. In contrast with arenes (see Section 8.3), the process does not usually start with a direct C(sp^2)–H palladation; instead, the formation of an alkoxycarbonylpalladium(II) intermediate takes place by CO migratory insertion into an alkoxypalladium(II) complex (formed in its turn by alcohol attack to Pd(II); Scheme 8.17b). This is followed by alkene coordination, double-bond insertion, β-H elimination, and Pd(0) reoxidation (in the presence of a suitable external oxidant) (Scheme 8.17).

This process is not easy to achieve, mainly because the [(β-alkoxycarbonyl)alkyl] palladium complex ensuing from olefin insertion tends to undergo a second carbon monoxide insertion, leading to dicarbonylated compounds (see later in the text).

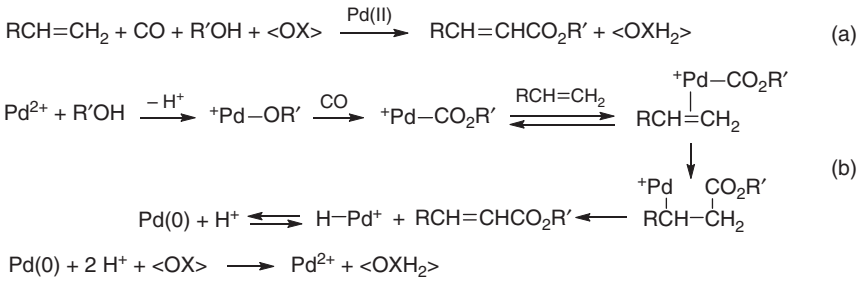

Scheme 8.17 (a) Pd(II)-catalyzed oxidative monoalkoxycarbonylation of olefins to α,β-unsaturated esters and (b) generally accepted reaction mechanism.

Following the seminal work by Yukawa and Tsutsumi [108], in 1979 Cometti and Chiusoli found that it was possible to slow down the second CO insertion by suitably diminishing the carbon monoxide partial pressure [109]. By carrying out the carbonylation under 1 atm of a 1 : 4 mixture of CO–N_2, with $PdCl_2$ as catalyst, $MgCl_2$ as additive, $CuCl_2$ as oxidant, and AcONa as base (to buffer the HCl ensuing from palladium reoxidation by $CuCl_2$), they were able to convert styrene into methyl cinnamate in 104% yield based on palladium [109]. Since then, considerable progress has been made in this field [110–116], and recently it was found that a combination of Pd/C (1 mol%) and CuI (10 mol%) (generating *in situ* a catalytically active Pd(II)–Cu bimetallic species) was able to convert styrenes into cinnamate esters in yields up to 95% under relatively mild conditions, with O_2 (from air) as simple and sustainable oxidant (Scheme 8.18) (with aliphatic α-olefins, a mixture of α,β- and β,γ-unsaturated esters was obtained) [116].

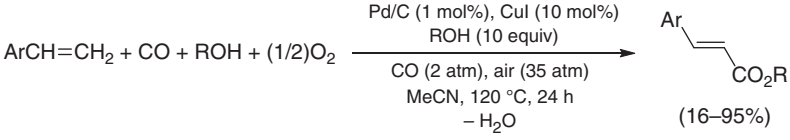

Scheme 8.18 Pd/C–CuI-catalyzed oxidative monoalkoxycarbonylation of styrenes to alkyl cinnamates. Source: Modified from Maffei et al. [116].

As said above, under oxidative conditions, Pd(II) catalysis usually tends to favor dicarbonylation, so the most common pathway followed by the [(β-alkoxycarbonyl) alkyl]palladium intermediate, deriving from olefin insertion into the Pd—CO_2R' bond, is a further CO insertion followed by nucleophilic displacement by R′OH. This leads to the formation of succinic diesters, as shown in Scheme 8.19. Also this process is of high applicative interest, considering the industrial importance of succinic acids and their derivatives [117–119].

Since the pioneering works by Tsutsumi [108], Fenton [120], Heck [121], and Stille [122–124], several catalytic systems and conditions have been proposed in the course of the years to perform this process in a selective manner (also enantioselective, using a suitable nonracemic ligand) [125–145]. These carbonylations were

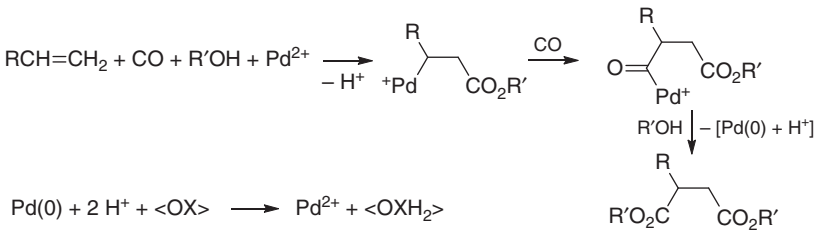

Scheme 8.19 Further CO insertion into the [(β-alkoxycarbonyl)alkyl]palladium intermediate (formed as shown in Scheme 8.17) followed by nucleophilic displacement to give succinic diesters.

mainly based on the use of α-olefins as substrates, which are more reactive with respect to higher substituted alkenes for steric reasons. Recently, however, it was found that a catalyst formed *in situ* from $Pd(TFA)_2$ (TFA = trifluoroacetate) and a suitable diamine ligand, with BQ as eternal oxidant, is able to efficiently promote the dialkoxycarbonylation not only of simple α-olefins (Scheme 8.20a) [142] but also of 1,2-disubstituted olefins (with total *syn* diastereospecificity) (Scheme 8.20b) [144] and even of strongly deactivated alkenes, such as acrylic esters and amides (Scheme 8.20c) [145].

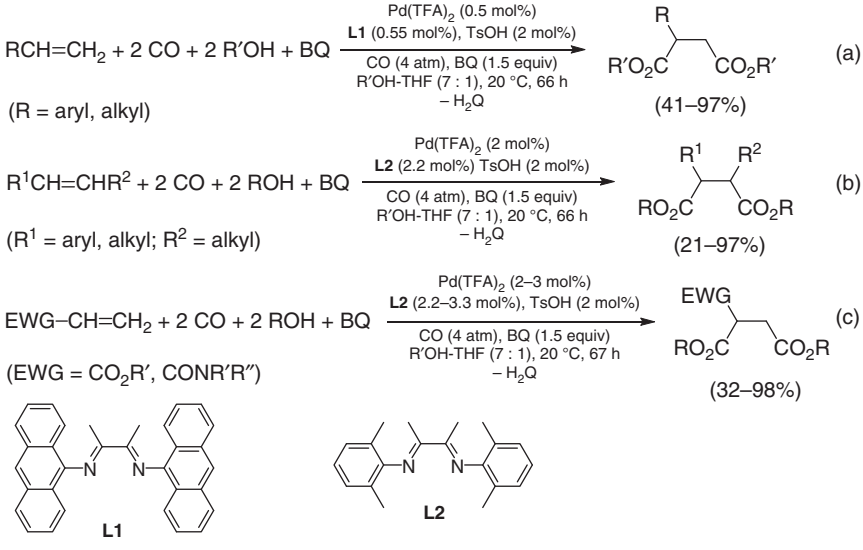

Scheme 8.20 Pd(II)-catalyzed oxidative dialkoxycarbonylation of (a) simple α-olefins [142], (b) 1,2-disubstituted olefins [144], and (c) acrylic esters and amides [145] (TFA = trifluoroacetate; BQ = benzoquinone; H_2Q = hydroquinone). Source: (a) Modified from Fini et al. [142], (b) Modified from Olivieri et al. [144], (c) Modified from Olivieri et al. [145].

Under suitable conditions, alkenes may also undergo a different oxidative carbonylation process, consisting in the alkoxy–alkoxycarbonylation of the double bond. This reaction initiates with *anti* nucleophilic attack by an alcohol to the most

substituted carbon of double bond coordinated to Pd(II), followed by alkoxycarbonylation of the ensuing (β-alkoxyalkyl)palladium(II) intermediate (Scheme 8.21). For example, with $PdCl_2$ as catalyst and $CuCl_2$ as the external oxidant, it was found by Stille in the 1970s that while dialkoxycarbonylation predominated under basic conditions, alkoxy–alkoxycarbonylation was the favored pathway under neutral conditions [122, 123]. Since then, not much progress has been made in this field, but recently it was reported that $PdCl_2$ in combination with Cu(I) and $SnCl_2$ and in the presence of 1,4-diazabicyclo[2.2.2]octane (DABCO) is able to catalyze the selective alkoxy–alkoxycarbonylation of vinylphenols. Unfortunately, however, potentially explosive conditions (1 : 1 CO–O_2 mixture) [1] were employed [146]. Apart from alcohols, other nucleophiles may oxidatively add to the double bond together with the alkoxycarbonyl group, including halides, amines, carboxylates, and carbanions [147–155].

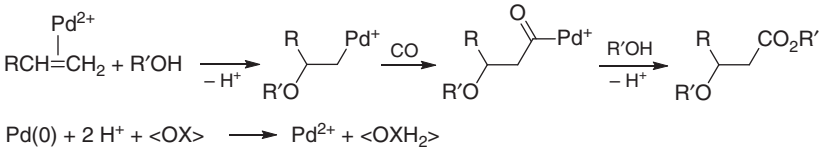

Scheme 8.21 Pd(II)-catalyzed oxidative alkoxy-alkoxycarbonylation of alkenes. Sources: Adapted from James et al. [122], James and Stille [123], Phan et al. [146].

The most studied Pd(II)-catalyzed carbonylation of alkenes is the additive alkoxycarbonylation with CO and an alcohol, with the formal addition to the double bond of a hydrogen atom on one carbon and the alkoxycarbonyl group to the other one (also called hydroesterification), disclosed by Reppe in the 1930s [156]. With respect to other metal catalysts, in this process, palladium tends to give better results (in terms of a lower degree of olefin polymerization and/or isomerization) and allows working under milder conditions [157–160]. The reaction is of high industrial interest for the production of esters from largely available feedstocks and, in particular, for the preparation of methyl propionate (an intermediate in the production of methyl methacrylate [161]) from ethylene [161–167]. It is important to note at this point that other very important and industrially relevant processes in alkene (and ethylene, in particular) carbonylation are the carbonylative di-, oligo-, and polymerization reactions [168–174], whose description, however, is beyond the scope of this chapter.

Hydroesterification of alkenes is quite sensible to the steric effects exerted by double-bond substitution, so, apart from ethylene, the most reactive and commonly used substrates are α-olefins, which, however, being unsymmetrically substituted, may lead to a mixture of regioisomeric products, as shown in Scheme 8.22 (R′ = alkyl). The regiochemical output of the process is strongly dependent on reaction conditions and, in particular, on the specific ligand used. Under suitable conditions, water can also be used instead of an alcohol to yield carboxylic acids (additive hydroxycarbonylation or hydrocarboxylation, R′ = H).

Mechanistically, two different pathways have to be considered. In the so-called alkoxycarbonylpalladium mechanism, double-bond insertion into the Pd—CO_2R′

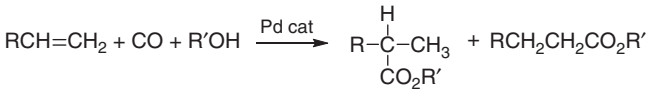

Scheme 8.22 Pd-catalyzed additive alkoxycarbonylation (hydroesterification, R′ = alkyl) and hydroxycarbonylation (hydrocarboxylation, R′ = H) of α-olefins.

bond (formed as already seen in Scheme 8.17b) is followed by protonolysis, with regeneration of the Pd(II) catalyst (Scheme 8.23a). On the other hand, in the "palladium hydride mechanism," which is believed to be the most common one at least in the presence of an acid additive, the catalytically active species is a $[Pd–H]^+$ complex, usually formed *in situ* from a Pd(0) species in the presence of an acidic co-catalyst. Olefin coordination is followed by double-bond insertion to give an alkylpalladium complex, which then undergoes alkoxycarbonylation, as exemplified in Scheme 8.23b for α-olefins.

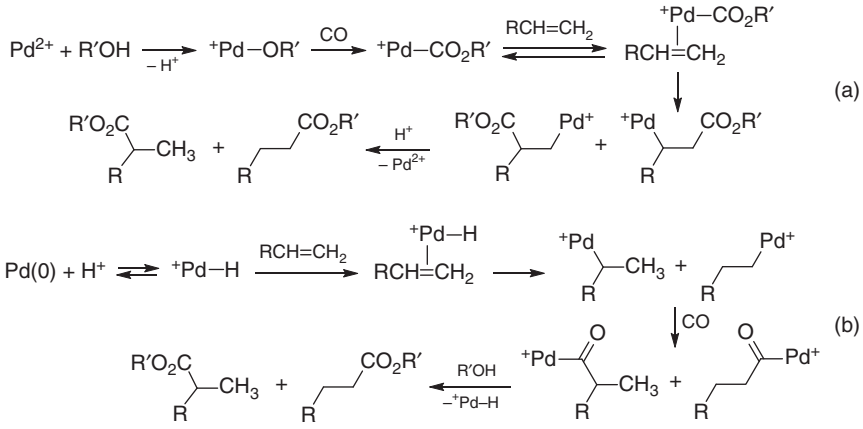

Scheme 8.23 Possible mechanisms in the Pd-catalyzed additive alkoxycarbonylation of alkenes: (a) alkoxycarbonylation mechanism and (b) palladium hydride mechanism.

Recent progress in catalysis, and especially in ligand design, has allowed achieving significant advances in the additive carbonylation of olefins [166, 167, 175–211]. This has permitted not only to improve the regioselectivity control toward either the "Markovnikov" (also enantioselectively) or the "anti-Markovnikov" regioisomer but also to significantly increase the catalytic efficiency of the process. Moreover, different kinds of olefinic substrates and alcohols, as well as various nucleophiles, such as amines (to give amides) and thiols (to give thioesters), have been successfully employed. In particular, recently the group of Beller found appropriate conditions for carrying out the reaction in an efficient manner not only for disubstituted but also for tri- and tetrasubstituted alkenes [166, 204]. In these protocols, tri- and tetrasubstituted alkenes are first isomerized *in situ* (by Pd–H) to α-olefins, which then undergo alkoxycarbonylation, as exemplified in Scheme 8.24 for tetramethylethylene [204].

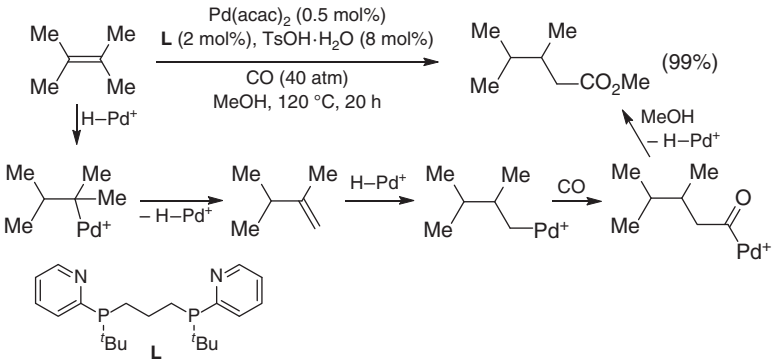

Scheme 8.24 Palladium-catalyzed additive carbonylation of tetramethylethylene, leading to methyl 3,4-dimethylpentanoate. Source: Modified from Liu et al. [204].

Dienes may also undergo Pd(II)-promoted carbonylations. For example, it was demonstrated many years ago that 1,4-cyclohexadienes react with bis(acetonitrile) palladium dichloride in methanol to give *trans*-bis(5-methoxy-1-3-η^3-cyclohexenyl) palladium chloride complexes, which were easily alkoxycarbonylated to give *trans*-5-methoxy-2-cyclohexene-1-carboxylates, as exemplified in Scheme 8.25 [212].

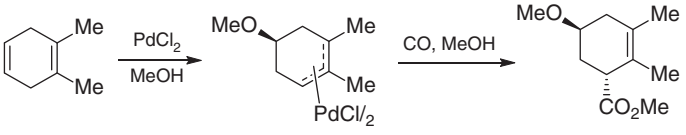

Scheme 8.25 Pd(II)-promoted alkoxy-alkoxycarbonylation of 1,2-dimethylcyclohexa-1,4-diene. Source: Modified from Söderberg et al. [212].

Carbonylation of 1,3-butadiene is of high applicative interest, owing to the possibility to convert it into adipic acid derivatives or their precursors. For example, the oxidative ethoxycarbonylation, carried out with $PdCl_2$ in the presence of chloranil and $MnCl_2$, afforded diethyl hex-3-enedioate [213], which could be converted into adipic acid upon hydrolysis and hydrogenation. Mechanistically, double-bond insertion into the Pd—CO_2Me bond generates a π-allyl complex, which is then regioselectively alkoxycarbonylated (Scheme 8.26). Under appropriate conditions, conjugated

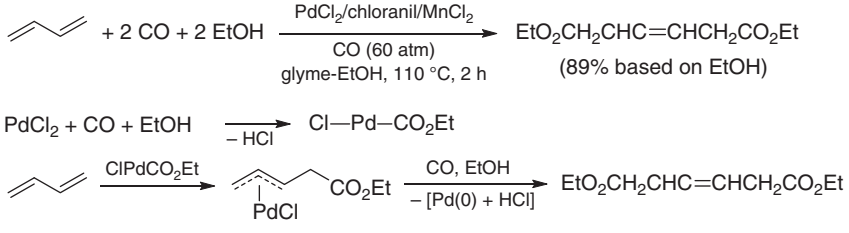

Scheme 8.26 Pd-catalyzed oxidative dialkoxycarbonylation of 1,3-butadiene to diethyl hex-3-enedioate. Source: Drent [213].

dienes can also undergo oxidative alkoxy-alkoxycarbonylation, as reported by Alper using $PdCl_2$ in the presence of $CuCl_2$, O_2, 3 Å molecular sieves, and Aliquat 336 [214]. In this case, the π-allyl intermediates formed by double-bond insertion into the Pd–CO_2Me species preferentially underwent MeOH attack rather than methoxycarbonylation with formation of methoxyesters.

Recently, Beller and coworkers found the appropriate conditions to directly convert butadiene into adipic esters under nonoxidative conditions with very high TON (>60 000), as exemplified in Scheme 8.27 for the synthesis of dibutyl adipate. The reaction, catalyzed by a Pd–H species formed *in situ*, initially led to the formation of butyl pent-3-enoate, which could be isolated after 90 minutes' reaction time. This intermediate then underwent Pd–H-promoted isomerization to the terminal olefin, which eventually converted into the final product (Scheme 8.27). The process could be applied also to other 1,3-dienes and alcohols [215]. The same research group was also able to work out suitable conditions for realizing the hydroamidocarbonylation of 1,3-dienes (using amides as nucleophiles) with formation of β,γ-unsaturated imides [216].

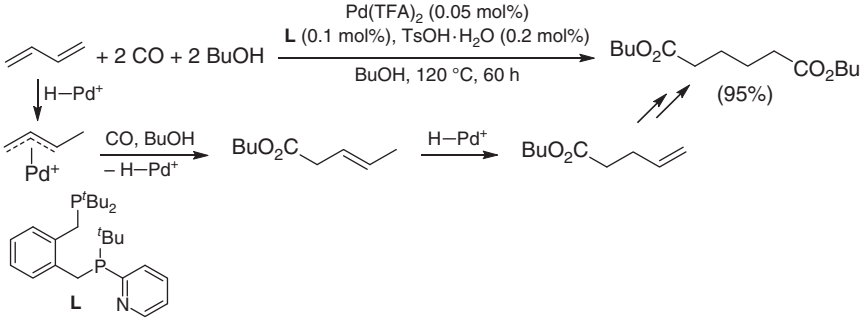

Scheme 8.27 Pd-catalyzed additive dialkoxycarbonylation of 1,3-butadiene to dibutyl adipate. Source: Modified from Yang et al. [215].

Allene has been carbonylated under oxidative conditions to give either dialkyl itaconate [217] or alkyl 2-(methoxymethyl)acrylate [218] depending on conditions. The first process begins with regiospecific allene insertion into a Pd—CO_2R bond to give a vinylpalladium intermediate, which is then alkoxycarbonylated (Scheme 8.28a). On the other hand, the alkoxy-alkoxycarbonylation reaction begins with alcohol attack to the terminal carbon of coordinated allene, which is then followed by alkoxycarbonylation (Scheme 8.28b). The alkoxy-alkoxycarbonylation reaction was also applied to substituted allenes [218]. Recent progress in Pd(II)-catalyzed oxidative carbonylation of allenes has allowed to achieve an enantioselective alkoxycarbonylative amination of terminal allenes, with formation of nonracemic methyl 2-(amino(aryl)methyl)acrylates by regiospecific allene insertion into the Pd—CO_2R bond followed by rearrangement and nucleophilic attack by an external amine [219].

Additive alkoxy- [220], amino- [221], and thioalkoxycarbonylation [222] of allenes to give unsaturated esters, amides, and thioesters, respectively, promoted by palladium hydride species, have also been reported, as exemplified in Scheme 8.29 for the

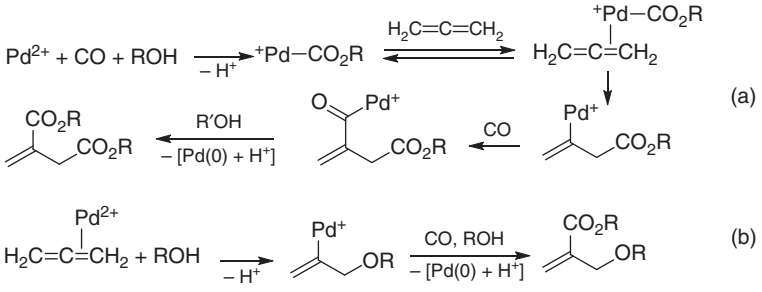

Scheme 8.28 (a) Pd-promoted oxidative dialkoxycarbonylation [217] and (b) alkoxy-alkoxycarbonylation [218] of allene to dialkyl itaconate and alkyl 2-(alkoxymethy)acrylate, respectively. Source: Modified from Tsuj and Susuki [217], (b) Modified from Alper et al. [218].

synthesis of β,γ-unsaturated esters through the formation of a π-allylpalladium complex (by ligand-directed regiospecific allene insertion into the Pd—H bond) [220].

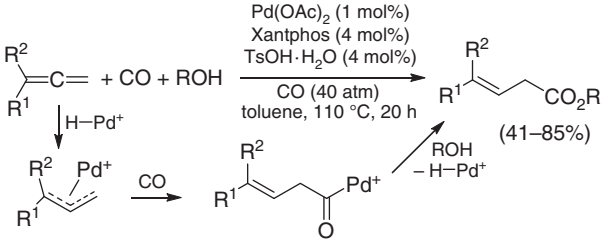

Scheme 8.29 Synthesis of β,γ-unsaturated esters by Pd-catalyzed additive alkoxycarbonylation of allenes. Source: Modified from Liu et al. [220].

8.4.2 Palladium(II)-Catalyzed Carbonylation of Functionalized Alkenes and Allenes

When suitably functionalized with a nucleophilic group in appropriate position, alkenes may lead to carbonylated heterocycles under Pd(II)-catalyzed carbonylation conditions. Different mechanistic pathways may be followed, under oxidative and nonoxidative conditions.

Under oxidative alkoxycarbonylation conditions, a first possibility corresponds to the nucleophilic attack of NuH to Pd(II), followed by CO insertion, to give an alkoxycarbonyl or carbamoylpalladium intermediate stabilized by intramolecular double-bond coordination. This intermediate then undergoes intramolecular double bond insertion followed by alkoxycarbonylation to give the final carbonylated heterocycle, with incorporation of one molecule of CO into the cycle (cyclocarbonylation) and another as ester group (Scheme 8.30a). A second possibility concerns the direct intramolecular nucleophilic attack by NuH to the double bond coordinated to Pd(II), followed by alkoxycarbonylation, as exemplified in Scheme 8.30b in the case of an *exo* cyclization (*endo* cyclization being, of course, also possible). In this case,

CO is only incorporated as ester group and not inside the cycle. A third possibility corresponds to a double cyclization process, which may take place when the olefin is functionalized with two suitably placed nucleophilic groups: the initial attack by NuH to the coordinated double bond in followed by CO insertion and intramolecular nucleophilic displacement (possibly occurring through the formation of a palladacycle), as exemplified in Scheme 8.30c.

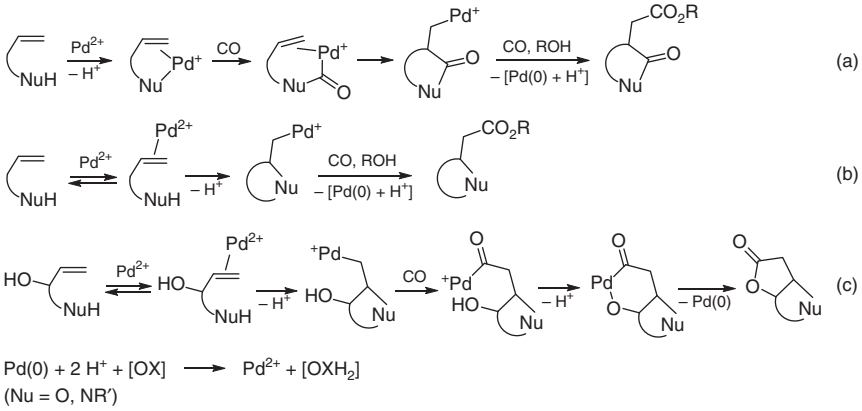

Scheme 8.30 Different mechanistic pathways in the Pd(II)-catalyzed oxidative alkoxycarbonylation of suitably functionalized alkenes to give carbonylated heterocycles: (a) cyclocarbonylation–alkoxycarbonylation, (b) cyclization–alkoxycarbonylation, and (c) cyclization–cyclocarbonylation.

Several examples of these kinds of reactivity (even enantioselective) have been reported in the literature, also applied to the synthesis of natural products, for all three mechanistic pathways (cyclocarbonylation–alkoxycarbonylation [126, 223, 224], cyclization–alkoxycarbonylation [225–239], and cyclization–cyclocarbonylation [240–260]), as shown in Scheme 8.31.

In some cases, the intermediate deriving from cyclization and CO insertion undergoes attack by other nucleophiles rather than an alcohol. An example is proffered by the oxidative aminochlorocarbonylation of *N*-tosylpentenamines, where the ensuing unstable acyl chloride derivative was trapped with an arene to give α-pyrrolidinyl ketones by In(III)-catalyzed Friedel–Crafts acylation (Scheme 8.32) [261]. In another example, the acylpalladium intermediate was converted into a formyl group or a keto group by one-pot addition of a hydride source, such as Ph_3SiH (oxidative cyclization–formylation), or of an organometallic reagent, such as Et_2Zn (oxidative cyclization–ketonylation) (Scheme 8.33) [262].

Oxidative carbonylation of functionalized alkenes may also lead to heterocycles through C(sp^2)–H activation. Two different kinds of mechanisms have been proposed for these processes. One possibility consists in the attack by the nucleophilic group present in the olefinic substrate on Pd(II), followed by CO insertion, double bond insertion- and β-H elimination (Scheme 8.34a) [263–265]. Alternatively, direct C(sp^2)–H palladation may take place, followed by CO insertion and intramolecular nucleophilic displacement (Scheme 8.34b) [266–269].

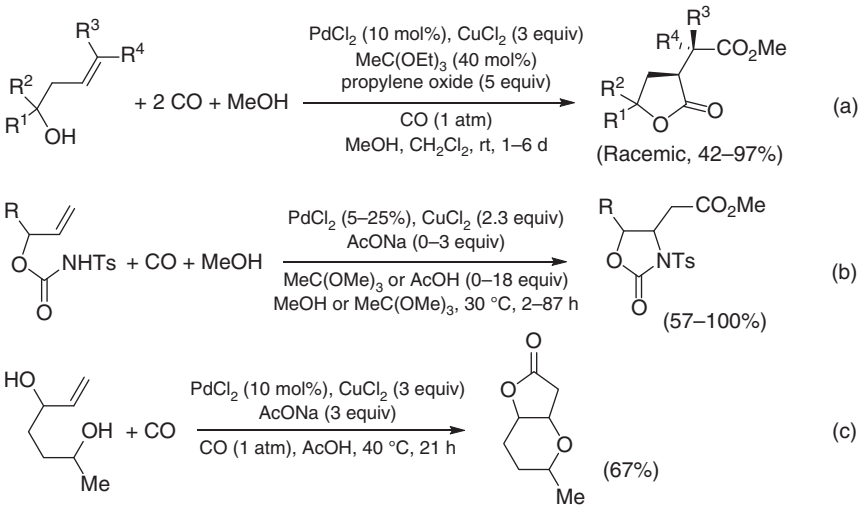

Scheme 8.31 Representative examples of the mechanistic pathways shown in Scheme 8.30. Source: (a) Modified from Tamaru et al. [223], (b) Modified from Harayama et al. [236], and (c) Modified from Cintulová et al. [260].

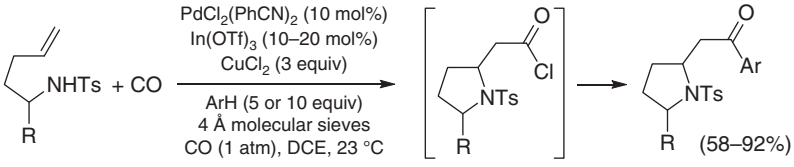

Scheme 8.32 Synthesis of 1-aryl-2-(1-tosylpyrrolidin-2-yl)ethan-1-ones by Pd(II)-catalyzed aminochlorocarbonylation of *N*-tosylpentenamines followed by In(III)-catalyzed Friedel–Crafts acylation. Source: Modified from Cernak and Lambert [261].

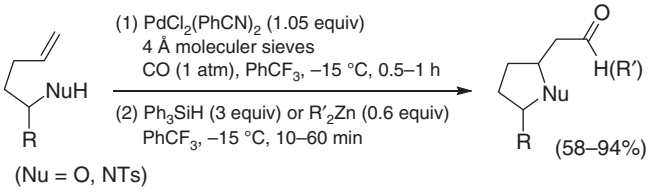

Scheme 8.33 Pd(II)-promoted oxidative cyclization–formylation or cyclization–ketonylation. Source: Modified from Ambrosini et al. [262].

Specific examples of both kinds of reactivity are shown in Scheme 8.35. In an interesting variant, the vinylpalladium complex deriving from *anti* chloropalladation of the triple bond of 3-arylpropiolates inserted the double bond of homoallylic alcohols, and this was followed by cyclocarbonylation to give the final γ-lactone derivative [270] (note, however, that the reaction conditions employed, $CO:O_2 = 3:1$, fell within the explosion limits for a CO/O_2 mixture [1]).

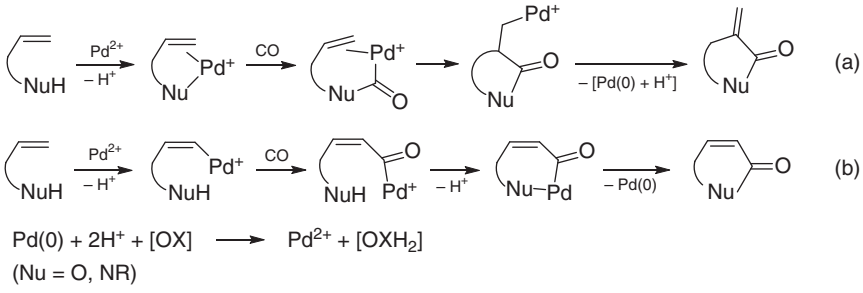

Scheme 8.34 Possible pathways in the Pd(II)-catalyzed oxidative cyclocarbonylation of suitably functionalized alkenes to give carbonylated heterocycles. Sources: (a) Li et al. [263], Ferguson et al. [264], Yang et al. [265], (b) Chen et al. [266], Liu et al. [267], Xie et al. [268], Wu et al. [269].

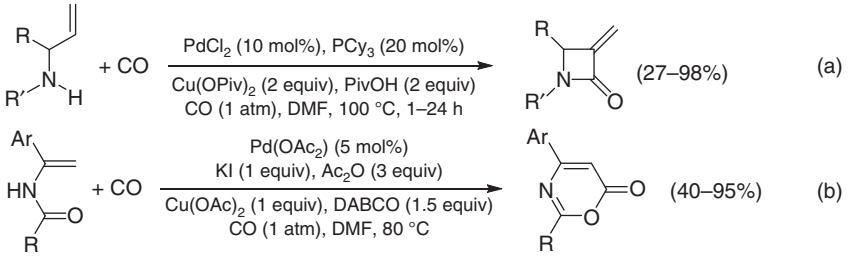

Scheme 8.35 Representative examples of the mechanistic pathways shown in Scheme 8.34. Source: (a) Modified from Li et al. [263], (b) Modified from Chen et al. [266].

Pd(II)-catalyzed carbonylation of functionalized alkenes may also occur under nonoxidative conditions. A first mechanistic possibility is very similar to that shown in Scheme 8.30a, with the difference that the vinylpalladium intermediate finally undergoes protonolysis rather than nucleophilic displacement (Scheme 8.36a). This pathway corresponds to the intramolecular version of the "alkoxycarbonylation mechanism" shown in Scheme 8.23a for simple alkenes with the external

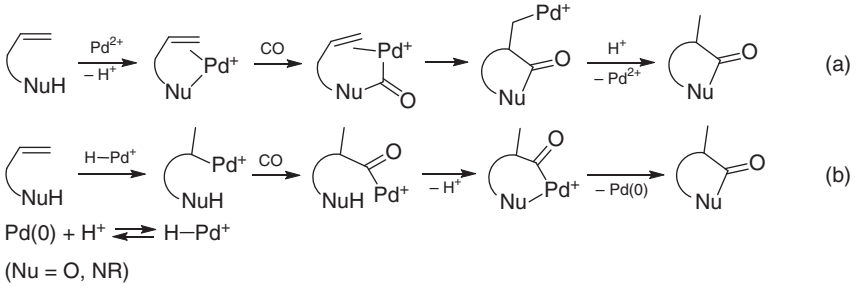

Scheme 8.36 Possible mechanistic pathways in the Pd(II)-catalyzed additive carbonylation of suitably functionalized alkenes to give carbonylated heterocycles: (a) cyclocarbonylation–protonolysis mechanism or (b) palladium hydride mechanism.

nucleophile corresponding to an alcohol. Another possibility consists in the double-bond insertion into an *in situ* formed palladium hydride complex, followed by CO insertion and intramolecular nucleophilic displacement (possibly, through the formation of a palladacycle followed by reductive elimination; Scheme 8.36b). This latter mechanism corresponds to the intramolecular version of the "palladium hydride mechanism" shown in Scheme 8.23b for simple alkenes, and it is the most commonly proposed one [271–283]. Scheme 8.37 shows, in particular, the synthesis of 1,4-dihydroisoquinolin-3(2*H*)-ones from 2-vinylbenzylamines [282].

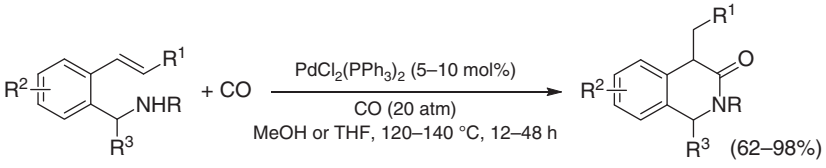

Scheme 8.37 Synthesis of 1,4-dihydroisoquinolin-3(2*H*)-ones by intramolecular Pd-catalyzed additive aminocarbonylation of 2-vinylbenzylamines. Source: Hu et al. [282].

Functionalized allenes are also excellent substrates for Pd(II) annulative carbonylation reactions. For example, the intramolecular attack of an oxygen [284–286] or nitrogen [287–290] nucleophilic group to the allene moiety of hexa-4,5-dien-1-ol or hexa-4,5-dien-1-amine derivatives coordinated to Pd(II), followed by alkoxycarbonylation, leads, under oxidative conditions, to the formation of alkyl α-(heterocyclic)acrylates, as shown in Scheme 8.38. The process can also be performed in an enantiospecific manner when starting from an enantiopure substrate, as exemplified in Scheme 8.39 [288]. Oxidative cyclocarbonylation is also possible, as shown in Scheme 8.40 [291].

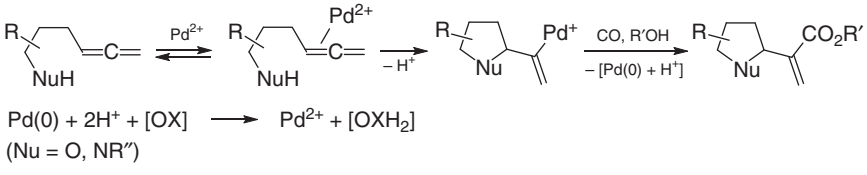

Scheme 8.38 Formation of alkyl α-(heteroaryl)acrylates by Pd(II)-catalyzed oxidative cyclization–alkoxycarbonylation of suitably functionalized allenes.

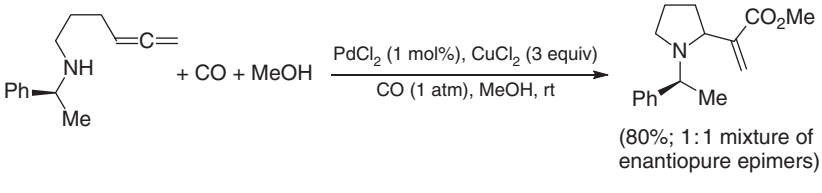

Scheme 8.39 Enantiospecific synthesis of methyl 2-(1-((*S*)-1-phenylethyl)pyrrolidin-2-yl) acrylate (1 : 1 mixture of enantiopure epimers). Source: Modified from Fox et al. [288].

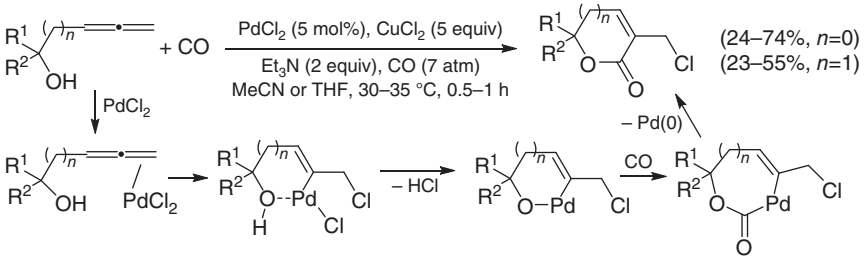

Scheme 8.40 Pd(II)-catalyzed oxidative cyclocarbonylation of allenols to 3-chloromethyl-2-(5*H*)-furanones and 3-chloromethyl-5,6-dihydropyranones. Source: Modified from Cheng et al. [291].

Recently, considerable progress has been made in Pd-catalyzed carbonylative carbocyclization of functionalized allenes [292–294]. As an example, Scheme 8.41 shows the Pd(II)-catalyzed oxidative carbonylation (with benzoquinone as oxidant) of enallenes with terminal alkynes to give dimethyl 4-(2-oxobut-3-yn-1-yl)-3-(prop-1-en-2-yl)cyclopent-2-ene-1,1-dicarboxylates after carbocyclization, CO insertion, and coupling [292].

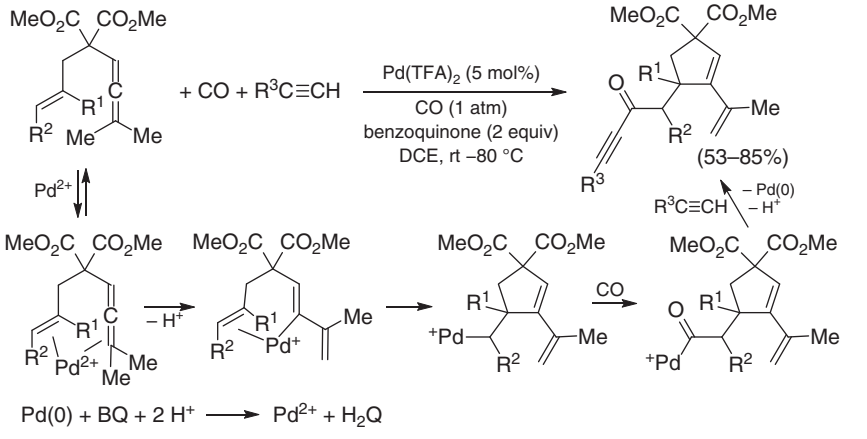

Scheme 8.41 Pd(II)-catalyzed oxidative carbonylation of enallene derivatives to give dimethyl 4-(2-oxobut-3-yn-1-yl)-3-(prop-1-en-2-yl)cyclopent-2-ene-1,1-dicarboxylates (BQ = benzoquinone; H_2Q = hydroquinone). Source: Modified from Volla and Bäckvall [292].

8.5 Palladium(II)-Catalyzed Carbonylation of Alkynes

8.5.1 Palladium(II)-Catalyzed Carbonylation of Unfunctionalized Alkynes

Alkynes are excellent substrates for Pd(II)-catalyzed carbonylation reactions. They easily coordinate to a Pd(II) center, generally even more efficiently with respect to alkenes, so Pd(II)-promoted alkyne carbonylations are usually carried out under milder reaction conditions with respect to olefin carbonylation.

Alkynes may undergo several different carbonylation processes under the catalysis of a Pd(II) species. A first possibility concerns the oxidative carbonylation, which, in its turn, depending on the nature of the alkyne and reaction conditions, may result in diverse kinds of reactions that lead to different carbonylated products. The main alkyne oxidative carbonylation processes are summarized in Scheme 8.42. In the presence of alcohols or water as external nucleophiles, an oxidative dialkoxy- or dihydroxycarbonylation may take place with formation of maleic esters or acids, respectively (sometimes together with smaller amounts of their fumaric isomers) (Scheme 8.42a). In the presence of water, maleic anhydrides can also be obtained from an oxidative oxycyclodicarbonylation process (also known as oxydicarbonylative cyclization) (Scheme 8.42b). On the other hand, with alcohols as nucleophiles, an oxidative alkoxy-alkoxycarbonylation is also possible, affording β-alkoxyacrylic esters (Scheme 8.42c). With terminal alkynes, C(sp)–H activation may occur under suitable conditions, resulting in monoalkoxycarbonylation or monoaminocarbonylation of the triple bond using alcohols or amines as nucleophiles, with formation of 2-ynoate esters or 2-ynamides, respectively (Scheme 8.42d).

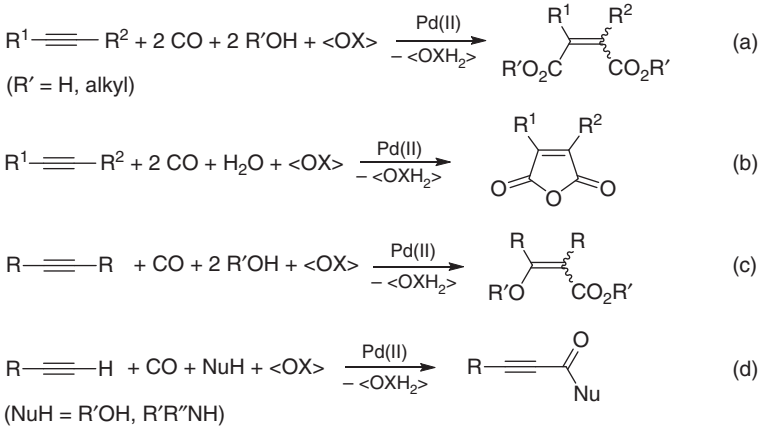

Scheme 8.42 Main Pd(II)-catalyzed oxidative carbonylations of alkynes: (a) dihydroxy- or dialkoxycarbonylation, (b) oxycyclodicarbonylation (or oxydicarbonylative cyclization), (c) alkoxy-alkoxycarbonylation, (d) monoalkoxy- or monoaminocarbonylation with C–H activation.

The first examples of alkyne oxidative carbonylations date back to the 1960s. Pioneering studies were performed by Jacobsen and Spaethe [295], Tsuji et al. [296], Chiusoli et al. [297], and Lines and Long [298]. In particular, Tsuji et al. reported the $PdCl_2$-promoted stoichiometric dichlorocarbonylation of acetylene with formation of muconyl chloride as the major product and fumaryl and maleyl chlorides as minor products, which were then transformed into the corresponding diesters by alcoholysis [296]. Later on, Chiusoli et al. reported the direct formation of dimethyl maleate (Scheme 8.42a, R′ = Me), together with smaller amounts of muconate and fumarate, using $PdCl_2$ in the presence of thiourea as ligand at room temperature

under catalytic conditions with oxygen as external oxidant and MeOH as solvent and nucleophile [297, 299].

The oxidative dialkoxycarbonylation of terminal alkynes was then studied by Alper et al., who found that maleic (major) and fumaric (minor) diesters could be obtained in high yields with a $PdCl_2/CuCl_2/O_2$ system in alcoholic solvents [300]. A breakthrough in this kind of process was subsequently realized by Gabriele and coworkers, who found that a very simple catalytic system, consisting of PdI_2 in conjunction with KI, was able to catalyze the dialkoxycarbonylation of terminal alkynes in a very efficient manner (up to c. 4000 TONs, with respect to the <10 TONs previously obtained) without using any additional ligand or additive and with oxygen (from air, under non-explosive conditions [301]) as the external oxidant. The excess of KI, besides helping to solubilize PdI_2 in the alcoholic solvents, was useful to stabilize the *in situ* formed catalytically active species PdI_4^{2-} [302, 303]. The method was successfully applied to both alkyl- and arylacetylenes and to simple acetylene and propargyl alcohol, to afford maleic diesters as the main reaction products, together with smaller amounts of fumarates and of cyclic isomers of maleic diesters, corresponding to 5,5-dialkoxyfuran-2-(5*H*)-ones. These latter derivatives, however, could be easily converted into maleic diesters by heating and/or acid-promoted isomerization, making the overall process very selective (Scheme 8.43a) [303]. This protocol was successfully employed as a key step for the synthesis of the core of natural product phomoidride B [304, 305]. Moreover, with 1,4-diyne substrates, ring closure takes place as shown by the synthesis of 2,2′-(thiophene-3,4-diyl)diacetate derivatives from dipropargyl sulfides [306]. Although other methods have subsequently appeared in the literature for realizing the terminal alkyne dialkoxycarbonylation [307–311] (including a method for the electrochemical reoxidation of Pd(0) [307] and methods [309, 311] employing potentially explosive reaction conditions [1]), the PdI_2/KI-catalyzed reaction still remains the most efficient one to date. As regards the reaction mechanism, the formation of an alkoxycarbonylpalladium iodide complex by the reaction between PdI_2, CO, and R′OH occurs first, followed by *syn* triple-bond insertion into the Pd—CO_2R′ bond (Scheme 8.43b). Nucleophilic displacement by R′OH gives a tetrahedral intermediate, from which the maleic diester is formed by β-H elimination from the H–O–Pd–I moiety (Scheme 8.43b, pathway a). On the other hand, lactonization (by intramolecular transesterification) may lead to a lactonyl π-allylpalladium complex, which undergoes regiospecific nucleophilic attack by R′OH to give the dialkoxyfuranone derivative (Scheme 8.43b, pathway b). The minor amounts of fumaric diesters are formed from double-bond isomerization, most likely at the vinylpalladium intermediate level. In any case, Pd(0) is formed at the end of the process, which is very efficiently reoxidized back to PdI_2 by oxidative addition of I_2, formed in its turn by oxidation of HI with oxygen (Scheme 8.43b) [303, 312].

One limitation of this process was that it did not work well for internal alkynes [303]. Recently, however, it was found by the groups of Carfagna and Gabriele that $(PhCN)_2PdCl_2$, stabilized by a suitable 1,4-diaryl-2,3-diazabutene ligand and in the presence of AgOTf, is able to perform the process for both dialkylacetylenes and alkylarylacetylenes under mild conditions (room temperature and 4 atm of CO) and using benzoquinone as external oxidant (Scheme 8.44) [313].

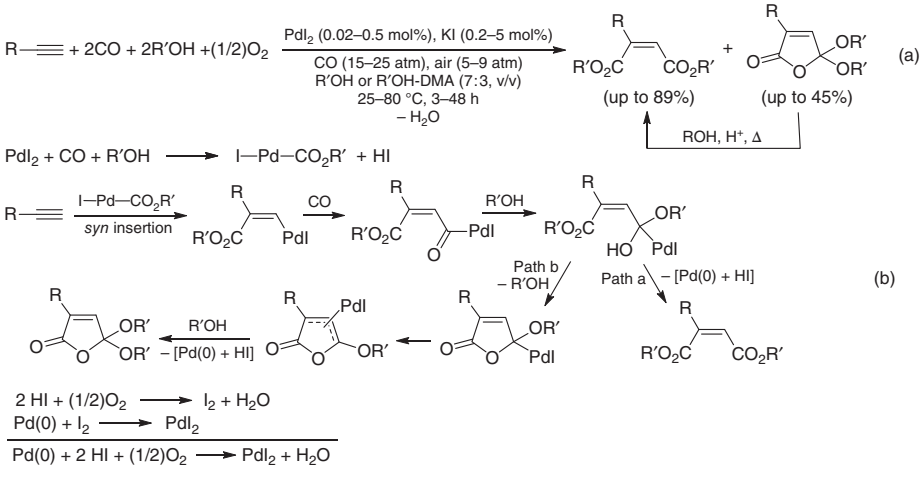

Scheme 8.43 PdI_2/KI-catalyzed oxidative dialkoxycarbonylation of terminal alkynes (a) and related reaction mechanism (b). Source: Modified from Gabriele et al. [302, 303].

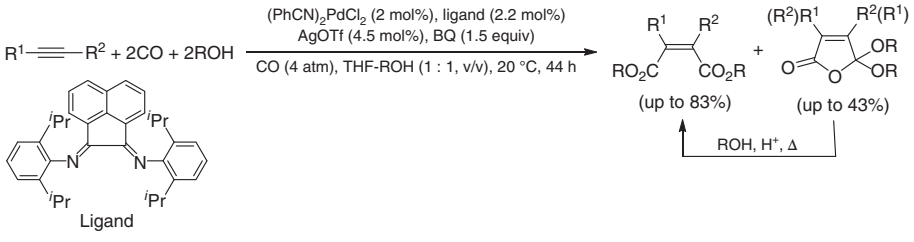

Scheme 8.44 Pd(II)-catalyzed oxidative dialkoxycarbonylation of internal alkynes. Source: Modified from Beltrani et al. [313].

With water as nucleophile, alkynes can be converted into maleic acids (Scheme 8.42a, R′ = H) or anhydrides (Scheme 8.42b), depending on reaction conditions [314–318]. In particular, the PdI_2/KI system was also able to efficiently catalyze the oxidative dihydroxycarbonylation of terminal alkynes with formation of maleic acids when the process was performed in a 3 : 1 DME–H_2O mixture (Scheme 8.45a) [318]. The same catalyst promoted the formation of maleic anhydrides when the reaction was carried out in dioxane in the presence of small amount of water (Scheme 8.45b) [318]. The formation of maleimides with primary amines as nucleophiles has also been recently reported with $PdCl_2$ as catalyst in toluene at 120 °C and oxygen (from air) as oxidant [319].

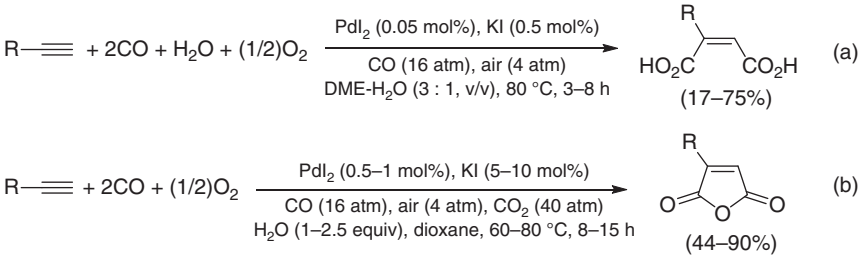

Scheme 8.45 Synthesis of (a) maleic acids and (b) maleic anhydrides by PdI_2/KI-catalyzed oxidative carbonylation of terminal alkynes. Source: Modified from Gabriele et al. [318].

Oxidative alkoxy-alkoxycarbonylation of alkynes (Scheme 8.42c) to give β-alkoxyacrylic ester derivatives is a less studied process. An example is represented by the synthesis of γ-acetoxy-β-methoxyacrylates from α,α-disubstituted propargyl acetates [320]. Oxidative haloalkoxycarbonylation to give 3-haloacrylate derivatives has also been reported [270, 321–324].

On the other hand, the oxidative monoalkoxycarbonylation of terminal alkynes with C(sp-H) activation and formation of 2-ynoate esters is a well-studied and important process for the production of useful compounds (Scheme 8.42d, NuH = R′OH). The first example of this kind of process was reported in 1980 by Tsuji et al., who employed $PdCl_2$ as catalyst in the presence of $CuCl_2$ and NaOAc as base [325]. Probably, the role of $CuCl_2$ was not only to act as external oxidant but also to promote C(sp-H) palladation via initial formation of an alkynylcopper intermediate followed by transmetalation [326]. The final product was then obtained by CO insertion and nucleophilic displacement by R′OH (Scheme 8.46).

Since then, many efforts have been made to expand the usefulness of the process [311, 313, 327–332], which have led to the development of methods with electrochemical reoxidation of Pd(0) [328], copper-free processes [311, 313, 329–332], recyclable catalysts [311], successful use of phenols instead of alcohols as nucleophiles [332], and base-free reactions under neutral conditions [311, 313, 329–332]. In particular, our research group in collaboration with Carfagna and coworkers has recently reported a general base-free oxidative monoalkoxycarbonylation of aryl- and alkylacetylenes to give alkynoates via β-H elimination from the *E* alkoxycarbonylpalladium intermediate formed by isomerization of the initially formed *Z* isomer (Scheme 8.47) [313].

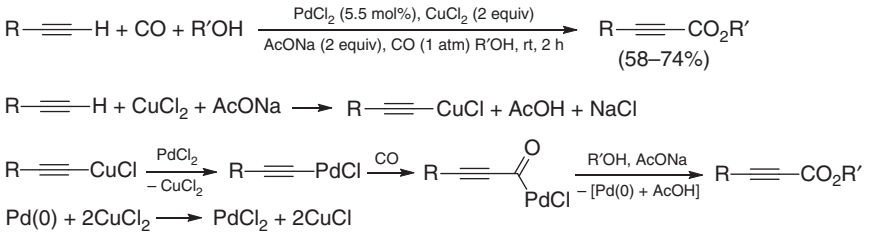

Scheme 8.46 Tsuji's oxidative monoalkoxycarbonylation of terminal alkynes to 2-ynoate esters. Sources: Adapted from Tsuji et al. [325], Bruk et al. [326].

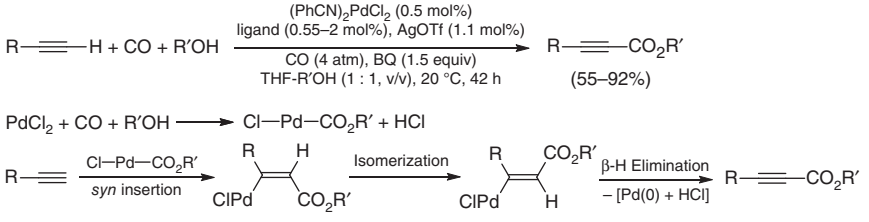

Scheme 8.47 An example of Pd(II)-catalyzed oxidative monoalkoxycarbonylation of terminal alkynes to alkyl 2-ynoates under neutral conditions (the ligand is the same as that shown in Scheme 8.44). Source: Modified from Beltrani et al. [313].

2-Ynamides, which are important intermediates for the formation of heterocycles and bioactive compounds, can also be obtained by Pd(II)-catalyzed oxidative monocarbonylation of terminal alkynes. The first example was reported in 2001 by Gabriele et al., who employed their PdI_2/KI catalytic system in the presence of nucleophilic secondary amines [333]. The latter had a double role, that is, to act as base for promoting the formation of the alkynylpalladium intermediate and to perform the final nucleophilic displacement after CO insertion (Scheme 8.48) [333]. Recently, other catalytic systems and conditions have also been developed to realize this kind of process [334–339].

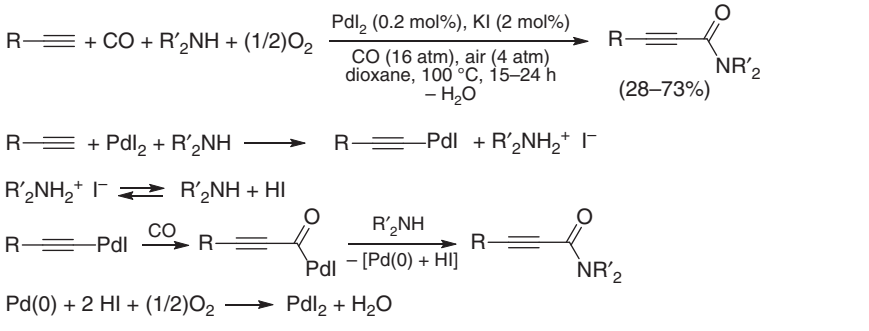

Scheme 8.48 PdI_2/KI-catalyzed oxidative monoaminocarbonylation of terminal alkynes to 2-ynamides. Source: Gabriele et al. [333].

Pd(II)-catalyzed additive carbonylations of alkynes are very important processes, which allow synthesizing very important carbonyl derivatives under relatively mild

conditions. The reaction can be exploited for the production of industrially relevant products from largely available feedstocks, such as methyl methacrylate from 1-propyne. Since the pioneering studies by Knifton [340], Alper [341], and Drent [342], among others, considerable progress has been made in this field, which has allowed to improve the catalyst performance and selectivity and the process sustainability [157–160].

The additive alkoxycarbonylation of alkynes leads to α,β-unsaturated esters, and, when starting from unsymmetrically substituted substrates such as terminal alkynes, the regiochemical output of the process strongly depends on reaction conditions [343–352], as exemplified in Scheme 8.49.

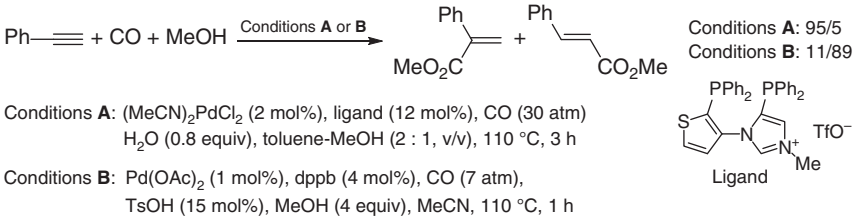

Scheme 8.49 Regiodivergent methoxycarbonylation reactions of phenylacetylene under different conditions (**A** [352] or **B** [345]). Sources: Modified from Yang et al. [352], Modified from Suleiman and Tijani [345].

As already seen in the case of olefins (Scheme 8.23), two different mechanisms are possible, that are, the alkoxycarbonylpalladium mechanism and the palladium hydride mechanism, the latter one being the most commonly proposed one (Scheme 8.50) [353, 354].

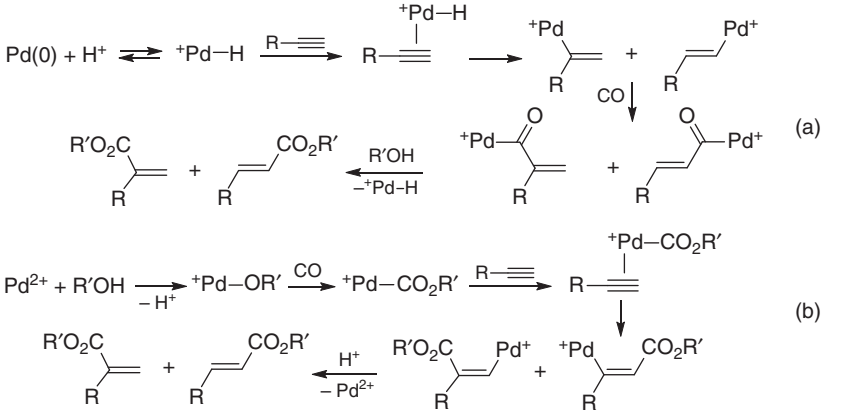

Scheme 8.50 Possible mechanisms in the Pd-catalyzed additive alkoxycarbonylation of alkynes: (a) palladium hydride mechanism and (b) alkoxycarbonylation mechanism. Sources: Adapted from Crawford et al. [353], Ahmad et al. [354].

Besides alkoxycarbonylation, alkyne additive hydroxy- [355], amino- [356–362], and thiocarbamoylations [363] have also been reported, as exemplified in

Scheme 8.51 for the synthesis of acrylamides from terminal alkynes and amines [362].

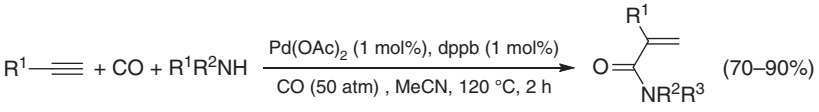

Scheme 8.51 Pd(II)-catalyzed additive aminocarbonylation of terminal alkynes to give acrylamides. Source: Wang et al. [362].

Under suitable conditions, the initially formed acrylic derivative may undergo *in situ* a second regiospecific additive carbonylation, as exemplified in Scheme 8.52 for the formation of succinate esters by sequential double additive alkoxycarbonylation of terminal alkynes [364–366]. Formation of succinimides by cyclizative aminocarbonylation of alkynes with primary amines has also been reported [367].

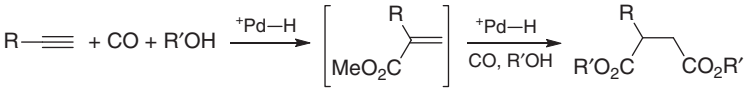

Scheme 8.52 Formation of succinate esters by sequential double additive alkoxycarbonylation of terminal alkynes. Sources: Liu et al. [364], Yang et al. [365], Guo et al. [366].

Pd(II)-catalyzed additive carbonylation of alkynes may also lead to ketones. For example, Alper reported the reaction between indoles and propiolate esters with formation of methyl (*E*)-4-(1*H*-indol-3-yl)-4-oxobut-2-enoates (Scheme 8.53) [368]. [2+2+1]-Cyclocarbonylation involving two molecules of alkyne and one of CO with formation of cyclopentadienones has also been reported [369, 370].

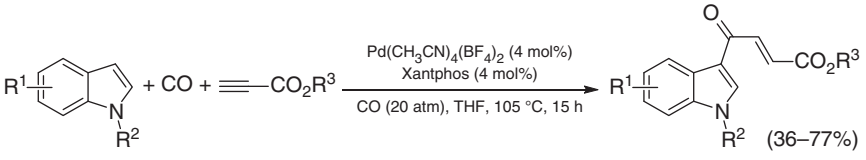

Scheme 8.53 Synthesis of (*E*)-4-(1*H*-indol-3-yl)-4-oxobut-2-enoates by Pd(II)-catalyzed carbonylation of indoles with alkyl propiolates. Source: Zeng and Alper [368].

Sometimes, the oxidative carbonylation of an alkyne may occur with simultaneous substrate reduction, thus overall leading to a formal additive or substitutive carbonylation process. The Pd(II)-catalyzed combination between an alkyne oxidative carbonylation process and reduction (in particular, a reductive carbonylation process) was first observed in 1966 by Tsuji and Nogi, who converted diphenylacetylene in a mixture of dimethyl 2,3-diphenylmaleate (from oxidative carbonylation) and 3,4-diphenylfuran-2(5*H*)-one (from reductive carbonylation) under quite drastic reaction conditions (100 atm of CO at 100 °C in the presence of $PdCl_2$ and HCl)

[371]. Later on, this formal additive carbonylation process was generalized to different terminal alkynes by Gabriele et al. using PdI_2 in conjunction with thiourea as ligand under particularly mild conditions (Scheme 8.54) [372].

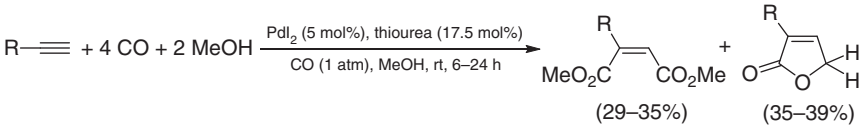

Scheme 8.54 Combined Pd(II)-catalyzed oxidative carbonylation and reductive carbonylation of terminal alkynes, resulting in a formal additive carbonylation process. Source: Modified from Gabriele et al. [372].

The same research group subsequently reported the possibility to selectively synthesize the 2(5*H*)-furanone derivatives by carrying out the carbonylation process under reductive conditions, using water as formal reducing agent and with formation of CO_2 as coproduct (Scheme 8.55) [373, 374].

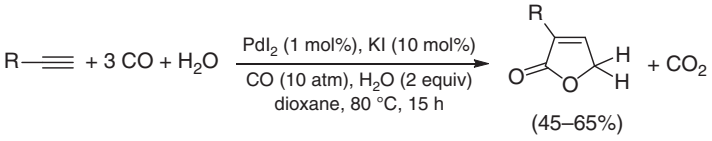

Scheme 8.55 Reductive carbonylation of terminal alkynes to 2(5*H*)-furanones under water-shift conditions. Sources: Adapted from Gabriele et al. [374], Chiusoli et al.[373].

Another example of reductive carbonylation of alkynes is represented by the hydroformylation reaction, as shown in Scheme 8.56 [375].

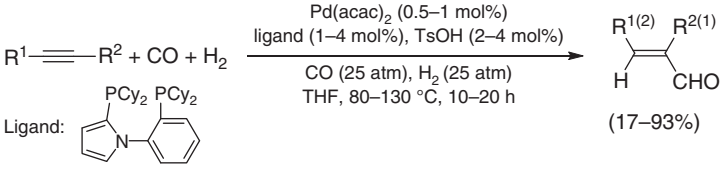

Scheme 8.56 Pd-catalyzed hydroformylation of alkynes to α,β-unsaturated aldehydes. Source: Modified from Feng et al. [375].

8.5.2 Palladium(II)-Catalyzed Carbonylation of Functionalized Alkynes

Suitably functionalized alkynes may undergo several important Pd(II)-catalyzed carbonylation processes, with formation of high-value-added compounds. Different mechanistic pathways may be followed, depending on the kind of alkyne functionalization and reaction conditions.

When the alkyne is functionalized with a suitably placed nucleophilic group, Pd(II)-catalyzed oxidative carbonylation usually occurs with simultaneous cyclization, with formation of carbonylated cyclic compounds (heterocycles in particular), with or without incorporation of CO into the cycle.

The most commonly encountered mechanisms with incorporation of CO into the cycle are shown in Scheme 8.57. A first possibility corresponds to the use of an alkyne bearing a suitable functionalized nucleophilic group, which undergoes *syn* triple-bond insertion into a Pd—CO_2R' bond (formed by the reaction between Pd(II), CO, and R′OH). This is followed by CO insertion and intramolecular nucleophilic displacement to give the final dicarbonylated product (oxidative alkoxycarbonylation–cyclocarbonylation; Scheme 8.57a) [376, 377]. The same product can also be obtained through the formation of an alkoxycarbonyl or carbamoyl complex from the nucleophilic function of the substrate followed by intramolecular *syn* triple-bond insertion and alkoxycarbonylation (oxidative cyclocarbonylation–alkoxycarbonylation; Scheme 8.57b) [223, 376, 378–381]. When Pd(II) is bonded to a halide ligand (chloride, in particular), *syn* insertion of the triple bond into the Pd—X bond may also take place, followed by cyclocarbonylation (oxidative *syn* halogenation–cyclocarbonylation; Scheme 8.57c) [382, 383]. Alternatively, the halide may attack the triple bond coordinated to Pd(II), followed by CO insertion and intramolecular nucleophilic displacement (oxidative *anti* halogenation–cyclocarbonylation; Scheme 8.57d, Nu′H = HX) [382–384]. The initial nucleophilic attack to coordinated triple bond can also be given by another external nucleophile, such as an alcohol, as shown in Scheme 8.57d (Nu′H = R′OH; oxidative alkoxylation–cyclocarbonylation) [223, 385, 386].

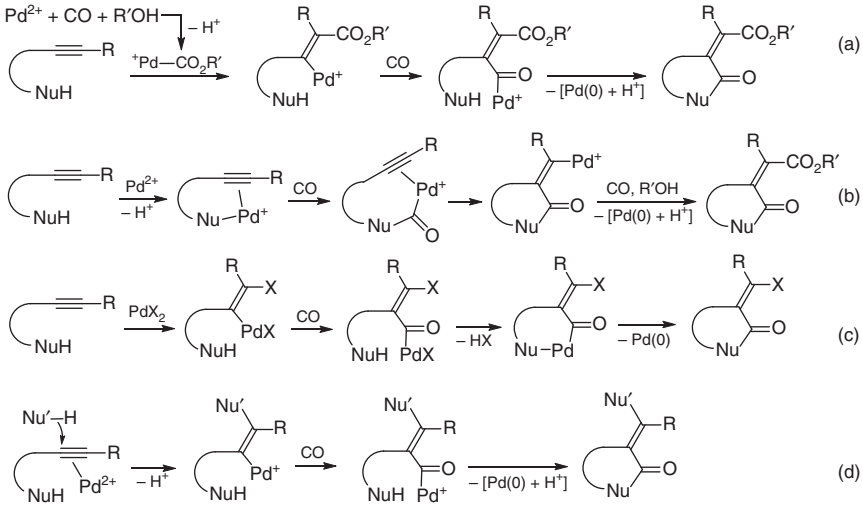

Scheme 8.57 Multiple pathways in the oxidative carbonylation of acetylenic substrates functionalized with a suitably placed nucleophilic group, with incorporation of CO into the cycle: (a) alkoxycarbonylation–cyclocarbonylation, (b) cyclocarbonylation–alkoxycarbonylation, (c) *syn* halogenation–cyclocarbonylation, and (d) *anti* halogenation–cyclocarbonylation (Nu′H = HX) or alkoxylation–cyclocarbonylation (Nu′H = R′OH).

Several examples have been reported in the literature of these kinds of reactivity, in particular employing the PdI_2/KI catalytic system, which have led to the synthesis

of important carbonylated heterocyclic derivatives, including β-lactones [376, 382], γ-lactones [223, 376, 385], δ-lactones [386], β-lactams [377, 384], γ-lactams [377], ζ-lactams [380], oxindoles [378, 383], pyridinones [379], and benzimidazopyrimidinones [381]. Scheme 8.58 illustrates the synthesis of ζ-lactam derivatives with antitumor activity, formed through mechanism (b) of Scheme 8.57, as confirmed by density functional theory (DFT) calculations [380].

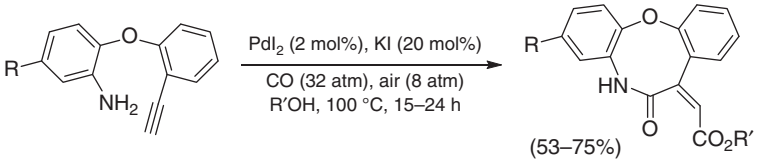

Scheme 8.58 Synthesis of ζ-lactams with antitumor activity by PdI_2/KI-catalyzed oxidative cyclocarbonylation–alkoxycarbonylation of 2-(2-ethynylphenoxy)anilines. Source: Modified from Mancuso et al. [380].

Under oxidative C(sp)–H aminocarbonylation conditions (Scheme 8.48, Section 8.5.1), and with suitable substrates, an oxidative cyclocarbonylation may also be the indirect result of a sequence of steps involving terminal triple-bond monoaminocarbonylation, followed by conjugated addition of the nucleophilic amine to the ensuing 2-ynamide intermediate and intramolecular alcoholysis or aminolysis. This reactivity has been reported in the PdI_2/KI-catalyzed conversion of propargyl alcohols and amines into dialkylaminofuranones [387] and dialkylaminodihydropyrrolones [388], respectively, as shown in Scheme 8.59.

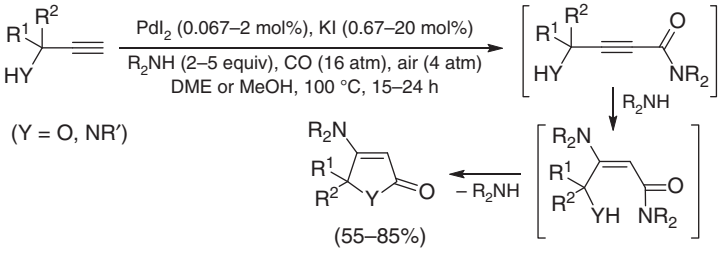

Scheme 8.59 Sequential PdI_2/KI-catalyzed oxidative monoaminocarbonylation–intermolecular conjugate addition–cyclization, leading to dialkylaminofuranones (Y = O) [387] and dialkylaminodihydropyrrolones (Y = NR′) [388]. Sources: Adapted from Gabriele et al. [387], Gabriele et al. [388].

Interestingly, when the PdI_2/KI-catalyzed oxidative aminocarbonylation of propargyl amines was carried out in the presence of water in dioxane [389] or $EmimEtSO_4$ [390] as the solvent instead of MeOH, the 2-ynamide intermediate followed a different route, as it underwent nitrogen palladation followed by CO insertion, water attack with concomitant cyclization, and β-H elimination from the H–O–C–Pd–I moiety (Scheme 8.60). The overall process, leading to oxazolidinones with anticancer activity [391], is an example of auto-tandem catalysis, as it

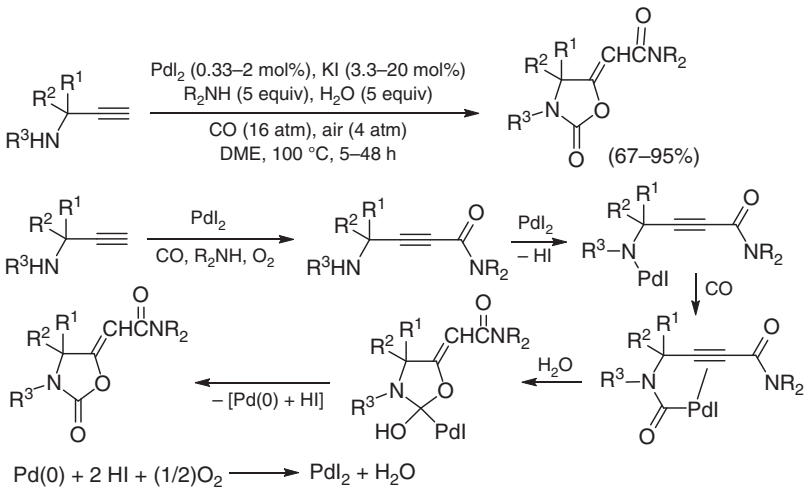

Scheme 8.60 Auto-tandem catalysis leading to oxazolidinones from propargyl amines: PdI_2/KI-catalyzed C–H aminocarbonylation, followed by PdI_2/KI-catalyzed cyclocarbonylation. Source: Modified from Gabriele et al. [389].

corresponds to two concatenated catalytic cycles (oxidative monoaminocarbonylation followed by cyclocarbonylation) catalyzed by the same species (PdI_2/KI) [389–391].

PdI_2/KI auto-tandem-catalyzed oxidative monoaminocarbonylation followed by cyclocarbonylation was also recently observed in the synthesis of imidazothiazinones [392] and benzimidazothiazinones [393] from 2-(prop-2-ynylthio)imidazoles and 2-(prop-2-ynylthio)benzimidazoles, respectively. Also in this case, the initially formed 2-ynamide intermediate underwent nitrogen palladation (at N-3) and CO insertion, which was followed by intramolecular triple-bond insertion, protonolysis, and isomerization, as exemplified in Scheme 8.61 for imidazothiazinones [392].

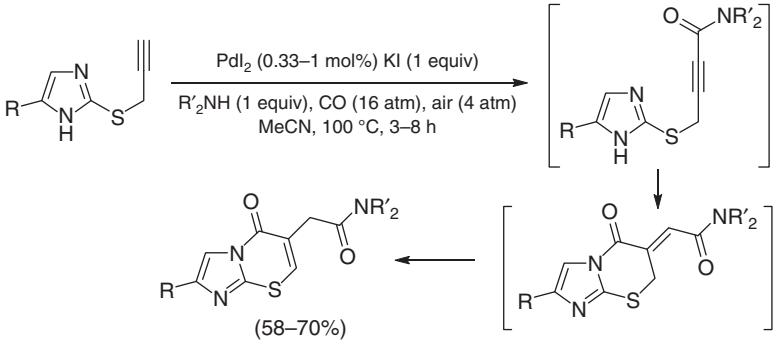

Scheme 8.61 Synthesis of imidazothiazinones by PdI_2/KI-catalyzed sequential oxidative monoaminocarbonylation–cyclocarbonylation of 2-(prop-2-ynylthio)imidazoles. Source:Veltri et al. [392].

The Pd(II)-catalyzed oxidative carbonylation of functionalized alkynes may also occur without incorporation of CO into the cycle and with exocyclic CO fixation. This approach represents another powerful methodology for the synthesis of carbonylated heterocyclic derivatives. A first possible mechanism consists in the *anti* intramolecular nucleophilic attack (either *exo* or *endo*) of the nucleophilic group (present in the acetylenic substrate in suitable position) to the triple bond coordinated to Pd(II), followed by alkoxy- [379, 394–425], hydroxy- [426], or aminocarbonylation [427] (Scheme 8.62).

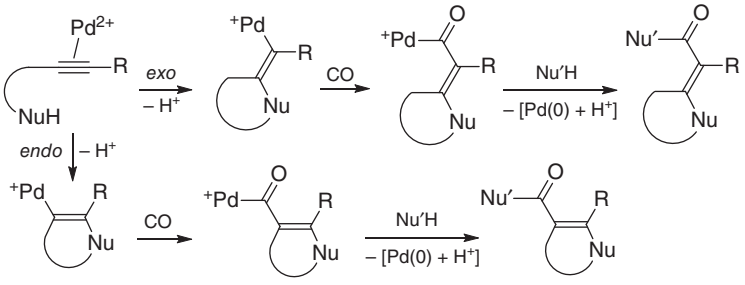

Scheme 8.62 Pd(II)-catalyzed oxidative *exo* and *endo* cyclization–carbonylation: alkoxycarbonylation (Nu′ = OR′), hydroxycarbonylation (Nu′ = OH), and aminocarbonylation (Nu′ = NR^1R^2).

Several important heterocyclic derivatives have been synthesized by this approach, including benzofurans [394, 396, 415, 426], indoles [394, 413], furans [395], tetrahydrofurans [397, 399–401, 409, 410, 412], pyrroles [379, 404], oxazolines [403], and imidazopyridines [425], among others, as exemplified in Scheme 8.63 for the synthesis of isobenzofuranimines [419] with herbicidal activity [420] from 2-alkynylbenzamides.

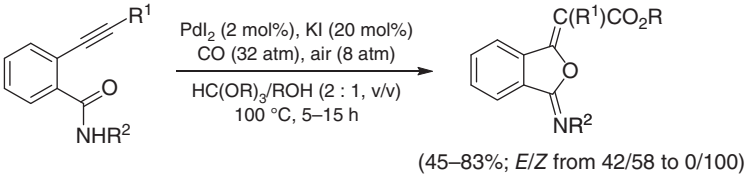

Scheme 8.63 Synthesis of isobenzofuranimine derivatives by PdI_2/KI-catalyzed oxidative O-cyclization–alkoxycarbonylation of 2-alkynylbenzamides. Sources: Adapted from Mancuso et al. [419].

In some cases, the process occurs with concomitant dehydration and aromatization, with formation of very important heterocycles such as quinolines [428], furans [429], pyrroles [430], and thiophenes [431], as shown in Scheme 8.64 for the synthesis of furan-3-carboxylic esters from 3-yne-1,2-diols [429].

Of particular interest is the possibility to realize the sequential incorporation of both carbon oxides (carbon dioxide and carbon monoxide) starting from

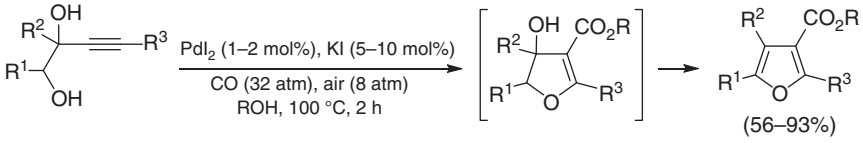

Scheme 8.64 PdI_2/KI-catalyzed oxidative cyclization–alkoxycarbonylation–dehydration of 3-yne-1,2-diols, leading to furan-3-carboxylic esters. Source: Modified from Gabriele et al. [429].

propargyl amines through the intermediate formation of a carbamate [432, 433]. As shown in Scheme 8.65, pathway a, an anionic carbamate would lead to the final oxazolidinone derivative with *E* stereochemistry by *anti* attack to the triple bond coordinated to Pd(II) followed by alkoxycarbonylation, according to the general mechanism shown in Scheme 8.62. On the other hand, the *Z* stereoisomer could be obtained from intramolecular *syn* triple-bond insertion into a palladium carbamate, followed by alkoxycarbonylation (Scheme 8.65, path b) [432, 433]. In a similar manner, recently it was reported the formation of (*Z*)-2-[oxoisobenzofuran-1-3(*H*)-ylidene]acetates from 2-ethynylbenzoic acids (obtained *in situ* by desilylation of 2-[(trimethylsilyl)ethynyl]benzoic acids) via the formation of a palladium carbamate as key intermediate (Scheme 8.66) [434].

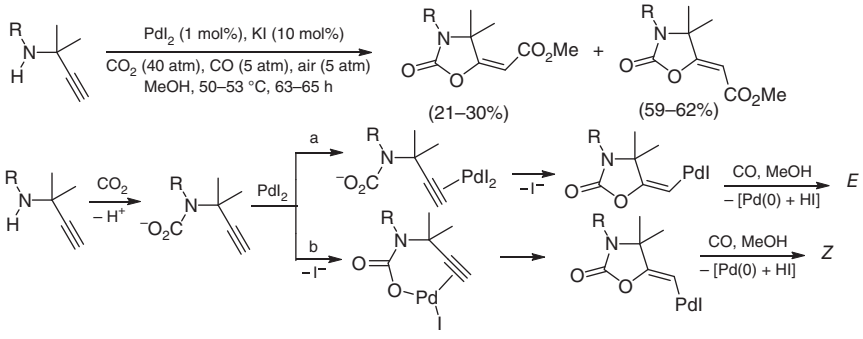

Scheme 8.65 PdI_2/KI-catalyzed oxidative sequential carboxylation–cyclization–alkoxycarbonylation of propargyl amines, leading to oxazolidinone derivatives. Sources: Adapted from Bacchi et al. [432], Chiusoli et al. [433].

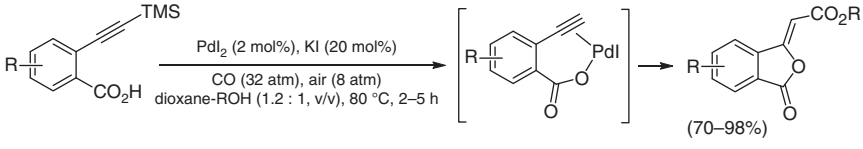

Scheme 8.66 Synthesis of isobenzofuranone derivatives by PdI_2/KI-catalyzed oxidative cyclization–alkoxycarbonylation of 2-[(trimethylsilyl)ethynyl]benzoic acids. Source: Mancuso et al. [434].

Another possible mechanism for the Pd(II)-catalyzed oxidative carbonylation of functionalized alkynes without incorporation of CO into the cycle concerns the

oxidative C–H aminocarbonylation of the triple bond, followed by intramolecular conjugate addition to the ensuing 2-ynamide intermediate [392, 393, 419, 435–442]. This is possible when cyclization is allowed by Baldiwn's rules (Scheme 8.67).

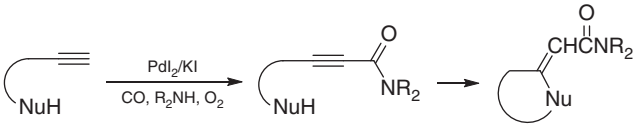

Scheme 8.67 Sequential PdI_2/KI-catalyzed oxidative monoaminocarbonylation–intramolecular conjugate addition, leading to heterocyclic (Nu = O, NR′) or carbocyclic (Nu = carbonucleophile) derivatives.

By this approach, several important carbonylated heterocyclic [392, 393, 435–438, 440–442] and carbocyclic [439] derivatives have been synthesized, including furans [437, 438], tetrahydrofurans [435, 438], benzoxazines [436], isoindolinones [419, 440], indanes [439], and fused heterocycles [392, 393, 441, 442], as shown in Scheme 8.68 in the case of the synthesis of imidazopyridinyl-*N*,*N*-dialkylacetamides from *N*-Boc-(prop-2-yn-1-yl)pyridin-2-amines [442].

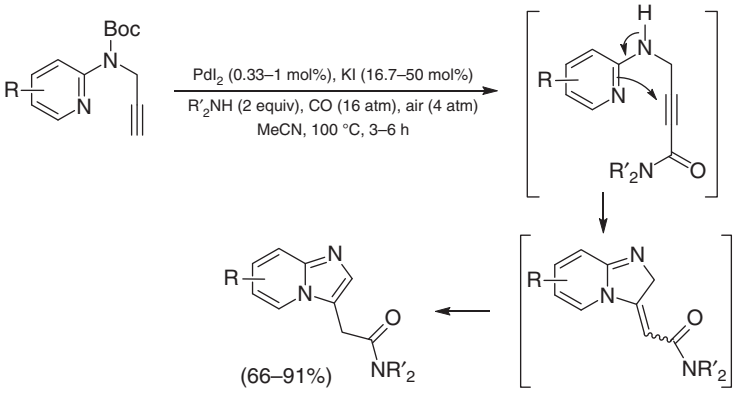

Scheme 8.68 Sequential PdI_2/KI-catalyzed monoaminocarbonylation–intramolecular conjugate addition–isomerization, leading to imidazopyridine derivatives. Source: Modified from Veltri et al. [442].

Under suitable conditions, a carbonylative double cyclization may occur, with formation of diheterocyclic ketones through heterocyclization followed by CO insertion, coordination of a second substrate molecule, further cyclization, and reductive elimination (Scheme 8.69). This kind of chemistry has been disclosed and studied by the group of Kato, who called the process "cyclization–carbonylation–cyclization coupling" or "CCC coupling" [443–451]. A particular example is shown in Scheme 8.70 [447].

A double cyclization process may also take place with alkyne substrates functionalized with two nucleophilic groups in suitable position, with formation of complex molecular architectures in one synthetic step [452–458]. In particular, by this

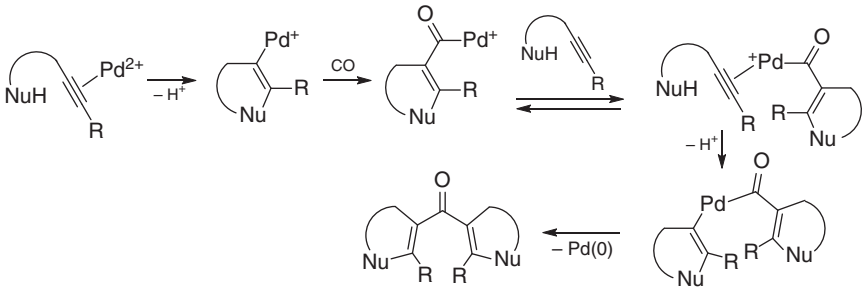

Scheme 8.69 Pd(II)-catalyzed cyclization–carbonylation–cyclization coupling (CCC coupling), leading to diaryl ketones.

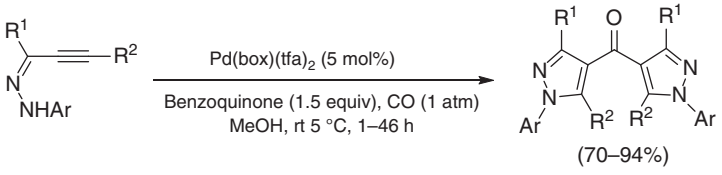

Scheme 8.70 Synthesis of di(1*H*-pyrazol-4-yl)ketones by the CCC coupling approach. Source: Modified from Kusakabe et al. [447].

approach, and employing the PdI_2/KI catalytic system, our research group was able to synthesize oxazolopyrimidines [452], dihydrofuroindolones [454], dihydrofurofuranones [455], furobenzofuranones [457], oxazinoquinolinones [458], and benzopyridopyrimidooxazinoquinolinediones [458], as exemplified in Scheme 8.71 for the synthesis of dihydrofurofuranones with anticancer activity [455] and of benzopyridopyrimidooxazinoquinolinediones [458].

Functionalized acetylenic derivatives may also be carbonylated under nonoxidative conditions. Scheme 8.72 shows, for example, an intramolecular additive aminocarbonylation, leading to medium-sized lactams, which occurs through triple-bond insertion into a Pd—H bond followed by isomerization, CO insertion, and intramolecular nucleophilic displacement [459].

Several examples of Pd(II)-catalyzed Pauson–Khand reaction have also be reported [460–462], and the mechanism of this process has been discussed in detail [463]. Scheme 8.73 shows as an example the synthesis of cyclopentenone derivatives from allylpropargyl ethers, *N*-tosyl allylpropargylamines, and diethyl 2-allyl-2-(prop-2-yn-1-yl)malonates under the catalysis of a palladacycle complex [462].

Of particular interest is the possibility to combine an oxidative carbonylation process with the reduction of a functional group present in the substrate, with formation of a single product formally corresponding to an additive or substitutive carbonylation. This may occur when the alkyne substrate possesses a functional group potentially reducible under the reaction conditions by the palladium hydride species ensuing from triple-bond oxidative carbonylation.

As shown in Scheme 8.74, a suitable functional group can be represented by a hydroxy group or an alkoxy group α to the triple bond, since the initially formed

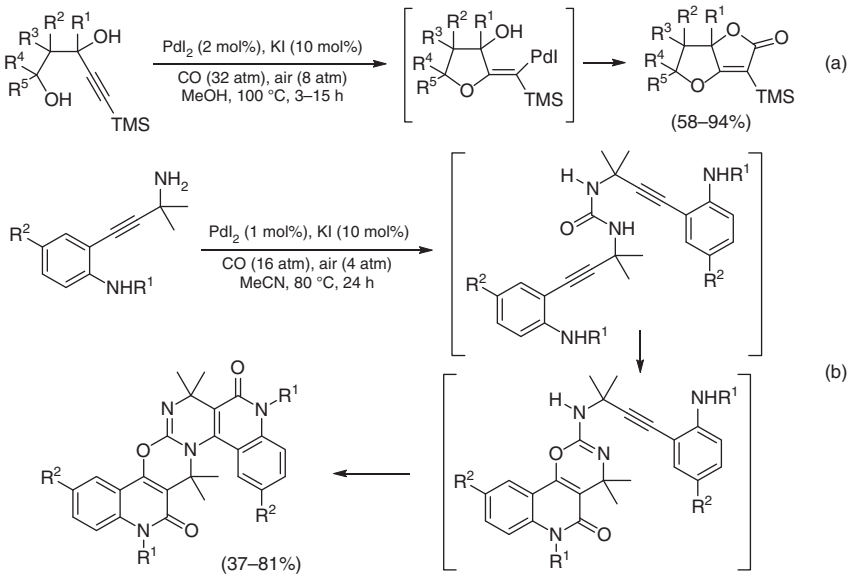

Scheme 8.71 Examples of PdI_2/KI-catalyzed oxidative carbonylative double cyclizations, leading to fused heterocycles: synthesis of (a) dihydrofurofuranone [455] and (b) benzopyridopyrimidooxazinoquinolinedione [458] derivatives. Source: (a) Modified from Mancuso et al. [455], (b) Modified from Pancrazzi et al. [458].

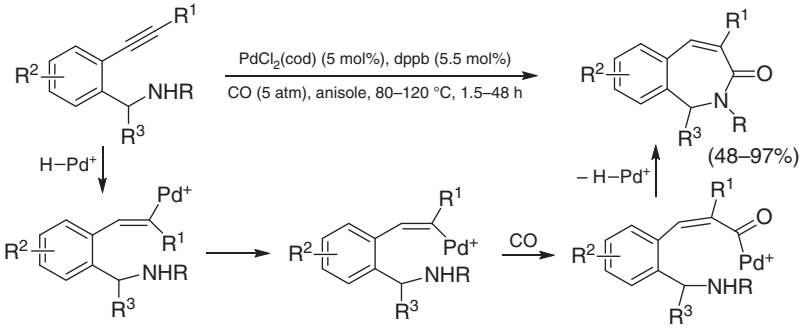

Scheme 8.72 Synthesis of ε-lactams by Pd(II)-catalyzed intramolecular additive carbonylation of 2-alkynylbenzyl amines. Source: Modified from Hu and Jiang [459].

maleic diester deriving from triple-bond oxidative dialkoxycarbonylation may react with Pd–H to give a π-allylpalladium intermediate [464], with simultaneous formation of water or an alcohol, respectively (see also Scheme 8.82; Section 8.6). Protonolysis of the complex then affords the final product with direct regeneration of the Pd(II) catalyst. This concept has been demonstrated in the conversion of 1,1′-(1,2-phenylene)bis(prop-2-yn-1-ol) into 2-(2-oxo-2,3-dihydronaphtho[1,2-*b*]furan-4-yl)acetate [465] and in the formation of diethyl (*E*)-2-(ethoxymethylene) succinate from 3,3-diethoxyprop-1-yne (Scheme 8.75) [466].

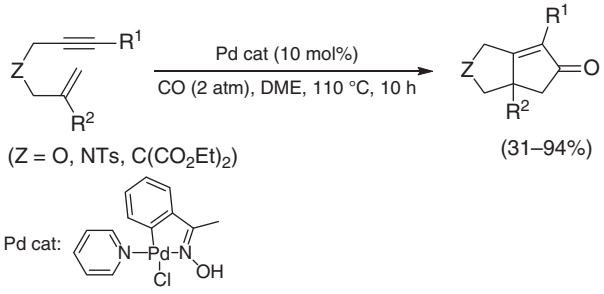

Scheme 8.73 Pd(II)-catalyzed Pauson–Khand reaction, leading to cyclopentenone derivatives. Source: Modified from Wang et al. [462].

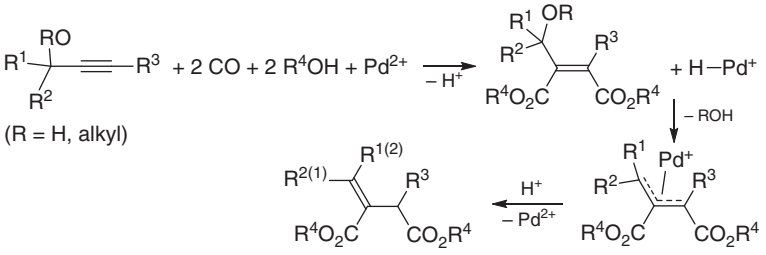

Scheme 8.74 Combination between triple-bond oxidative dialkoxycarbonylation and reduction of a propargylalcoholic or propargylethereal moiety within the same substrate, resulting in a formal substitutive carbonylation process.

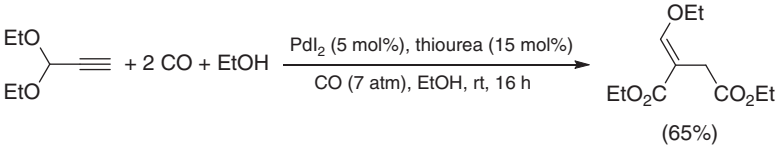

Scheme 8.75 Synthesis of diethyl (*E*)-2-(ethoxymethylene)succinate by formal substitutive carbonylation of 3,3-diethoxyprop-1-yne. Source: Modified from Bonardi et al. [466].

This concept was also further extended to the synthesis of important heterocyclic derivatives, that are, benzofurans [467–473], indoles [428], and coumarins [474, 475], starting from properly functionalized acyclic precursors. Scheme 8.76 shows, in particular, the synthesis of benzofuran derivatives [467–473] with antitumor activity [472, 473] from 1-(2-allyloxyphenyl)-2-yn-1-ols with internal triple bond, obtained *in situ* (owing to their instability at the pure state) by Pd(0)-catalyzed substrate deallylation. For the overall process, corresponding to a concatenation of two catalytic cycles promoted by the same metal (Pd) but in two different oxidation states (Pd(0) for deallylation; Pd(II) for carbonylation), in 2005, we coined the term "sequential homobimetallic catalysis" [467].

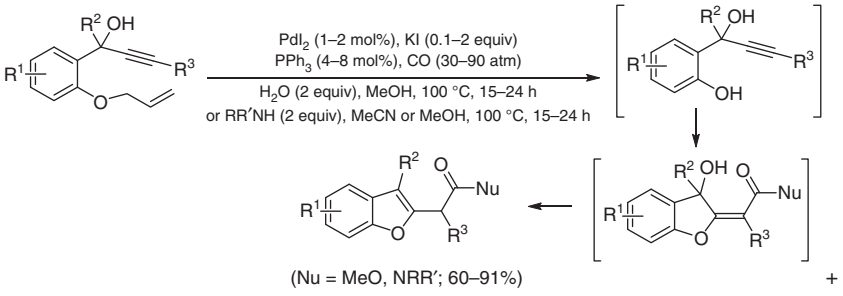

Scheme 8.76 Synthesis of benzofuran derivatives by sequential homobimetallic catalysis: Pd(0)-catalyzed deallylation of 1-(2-allyloxyphenyl)-2-yn-1-ols followed by formal substitutive carbonylation (oxidative carbonylative cyclization-reduction of the allylalcoholic moiety). Sources: Gabriele et al., Mancuso and Gabriele, Giordano et al., Iannazzo et al. [467–473].

8.6 Palladium(II)-Catalyzed Carbonylation of Other Substrates

Among the other substrates that can undergo a Pd(II)-catalyzed process, alcohols, phenols, and amines are surely the most important ones, owing to the significance, also at industrial level, of their carbonylation products.

The most important Pd(II)-catalyzed carbonylation processes of alcohols, phenols, and amines are oxidative carbonylations, which, depending on reaction conditions, may lead to different products, that are, carbonates, oxalates, ureas, oxamides, carbamates, and oxamates (Scheme 8.77) [476].

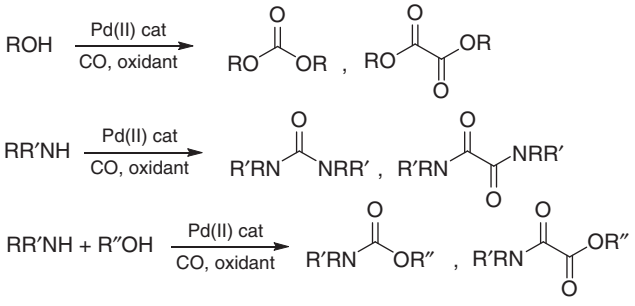

Scheme 8.77 Pd(II)-catalyzed oxidative carbonylation processes of alcohols and amines, leading to different carbonylated products. Source: Gabriele et al. [476].

The generally accepted mechanism for the formation of carbonates from alcohols involves the formation of an alkoxy-alkoxycarbonylpalladium complex followed by reductive elimination, as shown in Scheme 8.78. Further insertion of CO followed by reductive elimination may lead to oxalates under suitable conditions. A plethora of catalytic systems and reaction conditions have been used for optimizing the productivity and selectivity of the process, particularly for the synthesis of

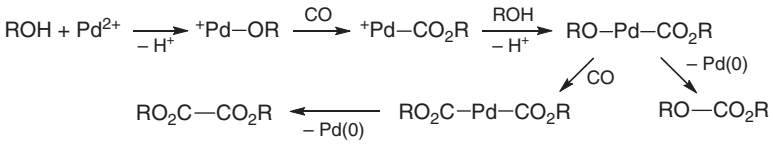

Scheme 8.78 Mechanistic pathways for the formation of carbonates and oxalates by Pd(II)-catalyzed oxidative carbonylation of alcohols.

highly industrially relevant dimethyl carbonate (DMC) [477, 478], diethyl carbonate (DEC) [479, 480], and diphenyl carbonate (DPC) [481], which are important industrial intermediates for the production of polycarbonates. The intramolecular version of the reaction, that is, the oxidative carbonylation of diols to give cyclic carbonates, is also of elevated practical importance [482–484] as it allows obtaining high-value-added products starting from readily available feedstocks, including glycerol carbonate from glycerin [482, 483], as exemplified in Scheme 8.79 [482].

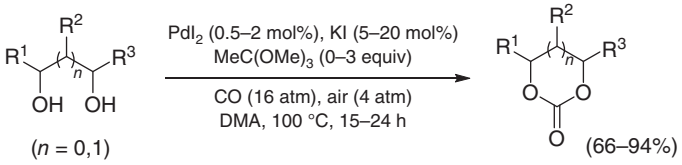

Scheme 8.79 Synthesis of cyclic carbonates by PdI_2/KI-catalyzed oxidative carbonylation of 1,2- and 1,3-diols. Source: Gabriele et al. [482].

Ureas are also very important carbonyl compounds, widely used as agrochemicals, dyes, antioxidants, resin precursors, antiviral agents (anti-HIV, in particular), and synthetic intermediates. The possibility to synthesize them by oxidative carbonylation of amines is particularly attractive. Also in this case, many different catalytic systems and reactions conditions have been employed so far to realize this important transformation [476]. To date, the most active catalytic system is Gabriele's catalyst (PdI_2 in conjunction with KI), employed in this process for the first time in 2003 [485]. With this catalyst, symmetrically disubstituted ureas were obtained from primary amines (Scheme 8.80a), while trisubstituted ureas were formed by carbonylation of a mixture of a primary amine and a secondary amine (Scheme 8.80b) through the intermediate formation of an isocyanate (the latter being obtained by β-H elimination from the initially formed carbamoylpalladium iodide complex; Scheme 8.80c) [485–488]. By employing this catalytic system in supercritical CO_2 as the solvent, aniline could be converted into diphenylurea (DPU) in 87% isolated yield and with an unprecedented TON of 43 500 (Scheme 8.80d) [487]. It should be mentioned at this point that, although recently it has been proposed that iron salts could act as (co)promoters for the PdI_2/KI-catalyzed oxidative carbonylation of aniline to DPU [489, 490], their real effect on the reaction has been questioned [491] and very recently demonstrated to be unimportant [492].

Under suitable conditions, a mixture of an alcohol and an amine may lead to carbamates [476], as shown in Scheme 8.81a [493]. The reaction is of particular

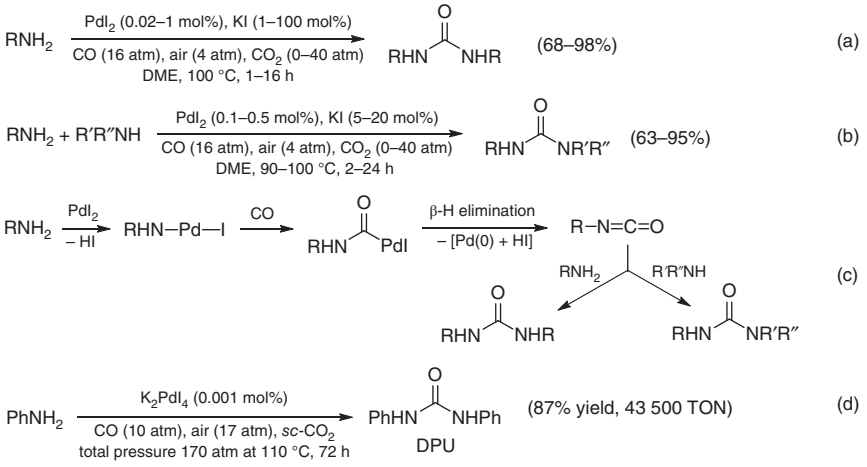

Scheme 8.80 PdI_2/KI-catalyzed oxidative carbonylation of (a) primary amines to give 1,3-disubstituted ureas. Sources: Adapted from Gabriele et al. [485, 486] and (b) primary amines in the presence of secondary amines to give trisubstituted ureas. Sources: Adapted from Gabriele et al. [485, 486]. (c) Proposed reaction mechanism. Source: Adapted from Gabriele et al. [486]. (d) Oxidative carbonylation of aniline in supercritical CO_2 to give DPU with a TON of 43 500. Source: Modified from Della Ca' et al. [487].

industrial interest, since carbamates are useful intermediates for the production of polyurethanes. When applied to β-amino alcohols, the intramolecular process leads to oxazolidin-2-ones [476], which are important intermediates in organic synthesis and compounds characterized by a high bioactivity (in particular, antimicrobial [497] and antitumor [391] activities). Also in this case, the PdI_2/KI catalytic system has proved to be an efficient catalyst for promoting this transformation (Scheme 8.81b) [494–496].

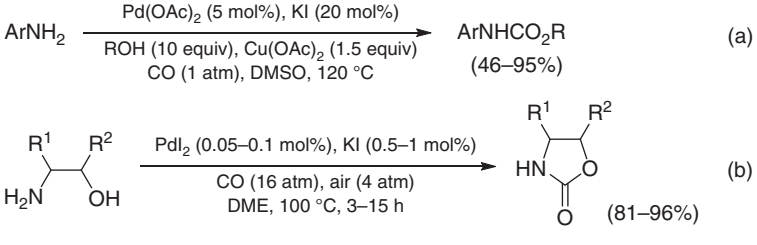

Scheme 8.81 (a) Synthesis of carbamates by $Pd(OAc)_2$/KI-catalyzed oxidative alkoxycarbonylation of amines. Source: Modified from Guan et al. [493] and (b) synthesis of 2-oxazolidinones by PdI_2/KI-catalyzed oxidative carbonylation of β-amino alcohols. Sources: Gabriele et al., Mancuso et al. [494–496].

Recently, the group of Beller has reported the possibility to alkoxycarbonylate secondary, tertiary, and benzylic alcohols [498] as well as secondary benzylic ethers [499] in the presence of an *in situ* generated palladium hydride catalyst. These reactions are believed to proceed through the initial formation of olefins, which then undergo additive alkoxycarbonylation as shown in Section 8.4.1.

In the presence of palladium hydride species, again obtained *in situ* under the reaction conditions, allyl alcohols may undergo direct or substitutive carbonylation with formation of β,γ-unsaturated acids or esters, respectively, through the formation of a π-allylpalladium complex with elimination of water followed by hydroxy- or alkoxycarbonylation (Scheme 8.82a). The reaction was disclosed by Gabriele et al. in 1996 [464], and, since then, only a few examples of successful realization of this process have been reported in the literature [500]. Scheme 8.82b shows, in particular, the use of PdI_2 in the presence of thiourea (tu) as ligand as an efficient catalyst precursor for the reaction, which has also allowed the synthesis of high-valued-added dimethyl hex-3-ene-1,6-dioate (a precursor of adipic acid, used for the production of nylon 6,6) from but-2-ene-1,4-diol (Scheme 8.82c) [464].

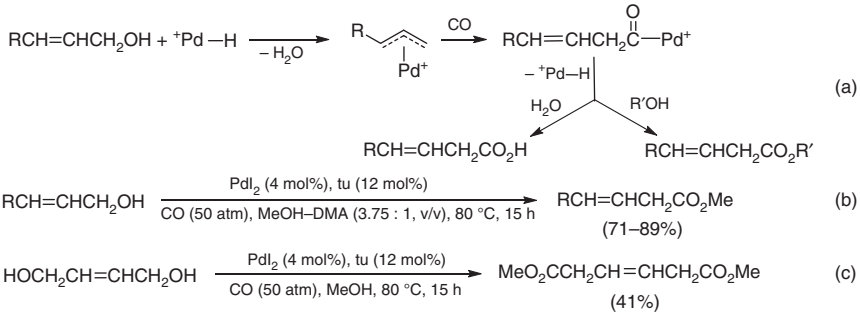

Scheme 8.82 (a) Mechanism of the palladium-catalyzed direct and substitutive carbonylation of allyl alcohols to give β,γ-unsaturated acids or esters, respectively. (b) PdI_2/thiourea-catalyzed substitutive carbonylation of allyl alcohols to β,γ-unsaturated esters. (c) PdI_2/thiourea-catalyzed substitutive carbonylation of but-2-ene-1,4-diol to dimethyl hex-3-ene-1,6-dioate. Source: Modified from Gabriele et al. [464].

8.7 Summary and Conclusions

In this chapter, we have described the most important carbonylation processes catalyzed by Pd(II) species with CO as the carbonylating agent. Paradigmatic examples of different types of mechanistic pathways leading to carbonylated products have been presented and discussed, with a particular emphasis on oxidative carbonylations, for which Pd(II) is the most important catalyst.

In the course of the last decades, Pd(II)-based catalysts have proved to be particularly efficient and versatile and have allowed the realization of very important synthetic transformations, for the production of industrially relevant carbonylated compounds and of fine chemicals (heterocyclic derivatives in particular). The modulation of the catalyst composition (Pd source, ligand, additives) associated to the optimization of the reaction conditions have result in achieving important processes in one synthetic step, which otherwise would have required much more complex synthetic routes. Moreover, the use of suitably functionalized substrates, combined with Pd(II) activity and functional group compatibility, has permitted the direct formation of complex molecular architectures in one step from relatively simple substrates.

This clearly presents positive implications toward the development of greener and more sustainable synthetic processes, as required by modern chemistry.

On these grounds, it is clear the Pd(II)-catalyzed carbonylation is expected to continue to play a leading role in this fascinating area of synthesis, making use of the simplest C-1 unit as the key building block for introducing, in the final product, what is considered to be the most important and versatile functional group in organic chemistry, i.e. the carbonyl group.

References

1 It is very important to point out that, unfortunately, many metal-catalyzed (including palladium-catalyzed) oxidative carbonylation processes reported in the literature (even among the most recent ones) that employ molecular oxygen as external oxidant have been carried out using $CO–O_2$ compositions that fall within the explosion limits for $CO–O_2$ mixtures. The flammability range, as reported by Bartish, C.M. and Drissel, G.M. (1978). *Kirk-Othmer Encyclopedia of Chemical Technology*, 3rd ed., vol. 4 (eds. M. Grayson, D. Eckroth, G.J. Bushey, et al.), 774. New York: Wiley, is 16.7–93.5% at room temperature and it becomes even larger at higher temperatures.

2 Fujiwara, Y., Takaki, K., Watanabe, J. et al. (1989). *Chem. Lett.*: 1687–1688.

3 Nakata, K., Watanabe, J., Takaki, K., and Fujiwara, Y. (1991). *Chem. Lett.*: 1437–1438.

4 Satoh, K. -i., Watanabe, J., Takaki, K., and Fujiwara, Y. (1991). *Chem. Lett.*: 1433–1436.

5 Nishiguchi, T., Nakata, K., Takaki, K., and Fujiwara, Y. (1992). *Chem. Lett.*: 1141–1142.

6 Kurioka, M., Nakata, K., Jintoku, T. et al. (1995). *Chem. Lett.*: 244–244.

7 Nakata, K., Miyata, T., Jintoku, T. et al. (1993). *Bull. Chem. Soc. Jpn.* 66: 3755–3759.

8 Periana, R.A., Mironov, O., Taube, D. et al. (2005). *Top. Catal.* 32: 169–174.

9 Lu, L., Shi, R., Liu, L. et al. (2016). *Chem. Eur. J.* 22: 14484–14488.

10 Liu, H., Laurenczy, G., Yan, N., and Dyson, P.J. (2014). *Chem. Commun.* 50: 341–343.

11 Xie, P., Xie, Y., Qian, B. et al. (2012). *J. Am. Chem. Soc.* 134: 9902–9905.

12 Xie, P., Xia, C., and Huang, H. (2013). *Org. Lett.* 15: 3370–3373.

13 Chen, H., Cai, C., Liu, X. et al. (2011). *Chem. Commun.* 47: 12224–12226.

14 Tanaka, K., Ewig, W.R., and Yu, J.-Q. (2019). *J. Am. Chem. Soc.* 141: 15494–15497.

15 Yoo, E.J., Wasa, M., and Yu, J.-Q. (2010). *J. Am. Chem. Soc.* 132: 17378–17380.

16 McNally, A., Haffemayer, B., Collins, B.S.L., and Gaunt, M.J. (2014). *Nature* 510: 129–133.

17 Li, S., Chen, G., Feng, C.-G. et al. (2014). *J. Am. Chem. Soc.* 136: 5267–5270.

18 Wang, P.-L., Li, Y., Wu, Y. et al. (2015). *Org. Lett.* 17: 3698–3701.

19 Wang, C., Zhang, L., Chen, C. et al. (2015). *Chem. Sci.* 6: 4610–4614.

20 Calleja, J., Pla, D., Gorman, T.W. et al. (2015). *Nat. Chem.* 7: 1009–1016.
21 Hernando, E., Villalva, J., Martínez, A.M. et al. (2016). *ACS Catal.* 6: 6868–6882.
22 Willcox, D., Chappell, B.G.N., Hogg, K.F. et al. (2016). *Science* 354: 851–857.
23 Cabrera-Pardo, J.R., Trowbridge, A., Nappi, M. et al. (2017). *Angew. Chem. Int. Ed.* 56: 11958–11962.
24 Hogg, K.F., Trowbridge, A., Alvarez-Pérez, A., and Gaunt, M.J. (2017). *Chem. Sci.* 8: 8198–8203.
25 Png, Z.M., Cabrera-Pardo, J.R., Cadahía, J.P., and Gaunt, M.J. (2018). *Chem. Sci.* 9: 7628–7633.
26 Ho, D.K.H., Calleja, J., and Gaunt, M.J. (2019). *Synlett* 30: 454–458.
27 Fujiwara, Y., Kawauchi, T., and Taniguchi, H. (1980). *J. Chem. Soc., Chem. Commun.*: 220–221.
28 Fujiwara, Y., Kawata, I., Kawauchi, T., and Taniguchi, H. (1982). *J. Chem. Soc., Chem. Commun.*: 132–133.
29 Arzoumadinis, G.G. and Rauch, F.C. (1980). *J. Mol. Catal.* 9: 335–338.
30 Itahara, T. (1982). *Chem. Lett.*: 1151–1152.
31 Itahara, T. (1983). *Chem. Lett.*: 127–128.
32 Fujiwara, Y., Kawata, I., Sugimoto, H., and Taniguchi, H. (1983). *J. Organomet. Chem.* 256: C35–C36.
33 Jintoku, T., Tanigichi, H., and Fujiwara, Y. (1987). *Chem. Lett.*: 1159–1162.
34 Ugo, R. and Chiesa, A. (1987). *J. Chem. Soc., Perkin Trans. 1*: 2625–2629.
35 Jintoku, T., Fujiwara, Y., Kawata, T. et al. (1990). *J. Organomet. Chem.* 385: 297–306.
36 Taniguchi, Y., Yamaoka, Y., Nakata, K. et al. (1995). *Chem. Lett.*: 345–346.
37 Fujiwara, Y., Takaki, K., and Taniguchi, Y. (1996). *Synlett*: 591–599.
38 Lu, W., Yamaoka, Y., Taniguchi, Y. et al. (1999). *J. Organomet. Chem.* 580: 290–294.
39 Kalinovskii, I.O., Pogorelov, V.V., Gelbshtein, A.I., and Akhmetov, N.G. (2001). *Russ. J. Gen. Chem.* 71: 1457–1462.
40 Kalinovskii, I.O., Gel'bshtein, A.I., and Pogorelov, V.V. (2001). *Russ. J. Gen. Chem.* 71: 1463–1466.
41 Behn, A., Zakzeski, J., Head-Gordon, M., and Bell, A.T. (2012). *J. Mol. Catal. A: Chem.* 361, 362: 91–97.
42 Zhang, H., Liu, D., Chen, C. et al. (2011). *Chem. Eur. J.* 17: 9581–9585.
43 Lang, R., Shi, L., Li, D. et al. (2012). *Org. Lett.* 14: 4130–4133.
44 Ohashi, S., Sakaguchi, S., and Ishii, Y. (2005). *Chem. Commun.*: 486–488.
45 Giri, R. and Yu, J.-Q. (2008). *J. Am. Chem. Soc.* 130: 14082–14083.
46 Houlden, C.E., Hutchby, M., Bailey, C.D. et al. (2009). *Angew. Chem. Int. Ed.* 48: 1830–1833.
47 Giri, R., Lam, J.K., and Yu, J.-Q. (2010). *J. Am. Chem. Soc.* 132: 686–693.
48 Li, H., Cai, G.-X., and Shi, Z.-J. (2010). *Dalton Trans.* 39: 10442–10446.
49 Liu, B. and Shi, B.-F. (2013). *Synlett*: 2274–2278.
50 Liu, B., Jiang, H.-Z., and Shi, B.-F. (2014). *Org. Biomol. Chem.* 12: 2538–2542.

51 Chen, M., Ren, Z.-H., Wang, Y.-Y., and Guan, Z.-H. (2015). *J. Org. Chem.* 80: 1258–1263.
52 Li, W., Duan, Z., Jiang, R., and Lei, A. (2015). *Org. Lett.* 17: 1397–1400.
53 Zhang, X., Dong, S., Niu, X. et al. (2016). *Org. Lett.* 18: 4634–4637.
54 Wang, Y. and Gevorgyan, V. (2017). *Angew. Chem. Int. Ed.* 56: 3191–3195.
55 Yin, D.-W. and Liu, G. (2018). *J. Org. Chem.* 83: 3987–4001.
56 Orito, K., Horibata, A., Nakamura, T. et al. (2004). *J. Am. Chem. Soc.* 126: 14342–14343.
57 Orito, K., Miyazawa, M., Nakamura, T. et al. (2006). *J. Org. Chem.* 71: 5951–5958.
58 Haffemayer, B., Gulias, M., and Gaunt, M.J. (2011). *Chem. Sci.* 2: 312–315.
59 Ma, B., Wang, Y., Peng, Y., and Zhu, Q. (2011). *J. Org. Chem.* 76: 6362–6366.
60 López, B., Rodríguez, A., Santos, D. et al. (2011). *Chem. Commun.* 47: 1054–1056.
61 Dai, H.-X., Stepan, A.F., Plummer, M.S. et al. (2011). *J. Am. Chem. Soc.* 126: 7222–7228.
62 Wrigglesworth, J.W., Cox, B., Lloyd-Jones, G.C., and Booker-Milburn, K.I. (2011). *Org. Lett.* 13: 5326–5329.
63 Lu, Y., Leow, D., Wang, X. et al. (2011). *Chem. Sci.* 2: 967–971.
64 Kumazawa, E., Tokuhashi, T., Horibata, A. et al. (2012). *Eur. J. Org. Chem.*: 4622–4633.
65 Guan, Z.-H., Chen, M., and Ren, Z.-H. (2012). *J. Am. Chem. Soc.* 134: 17490–17493.
66 Liang, D., Hu, Z., Peng, J. et al. (2013). *Chem. Commun.* 49: 173–175.
67 Rajeshkumar, V., Lee, T.-H., and Chuang, S.-C. (2013). *Org. Lett.* 15: 1468–1471.
68 Luo, S., Luo, F.-X., Zhang, X.-S., and Shi, Z.-J. (2013). *Angew. Chem. Int. Ed.* 52: 10598–10601.
69 Lee, T.-H., Jayakumar, J., Cheng, C.-H., and Chuang, S.-C. (2013). *Chem. Commun.* 49: 11797–11799.
70 Shun, S., Jeong, Y., Jeon, W.H., and Lee, P.H. (2014). *Org. Lett.* 16: 2930–2933.
71 Ji, F., Li, X., Wu, W., and Jiang, H. (2014). *J. Org. Chem.* 79: 11246–11253.
72 Liang, D., He, Y., and Zhu, Q. (2014). *Org. Lett.* 16: 2748–2751.
73 Xu, Y., Hu, W., Tang, X. et al. (2015). *Chem. Commun.* 51: 6843–6846.
74 Chen, J., Feng, J.-B., Natte, K., and Wu, X.-F. (2015). *Chem. Eur. J.* 21: 16370–16373.
75 Chen, J., Natte, K., and Wu, X.-F. (2015). *Tetrahedron Lett.* 56: 6413–6416.
76 Taneda, H., Inamoto, K., and Kondo, Y. (2016). *Org. Lett.* 18: 2712–2715.
77 Wang, P.-L., Li, Y., Ma, L. et al. (2016). *Adv. Synth. Catal.* 358: 1048–1053.
78 Shi, R., Lu, L., Xie, H. et al. (2016). *Chem. Commun.* 52: 13307–13310.
79 Xie, Z., Luo, S., and Zhu, Q. (2016). *Chem. Commun.* 52: 12873–12876.
80 Fox, J.C., Gilligan, R.E., Pitts, A.K. et al. (2016). *Chem. Sci.* 7: 2706–2710.
81 Shi, R., Nius, H., Lu, L., and Lei, A. (2017). *Chem. Commun.* 53: 1908–1911.
82 Wang, Z., Yin, Z., Zhu, F. et al. (2017). *ChemCatChem* 9: 3637–3640.
83 Wang, Z., Zhu, F., Li, Y., and Wu, X.-F. (2017). *ChemCatChem* 9: 94–98.
84 Guo, S., Wang, F., Sun, L. et al. (2018). *Adv. Synth. Catal.* 360: 2537–2545.

85 Chandrasekhar, A., Ramkumar, S., and Sankararaman, S. (2018). *Org. Biol. Chem.* 16: 8629–8638.
86 Yang, R., Yu, J.-T., Sun, S., and Cheng, J. (2018). *Org. Chem. Front.* 5: 962–966.
87 Zhang, C., Ding, Y., Gao, Y. et al. (2018). *Org. Lett.* 20: 2595–2598.
88 Cheng, X.-F., Wang, T., Li, Y. et al. (2018). *Org. Lett.* 20: 6530–6533.
89 Pérez-Gómez, M., Hernández-Ponte, S., García-López, A. et al. (2018). *Organometallics* 37: 4648–4663.
90 Bai, X.-F., Mu, Q.-C., Xu, Z. et al. (2019). *ACS Catal.* 9: 1431–1436.
91 Fu, L.-Y., Ying, J., Qi, X. et al. (2019). *J. Org. Chem.* 84: 1421–1429.
92 Zhang, X., Li, Z., Ding, Q. et al. (2019). *Adv. Synth. Catal.* 361: 976–982.
93 Mu, Q.-C., Nie, Y.-X., Bai, X.-F. et al. (2019). *Chem. Sci.* 10: 9292–9301.
94 Ying, J., Gao, Q., and Wu, X.-F. (2019). *J. Org. Chem.* 84: 14297–14305.
95 Han, H., Zhang, T., Yang, S.-D. et al. (2019). *Org. Lett.* 21: 1749–1754.
96 Chandrasekhar, A. and Sankararaman, S. (2020). *Org. Biomol. Chem.* 18: 1612–1622.
97 Li, W., Duan, Z., Zhang, X. et al. (2015). *Angew. Chem. Int. Ed.* 54: 1893–1896.
98 Zhang, H., Shi, R., Gan, P. et al. (2012). *Angew. Chem. Int. Ed.* 51: 5204–5207.
99 Wen, J., Tang, S., Zhang, F. et al. (2017). *Org. Lett.* 19: 94–97.
100 Liao, F., Shi, R., Sha, Y. et al. (2017). *Chem. Commun.* 53: 4354–4357.
101 Feng, M., Tang, B., Xu, H.-X., and Jiang, X. (2016). *Org. Lett.* 18: 4352–4355.
102 Shi, R., Lu, L., Zhang, H. et al. (2013). *Angew. Chem. Int. Ed.* 52: 10582–10585.
103 Chen, J., Natte, K., Spannenberg, A. et al. (2014). *Chem. Eur. J.* 20: 14189–14193.
104 Li, S., Li, F., Gong, J., and Yang, Z. (2015). *Org. Lett.* 17: 1240–1243.
105 Chen, J., Natte, K., and Wu, X.-F. (2016). *J. Organomet. Chem.* 803: 9–12.
106 Liu, J., Wei, Z., Jiao, H. et al. (2018). *ACS Cent. Sci.* 4: 30–38.
107 Sharma, P. (2011). *J. Chem. Pharm. Res.* 3: 403–423.
108 Yukawa, T. and Tsutsumi, S. (1969). *J. Org. Chem.* 34: 738–740.
109 Cometti, G. and Chiusoli, G.P. (1979). *J. Organomet. Chem.* 181: C14–C16.
110 El'man, A.R., Boldyreva, O.V., Slivinskii, E.V., and Loktev, S.M. (1992). *Russ. Chem. Bull.* 41: 435–438.
111 Bianchini, C., Mantovani, G., Meli, A. et al. (2001). *J. Chem. Soc., Dalton Trans.*: 690–698.
112 Bianchini, C., Meli, A., Oberhauser, W. et al. (2004). *J. Mol. Catal. A: Chem.* 224: 35–49.
113 Malkov, A.V., Derrien, N., Barłog, M., and Kočovský, P. (2014). *Chem. Eur. J.* 20: 4542–4547.
114 Wang, L., Wang, Y., Liu, C., and Lei, A. (2014). *Angew. Chem. Int. Ed.* 53: 5657–5661.
115 Chen, M., Yu, L., Ren, Z.-H. et al. (2017). *Chem. Commun.* 53: 6243–6246.
116 Maffei, M., Giacoia, G., Mancuso, R. et al. (2017). *J. Mol. Catal. A: Chem.* 426: 435–443.
117 Jamarani, R., Erythropel, H.C., Burkat, D. et al. (2017). *Processes* 5: 43–56.
118 Stuart, A., Le Captain, D.J., Lee, C.Y., and Mohanty, D.K. (2013). *Eur. Polym. J.* 49: 2785–2791.

119 Jiang, Y., Woortman, A.J.J., van Ekenstein, G.O.R.A., and Loos, K. (2013). *Biomolecules* 3: 461–480.
120 Fenton, D.M. and Steinwand, P.J. (1972). *J. Org. Chem.* 37: 2034–2035.
121 Heck, R.F. (1972). *J. Am. Chem. Soc.* 94: 2712–2716.
122 James, D.E., Hines, L.F., and Stille, J.K. (1976). *J. Am. Chem. Soc.* 98: 1806–1809.
123 James, D.E. and Stille, J.K. (1976). *J. Am. Chem. Soc.* 98: 1810–1823.
124 Stille, J.K. and Divakaruni, R.J. (1979). *J. Org. Chem.* 44: 3474–3482.
125 Bréchot, P., Chauvin, Y., Commereuc, D., and Saussine, L. (1990). *Organometallics* 9: 26–30.
126 Toda, S., Miyamoto, M., Kinoshita, H., and Inomata, K. (1991). *Bull. Chem. Soc. Jpn.* 64: 3600–3606.
127 Pisano, C., Nefkens, S.C.A., and Consiglio, G. (1992). *Organometallics* 11: 1975–1978.
128 Nefkens, S.C.A., Sperrle, M., and Consiglio, G. (1993). *Angew. Chem. Int. Ed.* 32: 1719–1720.
129 Sperrle, M. and Consiglio, G. (1996). *J. Organomet. Chem.* 506: 177–180.
130 Hayashi, M., Takezaki, H., Hashimoto, Y. et al. (1998). *Tetrahedron Lett.* 39: 7529–7532.
131 Sperrle, M. and Consiglio, G. (1999). *J. Mol. Catal. A: Chem.* 143: 263–277.
132 Sperrle, M. and Consiglio, G. (2000). *Inorg. Chim. Acta* 300–302: 264–271.
133 Bianchini, C., Lee, H.M., Mantovani, G. et al. (2002). *New J. Chem.* 26: 387–397.
134 Takeuchi, S., Ukaji, Y., and Inomata, K. (2001). *Bull. Chem. Soc. Jpn.* 74: 955–958.
135 Yokota, T., Sakaguchi, S., and Ishii, Y. (2002). *J. Org. Chem.* 67: 5005–5008.
136 Wang, L., Kwok, W., Wu, J. et al. (2003). *J. Mol. Catal. A: Chem.* 196: 171–178.
137 Aratani, T., Tahara, K., Takeuchi, S. et al. (2007). *Chem. Lett.* 37: 1328–1329.
138 Gao, Y.-X., Chang, L., Shi, H. et al. (2010). *Adv. Synth. Catal.* 352: 1955–1966.
139 Hamed, O., Henry, P.M., and Becker, D.P. (2010). *Tetrahedron Lett.* 51: 3514–3517.
140 Aratani, T., Tahara, K., Takeuchi, S. et al. (2012). *Bull. Chem. Soc. Jpn.* 85: 1225–1232.
141 Cavinato, G., Facchetti, S., and Toniolo, L. (2012). *J. Mol. Catal. A: Chem.* 352: 63–69.
142 Fini, F., Beltrani, M., Mancuso, R. et al. (2015). *Adv. Synth. Catal.* 357: 177–184.
143 Cho, Y.J., Lim, Y.N., Yoon, W. et al. (2017). *Eur. J. Org. Chem.*: 1139–1142.
144 Olivieri, D., Fini, F., Mazzoni, R. et al. (2018). *Adv. Synth. Catal.* 360: 3507–3517.
145 Olivieri, D., Tarroni, R., Della Ca', N. et al. (2020). *Adv. Synth. Catal.* 362: 533–544.
146 Phan, N.H.T., Furuya, T., Soeta, T., and Ukaji, Y. (2016). *Chem. Lett.* 45: 1431–1433.
147 Tsuji, J. (1969). *Acc. Chem. Res.* 2: 144–152.
148 Hegedus, L.S. and Darlington, W.H. (1980). *J. Am. Chem. Soc.* 102: 4980–4983.
149 Urata, H., Fujita, A., and Fuchikami, T. (1988). *Tetrahedron Lett.* 29: 4435–4436.

150 Wieber, G.M., Hegedus, L.S., Åkermark, B., and Michalson, E.T. (1989). *J. Org. Chem.* 54: 4649–4653.

151 Tsuji, J. (1990). *Synthesis*: 139–149.

152 Cheng, J., Qi, X., Li, M. et al. (2015). *J. Am. Chem. Soc.* 137: 2480–2483.

153 Li, M., Yu, F., Qi, X. et al. (2016). *Angew. Chem. Int. Ed.* 55: 13843–13848.

154 Qi, X., Yu, F., Chen, P., and Liu, G. (2017). *Angew. Chem. Int. Ed.* 56: 12692–12696.

155 Li, M., Yu, F., Chen, P., and Liu, G. (2017). *J. Org. Chem.* 82: 11682–11690.

156 Reppe, W. (1939). Verfahren zur Herstellung von Acrylsaeure oder ihren Substitutionserzeugnissen. German Patent 855110. IG Farben, filed 02 August 1939 and filed 10 November 1952.

157 Kiss, G. (2001). *Chem. Rev.* 101: 3435–3456.

158 Sarkar, B.R. and Chaudhari, R.V. (2005). *Catal. Surv. Asia* 9: 193–205.

159 Brennführer, A., Neumann, H., and Beller, M. (2009). *ChemCatChem* 1: 29–41.

160 Wu, X.-F., Fang, X., Wu, L. et al. (2014). *Acc. Chem. Res.* 47: 1041–1053.

161 Tullo, A.H. (2009). *Chem. Eng. News* 87: 22–23.

162 Tooze, R.P., Eastham, G.R., Whiston, K., Wang, X. (1996). Process for the Carbonylation of Ethylene and Catalyst System for Use Therein, International Patent Application WO 96/19434. Imperial Chemical Industries PLC, UK, filed 22 December 1994 and 27 June 1996.

163 Clegg, W., Eastham, G.R., Elsegood, M.R.J. et al. (1999). *Chem. Commun.*: 1877–1878.

164 Ferreira, A.C., Crous, R., Bennie, L. et al. (2007). *Angew. Chem. Int. Ed.* 46: 2273–2275.

165 García-Suárez, E.J., Khokarale, S.G., van Buu, O.N. et al. (2014). *Green Chem.* 16: 161–166.

166 Dong, K., Fang, X., Gülak, S. et al. (2017). *Nat. Commun.* 8: 14117.

167 Dong, K., Sang, R., Fang, X. et al. (2017). *Angew. Chem. Int. Ed.* 56: 5267–5271.

168 Drent, E. and Budzelaar, H.M. (1996). *Chem. Rev.* 96: 663–681.

169 Bianchini, C. and Meli, A. (2002). *Coord. Chem. Rev.* 225: 35–66.

170 Durand, J. and Milani, B. (2006). *Coord. Chem. Rev.* 250: 542–560.

171 Vavasori, A., Dell'Acqua, F., Cavinato, G., and Toniolo, L. (2010). *J. Mol. Catal. A: Chem.* 332: 158–164.

172 Wu, X.-F., Neumann, H., and Beller, M. (2012). *Chem. Asian J.* 7: 1199–1202.

173 Carfagna, C., Gatti, G., Paoli, P. et al. (2014). *Organometallics* 33: 129–144.

174 Vogelsang, D., Dittmar, M., Seidensticker, T., and Vorholt, A.J. (2018). *Catal. Sci. Technol.* 8: 4332–4337.

175 Frew, J.J.R., Clarke, M.L., Mayer, U. et al. (2008). *Dalton Trans.*: 1976–1978.

176 Estorach, C.T. and Masdeu-Bultó, A.M. (2008). *Catal. Lett.* 122: 76–79.

177 Frew, J.J.R., Damian, K., Van Rensburg, H. et al. (2009). *Chem. Eur. J.* 15: 10504–10513.

178 Konrad, T.M., Fuentes, J.A., Slawin, A.M.Z., and Clarke, M.L. (2010). *Angew. Chem. Int. Ed.* 49: 9197–9200.

179 Fuentes, J.A., Slawin, A.M.Z., and Clarke, M.L. (2012). *Catal. Sci. Technol.* 2: 715–718.

180 Roberts, G.M., Pierce, P.J., and Woo, L.K. (2013). *Organometallics* 32: 2033–2036.

181 Fang, X., Jackstell, R., and Beller, M. (2013). *Angew. Chem. Int. Ed.* 52: 14089–14093.

182 Liu, H., Yan, N., and Dyson, P.J. (2014). *Chem. Commun.* 50: 7848–7851.

183 Pews-Davtyan, A., Fang, X., Jackstell, R. et al. (2014). *Chem. Asian J.* 9: 1168–1174.

184 Pruvost, R., Boulanger, J., Léger, B. et al. (2014). *ChemSusChem* 7: 3157–3163.

185 Amézquita-Valencia, M., Achonduh, G., and Alper, H. (2015). *J. Org. Chem.* 80: 6419–6424.

186 Li, H., Dong, K., Neumann, H., and Beller, M. (2015). *Angew. Chem. Int. Ed.* 54: 10239–10243.

187 Tshabalala, T.A., Ojwach, S.O., and Akerman, M.A. (2015). *J. Mol. Catal. A: Chem.* 406: 178–184.

188 Holzapfel, C. and Bredenkamp, T. (2015). *ChemCatChem* 7: 2598–2606.

189 Fuentes, J.A., Durrani, J.T., Leckie, S.M. et al. (2016). *Catal. Sci. Technol.* 6: 7477–7485.

190 Gaide, T., Behr, A., Arns, A. et al. (2016). *Chem. Eng. Process.* 99: 197–204.

191 Zhang, G., Ji, X., Yu, H. et al. (2016). *Tetrahedron Lett.* 57: 383–386.

192 Mgaya, J.E., Barlett, S.A., Mubofu, E.B. et al. (2016). *ChemCatChem* 8: 751–757.

193 Liu, J., Li, H., Spannenberg, A. et al. (2016). *Angew. Chem. Int. Ed.* 55: 13544–13548.

194 Li, H., Dong, K., Jiao, H. et al. (2016). *Nat. Chem.* 8: 1159–1166.

195 Goldbach, V., Falivene, L., Caporaso, L. et al. (2016). *ACS Catal.* 6: 8229–8238.

196 Hirschbeck, V. and Fleischer, I. (2016). *J. Am. Chem. Soc.* 138: 16794–16799.

197 Nobbs, J.D., Low, C.H., Stubbs, L.P. et al. (2017). *Organometallics* 36: 391–398.

198 Bredenkamp, T. and Holzapfel, C. (2017). *Catal. Commun.* 96: 74–78.

199 Zhao, L., Pudasaini, B., Genest, A. et al. (2017). *ACS Catal.* 7: 7070–7080.

200 Gao, B., Zhang, G., Zhou, X., and Huang, H. (2018). *Chem. Sci.* 9: 380–386.

201 Tshabalala, T.A. and Ojwach, S.O. (2018). *Transition Met. Chem.* 43: 339–346.

202 Zhou, X., Zhang, G., Gao, B., and Huang, H. (2018). *Org. Lett.* 20: 2208–2212.

203 Huang, Z., Cheng, Y., Chen, X. et al. (2018). *Chem. Commun.* 54: 3967–3970.

204 Liu, J., Dong, K., Franke, R. et al. (2018). *Chem. Commun.* 54: 12238–12241.

205 Sang, R., Kucmierczyk, P., Düren, R. et al. (2019). *Angew. Chem. Int. Ed.* 58: 14365–14373.

206 Wang, X., Wang, B., Yin, X. et al. (2019). *Angew. Chem. Int. Ed.* 58: 12264–12270.

207 Akiri, S.O. and Ojwach, S.O. (2019). *Inorg. Chim. Acta* 489: 236–243.

208 Liu, J., Yang, J., Ferretti, F. et al. (2019). *Angew. Chem. Int. Ed.* 58: 4690–4694.

209 Vavasori, A., Bravo, S., Pasinato, F. et al. (2020). *Mol. Catal.* 484: 110742.

210 Lang, W.-Y., Liu, L., Zhou, Q. et al. (2020). *Mol. Catal.* 482: 110221.

211 Zulu, Z., Nyamato, G.S., Tshabalala, T.A., and Ojwach, S.O. (2020). *Inorg. Chim. Acta* 501: 119270.

212 Söderberg, B.C., Åkermark, B., and Hall, S.S. (1988). *J. Org. Chem.* 53: 2925–2937.

213 Drent, E. (1988). Process for the selective oxidative carbonylation of conjugated dienes. European Patent Application 275591A2, filed 24 December 1986 and 30 June 1988.

214 Fergusson, S.B. and Alper, H. (1986). *J. Mol. Catal.* 34: 381–384.

215 Yang, L., Liu, J., Neumann, H. et al. (2019). *Science* 366: 1514–1517.

216 Li, H., Fang, X., Jackstell, R. et al. (2016). *Chem. Commun.* 52: 7142–7145.

217 Tsuji, J. and Susuki, T. (1965). *Tetrahedron Lett.*: 3027–3031.

218 Alper, H., Hartstock, F.W., and Despeyroux, B. (1984). *J. Chem. Soc., Chem. Commun.*: 905–906.

219 Liu, J., Han, Z., Wang, X. et al. (2015). *J. Am. Chem. Soc.* 137: 15346–15349.

220 Liu, J., Liu, Q., Franke, R. et al. (2015). *J. Am. Chem. Soc.* 137: 8556–8563.

221 Grigg, R., Monteith, M., Sridharan, V., and Terrier, C. (1998). *Tetrahedron* 54: 3885–3894.

222 Xiao, W.-J., Vasapollo, G., and Alper, H. (1998). *J. Org. Chem.* 63: 2609–2612.

223 Tamaru, Y., Hojo, M., and Yoshida, Z.-i. (1991). *J. Org. Chem.* 56: 1099–1105.

224 Ukaji, Y., Miyamoto, M., Mikuni, M. et al. (1996). *Bull. Chem. Soc. Jpn.* 69: 735–742.

225 Hegedus, L.S., Allen, G.F., and Olsen, D.J. (1980). *J. Am. Chem. Soc.* 102: 3583–3597.

226 Semmelhack, M.F., Bozell, J.J., Sato, T. et al. (1982). *J. Am. Chem. Soc.* 104: 5850–5852.

227 Semmelhack, M.F. and Zask, A. (1983). *J. Am. Chem. Soc.* 105: 2034–2043.

228 Semmelhack, M.F. and Bodurow, C. (1984). *J. Am. Chem. Soc.* 106: 1496–1498.

229 Tamaru, Y., Hojo, M., Higashimura, H., and Yoshida, Z.-i. (1988). *J. Am. Chem. Soc.* 110: 3994–4002.

230 Holmes, C.P. and Bartlett, P.A. (1989). *J. Org. Chem.* 54: 98–108.

231 Semmelhack, M.F. and Zhang, N. (1989). *J. Org. Chem.* 54: 4483–4485.

232 McCormick, M., Monahan, R. III, Soria, J. et al. (1989). *J. Org. Chem.* 54: 4485–4487.

233 Yadav, J.S., Sreenivasa Rao, E., Rao, C.S., and Choudary, B.M. (1989). *J. Mol. Catal.* 49: L61–L63.

234 Yadav, J.S., Sreenivasa Rao, E., Sreenivasa Rao, V., and Choudary, B.M. (1990). *Tetrahedron Lett.* 31: 2491–2492.

235 Semmelhack, M.F., Kim, C., Zhang, N. et al. (1990). *Pure Appl. Chem.* 62: 2035–2040.

236 Harayama, Y., Abe, A., Sakado, T. et al. (1997). *J. Org. Chem.* 62: 2113–2122.

237 White, J.D., Hong, J., and Robarge, L.A. (1999). *Tetrahedron Lett.* 40: 1463–1466.

238 White, J.D., Kranemann, C.L., and Kuntiyong, P. (2001). *Org. Lett.* 3: 4003–4006.

239 Kuntiyong, P., Lee, T.H., Kranemann, C.L., and White, J.D. (2012). *Org. Biomol. Chem.* 10: 7884–7899.

240 Semmelhack, M.F., Bodurow, C., and Baum, M. (1984). *Tetrahedron Lett.* 25: 3171–3174.

241 Tamaru, Y., Higashimura, H., Naka, K. et al. (1985). *Angew. Chem. Int. Ed.* 24: 1045–1046.

242 Tamaru, Y., Kobayashi, T., Kawamura, S. -i. et al. (1985). *Tetrahedron Lett.* 26: 3207–3210.

243 Tamaru, Y., Hojo, M., and Yoshida, Z. -i. (1988). *J. Org. Chem.* 53: 5731–5741.

244 Kraus, G.A., Li, J., Gordon, M.S., and Jensen, J.H. (1993). *J. Am. Chem. Soc.* 115: 5859–5860.

245 Paddon-Jones, G.C., McErlean, C.S.P., Hayes, P. et al. (2001). *J. Org. Chem.* 66: 7487–7495.

246 Babjak, M., Kapitán, P., and Gracza, T. (2005). *Tetrahedron* 61: 2471–2479.

247 Szolcsányi, P., Grazca, T., and Špánik, I. (2007). *Tetrahedron Lett.* 49: 1357–1360.

248 Li, Z., Gao, Y., Tang, Y. et al. (2008). *Org. Lett.* 10: 3017–3020.

249 Kapitán, P. and Grazca, T. (2008). *Tetrahedron: Asymmetry* 19: 38–44.

250 Kapitán, P. and Grazca, T. (2008). *Arkivoc* viii: 8–17.

251 Tsujihara, T., Shinohara, T., Takenaka, K. et al. (2009). *J. Org. Chem.* 74: 9274–9279.

252 Nesbitt, C.L. and McErlean, C.S.P. (2009). *Tetrahedron Lett.* 50: 6318–6320.

253 Kubizna, P., Špánik, I., Kožíšek, J., and Szolcsányi, P. (2010). *Tetrahedron Lett.* 66: 2351–2355.

254 Hayes, P.Y., Chow, S., Rahm, F. et al. (2010). *J. Org. Chem.* 75: 6489–6501.

255 Nesbitt, C.L. and McErlean, C.S.P. (2011). *Org. Biomol. Chem.* 9: 2198–2208.

256 Karlubíková, O., Babjak, M., and Gracza, T. (2011). *Tetrahedron* 67: 4980–4987.

257 Doháňošová, J., Lásiková, A., Toffano, M. et al. (2012). *New J. Chem.* 36: 1744–1750.

258 Markovič, M., Ďuranová, M., Kóš, P. et al. (2013). *Tetrahedron* 69: 4185–4189.

259 Babjak, M., Markovič, M., Kandríková, B., and Grazca, T. (2014). *Synthesis* 46: 809–816.

260 Cintulová, D., Slahúčková, M., Paštrnák, J. et al. (2017). *Synthesis* 49: 755–762.

261 Cernak, T.A. and Lambert, T.H. (2009). *J. Am. Chem. Soc.* 131: 3124–3125.

262 Ambrosini, L.M., Cernak, T.A., and Lambert, T.H. (2010). *Synthesis*: 870–881.

263 Li, W., Liu, C., Zhang, H. et al. (2014). *Angew. Chem. Int. Ed.* 53: 2443–2446.

264 Ferguson, J., Zeng, F., and Alper, H. (2012). *Org. Lett.* 14: 5602–5605.

265 Yang, X.-H., Li, K., Song, R.-J., and Li, J.-H. (2014). *Eur. J. Org. Chem.*: 616–623.

266 Chen, M., Ren, Z.-H., Wang, Y.-Y., and Guan, Z.-H. (2013). *Angew. Chem. Int. Ed.* 52: 14196–14199.

267 Liu, K., Zou, M., and Lei, A. (2016). *J. Org. Chem.* 81: 7088–7092.

268 Xie, Y., Chen, T., Fu, S. et al. (2015). *Chem. Commun.* 51: 9377–9380.

269 Wu, J., Zhou, Y., Wu, T. et al. (2017). *Org. Lett.* 19: 6432–6435.

270 Li, J., Yang, S., Wu, W., and Jiang, H. (2014). *Chem. Commun.* 50: 1381–1383.

271 Alper, H. and Leonard, D. (1985). *J. Chem. Soc., Chem. Commun.*: 511–512.

272 Alper, H. and Leonard, D. (1985). *Tetrahedron Lett.*: 5639–5642.

273 Alper, H. and Hamel, N. (1990). *J. Chem. Soc., Chem. Commun.*: 135–136.

274 El Ali, B. and Alper, H. (1991). *J. Org. Chem.* 56: 5357–5360.

275 El Ali, B., Okuro, K., Vasapollo, G., and Alper, H. (1996). *J. Am. Chem. Soc.* 118: 4264–4270.

276 Orejon, A. and Alper, H. (1999). *J. Mol. Catal. A: Chem.* 143: 137–142.

277 Vasapollo, G., Mele, G., and El Ali, B. (2003). *J. Mol. Catal. A: Chem.* 204, 205: 97–105.

278 Chanthateyanonth, R. and Alper, H. (2004). *Adv. Synth. Catal.* 346: 1375–1384.

279 Touzani, R. and Alper, H. (2005). *J. Mol. Catal.* 227: 197–207.

280 Ye, F. and Alper, H. (2006). *Adv. Synth. Catal.* 348: 1855–1861.

281 Amézquita-Valencia, M. and Alper, H. (2014). *Org. Lett.* 16: 5827–5829.

282 Hu, Y., Shen, Z., and Huang, H. (2016). *ACS Catal.* 6: 6785–6789.

283 Hirschbeck, V. and Fleischer, I. (2018). *Chem. Eur. J.* 24: 2854–2857.

284 Walkup, R.D. and Park, G. (1987). *Tetrahedron Lett.* 28: 1023–1026.

285 Walkup, R.D. and Park, G. (1990). *J. Am. Chem. Soc.* 112: 1597–1603.

286 Walkup, R.D. and Mosher, M.D. (1993). *Tetrahedron* 49: 9285–9294.

287 Lathhury, D., Vernon, P., and Gallagher, T. (1986). *Tetrahedron Lett.* 27: 6009–6012.

288 Fox, D.N.A., Lathbury, D., Mahon, M.F. et al. (1991). *J. Am. Chem. Soc.* 113: 2652–2656.

289 Gallagher, T., Davies, I.W., Jones, S.W. et al. (1992). *J. Chem. Soc., Perkin Trans. 1*: 433–440.

290 Kimura, M., Saeki, N., Uchida, S. et al. (1993). *Tetrahedron Lett.* 34: 7611–7614.

291 Cheng, X., Jiang, X., Yu, Y., and Ma, S. (2008). *J. Org. Chem.* 73: 8960–8965.

292 Volla, C.M.R. and Bäckvall, J.-E. (2014). *Org. Lett.* 16: 4174–4177.

293 Yang, B., Qiu, Y., and Bäckvall, J.-E. (2018). *Acc. Chem. Res.* 51: 1520–1531.

294 Zhu, C., Liu, J., Li, M.-B., and Bäckvall, J.-E. (2020). *Chem. Soc. Rev.* 49: 341–353.

295 Jacobsen, G., and Spaethe, H. (1962). Verfahren zur Herstellung von gesaettigten und ungesaettigten Carbon saeureestern aus Acetylen, Kohlenmonoxyd und aliphatischen Alkoholen. German Patent DE1138760B. Hoeschst AG, filed 14 January 1960 and 31 October 1962.

296 Tsuji, J., Morikawa, M., and Iwamoto, N. (1964). *J. Am. Chem. Soc.* 86: 2095–2095.

297 Chiusoli, G.P., Venturello, C., and Merzoni, S. (1968). *Chem. Ind. (London)*: 977–977.

298 Lines, C.B. and Long, R. (1969). *Prepr. – Am. Chem. Soc., Div. Pet. Chem.* 14 (2): B159.

299 Cassar, L., Chiusoli, G.P., and Guerrieri, F. (1973). *Synthesis*: 509–523.

300 Alper, H., Despeyroux, B., and Woell, J.B. (1983). *Tetrahedron Lett.* 24: 5691–5694.

301 The explosion limits for CO in air are ca. 16–70% at 18–20 °C and atmospheric pressure, 14.8–71.4% at 100 °C and atmospheric pressure; at higher total pressure, the range of flammability decreases: for example, at 20 atm and 20 °C, the limits are ca. 19% and 60%. See: Bartish, C.M. and Drissel, G.M. (1978). *Kirk-Othmer Encyclopedia of Chemical Technology*, 3rd ed., vol. 2 (eds. M. Grayson, D. Eckroth, G.J. Bushey, et al.), 775. New York, NY: Wiley-Interscience.

302 Gabriele, B., Costa, M., Salerno, G., and Chiusoli, G.P. (1992). *J. Chem. Soc., Chem. Commun.*: 1007–1008.

303 Gabriele, B., Costa, M., Salerno, G., and Chiusoli, G.P. (1994). *J. Chem. Soc., Perkin Trans. 1*: 83–87.

304 Njardarson, J.T. and Wood, J.L. (2001). *Org. Lett.* 3: 2431–2434.

305 Njardarson, J.T., McDonald, I.M., Spiegel, D.A. et al. (2001). *Org. Lett.* 3: 2435–2438.

306 Fazio, A., Gabriele, B., Salerno, G., and Destri, S. (1999). *Tetrahedron* 55: 485–502.

307 Hartstock, F.W., McMahon, L.B., and Tell, P. (1993). *Tetrahedron Lett.* 34: 8067–8070.

308 Li, J., Jiang, H., and Jia, L. (1999). *Synth. Commun.* 29: 3733–3738.

309 Giannoccaro, P., Aresta, M., Doronzo, S., and Ferragina, C. (2000). *Appl. Organomet. Chem.* 14: 581–589.

310 Li, J., Jiang, H., and Chen, M. (2001). *Synth. Commun.* 31: 3131–3134.

311 Gadge, S.T. and Bhanage, B.M. (2013). *Synlett* 24: 981–986.

312 The calculated Gibbs free energy for the reaction: $Pd(0) + 2HI + (1/2)O_2 \rightarrow PdI_2 + H_2O$ is −65.4 kcal/mol. See:Pancrazzi, F., Sarti, N., Mazzeo, P.P. et al. (2020). *Org. Lett.* 22: 1569–1574.

313 Beltrani, M., Carfagna, C., Milani, B. et al. (2016). *Adv. Synth. Catal.* 358: 3244–3243.

314 Zargarian, D. and Alper, H. (1991). *Organometallics* 10: 2914–2921.

315 Gabriele, B., Salerno, G., Costa, M., and Chiusoli, G.P. (1999). *Chem. Commun.*: 1381–1382.

316 Sakurai, Y., Sakaguchi, S., and Ishii, Y. (1999). *Tetrahedron Lett.* 40: 1701–1704.

317 Li, J., Li, G., Jiang, H., and Chen, M. (2001). *Tetrahedron Lett.* 42: 6923–6924.

318 Gabriele, B., Veltri, L., Salerno, G. et al. (2003). *Eur. J. Org. Chem.*: 1722–1728.

319 Yang, J., Liu, J., Jackstell, R., and Beller, M. (2018). *Chem. Commun.* 54: 10710–10713.

320 Okumoto, H., Nishihara, S., Nakagawa, H., and Suzuki, A. (2000). *Synlett*: 217–218.

321 Li, J., Jing, H., Feng, A., and Jia, L. (1999). *J. Org. Chem.* 64: 5984–5987.

322 Li, J.-H., Tang, S., and Xie, Y.-X. (2005). *J. Org. Chem.* 70: 477–479.

323 Wu, N., Dang, L., Liu, L. et al. (2013). *Chem. Asian J.* 8: 65–68.

324 Huang, L., Wang, Q., Wu, W., and Jiang, H. (2014). *ChemCatChem* 6: 561–566.

325 Tsuji, J., Takahashi, M., and Takahashi, T. (1980). *Tetrahedron Lett.* 21: 849–850.

326 Bruk, L.G., Gorodskii, S.N., Zeigarnik, A.V. et al. (1998). *J. Mol. Catal. A: Chem.* 130: 29–40.

327 Vasilevsky, S.F., Trofimov, B.A., Mal'kina, A.G., and Brandsma, L. (1994). *Synth. Commun.* 24: 85–88.

328 Chiarotto, I. and Carelli, I. (2002). *Synth. Commun.* 32: 881–886.

329 Izawa, Y., Shimizu, I., and Yamamoto, A. (2004). *Bull. Chem. Soc. Jpn.* 77: 2033–2045.

330 Izawa, Y., Shimizu, I., and Yamamoto, A. (2005). *Chem. Lett.* 34: 1060–1061.

331 Cao, Q., Hughes, N.L., and Muldoon, M.J. (2016). *Chem. Eur. J.* 22: 11982–11985.

332 Zhu, F. and Wu, X.-F. (2018). *Org. Lett.* 20: 3422–3425.

333 Gabriele, B., Salerno, G., Veltri, L., and Costa, M. (2001). *J. Organomet. Chem.* 622: 84–88.

334 Gadge, S.T., Khedkar, M.V., Lanke, S.R., and Bhanage, B.M. (2012). *Adv. Synth. Catal.* 354: 2049–2056.

335 Hwang, J., Choi, J., Park, K. et al. (2015). *Eur. J. Org. Chem.*: 2235–2243.

336 Zhang, C., Liu, J., and Xia, C. (2015). *Catal. Sci. Technol.* 5: 4750–4754.

337 Hughes, N.L., Brown, C.L., Irwin, A.A. et al. (2017). *ChemSusChem* 10: 675–680.

338 Idris, M.A., Kim, M., Kim, J.G., and Lee, S. (2019). *Tetrahedron* 75: 4130–4137.

339 Li, Z., Li, H., Hu, J. et al. (2020). *Nat. Catal.* 3: 438–445.

340 Knifton, J.F. (1977). *J. Mol. Catal.* 2: 293–299.

341 El Ali, B. and Alper, H. (1991). *J. Mol. Catal.* 67: 29–33.

342 Drent, E., Arnoldy, P., and Budzelaar, P.H.M. (1993). *J. Organomet. Chem.* 455: 247–253.

343 Doherty, S., Knight, J.G., and Betham, M. (2006). *Chem. Commun.*: 88–90.

344 Kuniyasu, H., Yoshizawa, T., and Kambe, N. (2010). *Tetrahedron Lett.* 51: 6818–6821.

345 Suleiman, R., Tijani, J., and El Ali, B. (2010). *Appl. Organomet. Chem.* 24: 38–46.

346 Williams, D.B., Shaw, M.L., and Hughes, T. (2011). *Organometallics* 30: 4968–4973.

347 Oberhauser, W., Ienco, A., Vizza, F. et al. (2012). *Organometallics* 31: 4832–4837.

348 Queirolo, M., Vezzani, A., Mancuso, R. et al. (2015). *J. Mol. Catal. A: Chem.* 398: 115–126.

349 Chen, X., Zhu, H., Wang, W. et al. (2016). *ChemSusChem* 9: 2451–2459.

350 Scrivanti, A., Beghetto, V., and Bertoldini, M. (2017). *Mol. Catal.* 443: 38–42.

351 Qi, H., Huang, Z., Wang, M. et al. (2018). *J. Catal.* 363: 63–68.

352 Yang, D., Liu, L., Wang, D.-L. et al. (2019). *J. Catal.* 371: 236–244.

353 Crawford, L., Cole-Hamilton, D.J., and Bühl, M. (2015). *Organometallics* 34: 438–449.

354 Ahmad, S., Lockett, A., Shuttleworth, T.A. et al. (2019). *Phys. Chem. Chem. Phys.* 21: 8543–8552.

355 Yang, D., Liu, H., Liu, L. et al. (2019). *Green Chem.* 21: 5336–5344.

356 Li, Y., Alper, H., and Yu, Z. (2006). *Org. Lett.* 8: 5199–5201.

357 Suleiman, R. and El Ali, B. (2010). *Tetrahedron Lett.* 51: 3211–3215.

358 Hussain, S.M.S., Suleiman, R., and El Ali, B. (2012). *Tetrahedron Lett.* 53: 6535–6539.

359 Sha, F. and Alper, H. (2017). *ACS Catal.* 7: 2220–2229.

360 Gao, B. and Huang, H. (2017). *Org. Lett.* 19: 6260–6263.

361 Wang, D.-L., Guo, W.-D., Zhou, Q. et al. (2018). *ChemCatChem* 10: 4264–4268.

362 Wang, D.-L., Guo, W.-D., Liu, L. et al. (2019). *Catal. Sci. Technol.* 9: 1334–1337.

363 Kuniyasu, H., Kato, T., Asano, S. et al. (2006). *Tetrahedron Lett.* 47: 1141–1144.

364 Liu, J., Dong, K., Franke, R. et al. (2018). *J. Am. Chem. Soc.* 140: 10282–10288.

365 Yang, D., Liu, H., Wang, D.-L. et al. (2018). *Green Chem.* 20: 2588–2595.

366 Guo, W.-D., Liu, L., Yang, S.-Q. et al. (2020). *ChemCatChem* 12: 1376–1384.
367 Liu, H., Lau, G.P.S., and Dyson, P.J. (2015). *J. Org. Chem.* 80: 386–391.
368 Zeng, F. and Alper, H. (2013). *Org. Lett.* 15: 2034–2037.
369 Xu, Y., Zhao, J., Chen, H. et al. (2014). *Chem. Commun.* 50: 2488–2490.
370 Murakami, S., Sonehara, T., Iwakami, K. et al. (2019). *Tetrahedron Lett.* 60: 598–601.
371 Tsuji, J. and Nogi, T. (1966). *J. Am. Chem. Soc.* 88: 1289–1292.
372 Gabriele, B., Salerno, G., Costa, M., and Chiusoli, G.P. (1995). *J. Organomet. Chem.* 503: 21–28.
373 Chiusoli, G.P., Costa, M., Cucchia, L. et al. (2003). *J. Mol. Catal. A: Chem.* 204: 133–142.
374 Gabriele, B., Salerno, G., Costa, M., and Chiusoli, G.P. (1999). *Tetrahedron Lett.* 40: 989–990.
375 Feng, X., Zhang, M., Jackstell, R., and Beller, M. (2013). *Angew. Chem. Int. Ed.* 52: 4645–4649.
376 Gabriele, B., Salerno, G., De Pacali, F. et al. (1997). *J. Chem. Soc., Perkin Trans. 1*: 147–154.
377 Bonardi, A., Costa, M., Gabriele, B. et al. (1995). *Tetrahedron Lett.* 36: 7495–7498.
378 Gabriele, B., Salerno, G., Veltri, L. et al. (2001). *Eur. J. Org. Chem.*: 4607–4613.
379 Gabriele, B., Salerno, G., Fazio, A., and Veltri, L. (2006). *Adv. Synth. Catal.* 348: 2212–2222.
380 Mancuso, R., Raut, D.S., Marino, N. et al. (2016). *Chem. Eur. J.* 22: 3053–3064.
381 Mancuso, R., Veltri, L., Russo, P. et al. (2018). *Synthesis* 50: 267–277.
382 Ma, S., Wu, B., Jiang, X., and Zhao, S. (2005). *J. Org. Chem.* 70: 2568–2575.
383 Tang, S., Yu, Q.-F., Peng, P. et al. (2007). *Org. Lett.* 9: 3413–3416.
384 Ma, S., Wu, W., and Jiang, X. (2005). *J. Org. Chem.* 70: 2588–2593.
385 Kato, K., Motodate, S., Mochida, T. et al. (2009). *Angew. Chem. Int. Ed.* 48: 3326–3328.
386 Motodate, S., Kobayashi, T., Fujii, M. et al. (2010). *Chem. Asian J.* 5: 2221–2230.
387 Gabriele, B., Salerno, G., Plastina, P. et al. (2004). *Adv. Synth. Catal.* 346: 351–358.
388 Gabriele, B., Plastina, P., Salerno, G., and Costa, M. (2005). *Synlett*: 935–938.
389 Gabriele, B., Plastina, P., Salerno, G. et al. (2007). *Org. Lett.* 9: 3319–3322.
390 Mancuso, R., Maner, A., Ziccarelli, I. et al. (2016). *Molecules* 21: 897.
391 Armentano, B., Curcio, R., Brindisi, M. et al. (2020). *Biomedicines* 8: 35.
392 Veltri, L., Mancuso, R., Altomare, A., and Gabriele, B. (2015). *ChemCatChem* 7: 2206–2213.
393 Veltri, L., Grasso, G., Rizzi, R. et al. (2016). *Asian J. Org. Chem.* 5: 560–567.
394 Kondo, Y., Shiga, F., Murata, N. et al. (1994). *Tetrahedron* 50: 11803–11812.
395 Gabriele, B., Salerno, G., De Pascali, F. et al. (1999). *J. Org. Chem.* 64: 7693–7699.
396 Lütjens, H. and Scammels, P.J. (1999). *Synlett*: 1079–1081.
397 Gabriele, B., Salerno, G., De Pascali, F. et al. (2000). *J. Organomet. Chem.* 593: 409–415.

398 Marshall, J.A. and Yanik, M.M. (2000). *Tetrahedron Lett.* 41: 4717–4721.

399 Kato, K., Nishimura, A., Yamamoto, Y., and Akita, H. (2001). *Tetrahedron Lett.* 42: 4203–4205.

400 Kato, K., Tanaka, M., Yamamoto, Y., and Akita, H. (2002). *Tetrahedron Lett.* 43: 1511–1513.

401 Kato, K., Yamamoto, Y., and Akita, H. (2002). *Tetrahedron Lett.* 43: 4915–4917.

402 Kato, K., Yamamoto, Y., and Akita, H. (2002). *Tetrahedron Lett.* 43: 6587–6590.

403 Bacchi, A., Costa, M., Gabriele, B. et al. (2002). *J. Org. Chem.* 67: 4450–4457.

404 Gabriele, B., Salerno, G., Fazio, A., and Campana, F. (2002). *Chem. Commun.*: 1408–1409.

405 Bacchi, A., Costa, M., Della Ca', N. et al. (2004). *Eur. J. Org. Chem.*: 574–585.

406 Costa, M., Della Ca', N., Gabriele, B. et al. (2004). *J. Org. Chem.* 69: 2469–2477.

407 Bacchi, A., Costa, M., Della Ca', N. et al. (2005). *J. Org. Chem.* 70: 4971–4979.

408 Kato, K., Nouchi, H., Ishikura, K. et al. (2006). *Tetrahedron* 62: 2545–2554.

409 Kato, K., Matsuba, C., Kusakabe, T. et al. (2006). *Tetrahedron* 62: 9988–9999.

410 Kusakabe, T., Kato, K., Takaishi, S. et al. (2008). *Tetrahedron* 64: 319–327.

411 Kato, K., Teraguchi, R., Motodate, S. et al. (2008). *Chem. Commun.*: 3687–3689.

412 Della Ca', N., Campanini, F., Gabriele, B. et al. (2009). *Adv. Synth. Catal.* 351: 2423–2432.

413 Gabriele, B., Veltri, L., Salerno, G. et al. (2010). *Adv. Synth. Catal.* 352: 3355–3363.

414 Gabriele, B., Veltri, L., Maltese, V. et al. (2011). *Eur. J. Org. Chem.*: 5626–5635.

415 Fischer, J., Savage, G.P., and Coster, M.J. (2011). *Org. Lett.* 13: 3376–3379.

416 Gabriele, B., Veltri, L., Mancuso, R. et al. (2012). *Eur. J. Org. Chem.*: 2549–2559.

417 Kusakabe, T., Takahashi, T., Shen, R. et al. (2013). *Angew. Chem. Int. Ed.* 52: 7845–7849.

418 Kusakabe, T., Kawai, Y., and Kato, K. (2013). *Org. Lett.* 15: 5102–5105.

419 Mancuso, R., Ziccarelli, I., Armentano, D. et al. (2014). *J. Org. Chem.* 79: 3506–3518.

420 Araniti, F., Mancuso, R., Ziccarelli, I. et al. (2014). *Molecules* 19: 8261–8275.

421 Dhage, Y.D., Daimon, H., Peng, C. et al. (2014). *Org. Biomol. Chem.* 12: 8619–8626.

422 Matsuda, Y., Koyama, T., Kato, M. et al. (2015). *Tetrahedron* 71: 2134–2148.

423 Xu, T. and Alper, H. (2015). *Org. Lett.* 17: 4526–4529.

424 Pancrazzi, F., Motti, E., Costa, M. et al. (2017). *Molbank* 2017: M927.

425 Veltri, L., Prestia, T., Russo, P. et al. (2021). *ChemCatChem* **13**, 990–998. https://doi.org/10.1002/cctc.202001693

426 Liao, Y., Smith, J., Fathi, R., and Yang, Z. (2005). *Org. Lett.* 7: 2707–2709.

427 Li, J., Yu, J., Xiong, W. et al. (2020). *Green Chem.* 22: 465–470.

428 Gabriele, B., Mancuso, R., Salerno, G. et al. (2008). *J. Org. Chem.* 73: 4971–4977.

429 Gabriele, B., Mancuso, R., Maltese, V. et al. (2012). *J. Org. Chem.* 77: 8657–8668.

430 Gabriele, B., Veltri, L., Mancuso, R. et al. (2012). *J. Org. Chem.* 77: 4005–4016.

431 Mancuso, R., Strangis, R., Ziccarelli, I. et al. (2021). *J. Catal.* 393: 335–343.

432 Bacchi, A., Chiusoli, G.P., Costa, M. et al. (1997). *Chem. Commun.*: 1209–1210.

433 Chiusoli, G.P., Costa, M., Gabriele, B., and Salerno, G. (1999). *J. Mol. Catal. A: Chem.* 143: 297–310.

434 Mancuso, R., Ziccarelli, I., Fini, F. et al. (2019). *Adv. Synth. Catal.* 361: 690–695.

435 Gabriele, B., Salerno, G., and Plastina, P. (2004). *Lett. Org. Chem.* 1: 134–136.

436 Gabriele, B., Salerno, G., Veltri, L. et al. (2006). *J. Org. Chem.* 71: 7895–7898.

437 Gabriele, B., Plastina, P., Salerno, G., and Mancuso, R. (2006). *Synthesis*: 4247–4251.

438 Plastina, P., Gabriele, B., and Salerno, G. (2007). *Synthesis*: 3083–3087.

439 Gabriele, B., Veltri, L., Mancuso, R., and Carfagna, C. (2014). *Adv. Synth. Catal.* 356: 2547–2558.

440 Giofrè, S.V., Cirmi, S., Mancuso, R. et al. (2016). *Beilstein J. Org. Chem.* 12: 2793–2807.

441 Veltri, L., Giofrè, S.V., Devo, P. et al. (2018). *J. Org. Chem.* 83: 1680–1685.

442 Veltri, L., Russo, P., Prestia, T. et al. (2020). *J. Catal.* 386: 53–59.

443 Yasuhara, S., Sasa, M., Kusakabe, T. et al. (2011). *Angew. Chem. Int. Ed.* 50: 3912–3915.

444 Kusakabe, T., Kawai, Y., Shen, R. et al. (2012). *Org. Biomol. Chem.* 10: 3192–3194.

445 Kusakabe, T., Kawaguchi, K., Kawamura, M. et al. (2012). *Molecules* 17: 9220–9230.

446 Kusakabe, T., Sekiyama, E., Ishino, Y. et al. (2012). *Synthesis* 44: 1825–1832.

447 Kusakabe, T., Sagae, H., and Kato, K. (2013). *Org. Biomol. Chem.* 11: 4943–4948.

448 Jiang, Y., Kusakabe, T., Takahashi, K., and Kato, K. (2014). *Org. Biomol. Chem.* 12: 3380–3385.

449 Shen, R., Kusakabe, T., Takahashi, K., and Kato, K. (2014). *Org. Biomol. Chem.* 12: 4602–4609.

450 Shen, R., Kusakabe, T., Yatsu, T. et al. (2016). *Molecules* 21: 1177.

451 Ariyama, T., Kusakabe, T., Sato, K. et al. (2016). *Heterocycles* 93: 512–528.

452 Bacchi, A., Chiusoli, G.P., Costa, M. et al. (1998). *J. Organomet. Chem.* 562: 35–43.

453 Hu, Y. and Yang, Z. (2001). *Org. Lett.* 3: 1387–1390.

454 Acerbi, A., Carfagna, C., Costa, M. et al. (2018). *Chem. Eur. J.* 24: 4835–4840.

455 Mancuso, R., Ziccarelli, I., Chimento, A. et al. (2018). *iScience* 3: 279–288.

456 Ding, D., Zhu, G., and Jiang, X. (2018). *Angew. Chem. Int. Ed.* 57: 9028–9032.

457 Mancuso, R., Miliè, R., Palumbo Piccionello, A. et al. (2019). *J. Org. Chem.* 84: 7303–7311.

458 Pancrazzi, F., Sarti, N., Mazzeo, P.P. et al. (2020). *Org. Lett.* 22: 1569–1574.

459 Hu, Y. and Jiang, H. (2017). *Org. Lett.* 19: 5070–5073.

460 Tang, Y., Deng, L., Zhang, Y. et al. (2005). *Org. Lett.* 7: 1657–1659.

461 Deng, L.-J., Liu, J., Huang, J.-Q. et al. (2007). *Synthesis*: 2565–2570.

462 Wang, X.-R., Lu, F.-H., Song, Y., and Lu, Z.-L. (2012). *Tetrahedron Lett.* 53: 589–592.

463 Lan, Y., Deng, L., Liu, J. et al. (2009). *J. Org. Chem.* 74: 5049–5058.

464 Gabriele, B., Salerno, G., Costa, M., and Chiusoli, G.P. (1996). *J. Mol. Catal. A: Chem.* 111: 43–48.

465 Costa, M., De Souza Santos, L., Chiusoli, G.P. et al. (1993). *J. Mol. Catal.* 78: 151–158.

466 Bonardi, A., Costa, M., Gabriele, B. et al. (1994). *J. Chem. Soc., Chem. Commun.*: 2429–2430.

467 Gabriele, B., Mancuso, R., Salerno, G., and Veltri, L. (2005). *Chem. Commun.*: 271–273.

468 Gabriele, B., Mancuso, R., Salerno, G., and Costa, M. (2006). *Adv. Synth. Catal.* 37: 1101–1109.

469 Gabriele, B., Mancuso, R., Salerno, G., and Costa, M. (2007). *J. Org. Chem.* 72: 9278–9282.

470 Gabriele, B., Mancuso, R., Lupinacci, E. et al. (2010). *Tetrahedron* 66: 6156–6161.

471 Mancuso, R. and Gabriele, B. (2014). *Chem. Heterocycl. Compd.* 50: 160–170.

472 Giordano, C., Rovito, D., Barone, I. et al. (2017). *DNA Repair* 51: 20–30.

473 Iannazzo, D., Pistone, A., Celesti, C. et al. (2019). *Nanomaterials* 9: 282.

474 Gabriele, B., Mancuso, R., Salerno, G., and Plastina, P. (2008). *J. Org. Chem.* 73: 756–759.

475 Araniti, F., Mancuso, R., Lupini, A. et al. (2015). *Molecules* 20: 17883–17902.

476 Gabriele, B., Salerno, G., and Costa, M. (2006). *Top. Organomet. Chem.* 18: 239–272.

477 Kumar, P., Srivastava, V.C., Štangar, U.L. et al. (2019). *Catal. Rev.* https://doi.org/10.1080/01614940.2019.1696609.

478 Tan, H.-Z., Wang, Z.-Q., Xu, Z.-N. et al. (2018). *Catal. Today* 316: 2–12.

479 Shukla, K. and Srivastava, V.C. (2016). *RSC Adv.* 6: 32624–32645.

480 Huang, S., Yan, B., Wang, S., and Ma, X. (2015). *Chem. Soc. Rev.* 44: 3079–3116.

481 Gong, J., Ma, X., and Wang, S. (2007). *Appl. Catal. A:Gen.* 316: 1–21.

482 Gabriele, B., Mancuso, R., Salerno, G. et al. (2011). *ChemSusChem* 4: 1778–1786.

483 Hu, J., Gu, Y., Guan, Z. et al. (2011). *ChemSusChem* 4: 1767–1772.

484 Pearson, D.M., Conley, N.R., and Waymouth, R.M. (2011). *Adv. Synth. Catal.* 353: 3007–3013.

485 Gabriele, B., Mancuso, R., Salerno, G., and Costa, M. (2003). *Chem. Commun.*: 486–487.

486 Gabriele, B., Salerno, G., Mancuso, R., and Costa, M. (2004). *J. Org. Chem.* 69: 4741–4750.

487 Della Ca', N., Bottarelli, P., Dibenedetto, A. et al. (2011). *J. Catal.* 282: 120–127.

488 Mancuso, R., Raut, D.S., Della Ca', N. et al. (2015). *ChemSusChem* 8: 2204–2211.

489 Ferretti, F., Barraco, E., Gatti, C. et al. (2019). *J. Catal.* 369: 257–266.

490 Ragaini, F., Ferretti, F., Gatti, C., and Ramadan, D.R. (2019). *J. Catal.* 380: 391–395.

491 Gabriele, B., Mancuso, R., Veltri, L., and Della Ca', N. (2019). *J. Catal.* 380: 387–390.

492 Madej, D., Konopko, A., Piotrowski, P., and Krogul-Sobczak, A. (2020). *Catalysts* 10: 877.

493 Guan, Z.-H., Lei, H., Chen, M. et al. (2012). *Adv. Synth. Catal.* 354: 489–496.
494 Gabriele, B., Salerno, G., Brindisi, D. et al. (2000). *Org. Lett.* 2: 625–627.
495 Gabriele, B., Mancuso, R., Salerno, G., and Costa, M. (2003). *J. Org. Chem.* 68: 601–604.
496 Mancuso, R., Miliè, R., Ziccarelli, I. et al. (2018). *Molbank*: M1017.
497 Cattaneo, D., Alffenaar, J.W., and Neely, M. (2016). *Expert Opin. Drug Metab. Toxicol.* 12: 533–544.
498 Dong, K., Sang, R., Liu, J. et al. (2017). *Angew. Chem. Int. Ed.* 56: 6203–6207.
499 Schneider, C., Jackstell, R., Maes, B.U.W., and Beller, M. (2020). *Eur. J. Org. Chem.*: 932–936.
500 Liu, Q., Wu, L., Jiao, H. et al. (2013). *Angew. Chem. Int. Ed.* 52: 8064–8068.

9

Carbonylations Catalyzed by Other Second-Row Transition Metal Catalysts

Francesca Foschi and Gianluigi Broggini

Università degli Studi dell'Insubria, Dipartimento di Scienza e Alta Tecnologia, Via Valleggio 9, 22100, Como, Italy

9.1 Introduction

In the wide-spreading field of metal-catalyzed carbonylative reactions, the second-row transition metals are neglected catalysts. However, it is worth emphasizing their usefulness in synthetic and industrial applications on carbon monoxide chemistry given the variety of products they could be accessed by avoiding the use of high-value metals, reducing the cost of chemicals, and increasing profitability. Furthermore, in view of the fact that the few reports about carbonylation reactions in the presence of Y, Nb, and Cd are covered by patents, specific attention is given to zirconium-, molybdenum-, and silver-catalyzed carbonylation reactions.

9.2 Zirconium Compounds as Carbonylation Catalysts

Zirconium compounds can act as effective carbonylation catalysts in the form of sulfated zirconia (SZ), as zirconocene complexes, or as support of the catalysts in palladium-catalyzed carbonylative reactions.

9.2.1 Carbonylation with Carbon Monoxide on Sulfated-Doped Zirconia as the Solid Acid Catalyst

Over the past two decades, applications of anion-modified zirconium oxides for catalysis has received increasing attention. Even though zirconium oxides in general are used as the catalyst support, strong acid sites can be generated on zirconium oxides by modification with anions. In particular, functionalization with sulfate ions generates Brønsted and Lewis acid active sites on zirconium oxides, leading super acidity properties to the resulting SZ material (Figure 9.1).

Due to the excellent thermal stability, resistance to thermal extrusion, and high activity at low temperature and low cost, environmentally friendly SZ was found

Carbon Monoxide in Organic Synthesis: Carbonylation Chemistry,
First Edition. Edited by Bartolo Gabriele.

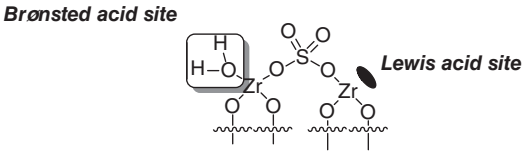

Figure 9.1 SZ structure.

to be suitable for promoting formal strongly acid-catalyzed bulk petrochemical processes involving the formation of carbonium ion (i.e. isomerization of alkanes). Eventually, the straightforward ability of SZ to form carbonium ion was exploited to promote carbonylation reactions under carbon monoxide atmosphere.

In this field, one of the first reports on an SZ-acid-catalyzed C–H activation/carbonylation reaction was published in 1997 by the Biaglow's research group, who performed spectroscopic measurements of the benzene carbonylation under CO atmosphere (Gatterman–Koch reaction) [1]. Both SZ and pure zirconia were tested after pretreatment by heating the materials to 600 °C for one hour in flowing dry O_2. A possible mechanism of the reaction is outlined in Scheme 9.1.

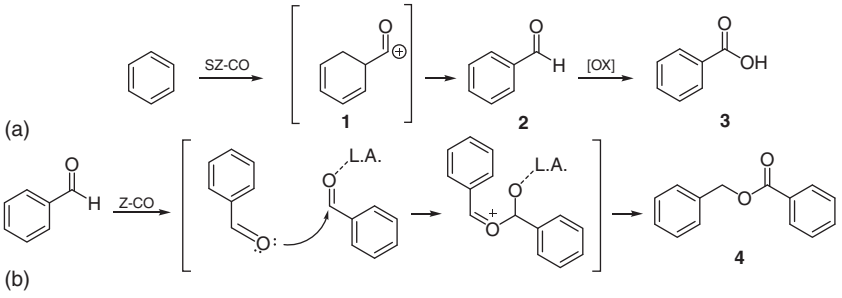

Scheme 9.1 SZ- and zirconia-catalyzed Gatterman–Koch reaction.

The reaction pathway can be explained through the trapping of the alkyl carbenium ion, generated from benzene inside SZ material, by CO to form the intermediate acylium cation **1**. Then, **1** is probably converted to benzaldehyde **2** via a hydride shift. An additional oxidation of benzaldehyde produces benzoic acid **3**, in agreement with the redox properties of SZ (Eq. (a), Scheme 9.1). Furthermore, the authors observed the ^{13}C carbonyl chemical shift of **2** at 206 ppm. This value is close to that of benzaldehyde in *magic acid* (205.7 ppm; the carbonyl resonance for benzaldehyde in $CDCl_3$ is 192.15 ppm). The NMR spectra does not change with time, suggesting that the benzaldehyde molecules are adsorbed as a stable complex at the Brønsted sites. The number of Brønsted acid sites on the materials became crucial for the reaction progress and the stabilization of the benzaldehyde molecules on the surface of the SZ. In fact, pure zirconia was inactive in the carbonylation reaction, while benzyl benzoate **4** was rapidly formed (Eq. (b), Scheme 9.1) when pure zirconia was exposed to benzaldehyde.

SZ was used also as a catalyst for Koch carbonylation reaction [2]. Authors found that the reaction at 150 °C under 5 MPa pressure of CO in chlorine-containing

Table 9.1 SZ-catalyzed Koch reaction.

ROH $\xrightarrow[CH_2Cl_2,\ 150\ °C,\ 18\ h]{SZ/CO}$ *t*-RCO_2H or ROR

Entry	Substrate	Main product	Main product (%)	Total carboxylic acids (%)
1	*t*-BuOH	*t*-$BuCO_2H$	52	69
2	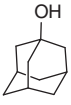	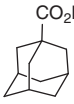	72	79
3		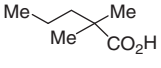	34	71
4		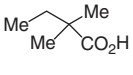	47	76
5	1-Butanol	$(C_4H_8)_2O$	62	—
6	1-Hexanol	$(C_6H_{13})_2O$	72	—
7	1-Octanol	$(C_8H_{17})_2O$	58	—
8	2-Hexanol	—		
9	Cyclohexanol	—		

solvents was the most suitable to achieve high-yield conversion of tertiary alcohols into the corresponding *tert*-carboxylic acid compounds (entries 1–4, Table 9.1).

The solvent effect could be understood by either the *in situ* formation of HCl gas or the generation of superacidic halomethyl cation, which would be produced from solvent and Lewis acidic SZ. The polymerization side reaction was the main drawback under these reaction conditions. C_{N+1} carboxylic acids were formed due to fragmentation and dimerization of carbon monoxide-derived carbenium ion.

The SZ ability to promote the Koch reaction was also tested on primary and secondary alcohols. It showed no ability to promote carbonylation of primary alcohols, providing the corresponding ethers in good yield (entries 5–7, Table 9.1). In the case of secondary alcohols, complex mixtures lacking of carboxylic acids or ethers were isolated (entries 8, 9, Table 9.1).

NMR spectroscopic measurements related to the direct conversion of saturated hydrocarbons into carboxylic acids using SZ catalysts were extensively investigated by Stepanov's research group. They found that the co-adsorption of CO and tertiary inert alkanes on SZ in the presence of water or methyl ketone furnished high yield of the corresponding carboxylic acid after heating at 70 °C for one hour (Scheme 9.2) [3].

Both direct formylation of isobutane with the acylium cation [HC^+O] (pathway a, Scheme 9.2) and reduction of pivaloyl cation with hydride ion (pathway b, Scheme 9.2) are possible for the formation of pivalic aldehyde **5**. This key intermediate, which was not isolated even in trace, could be quenched with water under oxidizing conditions to give carboxylic acid **6** as the main reaction

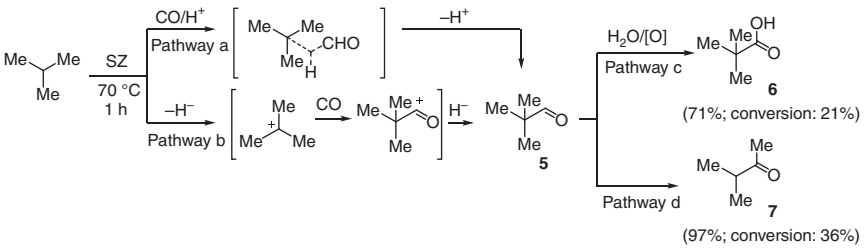

Scheme 9.2 SZ-catalyzed isobutane carbonylation. Source: Modified from Stepanov et al. [3].

product (pathway c, Scheme 9.2). On the other hand, the SZ acidity drives the rearrangement from **5** to **7** when the reaction is carried out under dry conditions (pathway d, Scheme 9.2). This is due to the property of α-quaternary aldehydes to rearrange in the presence of an acidic source.

The same synthetic approach was then extended to straight-chain alkanes. The co-adsorption of medium long-chain alkanes (*n*-pentane) and CO on SZ solid catalyst, followed by heating at 70 °C, furnished a complex mixture of branched products (Scheme 9.3) [4].

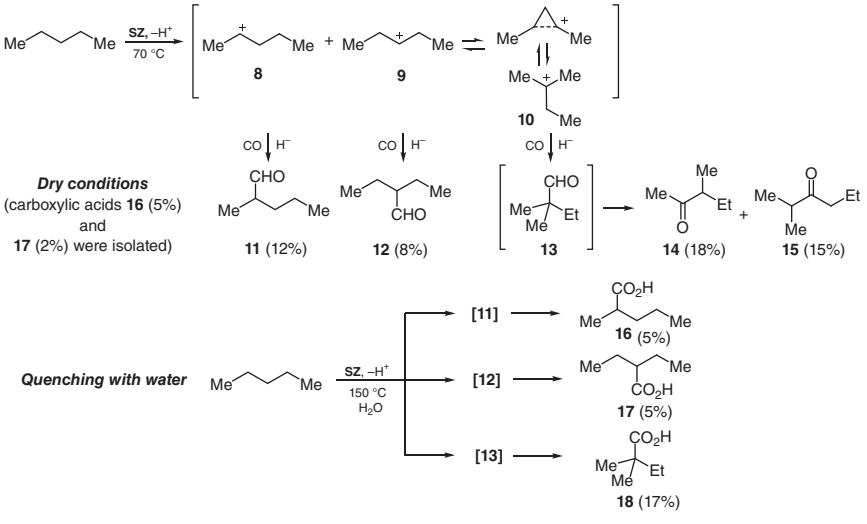

Scheme 9.3 *n*-Pentane carbonylation on SZ. Source: Modified from Luzgin et al. [4].

Hydride abstraction from *n*-pentane by SZ leads to the generation of two secondary carbenium ions **8** and **9**. In addition, **8** undergoes isomerization to the most stable tertiary cation **10**. While **8** and **9** react with CO and the hydride ion to produce isolable aldehydes **11** and **12** under anhydrous conditions, carbonylation of **10** furnished an unstable α-quaternary aldehyde. Rearrangement of 2,2-dimethylbutanal **13** occurs, allowing generation and isolation of ketones **14** and **15**. In this study, the formation of acids **16** and **17** was observed when *n*-pentane and carbon monoxide were allowed

to react on SZ in the absence of water. Once again, carboxylic acids **16**–**18** deriving from aldehydes **11–13** were formed as the only products of *n*-pentane carbonylation when the reaction was carried out in the presence of water.

Enhanced selectivity was achieved using the strongly inert propane as the starting alkane (Scheme 9.4) [5].

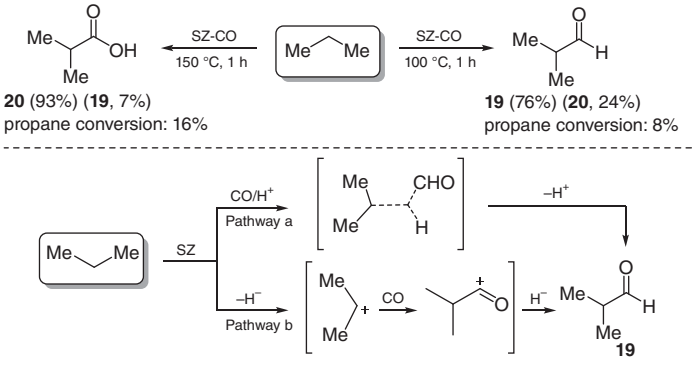

Scheme 9.4 Propane carbonylation on SZ. Source: Modified from Luzgin et al. [5].

The treatment of propane at 100 °C for one hour gave a conversion of 8% with formation of **19** and **20** in 76% and 24%, respectively. At 150 °C, alongside the doubling of the propane conversion, the selectivity toward acid **20** was almost complete. Even though the mechanism that provides the activation of the C—H bond followed by CO trapping was not clarified (pathway a and pathway b, Scheme 9.4), evidence of the oxidation step emerges. The infrared monitoring of the reaction indicates that the sulfate groups of SZ were the source of oxygen for the oxidative step and were reduced to dithionates during the course of the process. The reduction of sulfate groups results in a deactivation of the SZ catalyst. To restore the catalytic activity of SZ, it would be necessary to provide reoxidation by a molecular oxygen treatment.

9.2.2 Carbonylation of Zirconocene Complexes

The chemistry of zirconocene (Cp_2ZrII) and related complexes has been extensively explored since 1980s. Reactivity of Cp_2ZrII compounds is similar to that of carbenes since they have two vacant valence orbitals and one lone electron pair. Typical substrates for hydrozirconation are unsaturated compounds that then can give reductive coupling or insertion reactions to form zirconocycles after the addition of another unsaturated partner (Figure 9.2 – general structure of zirconacycles).

After cleavage, these types of structures are key intermediates for the synthesis of a large variety of compounds. Concerning reactions with CO, this method provides a way to cyclic ketones or alcohols through a formal [2+2+1] process (general structures **A** or **B**, Figure 9.2).

The first carbonylation reaction of a zirconacyclic substrate was reported by Erker [6]. The authors found that zirconaindane **21**, which is readily prepared by

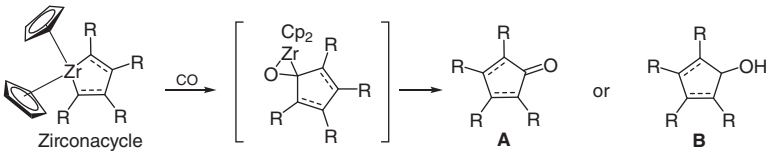

Figure 9.2 General structure of zirconacycles.

thermolysis of diphenylzirconocene under ethylene atmosphere (20 bar), rapidly takes up CO into the ZrC(sp^3) bond generating, by hydrolysis, the indanone **22** as the main product (~50% yield, independently on the reaction conditions) together with 3-phenylpropanol (**23**), 1-tetralone (**24**), and indane (**25**) as by-products (Scheme 9.5).

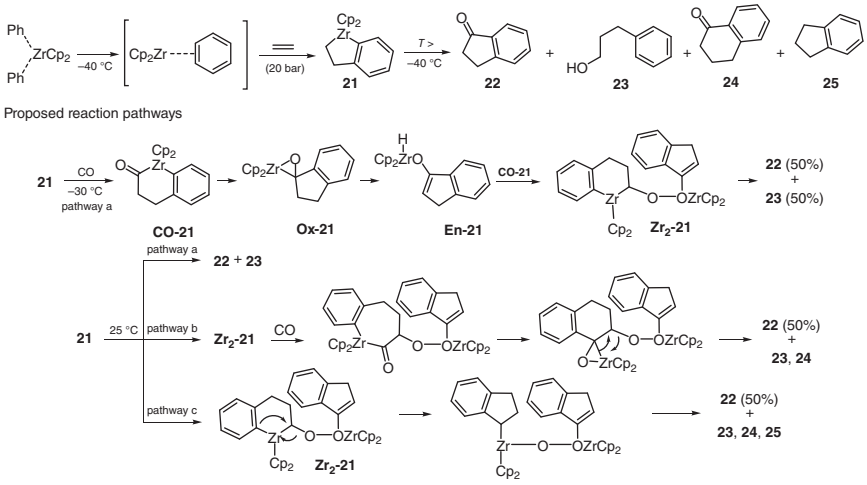

Scheme 9.5 First example of carbonylation of zirconacyclic structure.

The ratio of the products seems to be strictly related to the reaction temperature. Below −40 °C, zirconindane **21** is stable and no organic products were generated. The increase of the temperature at −30 °C resulted in the formation of an equimolar mixture of **22** and **23**, after hydrolysis of the binuclear zirconocene complex **Zr_2-21** arising from the combination of the enolate of **Ox-21** with the indanone **CO-21** (pathway a, Scheme 9.5). The further warming at 25 °C resulted in the activation of other two reaction routes. **Zr_2-21** could take up another equivalent of CO to form a mixed enolate complex. The corresponding 1-indanone **22** and 1-tetralone **24** were synthesized by this way (pathway b, Scheme 9.5). In the absence of carbon monoxide addition (pathway c, Scheme 9.5), rearrangement of **Zr_2-21** to a zirconium-substituted indane occurred, leading to the formation of **22**, and then of the hydrocarbon **25** upon hydrolysis.

After the discovery of zirconacycles carbonylation, many efforts have been made to induce specific reactivity toward the selective synthesis of carbonylated compounds.

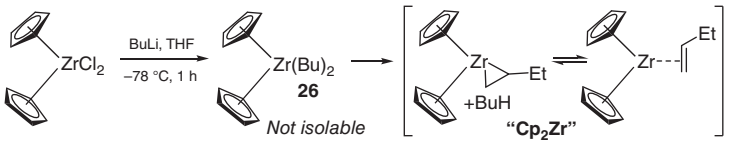

Figure 9.3 Synthesis of Negishi reagent.

A widely used source of "**Cp_2Zr**" in oxidative cyclisation reactions is given by the $Cp_2Zr(\eta^2$-butene) complex, also known as "Negishi reagent," prepared by treating zirconocene dichloride with 2 equiv of butyllithium (BuLi) in THF at low temperature. The first-formed dibutyl compound (**26**, Figure 9.3) undergoes β-hydride elimination to give a η^2-butenyl ligand ("**Cp_2Zr**"), with loss of a butyl group via reductive elimination. "**Cp_2Zr**" exists as a mixture of tautomers: zirconocene–butene Cp_2Zr^{iv} and Cp_2Zr^{ii} complexes.

In the absence of phosphine ligands, the Negishi reagent "**Cp_2Zr**" is not stable and highly reactive. Thus, it is *in situ* generated and directly coupled with unsaturated partners, such as alkenes, alkynes, dienes, and, in particular, enynes via a concerted process (Scheme 9.6).

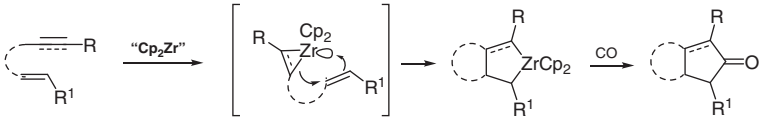

Scheme 9.6 Carbonylation reaction via Negishi reagent: general behavior.

Specifically, Negishi and co-workers found that the treatment of Cl_2ZrCp_2 with 2 mol of BuLi for one hour at −78 °C in THF, followed by addition of a nonterminal enyne at −78 °C and heating of the mixture to room temperature, produced the corresponding zirconabicycle **27a–g** in high yield. Compounds **27a–g** became susceptible to CO insertion and thus could be treated *in situ* with CO (1.1 atm) to give the corresponding α-cyclopentenone **28a–g** in good yield (Scheme 9.7) [7].

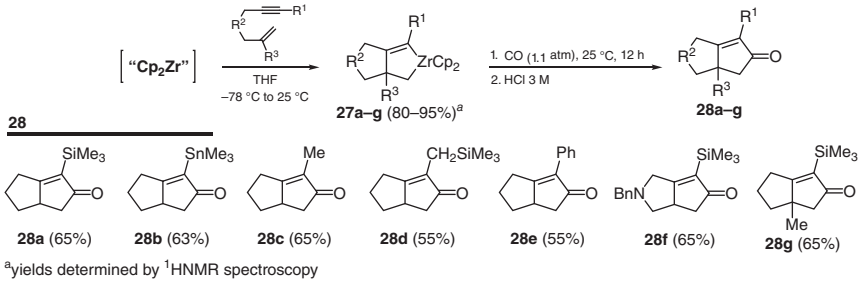

[a]yields determined by ^{1}HNMR spectroscopy

Scheme 9.7 Carbonylation of nonterminal enynes.

While both nitrogen-containing enynes and substituents at the alkenyl residue were well tolerated (**28f** and **28g**, Scheme 9.7), a limitation of this strategy was the

inability to induce CO coupling on zirconabicyclic derived from terminal enynes in a selective manner, giving complex mixtures of carbonylation products. This is probably due to the oxidative addition of the electron-rich metallocene to the acidic acetylene hydrogen. This process has been successfully used as the key step for the stereoselective synthesis of pentalenic acid (Eq. (1), Scheme 9.8) [8] and (+)-iridomyrmecin (Eq. (2), Scheme 9.8) [9].

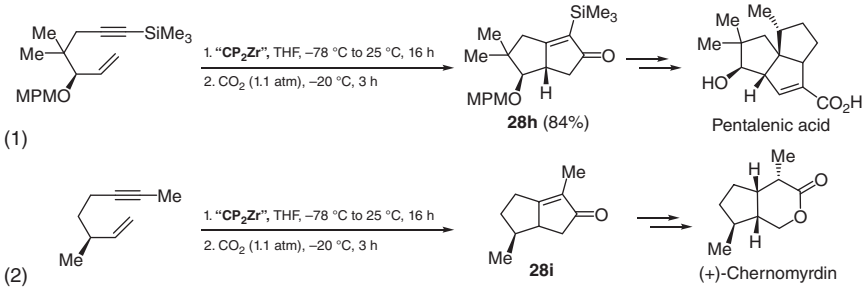

Scheme 9.8 Application of the zirconocene-promoted bicyclization–carbonylation protocol of nonterminal enynes. Source: Modified from Agnel et al. [8].

Concerning the synthesis of pentalenic acid, the relative stereochemistry of the two adjacent stereocenters in **28h** was determined by NMR experiments. The enantiomeric purity of pentalenic acid (>98%) was confirmed by NMR analysis of its (+)-methoxy(trifluoromethyl)phenylacetic ester. The stereochemistry of **28i** was confirmed by comparison with that reported for its enantiomer.

α,β-Disubstituted cyclopentenones were also prepared through intermolecular three-component coupling reaction [10]. The treatment of ethylene, disubstituted alkynes, and CO in the presence of "**Cp_2Zr**" provided the access to α,β-alkyl, α,β-aryl, α-silyl, α-aryl, α-alkynyl, β-alkyl, and α,α′-bridged cyclopentenones (Scheme 9.9).

A complete regioselectivity was detected when unsymmetrical alkynyl compounds were employed. The authors also found that the use of I_2 in the work-up step led to better yield of ketones **30j**,**k**. Normal quenching with HCl gave a mixture of cyclopentenone and its corresponding alcohol.

A similar reactivity was observed with zirconacycles generated by treatment of "**Cp_2Zr**" with alkenes (Scheme 9.10).

In fact, **31a** was isolated in 88% yield when "**Cp_2Zr**" was allowed to react with an excess of 1-butene. Treatment of **31a** with 1.1 atm of CO at −78 °C followed by protonolysis with saturated HCl in ether at low temperature (−78 °C) furnished the alcohol **32a** (45%). Carbonylation of **31a** at 0 °C followed by treatment with 1.1 mol equiv of iodine at 0 °C afforded ketone **33a** in 65% yield. Each compound was isolated as single regioisomer [11]. The reaction showed high regioselectivity toward the cross-coupling products using alkenyl compounds of various natures. This evidence indicates that probably the unsymmetrical zirconacycle compounds **31** are the thermodynamically favored products. Carbonylation of **31b** at 0 °C followed by treatment with iodine provided compounds **33b** essentially as the only

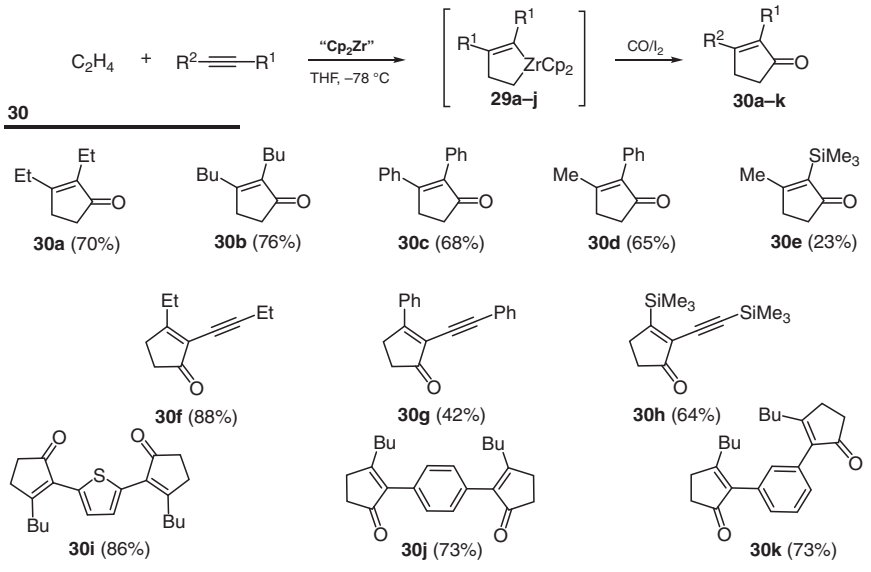

Scheme 9.9 Zirconium-promoted intermolecular coupling of disubstituted alkynes, ethylene, and CO.

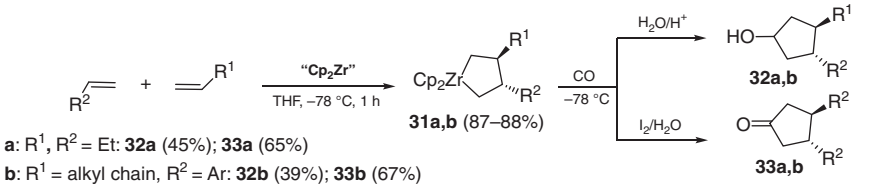

a: R^1, R^2 = Et: **32a** (45%); **33a** (65%)
b: R^1 = alkyl chain, R^2 = Ar: **32b** (39%); **33b** (67%)

Scheme 9.10 Zirconium-promoted alkene intermolecular coupling.

cyclization products while quenching with HCl at −78 °C gave the alcohol **32b**, without generating **33b** in a detectable amount.

On the other hand, the reaction of nonconjugated dienes involved isomerization of the less substituted double bond of the starting diene, forming a conjugated diene-zirconocene complex instead of the expected zirconabicycle (**34**, Eq. (1), Scheme 9.11). For this type of substrates, the formation of zirconabicycles was realized only when the diene chain was substituted with a bridgehead amino group (**35a,b**, Eqs. (2) and (3), Scheme 9.11) [12] or an alkyl-substituted tether (**35c**, Eq. (4), Scheme 9.11) [13].

Furthermore, reaction to **35a** proceeds with complete diastereoselectivity, probably due to the steric interaction between the substituents of **35a** and the two cyclopentadienyl rings.

This type of process has been as the key step in the total synthesis of (−)-dendrobine (synthesis of **36**, Scheme 9.12) [14].

Differently from zirconacyclopentane and zirconacyclopentene, zirconacyclopentadienes arising from two alkynes are inert toward the CO insertion under classical

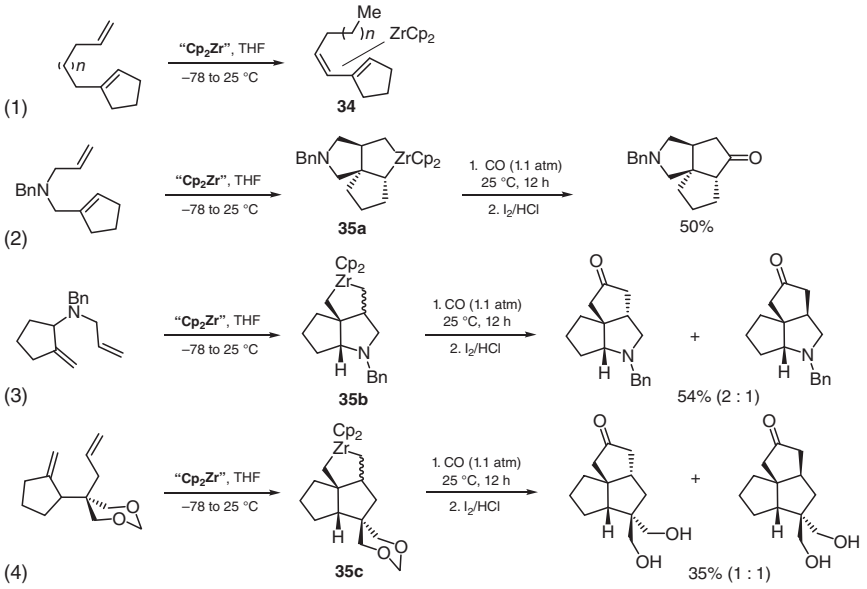

Scheme 9.11 Zirconocene-promoted bicyclization–carbonylation of dienes. Source: Modified from Mori et al. [12].

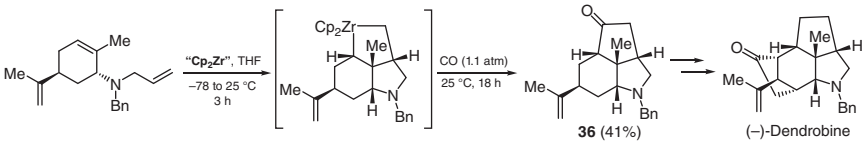

Scheme 9.12 Example of zirconocene-promoted bicyclization–carbonylation of dienes. Source: Modified from Saitoh et al. [14].

reaction conditions (**37**, Scheme 9.13) [15]. However, it is possible to induce CO insertion and cyclopentadiene formation by slightly varying the reaction conditions.

The crucial point for the CO activation toward **37** is the use of BuLi. By this way, independently from the nature of the alkynyl compounds used as starting material, general behavior and coherent results were observed. Furthermore, unsymmetrical cyclopentenones (**38c**,**d**, Scheme 9.13) were selectively formed when two different alkynes were tested, without detection of different cyclopentenones. As usual, the reaction was not selective when terminal alkynes were employed.

Experimental data and NMR studies plausibly indicate that BuLi is able to coordinate the zirconium atom, leading to the formation of complex **A**, in equilibrium with **B** (Scheme 9.14). The reaction of **B** with CO generates **C** by coordination to the zirconium atom, making it susceptible of nucleophilic attack by the alkenyllithium moiety to generate **D**. This latter rearranges to **E** and then in the much stable anionic species **F**. The final hydrolysis of **F** affords **38**.

Zirconacyclopentadienes **37a–c** could be also converted into the corresponding cyclopentadienones **39a–c** in fairly good yield when the reaction was carried out in the presence of $NiCl_2(PPh_3)_2$ (Scheme 9.15) [16].

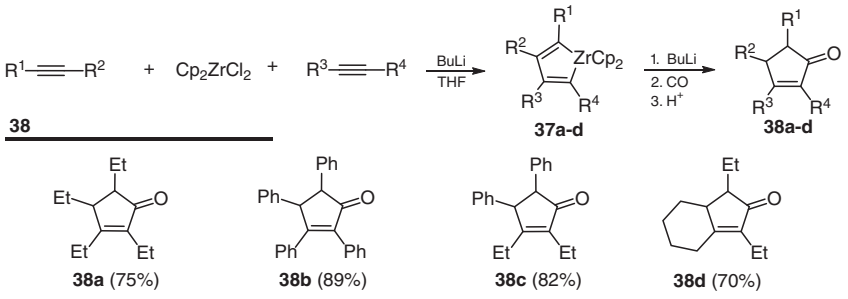

Scheme 9.13 Reaction of zirconacyclopentadienes derived from two alkynes with CO in the presence of BuLi. Sources: Adapted from Takahashi et al. [15a], Xi et al. [15b].

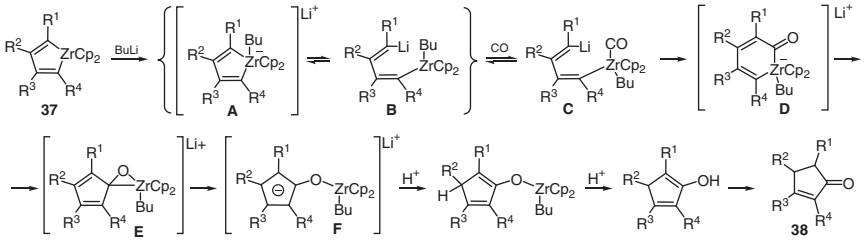

Scheme 9.14 Proposed reaction mechanism.

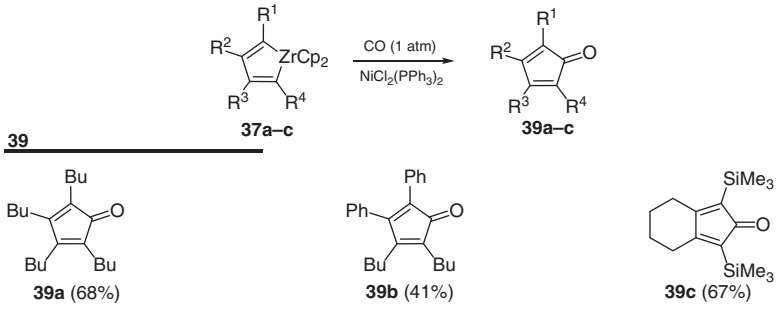

Scheme 9.15 Synthesis of cyclopentadienones. Source: Modified from Takahashi et al. [16].

A possible mechanism involves transmetalation of zirconacyclopentadienes to nickel, forming nickelacyclopentadienes together with zirconocene dichloride. The final insertion of CO into nickelacyclopentadienes leads to the formation of free cyclopentadienones.

"**Cp_2Zr**" stabilized with phosphine ligands became useful for the synthesis of hydroxycyclobutenones [17]. As reported in Scheme 9.16, zirconocene–cyclobutenones **41** are the products of the reaction between zirconium–alkyne complex **40** and CO.

This four-membered intermediate could be reactive toward a second CO molecule so that a double carbonylation occurred. A possible mechanism involves the initial

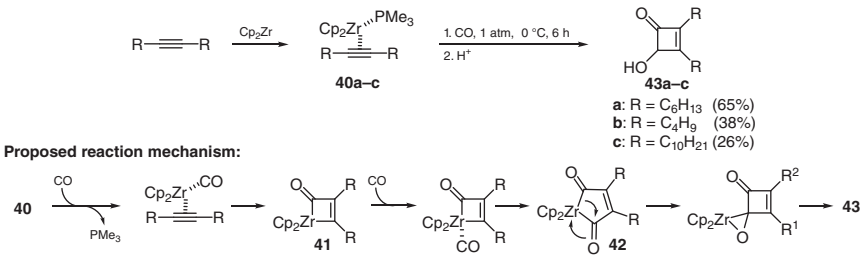

Scheme 9.16 Double carbonylation of zirconocene–alkyne complexes.

replacement of the phosphine ligand with CO, followed by insertion of CO into the zirconocene–alkyne bond to give **41**. This latter is susceptible to a second CO insertion, affording the zirconacyclopentadienones **42**. Subsequent skeletal rearrangement and hydrolysis produce **43**, in which one carbonyl group is reduced to a hydroxyl group. While saturated alkylic residue on the alkynes moiety were well tolerated, as exemplified by the synthesis of **43a–c**, in the case of aryl- or trimethylsilyl-substituted alkynes the reaction did not proceed. Probably, these types of alkynyl carbons are not nucleophilic enough toward CO when complexed with "**Cp_2Zr**." Once again, when a terminal alkyne was employed, a complex reaction mixture was obtained.

Zirconium-mediated intramolecular coupling–carbonylation of formally terminal alkynyl substrates (allyl-2-bromoallyl substrates) was investigated by Barluenga (Scheme 9.17) [18].

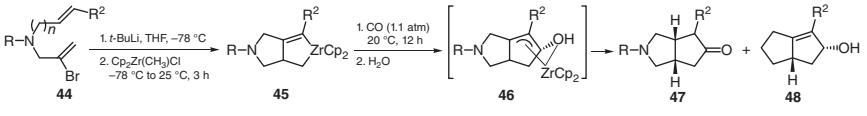

Scheme 9.17 Carbonylation of zirconacycle formally derived from terminal alkynes. Sources: Adapted from Barluenga et al. [18].

Treatment of substituted *N*-allyl-*N*-(2-bromoallyl)amines **44** with *t*-BuLi and zirconocene methylchloride led to zirconabicyclopentenes **45**. When a diethyl ether solution of **45** was stirred under carbon monoxide and then quenched with water, cyclopentanones **47** and the corresponding allylic alcohols **48** were isolated. The expected enone was never detected. This is probably due to the insertion of carbon monoxide into zirconacycle **45**, which produces a π-allyl-zirconium complex **46**. Hydrolysis of **46** occurs at the bridge carbon atom (**47**) or at the carbon nearest the oxygen (**48**). Reaction proceeds with various substituted amines **49** in satisfactory yields, even though a mixture of compounds **47** and **48** was usually formed (Scheme 9.18). Nevertheless, this methodology gave access to polyfunctionalized molecules in a one-pot procedure.

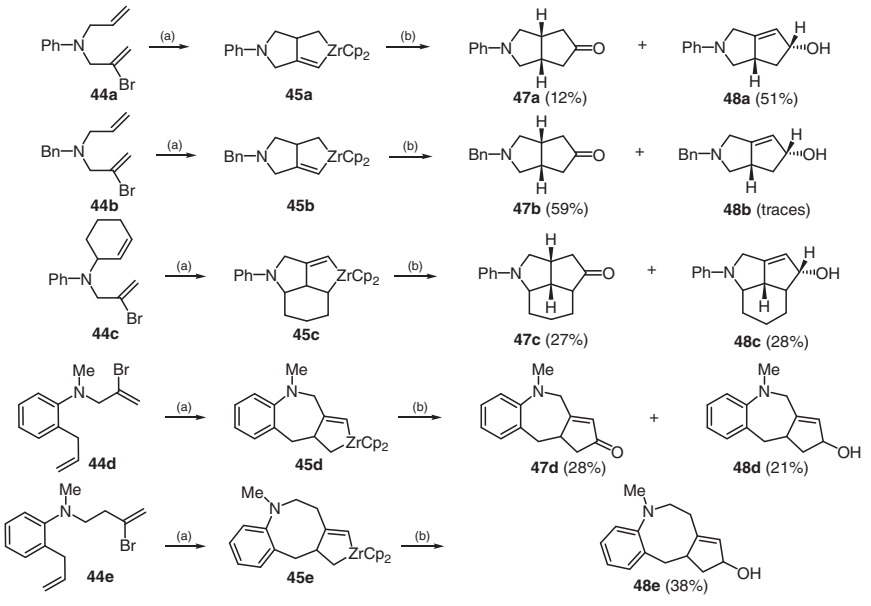

Reaction conditions: (a) *t*-BuLi, THF, –78 °C; $Cp_2Zr(CH_3)Cl$, –78 °C to 25 °C; (b) CO, 20 °C, 12 h

Scheme 9.18 Reaction scope.

9.3 Silver Compounds in Carbonylation Reactions

Unlike zirconium, the use of silver compounds in carbonylation reactions is due to their properties to enhance or promote the activity of other carbonylation catalysts. This synergic effect was observed by using systems of different nature, i.e. in silver carbonyl catalysis under acidic medium (Koch-type reactions), in Lewis acid system, or in the presence of bimetallic catalysts.

9.3.1 Koch-Type Reactions in the Presence of Silver Carbonyl Ion Catalyst

Tertiary carboxylic acids were prepared by carbonylation of olefins or alcohols in strong acids, such as H_2SO_4. These reactions need high carbon monoxide pressure and high reaction temperature. The same branched compounds could be achieved under milder reaction conditions when Ag(I) carbonyl ions were employed [19]. In this type of transformation, silver compounds (Ag_2O, Ag_2SO_4, or $AgClO_4$) were reported to form a "CO carrier" [$Ag(CO)^+$ or $Ag(CO)_2^+$] absorbing carbon monoxide from the gas phase in H_2SO_4 solution. In the presence of carbon ions, carbon monoxide is released from the unstable $Ag(CO)_n^+$ cation allowing its immediate reaction with the carbon ions. The use of both concentrate H_2SO_4 and an excess

of silver compounds is recognized to be essential to rule out polymerization processes. In addition, neither primary nor secondary carboxylic acids were obtained by this way independently from the conformation of the starting substrate. This is due to the isomerization of the carbon ion intermediate and the rearrangement of a methyl residue to generate the most stable tertiary carbon ion prior to the carbonylation reaction. Mixtures of isomers of tertiary carboxylic acids were isolated when terminal olefins or primary alcohols were used (entries 1, 2, and 4, Table 9.2). Saturated tertiary hydrocarbons were also selectively carbonylated when the reaction was conducted in the presence of alcohols or olefins as carbon precursors (entry 7, Table 9.2).

As described in Section 9.2.1, carbonylation reactions of unstable tertiary carbocations have been accomplished using solid superacids (i.e. Nafion, ZSM-5, or SO_4/ZrO_2). Furthermore, their activity toward the carbonylation of tertiary alcohols could be increased by ion exchanging with silver cations [20]. For example, silver-doped Nafion was prepared, salinizing the sulfonic group of Nafion with $AgNO_3$ (Scheme 9.19). When Ag/Nafion was exposed to CO, silver carbonyl ions were formed on the surface.

Comparison between the activity of **Nafion** and **Ag/Nafion** in the Koch reaction of 1-adantanol showed a slightly acceleration of the carbonylation process when the silver carbonyl catalysts was used.

Table 9.2 Carbonylation reactions in the presence of the Ag(I)/H_2SO_4 system.

Substrate $\xrightarrow[30\ °C,\ 1–3\ h]{AgO_2/H_2SO_4}$ 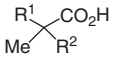

Entry	Substrate	Main product	Main product (%)	Carboxylic acids (%)
1	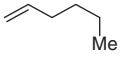	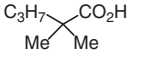	80	96
2	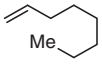	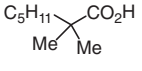	61	97
3		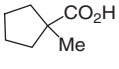	84	84
4	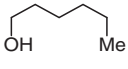	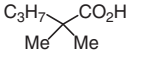	79	98
5	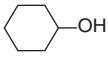	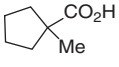	81	81
6	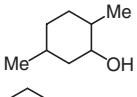	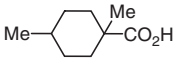	66	66
7		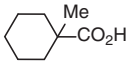	45	45
8	*n*-Octane	—	—	—

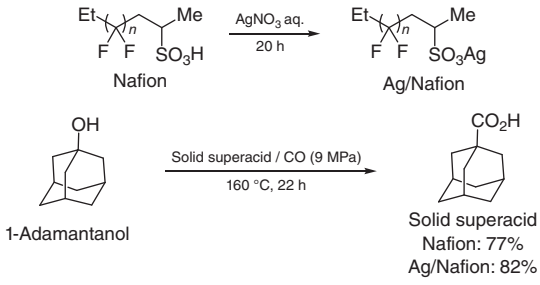

Scheme 9.19 Carbonylation of alcohols by solid superacids.

9.3.2 Koch-Type Reactions in the Presence of Silver Lewis Acids under CO Atmosphere

Koch-type reactions of methoxymethyl chloride under CO pressure required milder catalysts to generate the reactive cationic species in comparison with those described in Section 9.2.1. Actually, this reaction can proceed in the presence of a catalytic amount (5%) of $AgSbF_6$ (Scheme 9.20) [21]. Even though silver metal atom is not involved in the catalytic cycle, its presence was essential to easily promote the formation of the key species methoxymethyl cation.

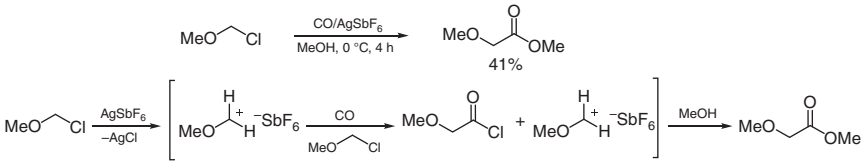

Scheme 9.20 Carbonylation of methoxymethyl chloride with $AgSbF_6$. Source: Modified from Ohga et al. [21].

9.3.3 Carbonylative Coupling Reactions Promoted by Metal–Silver Bimetallic Catalysts

The redox properties of silver(I) compounds can help avoid the deactivation of other metal catalysts. This redox nature combined with the Lewis acid property made Ag(I) an effective co-catalyst in palladium- or cobalt-catalyzed carbonylation reactions.

The promotional effect of silver(I) salts have been studied in reductive carbonylation of nitrobenzene under palladium catalysis (Table 9.3) [22].

The reaction carried out under CO atmosphere in methanol afforded urethane **49**. Furthermore, the catalytic systems containing a nitrogen ligand in the presence of AgF or AgTFA in 1 : 1 ratio Pd/Ag showed slightly higher nitrobenzene conversion and selectivity toward carbamate **49** in comparison with the experiment conducted solely with the palladium catalyst (entries 2, 3, 5 vs. 1, 4, Table 9.3). On the other hand, experiments conducted in the absence of palladium source indicated that Ag(I) salts alone were inactive as catalysts (entry 6, Table 9.3). Probably, the

Table 9.3 Reductive carbonylation of nitrobenzene[a].

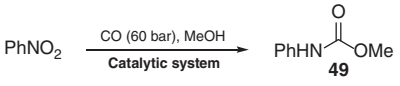

Entry	Catalytic system	49 (%)
1	$Pd(OAc)_2$	75
2	$Pd(OAc)_2$/AgF[b]	79
3	$Pd(OAc)_2$/AgTFA[b]	81
4	$Pd(TFA)_2$	78
5	$Pd(TFA)_2$/AgTFA[b]	83
6	Ag(I)salts	—

a) Reaction conditions: cat. (0.1%), 1,10-phenanthroline (3.0%), *p*-toluenesulfonic acid (2.0%), 135 °C, two hours.
b) Pd/Ag ratio = 1 : 1.

redox nature of Ag(I) salts avoids the formation of the inactive palladium black, improving the selectivity toward phenylcarbamate **49**.

Another application of the Pd/Ag bimetallic synergic catalysis regards the carbonylation of C(sp^2)–H in the presence of dimethylformamide (DMF) and atmospheric oxygen as cheap and safe CO surrogate [23]. The developed catalytic system did not require the use of base or additives, while atmospheric oxygen was found to be the best oxidizing agent. Using $Pd(OAc)_2$ and AgOTf as palladium and silver sources, the reactivity of a range of substituted *N*-aryl-2-aminopyridines **50a–t** was investigated (Scheme 9.21). In general, both electron-donating groups and electron-withdrawing groups on the aromatic rings are well tolerated, and quinazolinones **51a–t** were isolated in good yields.

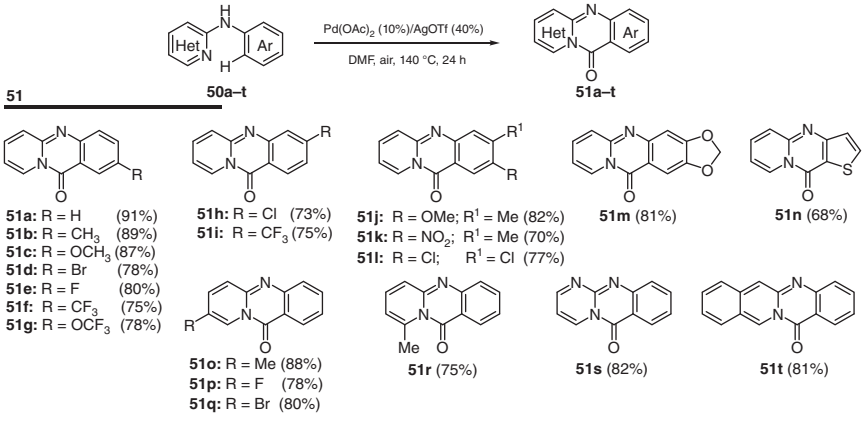

Scheme 9.21 Pd/Ag as synergic catalysts for the tandem CO functionalization of C(sp^2)—H bonds/C–N cyclization.

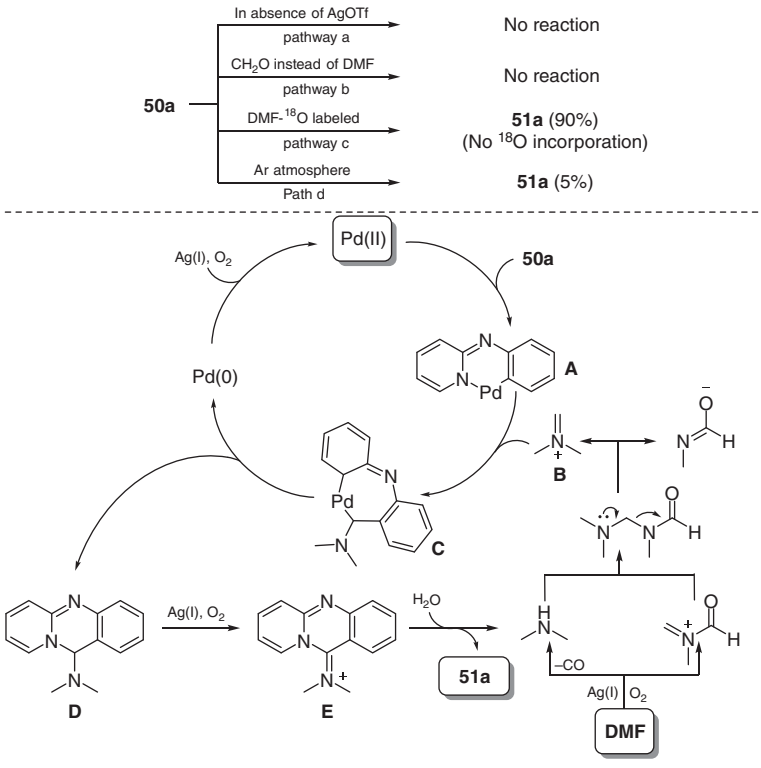

Scheme 9.22 Control experiments and reaction mechanism.

Substrate **50a** was used as the model compound to better understand the outcome of this process (Scheme 9.22).

Reactions conducted either in the absence of AgOTf or using formamide instead of DMF did not furnish the product **51a**, suggesting that AgOTf acted as a co-catalyst (pathway a, Scheme 9.22) and the methyl groups of DMF could be involved in the catalytic cycle (pathway b, Scheme 9.22). Interestingly, when labeled DMF-O^{18} was used as solvent, no incorporation of O^{18} in **51a** was detected (pathway c, Scheme 9.22). Finally, argon atmosphere was detrimental for the reaction progress, indicating that the quinazolinone oxygen atom is coming from environmental oxygen sources (pathway d, Scheme 9.22). These results, on the whole, indicated that palladium(II) catalyzes the C–H activation/intramolecular amination of **50a**, providing palladacycle **A**. At the same time, DMF was converted to the iminium species **B** via a domino "decarbonylation/nucleophilic addition/elimination process" mediated by the silver(I) salt under oxidative conditions. Nucleophilic addition of complex **A** to ion **B** generated **C**, which underwent reductive elimination to **D** and Pd(0). The Pd(0) metal was reoxidized to the active catalyst Pd(II) by Ag(I) in the presence of O_2. On the other hand **51a** was formed after oxidation and hydrolysis of **D**. Following a similar pathway, a series of phenanthridinones (**52a**–**g**) bearing on the aromatics ring a range of functional groups with various electronic properties was synthesized (Scheme 9.23).

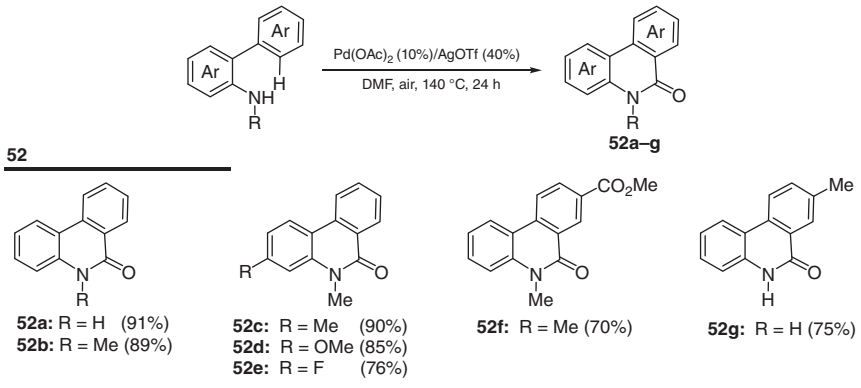

Scheme 9.23 Reaction scope.

9.4 Molybdenum Compounds in Carbonylation Reactions

In the field of second-row transition metals, molybdenum is the most employed element in many types of carbonylation reactions. Molybdenum can act as catalyst and/or carbon monoxide source, especially as molybdenum hexacarbonyl, in procedures such as formal carbonylations and intermolecular and intramolecular coupling reactions.

9.4.1 Formal Carbonylation Processes: Carbonylation of Ethylene and Methanol

Molybdenum hexacarbonyl was used as the effective catalyst and carbon monoxide source in formal carbonylation reactions of alkyl halides, alkenes, and primary alcohols. The first example of this reactivity was reported in 1992 in a procedure for carbonylation of alkyl halides in which $Mo(CO)_6$ was activated by fluoride ion to generate metal carbonyl anions providing the corresponding esters (Scheme 9.24) [24]. If dihalogenated compounds were used as starting materials, lactones **53b–d** were obtained as final products (entries 2–4, Scheme 9.24). Both the R residue in **53** are furnished by an electrophilic reagent while the oxygen atom necessary for the ester formation comes from a water molecule.

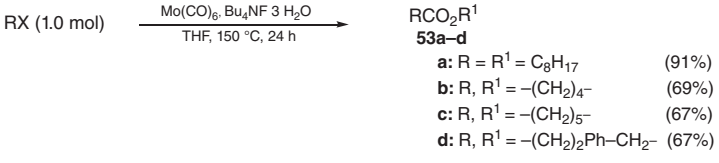

Scheme 9.24 $Mo(CO)_6$-promoted carbonylation of alkyl halides: synthesis of esters and lactones. Source: Modified from Imbeaux et al. [24].

Replacement of tetrabutylammonium fluoride with KF did not affect the reaction progress. Conversely, starting material or the nucleophilic substitution product was recovered when tetrabutylammonium iodide, bromide, or hydroxide was used. Catalytic amount of $Mo(CO)_6$ was enough to accomplish the carbonylation /esterification process. In this case, methyl formate was added to the reaction medium to provide the stoichiometric amount of CO necessary for the carbonylation.

Catalytic carbonylation of ethylene to propionic acid and the corresponding anhydride was realized in the presence of $Mo(CO)_6$, an alkyl halide, and a quaternary phosphonium iodide [25]. Two alternative mechanisms were proposed. The first involved a free radical pathway, in which the dissociated species $Mo(CO)_5$ reacted with EtI forming the $Mo(CO)_5I$ species and ethyl radicals, which in their turn generated the pivotal complex $Mo(EtCO)(CO)_5$ (pathway a, Scheme 9.25).

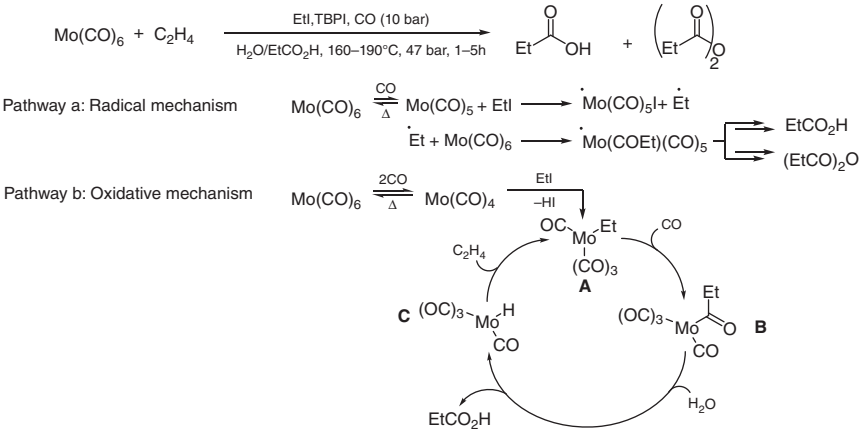

Scheme 9.25 Ethylene carbonylation with $Mo(CO_6)$.

Furthermore, the main termination process involved a dimerization of intermediate $Mo(EtCO)(CO)_5$ forming $[Mo(EtCO)(CO)_5]_2$ and propionic anhydride after intramolecular elimination. The second hypothesis of reaction mechanism was based on the oxidative addition of EtI to a $Mo(CO)_4$ intermediate (complex **A**, pathway b, Scheme 9.25). The subsequent CO migratory insertion/carbonylation generated **B**. Hydrolysis of **B** furnished propanoic acid and molybdenum hydride **C**, which could add to ethylene, thus regenerating complex **A**. Interestingly, the yield of propionic acid obtained by this strategy was dramatically improved soaking or condensing $Mo(CO)_6$ on a zeolite material [26]. Zeolite HY (Si : Al atomic ratio = 15, 30, or 40) as solid support are produced up to 40 ton of propionic acid in five hours. This straightforward activity could be ascribed to the Brønsted acidic site on the solid support.

Carbonylation of ethylene to related carbonyl compounds was accomplished under syngas atmosphere (1 MPa) in the presence of supported NiMo sulfide catalysts at 240 °C [27]. Many catalyst supports (i.e. carbon, alumina, magnesia,

and zirconia) were suitable for this transformation. In particular, carbon-supported catalysts became the most active and selective toward the production of diethyl ketone (25%).

Methanol is widely used in formal carbonylations promoted by molybdenum hexacarbonyl complex for the preparation of methyl acetate on supported materials and methyl formate under homogeneous conditions. Differently from carbonylation of ethylene, carbon-supported sulfided Co/Mo bi-catalysts were found to be active at atmospheric pressure and 250 °C for carbonylation of methanol without using methyl iodide as carbonylation promoter [28]. This process selectively leads the formation of methyl acetate. Sulfided Co/C catalysts were proven to be effective for the acetate formation even though the methanol conversion was higher using a Co/Mo bi-catalyst (CO/Mo ratio 3/10; methyl acetate 53% yield). On the other hand, no methyl acetate was detected when sulfided Mo/C catalysts were used under these reaction conditions.

The continuous production of methyl formate could be performed by conversion of methanol in the presence of syngas or CO, a bimetallic catalyst system ($Mo(CO)_6$ and potassium methoxide) in THF. In addition, the final result was recognized closely related to the $Mo(CO)_6/KOCH_3$ ratio [29]. The synthesis could be conducted in the presence of the potassium methoxide catalyst alone. However, the addition of molybdenum carbonyls enhanced the performance of the reaction. In particular, the use of a 1/2 $Mo(CO)_6$/KOMe molar ratio gave the best result. Finally, no reaction product was detected in the absence of KOMe. The mechanism proposed proceeds via the methoxycarbonyl salt intermediate **A**, which is then protonated by methanol to eliminate methyl formate and regenerating both potassium methoxide and molybdenum active species after CO addition (Scheme 9.26).

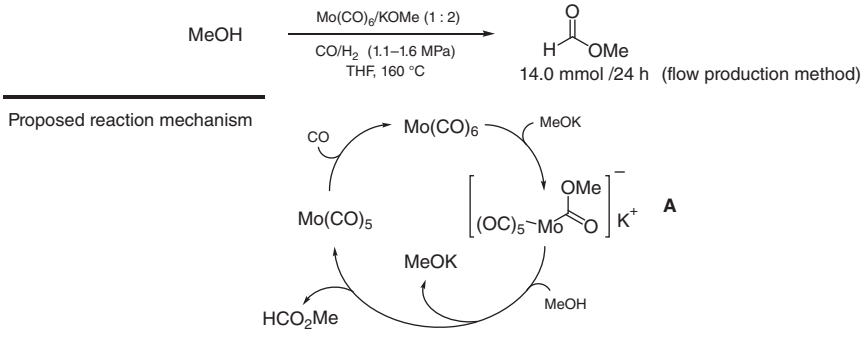

Scheme 9.26 Flow production of methyl formate via formal carbonylation of methanol: proposed reaction mechanism.

9.4.2 Molybdenum Carbonyl Complexes as Catalysts and CO Source in Intermolecular Carbonylation Coupling Reactions of Aryl or Alkenyl Halides

Reactions of aryl halides with several nucleophiles employing molybdenum carbonyl complexes as the reaction catalysts and carbon monoxide source were

described. Depending on the nature of the nucleophile used, a variety of carboxylic derivatives were accomplished avoiding the use of gaseous carbon monoxide.

In 2010, the Yamane research group found that the carbamoylation to the corresponding amide occurs in high yields when the aryl halide source was treated with a stoichiometric amount of molybdenum carbonyl amine complexes in the presence of a base (Scheme 9.27) [30]. Aryl iodide and bromide were suitable substrate for this transformation. The process tolerates a variety of electron-deficient and electron-rich (hetero)aryl halides, and the corresponding products **54** were isolated in good yield. Compound **54k**, bearing a 2-bromopyridine residue, was isolated in low yield (49%) due the strong coordination of pyridine nitrogen atom to the molybdenum metal center. Benzyl bromide and alkenyl bromides were also successfully tested.

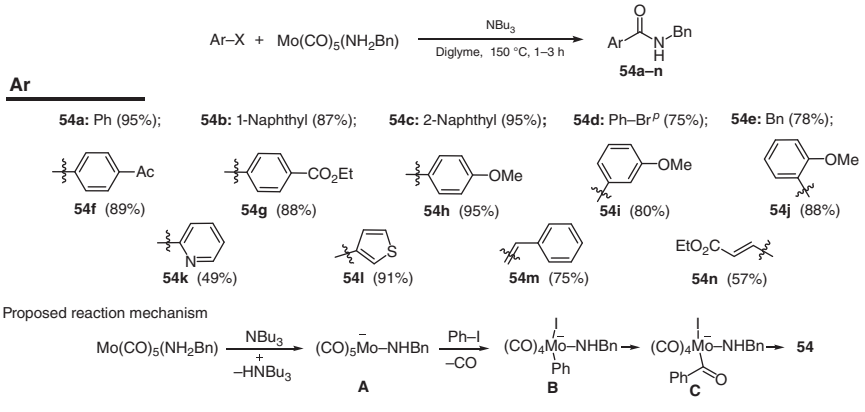

Scheme 9.27 Molybdenum-promoted carbamoylation of aryl halides.

The authors suggested that, most probably, the acyl metal intermediate **C** could be generated by the oxidative addition of the halobenzene to molybdenum complex **A** followed by insertion of carbon monoxide to phenyl-molybdenum bond. The final reductive elimination furnished the target compound **54**. A lower loading of the molybdenum source was then realized through the *in situ* generation of the active Mo carbonyl amino complex by reacting the amine and $Mo(CO)_6$ in the presence of tetraethylammonium chloride [31]. Also, the use of a catalytic amount of both $Mo(CO)_6$ and Et_4NCl in the presence of a stoichiometric amount of benzylamine, aryl halide, and NBu_3 in diglyme at 150 °C furnished amides **54a–n** (yields: 57–99%). It is worth of note that the 20% of $Mo(CO)_6$ corresponds to a slightly excess of CO. The scope of the process was extended varying the nature of the amine used in the presence of phenyl iodide (Scheme 9.28). Anilines, primary and secondary aliphatic amines, and heteroaromatic amines gave the corresponding amides **55a–j** in good yields. The authors described two plausible reaction mechanisms (pathway a-b, Scheme 9.28). Pathway a involved the formation of intermediate **B** by nucleophilic attack of the amine to a CO residue and oxidative addition of the aryl halide specie. On the other hand, molybdenum complex **A** could undergo oxidative addition of the aryl halide and a subsequent insertion of carbon monoxide generating C (pathway b).

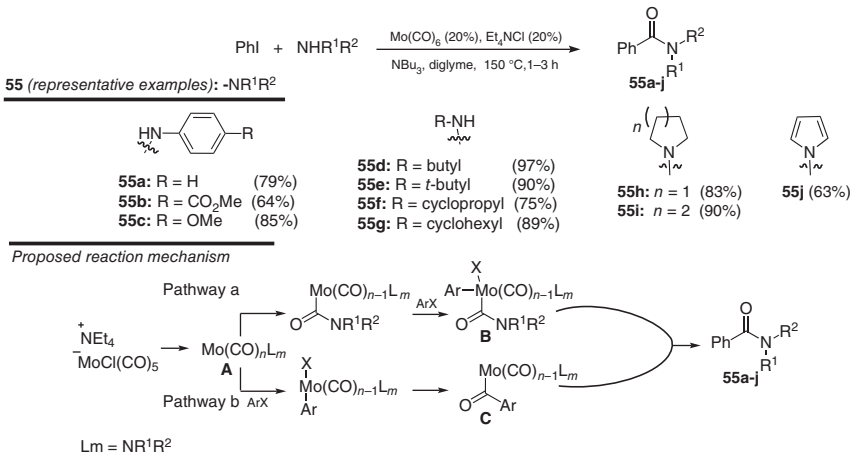

Scheme 9.28 Scope of catalytic $Mo(CO)_6$-mediated carbamoylation reaction.

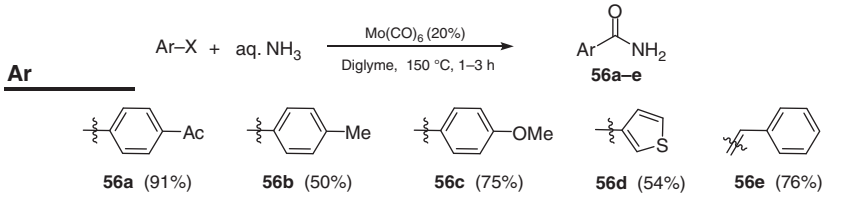

Scheme 9.29 Scope: primary amides synthesis.

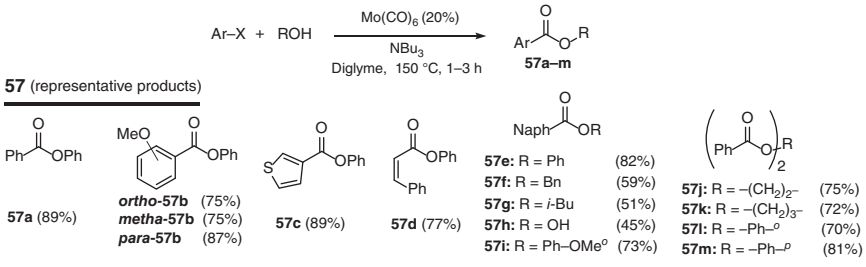

Scheme 9.30 Alkoxycarbonylation of aryl halides with a low loading of $Mo(CO)_6$ for the synthesis of esters. Source: Modified from Ren et al. [32].

Primary amides could be synthesized by simple treatment of $Mo(CO)_6$ with aqueous ammonia. Representative primary amides were isolated from moderate to good yields employing electron-rich and electron-deficient aryl, heteroaryl, or styryl halides (**56a**–**e**, Scheme 9.29).

This process was proven to be efficient also when the hydroxy group was employed as nucleophile (synthesis of **57a**–**m**, Scheme 9.30) [32].

A strictly related molybdenum-promoted carbonylation of aryl halides with nucleophiles was reported in 2010 [33]. In this one-pot process under MW irradiation, a range of carboxylated products were obtained combining a stoichiometric amount of $Mo(CO)_6$ and Et_4NCl in 1,4-dioxane at 140 °C for two minutes to form complex $Mo(CO)_5Cl{\cdot}NEt_4$. The following additions of a stoichiometric amount of aryl halide

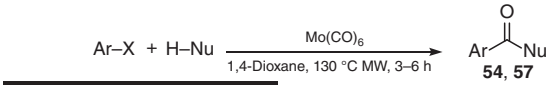

54: Nu = NHBn: Ar = EWG-aryl (80–99%), EDG-aryl (75–98%), heteroaryl (87–97%)
Ar = Ph: Nu = Ph–NH (99%); RSO_2NH (71–93%); R_1R_2N (96–95%)
57: Ar = Ph: Nu = OH (95%); OMe (65%)

Scheme 9.31 Mo-mediated carbonylation of aryl halides under microwave irradiation.

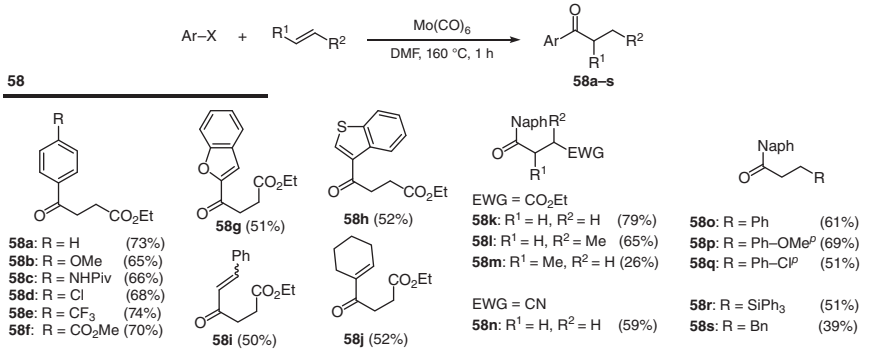

Scheme 9.32 Intermolecular molybdenum carbonyl promoted formation of ketones.

and nucleophile, and further MW heating at 130 °C (three to six hours), furnished the desired carbonylated compound (**54** and **57** Scheme 9.31).

Aryl or alkenyl halides could also react with alkenes in the presence of molybdenum carbonyl complexes, leading to the formation of ketones [34]. Treating a mixture of halides and a large excess of alkene with stoichiometric $Mo(CO)_6$ in DMF at 160 °C, the addition products **58** were obtained (Scheme 9.32). A range of halides were tested, showing that aryl residues with different electronic properties and functional groups and heteroaromatic or alkenyl halides were tolerated.

The effect on the reactivity of the olefin counterparts was also studied (**58k–s**, Scheme 9.32). In particular, acylmolybdenum addition to alkenes was realized on electron-rich alkenes **58r,s**, and a complete regioselectivity was obtained when substituted alkenyl moiety were employed (**58l,m**, Scheme 9.32). Most probably, the reaction proceeds through the formation of an acylmolybdenum species, generated by oxidative addition of aryl or alkenyl halides to $Mo(CO)_6$, followed by carbon monoxide insertion and addition to the olefinic counterparts. Isomerization of the alkylmolybdenum species could then occurs through β-hydride elimination and hydrometalation to form a molybdenum enolate intermediate. The final protonation generates **58**.

9.4.3 Molybdenum Carbonyl Complexes as Both Catalysts and CO Source in Intramolecular Carbonylation Coupling Reactions

The latter intermolecular procedure described in Section 9.4.2 was also realized at intramolecular level [34]. The one-pot intramolecular acylmolybdenum addition to alkenes gave the corresponding cyclized ketones when simple alkenes tethered to the iodobenzene ring were employed (**59a–d**, Scheme 9.33), while indanone **59e** and

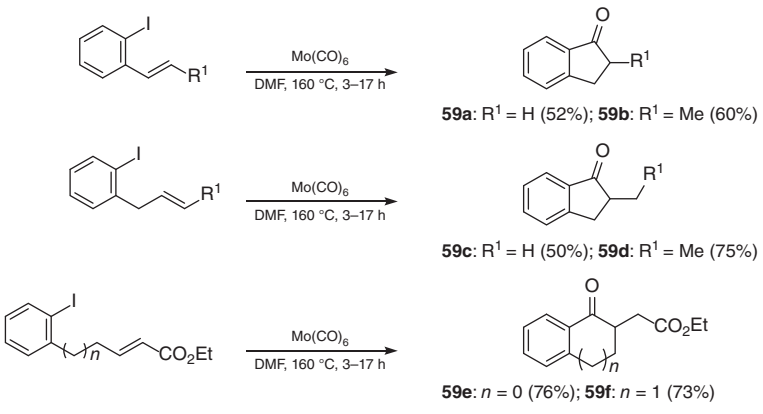

Scheme 9.33 Intramolecular acylmolybdenum addition to alkenes.

Table 9.4 Intramolecular Mo-carbonylative addition to haloaryl- and haloalkenyl-imines.

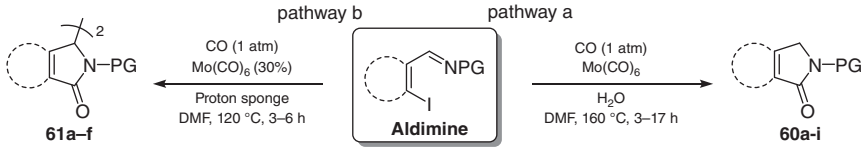

Entry	Aldimine	R^1	R^2		Pathway a: 60 (%)	Pathway b: 61 (%)
1	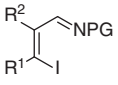	$CH_2CH_2CH_2$		a	49	90
2		$CH_2(CH_2)_2CH_2$		b	86	91
3		Ph	Me	c	94	50
4	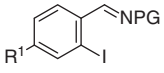	H	—	d	66	91
5		OMe	—	e	55	72
6		Cl	—	f	49	55
7	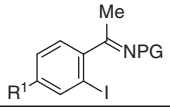	H	—	g	73	
8		OMe	—	h	81	
9		Cl	—	i	59	

α-tetralone **59f** were isolated working with iodobenzenes bearing a α,β-unsaturated ester group.

Haloaryl- and haloalkenyl-imines are suitable substrates for oxidative molybdenum-promoted carbonylative cyclizations [35]. A divergent synthesis of γ-lactams could be achieved working in the presence of $Mo(CO)_6$, under CO atmosphere in DMF as the solvent (Table 9.4).

Thus, using a stoichiometric amount of molybdenum source and a proton donor (water), γ-lactams **60a–i** were isolated (pathway a, Table 9.4). On the other hand, $Mo(CO)_6$-catalyzed synthesis of bis(γ-lactam) derivatives **61a–f** was realized under anhydrous conditions in the presence of 30 mol% of $Mo(CO)_6$ and a stoichiometric amount of proton sponge (pathway b, Table 9.4).

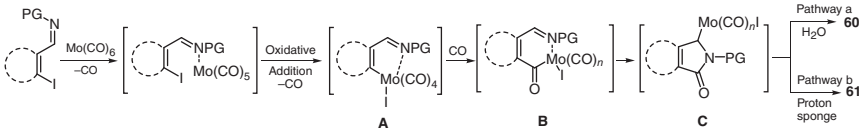

Scheme 9.34 Reaction mechanism.

Concerning the reaction mechanism (Scheme 9.34), intermediate **A** was formed after coordination of the imine nitrogen atom to the molybdenum, followed by oxidative addition to the carbon(sp^2)–halogen bond. The next insertion of a CO molecule generates an acyl molybdenum complex **B**, which undergoes migration to alkyl intermediate **C**. Protonation of **C** to **60** occurs in the presence of water, while in the presence of proton sponge transmetalation and reductive elimination of **C** furnished **61** and the active molybdenum(0) catalyst.

$Mo(CO)_6$ was reported as promoter for cyclocarbonylations of allenyl carbonyl compounds to fused bicyclic γ-butyrolactones [36]. A stoichiometric amount of $Mo(CO)_6$ in association with DMSO were required for the reaction carried out on substrates **62a–h** (Scheme 9.35). By this way, carbo- and heterocycles **63a–h** were isolated as single diastereoisomers. A probable stereochemical outcome was explained by assuming that DMSO acts as ligand exchanging with CO and generating the intermediate **A**, which contained a vacant orbital able to interact with the allenyl moiety. Intermediate **A**, in its turn, transformed into metalacycle **B** via a *syn* stereochemical outcome. Migratory insertion of the vinyl group to carbonyl group was probably assisted by DMSO (complex **C**), and the final CO insertion followed by reductive elimination provided product **63**.

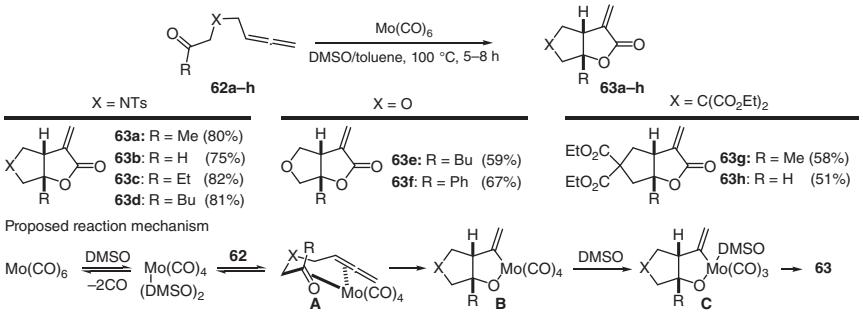

Scheme 9.35 Molybdenum-mediated cyclocarbonylation of allenyl compounds.

An analogous molybdenum-promoted cyclocarbonylation of allenyl compounds was also realized starting from the 1-ethynyl-2-allenylbenzenes **64** (synthesis of **65a–h**, Scheme 9.36) [37]. The reaction proceeded smoothly using $Mo(CO)_3(CH_3CN)_3$ as the stoichiometric carbonyl reagent under very mild reaction conditions.

9.4.4 Metal-Catalyzed Coupling Procedures Using Molybdenum as the CO Source

The $Mo(CO)_6$ complex has been widely used as a condensed source of carbon monoxide in palladium-catalyzed carbonylation coupling reactions of

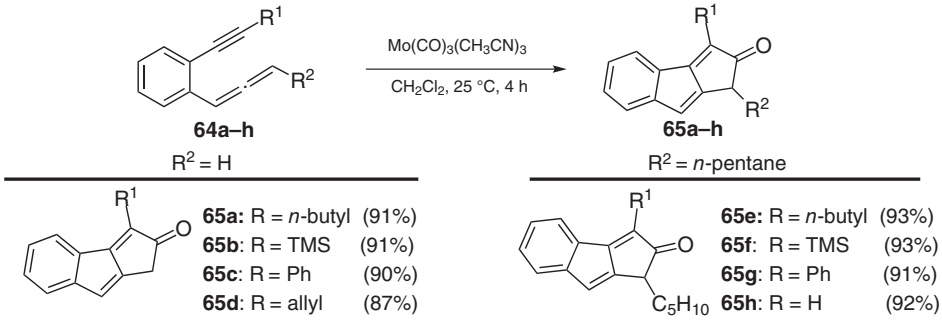

Scheme 9.36 Molybdenum-mediated cyclocarbonylation of 1-ethynyl-2-allenyl benzenes.

C(sp^2)–halogen bonds by a Pd(0)/Pd(II) catalytic cycle. Some examples on molybdenum-promoted palladium-catalyzed C(sp^2)– or C(sp^3)–H activation or transmetalation reactions are also reported. In this type of reactions, the addition of the electrophile to the palladium species generates the key organopalladium(II) intermediate susceptible of CO insertion. The generated palladium(II) complex is finally attacked by the nucleophile, giving the product and regenerating the Pd catalyst. Usually a base is required to promote the release of CO from the molybdenum complex and to abstract a proton from the nucleophile. Furthermore, the use of $Mo(CO)_6$ complex represents one of the most convenient and safer methods for handling the toxic carbon monoxide gas due to its ability to release CO into the reaction mixture at atmospheric pressure and temperatures above 150 °C [38].

Palladium-catalyzed procedures involving molybdenum carbonyl complexes are shown below. Finally, the nickel-catalyzed carbonylation reactions promoted by molybdenum reported in the literature are described.

9.4.4.1 Intermolecular Cross-Coupling Procedures

The first palladium-catalyzed $Mo(CO)_6$-promoted carbonylation of C(sp^2)–halogen bonds was performed using Pd/C as the catalyst. Nitrogen- and oxygen-containing nucleophiles were successfully used (synthesis of **66**, Table 9.5) [39].

Furthermore, the oxidative addition of the aryl halide to the palladium(0) A formed aryl palladium B. B, in turn, is able to coordinate the carbon monoxide released treating $Mo(CO)_6$ under heating in the presence of ligands. Subsequently, the nucleophile reacts with complex C providing **66**. Further investigation showed that the process could be conducted under milder reaction conditions changing the Pd source. Working with a stoichiometric amount of a suitable additive accelerated the release of CO from $Mo(CO)_6$ via a ligand exchange process. In particular, the addition of the strong amidine base DBU generated a $Mo(DBU)_2(CO)_4$ species, allowing to extend the process on a variety of both electrophiles and nucleophiles [40]. Thus, a broad array of Pd-catalyzed carbonylative $Mo(CO)_6$-mediated strategies have been developed during the last decade. In Scheme 9.37, the representative Pd-catalyzed $Mo(CO)_6$/DBU-promoted carbonylation processes are summarized.

Aminocarbonylation of aryl halides with different electronic properties have been realized on sterically hindered amines (*tert*-butylamine) or poorly nucleophilic

Table 9.5 Palladium-catalyzed $Mo(CO)_6$-promoted carbonylation of aryl iodides.

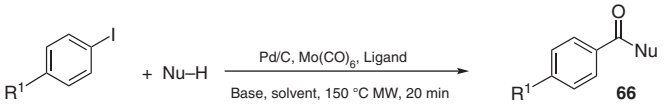

Proposed reaction mechanism

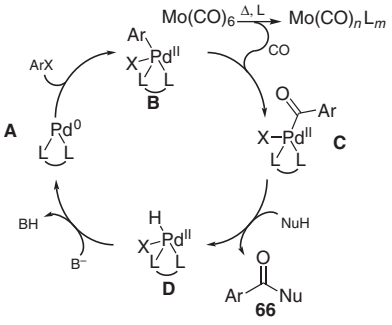

Entry	Nu–H	R^1	Base	Solvent	66 (%)
1	$BuNH_2$ or piperidine	EWG or EDG	K_2CO_3	Diglyme	65–83
2	H_2O or ROH	EWG or EDG	DMAP/DIPEA	1,4-Dioxane	33–98

Sources: Kaiser et al. [39a], Georgsson et al. [39b, c].

aniline (pathway a, Scheme 9.37) [41]. Heteroaryl amines were used by slightly varying the reaction conditions, i.e. using thermal heating at 120 °C in DMF as the reaction solvent [42], with addition of K_2CO_3 when indolyl compounds were used [43]. The same protocol was also useful in hydroxycarbonylation [44] or amidocarbonylation reaction using ureas, hydrazides (pathway b, Scheme 9.37) [45], sulfinimides (pathway c, Scheme 9.37) [46], sulfonamides [47], sulfamide [48], sulfonimidamides (pathway d, Scheme 9.37), or cyanamides (pathway e, Scheme 9.37) as nucleophiles [49, 50].

Several polyfunctionalized aryl iodides or bromides were effectively subjected to amino- or amidocarbonylation conditions (synthesis of **67**–**70**, Scheme 9.38) [51].

Substituted aryl chloride or sulfonate [52, 53] and heteroaryl or alkenyl halides were also found to be suitable electrophilic partners for this system [49, 54, 55]. The utility of the Pd-catalyzed $Mo(CO)_6$/DBU-mediated process was improved in CO functionalization of sulfonyl azides with nucleophiles. The use of aryl amides and amine or alcohol nucleophiles afforded acylsulfonyl and sulfonyl ureas or carbamates, respectively (Scheme 9.39) [56]. According to the general carbonylation mechanism, the oxidative addition on the sulfonyl azide group led to a nitrene–palladium complex, which underwent CO insertion and reductive elimination furnishing the key sulfonyl isocyanate. This latter was then trapped by the nucleophile.

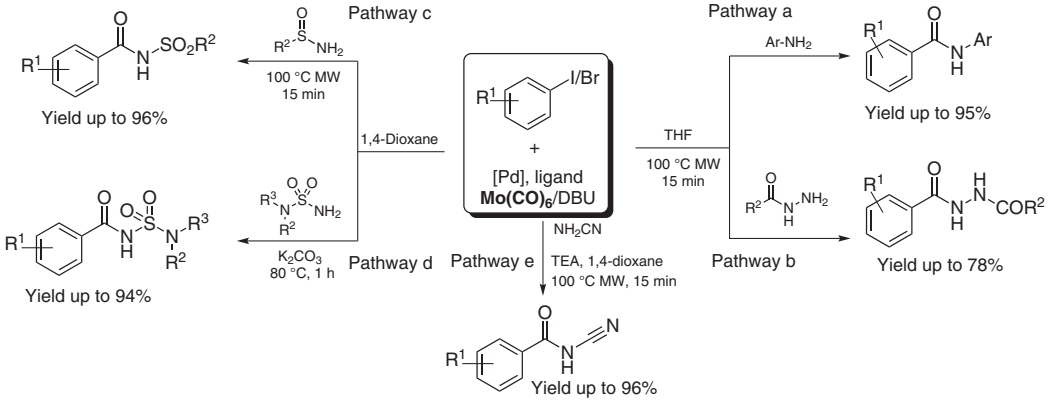

Scheme 9.37 DBU-mediated amino- and amidocarbonylation of aryl iodides and bromides. Source: Modifed from Wannberg and Larhed [41].

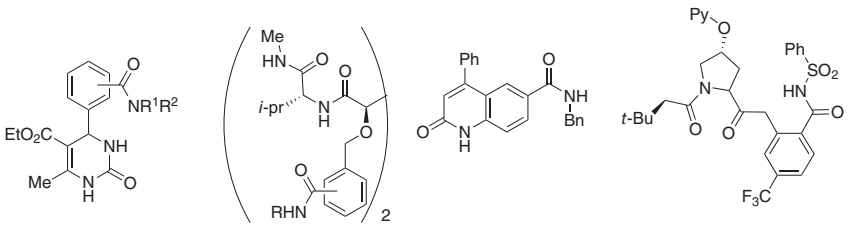

Scheme 9.38 DBU-mediated amino- and amidocarbonylation: synthesis of targets. Sources: Wannberg et al. [51a, c], Glasnov et al. [51b], Rönn et al. [51d].

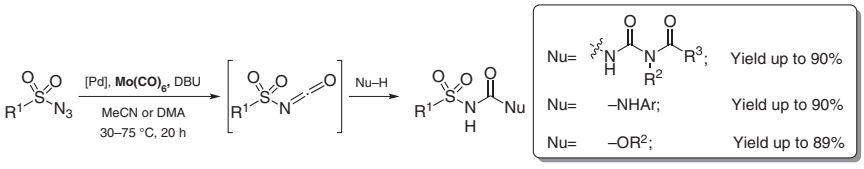

Scheme 9.39 Mo-promoted CO functionalization of sulfonyl azides. Sources: Adapted from Chow et al. [56].

9.4.4.2 Cascade and Intramolecular Cross-Coupling Procedures

Pd-catalyzed $Mo(CO)_6$-mediated carbonylation strategy was also recognized as a useful method for the synthesis of functionalized heterocycles. Starting from appropriately substituted aryl halides, different heterocyclic structures could be assembled by changing the nucleophilic coupling partner. Furthermore, 2-iodoaniline compounds were coupled with alkynes through Pd-catalyzed carbonylative Sonogashira/cyclization sequences (Scheme 9.40). This approach gave access to 4-quinolone and 4-chromone scaffolds (pathway a and b, respectively, Scheme 9.40) using terminal alkynes [58, 59] or 2-quinolones with internal alkynes either symmetric ($R^2 = R^3$; pathway c, Scheme 9.40) or nonsymmetric ($R^2 \neq R^3$; pathway d, Scheme 9.40) [57]. In the latter case, the use of alkynes bearing electron-rich and electron-poor substituents was essential to induce good regioselectivity. This reaction (pathway d, Scheme 9.40) has also been conducted on internal alkenyl compounds [60].

Isocyanates (pathway a, Scheme 9.41) [61], cyanamides (pathway b, Scheme 9.41) [63], nitroalkanes (pathway c, Scheme 9.41) [64], and amines (pathway d, Scheme 9.41) [62] were recognized as other nucleophiles useful in cascade Pd-catalyzed amino- and amidocarbonylation with $Mo(CO)_6$ as the CO source.

Intramolecular carboannulation procedures have been accomplished on 2-halostyrenes (Scheme 9.42) [65]. The carbopalladation of the double bond by the acylpalladium intermediate furnished the corresponding indanone.

Intramolecular cyclizations involving C—H bond functionalization have been reported in the literature. Direct $C(sp^2)$–H functionalization/aminocarbonylations were obtained on acyl hydrazine and azoarene substrates (pathway a and b, Scheme 9.43) [66, 67], while a $C(sp^3)$–H activation strategy was realized on *N*-protected aliphatic amines or amino acids bearing a γ-methyl residue (pathway c,

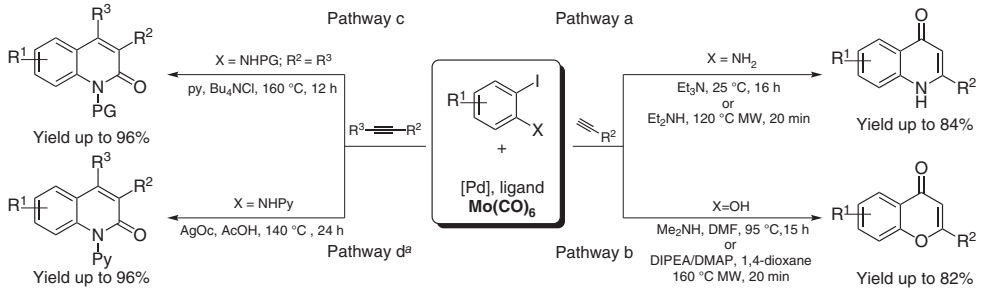

[a] Internal alkenes were also used under these conditions

Scheme 9.40 Pd-catalyzed $Mo(CO)_6$-promoted carbonylative Sonogashira/cyclization reactions. Sources: Adapted from Jafarpour and Otaredi-Kashani [57a], Chen et al. [57b].

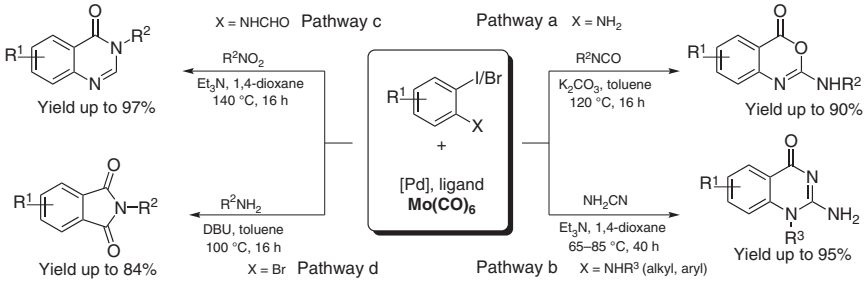

Scheme 9.41 Nucleophiles used in cascade Pd-catalyzed $Mo(CO)_6$-promoted carbonylative reactions. Sources: Wu et al. [61, 62], Åkerbladh et al. [63].

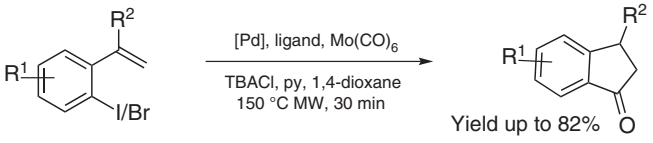

Scheme 9.42 Intramolecular C(sp^2)–halogen carbonylation. Source: Modified from Wu et al. [65].

Scheme 9.43) [68]. C(sp^2)–H carbonylative cyclization also occurred under these reaction conditions. For these transformations, the Pd(II)-catalyzed C–H activation is followed by CO insertion, reductive elimination, and reoxidation of the Pd(0) species by benzoquinone or AgOAc.

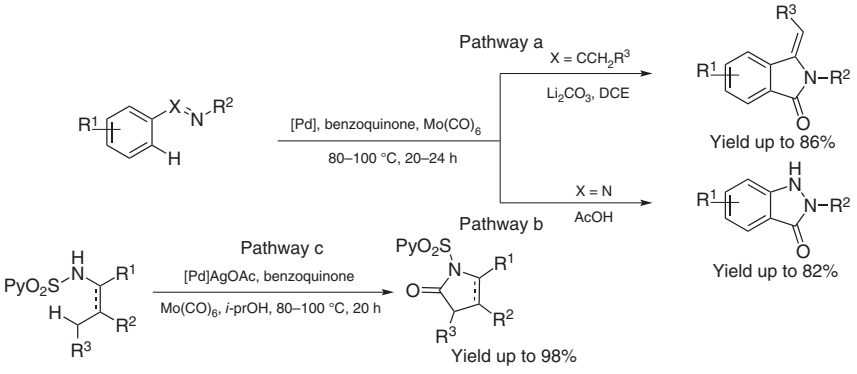

Scheme 9.43 $Mo(CO)_6$-promoted carbonylative intramolecular cyclizations via C–H activation. Sources: Adapted from Wang et al. [66, 67].

9.4.4.3 Carbonylative Cross-Coupling in the Presence of Transmetalation Partners

Organometallic nucleophiles in Pd-catalyzed $Mo(CO)_6$-promoted carbonylations allowed access to unsymmetrical ketones. Hiyama and Negishi cross-coupling performed on aryl halides led to the formation of aryl ketones (Scheme 9.44). Employing trimethylsilyl acetonitrile in the presence of CuF_2 as the activating agent various substituted acetonitriles have been synthesized (Hiyama type; pathway a, Scheme 9.44) [69], while benzylated compounds were obtained using benzylzinc bromide (Negishi; pathway b, Scheme 9.44) [70].

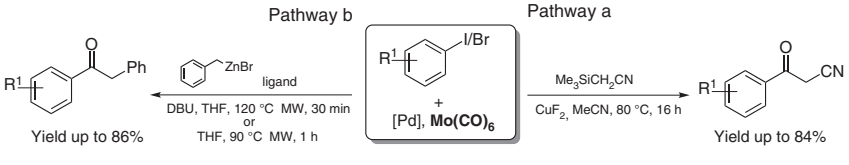

Scheme 9.44 $Mo(CO)_6$-promoted Hiyama and Negishi cross-coupling. Sources: Adapted from Pyo et al. [69], Motwani and Larhed [70].

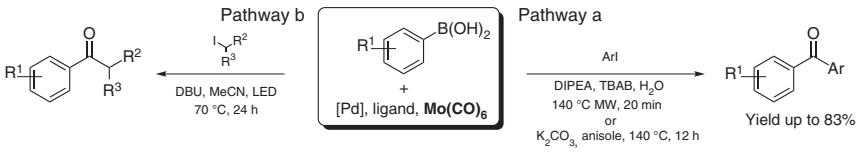

Scheme 9.45 $Mo(CO)_6$-promoted carbonylative Suzuki–Miyaura cross-coupling.

Aryl and alkyl halides [71, 72] have been used as coupling partners in Pd-catalyzed $Mo(CO)_6$-promoted carbonylative Suzuki–Miyaura cross-coupling reactions of arylboronic acids (pathway a and b, Scheme 9.45). In particular, using alkyl halides as substrates, visible-light photocatalysis has been applied under Pd(0)-catalyzed conditions (pathway b, Scheme 9.45).

Aryl and heteroaryl stannanes were also coupled with aryl (pathway a, Scheme 9.46) or benzyl halides (pathway b, Scheme 9.46) [75, 76]. Both electron-rich and neutral stannanes and heteroaromatic stannanes (i.e. furanyl or thienyl stannanes) afforded the corresponding ketones in good yield.

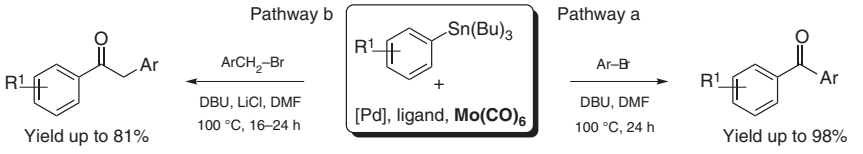

Scheme 9.46 $Mo(CO)_6$-promoted carbonylative Stille coupling reactions. Sources: Adapted from Jenner et al. [73], Kelkar et al. [74].

A Stille coupling procedure was performed under nickel catalysis and $Mo(CO)_6$ as the CO source (pathway a, Scheme 9.47) [79]. Finally, a nickel-catalyzed molybdenum-promoted carbonylative homocoupling reaction of aryl halides was applied in the synthesis of symmetrical benzophenones (pathway b, Scheme 9.47) [80]. In the latter case, most probably, zinc acted as reducing agent to generate the Ni(0) active species *in situ*.

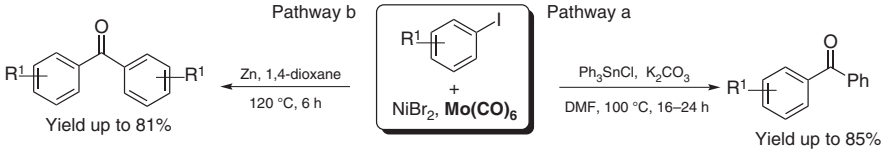

Scheme 9.47 Ni-catalyzed $Mo(CO)_6$-promoted carbonylative coupling reactions. Sources: Whyman et al. [77], Gautron et al. [78].

9.5 Summary and Conclusions

In this chapter, the advancement in the field of second-row transition metal-promoted carbonylative reactions has been discussed. The catalytic efficiency in

these procedures is still limited compared with other more "noble" and precious metals. However, zirconium, silver, and molybdenum catalysis may give access to a plethora of carbonylated compounds via coupling or formal carbonylative reactions. Fundamental differences concern the applications and reaction mechanisms of these metals. Zirconium acts as the effective carbonylation catalyst in the form of sulfated zirconia or zirconocene complexes under CO pressure, while silver is typically used as salts to enhance or promote the activity of other carbonylation catalysts. Furthermore, molybdenum, in particular molybdenum hexacarbonyl, is the most employed second-row transition metal in carbonylation reactions due to its ability to act as catalyst and/or carbon monoxide source, avoiding the use of CO atmosphere. Despite the progress in the last decades, the use of "neglected" second-row transition metals in carbonylation reactions today remains largely unexplored and much has yet to be discovered. The ongoing research in this field may pave the way for new sustainable carbonylation reactions, which is a topic of remarkable interest to the chemical community.

References

1 Clingenpeel, T.H., Wessel, T.E., and Biaglow, A.I. (1997). *J. Am. Chem. Soc.* 119: 5469–5470.
2 Mori, H., Wada, A., Xu, Q., and Souma, Y. (2000). *Chem. Lett.*: 136–137.
3 Stepanov, A.G., Luzgin, M.V., Krasnoslobodtsev, A.V. et al. (2000). *Angew. Chem. Int. Ed.* 39: 3658–3660.
4 Luzgin, M.V., Stepanov, A.G., Shmachkova, V., and Kotsarenko, N. (2001). *Mendeleev Commun.* 11 (290): 23–25.
5 Luzgin, M.V., Thomas, K., Van Gestel, J. et al. (2004). *J. Catal.* 223: 290–295.
6 Erker, G. (1984). *Acc. Chem. Res.* 17: 103–109.
7 (a) Negishi, E., Holmes, S.J., Tour, J.M. et al. (1989). *J. Am. Chem. Soc.* 111: 3336–3346. (b) for an alternative procedure for generating "Cp_2Zr" ($Mg/HgCl_2$ instead of BuLi) applied to the synthesis of **27a**, see: Negishi, E., Holmes, S.J., Tour, J.M., and Miller, J.A. (1985). *J. Am. Chem. Soc.* 107: 2568–2569.
8 Agnel, G. and Negishi, E. (1991). *J. Am. Chem. Soc.* 113: 7424–7426.
9 Agnel, G., Owczarczyk, Z., and Negishi, E. (1992). *Tetrahedron Lett.* 33: 1543–1546.
10 Takahashi, T., Xi, Z., Nishihara, Y. et al. (1997). *Tetrahedron* 53: 9123–9134.
11 Swanson, D.R., Christophe, J.R., and Negishi, E. (1989). *J. Organomet. Chem.* 54: 3521–3523.
12 (a) Negishi, E., Maye, J.P., and Choueiry, D. (1995). *Tetrahedron* 51: 4447–4462. (b) Mori, M., Uesaka, N., Saitoh, F., and Shibasaki, M. (1994). *J. Organomet. Chem.* 59: 5643–5649.
13 Mori, M., Saitoh, F., Uesaka, N., and Shibasaki, M. (1993). *Chem. Lett.*: 213–216.
14 Saitoh, F., Mori, M., Okamura, K., and Date, T. (1995). *Tetrahedron* 51: 4439–4446.

15 (a) Takahashi, T., Huo, S., Hara, R. et al. (1999). *J. Am. Chem. Soc.* 121: 1094–1095. (b) Xi, Z., Fan, H.-T., Mito, S., and Takahashi, T. (2003). *J. Organomet. Chem.* 682: 108–112.

16 Takahashi, T., Tsai, F.-H., Li, Y., and Nakajima, K. (2001). *Organometallics* 20: 4122–4125.

17 Mito, S. and Takahashi, T. (2005). *Chem. Commun.*: 2495–2496.

18 (a) Barluenga, J., Sanz, R., and Fananas, F.J. (1995). *J. Chem. Soc., Chem. Commun.*: 1009–1010. (b) Barluenga, J., Sanz, R., and Fananas, F.J. (1997). *Chem. Eur. J.* 3: 1324–1336.

19 Souma, Y. and Sano, H. (1974). *Bull. Chem. Soc. J.* 47: 1717–1719.

20 Souma, Y., Tsumori, N., Willner, H. et al. (2002). *Catal. A Chem.* 189: 67–77.

21 Ohga, Y., Netsu, F., Mori, S. et al. (1995). *Tetrahedron*: 11119–11124.

22 Santi, R., Romano, A.M., Panella, F. et al. (1997). *Catal. A Chem.* 127: 95–99.

23 Nageswar, R.D., Rasheed, S., and Parthasarathi, D. (2016). *Org. Lett.* 18: 3142–3145.

24 Imbeaux, M., Mestdagh, H., Moughamir, K., and Rolando, C. (1992). *J. Chem. Soc., Chem. Commun.*: 1678–1679.

25 (a) Zoeller, J.R., Blakely, E.M., Moncier, R.M., and Dickson, T.J. (1997). *Catal. Today* 36: 227–241. (b) Zoeller, J.R. (2016). *Org. Process Res. Dev.* 20: 1016–1025. (c) Yang, C.-C., Kilos, B.A., Barton, D.G. et al. (2014). *J. Catal.* 319: 211–219.

26 Yang, C.-C., Yacob, S., Kilos, B.A. et al. (2016). *J. Catal.* 338: 313–320.

27 Vit, Z., Portefaix, J.L., and Breysse, M. (1997). *Collect. Czech. Chem. Commun.* 62: 1015–1022.

28 Calafat, A. and Laine, J. (1994). *Catal. Lett.* 28: 69–77.

29 Jali, S., Friedrich, H.B., Julius, G.R., and Mol, J. (2011). *Catal. A Chem.* 348: 63–69.

30 Ren, W. and Yamane, M. (2010). *J. Organomet. Chem.* 75: 3017.

31 Ren, W. and Yamane, M. (2010). *J. Organomet. Chem.* 75: 8410.

32 Ren, W., Emi, A., and Yamane, M. (2011). *Synthesis*: 2303.

33 Roberts, B., Liptrot, D., Alcaraz, L. et al. (2010). *Org. Lett.* 12: 4280–4283.

34 Sangu, K., Watanabe, T., Takaya, J., and Iwasawa, N. (2007). *Synlett*: 929–933.

35 Takaya, J., Sangu, K., and Iwasawa, N. (2009). *Angew. Chem. Int. Ed.* 48: 7090–7093.

36 Yu, C.-M., Hong, Y.-T., and Lee, J.-H. (2004). *J. Organomet. Chem.* 69: 8506.

37 Datta, S. and Lui, R.-S. (2005). *Tetrahedron Lett.* 46: 7985–7988.

38 For recent reviews about Pd catalysed coupling procedures using molybdenum as CO source see:(a)Odell, L.R., Russo, F., and Larhed, M. (2012). *Synlett* 23: 685–698. (b) Peng, J.-P., Qi, X., and Wu, X.-F. (2017). *Synlett* 28: 175–195. (c) Åkerbladh, L., Odell, L.R., and Larhed, M. (2019). *Synlett* 30: 141–155.

39 (a) Kaiser, N.-F.K., Hallberg, A., and Larhed, M. (2002). *J. Comb. Chem.* 4: 109–111. (b) Georgsson, J., Hallberg, A., and Larhed, M. (2003). *J. Comb. Chem.* 5: 350–352. (c) Georgsson, J., Sköld, C., Plouffe, B. et al. (2005). *J. Med. Chem.* 48: 6620.

40 (a) Friis, S.D., Lindhardt, A.T., and Skrydstrup, T. (2016). *Acc. Chem. Res.* 49: 594–605. (b) Gautam, P. and Bhanage, B.M. (2015). *Catal. Sci. Technol.* 5:

4663–4702. (c) Wang, L., Sun, W., and Liu, C. (2018). *Chin. J. Chem.* 36: 353. (d) Nordeman, P., Odell, L.R., and Larhed, M. (2012). *J. Organomet. Chem.* 77: 11393–11398. (e) Iizuka, M. and Kondo, Y. (2006). *Chem. Commun.*: 1739–1741.

41 Wannberg, J. and Larhed, M. (2003). *J. Organomet. Chem.* 68: 5750–5753.

42 (a) Mamone, M., Aziz, J., Le Bescont, J., and Piguel, S. (2018). *Synthesis* 50: 1521–1526. (b) Wu, X.-F., Oschatz, S., Sharif, M. et al. (2014). *Tetrahedron* 70: 23–29.

43 Wu, X.-F., Oschatz, S., Sharif, M., and Langer, P. (2015). *Synthesis* 47: 2641–2646.

44 Skogh, A., Fransson, R., Sköld, C. et al. (2013). *J. Organomet. Chem.* 78: 12251–12256.

45 (a) Liptrot, D., Alcaraz, L., and Roberts, B. (2010). *Adv. Synth. Catal.* 352: 2183–2188. (b) Herrero, M.A., Wannberg, J., and Larhed, M. (2004). *Synlett* 4: 2335–2338.

46 Belfrage, A.K., Wakchaure, P., Larhed, M., and Sandström, A. (2015). *Eur. J. Org. Chem.* 32: 7069–7074.

47 Wu, X., Ronn, R., Gossas, T., and Larhed, M. (2005). *J. Organomet. Chem.* 70: 3094–3098.

48 Liptrot, D., Alcaraz, L., and Roberts, B. (2010). *Tetrahedron Lett.* 51: 5341–5343.

49 (a) Borhade, S.R., Sandström, A., and Arvidsson, P.I. (2013). *Org. Lett.* 15: 1056–1059. (b) Wakchaure, P.B., Borhade, S.R., Sandström, A., and Arvidsson, P.I. (2015). *Eur. J. Org. Chem.*: 213–219.

50 (a) Mane, R.S., Nordeman, P., Odell, L.R., and Larhed, M. (2013). *Tetrahedron Lett.* 54: 6912–6915. (b) Lian, Z., Friis, S.D., Lindhardt, A.T., and Skrydstrup, T. (2014). *Synlett* 25: 1241–1245. (c) Nordeman, P., Chow, S.Y., Odell, A. et al. (2017). *Org. Biomol. Chem.* 15: 4875.

51 (a) Wannberg, J., Dallinger, D., Kappe, C.O., and Larhed, M. (2005). *J. Comb. Chem.* 7: 574–583. (b) Glasnov, T.N., Stadlbauer, W., and Kappe, C.O. (2005). *J. Organomet. Chem.* 70: 3864–3870. (c) Wannberg, J., Kaiser, N.-F.K., Vrang, L. et al. (2005). *J. Comb. Chem.* 7: 611–617. (d) Rönn, R., Lampa, A., Peterson, S.D. et al. (2008). *Bioorg. Med. Chem.* 16: 2955–2967.

52 Lagerlund, O. and Larhed, M. (2006). *J. Comb. Chem.* 8: 4–6.

53 Odell, L.R., Sävmarker, J., and Larhed, M. (2008). *Tetrahedron Lett.* 49: 6115–6118.

54 (a) Letavic, M.A. and Ly, K.S. (2007). *Tetrahedron Lett.* 48: 2339–2343. (b) Begouin, A. and Queiroz, M.-J.R.P. (2009). *Eur. J. Org. Chem.*: 2820–2827.

55 Lagerlund, O., Mantel, M.L.H., and Larhed, M. (2009). *Tetrahedron* 65: 7646–7652.

56 (a) Chow, S.Y. and Odell, L.R. (2017). *J. Organomet. Chem.* 82: 2515–2522. (b) Chow, S.Y., Stevens, M.Y., and Odell, L.R. (2016). *J. Organomet. Chem.* 81: 2681–2691.

57 (a) Jafarpour, F. and Otaredi-Kashani, A. (2014). *ARKIVOC* 4: 193–203. (b) Chen, J., Natte, K., Spannenberg, A. et al. (2014). *Chem. Eur. J.* 20: 14189–14193.

58 (a) Yamazaki, K. and Kondo, Y. (2004). *J. Comb. Chem.* 6: 121–125. (b) Åkerbladh, L., Nordeman, P., Wejdemar, M. et al. (2015). *J. Organomet. Chem.* 80: 1464–1471. (c) Iizuka, M. and Kondo, Y. (2007). *Eur. J. Org. Chem.*:

5180–5182. (d) Schembri, L.S., Eriksson, J., and Odell, L.R. (2019). *J. Organomet. Chem.* 84: 6970–6981.
59 Ghosh, P., Nandi, A.K., and Das, S. (2018). *Tetrahedron Lett.* 59: 2025–2029.
60 Chen, J., Natte, K., and Wu, X.-F. (2016). *J. Organomet. Chem.* 803: 9–12.
61 Wu, X.F., Sharif, M., Shoaib, K. et al. (2013). *Chem. Eur. J.* 19: 6230–6233.
62 Wu, X.-F., Oschatz, S., Sharif, M. et al. (2013). *Adv. Synth. Catal.* 355: 3581–3585.
63 (a) Åkerbladh, L. and Odell, L.R. (2016). *J. Organomet. Chem.* 81: 2966–2973. (b) Åkerbladh, L., Chow, S.Y., Odell, L.R., and Larhed, M. (2017). *ChemistryOpen* 6: 620–628.
64 He, L., Sharif, M., Neumann, H. et al. (2014). *Green Chem.* 16: 3763–3767.
65 Wu, X., Nilsson, P., and Larhed, M. (2005). *J. Organomet. Chem.* 70: 346–349.
66 Wang, Z., Zhu, F., Li, Y., and Wu, X.-F. (2017). *ChemCatChem* 9: 94–98.
67 Wang, Z., Yin, Z., Zhu, F. et al. (2017). *ChemCatChem* 9: 3637–3640.
68 Hernando, E., Villalva, J., Martínez, Á.M. et al. (2016). *ACS Catal.* 6: 6868–6882.
69 Pyo, A., Park, A., Jung, H.M., and Lee, S. (2012). *Synthesis* 44: 2885–2888.
70 Motwani, H.V. and Larhed, M. (2013). *Eur. J. Org. Chem.*: 4729–4733.
71 (a) Jafarpour, F., Rashidi-Ranjbar, P., and Kashani, A.O. (2011). *Eur. J. Org. Chem.*: 2128–2132. (b) Cho, S.K., Song, J.H., Hahn, J.T., and Jung, D. (2016). *Bull. Korean Chem. Soc.* 37: 1567.
72 Roslin, S. and Odell, L.R. (2017). *Chem. Commun.* 53: 6895–6898.
73 Jenner, G. and Bitsi, G. (1987). *J. Mol. Catal.* 40: 71–82.
74 Kelkar, A.A., Kohle, D.S., and Chaudhari, R.V. (1992). *J. Organomet. Chem.* 430: 111–116.
75 Sävmarker, J., Lindh, J., and Nilsson, P. (2010). *Tetrahedron Lett.* 51: 6886–6889.
76 Lindh, J., Fardost, A., Almeida, M., and Nilsson, P. (2010). *Tetrahedron Lett.* 51: 2470–2472.
77 Whyman, R., Wright, A.P., Iggo, J.A., and Heaton, B.T. (2002). *J. Chem. Soc., Dalton Trans.*: 771–777.
78 Gautron, S., Lassauque, N., Le Berre, C. et al. (2006). *Eur. J. Inorg. Chem.*: 1121–1126.
79 Iranpoor, N., Firouzabadi, H., and Etemadi-Davan, E. (2015). *J. Organomet. Chem.* 794: 282–287.
80 Peng, J.-B., Wu, F.-P., Da, L. et al. (2018). *J. Organomet. Chem.* 83: 6788–6792.

Part III

Miscellaneous Carbonylation Reactions

10

Carbonylations Promoted by Third-Row Transition Metal Catalysts

Anthony Haynes

University of Sheffield, Department of Chemistry, Dainton Building, Brook Hill, Sheffield, S3 7HF, UK

10.1 Introduction

Many transition metals form complexes that are active as catalysts for carbonylation of organic substrates. Perhaps the best known are those based on cobalt, rhodium, and palladium. For example, the earliest commercial processes for both alkene hydroformylation and methanol carbonylation were based on cobalt. However, in both cases, rhodium-based catalysts were introduced that were more active and operated under milder conditions. Third-row metals are often regarded as less active catalysts than their lighter analogs, although there are exceptions to this general rule. For example, iridium catalysts are well known to show high activity in many hydrogenation reactions [1].

Catalytic carbonylation reaction mechanisms generally involve binding carbon monoxide to a metal and migratory insertion of CO into a metal alkyl to give a metal acyl species (Scheme 10.1). Established metal-ligand bonding trends show that M—C bond strengths for metal alkyls generally increase descending a triad of transition metals. Since an M—alkyl bond is broken during migratory CO insertion, activation energies for this step are greater for third-row metals. Hence, the reactions are typically slower under equivalent conditions as demonstrated in model systems such as the reaction of $[(\eta^5\text{–}C_5H_5)M(CO)_2R]$ with PPh_3 to give $[(\eta^5\text{–}C_5H_5)M(CO)(PPh_3)(COR)]$ (M = Fe, Ru, Os; R = CH_3 to $C_{18}H_{37}$) [2]. At 137 °C in xylene, the rate for M = Ru was $\sim 10^3$ times slower than the corresponding Fe complex, while no reaction was detectable for Os. However, this would appear to be an extreme example as many third-row metal alkyl complexes undergo CO insertion reactions under accessible conditions.

Another significant consideration is that π-backdonation from metal to CO is generally stronger for third-row than for second-row metals. A theoretical explanation for this involves relativistic effects, which raise the 5d orbital energies for heavy metals [3]. This can also inhibit the CO insertion step since one of the two M—CO π-backbonding interactions is lost on the conversion of RM(CO) to M(COR). Furthermore, stronger metal-ligand bonding (e.g. to CO and phosphines) makes

Carbon Monoxide in Organic Synthesis: Carbonylation Chemistry,
First Edition. Edited by Bartolo Gabriele.

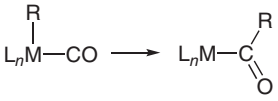

Scheme 10.1 Migratory CO insertion.

third-row metal complexes inherently less labile, thus inhibiting coordination of substrates such as alkenes requiring a coordination site to be vacated to bind to a metal center.

Although some organometallic reaction steps are typically slower for a third-row metal, other steps can be faster. Typically, this applies to reactions in which metal-ligand bonds are formed, such as oxidative addition of reactants like H_2 or alkyl halides. This can be beneficial when the reaction is a step within the main catalytic cycle. However, it can also result in loss of selectivity due to a competitive reaction (for example, alkane formation due to hydrogenation in competition with hydroformylation).

Stronger metal-ligand bonding for third-row metals can lead to more robust catalysts that are less prone to degradation. This can be at the expense of catalytic activity, so there is often a trade-off between these considerations to achieve the optimum desired behavior. Selection of the best catalyst system for a given process involves consideration of several variables, including metal, ligands, solvent, temperature, pressure, and their effects on activity, selectivity, and catalyst stability. Sometimes these criteria can allow the selection of a catalyst based on a third-row metal. A notable industrial example uses an iridium catalyst for imine hydrogenation leading to an important agrochemical product [4]. In carbonylation catalysis, the biggest commercial success story for a third-row metal also involves iridium, in the BP Cativa™ process for methanol carbonylation. This chapter will discuss that process in detail and other significant carbonylations promoted by third-row metal catalysts.

10.2 Methanol Carbonylation

10.2.1 Acetic Acid Production

Acetic acid is an important bulk commodity chemical with a global annual demand that exceeds 10 million tonnes and continues to grow, for example, in Asia. Significant uses of acetic acid include the manufacture of vinyl acetate (an important monomer for the polymer industry), other acetate esters, and acetic anhydride. Acetic acid is also used as a solvent for the process where para-xylene is oxidized to terephthalic acid, a precursor to polyethylene terephthalate (PET), commonly employed in plastic bottles and textiles. A derivative, monochloroacetic acid, is important in the production of pesticides. Older routes to acetic acid include oxidation of ethanol (e.g. from fermentation), hydrolysis of acetylene, and the oxidation of hydrocarbons such as butane or naphtha. In the late 1950s, a new route to acetaldehyde (which could subsequently be oxidized to acetic acid) was provided by the Wacker process involving ethene oxidation using a homogeneous

$PdCl_2/CuCl_2$ catalyst [5]. The 1960s then saw the introduction of processes in which the catalytic methanol carbonylation Eq. (10.1) was used for large-scale acetic acid production, and variants of this process have since dominated.

$$MeOH + CO \xrightarrow{cat} MeCO_2H \quad (10.1)$$

The first commercial methanol carbonylation process was developed by BASF [6, 7] and used a cobalt/iodide catalyst with relatively high temperatures and pressures (~250 °C, 600 bar) [8, 9]. The selectivity to acetic acid (90% based on methanol; 70% based on CO) was quite low compared to subsequent catalysts based on heavier group 9 metals. Demanding separation procedures were required to remove by-products such as higher alcohols, aldehydes, and carboxylic acids. In 1968 it was reported by Paulik and Roth at Monsanto that much greater catalytic activity and selectivity could be achieved under milder conditions (~175 °C, 30 bar) using rhodium or iridium catalysts [10]. A full-scale plant based on a rhodium/iodide catalyst began production in Texas City in 1970. The so-called Monsanto process became the dominant method for the manufacture of acetic acid during the 1970s and 1980s, and by 1991 it accounted for more than 50% of global acetic acid production. It achieved very good selectivity of >99% (based on methanol) and ~85% (based on CO) due to consumption of CO by the water-gas shift (WGS) reaction (Eq. (10.2)).

$$CO + H_2O \longrightarrow CO_2 + H_2 \quad (10.2)$$

Although rhodium-catalyzed carbonylation had proved highly successful, there were still opportunities to improve process efficiency and catalyst stability. Consequently, during the early 1990s, BP Chemicals developed an iridium/iodide-based catalyst commercialized in 1995 in the Cativa process, which now operates on several plants worldwide. This section will summarize the main features of catalytic methanol carbonylation processes and examine the mechanisms operating for iridium catalysts and how they compare with rhodium-catalyzed systems. Examples of other catalyst systems for methanol carbonylation involving third-row metals will also be discussed.

10.2.2 Process Considerations and Mechanism for Rh Catalyst

Methanol carbonylation has been the subject of numerous reviews [11–24]. Processes using either rhodium or iridium catalysts operate under similar conditions and have many features in common. For both metals, an iodide co-catalyst is employed, which provides ligands for the participating metal complexes and plays an important role in activating the methanol reactant. The methanol fed to the reactor initially undergoes esterification (Eq. (10.3)) under process conditions by reaction with acetic acid (the principal component of the reaction medium). The resulting methyl acetate is activated by reaction with HI (Eq. (10.4)), the net result of Eqs. (10.3) and (10.4) being the conversion of MeOH into MeI.

$$MeOH + AcOH \longrightarrow MeOAc + H_2O \quad (10.3)$$

$$MeOAc + HI \longrightarrow MeI + AcOH \quad (10.4)$$

The rhodium-based catalyst developed by Monsanto has been thoroughly investigated and represents one of the classic examples of homogeneous organometallic catalysis (for leading references, see [11–17, 21, 23, 25]). The overall carbonylation process is zero-order in MeOH and CO but first-order in Rh and methyl iodide. The well-established catalytic mechanism shown in Scheme 10.2 comprises an outer cycle with reactions of anionic rhodium complexes and an inner cycle of organic reaction steps. The active catalyst, identified by *in situ* high-pressure infrared (HPIR) spectroscopy [26], is a square-planar Rh(I) complex, *cis*-$[Rh(CO)_2I_2]^-$ **1**. The rate-determining step of the Rh cycle is the oxidative addition of methyl iodide to this Rh(I) complex [27, 28]. The S_N2 transition state structure for nucleophilic attack by the metal center on methyl iodide has been probed in computational studies [29–35]. The Rh(III) methyl complex **2** cannot be isolated but was detected at low concentration by IR and ^{13}C NMR spectroscopy [28, 36]. It undergoes rapid migratory CO insertion to give the acetyl complex, **3**. The Rh cycle is completed by fast coordination of CO to give a dicarbonyl **4** and reductive elimination of acetyl iodide, with subsequent hydrolysis to acetic acid.

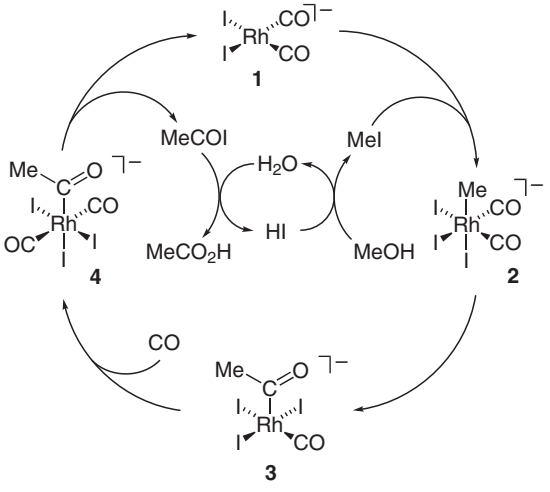

Scheme 10.2 Catalytic cycle for Rh-catalyzed methanol carbonylation.

As noted earlier, the WGS reaction (Eq. (10.2)) occurs in competition with methanol carbonylation [37–39]. This proceeds via the reactions shown in Eqs. (10.5) and (10.6), involving a Rh(III) tetraiodide complex **5** that can accumulate the expense of **1** and resulting in lower methanol carbonylation activity.

$$[Rh(CO)_2I_2]^-(\mathbf{1}) + 2HI \longrightarrow [Rh(CO)_2I_4]^-(\mathbf{5}) + H_2 \qquad (10.5)$$

$$[Rh(CO)_2I_4]^-(\mathbf{5}) + H_2O + CO \longrightarrow [Rh(CO)_2I_2]^-(\mathbf{1}) + 2HI + CO_2 \qquad (10.6)$$

Complex **5** is also prone to dissociation of CO, leading to precipitation of insoluble rhodium(III) species (e.g. RhI_3) during product/catalyst separation. In order to maintain the rhodium catalyst in its active form, a relatively high water concentration (10–15% w/w) is employed in the conventional Monsanto process to promote

the reduction of **5** back to the active Rh(I) catalyst, as shown in Eq. (10.6). However, the high water concentration necessitates a costly separation process to dry the acetic acid product. It would be beneficial to operate the process at a lower water concentration, provided that catalyst stability can be maintained. One solution is the addition of an iodide salt, which can help stabilize the Rh catalyst under these conditions, such as in Celanese's Acid Optimization (AO Plus) technology, which uses lithium iodide [16, 40]. Replacement of the rhodium catalyst by iridium provides another solution, as discussed below.

10.2.3 Iridium Catalysts

During the development of their rhodium-based process, Monsanto discovered that iridium/iodide catalysts could also be effective for methanol carbonylation [10] and others reported analogous carbonylation of ethanol [41, 42]. Studies by Forster using *in situ* HPIR spectroscopy revealed a more complex mechanism for the iridium system (see below) [43]. Although iridium was cheaper and displayed good catalytic activity, Monsanto selected the rhodium-based process for commercialization, in part due to its high selectivity and simpler kinetic behavior. BP Chemicals initiated further development of iridium-based catalysts in the 1990s. Most significant was the discovery of promoters that enhance the carbonylation activity and give optimum rates at relatively low water concentration (e.g. 5 wt% compared with >10 wt% for Rh) [44–47]. BP commercialized the Cativa process in 1995 [48–52], retrofitting existing plants in Texas City (USA), followed by plants in the UK, South Korea, China, and India. The first new plant to employ the Cativa process was built in Malaysia, and further plants were commissioned in Southeast Asia to meet increasing regional demand.

The high activity of the Cativa process is illustrated by the 75% increase in throughput that was achieved at the Samsung-BP plant in Ulsan, South Korea, on replacement of the rhodium catalyst [51]. It is also highly selective (>99% based on methanol) with reduced formation of liquid (e.g. propionic acid) and gaseous (CO_2 and CH_4) by-products compared to the rhodium system. The lower water concentration used allows for lower product purification costs, with steam and cooling water requirements being reduced by 30%. Amounts of acetaldehyde by-product are lower than in the rhodium process, which in turn reduces levels of higher organic iodides formed by condensation reactions in low-water rhodium systems. Organic iodides can poison downstream processes such as vinyl acetate manufacture, and their removal can require further treatment steps. All of these benefits help to reduce the environmental impact of the Cativa process. Overall CO_2 emissions (both direct and indirect) per tonne of product are estimated to be lowered by c. 30% compared to the Monsanto process.

10.2.3.1 Mechanism for Iridium Catalyst

Forster's investigations of the iridium/iodide-based process revealed quite a complicated dependence of carbonylation rate and catalyst speciation on process conditions [11, 12, 26, 43, 53–56]. Three distinct regimes were identified: (i) at relatively low

water and methyl iodide concentrations, the dominant complex is a neutral iridium(I) species $[Ir(CO)_3I]$, and carbonylation rate is inhibited by increasing CO pressure; (ii) in the presence of small amounts of iodide salt the dominant iridium species is an Ir(III) methyl complex, $[Ir(CO)_2I_3Me]^-$ and the rate increases with CO pressure but is inhibited by ionic iodide; (iii) at higher concentrations of MeI and H_2O, an Ir(III) hydride $[Ir(CO)_2I_3H]^-$ is the major species and the WGS reaction competes with carbonylation.

Forster proposed two linked cycles: one involving neutral iridium complexes and the other containing predominantly anionic species (Scheme 10.3). At low concentrations of water and iodide, the "neutral cycle" operates, with $[Ir(CO)_3I]$ **12** as the resting state and rate-determining oxidative addition of MeI to $[Ir(CO)_2I]$ **13**. At higher iodide concentrations, the "anionic cycle" predominates, with rate-determining carbonylation of $[Ir(CO)_2I_3Me]^-$ **7** via an iodide loss mechanism. The competing WGS reaction can also proceed via anionic or neutral intermediates, as shown in the cycles at the top of Scheme 10.3.

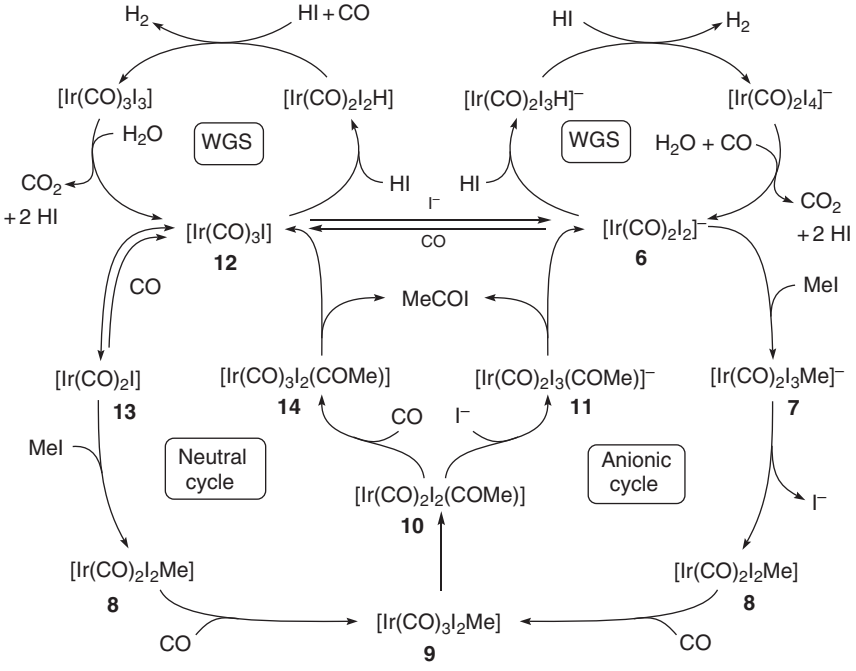

Scheme 10.3 Catalytic cycles for iridium-catalyzed methanol carbonylation and WGS reaction. Source: Forster [43].

Under the conditions normally employed for catalysis, the anionic cycle is dominant, with zero-order dependence on [MeI] and Ir(III) methyl complex **7** identified as the major Ir species by *in situ* HPIR spectroscopy. Kinetic studies have shown that oxidative addition of MeI to $[Ir(CO)_2I_2]^-$ **6** is c. 100 times faster than the Rh analog **1** [57, 58]. The oxidative addition product **7** is stable and was characterized crystallographically as its *cis*, *fac* isomer [59]. Carbonylation of **7** (to give **11**) is regarded as rate-determining under normal process conditions and proceeds via several steps

as shown in Scheme 10.4. Dissociative substitution of iodide by CO gives a neutral tricarbonyl **9**, characterized as the fac isomer by HPIR and HPNMR spectroscopy [60, 61]. This complex undergoes methyl migration more readily than the anionic precursor **7**.

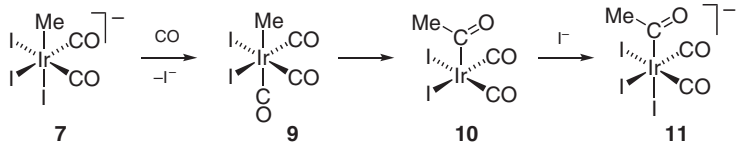

Scheme 10.4 Iodide loss mechanism for stoichiometric carbonylation of $[Ir(CO)_2I_3Me]^-$ **7**.

The iodide-loss mechanism depicted in Scheme 10.4 means that carbonylation of **7** is inhibited by added iodide salts but accelerated in reaction media that can solvate iodide anions. For example, the reaction is slow in chlorinated solvents even at temperatures >80 °C. However, the addition of a protic solvent (e.g. methanol) has a dramatic accelerating effect, and carbonylation proceeds readily at <50 °C [60, 62, 63]. The promotional effect of several metal compounds on the iridium-catalyzed process is ascribed to their ability to scavenge iodide and hence accelerate the carbonylation of **7**, as discussed later.

Theoretical calculations confirm a lower activation barrier for methyl migration in **9** relative to **7**. It suggest that a π-acceptor CO ligand *trans* to methyl stabilizes the transition state for migratory insertion [32, 64]. The *cis*, *mer* isomer of **7** undergoes even faster methyl migration. Ford and coworkers found the carbonylation of *cis,fac*-**7** to be promoted by UV irradiation and proposed the mechanism shown in Scheme 10.5 involving photo-induced isomerization [65]. Haynes et al. demonstrated a thermal pathway to generate *cis,mer*-**7** and showed that this species is carbonylated rapidly at room temperature [66]. This isomerization route may contribute to catalytic turnover, although the iodide loss mechanism (Scheme 10.4) is likely the dominant pathway.

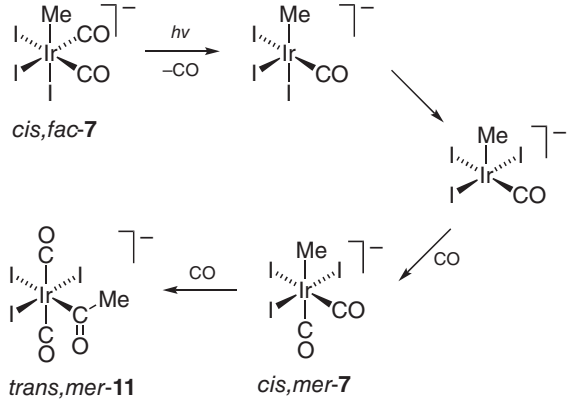

Scheme 10.5 Proposed CO-loss mechanism for photochemical carbonylation of $[Ir(CO)_2I_3Me]^-$ **7**.

Methane is a known by-product of iridium-catalyzed carbonylation. It has been shown that this can originate from the methyl ligand of **7** by protonolysis with carboxylic acids or hydrogenolysis at elevated temperatures [67]. In both cases, the reaction is inhibited by the presence of CO, suggesting that CO dissociation from the reactant complex is required. An alternative pathway to gaseous by-products was proposed based on the observation that Ir(III) methyl and acetyl complexes such as **7** and **11** release CO_2 and CH_4 on reaction with water under mild conditions [68]. It was proposed that nucleophilic attack by H_2O on a CO ligand (as in the WGS cycle) gives a hydroxycarbonyl ligand that can eliminate CO_2 and provide a proton to release the methyl group as methane (Scheme 10.6).

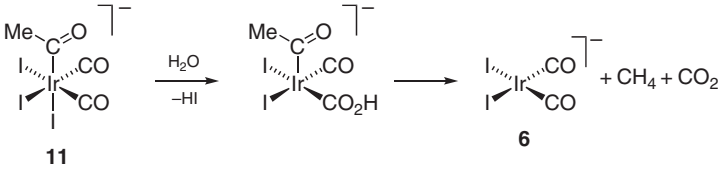

11 **6**

Scheme 10.6 Proposed mechanism for methane formation from Ir(III) acetyl species.

10.2.3.2 Role of Promoters in Iridium-Catalyzed Methanol Carbonylation

The promoters identified by BP to enhance the rate of iridium-catalyzed methanol carbonylation fall into two categories: (i) carbonyl or halocarbonyl complexes of W, Re, Ru, and Os; (ii) simple iodides of Zn, Cd, Hg, Ga, and In [44, 45, 47]. None is active in the absence of iridium catalyst (although ruthenium has been reported to catalyze methanol carbonylation under harsh conditions with relatively low selectivity [69–74]). Notably, ionic iodides such as LiI and Bu_4NI are strong catalyst inhibitors [50, 51, 60]. Figure 10.1 illustrates the effect of a ruthenium promoter as a function of $[H_2O]$ compared to Ir-only and Rh catalysts.

The promoters are believed to operate by acting as iodide acceptors, thus facilitating the carbonylation mechanism of **7** shown in Scheme 10.4. Model kinetic studies on this reaction have confirmed the promotional effect of neutral ruthenium

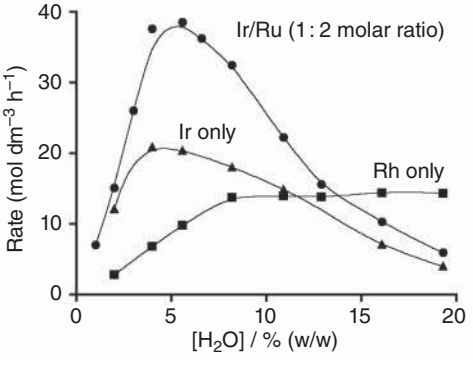

Figure 10.1 Comparison of methanol carbonylation rates as a function of water concentration for Rh, Ir, and Ir/Ru-based catalysts (190 °C, 28 bar, 30% MeOAc (w/w), 8.4% MeI (w/w), 1950 ppm Ir or equimolar Rh). Source: Haynes et al. [60].

complexes such as $[Ru(CO)_3I_2]_2$, $[Ru(CO)_4I_2]$, and simple metal iodides such as InI_3 and GaI_3 [60]. These species can accept iodide reversibly to form the anions $[Ru(CO)_3I_3]^-$ and MI_4^- [59–61, 75]. Under catalytic conditions for a ruthenium promoter, *in situ* HPIR spectroscopy shows that $[Ru(CO)_3I_3]^-$ is the dominant Ru complex during catalysis [18, 52, 60]. Kalck and coworkers also reported similar iodide abstraction behavior for $[Pt(CO)_2I_2]$ [63, 76, 77] and some evidence for carbonylation activity of $[Pt(CO)I_3]^-$ had been noted [78].

A simplified catalytic mechanism that includes the role played by a ruthenium promoter is shown in Scheme 10.7. The neutral Ru species $[Ru(CO)_3I_2]$ scavenges iodide (represented as $HI_{(aq)}$) that is released from the Ir methyl complex **7**, thus aiding the formation of the reactive neutral tricarbonyl, **9** and enhancing turnover in the Ir cycle. There is no necessity for direct iodide transfer from Ru back to Ir after the CO insertion step. The iodide can be recycled in a ruthenium-catalyzed activation of methyl acetate to form MeI. Experimental evidence for this is provided by the observation that the exchange of isotopically labeled methyl groups between MeI and MeOAc is accelerated in the presence of $[Ru(CO)_3I_3]^-H_3O^+$ [18, 60]. The high concentration of $[Ru(CO)_3I_3]^-H_3O^+$ (or other promoters such as $[InI_4]^-H_3O^+$) can be considered to increase the Brønsted acidity, resulting in acid catalysis of the reaction of methyl acetate with $HI_{(aq)}$. The promoter's role is rather subtle, acting to moderate the steady-state iodide concentration, thereby enhancing carbonylation rate in the iridium cycle.

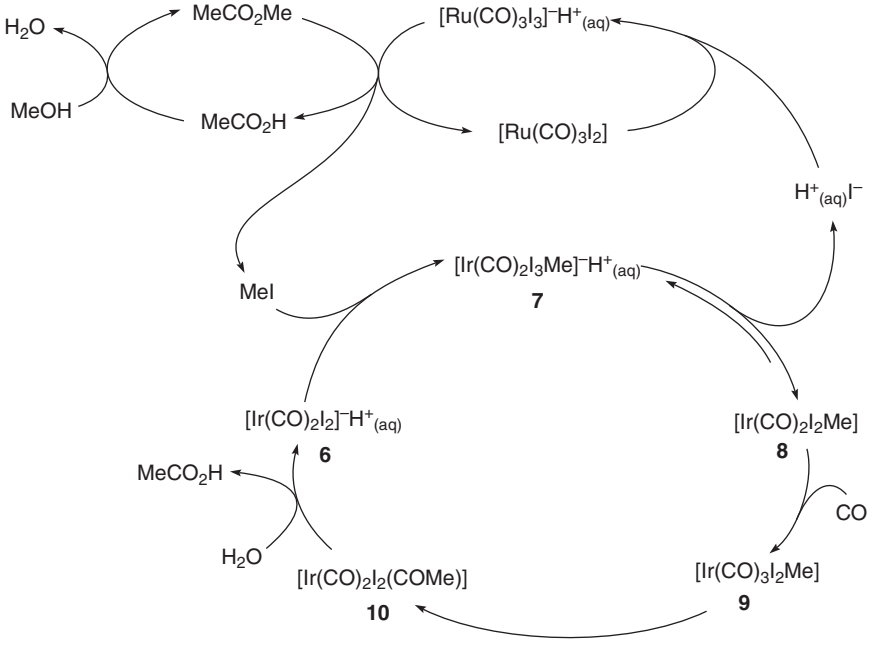

Scheme 10.7 Mechanism for iridium-catalyzed methanol carbonylation with a ruthenium promoter.

10.2.3.3 Recent Developments

Heterogeneous carbonylation of methanol catalyzed by atomically dispersed iridium and lanthanum halides supported on carbon was reported by Kwak et al. [79]. The catalysts are reported to have high activity and selectivity, maintained for more than a month of continuous operation. Characterization of the catalyst by high-angle annular dark-field scanning transmission electron microscopy (HAADF STEM) gave evidence for discrete heterobimetallic Ir–La sites. A mechanism in which the Lewis acidic La facilitates iodide dissociation from iridium and promotes CO insertion, similar to promoters' role in the homogeneous process, was proposed. It was also suggested that lanthanum might play a more direct role in promoting CO insertion by acting as a Lewis acid toward an Ir–CO species and facilitating acetyl formation (Scheme 10.8). Supported iridium catalysts of this sort have attracted further recent attention [80–83].

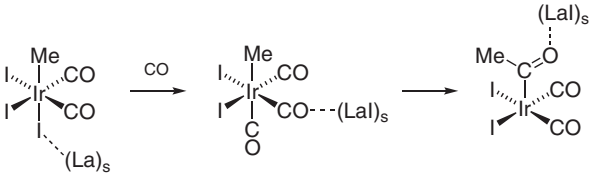

Scheme 10.8 Proposed steps in Ir-La/C-catalyzed methanol carbonylation (s = support).

Some other third-row metals have been reported for their activity as heterogeneous catalysts for methanol carbonylation. For example, patents from Zoeller et al. reported that a gold catalyst supported on carbon had comparable activity to related

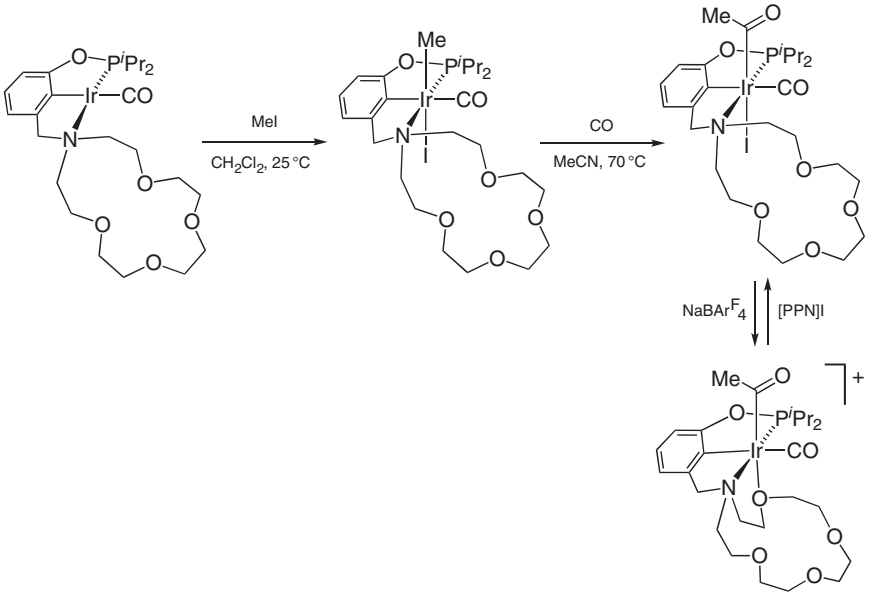

Scheme 10.9 Stoichiometric reaction steps for iridium pincer-crown ether complexes.

iridium systems [84]. A study of the Au/C catalysts by Goguet et al. identified Au dimers or trimers as the active sites. It showed that iodide plays an important role in activating the catalyst and maintaining activity [85]. A study of gold catalysts supported on silica included measurement of *in situ* infrared data, which indicated the formation of Au carbonyl species that reacted with surface methoxy groups [86]. A halide-free atomically dispersed ReO_4/SiO_2 catalyst for the gas phase carbonylation of methanol was reported by Christopher and coworkers in 2020 [87].

Miller and coworkers have investigated iridium pincer-crown ether complexes of the type shown in Scheme 10.9 as pre-catalysts for homogeneous methanol carbonylation [88]. The effects of a range of salt additives were tested to determine whether binding of a metal cation by the crown ether would promote catalysis. The highest turnover numbers were found with LiCl or $HfCl_4$ additives. Mechanistic studies demonstrated MeI oxidative addition, CO insertion, and iodide abstraction steps (Scheme 10.9) and showed that Li^+ and La^{3+} salts cause acceleration of migratory CO insertion in these systems [89]. However, in the catalytic reactions, evidence for pincer ligand degradation by methanolysis was found.

10.3 Hydroformylation

Hydroformylation of alkenes is carried out on a bulk scale to give aldehydes (Scheme 10.10) or alcohols by further addition of H_2. Propene hydroformylation to butanal/butanol is the largest scale process, but longer chain alkene feedstocks are also used to give detergent-precursor higher alcohols. Homogeneous catalysts based on cobalt or rhodium are widely applied, generally with phosphine ligands. For cobalt, trialkyl phosphines such as P^nBu_3 are employed, whereas, for rhodium, PPh_3 is often used. However, many mondenatate and bidentate P-donor ligands have been investigated for their effects on catalyst activity, stability, and selectivity [90]. The established catalytic cycle has common steps for group 9 metal catalysts, as shown in Scheme 10.11. Linear or branched aldehyde products are formed because the alkene insertion step can give isomeric alkyl species before CO insertion and hydrogenolysis of the acyl intermediates. It is often desired to achieve selectivity to the more valuable linear products (high *n*:*iso* ratio). Rhodium is generally considered to form the most active hydroformylation catalysts and typically operates under milder temperature and pressure conditions than cobalt-based systems. Addition of other metal compounds can have a promotional effect on the catalytic rate. For example, Garland and coworkers reported that the rhenium hydride, $[Re(CO)_5H]$, enhances the rate of Rh-catalyzed hydroformylation [91]. High-pressure IR spectroscopy

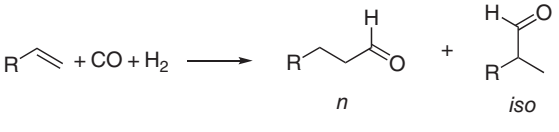

Scheme 10.10 Hydroformylation of an alkene to give linear and branched aldehydes.

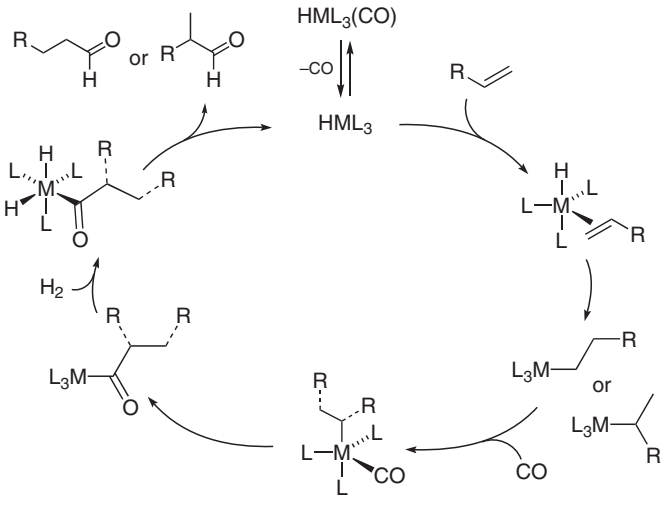

Scheme 10.11 General hydroformylation mechanism for group 9 metal catalysts (in phosphine modified systems $L_3 = (CO)_n(PR_3)_{3-n}$).

provided evidence for heterodinuclear complexes such as $[RhRe(CO)_9]$, and a mechanism was proposed involving reaction of $[Rh(CO)_4(COR)]$ with $[Re(CO)_5H]$ to eliminate aldehyde, in parallel to the hydrogenolysis of $[Rh(CO)_4(COR)]$ [92]. The use of alternative metals for homogeneous catalytic hydroformylation was reviewed in 2013 by Pospech et al. [93].

10.3.1 Iridium Catalysts

Iridium is significantly less active for hydroformylation than the lighter group 9 metals, with relative activities of 1 : 1000 : 0.1 estimated for Co, Rh, and Ir [94]. This can be ascribed to stronger metal-ligand bonding for the third-row metals, leading to lower lability and slower migratory CO insertion in Ir(alkyl)(CO) species, as discussed above for methanol carbonylation catalysts. Moreover, the greater propensity for H_2 oxidative addition to iridium means that it shows greater activity as a hydrogenation catalyst leading to significantly more alkane by-product formation.

Iridium complexes have, however, often been studied as more robust models for mechanistic and structural investigations. For example, chelating diphosphines have frequently been investigated in rhodium-catalyzed hydroformylation for their effects on catalytic activity and selectivity. Iridium complexes of such ligands can be useful as stable models for reactive intermediates. Deutsch and Eisenberg studied the reactivity of iridium complexes of bis(diphenylphosphino)ethane (dppe) [95, 96]. The ethene complex $[Ir(CO)(dppe)(\eta^2\text{–}C_2H_4)Et]$ reacted with H_2 to give $[Ir(CO)(dppe)H_2Et]$, for which the kinetics of competitive reductive elimination of ethane or H_2 were measured. The reaction of $[Ir(CO)(dppe)(\eta^2\text{–}C_2H_4)Et]$ with CO initially gave $[Ir(CO)_2(dppe)Et]$ which was carbonylated to form the propionyl complex $[Ir(CO)_2(dppe)(COEt)]$ (Scheme 10.12a). Subsequent reaction with H_2 gave

$[Ir(CO)(dppe)H_2(COEt)]$ from which reductive elimination of propionaldehyde could be followed.

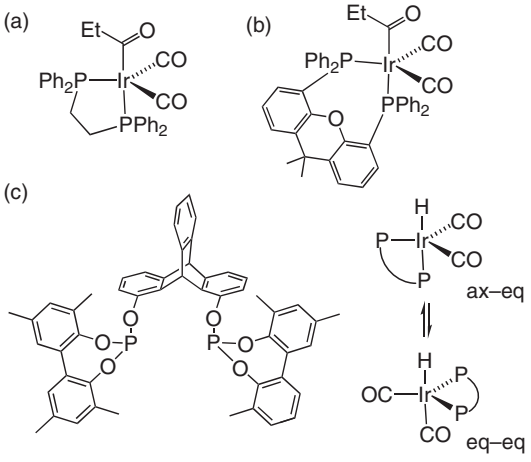

Scheme 10.12 Ir-propionyl complexes of diphosphines dppe (a), xantphos (b), and isomeric Ir hydride complexes of tMe-triptylphosphite (c).

Eisenberg and coworkers also investigated iridium complexes of the wide bite-angle ligand, xantphos, which gives good activity and *n*:*iso* selectivity in rhodium-catalyzed hydroformylation [97]. Halide complexes, $[Ir(CO)_2(xantphos)X]$ were structurally characterized, and their fluxional behavior in solution examined by NMR spectroscopy. The addition of hydrogen to these complexes to give dihydride species $[Ir(CO)(xantphos)H_2X]$ was probed using the para-hydrogen induced polarization (PHIP) technique. The reaction of $[Ir(CO)_2(xantphos)X]$ with $NaBH_4$ gave $[Ir(CO)_2(xantphos)H]$ and $[Ir(CO)(xantphos)H_3]$. The trihydride complex reacted with ethene and CO to give the propionyl complex $[Ir(CO)_2(xantphos)(COEt)]$ (Scheme 10.12b). An X-ray crystal structure showed a distorted trigonal bipyramidal geometry with the acyl group in an axial position and the xantphos P-donor groups spanning equatorial and axial sites. These hydride and propionyl complexes, along with $[Ir(CO)_2(dppe)(COEt)]$, exhibited some activity for the hydroformylation of 1-hexene at 75 °C, but alkene isomerization occurred in competition. Duckett and coworkers also employed the PHIP method to study the reactions of $[Ir(CO)(PR_3)_2(\eta^3\text{-}C_3H_5)]$ with hydrogen and CO and identified a number of hydride and acyl species [98].

Hofmann and coworkers reported iridium hydride complexes of a bulky bis(phosphite) ligand, $[Ir(CO)_2$(tMe-triptylphosphite)H] (Scheme 10.12c) [99]. Both eq–eq and eq–ax isomers were observed in solution. Crystallization from different solvents enabled the isolation and crystallographic characterization of the individual isomers in the solid-state. A related bis(phosphite) ligand was used by Ternel et al. in combination with iridium precursors, $[Ir(cod)Cl]_2$ or [Ir(cod)(acac)], for the tandem hydroformylation/isomerization of unsaturated fatty substrates, $H_2C{=}CH(CH_2)_7CH_2R$ (e.g. R = CN, CO_2Me) [100]. The catalytic turnover frequency

was only ~5 times lower than for the corresponding rhodium system and gave more control of the distribution of internal olefins formed by isomerization.

In 1994, Crudden and Alper reported that the iridium complex $[Ir(cod)_2]BF_4$ (cod = 1,5 cyclooctadiene) catalyzed the hydroformylation of trialkylvinylsilanes (without the addition of phosphine) to give the linear product 3-(trialkylsilyl)-propanal with good regioselectivity [101]. This contrasted with the results using a $[Rh(cod)BPh_4]$ catalyst, which gave the branched 2-(trialkylsilyl)propanal as the major product unless PPh_3 was added. Competing hydrogenation of the substrate was significant but could be suppressed to a degree by using a high $CO:H_2$ ratio (e.g. 7 : 1) in the syn-gas feed. Hydroformylation activity was lost upon the addition of PPh_3 to this iridium catalyst. However, Rosales et al. found that phosphine complexes $[M(cod)(PPh_3)_2]PF_6$ (M = Rh, Ir) were active for the hydroformylation of 1-hexene, although a higher temperature (100 vs. 60 °C) was required for the Ir catalyst to achieve comparable rates, and *n*:*iso* selectivity was lower [102]. A mechanism was proposed with H_2 addition to the M(I) cation to give $[MH_2(CO)_2(PPh_3)_2]^+$ followed by alkene and CO insertion steps.

Trzeciak and coworkers reported that the phosphine-containing iridium siloxide complex $[Ir(cod)(OSiMe_3)(PCy_3)]$ had activity comparable to $[Ir(cod)(OSiMe_3)]_2$ for the hydroformylation and hydrogenation of vinylsilanes [103]. For the hydroformylation of styrene using Vaska-type complexes $[IrCl(CO)L_2]$, Franciò et al. found a markedly higher activity for the 2-pyridyldiphenylphosphine, L = PPh_2Py than for L = PPh_3 (for which the activity was negligible under the same conditions) [104]. A mechanism involving proton transfer from Ir to the pendant pyridyl group and subsequent transfer to an acetyl ligand to release aldehyde was proposed.

Moreno et al. investigated the use of inorganic salts (e.g. metal halides and carbonates) as promoters for iridium-catalyzed hydroformylation of 1-hexene, using several iridium compounds as catalyst precursors (in the absence of phosphine ligands) [105]. The hydroformylation activity was found to increase in the order $IrCl_3 < [IrCl(CO)_3]_n < Ir_4(CO)_{12}$. The addition of halide salts, notably LiCl and $CaCl_2$, enhanced the selectivity to aldehyde formation by suppressing the competing hydrogenation. IR spectra of the recovered catalyst suggested conversion of $Ir_4(CO)_{12}$ into halocarbonyl species, although a detailed mechanism based on these was not proposed.

In 2011, Beller and coworkers reported an investigation of the hydroformylation of 1-octene using a range of solvents, iridium precursors, and phosphine ligands [106]. The pre-catalyst [Ir(cod)(acac)] (acac = acetylacetonate) with 2.2 equiv PPh_3 in tetrahydrofuran (100 °C, 20 bar 2 : 1 CO/H_2) gave aldehyde products with an *n*:*iso* ratio of ~3 : 1 and ~12% hydrogenation to octane. Similar catalytic behavior was observed for the hydride complex, $[IrH(CO)(PPh_3)_3]$ and a dinuclear complex, $[Ir_2(CO)_6(PPh_3)_2]$, isolated from the reaction mixture after catalysis also showed activity on recycling. Improved regioselectivity (*n*:*iso* 86 : 14) was obtained using the sterically hindered methoxy substituted ligand $P\{2,4,6\text{-}(MeO)_3C_6H_2\}_3$. Comparison of Ir and Rh catalysts under identical conditions ([M(cod)(acac)], 8 equiv PPh_3 (120 °C, 20 bar 2 : 1 CO/H_2) gave TOF values (based on aldehyde yields) of 163 and 1255 h^{-1} respectively, indicating that the Ir catalyst has a lower activity by a factor

of ~8. More hydrogenation occurred for Ir, but alkene isomerization was lower than for Rh.

In situ high pressure IR studies of the [Ir(cod)(acac)]/PPh_3 catalyst system by Hess et al. [107] showed the formation of ν(CO) absorptions assigned to $[IrH(CO)_3(PPh_3)]$ and $[IrH(CO)_2(PPh_3)_2]$ on heating under syn-gas, with relative concentrations of the dicarbonyl and tricarbonyl complexes varying with CO and H_2 partial pressures. DFT calculations aided the assignment of the IR spectra. This work was extended by using a combination of *in situ* high-pressure IR and ^1H and ^{31}P NMR spectroscopy to quantify the equilibria between iridium hydride species, including eq–eq and ax–eq geometrical isomers of $[IrH(CO)_2(PPh_3)_2]$ and an Ir(III) trihydride complex, $[IrH_3(CO)(PPh_3)_2]$ [108]. Rate constants and activation energies for the reactions that interconvert these species were obtained using stopped-flow methods at lower temperatures.

Behr et al. demonstrated that modification of the [Ir(cod)(acac)]/PPh_3 catalyst system by the addition of inorganic salts such as LiCl increases the chemoselectivity to aldehyde products and suppresses akene hydrogenation [109]. The solvent for these experiments was *N*-methyl-2-pyrrolidone (NMP). A LiCl/Ir ratio of 2 : 1 increased the chemoselectivity to aldehydes from 77% to 94% while maintaining the *n*:*iso* ratio of ~3 : 1. Hydrogenation was reduced from 12% to 4%, and alkene isomerization from 4% to 1%. The effect of LiCl occurs for relatively small amounts of the additive, and no significant change in activity or selectivity was found above 1 : 1 LiCl/Ir.

Further studies by Behr et al. were directed at developing a biphasic fluid system to facilitate catalyst recycling [110]. It was found that the monosulfonated and trisulfonated triphenylphosphine ligands, $PPh_2(3\text{-}C_6H_4SO_3)^-$ (TPPMS) and $P(3\text{-}C_6H_4SO_3)_3{}^{3-}$ (TPPTS), gave comparable catalytic performances to PPh_3 in NMP with the [Ir(cod)(acac)]/LiCl (1 : 2) catalyst system. Catalyst recycling experiments using TPPMS were conducted using either propylene carbonate (PC) or dimethylformamide (DMF) as polar solvents. Chemoselectivity to the desired aldehyde products remained high (~90%), and non-polar components (1-octene, octane, and aldehyde products) formed a phase that could be separated from the catalyst-containing polar solvent after the reaction. Different recycling strategies were assessed, and a DMF/H_2O system was found to give selective hydroformylation and efficient product/catalyst separation employing extraction with *iso*-octane. Leaching of iridium catalyst was found to be ~0.2%. Continuous operation of this catalytic system in a mini-plant was demonstrated by Behr and coworkers in 2016 [111]. The mini-plant includes a continuous stirred tank reactor (volume ~800 mL) and a settler vessel. Experiments over 90 hours under steady-state conditions (120 °C, 20 bar CO/H_2, 2 : 1) gave 1-octene conversion of 84% with 85% chemoselectivity to aldehydes and an *n*:*iso* ratio of 78 : 22. Leaching rates for Ir and P were ~0.1% h^{-1}.

10.3.2 Platinum Catalysts

Hydroformylation catalysts based on the group 10 metals palladium and platinum have received significant attention. In the case of platinum, tin(II) chloride is frequently used as a co-catalyst. Some Pt/Sn catalyst systems can exhibit higher

regioselectivity for linear aldehyde products (high *n*:*iso* ratio) than cobalt or rhodium catalysts. For example, Clark and Davies reported that whereas $[Pt(CO)(PPh_3)Cl_2]$ is completely inactive for the hydroformylation of 1-hexene in acetonitrile at 80 °C, the addition of $SnCl_2$ (2 equiv) resulted in formation of aldehyde products with an *n*:*iso* ratio of 11 : 1 [112]. The $SnCl_2$ co-catalyst can potentially play many different roles. It can act as a Lewis acid or form $SnCl_3^-$ which can act as a counterion for cationic Pt species or coordinate to Pt as a ligand, in which case it can stabilize five-coordinate intermediates. Based on a Pt-hydride complex, the catalytic mechanism is thought to follow a similar sequence to those for Co and Rh catalysts. Hence, a Pt-hydride undergoes alkene insertion, then CO insertion into a Pt-alkyl, followed by hydrogenolysis of the resulting Pt-acyl species as shown in Scheme 10.13. Goméz et al. [113] reported mechanistic model studies of these steps and showed that *trans*-$[Pt(PPh_3)_2H(SnCl_3)]$ undergoes facile insertion of 1-pentene whereas *trans*-$[Pt(PPh_3)_2HCl]$ does not. The reaction of the acyl complex *trans*-$[Pt(PPh_3)_2(COC_5H_{11})(SnCl_3)]$ with hydrogen results in hydrogenolysis to give *n*-hexanal in competition with decarbonylation and β-elimination. A series of studies by Toniolo and coworkers investigated the structure and reactivity of Pt complexes with relevance to the catalytic mechanism. They demonstrated that coordination of an $SnCl_3^-$ ligand plays a key role in promoting the hydrogenolysis of Pt-acyl species to form aldehydes [114–123].

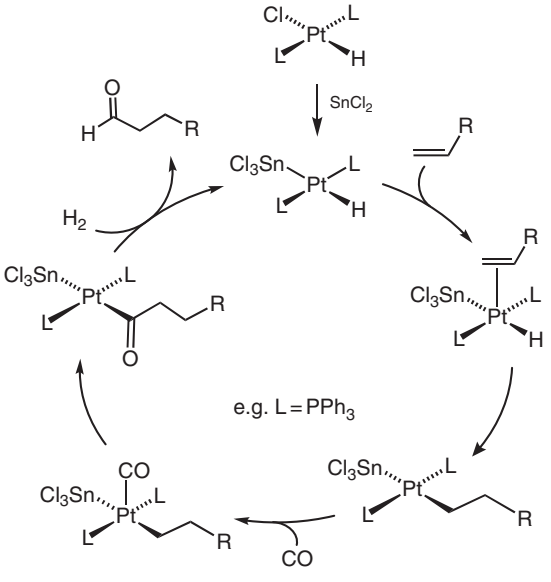

Scheme 10.13 Simplified mechanism for Pt/$SnCl_2$-catalyzed alkene hydroformylation.

Hydroformylation of 1-octene or methyl-3-pentenoate has also been studied using $[Pt(PPh_3)_2Cl_2]$ in chlorostannate ionic liquid media generated from mixtures of $SnCl_2$ with 1-butyl-3-methylimidazolium chloride or 1-butyl-4-methylpyridinium chloride [124].

Kawabata et al. reported the effect of diphosphine ligands on the $PtCl_2/SnCl_2$ catalyst system for the hydroformylation of 1-pentene [125, 126]. Changing the backbone spacer length for ligands $Ph_2P(CH_2)_nPPh_2$ gave a maximum catalytic rate for the ligand with $n = 4$, which forms a seven-membered chelate ring. Further rate enhancement was achieved, along with a very high product *n*:*iso* ratio (99 : 1), by incorporating a cyclobutane unit into the ligand backbone to increase chelate ring rigidity.

van Leeuwen and coworkers investigated the use of some wide bite-angle ligands for Pt/Sn-catalyzed hydroformylation of 1-octene [127]. Notably, high activity and selectivity were found for xantphos variants with one or both phosphorus donor atoms replaced by arsenic and attributed to the enhanced preference (relative to xantphos) for the formation of *cis*-chelate as opposed to *trans*-chelate complexes. Vogt and coworkers reported good activity and selectivity for wide bite-angle terphenyl-derived diphosphines in 1-octene hydroformylation and for xantphos-type ligands in the hydroformylation of functionalized internal alkenes such as methyl-3-pentenoate [128, 129]. Enantioselective hydroformylation reactions have been achieved using Pt/Sn halide catalysts with chiral diphosphine ligands. For example, Kollár and coworkers reported moderate enantioselectivity in the asymmetric hydroformylation of styrene using 2,4-bis(diphenylphosphino)pentane or bis(binapthophosphole) ligands [130, 131]. The same reaction has been investigated under more sustainable conditions using γ-valerolactone as a reaction solvent, achieving higher enantioselectivity than in toluene [132]. Polymer-bound chiral phosphines have also been used to support Pt/Sn chloride catalysts for styrene hydroformylation [133].

10.3.3 Osmium Catalysts

Although ruthenium compounds have been widely investigated in hydroformylation catalysis [93], examples of catalysts that employ the third-row group 8 metal, osmium, are rare. Some activity was reported for the hydroformylation of 1-hexene using $[Os(CO)(PPh_3)_3HBr]$ at 100 °C under 100 bar CO/H_2 (2 : 1) with a product *n*:*iso* ratio of ∼2 : 1 [134]. A polymer-supported anionic cluster, $[Os(CO)_{11}H]^-$, showed low activity but a high *n*:*iso* ratio for 1-hexene hydroformylation [135]. More recently, a range of monodentate and bidentate phosphine ligands was tested in combination with $[Os(CO)_{12}]$ for the hydroformylation of 1-octene and some other olefins [136]. The most promising results were obtained using imidazoyl-substituted bulky phosphine ligands, achieving good conversion, and high regioselectivity (*n*:*iso* 24 : 1 or greater).

10.4 Other Carbonylation Reactions

Third-row metals have been used in several other catalytic carbonylation reactions. Selected notable examples are summarized in this section.

10.4.1 Alkoxycarbonylation of Alkenes

In addition to methanol carbonylation and alkene hydroformylation, another catalytic carbonylation process to be operated industrially is the hydroxycarbonylation or methoxycarbonylation of ethene. This gives propionic acid or methyl propionate (Scheme 10.14), typically using Co, Ni, or Pd catalysts. The most notable recent development in this field is the commercialization by Lucite of an ethene methoxycarbonylation process that uses a highly active and selective Pd catalyst incorporating a bulky diphosphine ligand, 1,2-$(CH_2P^tBu_2)_2C_6H_4$ (dtbpx) [137].

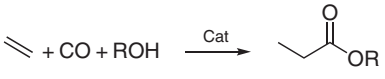

Scheme 10.14 Hydroxycarbonylation (R = H) or methoxycarbonylation (R = Me) of ethene.

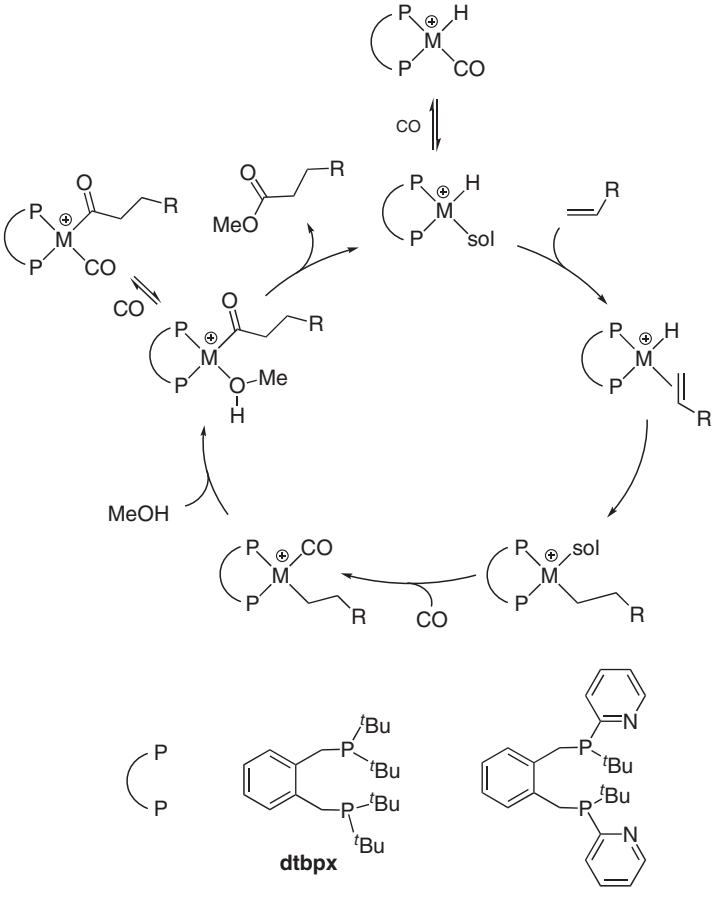

Scheme 10.15 Mechanism for Pd or Pt diphosphine-catalyzed methoxycarbonylation of ethene (R = H) or higher alkenes (showing only linear ester product). Structures of dtbpx and the pyridyl variant from Ref. [136] are shown. Source: Modified from Yang et al. [136].

The mechanism involves ethene insertion into a cationic Pd-hydride followed by CO insertion and methanolysis of a Pd-COEt species (Scheme 10.15) [139]. Iggo and coworkers' investigation showed that the much slower rates ($\sim 10^4$ fold) obtained for the corresponding platinum system are due to the stronger coordination of CO to Pt. This resulted in the formation of carbonyl complexes, $[Pt(CO)(diphosphine)R]^+$ (R = H, COEt), that act as thermodynamic sinks lying off the active catalytic cycle [140]. In 2020, Beller and coworkers reported that modification of the diphosphine ligand to include pyridyl substituents (as shown in Scheme 10.15) resulted in a notable increase in the rate of Pt-catalyzed methoxycarbonylation of 1-octene [138]. The pyridyl substituents were intended to act as proton shuttles to aid the formation of hydride species and to impart greater catalyst stability due to hemilabile properties. Comparison of Pd and Pt catalysts under the same conditions showed a longer induction period for Pt but only marginally lower activity after that and a $\sim 3:1$ *n*:*iso* ratio for the ester products. This catalyst system was screened against other alkene substrates and showed good tolerance of functional groups. Hydroxycarbonylation of alkenes by cationic gold carbonyl complexes $[Au(CO)_n]^+$, generated from Au_2O_3 in concentrated sulfuric acid, has also been noted [141].

10.4.2 Carbonylation Reactions Involving Alkynes

The Pauson–Khand reaction involves the coupling of an alkene, an alkyne, and CO to give a cyclopentenone. The most well-known catalysts are based on dinuclear cobalt carbonyl complexes, but iridium catalysts have been exemplified. For example, Shibita and Takagi reported the enantioselective intramolecular carbonylative coupling shown in Scheme 10.16a, using $[Ir(cod)Cl]_2$ with chiral BINAP-type diphosphine ligands [144]. Several other iridium-catalyzed Pauson–Khand and related reactions have been reported [145–149]. In 2016, Wu and coworkers reported the use of iridium catalysts for the carbonylative annulation of alkynes with amines or phenols to give heterocyclic products, as shown in Scheme 10.16b [142, 143]. Hydroalkoxycarbonylation of alkynes can be promoted by Pt or Pt/Sn catalysts similar to the hydroformylation catalysts discussed in Section 3.2 [150, 151].

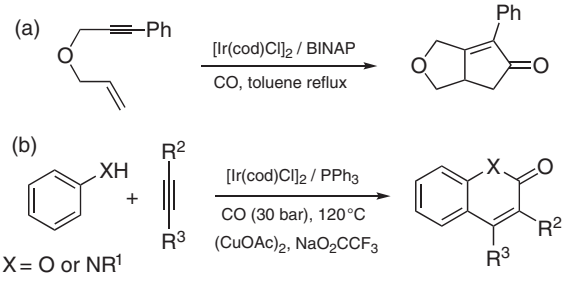

Scheme 10.16 Ir-catalyzed reactions of alkynes: (a) intramolecular Pauson–Khand reaction. (b) Carbonylative annulation with anilines or phenols. Source: Adapted from Zhu et al. [142, 143].

10.4.3 Oxidative Carbonylations

The functionalization of alkanes has long been a significant goal, and platinum-based catalysts have been the subject of considerable attention in the oxidation of methane to methanol and derivatives [152]. Related to this, Zerella and Bell reported that $PtCl_2$ in concentrated sulfuric acid could catalyze the oxidative carbonylation of methane to acetic acid (Eq. (10.7)) [153]. A mechanism was proposed involving C–H activation of methane followed by insertion of CO into a Pt-methyl species to give acetyl, which is hydrolyzed to give acetic acid.

$$CH_4 + CO + 0.5O_2 \longrightarrow MeCO_2H \tag{10.7}$$

Other oxidative carbonylation reactions include the tungsten-catalyzed conversion of primary amines into ureas. McElwee-White and coworkers initially used an iodide-bridged tungsten(IV) complex, $[W(CO)_2(NPh)I_2]_2$, and proposed the mechanism shown in Scheme 10.17 [154]. Cleavage of the dimer and substitution of an iodide ligand by amine gives a cationic complex that undergoes nucleophilic attack by amine on a CO ligand to give a carbamoyl complex. In the presence of an oxidant, deprotonation by excess amine gives an isocyanate complex. This can yield urea following a nucleophilic attack by amine. Subsequent studies showed that the use of $[W(CO)_6]$ with an oxidant such as I_2 is effective for this type of reaction for primary and secondary amines [155–157].

Polynuclear gold complexes have also been reported to catalyze the oxidative carbonylation of primary amines to ureas. For example, Bertrand and coworkers demonstrated the activity of a trinuclear complex, $[Au_3L_3]BF_4$ (L = cyclic (alkyl)(amino)carbene) [158] and Smirnova et al. used a bimetallic Au(I)/Ag(I) complex, $[Au_4Ag\{2,6\text{-}(Ph_2P)_2C_5H_3N\}_2(OAc)_2](SbF_6)_3$ [159]. Oxidative carbonylation of amines can also give carbamates (Eq. (10.8)), for example using gold(I) complexes such as $Au(PPh_3)_nCl$ (n = 1, 2) [160] or polymer-immobilized gold catalysts prepared from $HAuCl_4$ and an ion exchange resin [161]. No mechanistic studies of these systems are reported. Probably, nucleophilic attack by amine on coordinated CO (analogous to the tungsten system in Scheme 10.17) is followed by interception of an intermediate carbamoyl species by alcoholysis to give the carbamate product.

$$RNH_2 + CO + 0.5O_2 + R'OH \xrightarrow{\text{Au cat}} RNHCO_2R' + H_2O \tag{10.8}$$

Gold-based catalysts have also been applied in oxidative carbonylation of methanol to dimethyl carbonate (Eq. (10.9)) (a reaction that is more commonly promoted by copper-based catalysts). Li et al. reported that Au(III) Schiff base complexes such as $[Au(phen)Cl_2]^+$ (phen = 1,10-phenanthroline) are active at 120 °C and a pressure of 3 MPa (2 : 1 $CO:O_2$) provided that a halide promoter is added, with KI being the most effective [162]. A proposed mechanism is shown in Scheme 10.18, involving Au(phen) iodide complexes. An Au(III)-methoxy species undergoes CO insertion to give a methoxycarbonyl ligand which couples with another methanol-derived methoxy unit to eliminate dimethyl carbonate. Oxidation of Au(I) back to Au(III)

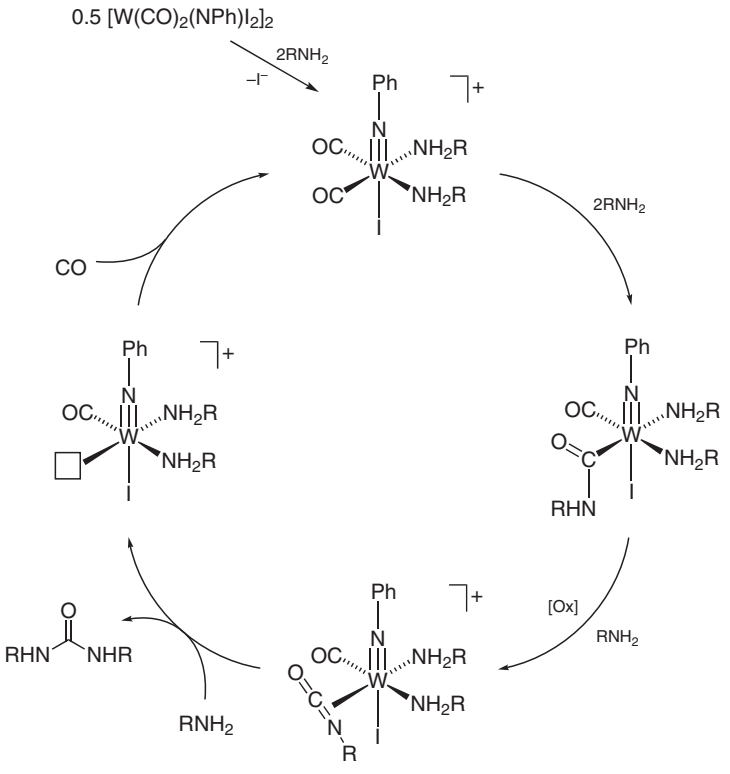

Scheme 10.17 Proposed mechanism for tungsten-catalyzed oxidative carbonylation of amines. Source: Modified from McCusker et al. [154].

is required to complete the cycle.

$$2\mathrm{MeOH} + \mathrm{CO} + 0.5\mathrm{O_2} \xrightarrow{\text{cat}} (\mathrm{MeO})_2\mathrm{CO} + \mathrm{H_2O} \tag{10.9}$$

10.5 Summary and Conclusions

This chapter has illustrated the application of third-row transition metal catalysts in a variety of carbonylation reactions. The most prominent large-scale commercial carbonylation employing a third-row metal catalyst is the Cativa process developed and operated successfully by BP. This showed that by careful selection of reaction conditions and promoters, an iridium-based catalyst could compete with and even out-perform the long-established rhodium-catalyzed Monsanto process. Although mechanistically similar, the rate-determining step changes on going from Rh to Ir, with the crucial C—C bond-forming migratory CO insertion being much slower on Ir. However, additives including Ru compounds promote this step, and high catalytic activity can be achieved. Adjustments to process conditions improve catalyst stability and efficiency, reducing by-product formation and lowering product purification costs. This successful implementation of a third-row metal catalyst

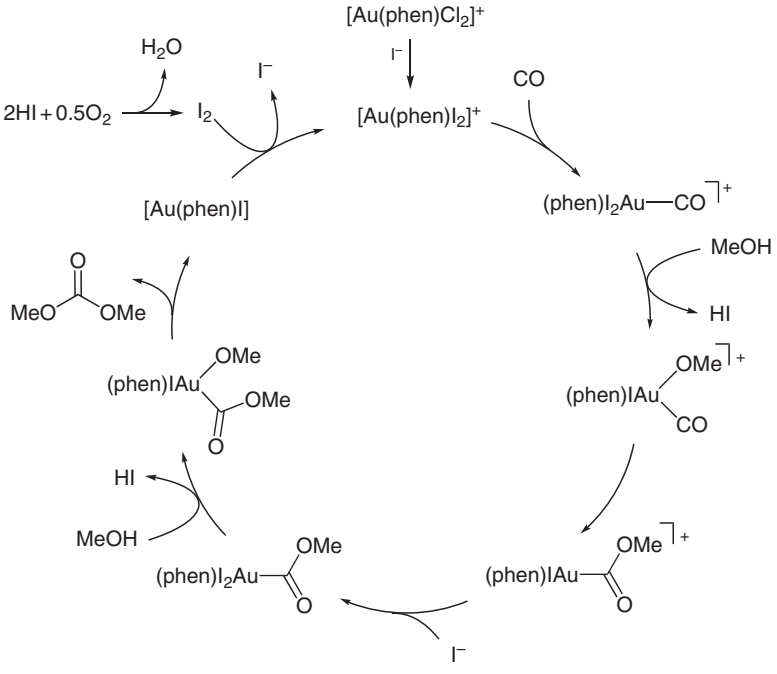

Scheme 10.18 Proposed mechanism for oxidative carbonylation of methanol catalyzed by $[Au(phen)Cl_2]Cl/KI$.

suggests that a similar approach could be applied to other important carbonylation reactions, and recent progress supports this. The beneficial effects of tin halide promoters for platinum-catalyzed alkene hydroformylation are well-established. Recent results show that appropriate choice of ligands, additives, and reaction conditions can improve the activity of iridium hydroformylation catalysts beyond what was previously assumed. Likewise, platinum catalysts for alkoxycarbonylation have recently been developed that show comparable activity to palladium in some cases. Notable progress has been made in applying third-row metals in other carbonylation reactions, for example, those involving alkynes to produce cyclic products. In conclusion, the developments discussed in this chapter demonstrate a strong potential for growth in the application of third-row metals in carbonylation chemistry.

References

1 Hartwig, J. (2010). *Organotransition Metal Chemistry. From Bonding to Catalysis*. University Science Books, Sausalito.

2 George, R., Andersen, J.A.M., and Moss, J.R. (1995). *J. Organomet. Chem.* 505: 131–133.

3 Li, J., Schreckenbach, G., and Ziegler, T. (1995). *J. Am. Chem. Soc.* 117: 486–494.

4 Blaser, H.U. (2002). *Adv. Synth. Catal.* 344: 17–31.
5 Jira, R. (2009). *Angew. Chem. Int. Ed.* 48: 9034–9037.
6 Hohenschutz, H., von Kutepow, N., and Himmele, W. (1966). *Hydrocarb. Process.* 45: 141–144.
7 von Kutepow, N., Himmele, W., and Hohenschutz, H. (1965). *Chem.-Ing.-Tech.* 37: 383–388.
8 Reppe, W., Friederich, H., von Kutepow, N., and Morsch, W. (1956). BASF. US Patent 2, 729, 651.
9 Reppe, W. and Friederich, H. (1957). BASF. US Patent 2, 789, 137.
10 Paulik, F.E. and Roth, J.F. (1968). *Chem. Commun.*: 1578.
11 Forster, D. (1979). *Adv. Organomet. Chem.* 17: 255–267.
12 Dekleva, T.W. and Forster, D. (1986). *Adv. Catal.* 34: 81–130.
13 Howard, M.J., Jones, M.D., Roberts, M.S., and Taylor, S.A. (1993). *Catal. Today* 18: 325–354.
14 Maitlis, P.M., Haynes, A., Sunley, G.J., and Howard, M.J. (1996). *J. Chem. Soc. Dalton Trans.*: 2187–2196.
15 Yoneda, N., Kusano, S., Yasui, M. et al. (2001). *Appl. Catal. A* 221: 253–265.
16 Steinhoff, B.A. and Zoeller, J.R. (2018). Carbonylation of methanol and its derivatives to acetic acid and acetic anhydride. In: *Applied Homogeneous Catalysis with Organometallic Compounds*, 3e, vol. 1 (eds. B. Cornils and W.A. Herrmann), 93–117. Weinheim: Wiley-VCH.
17 Thomas, C.M. and Süss-Fink, G. (2003). *Coord. Chem. Rev.* 243: 125–142.
18 Morris, G.E. (2005). Carbonylation of methanol to acetic acid and methyl acetate to acetic anhydride. In: *Mechanisms in Homogeneous Catalysis; A Spectroscopic Approach* (ed. B.T. Heaton), 195–230. Weinheim: Wiley-VCH.
19 Maitlis, P. and Haynes, A. (2006). Syntheses based on carbon monoxide. In: *Metal-Catalysis in Industrial Organic Processes* (eds. P. Maitlis and G.P. Chiusoli), 114–162. RSC.
20 Haynes, A. (2006). Commercial applications of iridium complexes in homogeneous catalysis. In: *Comprehensive Organometallic Chemistry III*, vol. 7 (eds. R.H. Crabtree and D.M.P. Mingos), 427–444. Elsevier.
21 Haynes, A. (2006). Acetic acid synthesis by catalytic carbonylation of methanol. In: *Catalytic Carbonylation Reactions, Topics in Organometallic Chemistry*, vol. 18 (ed. M. Beller), 179–205. Berlin: Springer.
22 Kalck, P. and Serp, P. (2009). Iridium-catalyzed methanol carbonylation. In: *Iridium Complexes in Organic Synthesis* (eds. L.A. Oro and C. Claver), 195–209. Weinheim: Wiley-VCH.
23 Haynes, A. (2010). *Adv. Catal.* 53: 1–45.
24 Kalck, P., Le Berre, C., and Serp, P. (2020). *Coord. Chem. Rev.* 402: 213078.
25 Forster, D. and Dekleva, T.W. (1986). *J. Chem. Educ.* 63: 204–206.
26 Forster, D. (1977). *Ann. N. Y. Acad. Sci.* 295: 79–82.
27 Fulford, A., Hickey, C.E., and Maitlis, P.M. (1990). *J. Organomet. Chem.* 398: 311–323.
28 Haynes, A., Mann, B.E., Morris, G.E., and Maitlis, P.M. (1993). *J. Am. Chem. Soc.* 115: 4093–4100.

29 Griffin, T.R., Cook, D.B., Haynes, A. et al. (1996). *J. Am. Chem. Soc.* 118: 3029–3030.

30 Ivanova, E.A., Gisdakis, P., Nasluzov, V.A. et al. (2001). *Organometallics* 20: 1161–1174.

31 Kinnunen, T. and Laasonen, K. (2001). *J. Mol. Struct. (THEOCHEM)* 540: 91–100.

32 Kinnunen, T. and Laasonen, K. (2001). *J. Mol. Struct. (THEOCHEM)* 542: 273–288.

33 Kinnunen, T. and Laasonen, K. (2001). *J. Organomet. Chem.* 628: 222–232.

34 Cheong, M. and Ziegler, T. (2005). *Organometallics* 24: 3053–3058.

35 Feliz, M., Freixa, Z., van Leeuwen, P.W.N.M., and Bo, C. (2005). *Organometallics* 24: 5718–5723.

36 Haynes, A., Mann, B.E., Gulliver, D.J. et al. (1991). *J. Am. Chem. Soc.* 113: 8567–8569.

37 Baker, E.C., Hendriksen, D.E., and Eisenberg, R. (1980). *J. Am. Chem. Soc.* 102: 1020–1027.

38 Roe, D.C., Sheridan, R.E., and Bunel, E.E. (1994). *J. Am. Chem. Soc.* 116: 1163–1164.

39 Haynes, A., McNish, J., and Pearson, J.M. (1997). *J. Organomet. Chem.* 551: 339–347.

40 Smith, B.L., Torrence, G.P., Aguilo, A., and Alder, J.S. (1991). Hoechst celanese corporation. US Patent 5, 001, 259.

41 Patil, R.P., Kelkar, A.A., and Chaudhari, R.V. (1992). *J. Mol. Catal.* 72: 153–165.

42 Patil, R.P., Kelkar, A.A., and Chaudhari, R.V. (1988). *J. Mol. Catal.* 47: 87–97.

43 Forster, D. (1979). *J. Chem. Soc. Dalton Trans.*: 1639–1645.

44 Garland, C.S., Giles, M.F., and Sunley, J.G. (1995). BP chemicals. EP0643034.

45 Baker, M.J., Giles, M.F., Garland, C.S., and Rafeletos, G. (1996). BP chemicals. EP0749948.

46 Garland, C.S., Giles, M.F., Poole, A.D., and Sunley, J.G. (1996). BP chemicals. EP0728726.

47 Baker, M.J., Giles, M.F., Garland, C.S. et al. (1997). BP chemicals. EP0752406.

48 (1996). *Chem. Br.* 32: 7.

49 (1996). *Chem. Ind.*: 483.

50 Sunley, G.J. and Watson, D.J. (2000). *Catal. Today* 58: 293–307.

51 Jones, J.H. (2000). *Platin. Met. Rev.* 44: 94–105.

52 Howard, M.J., Sunley, G.J., Poole, A.D. et al. (1999). *Stud. Surf. Sci. Catal.* 121: 61–68.

53 Forster, D. (1969). *Inorg. Nucl. Chem. Lett.* 5: 433–436.

54 Forster, D. (1972). *Inorg. Chem.* 11: 473–475.

55 Forster, D. (1972). *Inorg. Chem.* 11: 1686–1687.

56 Forster, D. and Singleton, T.C. (1982). *J. Mol. Catal.* 17: 299–314.

57 Ellis, P.R., Pearson, J.M., Haynes, A. et al. (1994). *Organometallics* 13: 3215–3226.

58 Bassetti, M., Monti, D., Haynes, A. et al. (1992). *Gazz. Chim. Ital.* 122: 391–393.

59 Gautron, S., Giordano, R., Le Berre, C. et al. (2003). *Inorg. Chem.* 42: 5523–5530.

60 Haynes, A., Maitlis, P.M., Morris, G.E. et al. (2004). *J. Am. Chem. Soc.* 126: 2847–2861.

61 Ghaffar, T., Adams, H., Maitlis, P.M. et al. (1998). *Chem. Commun.*: 1023–1024.

62 Pearson, J.M., Haynes, A., Morris, G.E. et al. (1995). *J. Chem. Soc. Chem. Commun.*: 1045–1046.

63 Gautron, S., Lassauque, N., Le Berre, C. et al. (2006). *Organometallics* 25: 5894–5905.

64 Cheong, M., Schmid, R., and Ziegler, T. (2000). *Organometallics* 19: 1973–1982.

65 Volpe, M., Wu, G., Iretskii, A., and Ford, P.C. (2006). *Inorg. Chem.* 45: 1861–1870.

66 Haynes, A., Meijer, A.J.H.M., Lyons, J.R., and Adams, H. (2009). *Inorg. Chem.* 48: 28–35.

67 Ghaffar, T., Charmant, J.P.H., Sunley, G.J. et al. (2000). *Inorg. Chem. Commun.* 3: 11–12.

68 Elliott, P.I.P., Haak, S., Meijer, A.J.H.M. et al. (2013). *Dalton Trans.* 42: 16538–16546.

69 Braca, G., Sbrana, G., Valentini, G. et al. (1978). *J. Am. Chem. Soc.* 100: 6238–6240.

70 Braca, G., Paladini, L., Sbrana, G. et al. (1981). *Ind. Eng. Chem. Prod. Res. Dev.* 20: 115–122.

71 Braca, G., Sbrana, G., Valentini, G., and Cini, M. (1982). *J. Mol. Catal.* 17: 323–330.

72 Gautier-Lafaye, J., Perron, R., Leconte, P., and Colleuille, Y. (1985). *Bull. Soc. Chim. Fr.*: 353–360.

73 Jenner, G. and Bitsi, G. (1987). *J. Mol. Catal.* 40: 71–82.

74 Kelkar, A.A., Kohle, D.S., and Chaudhari, R.V. (1992). *J. Organomet. Chem.* 430: 111–116.

75 Whyman, R., Wright, A.P., Iggo, J.A., and Heaton, B.T. (2002). *J. Chem. Soc. Dalton Trans.*: 771–777.

76 Gautron, S., Lassauque, N., Le Berre, C. et al. (2006). *Eur. J. Inorg. Chem.* 2006: 1121–1126.

77 Gautron, S., Lassauque, N., Le Berre, C. et al. (2006). *Top. Catal.* 40: 83–90.

78 Yang, J., Haynes, A., and Maitlis, P.M. (1999). *Chem. Commun.*: 179–180.

79 Kwak, J.H., Dagle, R., Tustin, G.C. et al. (2014). *J. Phys. Chem. Lett.* 5: 566–572.

80 Peng, S.Q., Lin, X.S., Song, X.G. et al. (2020). *J. Catal.* 381: 193–203.

81 Feng, S.Q., Lin, X.S., Song, X.G. et al. (2019). *J. Catal.* 377: 400–408.

82 Ren, Z., Lyu, Y., Feng, S.Q. et al. (2018). *Chin. J. Catal.* 39: 1060–1069.

83 Hensley, A.J.R., Zhang, J.H., Vincon, I. et al. (2018). *J. Catal.* 361: 414–422.

84 Zoeller, J.R., Singleton, A.H., Tustin, G.C., and Carver, D.L. (2003). Eastman. US Patent 6, 506, 933 and 6, 509, 293.

85 Goguet, A., Hardacre, C., Harvey, I. et al. (2009). *J. Am. Chem. Soc.* 131: 6973–6975.

86 Martinez-Ramirez, Z., Flores-Escamilla, G.A., Berumen-Espana, G.S. et al. (2015). *Appl. Catal. A Gen.* 502: 254–261.

87 Qi, J., Finzel, J., Robatjazi, H. et al. (2020). *J. Am. Chem. Soc.* 142: 14178–14189.

88 Gregor, L.C., Grajeda, J., White, P.S. et al. (2018). *Catal. Sci. Tech.* 8: 3133–3143.

89 Gregor, L.C., Grajeda, J., Kita, M.R. et al. (2016). *Organometallics* 35: 3074–3086.

90 Franke, R., Selent, D., and Borner, A. (2012). *Chem. Rev.* 112: 5675–5732.

91 Li, C., Chen, L., and Garland, M. (2007). *J. Am. Chem. Soc.* 129: 13327–13334.

92 Klähn, M. and Garland, M.V. (2015). *ACS Catal.* 5: 2301–2316.

93 Pospech, J., Fleischer, I., Franke, R. et al. (2013). *Angew. Chem. Int. Ed.* 52: 2852–2872.

94 Pruchnik, F.P. (1990). *Organometallic Chemistry of the Transition Elements.* New York: Plenum Press.

95 Deutsch, P.P. and Eisenberg, R. (1990). *J. Am. Chem. Soc.* 112: 714–721.

96 Deutsch, P.P. and Eisenberg, R. (1990). *Organometallics* 9: 709–718.

97 Fox, D.J., Duckett, S.B., Flaschenriem, C. et al. (2006). *Inorg. Chem.* 45: 7197–7209.

98 Guan, D.X., Godard, C., Polas, S.M. et al. (2019). *Dalton Trans.* 48: 2664–2675.

99 Abkai, G., Schmidt, S., Rosendahl, T. et al. (2014). *Organometallics* 33: 3212–3214.

100 Ternel, J., Couturier, J.L., Dubois, J.L., and Carpentier, J.F. (2015). *ChemCatChem* 7: 513–520.

101 Crudden, C.M. and Alper, H. (1994). *J. Org. Chem.* 59: 3091–3097.

102 Rosales, M., Duran, J.A., Gonzalez, A. et al. (2007). *J. Mol. Catal. A-Chem.* 270: 250–256.

103 Mieczynska, E., Trzeciak, A.M., Ziolkowski, J.J. et al. (2005). *J. Mol. Catal. A-Chem.* 237: 246–253.

104 Franciò, G., Scopelliti, R., Arena, C.G. et al. (1998). *Organometallics* 17: 338–347.

105 Moreno, M.A., Haukka, M., and Pakkanen, T.A. (2003). *J. Catal.* 215: 326–331.

106 Piras, I., Jennerjahn, R., Jackstell, R. et al. (2011). *Angew. Chem. Int. Ed.* 50: 280–284.

107 Hess, D., Hannebauer, B., Konig, M. et al. (2012). *Z. Naturforsch., B: Chem. Sci.* 67: 1061–1069.

108 Kubis, C., Baumann, W., Barsch, E. et al. (2014). *ACS Catal.* 4: 2097–2108.

109 Behr, A., Kamper, A., Nickel, M., and Franke, R. (2015). *Appl. Catal. A Gen.* 505: 243–248.

110 Behr, A., Kamper, A., Kuhlmann, R. et al. (2016). *Catal. Sci. Tech.* 6: 208–214.

111 Kamper, A., Warrelmann, S.J., Reiswich, K. et al. (2016). *Chem. Eng. Sci.* 144: 364–371.

112 Clark, H.C. and Davies, J.A. (1981). *J. Organomet. Chem.* 213: 503–512.

113 Goméz, M., Muller, G., Sainz, D. et al. (1991). *Organometallics* 10: 4036–4045.

114 Bardi, R., Piazzesi, A.M., Cavinato, G. et al. (1982). *J. Organomet. Chem.* 224: 407–420.

115 Bardi, R., Piazzesi, A.M., Delpra, A. et al. (1982). *J. Organomet. Chem.* 234: 107–115.

116 Cavinato, G. and Toniolo, L. (1983). *J. Organomet. Chem.* 241: 275–279.

117 Scrivanti, A., Cavinato, G., Toniolo, L., and Botteghi, C. (1985). *J. Organomet. Chem.* 286: 115–120.

118 Ruegg, H.J., Pregosin, P.S., Scrivanti, A. et al. (1986). *J. Organomet. Chem.* 316: 233–241.

119 Scrivanti, A., Berton, A., Toniolo, L., and Botteghi, C. (1986). *J. Organomet. Chem.* 314: 369–383.

120 Moretti, G., Botteghi, C., and Toniolo, L. (1987). *J. Mol. Catal.* 39: 177–183.

121 Graziani, R., Cavinato, G., Casellato, U., and Toniolo, L. (1988). *J. Organomet. Chem.* 353: 125–131.

122 Scrivanti, A., Botteghi, C., Toniolo, L., and Berton, A. (1988). *J. Organomet. Chem.* 344: 261–275.

123 Cavinato, G., De Munno, G., Lami, M. et al. (1994). *J. Organomet. Chem.* 466: 277–282.

124 Wasserscheid, P. and Waffenschmidt, H. (2000). *J. Mol. Catal. A-Chem.* 164: 61–67.

125 Kawabata, Y., Hayashi, T., and Ogata, I. (1979). *J. Chem. Soc. Chem. Commun.*: 462–463.

126 Hayashi, T., Kawabata, Y., Isoyama, T., and Ogata, I. (1981). *Bull. Chem. Soc. Jpn.* 54: 3438–3446.

127 van der Veen, L.A., Keeven, P.K., Kamer, P.C.J., and van Leeuwen, P. (2000). *J. Chem. Soc. Dalton Trans.*: 2105–2112.

128 Meessen, P., Vogt, D., and Keim, W. (1998). *J. Organomet. Chem.* 551: 165–170.

129 van der Vlugt, J.I., van Duren, R., Batema, G.D. et al. (2005). *Organometallics* 24: 5377–5382.

130 Kollár, L., Kegl, T., and Bakos, J. (1993). *J. Organomet. Chem.* 453: 155–158.

131 Gladiali, S., Fabbri, D., and Kollar, L. (1995). *J. Organomet. Chem.* 491: 91–96.

132 Pongracz, P., Kollar, L., and Mika, L.T. (2016). *Green Chem.* 18: 842–847.

133 Stille, J.K. and Parrinello, G. (1983). *J. Mol. Catal.* 21: 203–210.

134 Sanchezdelgado, R.A., Andriollo, A., and Valencia, N. (1983). *J. Chem. Soc. Chem. Commun.*: 444–445.

135 Marrakchi, H, Nguini Effa, J.-B., Haimeur, M. et al. (1985). *J. Mol. Catal.* 30: 101–109.

136 Wu, L, Liu, Q, Spannenberg, A. et al. (2015). *Chem. Commun.* 51: 3080–3082.

137 Clegg, W., Elsegood, M.R.J., Eastham, G.R. et al. (1999). *Chem. Commun.*: 1877–1878.

138 Yang, J., Liu, J.W., Ge, Y. et al. (2020). *Chem. Commun.* 56: 5235–5238.

139 Eastham, G.R., Tooze, R.P., Heaton, B.T. et al. (2000). *Chem. Commun.*: 609–610.

140 Wolowska, J., Eastham, G.R., Heaton, B.T. et al. (2002). *Chem. Commun.*: 2784–2785.

141 Xu, Q., Imamura, Y., Fujiwara, M., and Souma, Y. (1997). *J. Org. Chem.* 62: 1594–1598.

142 Zhu, F.X., Li, Y.H., Wang, Z.C., and Wu, X.F. (2016). *Angew. Chem. Int. Ed.* 55: 14151–14154.

143 Zhu, F.X., Li, Y.H., Wang, Z.C., and Wu, X.F. (2016). *Adv. Synth. Catal.* 358: 3350–3354.

144 Shibata, T. and Takagi, K. (2000). *J. Am. Chem. Soc.* 122: 9852–9853.

145 Lu, Z.L., Neumann, E., and Pfaltz, A. (2007). *Eur. J. Org. Chem.* 2007: 4189–4192.

146 Shibata, T. (2006). *J. Synth. Org. Chem Jpn.* 64: 913–922.

147 Shibata, T., Toshida, N., Yamasaki, M. et al. (2005). *Tetrahedron* 61: 9974–9979.

148 Shibata, T., Kadowaki, S., Hirase, M., and Takagi, K. (2003). *Synlett*: 573–575.

149 Shibata, T., Yamashita, K., Katayama, E., and Takagi, A. (2002). *Tetrahedron* 58: 8661–8667.

150 Scrivanti, A., Chinellato, R., and Matteoli, U. (1993). *J. Mol. Catal.* 84: L141–L144.

151 Scrivanti, A., Menchi, G., and Matteoli, U. (1995). *J. Mol. Catal. A-Chem.* 96: 223–229.

152 Labinger, J.A. (2017). *Chem. Rev.* 117: 8483–8496.

153 Zerella, M. and Bell, A.T. (2006). *J. Mol. Catal. A-Chem.* 259: 296–301.

154 McCusker, J.E., Logan, J., and McElwee-White, L. (1998). *Organometallics* 17: 4037–4041.

155 Zhang, L., Darko, A.K., Johns, J.I., and McElwee-White, L. (2011). *Eur. J. Org. Chem.* 2011: 6261–6268.

156 McCusker, J.E., Qian, F., and McElwee-White, L. (2000). *J. Mol. Catal. A-Chem.* 159: 11–17.

157 McCusker, J.E., Main, A.D., Johnson, K.S. et al. (2000). *J. Org. Chem.* 65: 5216–5222.

158 Jin, L.Q., Weinberger, D.S., Melaimi, M. et al. (2014). *Angew. Chem. Int. Ed.* 53: 9059–9063.

159 Smirnova, E.S., Molina, J.M.M., Johnson, A. et al. (2016). *Angew. Chem. Int. Ed.* 55: 7487–7491.

160 Shi, F. and Deng, Y.Q. (2001). *Chem. Commun.*: 443–444.

161 Shi, F. and Deng, Y.Q. (2002). *J. Catal.* 211: 548–551.

162 Li, J.J., Hu, J.L., Gu, Y.L. et al. (2011). *J. Mol. Catal. A-Chem.* 340: 53–59.

11

Transition Metal-Free Carbonylation Processes

Lu Cheng[1], Binbin Liu[2], Fangning Xu[1] and Wei Han[1]

[1] Nanjing Normal University, School of Chemistry and Materials Science, Jiangsu Collaborative Innovation Center of Biomedical Functional Materials, Jiangsu Key Laboratory of Biofunctional Materials, Key Laboratory of Applied Photochemistry, Wenyuan Road NO 1, Qixia District, Nanjing 210023, P.R. China
[2] Technical University Munich, Department of Chemistry and Catalysis Research Center, Lichtenbergstrasse 4, 85748, Garching, Munich, Germany

11.1 Introduction

Transition-metal-catalyzed carbonylation employing gaseous CO as the carbonyl source is a fundamental and key chemical process for transforming inexpensive and readily accessible feedstocks to valuable products (typical industrial processes: Oxo process, Monsanto process, and Fischer–Tropsch synthesis) [1]. High added-value compounds, such as ketones, aldehydes, acids, amides, esters, and anhydrides, can be readily prepared by the insertion of CO into an existing bond, e.g. C–X (X = Cl, Br, I), or by the addition of CO to alkynes or alkenes in the presence of nucleophiles (NuH) [1, 2]. Generally, these carbonylation processes require the employment of a transition metal and an expensive ligand (often organophosphine or *N*-heterocyclic carbene) to ensure high efficiency and a wide variety of substrate, as gaseous carbon monoxide is relatively inert (bond energy, 257 kcal/mol) and causes mass transfer resistance in a liquid system [1, 2].

Although transition-metal catalysis has become an indispensable tool in the synthetic community, this strategy may also present limitations, such as the cost of the transition metal catalyst and the deactivation of the catalyst (CO is a strong π-acidic ligand), and generation of residual metal contamination [3]. Trace metals in products for human consumption are strictly regulated by stringent specifications [3]. Similar concerns are also observed in the modern electronics industry, where metal residues may reduce organic electronic devices [4]. Therefore, the development of efficient and practical strategies devoid of metal catalysts is highly attractive but also represents a formidable challenge [5]. We will endeavor to highlight the recent advances in transition-metal-free carbonylation to synthesize aldehydes and ketones, esters and lactones, amides, acids and anhydrides, acyl chlorides, and alcohols. We hope that this review will be useful for synthetic organic chemists and

Carbon Monoxide in Organic Synthesis: Carbonylation Chemistry,
First Edition. Edited by Bartolo Gabriele.

inspire further reaction development in the interesting transition-metal-free carbonylation area.

11.2 Transition-Metal-Free Carbonylation for the Synthesis of Aldehydes and Ketones

The first transition-metal-free carbonylation to synthesize ketones was reported in 1952. It was reported that treatment of ethylene and CO under high pressures (180–1000 bar) and temperatures (120–165 °C) led to the formation of polyketones via a radical process [6]. In 1956, Foster et al. reported that the peroxide-initiated reaction of mercaptans with ethylene and carbon monoxide (3000 atm at 130 °C) afforded 3-(alkylthio)propanal in 11–18% yields [7]. While these reactions were noteworthy as pioneering efforts to effect trapping of acyl radicals for the formation of carbonyl compounds, the extremely high pressures of CO and low product yields limited their utility.

Subsequently, Ryu et al. disclosed the first example of the highly efficient carbon monoxide trapping by a free-radical process [8] (Scheme 11.1). In general, the reactions were carried out at 80–100 °C for three to five hours under 65–80 atm of CO using azobisisobutyronitrile (AIBN) as the radical initiator and Bu_3SnH as the hydride source. Thus, primary, secondary, tertiary alkyl bromides, and aryl iodides [9] were carbonylated to provide the corresponding aldehydes in moderate to good yields.

Furthermore, Nishii et al. reported the radical carbonylations of *gem*-dihalocyclopropanes **3** using CO (80 atm) and Bu_3SnH (formylation) or $Bu_3Sn(CH_2CH{=}CH_2)$ to give *trans* and *cis* adducts **4** and **5** with good to excellent stereoselectivity (*trans*/*cis*) >99/1–75/25 or 17/83–1/99) (Scheme 11.2) [10]. Initially generated

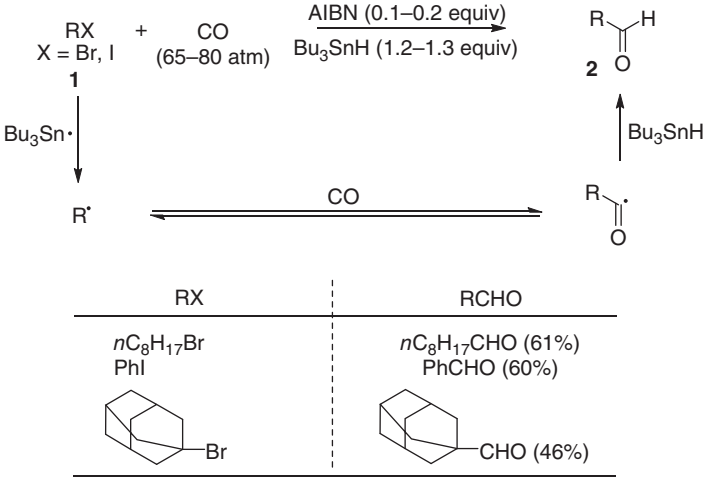

Scheme 11.1 Conversion of organohalides into aldehydes by free-radical carbonylation. Source: Modified from Ryu et al. [8].

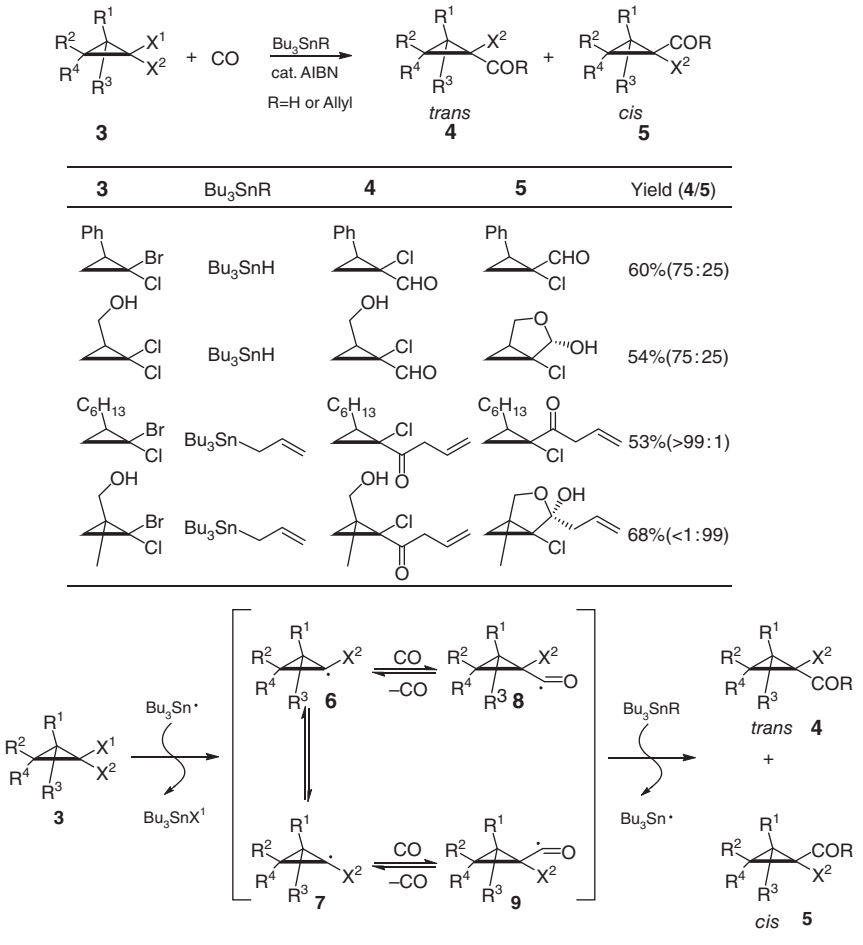

Scheme 11.2 Radical carbonylations of *gem*-dihalocyclopropane derivatives with CO. Source: Modified from Nishii et al. [10].

trans-radical **6** more preferentially adds to CO than *cis*-radical **7** to give mainly **4** due to the stereocongestion between R^1 (and/or R^2) and CO. The allylacylation amplifies stereoselectivity because of the additional stereocongestion in the final product-determining allylation step.

A seminal example of radical carbonylation was reported by the Ryu group and involved the double CO-trapping reaction by pent-4-enyl radicals **12**, from pent-4-enyl iodides **10**, to afford keto aldehyde **11**. Reactions were carried out under 90 atm of CO using a combination of AIBN/Bu_3SnH (Scheme 11.3) [11]. The pent-4-enyl radical **12** was trapped by CO to form hex-5-enoyl radical **13**. The subsequent 5-*exo* cyclization of radical **13** generated 3-oxocyclopentyl carbinyl radical **14**, and under high CO concentrations, **14** would be trapped by a second molecule of CO to yield acyl radical **15**. Finally, the acyl radical **15** abstracted a

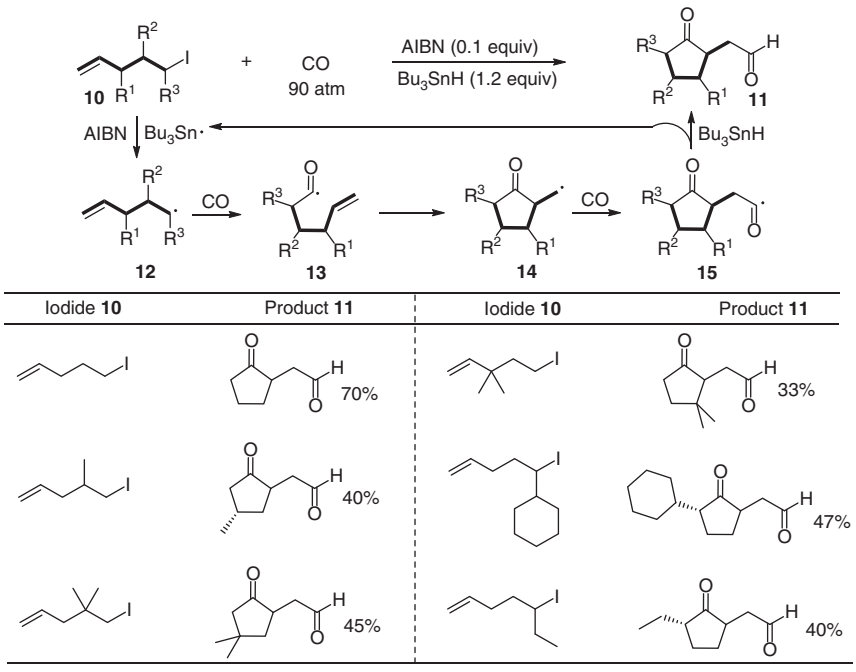

Scheme 11.3 Radical-mediated double carbonylations of alk-4-enyl iodides. Source: Modified from Tsunoi et al. [11].

hydrogen atom to give the double carbonylated product and generate tributyltin radical for the next run.

Despite the broad applications of Bu_3SnH, it is relatively expensive, unstable, and toxic. The Ryu group further demonstrated the use of TTMSS [tris(trimethylsilyl) silane] instead of tin hydride as a free-radical mediator that enabled the carbonylation of an aliphatic halide **16** to an aldehyde under lower CO pressure (15–30 atm) [12]. Furthermore, the key acyl radical intermediate **20** was trapped by an electron-deficient alkene **17**. This allowed a three-component carbonylative coupling reaction with the formation of unsymmetrical ketones **18** (Scheme 11.4) [12]. When Bu_3SnH [13] or tetrabutylammonium cyanoborohydride [14] was used as the hydride source, an excess (2–4 equiv) of an alkene was required to ensure an effective cross-coupling.

Subsequently, Ryu and co-workers exploited CO trapping by carbon-centered radical **26**, *in situ*-generated from the thermolysis of 5-alkenyloxyamines, by reporting a new route for tin-free radical carbonylation (Scheme 11.5) [15]. This process involves a two-step procedure: (i) a persistent radical effect-mediated cyclization/carbonylation of 1-phenyl-substituted 5-hexenyloxyamines under thermolysis conditions, and (ii) an intramolecular Friedel–Crafts-type acylation using Otera's conditions [16], as depicted in Scheme 11.5.

Visible-light-initiated photocatalysis is emerging as a powerful tool for developing novel radical synthetic methods due to the natural abundance of visible

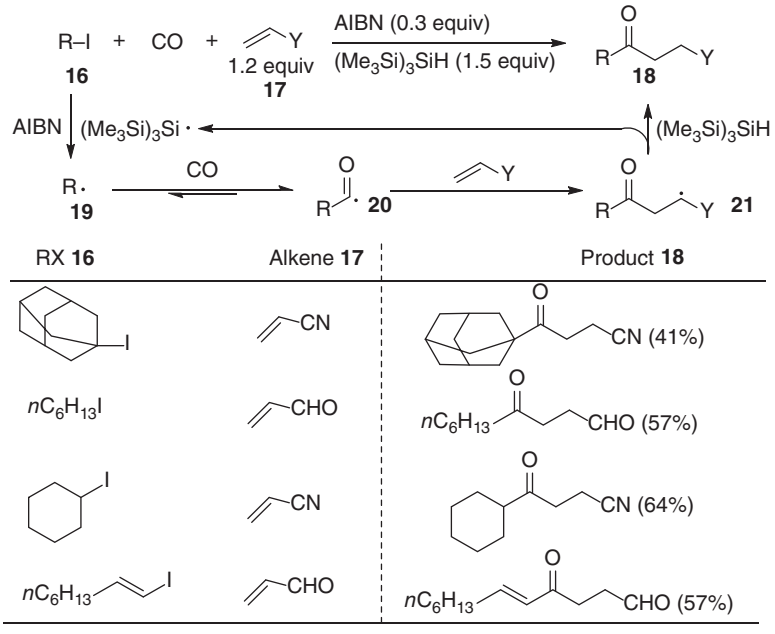

Scheme 11.4 Free-radical carbonylation of organoiodides, carbon monoxide, and alkenes. Source: Modified from Ryu et al. [12].

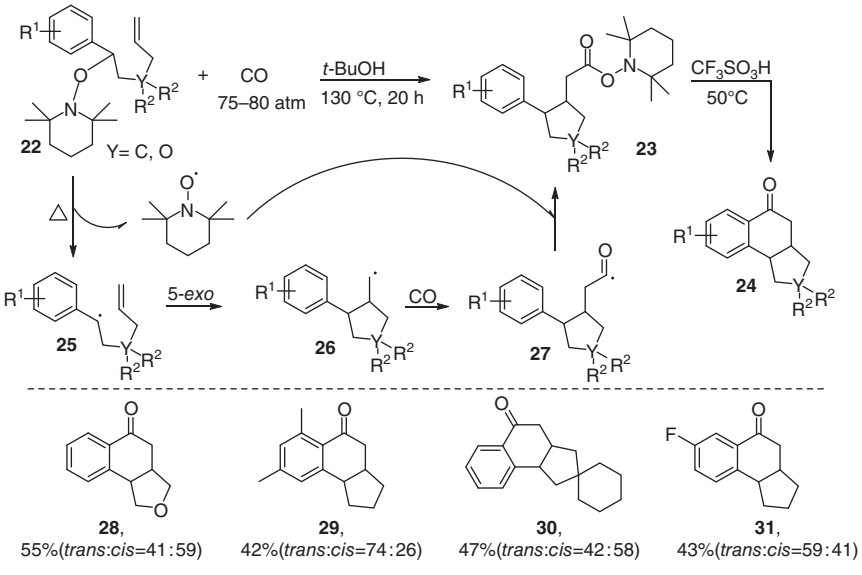

Scheme 11.5 CO-trapping reaction under thermolysis of alkoxyamines. Source: Modified from Uenoyama et al. [15].

light, thus inspiring potential applications and sustainability. In 2015, Gu et al. disclosed visible-light-induced radical carbonylation of aryldiazonium salts and (hetero)arenes to synthesize aryl ketones. It used a low-loading of an organic photosensitizer and low-energy visible light under base-free and transition-metal-free conditions under 70 atm of carbon monoxide (Scheme 11.6) [17]. In the proposed mechanism, aryl diazonium tetrafluoroborate **32** accepts one electron from the excited [Eosin Y*], which is generated by visible light excitation of [Eosin Y], to form Ar′· radical **35** and the oxidized dye radical cation [Eosin Y^+·]. Trapping of intermediate **35** by CO then gives aryoyl radical **36**. Further oxidation of **36** by [Eosin Y^+·] affords the aryl acylium cation **37**. Finally, electronic trapping of **37** by the arene generates the desired aryl ketone **34**.

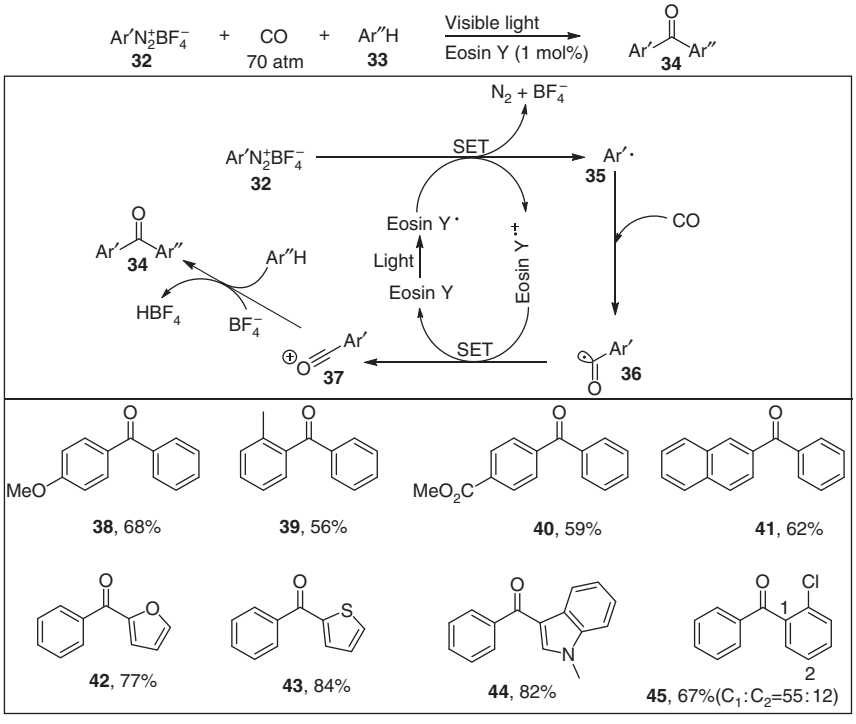

Scheme 11.6 Visible-light-induced radical carbonylation of aryldiazonium salts and (hetero)arenes. Source: Adapted from Gu et al and Zhang et al. [17].

Based on Gu's work that arylsulfonyl chlorides could generate aryl radicals **49** with the aid of the excited state [Eosin Y*] [18], the intermediate acyl radicals **50** could be readily and efficiently obtained from aryl radicals **49** in the presence of CO. Acyl radicals **50** would then be further oxidized to acylium ion **51** by the oxidized dye radical cation. When indoles were used as nucleophiles to attack the acylium ion intermediate **51**, indol-3-yl aryl ketones **48** were efficiently generated using visible-light-initiated photocatalysis under transition-metal-free, base-free, and acid-free conditions under carbon monoxide atmosphere (Scheme 11.7) [19].

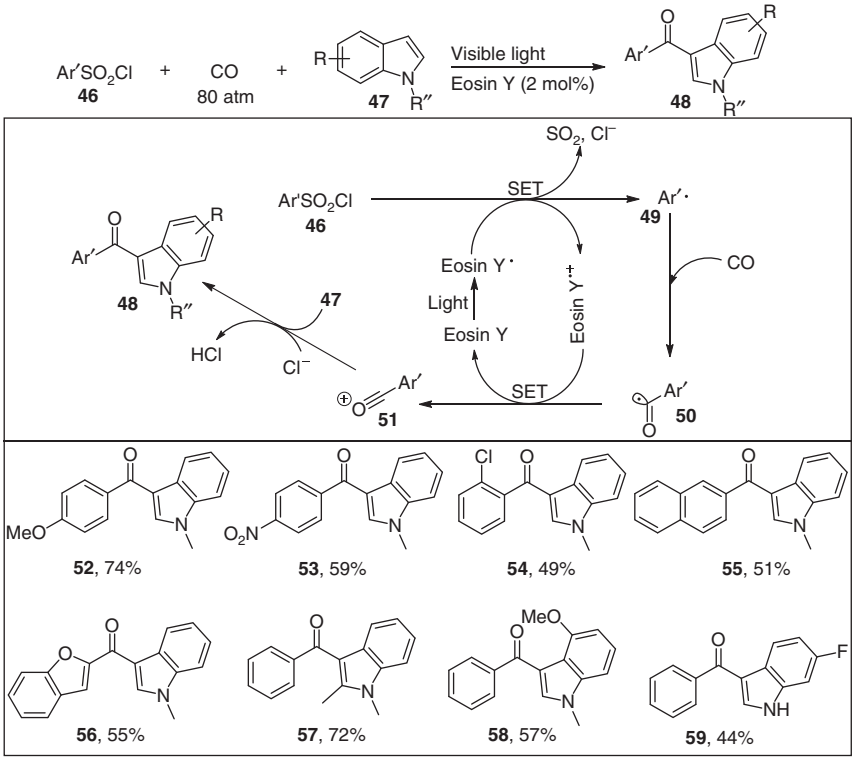

Scheme 11.7 Visible-light-induced radical carbonylation of arylsulfonyl chlorides and indoles. Source: Modified from Li et al. [19].

Generally, alkyl radical carbonylation derives from alkyl halides treated with a radical mediator, like tributyltin hydride [8a] or TTMSS [12]. Recently, Ryu and co-workers reported the first example of oxidative photocatalyzed carbonylation of alkyl radicals derived from bis(catecholato)silicates under mild visible-light photoredox conditions that require no traditional radical mediators (Scheme 11.8) [20]. Single-electron-transfer (SET) oxidation of the alkyl bis(catecholato)silicate **60** by the excited *4CzIPN leads to the reduced species $[4CzIPN]^{-}\cdot$ and generation of the alkyl radical **65** through homolytic cleavage of the C—Si bond of the silicate. Then, the alkyl radical **65** reacts with CO to form the acyl radical **66**, which adds to the acceptor alkene **61** to give the adduct radical **67**. The latter is reduced by [4CzIPN]—· to provide carbanionic intermediate **68** with photocatalyst regeneration. Finally, protonation of **68** by KH_2PO_4 yields the desired product **63**. In this transformation, primary, secondary, and tertiary alkyl radicals can be formed smoothly and undergo efficient carbonylation with carbon monoxide to afford various functionalized unsymmetrical ketones, including β,γ-unsaturated ketones (Scheme 11.8).

Alkylamines are widely present in natural products, pharmaceuticals, and materials and are attractive alkylating agents. The Wu group recently disclosed that alkylamines, after conversion into Katritzky salts **77**, can be utilized as alkyl

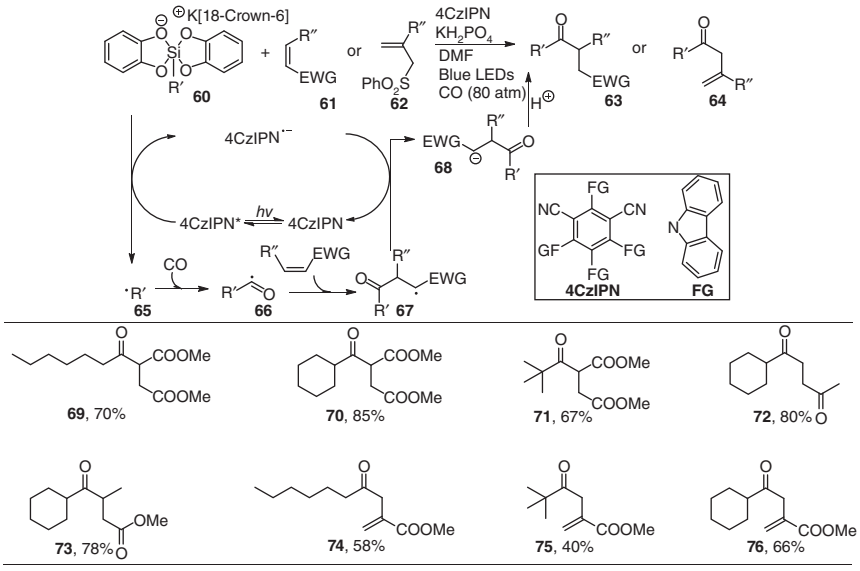

Scheme 11.8 Carbonylation of alkyl radicals derived from organosilicates. Source: Modified from Cartier et al. [20].

radical precursors to trigger a deaminative carbonylation reaction of alkylamines with styrenes **78** to give α,β-unsaturated ketones (Scheme 11.9) [21]. Mechanistically, the alkyl radical **80** generated from **77** under the assistance of DBU (1,8-diazabicyclo[5.4.0]undec-7-ene) was trapped by CO to produce acyl radical **81**, which further reacted with styrenes **78** to give a more stable radical species **82**. The latter was oxidized into cationic intermediate **83** by the previously produced DBU radical cation, with the regeneration of DBU. Finally, deprotonation of **83** gave the corresponding product **79** with a base's assistance (Scheme 11.9).

Although the above-mentioned transition-metal-free carbonylations represent powerful tools for synthesizing aldehydes and ketones, high CO pressures (more than 20 atm) are required to ensure efficient catalysis. To address this issue, our group uncovered an unprecedented transition metal-free trimodular reaction of aryl halides with potassium aryl trifluoroborates under atmospheric pressure of CO (Scheme 11.10) [22]. The method shows good generality. Various synthetically valuable functional groups were compatible in this transformation. The simple method was successfully applied for synthesizing the marketed drug Fenofibrate and a complex drug-like molecule. The key to this protocol's success is polyethylene glycol (PEG), often used as a good phase transfer agent. This property favors the gas–liquid–solid multiphase catalytic reaction. Additionally, PEG is a highly polar solvent that can cause strong solvation effects on polar molecules such as carbon monoxide to reduce mass transfer resistance. The dual properties probably enabled PEG to show excellent performance in the transformation.

Compared with aryl halides, carbonylative Suzuki couplings of alkyl or benzyl halides have been scarcely reported. This is because C(sp^3)-halides are less

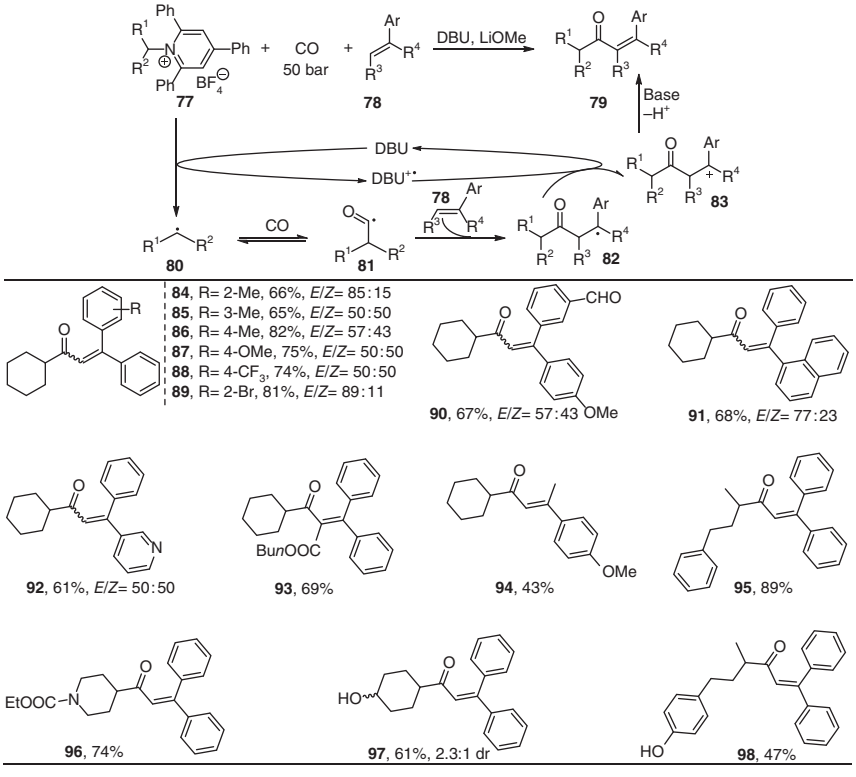

Scheme 11.9 Deaminative carbonylative coupling of alkylamines with styrenes.

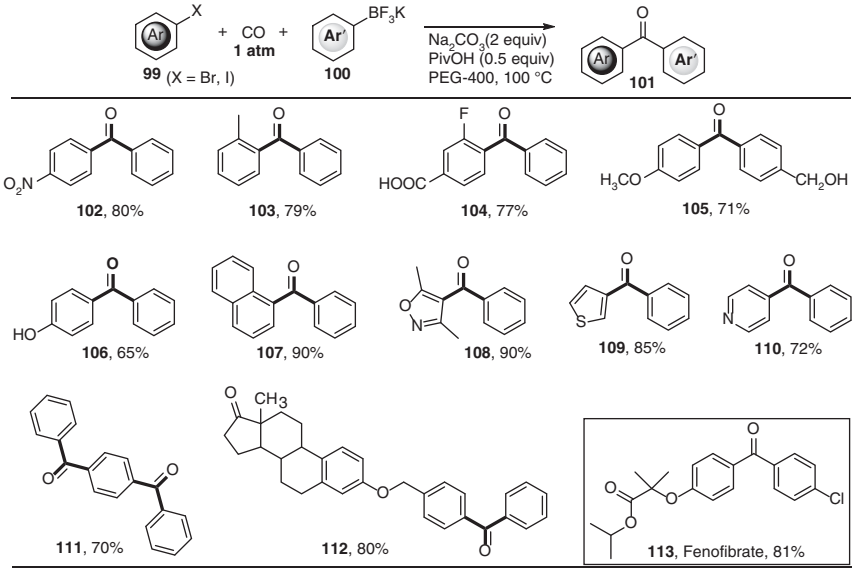

Scheme 11.10 Atmospheric-pressure carbonylative Suzuki reactions of aryl halides with potassium aryltrifluoroborates. Source: Modified from Jin et al. [22].

reactive toward oxidative addition to Pd^0 than their unsaturated analogs [23]. Pioneering works on carbonylative Suzuki couplings of benzyl halides were reported by Miyaura and co-workers and Beller and co-workers and required a palladium catalyst and/or high CO pressures [24]. Shortly after, we reported an alternative metal-free carbonylative Suzuki coupling of benzyl chlorides, which involved a hitherto unknown single-electron redox process driven by inorganic iodide (Scheme 11.11) [25]. The idea was based on the easy decomposition of benzyl iodide to reactive benzyl free-radical [26]. Considering the instability and high cost of benzyl iodides, we employed halogen exchange between sodium iodide (used in catalytic amount) and benzyl chloride to generate benzyl iodide *in situ*. Surprisingly, this transformation did not give the expected product 1,2-diarylethanone, but 1,2,3-triarylpropan-1-ones **116** instead, by a one-pot domino carbonylation–alkylation process. Notably, 1,2,3-triarylpropan-1-ones belong to a class of valuable synthetic building blocks to prepare triarylisoxazoles,

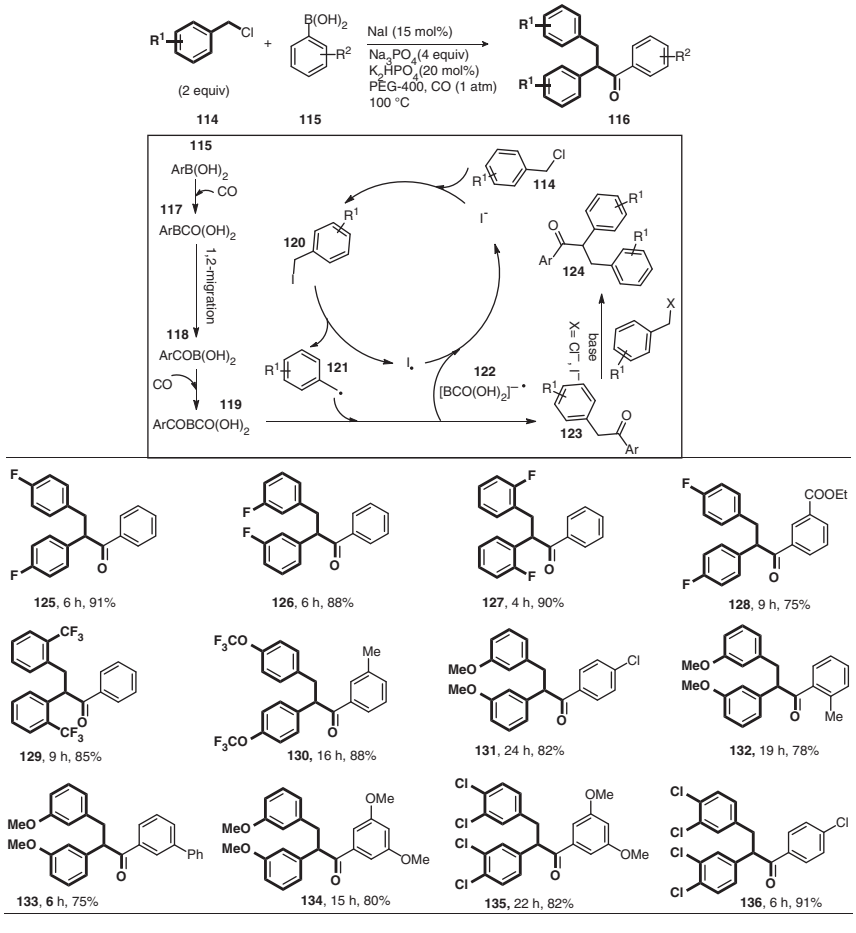

Scheme 11.11 Iodide-mediated domino carbonylation–benzylation of benzyl chlorides with arylboronic acids under carbon monoxide atmospheric pressure.

triarylpyrazoles, 2,3-diarylindenes, tri- and tetrasubstituted alkenes, and active pharmaceutical ingredients [27].

The process was mechanistically initiated by the reaction of aryl boronic acid **115** with carbon monoxide to give intermediate **117**, followed by carbonyl 1,2-migration insertion to give the key intermediate **118** [28]. The latter was further carbonylated in the presence of carbon monoxide to give intermediate **119** [28], which was intercepted by an active benzyl free radical (generated *in situ* from the decomposition of a benzyl iodide obtained from benzyl chloride and NaI) to generate 1,2-diarylethanone intermediate **123** and radical anion $[BCO(OH)_2]^-\cdot$ **122**. Finally, **123** underwent benzylation with the assistance of a base to give **124**. Simultaneously, **122** reacted with iodine-free radical through SET to regenerate the iodide ion, thus completing a radical chain (Scheme 11.11).

Organotrifluoroborates are known to be unreactive toward important classes of reagents (e.g. oxidants, bases, and nucleophiles) commonly utilized in organic synthesis. Accordingly, reports on the carbonylation of these species to give the corresponding carbonyl compounds are very limited [22, 24b, 29]. To our knowledge, only one example of carbonylative Suzuki reaction of $C(sp^3)$ halides with potassium aryltrifluoroborates has been reported [24b], albeit air-sensitive palladium catalyst and high pressure of CO gas were required. Based on our previous work [25], we further demonstrated a transition-metal-free, iodide-catalyzed radical carbonylation–benzylation of benzyl chlorides with potassium aryltrifluoroborates under atmospheric pressure of CO. This provided a wide range of 1,2,3-triarylpropan-1-one derivatives in high yields (Scheme 11.12) [30].

Carbon monoxide is a cheap, abundant, readily available, and atom-economical C1 source. However, its properties may limit its wide applications because carbon monoxide is an odorless, toxic, colorless, and flammable gas, difficult to handle and typically delivered in pressurized cylinders. Therefore, using a CO surrogate as the

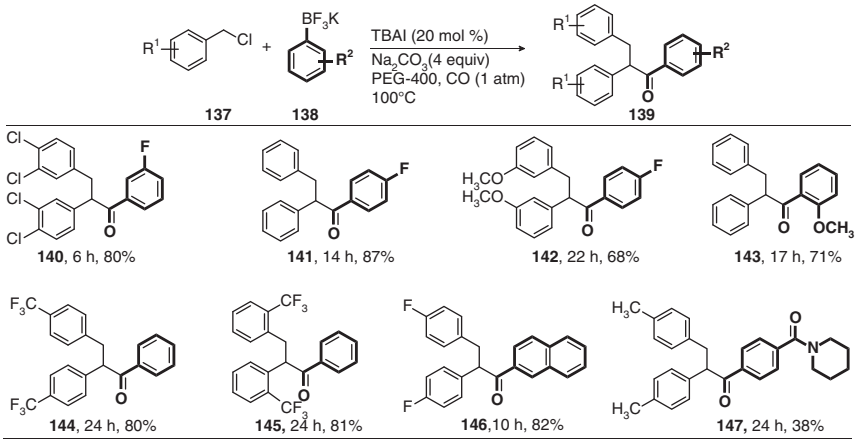

Scheme 11.12 Iodide-mediated domino carbonylation–benzylation of benzyl chlorides with arylboronic acids under carbon monoxide ambient pressure. Source: Modified from Han et al. [30].

carbonyl source may be of interest [31]. Our group recently reported an unprecedented, transition-metal-free carbonylative Suzuki reaction of aryl halides with arylboronic acids utilizing stoichiometric $CHCl_3$ as the CO precursor. This general and robust protocol was suitable for the synthesis of drugs such as Fenofibric acid **167** (a triglyceride and cholesterol regulator) and naphthyl phenstatin **168** (a tubulin polymerization and tumor cell growth inhibitor), and a ^{13}C-labeled active molecule **169** (Scheme 11.13a) [32]. A radical probe 1-(allyloxy)-2-iodobenzene was subjected to the standard reaction conditions. The reaction only afforded a cyclization product,

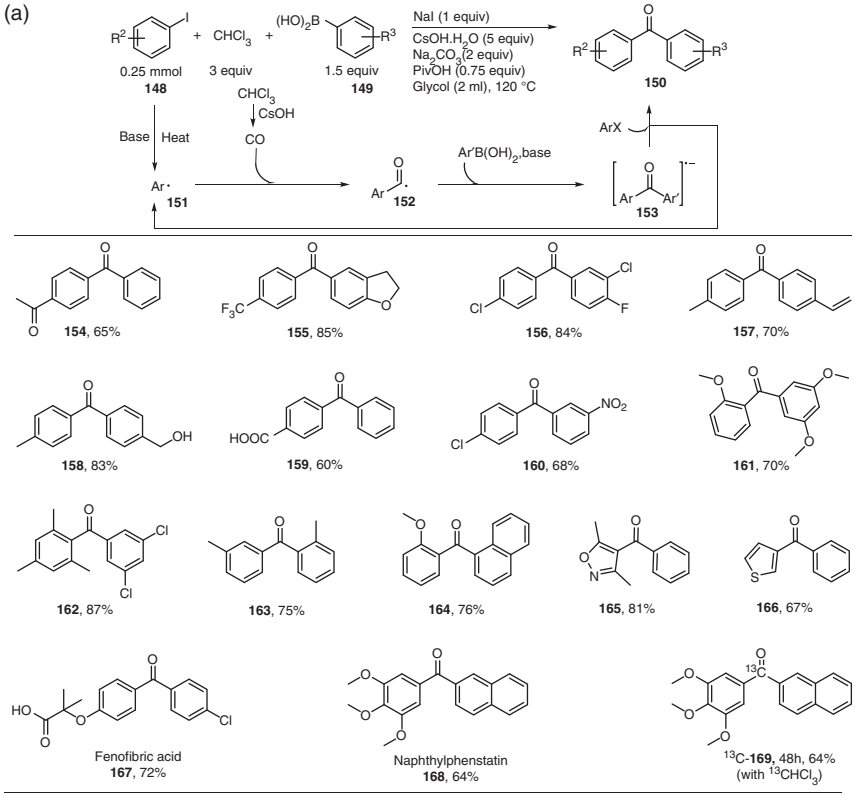

(b)

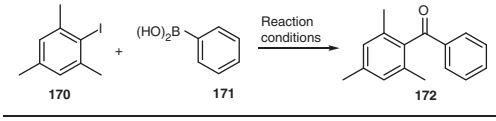

Entry	Reaction system	Ref.	Yield (%)
1	$CHCl_3$	*This work*	***94***
2	$Pd_2(dba)_3$/CO	37	72
3	$Pd(OAc)_2/CHCl_3$	38	50
4	$FeCl_2/CHCl_3$	39	6

Scheme 11.13 (a) Carbonylative Suzuki couplings of aryl halides with arylboronic acid using stoichiometric $CHCl_3$ as the carbonyl source. (b) Comparison of reaction conditions systems. Source: Modified from Xu et al. [32].

3-methyl-2,3-dihydrobenzofuran based on GC/MS analysis [33]. This implied that an aryl radical intermediate is present in the transition-metal-free carbonylation process. Hence, a plausible mechanism for the transformation involving aryl radical intermediate is proposed. Initially, aryl halide thermally dissociates with the assistance of a base [34] to give an aryl radical, which further reacts with CO (*in situ*-generated from chloroform and $CsOH{\cdot}H_2O$) [35] to provide an acyl radical intermediate. Subsequently, the acyl radical reacts with arylboronic acid under the assistance of a base to afford a biaryl ketone radical anion [36]. Then, SET from the biaryl ketone radical anion to an aryl halide gives the desired biarylketone product and regenerates a reactive aryl radical, thus completing a catalytic cycle [36]. The comparison between the transition-metal free method with previously reported transition-metal-catalyzed carbonylative Suzuki reactions [37–39] was made by performing the carbonylative cross-coupling of **170** with **171** and further highlighted the advantage of the transition-metal free protocol (Scheme 11.13b).

N-formylsaccharin **174** works as an easily accessible and highly reactive crystalline CO surrogate [40]. Bhanage and co-workers reported the first carbonylative Suzuki cross-coupling using *N*-formylsaccharin as a CO surrogate under palladium catalysis [41]. Inspired by our work mentioned earlier on transition-metal free carbonylative Suzuki coupling utilizing stoichiometric $CHCl_3$ as the CO precursor, we further disclosed a practical and convenient transition metal-free carbonylative Suzuki reaction of aryl iodide with arylboronic acid using *N*-formylsaccharin as CO surrogate. This method was demonstrated by synthesizing Fenofibrate (a triglyceride and cholesterol regulator), which was readily prepared in 69% yield under normal reaction conditions (Scheme 11.14).

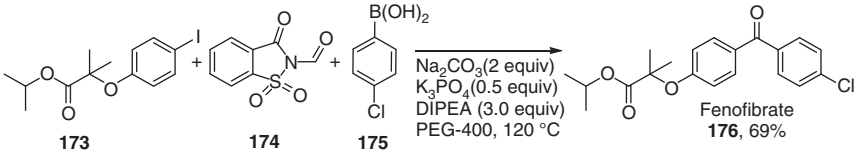

Scheme 11.14 Synthesis of Fenofibrate by transition metal-free carbonylative Suzuki reaction with *N*-formylsaccharin **174** as the carbonyl source.

11.3 Transition-Metal-Free Carbonylation for the Synthesis of Esters and Lactones

The Ryu group reported a seminal example of radical carbonylation for the synthesis of esters. A double CO-trapping reaction by pent-4-enyl radicals **179** derived from pent-4-enyl iodides **177** afforded the bicyclic γ-lactone **178** under 90 atm of CO using a combination of AIBN/Bu_3GeH-initiated catalytic cycle (Scheme 11.15) [11]. The pent-4-enyl radical **179** was initially trapped by CO to form hex-5-enoyl radical **180**. The subsequent 5-*exo-trig* cyclization of radical **180** generated 3-oxocyclopentyl

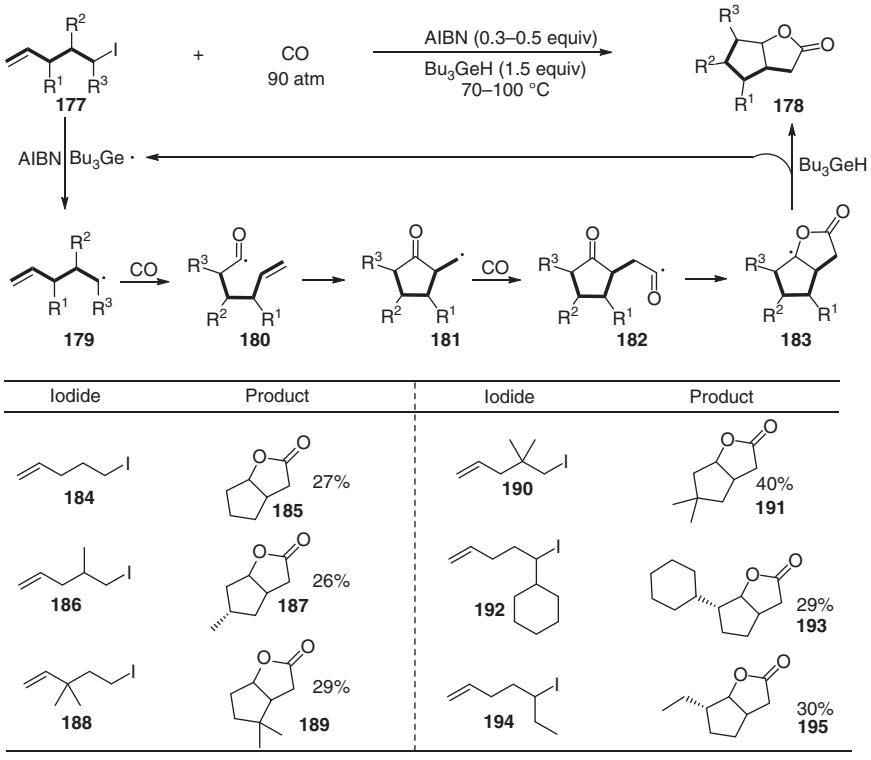

Scheme 11.15 Radical-mediated double carbonylation of alk-4-enyl iodides for the synthesis of bicyclic γ-lactones. Source: Modified from Tsunoi et al. [11].

carbinyl radical **181** and, under high CO concentrations, **181** was trapped by a second molecule of CO to yield acyl radical **182**. Finally, the acyl radical **182** cyclized to afford **183**, which abstracted a hydrogen atom to give the bicyclic γ-lactone product **178** with the regeneration of the tributyltin radical.

Subsequently, the same group reported an efficient method for the synthesis of carboxylic esters from a combination of alkyl iodides, alcohols, and CO (20–55 atm), carried out with photoirradiation in the absence of a metal catalyst (Scheme 11.16) [42]. The transformation involved an iodine transfer reaction, which could be driven by a subsequent ionic reaction of the acyl iodide with alcohol to furnish the ester (Scheme 11.16).

Furthermore, Ryu and coworkers reported the intramolecular variation of an atom transfer carbonylation starting with ω-hydroxyalkyl iodides. This represented a novel method for synthesizing five- to seven-membered ring lactones (Scheme 11.17) [43]. The reaction proceeded via a hybrid radical/ionic mechanism in which the intramolecular alcoholysis of a ω-hydroxyacyl iodide, arising from atom transfer carbonylation, afforded the lactone.

In 2012, the Lei group developed the first transition metal-free alkoxycarbonylation of aryl halides **216** for accessing *t*-butyl benzoates **217**. Heteroaryl iodides could also be carbonylated to provide the desired heterocyclic esters (**225** and

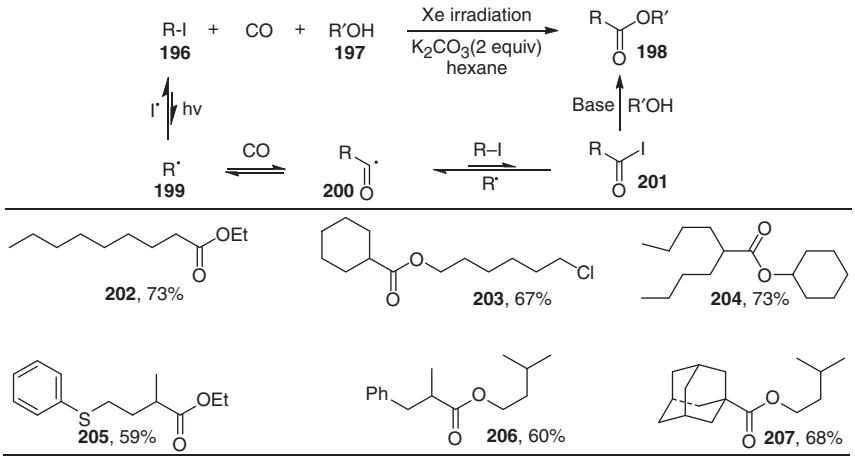

Scheme 11.16 Ester synthesis from alkyl iodides, carbon monoxide, and alcohols. Source: Modified from Nagahara et al. [42].

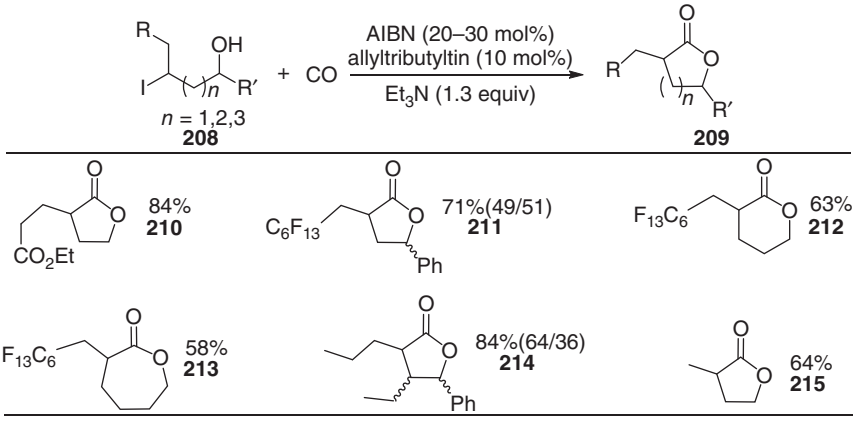

Scheme 11.17 Five- to seven-membered ring lactones synthesis from ω-hydroxyalkyl iodides and carbon monoxide. Source: Modified from Kreimerman et al. [43].

228) (Scheme 11.18) [36]. Electron paramagnetic resonance (EPR) experiments were run to reveal the participation of radicals in the reaction system. Thus, an aryl halide radical anion was generated from Ar-X **218** by SET in the presence of 1,10-phenanthroline/KO*t*Bu and converted into an aryl radical **220** upon elimination of X^-. The aryl radical **220** reacts with CO to afford an acyl radical **221**, which is attacked by tBuO$^-$ to give the ester radical anion **222**. Another SET from the ester radical anion to Ar-X **218** gives product and regenerates the aryl halide radical anion **219**. The reaction is terminated by the formation of product from the ester radical anion **222** by SET with 1,10-phenanthroline/KO*t*Bu.

Fukuoka et al. developed a novel transition metal catalyst-free and radical initiator/additive-free aryloxycarbonylation of aryl iodides to yield aryl esters (Scheme 11.19) [44], to be compared with the above-mentioned transition metal

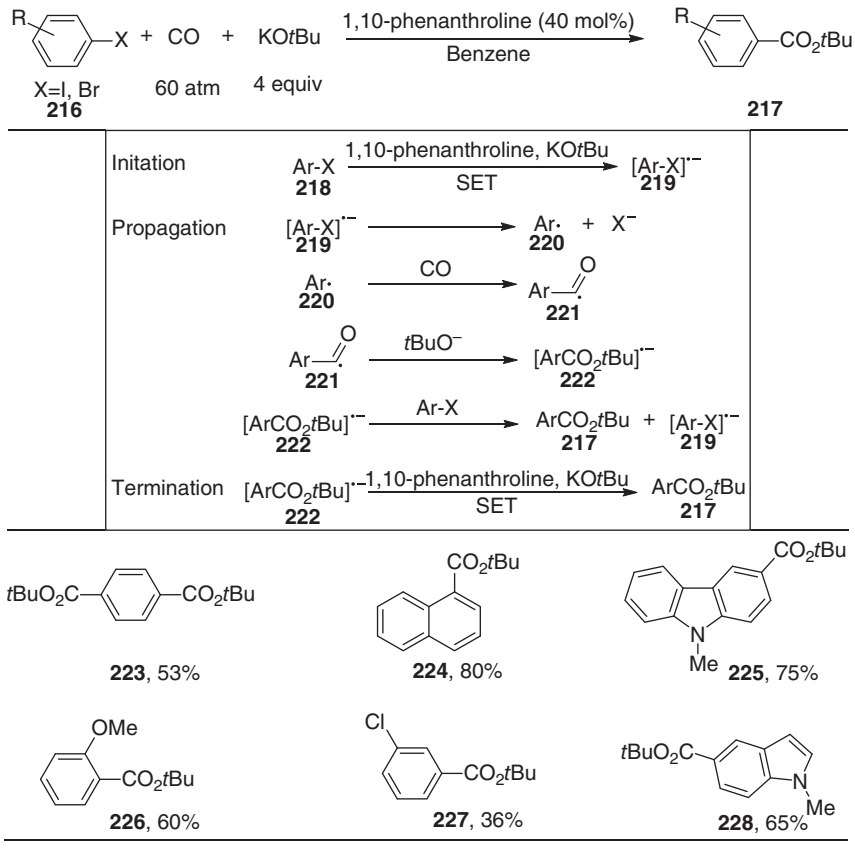

Scheme 11.18 Transition metal-free alkoxycarbonylation of aryl halides. Source: Modified from Zhang et al. [36].

catalyst-free *t*-butoxycarbonylation of aryl halides that required additives such as *t*-BuOK and 1,10-phenanthroline. Aryl iodide **229** reacted with CO and alkali metal aryloxide **230** (M = Li, Na, K) at 250–260 °C to give aryl ester **231** in 95–99% yields. Because of the high yields and no use of any reagents other than the substrates, the desired products could be readily obtained by a simple separation step (e.g. filtration) from the by-produced alkali metal iodides (MIs). Mechanistically, an aryl radical **232** generated by the thermal dissociation of Ar–I **229** reacts with CO to give an acyl radical **233**, which reacts with M–Nu **230** via nucleophilic addition to give an anionic radical intermediate **234**. The desired product **231** is formed from **234** by SET to the aryl iodide **229**, with the aryl radical **232** and iodine anion regeneration. Thus, the electron catalytic cycle and the radical chain reaction would complete, in which formally the electron acts as the catalyst. The left M^+ and iodine anion form MI (Scheme 11.19) [44].

Visible light-induced photoredox catalysis is a benign and useful tool in organic synthesis and has attracted great interest in carbonylation reactions. In 2015, Xiao and co-workers presented visible-light-catalyzed radical alkoxycarbonylation

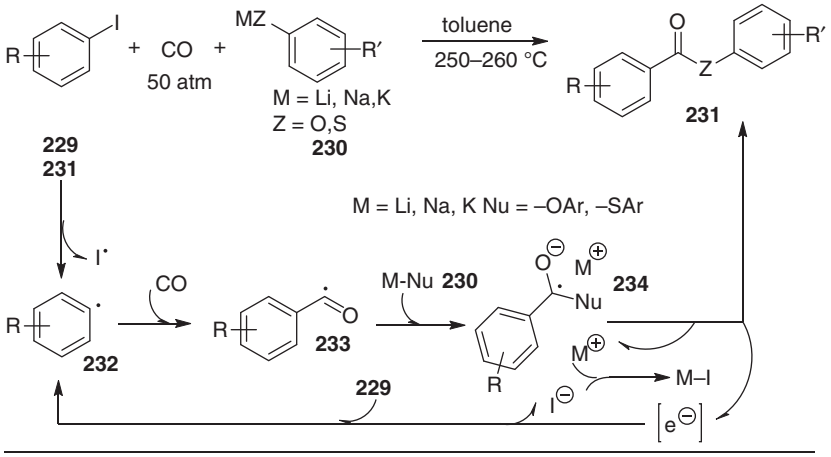

Iodide	Ar-OM	Product
 229a	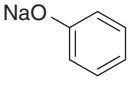 230a	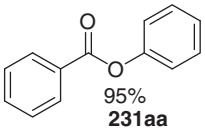 95% 231aa
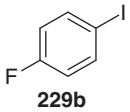 229b	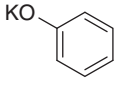 230a	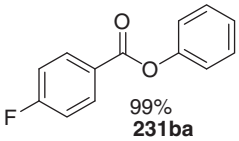 99% 231ba
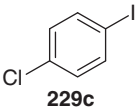 229c	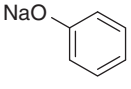 230a	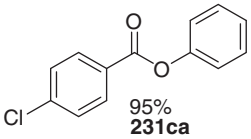 95% 231ca
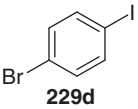 229d	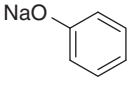 230a	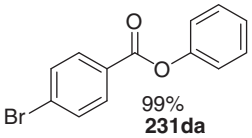 99% 231da
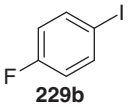 229b	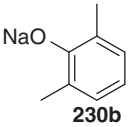 230b	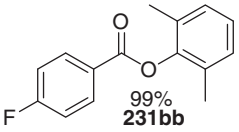 99% 231bb
 229a	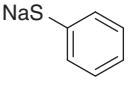 230c	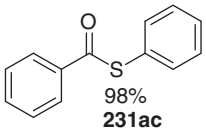 98% 231ac

Scheme 11.19 Transition metal-free and radical initiator-free alkoxycarbonylation of aryl iodides. Source: Modified from Fukuoka [44].

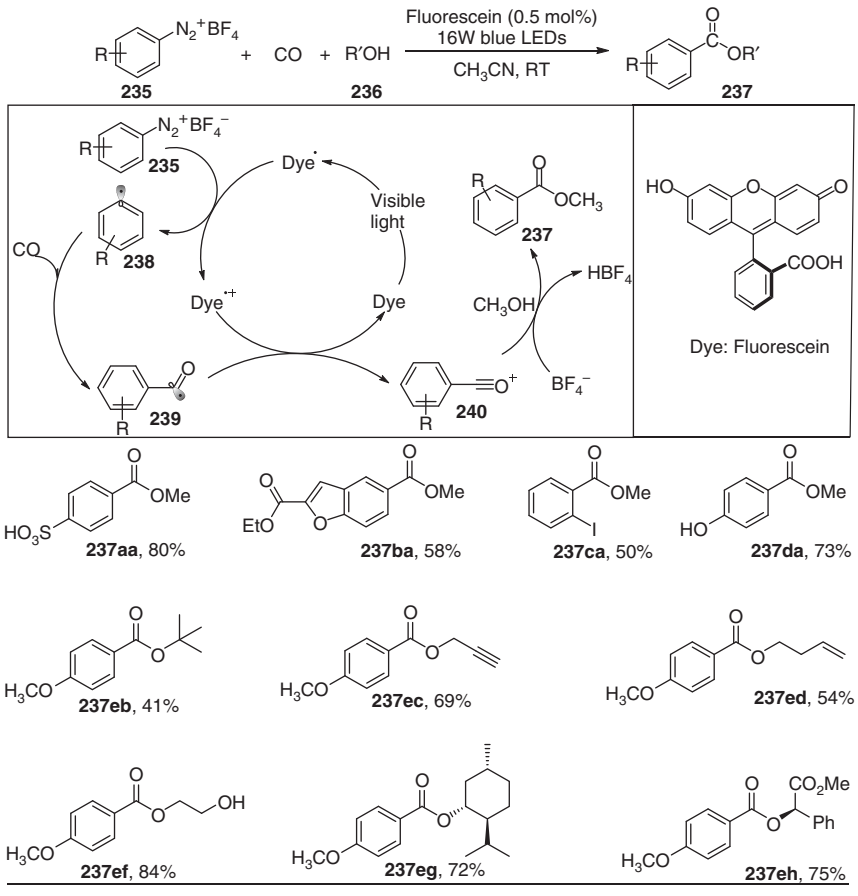

Scheme 11.20 Radical alkoxycarbonylation of aryldiazonium salts through visible-light photoredox catalysis. Source: Modified from Guo et al. [45].

photoredox reaction using aryldiazonium salt as a robust aryl radical source and low loading of an organic dye as a photocatalyst (Scheme 11.20) [45]. A wide range of aliphatic alcohols, including steric bulky alcohols such as isopropanol, cyclohexanol, and even *t*-butanol, could all be applied in this reaction. Notably, natural chiral alcohols such as (−)-menthol and their derivatives such as methyl D-(−)-mandelate and *N*-benzoyl L-(+)-prolinol resulted in the corresponding products in moderate-to-good yields with unchanged enantiopurities.

A plausible mechanism was also proposed. Initially, an aryl radical **238** was generated by single-electron reduction of the aryldiazonium salt **235** with the excited state of the Dye photocatalyst, along with an oxidized Dye radical cation (Dye·$^+$). Under high CO pressure (80 bar), **238** would be trapped by CO to yield acyl radical **239**, followed by Dye·$^+$ oxidation to provide acylium intermediate **240**, thus completing the photocatalytic cycle. Finally, nucleophilic attack of the alcohol to **240** generated the product (Scheme 11.20) [45].

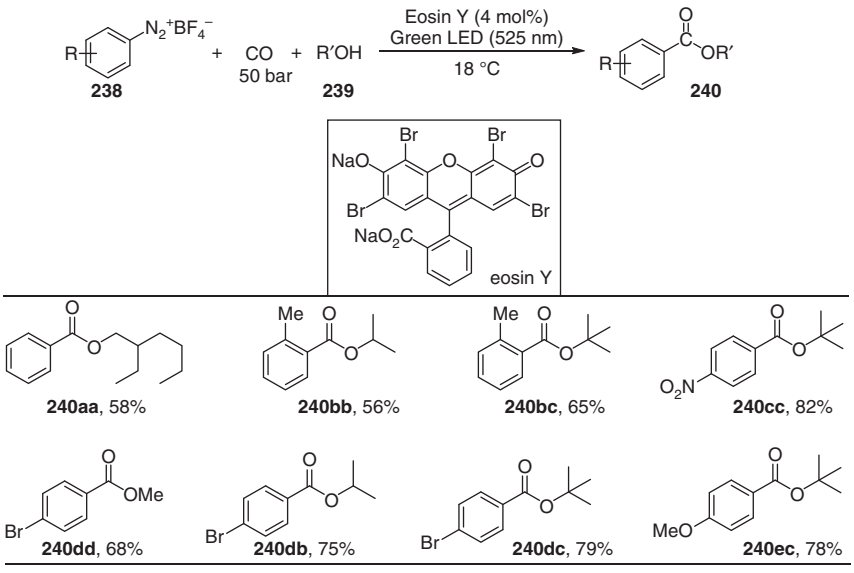

Scheme 11.21 Visible-light photoredox-catalyzed radical alkoxycarbonylation of aryldiazonium tetrafluoroborates. Source: Modified from Majek and Wangelin [46].

Meanwhile, Majek and Wangelin independently reported visible-light photoredox-catalyzed radical alkoxycarbonylation of aryldiazonium tetrafluoroborate used as an organic dye eosin Y photocatalyst (Scheme 11.21) [46]. A broad range of different substituted benzoates was prepared in good yields. Notably, *t*-butyl esters could also be produced, which are difficult to prepare by transition-metal-catalyzed carbonylation because of their steric hindrance. Mechanistic studies supported the sequential involvement of SET reduction, carbonylation, and back electron transfer to give aroylium cations, which underwent rapid addition to alcohols, similar to what was reported in Ref. [45] (Scheme 11.20).

Inspired by the formation of aryl radicals from arenediazonium salts with weak bases under ambient conditions [47], the group of Wangelin further demonstrated the HCO_2Na-mediated alkoxycarbonylation of arenediazonium salts with carbon monoxide and alcohols. This process did not require radical initiators, metal catalysts, inert conditions, or irradiation equipment (Scheme 11.22) [34]. Key mechanistic studies were conducted that supported the involvement of aryl and acyl radicals as intermediates (Scheme 11.22) [34]. Later on, the Wu group reported a phosphite-catalyzed alkoxycarbonylation of aryl diazonium salts. In the presence of tris(2,4-di-*t*-butylphenyl)phosphite (10 mol%) with no other bases or additives and under CO pressure (60 bar), the desired benzoates were produced in moderate to good yields at room temperature [48].

Although radical alkoxycarbonylation can afford carbonyl derivatives in the absence of transition-metal catalysts, the vast majority of reports involve organic halides/pseudohalides. It is an urgent need to develop radical oxidative alkoxycarbonylation of C—H bonds, which is regarded as an atom-economic and

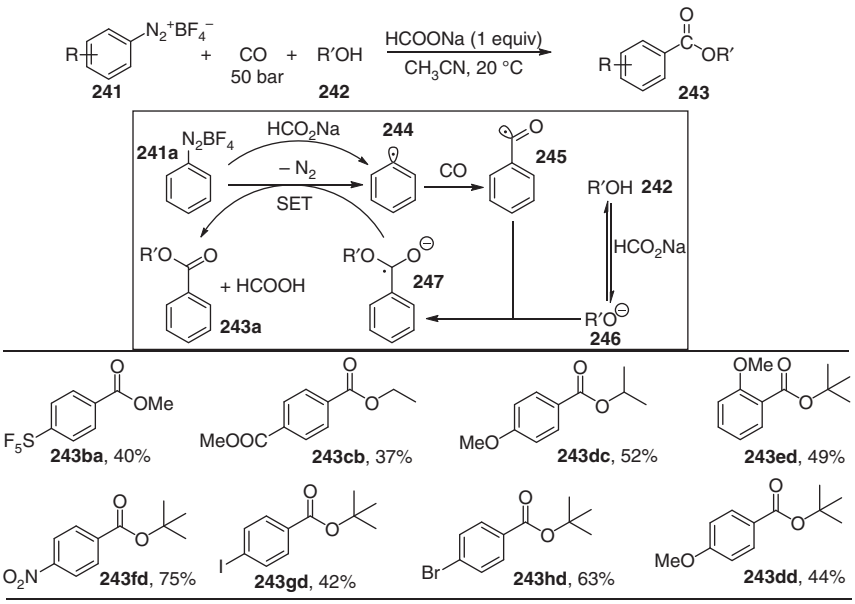

Scheme 11.22 HCOONa-mediated radical alkoxycarbonylation of aryldiazonium tetrafluoroborate. Source: Modified from Koziakov and Wangelin [34].

step-economic protocol. In this context, the Lei group disclosed the first example of an oxidant-induced alkane C—H bond activation and alkoxycarbonylation using alcohols as nucleophiles (Scheme 11.23) [49]. A series of esters (**250**) can be obtained in the absence of any metal and additives. Primary, secondary, and tertiary alcohols all showed good reaction efficiencies (**250aa**–**250ai**). Also, various functional groups such as keto, alkoxy, chloro, and alkenyl could be transformed into the corresponding esters smoothly. Natural products such as L-menthol, dehydroepiandrosterone, and stigmasterol, gave the corresponding products moderate-to-good yields with unchanged enantiopurities. A plausible reaction mechanism was also proposed (Scheme 11.23). Firstly, the *t*-butoxyl radical generated from the homolytic cleavage of DTBP abstracted a hydrogen atom from the alkane to afford the alkyl radical (**252**). Subsequently, CO was added to the alkyl radical **252** to form an acyl radical (**254**). Then, the acyl radical **254** reacted with the nucleophile by losing a proton to give a radical anion species (**255**). Ultimately, DTBP abstracted an electron from the radical anion (**255**) to provide the desired product **250** (Scheme 11.23) [49].

In 2005, Ryu et al. reported 1,1′-azobis(cyclohexanecarbonitrile) (V-40) as an initiator to mediate the carbonylation of alkyl allyl sulfones **256** and phenyl benzenethiosulfonate **257** under CO pressure (95 atm) to yield thioesters **258** (Scheme 11.24) [50]. A series of alkyl allyl sulfones **256** could afford the corresponding products with moderate to excellent yields. Long-chain alkanes, polycycloalkanes, and oxacycloalkanes were good substrates, and ester and alkynyl groups can also be well compatible in the system. The author proposed a possible

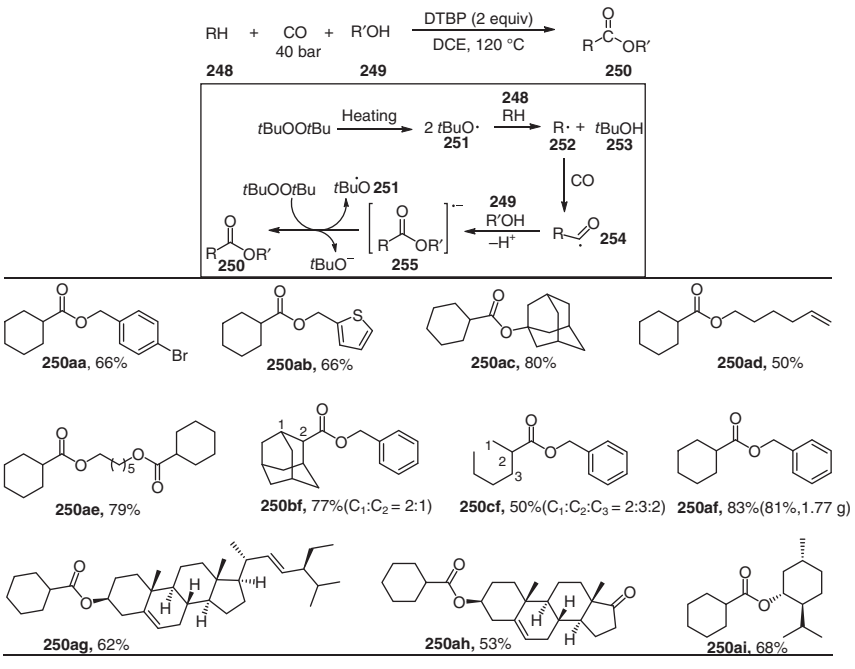

Scheme 11.23 Oxidative alkoxycarbonylation of alkanes. Source: Modified from Lu et al. [49].

radical mechanism: phenyl benzenethiosulfonate **257** reacts with 1,1′-azobis (cyclohexanecarbonitrile) to generate phenylsulfonyl radical **259**, which is substituted with alkyl allyl sulfone **256** to generate alkyl sulfonyl radical **261**. Subsequently, the alkyl sulfonyl radical **261** is decomposed with elimintaion of sulfur dioxide to obtain alkyl radical **262**, which then reacts with carbon monoxide to generate acyl radical **263**. The latter finally reacts with phenyl benzenethiosulfonate **257** to produce the thioester derivative **258** (Scheme 11.24).

Considering that the reaction also afforded allyl aryl sulfone as a side-product, the group developed a new radical reaction type, in which the substrate could act not only as a radical precursor but also as a radical acceptor [51]. This idea was based on the previously known thermal desulfonylation of alkylsulfonyl radicals to liberate alkyl radicals along with sulfur dioxide [52]. A plausible rationale for the direct conversion of alkylsulfonyl derivative **265** into alkylcarbonyl derivative **269** is shown in Scheme 11.25. The reaction is initiated by the reaction of **265** with a radical initiator to generate alkylsulfonyl radical **266**. The success of the present approach depends critically on the preferential formation of acyl radical **267** through radical carbonylation rather than direct reaction with **265** to afford byproduct **268**. This, in its turn, depends on the nature of alkyl radicals. In this context, alkylthiosulfonates, alkylsulfonyl cyanides, and alkylsulfonyl oxime ethers could be effectively converted into the corresponding alkyl thioesters, acyl cyanides, and acylated oxime ethers **269**.

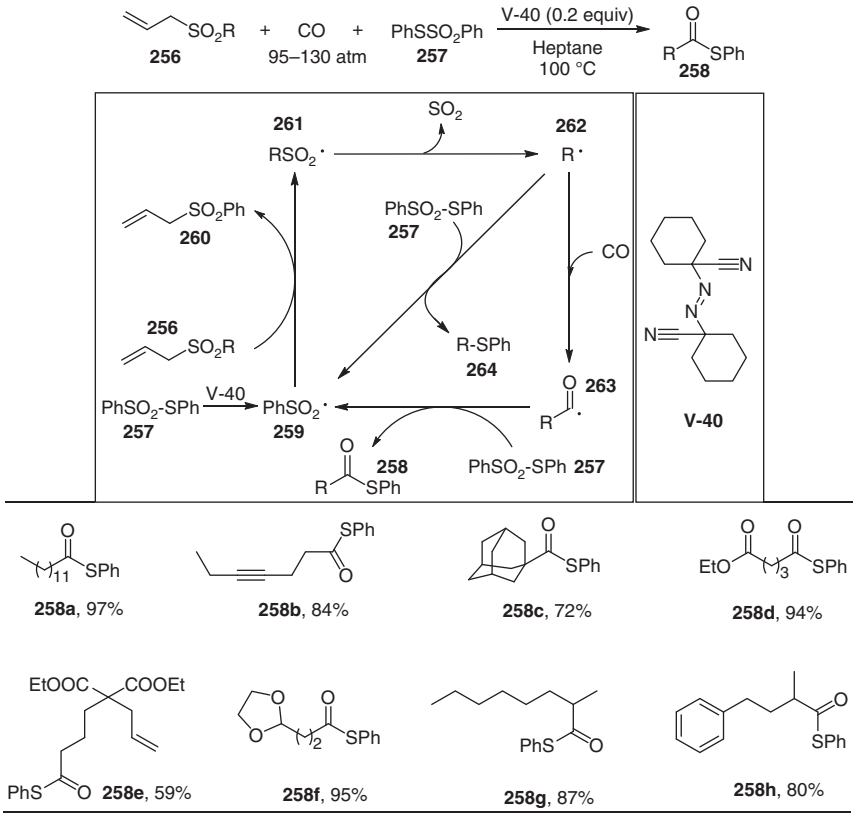

Scheme 11.24 Carbonylation of alkyl allyl sulfones with phenyl benzenethiosulfonate. Source: Modified from Kim et al. [50].

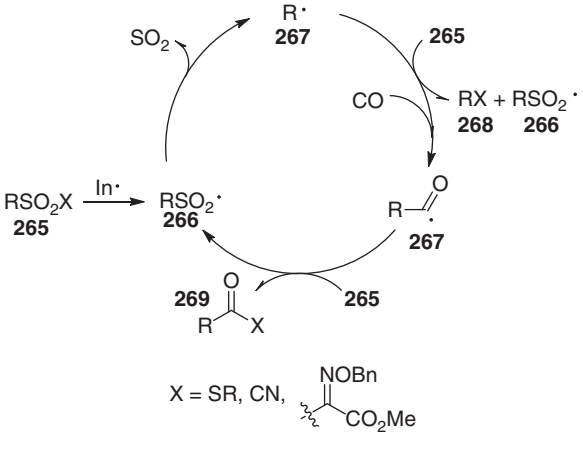

Scheme 11.25 Carbonylation of alkyl allyl sulfones with phenyl benzenethiosulfonate.

11.4 Transition-Metal-Free Carbonylation for the Synthesis of Amides

In 1998, the Ryu group reported that, under pressure of CO (20–25 atm), AIBN and allyltributyltin could be employed for realizing the aminocarbonylation of alkyl iodides with primary and secondary amines to form amides for the first time in the absence of a transition metal catalyst (Scheme 11.26) [53]. In general, carbonylation of tertiary radicals is relatively inefficient compared with secondary and primary alkyl radicals, due to the facile reverse reaction [54]. However, the unique radical/ionic cooperation driving the carbonylation/decarbonylation equilibrium in the forward direction provided an advantage for the carbonylation of tertiary radicals in this case. The corresponding products could be obtained with yields up to 97%. The authors proposed the following possible mechanism. Alkyl iodide **270** generates the alkyl radical **273** with the assistance of the radical initiator. Then the alkyl radical **273** is trapped by carbon monoxide to form an acyl radical **274**, which reacts with alkyl iodide **270** to form an acyl iodide intermediate **274**, attacked by the amine to give amides **272** (Scheme 11.26).

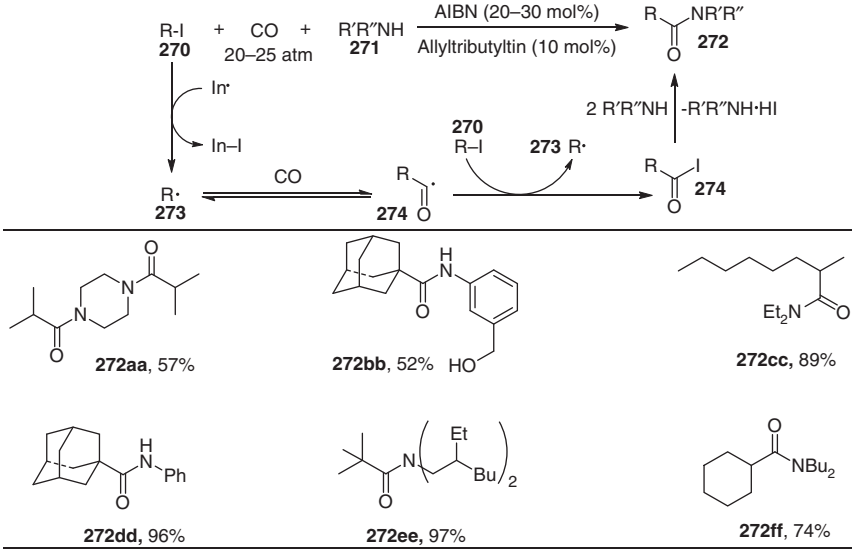

Scheme 11.26 Carbonylation of alkyl iodides with primary and secondary amines. Source: Modified from Ryu et al. [53].

Since aryl radicals add to CO to form the corresponding aromatic acyl radicals [55], and acyl radicals can be trapped by amines [56], the Ryu group reported that aryl iodides could react with amines to form amides under xenon lamp irradiation and CO pressure (70 atm) (Scheme 11.27) [57]. This methodology showed broad functional-group tolerance, including that of heteroaromatic amides. A possible reaction mechanism is as follows. Light-induced decomposition of an aryl iodide

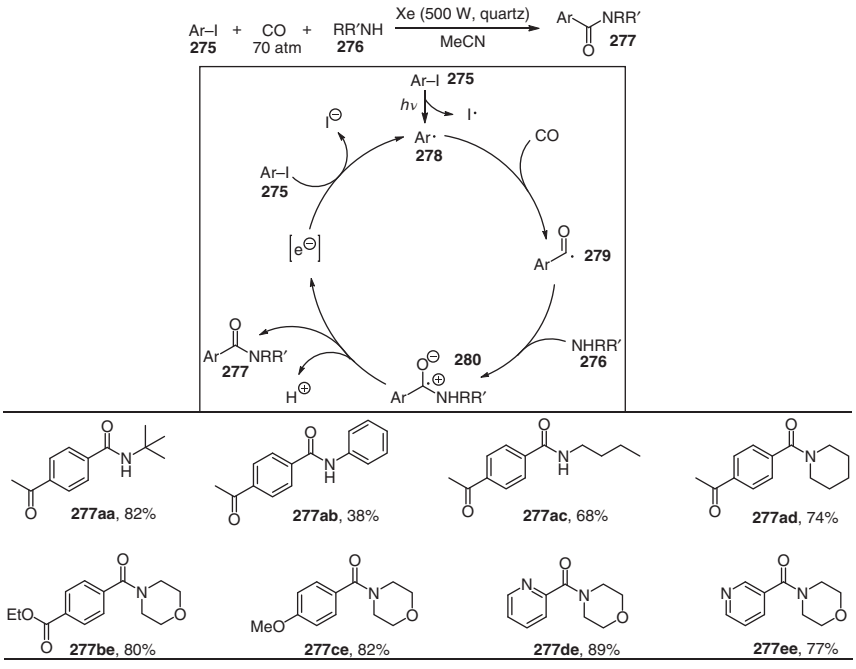

Scheme 11.27 Carbonylation of aryl iodides with primary and secondary amines. Source: Modified from Kawamoto et al. [57].

275 produces an aryl radical **278**, followed by a carbon monoxide reaction to give acyl radical **279**. Then, **279** is attacked by nucleophilic amine **276** to produce the zwitterionic radical intermediate **280**. Electron transfer to the aryl iodide **275** would give aryl radical **278**, thus completing the cycle and the radical chain reaction, where formally the electron acts as the catalyst (Scheme 11.27).

Recently, the Lei group demonstrated that under CO pressure (60 bar), DTBP-induced alkane C—H bond carbonylation employing amides **282** as nucleophiles produced a series of imides **283** (Scheme 11.28) [49]. The reaction has good compatibility with an amino acid derivative and was proposed to proceed through a radical process: DTBP was decomposed by heat to generate a *t*-butyl oxygen radical **284**, which abstracted a hydrogen atom from alkane to form an alkyl radical **285**. Subsequently, the alkyl radical **285** reacted with carbon monoxide to obtain an acyl radical **287**, followed by coupling with a nucleophilic amide to obtain an ionic radical intermediate **288**. The latter underwent SET with DTBP to give the imide product **283** (Scheme 11.28).

11.5 Transition-Metal-Free Carbonylation for the Synthesis of Acids and Anhydrides

As early as 1992, Sen and Lin reported the oxidative carbonylation of methane and ethane to the corresponding acetic and propanoic acids using $K_2S_2O_8$

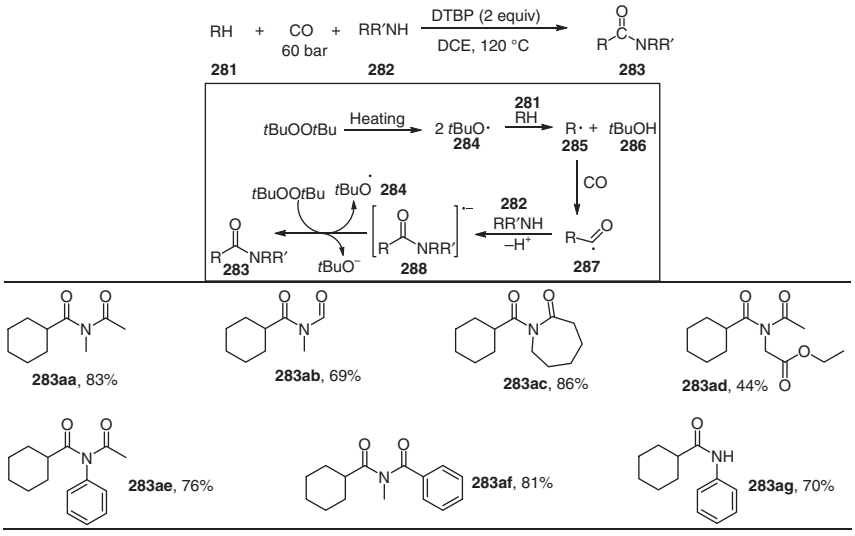

Scheme 11.28 Carbonylation of aryl iodides with primary and secondary amines. Source: Modified from Lu et al. [49].

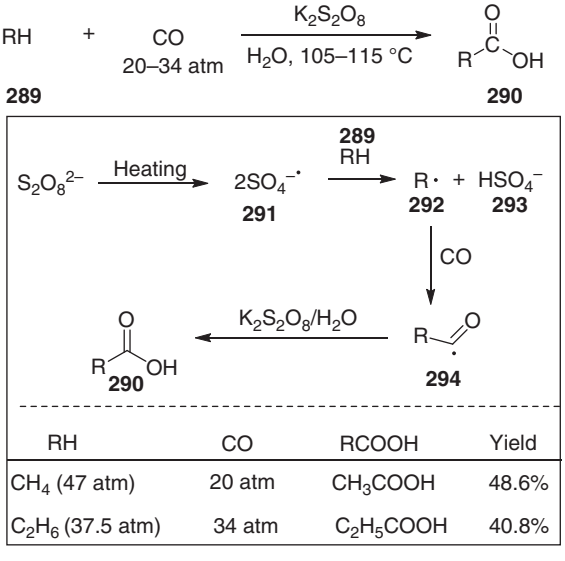

RH	CO	RCOOH	Yield
CH_4 (47 atm)	20 atm	CH_3COOH	48.6%
C_2H_6 (37.5 atm)	34 atm	C_2H_5COOH	40.8%

Scheme 11.29 Oxidative carbonylation of methane and ethane. Source: Modified from Lin et al. [58].

(Scheme 11.29) [58]. In an aqueous medium, at 105–115 °C, $K_2S_2O_8$ decomposes to form a radical anion **291**, which abstracts hydrogen from alkane **289** to give the alkyl radical **292**. Then, **292** is trapped by CO to yield an acyl radical **294**, which further undergoes oxidation and hydrolysis to provide the desired product **290** (Scheme 11.29).

Although Sen's work offered a mild and sustainable method for synthesizing valuable carboxylic acids, the process exhibited very low alkane conversions to the acids (their yields based on the alkanes did not exceed 0.4%) and modest selectivities. It was limited to the carbonylation of methane and ethane. To address these issues, Pombeiro and coworkers found out that a 1:1 mixture H_2O/MeCN as the solvent with peroxodisulfate as oxidant was suitable for realizing a facile, efficient, and selective hydroxycarbonylation of various alkanes to yield carboxylic acids bearing $(n+1)$ carbon atoms, in the absence of a transition-metal promoter and any acid additive [59]. Both gaseous (ethane, propane, and *n*-butane) and liquid (*n*-pentane, *n*-hexane, cyclopentane, and cyclohexane) C_n alkanes were efficiently and selectively converted into the corresponding carboxylic acids. The relevant hydroxylating role of H_2O and the radical mechanism were also confirmed by radical-trap and $H_2{}^{18}O$ experiments and DFT studies.

In 1998, Ishii and coworkers developed a new type of catalytic free-radical carboxylation of polycyclic alkanes, such as adamantanes, with CO/air using *N*-hydroxyphthalimide (NHPI) as an efficient radical catalyst [60]. A plausible mechanism of the NHPI-catalyzed radical carboxylation of adamantane with CO/air system was proposed. The first step is the generation of phthalimide *N*-oxyl (PINO) from NHPI and O_2. PINO then abstracts a tertiary hydrogen from adamantane to form the adamantyl radical. The latter is trapped by CO to give an adamantane-formyl radical, followed by a reaction with O_2 to give an adamantanecarboperoxy radical and eventually the carboxylic acid product.

Recently, Fukuoka demonstrated a novel transition metal catalyst-free and radical initiator/additive-free hydroxycarbonylation of aryl iodides to yield aryl carboxylic acids (Scheme 11.30) [44]. Aryl iodide **295** reacted with CO under the assistance of a base at 250–260 °C to give aryl carboxylic acids **296** in 96–98% yields. The desired products could be readily obtained by a simple separation step (e.g. filtration) from the by-produced alkali MIs. As the reaction did not occur at 150 °C, the generation of the aryl radical by thermal dissociation of Ar–I required temperatures higher than 150 °C, preferably more than 250 °C.

Furthermore, the same research group investigated the reaction of aryl halides with CO and alkali metal salt of aromatic carboxylic acid (Ar-COOM) (M = Li, Na, K) **298** at 260–270 °C to give the corresponding carboxylic anhydrides $[(Ar\text{-}CO)_2O]$ **299**–**300**. When the alkali metal carboxylate Ar′-COOM **298** presented a different aryl group from Ar–I, only the two symmetrically substituted anhydrides **299** and **300** were obtained. With 2-iodobenzoate as substrate, phthalic anhydride was obtained (Scheme 11.31).

11.6 Transition-Metal-Free Carbonylation for the Synthesis of Acyl Chlorides and Alcohols

Acid chlorides are among the most versatile building blocks employed for synthesizing esters, amides, and ketones. As early as 1966, Thaler et al. reported a new approach to the synthesis of acid chlorides via DTBP-initiated carbonylation of alkanes with CCl_4 (Scheme 11.32) [61]. Under 410 atm of CO at 130 °C, cyclohexane

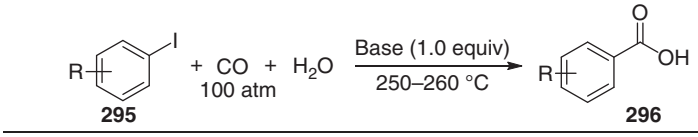

Iodide	Base	Product
 **295a**	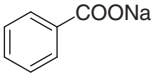	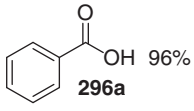 96% **296a**
 **295a**	NaOH	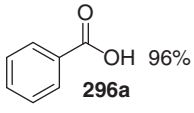 96% **296a**
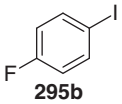 **295b**	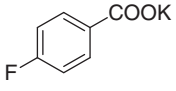	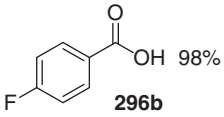 98% **296b**

Scheme 11.30 Hydroxycarbonylation of aryl iodides. Source: Modified from Fukuoka [44].

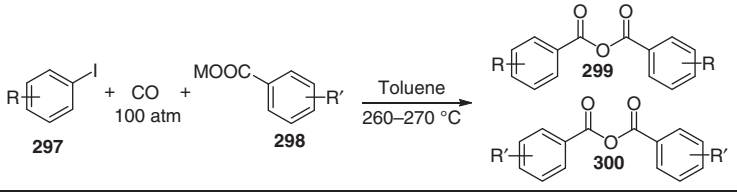

Iodide	Ar-COOM	Product
 **297a**	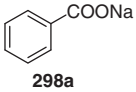 **298a**	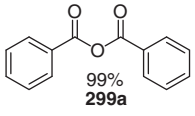 99% **299a**
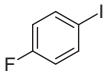 **297b**	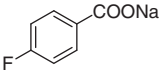 **298b**	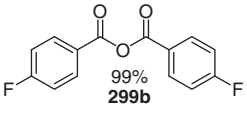 99% **299b**
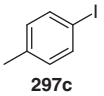 **297c**	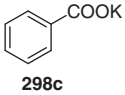 **298c**	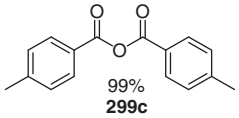 99% **299c** 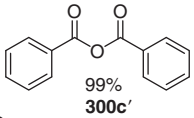 99% **300c′**
	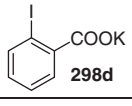 **298d**	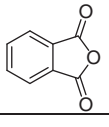 97% **300d**

Scheme 11.31 Carbonylation of aryl iodides for carboxylic acid anhydride synthesis.

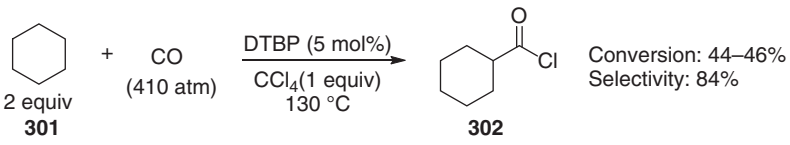

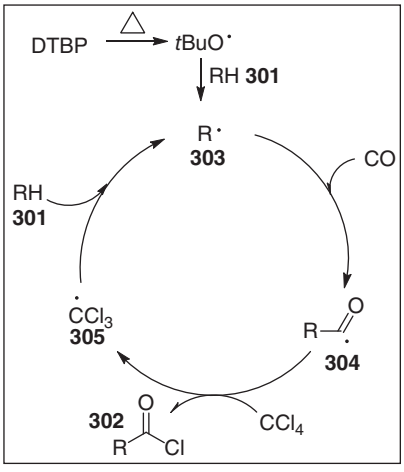

Scheme 11.32 Carbonylation of alkane for acid chloride synthesis. Source: Modified from Thaler [61].

was transformed to the corresponding acyl chloride in 44–46% conversion with 84% selectivity. Mechanistically, thermal dissociation of DTBP formed the *t*-butoxy radical, which abstracted a hydrogen from the alkane to give alkyl radical **303**. The latter was then trapped by CO to generate the acyl radical intermediate **304**, followed by the abstraction of a chlorine atom from CCl_4 to give the desired product acid chloride **302** along with trichlorocarbon radical **305**. Finally, **305** abstracts a hydrogen from an alkane to regenerate the reactive alkyl radical **303** and complete the cycle.

In 1993, Kahne et al. reported the Ph_3GeH/AIBN-induced addition of CO to alkyl radicals under high pressure and $NaBH_3CN$ reduction to form the corresponding hydroxymethyl compounds [62]. Under 96 atm of CO, primary, secondary, and tertiary alkanes reacted smoothly. This method could be employed to synthesize a B ring analog of the calicheamicin oligosaccharide, in which the hydroxylamine at C4 is replaced by a hydroxymethyl group (Eq. (11.1)).

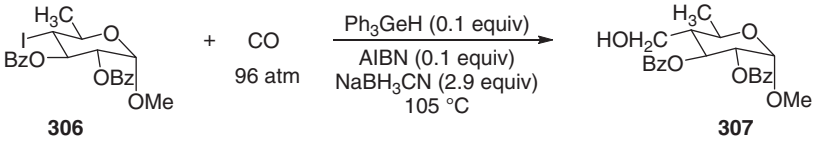

Subsequently, the Ryu group reported that a catalytic amount of fluorous tin hydride **309** could be used for the free-radical carbonylation of organic bromides **308** into the corresponding hydroxymethyl compounds using $NaBH_3CN$ as a

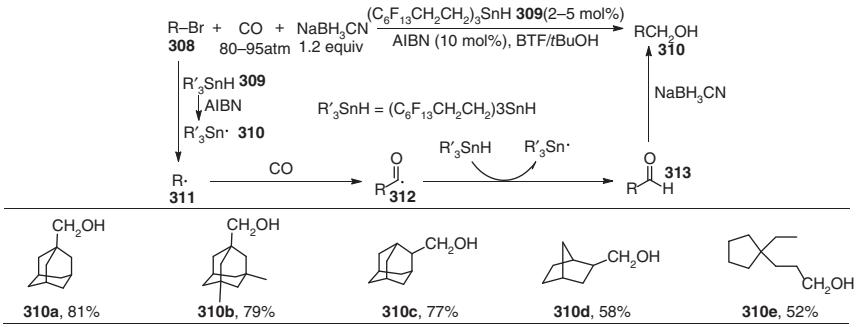

Scheme 11.33 Hydroxymethylation of organic bromides. Source: Modified from Ryu et al. [63].

reducing agent under 80–95 atm of CO and in a 1/1 mixture of BTF (benzotrifluoride) and *t*-butyl alcohol (Scheme 11.33) [63]. Notably, a three-phase workup (water-dichloromethane-perfluorohexane) was convenient for the separation of tin hydride and products. The reaction process involved alkyl radical **311**, acyl radical **312**, and reduction of aldehyde **313**. Since the use of high-pressure carbon monoxide gas may limit the application of the reaction, Ryu and coworkers further studied the hydroxymethylation of alkyl iodides to alcohols under atmospheric pressure of CO, using irradiation with near ultraviolet light and tetrabutylammonium borohydride as reducing agent [64, 65].

Recently, the Ryu group further demonstrated that the hydroxymethylation reaction of a variety of iodoarenes **314** proceeded effectively in the presence of CO, NHC-borane, diMeImd-BH_3 **315** as a radical mediator, and a catalytic amount of AIBN (Scheme 11.34) [66]. Under 80 atm of CO, a series of aryl iodides **314** reacted

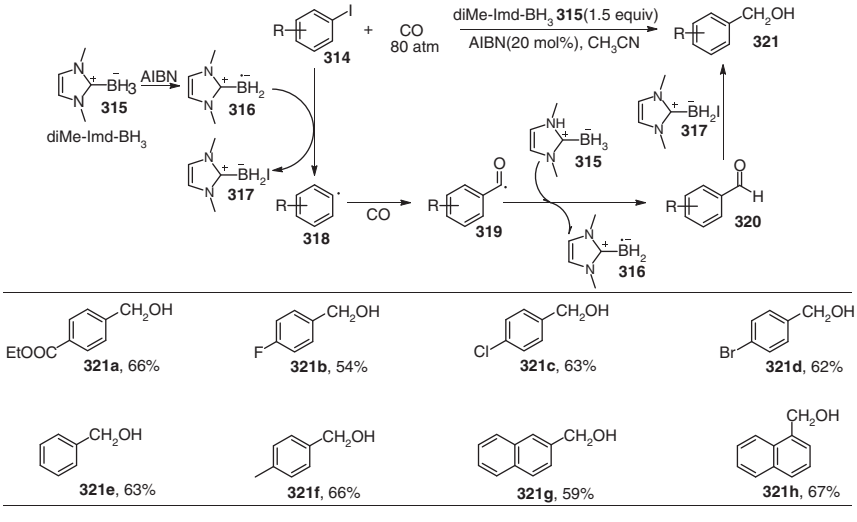

Scheme 11.34 Hydroxymethylation of organic bromides. Source: Modified from Kawamoto et al. [66].

well to give hydroxymethylated products in good yields. The proposed mechanism involves the radical initiation of aryl iodide **314** to give the aryl radical **318**, which adds to CO to form the corresponding acyl radical **319**. The acyl radical **319** can further abstract hydrogen from diMeImd-BH_3 **315** to give aldehyde **320** and the borane radical anion **316**. Subsequent iodine abstraction from aryl iodide **314** returns the aryl radical **318** and iodinated NHC **317**, thus completing the radical chain. The final alcohol is formed by hydride reduction of the aldehyde by the iodinated NHC **317** (Scheme 11.34).

Inspired by the previous work on radical hydroxymethylation of alkyl iodides with CO as a C1 source the Ryu group was interested in using more benign and easy-handling formaldehyde as a C1 synthon for the hydroxymethylation of alkyl halides. In the presence of tetrabutylammonium cyanoborohydride as a hydrogen source, the hydroxymethylation of alkyl iodides and bromides was achieved using paraformaldehyde as a radical C1 synthon (Scheme 11.35) [67].

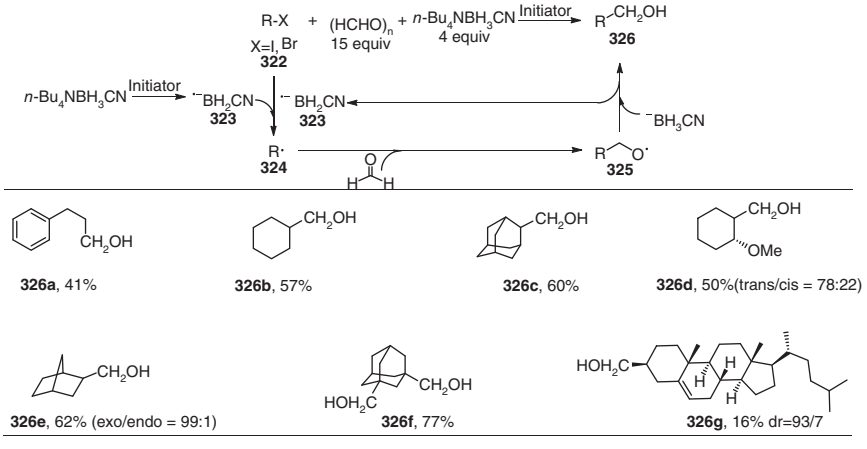

Scheme 11.35 Hydroxymethylation of organohalides. Source: Modified from Kawamoto et al. [67].

The reaction using thermal conditions with 2,2′-AIBN as a radical initiator, a 15 W black light (peak wavelength at 352 nm) in a Pyrex flask, or Hg lamp (peak wavelength at 254 nm) through a quartz tube proceeded smoothly, suggesting that the present reaction would proceed via a radical chain process. As shown in Scheme 11.35, radical initiation generates the alkyl radical **324** from **322**, which adds to formaldehyde to provide an alkoxy radical **325**. The alkoxy radical **325** abstracts hydrogen from BH_3CN^- to form alcohol product along with $BH_2CN\cdot^-$. The resulting borane radical anion $BH_2CN\cdot^-$ would abstract the bromine atom from **322** to form **324**.

11.7 Summary and Conclusions

Carbon monoxide is an important and abundant carbon resource, and carbonylation reactions are fundamental tools for synthesizing high value-added fine chemicals.

Classical carbonylation reactions require transition metal catalysis to obtain excellent catalytic activity. It may also present several limitations, such as cost of the transition-metal catalyst, deactivation of the catalyst (CO is a strong π-acidic ligand), and generation of residual metal contamination, which is difficult to be removed. Therefore, the development of transition metal catalyst-free processes has attracted more and more attention, and important progress has been achieved, especially in carbonylative cross-coupling reactions, alkoxycarbonylation, and aminocarbonylation. Moreover, some carbonylation processes may be carried out under mild reaction conditions, with good selectivity and high yield, which have great potential to replace traditional methods in practical organic synthesis.

However, compared with transition metal-catalyzed carbonylations, the transition metal-free process usually requires high pressureand shows a lower efficiency, because of the lack of the transition metal to directly activate inert carbon monoxide. Inert substrates such as organic chlorides and bromides are difficult to directly participate in the reaction directly, and the reaction types are relatively limited. Also, carbon monoxide precursors as carbonyl sources are rarely reported in transition metal-free carbonylation reactions. However, it is of great significance to develop new carbonylation reagents to introduce carbonyl groups and avoid the safety concerns of direct carbon monoxide gas use. It is also an important direction and trend to develop new strategies such as photocatalysis and electrocatalysis applied to transition metal-free carbonylation processes and carbon-hydrogen bond carbonylation reactions making the whole synthesis process simpler and producing less waste.

References

1 (a) Hagen, J. (2006). *Industrial Catalysis*. Weinheim: Wiley-VCH. (b) Beller, M. (2006). *Catalytic Carbonylation Reactions*. Heidelberg: Springer-Verlag Berlin. (c) Kollά, L. (2008). *Modem Carbonylation Methods*. Weinheim: Wiley-VCH. (d) Wu, X.-F. and Beller, M. (2013). *Transition Metal Catalyzed Carbonylation Reactions-Carbonylative Activation of C—X Bonds*. Heidelberg: Springer-Verlag Berlin.

2 Colquhoun, H.M., Thompson, D.J., and Twigg, M.V. (1991). *Carbonylation: Direct Synthesis of Carbonyl Compounds*. New York: Plenum Press.

3 (a) Garrett, C.E. and Prasad, K. (2004). *Adv. Synth. Catal.* 346: 889–900. (b) Welch, C.J., Albaneze-Walker, J., Leonard, W.R. et al. (2005). *Org. Process Res. Dev.* 9: 198–205. (c) Liu, Y.-Y., Xiong, J., Wei, L., and Chin, J. (2017). *Org. Chem.* 37: 1667–1680. (d) Yuan, S.-T., Wang, Y.-H., Qiu, G.-Y.-S., and Liu, J.-B. (2017). *Chin. J. Org. Chem.* 37: 566–576.

4 Usluer, Ö., Abbas, M., Wantz, G. et al. (2014). *ACS Macro Lett.* 3: 1134–1138.

5 Recent reviews on transition-metal-free processes, see:(a)Sun, C.-L. and Shi, Z.-J. (2014). *Chem. Rev.* 114: 9219–9280. (b) Yanagisawa, S. and Itami, K. (2011). *ChemCatChem* 3: 827–829. (c) Shirakawa, E. and Hayashi, T. (2012). *Chem. Lett.* 41: 130–134. (d) Mehta, V.P. and Punji, B. (2013). *RSC Adv.* 3: 11957–11986.

6 Brubaker, M.M., Coffman, D.D., and Hoehn, H.H. (1952). *J. Am. Chem. Soc.* 74: 1509–1515.
7 Foster, R.E., Larchar, A.W., Lipscomb, R.D., and McKusick, B.C. (1956). *J. Am. Chem. Soc.* 78: 5606.
8 Ryu, I., Kusano, K., Ogawa, A. et al. (1990). *J. Am. Chem. Soc.* 112: 1295–1297.
9 Ryu, I., Kusano, K., Masumi, N. et al. (1990). *Tetrahedron Lett.* 31: 6887–6890.
10 Nishii, Y., Nagano, T., Gotoh, H. et al. (2007). *Org. Lett.* 9: 563–566.
11 Tsunoi, S., Ryu, I., Yamasaki, S. et al. (1996). *J. Am. Chem. Soc.* 118: 10670–10671.
12 Ryu, I., Hasegawa, M., Kurihara, A. et al. (1993). *Synlett* 2: 143–145.
13 (a) Ryu, I., Kusano, K., Yamazaki, H., and Sonoda, N. (1991). *J. Org. Chem.* 56: 5003–5005. (b) Boger, D.L. and Mathvink, R.J. (1992). *J. Org. Chem.* 57: 1429–1443.
14 Ryu, I., Uehara, S., Hirao, H., and Fukuyama, T. (2008). *Org. Lett.* 10: 1005–1008.
15 Uenoyama, Y., Tsukida, M., Doi, T. et al. (2005). *Org. Lett.* 7: 2985–2988.
16 Otera, J. and Orita, A. (2000, 2000-351741). *Jpn. Kokai Tokkyo Koho* 2000.
17 (a) Gu, L.-J., Jin, C., and Liu, J.-Y. (2015). *Green Chem.* 17: 3733–3736. (b) Zhang, H.-T., Gu, L.-J., Huang, X.-Z. et al. (2016). *Chin. Chem. Lett.* 27: 256–260.
18 Gu, L., Jin, C., Liu, J. et al. (2014). *Chem. Commun.* 50: 4643–4645.
19 Li, X.-G., Liang, D.-Q., Huang, W.-Z. et al. (2016). *Tetrahedron* 72: 8442–8448.
20 Cartier, A., Levernier, E., Corcé, V. et al. (2019). *Angew. Chem. Int. Ed.* 58: 1789–1793.
21 Zhao, F., Li, C.-L., and Wu, X.-F. (2020). *Chem. Commun.* 56: 9182–9185.
22 Jin, F.-L. and Han, W. (2015). *Chem. Commun.* 51: 9133–9136.
23 (a) Cárdenas, D.J. (2003). *Angew. Chem. Int. Ed.* 42: 384–387. For recent reviews on carbonylation of C(sp^3) halides, see:(b)Liégault, B., Renaud, J.-L., and Bruneau, C. (2008). *Chem. Soc. Rev.* 37: 290–299. (c) Wu, L., Fang, X., Liu, Q. et al. (2014). *ACS Catal.* 4: 2977–2989.
24 (a) Ishiyama, T., Kizaki, H., Hayashi, T. et al. (1998). *J. Org. Chem.* 63: 4726–4731. (b) Wu, X.-F., Neumann, H., and Beller, M. (2011). *Adv. Synth. Catal.* 353: 788–792. (c) Wu, X.-F., Neumann, H., and Beller, M. (2010). *Tetrahedron Lett.* 51: 6146–6149.
25 Jin, F., Zhong, Y., Zhang, X. et al. (2016). *Green Chem.* 18: 2598–2603.
26 (a) Brouwer, L.D., Müller-Markgraf, W., and Troe, J. (1988). *J. Phys. Chem.* 92: 4905–4914. (b) Sumino, S., Ui, T., and Ryu, I. (2013). *Org. Lett.* 15: 3142–3145.
27 (a) Zhu, X., Wang, Y.-F., Ren, W. et al. (2013). *Org. Lett.* 15: 3214–3217. (b) Anstead, G.M., Altenbach, R.J., Wilson, S.R., and Katzenellenbogen, J.A. (1988). *J. Med. Chem.* 31: 1316–1326. (c) Wang, Z., Dufresne, C., Leblanc, Y., Li, C., Gauthier, J. Y., Lau, C. K., Therien, M., Roy, P., (2001). US 6174874; (d) Govek, S. P., Smith, N. D., (2011). WO 159769.
28 For a review on carbonylation of organoboranes, see:Brown, H.C. (1969). *Acc. Chem. Res.* 2: 65–72.
29 Zhao, H. and Han, W. (2016). *Eur. J. Org. Chem.* 2016: 4279–4283.
30 Han, W., Chen, J., Jin, F., and Yuan, X. (2018). *Synlett* 29: 369–374.

31 For selected reviews on carbonylations using CO surrogates, see: (a)Peng, J.-B., Qi, X., and Wu, X.-F. (2017). *Synlett* 28: 175–194. (b) Friis, S.D., Lindhardt, A.T., and Skrydstrup, T. (2016). *Acc. Chem. Res.* 49: 594–605. (c) Gautam, P. and Bhanage, B.M. (2015). *Catal. Sci. Technol.* 5: 4663–4702. (d) Wu, L., Liu, Q., Jackstell, R., and Beller, M. (2014). *Angew. Chem. Int. Ed.* 53: 6310–6320. (e) Konishi, H. and Manabe, K. (2014). *Synlett* 25: 1971–1986. (f) Odell, L.R., Russo, F., and Larhed, M. (2012). *Synlett* 23: 685–698. (g) Morimoto, T. and Kakiuchi, K. (2004). *Angew. Chem. Int. Ed.* 43: 5580–5588.

32 Xu, F., Li, D., and Han, W. (2019). *Green Chem.* 21: 2911–2915.

33 Annunziata, A., Galli, C., Marinelli, M., and Pau, T. (2001). *Eur. J. Org. Chem.* 2001: 1323–1329.

34 Koziakov, D. and Wangelin, A.J. (2017). *Org. Biomol. Chem.* 15: 6715–6719.

35 (a) Grushin, V.V. and Alper, H. (1993). *Organometallics* 12: 3846–3850. (b) Gockel, S.N. and Hull, K.L. (2015). *Org. Lett.* 17: 3236–3239. (c) Li, Z. and Wang, L. (2015). *Adv. Synth. Catal.* 357: 3469–3473.

36 Zhang, H., Shi, R., Ding, A. et al. (2012). *Angew. Chem. Int. Ed.* 51: 12542–12545.

37 Li, H., Yang, M., Qi, Y., and Xue, J. (2011). *Eur. J. Org. Chem.*: 2662–2667.

38 Sharma, P., Rohilla, S., and Jain, N. (2017). *J. Org. Chem.* 82: 1105–1113.

39 Zhao, H., Du, H., Yuan, X. et al. (2016). *Green Chem.* 18: 5782–5787.

40 Ueda, T., Konishi, H., and Manabe, K. (2013). *Angew. Chem. Int. Ed.* 52: 8611–8615.

41 Gautam, P., Gupta, R., and Bhanage, B.M. (2017). *Eur. J. Org. Chem.* 2017: 3431–3437.

42 Nagahara, K., Ryu, I., Komatsu, M., and Sonoda, N. (1997). *J. Am. Chem. Soc.* 119: 5465–5466.

43 Kreimerman, S., Ryu, I., Minakata, S., and Komatsu, M. (2000). *Org. Lett.* 2: 389–391.

44 Fukuoka, S. (2016). *Ind. Eng. Chem. Res.* 55: 4830–4835.

45 Guo, W., Lu, L.-Q., Wang, Y. et al. (2015). *Angew. Chem. Int. Ed.* 54: 2265–2269.

46 Majek, M. and Wangelin, A.J. (2015). *Angew. Chem. Int. Ed.* 54: 2270–2274.

47 (a) Galli, C. (1988). *Chem. Rev.* 88: 765–792. (b) Kindt, S., Wicht, K., and Heinrich, M.R. (2015). *Org. Lett.* 17: 6122–6125. (c) Fehler, S.K., Pratsch, G., Ostreicher, C. et al. (2016). *Tetrahedron* 72: 7888–7893. (d) Kindt, S., Wicht, K., and Heinrich, M.R. (2016). *Angew. Chem. Int. Ed.* 55: 8744–8747. (e) Hegmann, N., Prusko, L., and Heinrich, M.R. (2017). *Org. Lett.* 19: 2222–2225. (f) Hofmann, J., Gans, E., Clark, T., and Heinrich, M.R. (2017). *Chem. Eur. J.* 23: 9647–9656. (g) Koziakov, D., Majek, M., and Wangelin, A.J. (2016). *Org. Biomol. Chem.* 14: 11347–11352. (h) Gomberg, M. and Bachmann, W.E. (1924). *J. Am. Chem. Soc.* 46: 2339–2343. (i) Huisgen, R. and Krause, L. (1951). *Ann. Chem.* 574: 157–171. (j) Crisostomo, F.P., Martin, T., and Carrillo, R. (2014). *Angew. Chem. Int. Ed.* 53: 2181–2185.

48 Xu, J.-X., Franke, R., and Wu, X.-F. (2018). *Org. Biomol. Chem.* 16: 6180–6182.

49 Lu, L., Cheng, D., Zhan, Y. et al. (2017). *Chem. Commun.* 53: 6852–6855.

50 Kim, S., Kim, S., Otsuka, N., and Ryu, I. (2005). *Angew. Chem. Int. Ed.* 44: 6183–6186.

51 Kim, S., Lim, K.-C., and Kim, S. (2008). *Chem. Asian J.* 3: 1692–1701.

52 Bertrand, M.P. (1994). *Org. Prep. Proced. Int.* 26: 257–290.

53 Ryu, I., Nagahara, K., Kambe, N. et al. (1998). *Chem. Commun.* 18: 1953–1954.

54 (a) Ryu, I. and Sonoda, N. (1996). *Angew. Chem. Int. Ed.* 35: 1050–1066. (b) Tsentalovich, Y.P. and Fischer, H. (1994). *J. Chem. Soc., Perkin Trans.* 2: 729–733. (c) Brown, C.E., Neville, A.G., Rayner, D.M. et al. (1995). *Aust. J. Chem.* 48: 363–379. (d) Chatgilialoglu, C., Ferreri, C., Lucarini, M. et al. (1995). *Organometallics* 14: 2672–2676.

55 Ryu, I., Sonoda, N., and Curran, D.P. (1996). *Chem. Rev.* 96: 177–194.

56 Uenoyama, Y., Fukuyama, T., Nobuta, O. et al. (2005). *Angew. Chem. Int. Ed.* 44: 1075–1078.

57 Kawamoto, T., Sato, A., and Ryu, I. (2015). *Chem. Eur. J.* 21: 14764–14767.

58 Lin, M. and Sen, A. (1992). *J. Chem. Soc., Chem. Commun.* 12: 892–893.

59 (a) Kirillova, M.V., Kirillov, A.M., and Pombeiro, A.J.L. (2010). *Chem. Eur. J.* 16: 9485–9493. (b) Kirillova, M.V., Kirillov, A.M., Kuznetsov, M.L. et al. (2009). *Chem. Commun.* 2009: 2353–2355.

60 Kato, S., Iwahama, T., Sakaguchi, S., and Ishii, Y. (1998). *J. Org. Chem.* 63: 222–223.

61 Thaler, W.A. and Am, J. (1966). *Chem. Soc.* 88: 4278–4279.

62 Gupta, V. and Kahne, D. (1993). *Tetrahedron Lett.* 34: 591–594.

63 Ryu, I., Niguma, T., Minakata, S. et al. (1997). *Tetrahedron Lett.* 38: 7883–7886.

64 Kobayashi, S., Kawamoto, T., Uehara, S. et al. (2010). *Org. Lett.* 12: 1548–1551.

65 Kawamoto, T., Matsubara, H., and Ryu, I. (2014). *Chem. Lett.* 43: 1140–1142.

66 Kawamoto, T., Okada, T., Curran, D.P., and Ryu, I. (2013). *Org. Lett.* 15: 2144–2147.

67 Kawamoto, T., Fukuyama, T., and Ryu, I. (2012). *J. Am. Chem. Soc.* 134: 875–877.

12

Conclusions and Perspectives

Bartolo Gabriele

University of Calabria, Laboratory of Industrial and Synthetic Organic Chemistry (LISOC), Department of Chemistry and Chemical Technologies, Via Pietro Bucci 12/C, 87036 Arcavacata di Rende, Italy

The use of carbon monoxide as C-1 building block has become an essential tool in modern organic synthesis to directly prepare carbonyl compounds with high atom and step economy. Since the pioneering studies by Reppe and Roelen in the 1930s, impressive progress has been made in carbonylation chemistry, both at the industrial and academic levels. Carbonylation is now widely recognized as the most attractive approach for the direct insertion of the carbonyl functional group into an organic substrate.

This book discusses the synthetic applications of carbonylation chemistry, with particular reference to the most recent achievements in this field. Metal-catalyzed carbonylation processes have been presented on the basis of the metal species promoting them (Chapters 2–10). This classification has permitted us to better focus on the different catalytic abilities and specificities of different metal catalysts in promoting various carbonylation processes. A final chapter has been devoted to metal-free-catalyzed reactions (Chapter 11).

Part I of the book (Chapters 2–4) focused on Carbonylations promoted by first-row transition metal catalysts. Chapter 2 (by Jérôme Volkman and Philippe Kalck) described the carbonylations promoted by cobalt catalysts. Cobalt catalysts were the first kind of catalysts used in the hydroformylation of alkenes. They are still the most important catalysts for the hydroformylation of heavy alkenes and the Pauson–Khand reaction. Additional important applications involve the carbonylation of epoxides to yield lactones and, more recently, C–X and C–H carbonylations. Chapter 3 (by Debarati Das and Bhalchandra M. Bhanage) described the nickel-catalyzed carbonylations. Apart from being relatively inexpensive, Nickel may present four different oxidation states (from 0 to +3), which may allow peculiar mechanistic pathways leading to various carbonyl derivatives, which were illustrated in the chapter. Carbonylation processes catalyzed by other first-row transition metal catalysts (manganese, iron, copper) were treated in Chapter 4 (by Chong-Liang Li, Hai Wang, and Xiao-Feng Wu). These catalysts are based on relatively abundant and less toxic metals than traditional heavier metals. They may

Carbon Monoxide in Organic Synthesis: Carbonylation Chemistry,
First Edition. Edited by Bartolo Gabriele.

become very competitive when shown to efficiently catalyze a carbonylation process classically promoted by a heavier, more expensive metal-based catalyst. Although their versatility tends to be generally lower than heavier metal catalysts, their use in carbonylation chemistry is relatively recent, so there is room for improvement in future studies.

Part II of the book (Chapters 5–9) was devoted to carbonylations promoted by second-row transition metal catalysts, among which are the most important metal catalysts for these transformations (that are, Ru-, Rh-, and Pd-based catalysts). Chapter 5 (by Helfried Neumann and Jagadeesh Rajenahally) described ruthenium-based carbonylations. Ru-based catalysts are particularly efficient in carbonylative processes occurring with C–H activation and Pauson–Khand reactions. Moreover, their utility in carbonylative cyclization processes has been well-documented in recent studies. Rhodium-catalyzed carbonylations were the topic of Chapter 6 (by Oreste Piccolo and Stefano Paganelli). Rh catalysts are very active in the hydroformylation of light alkenes and the industrially relevant direct carbonylation of methanol to acetic acid. Chapters 7 and 8 were devoted to the most versatile carbonylation catalysts, that are, Pd-based catalysts. Palladium catalysts promote a plethora of different carbonylation processes, including cross-coupling carbonylative reactions, alkoxycarbonylations, hydroxycarbonylations, aminocarbonylations, and carbonylative cyclizations, often under mild reaction conditions. The large number and variety of carbonylations catalyzed by Pd-based catalysts have justified the dedication of two different chapters to these processes. Chapter 7 (by Jianming Liu, Chengtao Yue, and Fuwei Li) illustrated Pd(0)-catalyzed carbonylations, which are usually based on a general mechanistic pathway involving oxidative addition to Pd(0), carbon monoxide insertion, and reductive carbonylation to Pd(0) as the key elementary steps. Pd(II)-catalyzed carbonylations were treated in Chapter 8 (by Bartolo Gabriele, Nicola Della Ca', Raffaella Mancuso, Lucia Veltri, and Ida Ziccarelli). Palladium(II) complexes can catalyze carbonylation processes in a completely different manner compared to Pd(0), as Pd(II) does not usually undergo oxidative addition to give a rather unstable Pd(IV) species. The electrophilic character of Pd(II) makes Pd(II)-based catalysts able to electrophilically attack different organic substrates. They can undergo carbonylation with the formation of a variety of carbonyl compounds. Due to the "noble" character of palladium, in some cases and with specific substrates, these processes occur with concomitant reduction of Pd(II) to Pd(0). The use of a suitable external oxidant is therefore needed to oxidize back Pd(0) to catalytically active Pd(II), closing the catalytic cycle. Pd(II)-based catalysts are indeed the most effective, important, and versatile catalysts for performing these kinds of processes (oxidative carbonylations). Chapter 9 (by Francesca Foschi and Gianluigi Broggini) described the carbonylations catalyzed by other second-row transition metal catalysts (zirconium, silver, and molybdenum, in particular). Their catalytic efficiency is still rather limited compared to other more classical metals. However, being relatively unexplored, it is likely that future progress will lead to interesting novel results and applications.

The book ends with Part III (Chapters 10 and 11) dedicated to miscellaneous carbonylation reactions. Carbonylations promoted by third-row transition metal catalysts were the topic of Chapter 10 (by Anthony Haynes). Industrially relevant iridium-catalyzed carbonylation of methanol to acetic acid, as well as iridium and platinum-based catalysts for alkene hydroformylation and other carbonylation processes, were described. Chapter 11 (by Lu Cheng, Binbin Liu, Fangning Xu, and Wei Han) highlighted the potential of transition-metal-free carbonylation processes in synthesis, emphasizing radical carbonylations.

The use of CO as the simplest carbonyl precursor is destined to play a major role in the future, given the increasingly stringent sustainability requirements in organic synthesis. The availability of carbon monoxide as well as of its surrogates, associated with the high step and atom economy of the process, make carbonylation the most attractive and important approach for the direct synthesis of carbonyl compounds, which are very important at the industrial level and for the production of fine chemicals with different important applications (in material science, biomedical, and other fields). By combining the suitable catalyst with the appropriately functionalized starting materials, not only relatively simple and/or industrially important carbonyl compounds can be prepared in one step, but also complex molecular architectures (difficult to prepare by conventional synthetic techniques) can be made easily accessible.

In the future, progress in catalysis and catalytic system engineering (including bimetallic systems) is expected to lead to more performing catalysts, both in turnover numbers (TONs) and product selectivity. This includes enantioselectivity in the case of nonracemic catalysts leading to specific enantiomeric products with peculiar properties.

Another fascinating research field that will be implemented will concern the heterogenization of the catalytic system, aimed at synthesizing heterogeneous systems with activities and selectivities at least comparable to those achieved by the homogenous catalysts. Their use will allow easier separation of the catalyst from the reaction mixture, minimize metal contamination in the organic product, and possibly allow catalyst recycling. The progress in metal-free carbonylations (radical carbonylations, in particular) will also give a significant push in avoiding metal contamination in the carbonylated product, which is very important for biomedical applications.

Finally, research in the field of nonconventional solvents (such as ionic liquids and deep eutectic solvents), less toxic substitutes of “classical” volatile organic solvents, will permit to carry out more and more carbonylation processes under safer and more environmentally friendly conditions.

Index

Carbon Monoxide in Organic Synthesis: Carbonylation Chemistry,
First Edition. Edited by Bartolo Gabriele.

d

n

s

t

u

v